UNIV. OF
TORONTO
LIBRARY

BULLETIN

OF THE

UNIVERSITY OF WISCONSIN

ENGINEERING SERIES

VOLUME IV
1907-08

LIBRARY
MAR 4 1912
UNIVERSITY OF TORONTO.

122480
15/6/12

MADISON, WISCONSIN
1908

BULLETIN OF THE UNIVERSITY OF WISCONSIN

COMMITTEE OF PUBLICATION

Walter M. Smith, *Chairman*
Willard G. Bleyer, *Secretary*
Charles M. Gillett, *Editor*

John R. Commons, *Economics and Political Science Series*
William H. Lighty, *University Extension Series*
William S. Marshall, *Science Series*
Daniel W. Mead, *Engineering Series*
Julius E. Olson, *General Series*
Edward T. Owen, *Philology and Literature Series*
William L. Westermann, *History Series*

CONTENTS

PAGE

No. 1. Tests on plain and reinforced concrete, series of 1906, by Morton Owen Withey 1

No. 2. Tests on plain and reinforced concrete series of 1907, by Morton Owen Withey 67

No. 3. Investigation of the hydraulic ram, by LeRoy Francis Harza 137

No. 4. Investigation of flow through large submerged orifices and tubes, part I, by Clinton Brown Stewart 249

No. 5. Current practice in steam engine design, by Ole N. Trooien 333

No. 6. Self-excited polyphase asynchronous generators, by Lewis Fussell 413

BULLETIN OF THE UNIVERSITY OF WISCONSIN
NO. 175
ENGINEERING SERIES, VOL. 4, NO. 1, PP. 1-66

TESTS ON PLAIN AND REINFORCED CONCRETE

SERIES OF 1906

BY

MORTON OWEN WITHEY, C. E.
Instructor in Mechanics, University of Wisconsin

RESEARCHES IN APPLIED MECHANICS

EDWARD R. MAURER, PROFESSOR OF MECHANICS

*Published bi-monthly by authority of law with the approval of the Regents
of the University and entered at the post office at
Madison as second-class matter*

MADISON, WISCONSIN
NOVEMBER, 1907

CONTENTS.

PAGE
I. Introduction 5
II. Description of materials 6
III. Bond tests 10
IV. Compression tests 13
V. Beams 19
  1. Series A. Simple beam 28
  2. Series B. Reinforced in top and bottom 29
  3. Series C. Overhanging beams 40
  4. Series D. Overhanging beams 44
  5. Tee beams 60

ILLUSTRATIONS.

PLATES.

I. Compressometer apparatus 14
II. Overhanging beam N_2 ready to be tested 21
III. Failure cracks in beam P_1, V_2 and A_2 25
IV. Failure cracks in beams B_1 and B_2 54
V. Failure cracks in beams D_2 and K_1 56
VI. Failure cracks in beams E_1, E_2 and L_2 57
VII. Failure cracks in beams F_1, M_1 and M_2 59
VIII. Failure cracks in beams C_2, tee beams A_1 and D_2 64

FIGURES.

1. Relation between bond and compressive strength 11
2. Cylinders—stress-deformation curves 15
3, 4. Cylinders—stress-deformation curves 18
5. Forms 20
6. Stirrups 20
7. Deflectometer apparatus 23
8. Beams of series A—reinforcement 28
9. Beams of series A—moment deformation curves, etc 30
10. Beams of series A—moment deformation curves, etc 31

PAGE
11. Beams of series B—reinforcement curves 32
12. Beams of series B—moment-deformation curves, etc 35
13. Beams of series B—moment-deformation curves, etc... 36
14. Beams of series B—moment-deformation curves, etc........... 37
15. Beams of series B—moment-deformation curves, etc........... 38
16. Beams of series C—reinforcement 39
17. Beams of series D—reinforcement and cracks....... 44
18. Beams of series D—reinforcement and cracks.................. 45
19. Beams of series D—reinforcement and cracks.................. 46
20. Beams of series D—load-deflection curves 49
21. Beams of series D—load-deflection curves 50
22. Beams of series D—load-deflection curves 51
23. Beams of series D—load-deflection curves 52
24. Tee beams—reinforcement and cracks.......................... 61
25. Tee beams—reinforcement and cracks 62
26. Tee beams—moment-deflection curves 63

TABLES.

I. Tension tests of steel 7
II. Analysis of stone 7
III. Analysis of sand 8
IV. Tensile strength of cement 9
V. Variation of bond with the compressive strength 11
VI. Value of bond developed for rods of different diameters.. 12
VII. Comparison of bond of straight and bent rods 13
VIII. Comparison of compressive strength of cylinders and cubes 16
IX. Moduli of elasticity of cylinders.......................... 17
X. Stresses in tensile reinforcement computed by various methods 27
XI. Simple beams, series A 28
XII. Simple beams, series B 33
XIII. Beams, series B. Values of v and $\frac{M}{bd^2}$ 34
XIV. Series C. Reinforcement of overhanging beams 41
XV. Overhanging beams, series C. Values of v and $\frac{M}{bd^2}$ 42
XVI. Series C. Stresses in steel at center of span............. 42
XVII. Overhanging beams, series D. Values of v and $\frac{M}{bd^2}$ 47
XVIII. Overhanging beams, series D. Stresses in steel 48
XIX. Tee beams.......................... 66

TESTS ON PLAIN AND REINFORCED CONCRETE

I. INTRODUCTION.

This bulletin is a report of tests upon plain and reinforced concrete made in the testing laboratory of the University of Wisconsin during the summer of 1906. The following subjects were investigated: bond; compressive strength of concrete in cubes, cylinders and beams; effect of compression reinforcement in beams; overhanging beams; diagonal tension failures and methods of preventing the same; tee beams.

In the investigations, an effort was made to approach practical working conditions wherever possible. Materials were purchased in the open market. Concrete was mixed wet in accordance with standard methods. Experienced men were employed for this purpose. Specimens, except in special cases, were cured in air. As the air in the laboratory was considerably drier than that out-of-doors, the strength of the specimens doubtless suffered more from evaporation than if seasoned in the open air. The compressive strength of cubes and cylinders furnishes but little indication of the ability of the concrete to resist diagonal tensile stresses. Tensile tests made in connection with beams would, without doubt, be of much more value for this purpose.

A new computed quantity will be noted in the results of the compression tests called the 600 lbs./in^2 modulus of elasticity. The initial modulus and the secant modulus at the ultimate have been employed in working formulae. The first is evidently too high a value, while the second is too low. In order to approximate more closely a ratio of stress to deformation which will apply to working stresses, the slope of a line drawn from the origin of coordinates to a point on the stress-deformation curve representing a stress of 600 lbs./in^2. has been determined and reported. While it is recognized that the modulus of elasticity of concrete is a variable quantity, it is believed that values computed in this manner are sufficiently accurate for working conditions under static loading.

As the principles of continuity over supports has a wide application in all concrete structures, it was decided to make overhanging beams for the purpose of investigating web stresses. A constant amount of horizontal reinforcement, large enough to develop the full strength of the concrete in compression, was employed The ratio of span to depth was made small to secure high tensile web stresses.

A great deal of pains was taken to note the appearance and growth of cracks. In reporting failures, the primary one is in all cases tabulated. The diagrams of cracks and reinforcement are scale-drawn copies of sketches made from measurements taken on the beams. These are included here in order that the position of cracks with reference to reinforcement may be observed.

The inception of these experiments was due to Dean F. E. Turneaure. Much of the work was planned by him and carried out at his suggestion. Acknowledgement is also made to F. M. McCullough, H. F. Moore and E. A. Moritz, members of the instructional force, and E. P. Abbott of the class of 1908 for valuable assistance in these investigations. H. F. Lutze, of the class of 1908, assisted in preparing drawings for this bulletin. Funds for the work were provided by the University.

II. DESCRIPTION OF MATERIALS.

Metal:—All reinforcement was purchased in the local market. With one exception, round rods of mild steel were used as longitudinal reinforcement in all beams. In the compression beams, Series A, $\frac{1}{2}$-inch Johnson corrugated bars (new style) were employed. For web reinforcement, $\frac{1}{4}$-inch and $\frac{3}{16}$-inch round rods and expanded metal were used. Table I shows character of metal.

TABLE I.

Tension Tests of Steel.

Diameter of Specimen (in ins.)	Yield Point (in lbs./in.^{2})	Ultimate Strength (in lbs./in.^{2})
$\frac{3}{16}$	93,700	101,000
$\frac{1}{4}$	53,000	67,700
$\frac{3}{8}$	51,600	68,700
$\frac{1}{2}$	38,600	56,000
$\frac{9}{16}$	36,400	52,400
$\frac{5}{8}$	42,300	61,500
$\frac{3}{4}$	42,200	62,100

Stone:—Crushed limestone from Kankakee, Illinois, was used in this work. It was of good quality, weighed 83 pounds to the cubic foot, measured loose, and contained 48½ per cent voids. The proportion of the various sizes in a 40-pound sample is shown in Table II.

TABLE II.

Analysis of Stone.

Diameter of Mesh (in ins.)	Amount Retained (in lbs.)	Per Cent. Passing.
1		100
$\frac{3}{4}$	2.00	95
$\frac{1}{2}$	27.25	26.4
.2	9.00	3.8
No. 20	1.06	1.1
Dust	.44	

Sand:—The local market supplied the sand. Although fairly clean, it was too fine to give the best results. It weighed 103 pounds per cubic foot, loose, and contained 38 per cent voids. A mechanical analysis is given in Table III.

TABLE III.

ANALYSIS OF SAND.

Sieve No.	Diameter of Mesh. (in ins.)	Per cent Passing.
6	0.131	98.7
10	0.073	96.1
16	0.042	92.9
20	0.034	90.9
30	0.022	78.1
40	0.015	61.9
50	0.011	35.7
74	0.0078	14.0
100	0.0045	10.4

Cement:—The United States Geological Survey furnished all cement. Table IV contains the results of tests made upon the various brands of cement used in these experiments.

These tests were made in accordance with the rules of the American Society for Testing Materials. The mixed brands consisted of five Standard American Portland Cements. Saylors and Giant brands were used in the overhanging beams, Lehigh in the beams of Series B, Dragon in beams of Series A and the mixed brands in the tee beams.

Concrete:—A 1:2:4 mixture was adopted as being, on the whole, the most suitable for this work. All materials were measured loose except the cement which was weighed, 100 pounds being allowed to the cubic foot. The cement and sand were thoroughly mixed dry, and then the wetted stone was thrown upon the dry mortar. Water was added and the whole turned until it appeared of uniform consistency. About 8½ per cent of water by weight was required to produce a wet mixture which could be easily worked around the reinforcement.

Specimens were surfaced by running a large trowel around the inside of the mold, thus bringing the mortar to the outside and forming a smooth finish. This was necessary in order that cracks might readily be detected.

TABLE IV.

TENSILE STRENGTH OF CEMENTS.

BRIQUETTE No.	Ultimate Strength (in lbs. in.^{2})				Brand.
	Age 7 Days.		Age 28 Days		
	Neat.	1:3 Mortar.	Neat.	1:3 Mortar.	
1	550	260	542	330	Giant.
2	530	220	470	360	
3	630	240	542	346	
4	590	210	522	330	
Average	575	232	519	341	
1	610	238	585	340	Lehigh.
2	536	216	695	355	
3	506	206	690	370	
4	552	226	660	395	
Average	551	221	658	378	
1	440	160	530	250	Dragon.
2	560	220	580	225	
3	530	176	650	290	
4	476	152	520	290	
Average	501	177	570	264	
1	616	300	660	360	Saylors.
2	654	194	730	290	
3	696	236	700	358	
4	580	232	686	312	
Average	636	240	694	330	
1	380	160	680	248	Mixed Brands.
2	520	138	680	308	
3	538	160	680	222	
4	....	190	600	280	
Average	486	162	660	264	

III. BOND TESTS.

The form of specimen adopted in these tests was that of a prism, 8 inches by 8 inches in cross-section. Part of the blocks were 6 inches long and the remainder 8 inches. In all cases, one end of the rod was set flush with the face of the block while the other projected from the opposite face far enough to afford a hold for the grips of the testing machine. The rods were all of mild steel from the same lot as the steel used in the beams. Specimens were allowed to remain in the mold for two days and in the air for twenty-five. In testing, the rod was run up through the movable crosshead of the machine and gripped by the fixed crosshead. The movable head was then run down and the specimen adjusted to an even bearing. No plaster of paris or blotting paper was used between the specimen and crosshead. This method of testing is not ideal as a compressive stress is placed upon the concrete next to the pulling head which doubtless increases the bond. The maximum load was read and the bond computed from it. As soon as the rod had slipped an appreciable amount, the load which balanced the beam was noted and recorded as the frictional resistance. This reading was taken while the machine was still running.

Table V contains the results of tests made from various batches of concrete. Nos. 8 and 9 in this table were made from a concrete in which limestone screenings and sand were used as aggregate. The screenings contained about 40 per cent of dirt. From Fig. 1, it would seem that the bond of 1:2:4 concrete increases with the compressive strength. For these tests the bond developed averages about .3 of the compressive strength.

TABLE V.

VARIATION OF BOND WITH THE COMPRESSIVE STRENGTH. 1:2:4 CONCRETE.

Age of specimens 28 days.

Test No.	Size of Rod (in ins.)	Area (in sq. ins.)	Depth Imbedded (in ins.)	Maximum Load (in lbs.)	Unit Stress in Rod (in lbs./in.^{2})	Elastic Limit (in lbs./in.^{2})	Bond (in lbs./in.^{2})	Strength of Concrete (in lbs./in.^{2})
1	$\frac{9}{16}$	.248	$6\frac{1}{4}$	6,700	27,000	36,400	607	1,850
2	"	"	$6\frac{1}{8}$	5,500	22,200	"	509	2,000
3	"	"	$6\frac{1}{2}$	7,200	29,000	"	627	2,155
4	"	"	$6\frac{1}{4}$	4,625	18,600	"	418	1,485
5	"	"	$6\frac{1}{4}$	4,250	17,100	"	384	1,435
6	"	"	6	4,100	16,500	"	387	1,150
7	$\frac{1}{2}$	.196	6	3,600	18,400	38,600	382	1,150
8	"	"	$5\frac{3}{4}$	1,500	7,600	"	166	795
9	"	"	$6\frac{1}{4}$	1,840	9,400	"	187	584

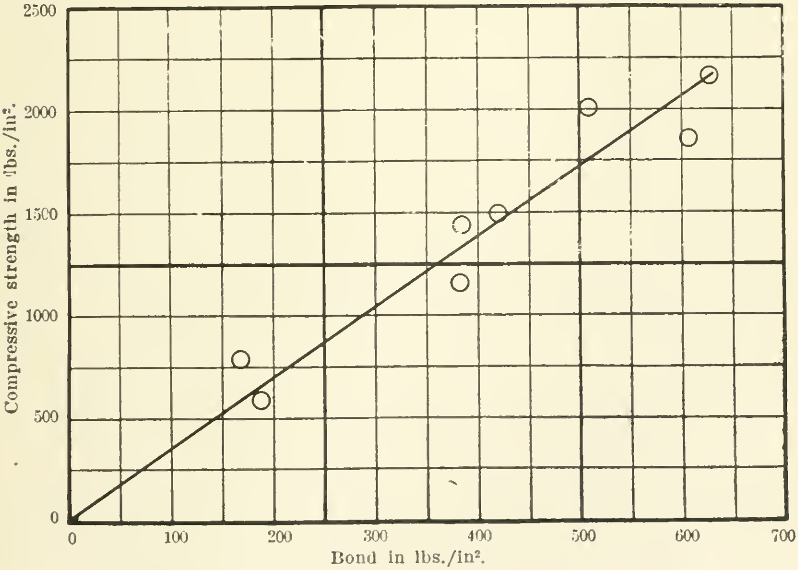

FIG. 1.—RELATION BETWEEN BOND AND COMPRESSIVE STRENGTH.

TABLE VI.

VALUES OF BOND DEVELOPED FOR RODS OF DIFFERENT DIAMETERS.
Age of specimens 28 days. Compressive Strength of 1:2:4 Concrete 1,150 lbs. in.^{2}

Test No.	Size of Rod (in ins.)	Area (in sq. in.)	Depth Imbedded (in ins.)	Maximum Load (in lbs.)	Stress in Rod (in lbs./in.^{2})	Elastic Limit (in lbs./in.^{2})	Bond (in lbs./in.^{2})	Fictional Resistance (in lbs./in.^{2})	Friction / Bond.
1	$\frac{3}{16}$	.0276	6	1,160	42,000	93,700	327	267	.82
2	$\frac{1}{4}$	.0491	”	2,525	51,500	53,000	535	445	.83
3	$\frac{3}{8}$	.1100	”	3,200	29,100	51,600	454	370	.82
4	$\frac{1}{2}$	.1960	”	3,600	18,400	38,600	382	276	.72
5	$\frac{9}{16}$	.2480	”	4,100	16,500	36,400	387	284	.75
6	$\frac{5}{8}$	.3070	”	4,600	15,000	42,300	391	340	.87
7	$\frac{3}{4}$	.4420	”	4,600	10,400	42,200	327	270	.82
						Average.	400	322	.80
8	$\frac{3}{16}$	.0276	8	1,750	63,400	93,700	372	350	.94
9	$\frac{1}{4}$	.0491	”	1,800	36,700	53,000	286	255	.89
10	$\frac{3}{8}$	.1100	”	3,200	29,100	51,600	340	170	.50
11	$\frac{1}{2}$	.1960	”	4,000	20,400	38,600	318	270	.85
12	$\frac{9}{16}$	.2480	”	4,400	17,700	36,400	311	276	.89
13	$\frac{5}{8}$	.3070	”	3,900	12,700	42,300	248	210	.85
14	$\frac{3}{4}$	.4420	”	5,500	12,400	42,200	292	265	.91
						Average.	310	257	.83

Table VI gives the results of tests, all of which were made from the same batch of concrete. It will be noted that the average bond of the 6-inch specimens was 400 lbs./in^2., while that developed by the 8-inch was only 310 lbs./in^2. The frictional resistance changed in a like manner. For the 6-inch and the 8-inch specimens, the frictional resistance averaged 80 per cent and 83 per cent respectively of the bond stress.

An attempt was made to ascertain the effect upon bond of bending over the end of the bar. For this purpose the bars were bent at right angles two inches from the end. In making the specimen, the bar was placed in the center of the mold with the bend on the bottom and extending towards a corner. These specimens were made from the same batch as those of Table VI. A comparison of the bond of straight and bent rods is given in Table VII.

TABLE VII.

Comparison Between Bond of Straight and Bent Rods.

Age of specimens 28 days. Compressive strength of concrete 1,150 lbs./in.^{2}

Test No.	Size of Rod (in ins.)	Depth of Block (in ins.)	Maximum Load on Bent Rod (in lbs.)	Maximum Load on Str. Rod (in lbs.)	Remarks.
1	$\frac{3}{16}$	6	1,655	1,160	Bent rod slipped.
2	$\frac{3}{16}$	8	....	1,750	"
3	$\frac{1}{4}$	6	2,780	2,525	"
4	$\frac{1}{4}$	8	2,600	1,800	"
5	$\frac{3}{8}$	6	3,450	3,200	In bent rod specimens.
6	$\frac{3}{8}$	8	3,600	3,200	Concrete split.
7	$\frac{1}{2}$	6	3,710	3,600	"
8	$\frac{1}{2}$	8	5,750	4,000	"
9	$\frac{9}{16}$	6	4,100	4,100	"
10	$\frac{9}{16}$	8	5,050	4,400	"
11	$\frac{5}{8}$	6	5,100	4,600	"
12	$\frac{5}{8}$	8	6,300	3,900	"
13	$\frac{3}{4}$	6	5,100	4,600	"
14	$\frac{3}{4}$	8	5,600	5,500	"

IV. COMPRESSION TESTS.

With every batch of concrete, one or more specimens were made to determine the compressive strength of the mixture. In general, two of these specimens were made at a mixing, a 4-inch cube and a cylinder 6 inches in diameter and 18 inches long. Particular care was taken in making the cylinders. Cast iron molds with ends planed parallel and the inside ground to a uniform bore were employed. These were oiled and set up on a horizontal slate slab. The concrete was puddled with a $\frac{1}{4}$-inch rod as it was poured into the mold so that the surface would be free from air holes. An excess of material was placed upon the top to allow for settling, it was found that at the end of a half hour most of the settling had ceased. The head of the cylinder was then carefully leveled off with a trowel. All cubes and cylinders except S_3 and S_4 were cured in air. These were stored in water after two days in the molds.

In testing, those cylinders whose tops were uneven were imbedded in plaster of paris. These are marked with an asterisk in the tables. The others were bedded on two sheets of blotting paper at the top and bottom. The cubes were also bedded on blotting paper.

Plate I shows the compressometer for measuring deformations of cylinders. The apparatus consists essentially of two collars which are separated, while the instrument is being put on, by a 12-inch gauge bar. On the back side of the upper collar is a slotted pin to which is attached one end of a No. 32 covered copper wire. The wire is carried vertically downward parallel to the axis of the cylinder to a pulley mounted on the lower collar. It is then led around the test piece by means of a pulley

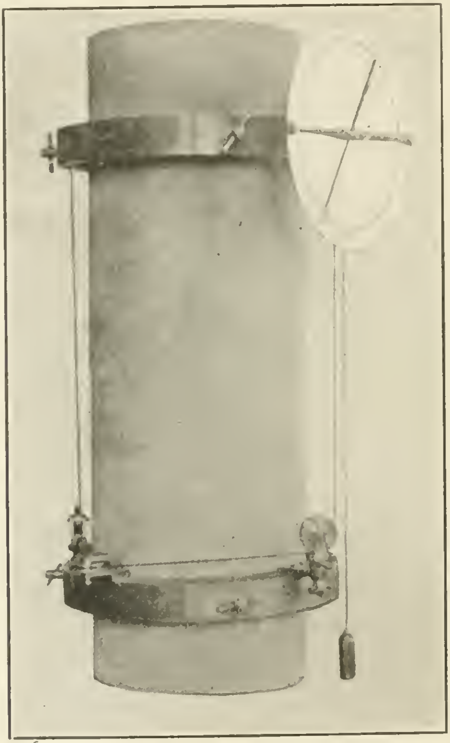

PLATE I. COMPRESSOMETER APPARATUS.

with its axis vertical, to a third pulley from which it is carried vertically to the drum of a dial fastened on the upper collar. A small weight serves to keep the wire taut. The dial has a screw and lock-nut attachment which allows it to be removed and placed upon other apparatus. The circumference of the dial is graduated into 1,000 parts. As the dial drum is 1 inch in circumference, the vernier attachment makes readings to one ten-thousandth of an inch possible.

This form of apparatus proved very efficient and satisfactory in this work. Its advantages are:—

An average deformation of both sides of the specimen is obtained by reading only one dial.

The apparatus can be quickly adjusted. Only a minimum amount of time is consumed in taking readings. In fact, this may be done without stopping the machine.

It is not necessary to touch the apparatus after the test is started.

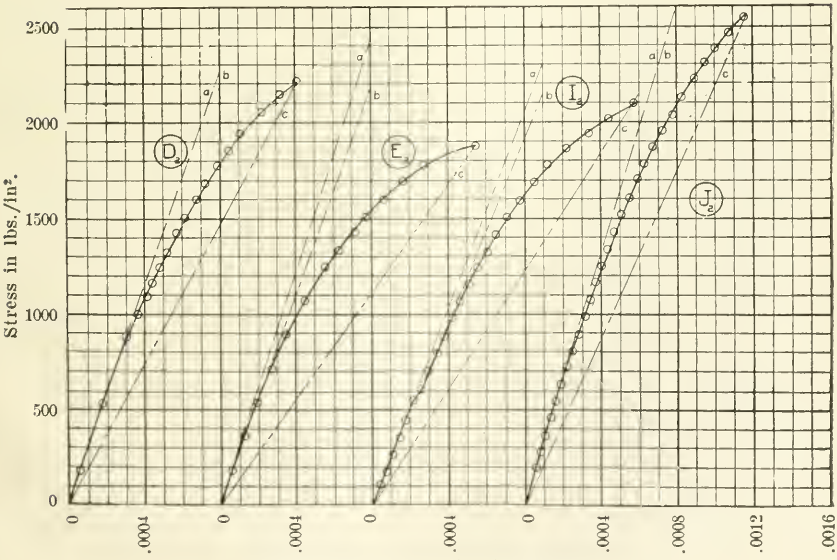

FIG. 2.—CYLINDERS—STRESS-DEFORMATION CURVES FOR D_2, E_2, I_2 AND J_2.

TABLE VIII.

COMPARISON OF COMPRESSIVE STRENGTH OF CYLINDERS AND CUBES.

CONCRETE 1:2:4.

Age of specimens 28 days.

Name.	Total Load on Cube (in lbs.)	Unit Stress on Cube (in lbs.)	Total Load on Cylinder (in lbs.)	Unit Stress on Cylinder (in lbs.)	$\frac{\text{Cyl.}}{\text{Cube.}}$
A_1	31,000	1,940	57,600	2,040	1.05
C_1	40,300	2,520	59,800	2,110	0.84
C_2	37,700	2,360	68,000	2,400	1.02
D_1	25,900	1,620	....	....	....
D_2	27,000	1,690	65,300	2,310	1.37
E_1	22,200	1,390	57,000	2,020	1.45
E_2	28,000	1,750	54,700	1,940	1.11
F_1	32,000	2,000	62,800	2,215	1.11
F_2	21,300	1,960	58,000	2,050	1.05
G_1	22,800	1,430	44,600	1,580	1.10
G_2	29,000	1,810	42,000	1,485	0.82
H_1	38,900	2,430	45,000	1,590	0.665
H_2	20,900	1,310	34,000	1,200	0.915
I_1	39,500	2,500	53,000	1,870	0.75
I_2	36,000	2,250	62,500	2,210	0.98
J_1	32,600	2,040	67,500	2,380	1.17
J_2	46,000	2,870	75,000	2,650	0.925
K_1	22,000	1,380	44,400	1,570	1.14
K_2	26,000	1,620	40,000	1,410	0.87
L_1	29,000	1,810	47,100	1,660	0.915
L_2	30,000	1,880	42,000	1,490	0.79
M_1	20,300	1,270	38,000	1,340	1.05
M_2	24,100	1,510	41,300	1,460	0.97
N_1	24,500	1,530	47,500	1,680	1.10
N_2	30,800	1,930	51,700	1,830	0.95
P_1	20,000	1,250	37,500	1,330	1.06
P_2	18,000	1,120	40,500	1,430	1.28
R_1	32,300	2,020	40,000	1,410	0.70
R_2	22,200	1,390	50,000	1,770	1.27
T_1	29,500	1,840	45,000	1,590	0.865
T_2	22,400	1,400	38,800	1,370	0.98
V_1	36,200	2,230	63,800	2,250	1.01
V_2	28,250	1,770	50,000	1,770	1.00
S_1 dry	21,600	1,350	39,000	1,380	1.02
S_2 "	19,000	1,190	36,700	1,300	1.09
S_3 wet	22,800	1,420	35,700	1,260	0.89
S_4 "	28,000	1.750	47.500	1,680	0.96
Average..........		1,755	....	1,750	1.00

TABLE IX.

MODULI OF ELASTICITY OF CYLINDERS.

CYL.	Max. Stress (in lbs. in.^{2})	Initial Modulus (in lbs. in.^{2})	600 lbs. per sq. in. Modulus (in lbs./in.^{2})	Ultimate Modulus (in lbs./in.^{2})
C_2	2,400	2,800,000	2,800,000	1,400,000
D_2	2,310	2,900,000	2,900,000	1,800,000
E_2	1,940	3,000,000	2,700,000	1,400,000
F_1	2,215	2,700,000	2,700,000	2,000,000
F_2	2,050	4,100,000	3,400,000	2,200,000
G_1	1,580	2,900,000	2,500,000	1,800,000
G_2	1,485	2,600,000	2,500,000	1,700,000
H_1	1,590	3,100,000	3,100,000	2,600,000
H_2	1,200	2,300,000	1,600,000	1,100,000
I_1	1,870	3,000,000	2,200,000	1,200,000
I_2	2,210	2,600,000	2,400,000	1,500,000
J_1	2,380	3,600,000	3,400,000	1,900,000
*J_2	2,650	3,300,000	3,300,000	2,200,000
*K_1	1,570	3,000,000	2,700,000	1,300,000
K_2	1,410	2,200,000	2,000,000	900,000
*L_1	1,660	2,900,000	2,400,000	1,600,000
*L_2	1,490	4,100,000	2,200,000	1,100,000
M_1	1,340	2,600,000	1,900,000	1,400,000
*M_2	1,460	6,500,000	3,500,000	1,100,000
N_1	1,680	2,100,000	1,700,000	1,100,000
N_2	1,830	3,800,000	2,800,000	1,200,000
P_1	1,330	2,500,000	2,300,000	1,500,000
P_2	1,430	2,300,000	2,000,000	1,200,000
R_1	1,410	3,200,000	2,700,000	1,800,000
R_2	1,770	3,100,000	2,700,000	1,600,000
*S_1	1,380	3,000,000	2,200,000	1,100,000
*T_1	1,590	3,100,000	2,500,000	1,400,000
*T_2	1,370	2,200,000	2,100,000	1,300,000
*V_1	2,250	2,700,000	3,000,000	1,700,000
*V_2	1,770	3,200,000	2,800,000	1,400,000
		Average......	2,560,000	
†*S_3	1,260	4,500,000	3,300,000	2,100,000
†*S_4	1,680	3,300,000	3,200,000	1,200,000
		Average.......	3,250,000	

*Cylinders bedded in plaster paris.

†Cylinders cured in water.

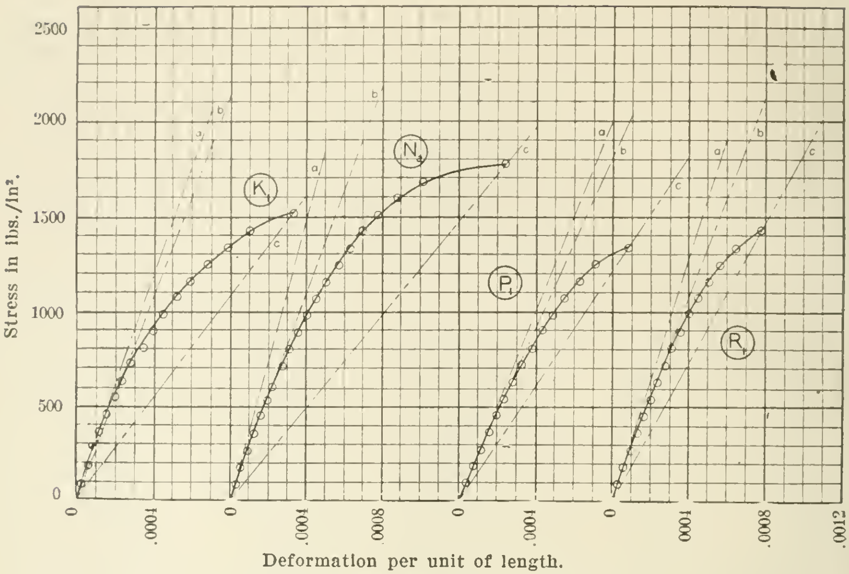

Fig. 3.—Cylinders—Stress-Deformation Curves for K_1, N_2, P_1 and R_1.

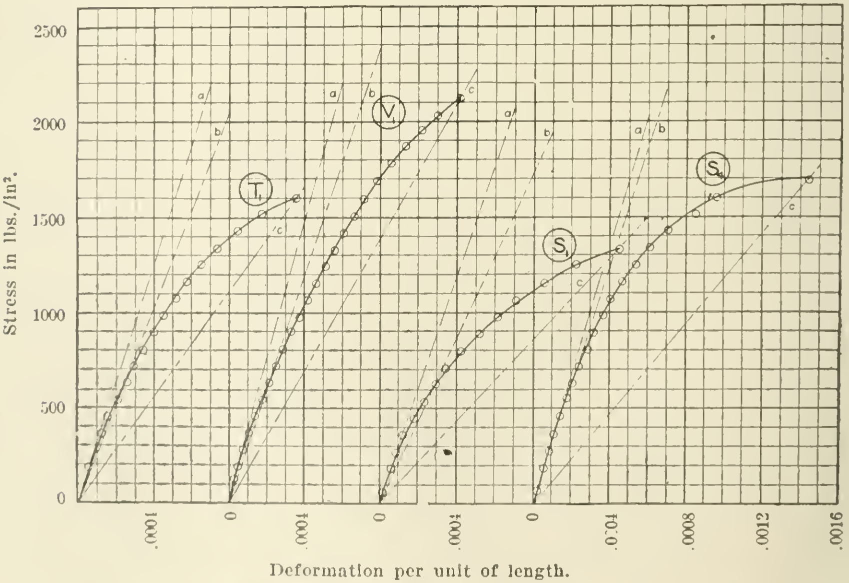

Fig. 4.—Cylinders—Stress-Deformation Curves for T_1, V_1, S_1 and S_4.

Table VIII shows a comparison between the strength of the cylinder and cubes. In spite of precautions taken in proportioning and mixing to secure a uniform product, a wide variation will be observed in the strength of the concrete. This is attributed largely to the poor quality of the sand. However, it will be noticed that the average strengths of both kinds of specimens are the same. This may be due to the fact that the cylinders, although weaker than the cubes on account of their height, had proportionally less surface to dry out. Consequently the interior of the cylinders suffered less from evaporation.

Table IX contains calculated values of moduli of elasticity. The quantities given in columns 3, 4 and 5 represent the slopes of lines a, b, and c, Figs. 2, 3, and 4, drawn on the stress deformation curves of the specimens. Figs. 2, 3, and 4 give a number of representative curves. In nearly all cases the curve is practically a straight line up to a stress of 400 lbs./in^2. In many instances, lines a and b coincide. The average slope of line b for the series is 2,600,000 lbs./in^2.

Cubes and cylinders S_1, S_2, S_3 and S_4 were made from the same batch of concrete. Cylinder S_3 and S_4, which were cured in water, showed greater stiffness and strength than cylinder S_1. The stress-deformation curve for cylinder S_2 was not obtained.

V. BEAMS.

Method of Making:—As the laboratory floor was uneven, it was necessary to use forms with bottom boards which could be leveled up. The general plan of mold is shown in Fig. 5. All lumber was dressed on the inside. The braces were spaced from 2½ feet to 3 feet apart. By shortening the lengths of the cleats c-c and using higher blocks under the bottom boards, beams of less depth could be molded in the same forms. For shorter beams, the cleats were moved towards the center of the span. At each end of the forms, ⅜-inch holes, h, were bored through the sides at points midway the depth of the beam and over the

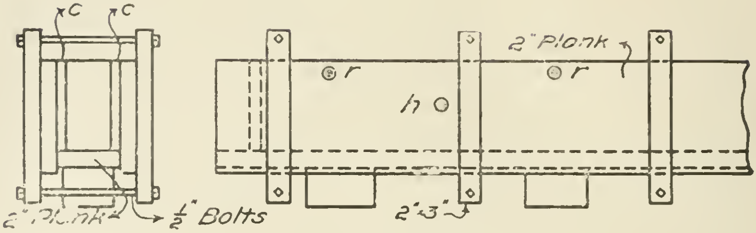

FIG. 5.—FORMS.

points of support. The $\frac{3}{16}$-inch rods were run through the holes and left in the beam. These served to hold the deflection apparatus. Where reinforcement was placed in the tops of beams, a constant vertical position was secured by resting it upon $\frac{3}{16}$-inch rods r-r stuck through the forms. These rods were pulled out when the forms were removed.

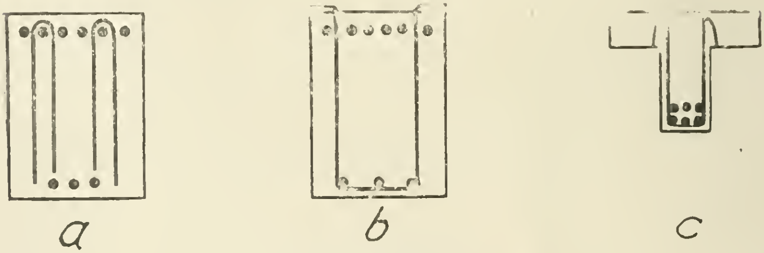

FIG. 6.—STIRRUPS.

Fig. 6 shows the kind of stirrups used for web reinforcement in the overhanging and tee beams. Stirrups shown at (a) were used in the overhanging beams where the bending moment was negative; those shown at (b) where it was positive. In tee beams the height of the rods above the bottom of the beam could be regulated by bending the wing of the stirrup. Longitudinal spacing of the stirrups is shown in Figs. 17, 18, 19, 24 and 25. Where expanded metal was used in tee beams, it was bent around the rods, forming a U. In the overhanging beams, two separate vertical sheets were used. These were not connected to the longitudinal reinforcement.

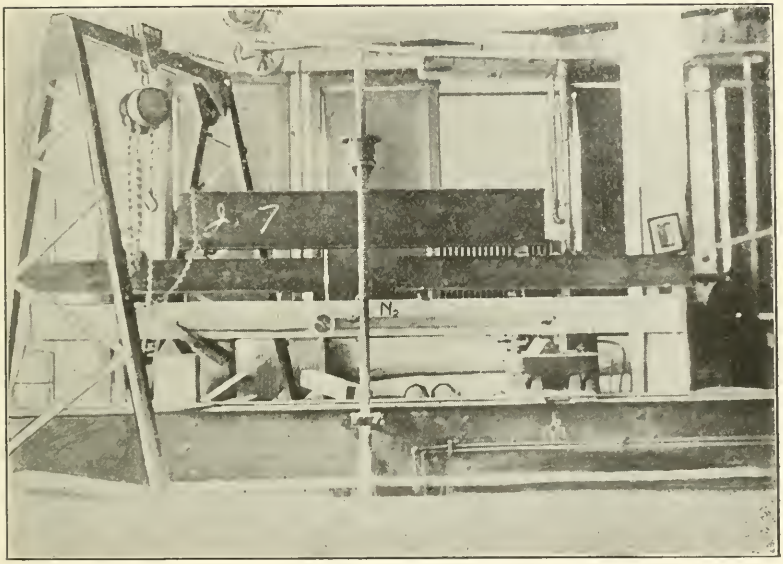

Plate II.—Overhanging Beam N_2 Ready to be Tested.

The method of mixing has already been outlined (see page 596). In placing the concrete, care was taken to keep all reinforcement in its proper position. This was especially necessary in putting concrete around the stirrups in tee beams.

Testing:—The machine used for this purpose was an Olsen 100,000-pound beam machine. Power was furnished by an oil pump operated by hand. All beams were supported on a knife edge at one end and a tipple at the other. Loads were applied through knife edges to flat plates resting upon the beams. Rocker bearings were used to secure an even distribution of pressure. In testing the simple beams, loads were applied at the third points of the span. Plate II shows how the load was applied to the overhanging beams. Precautions were taken in setting up these beams to secure uniformity in loading. As breaks occurred at either end of the span and in some cases simultaneously at both ends, it is believed that this method of loading was sufficiently exact for this class of work.

Deflections of the center of the span were taken in all cases. In the simple beams, the apparatus consisted of a taut thread attached to the pins over the points of support and a mirror and scale placed at the middle of the beam. The thread was lined up with its image in the mirror and the scale reading noted to the nearest hundredth of an inch. A much more accurate device was employed for the overhanging beams. Fig. 7 illustrates this device mounted upon a simple beam. Two wooden bars R-R, one on each side of the beam, are supported upon pins Z-Z. At the middle of the beam is placed an adjustible transverse yoke consisting of two small horizontal wooden pieces and vertical bolts on either side. Two pulleys I-I are attached to the lower part of the yoke with their planes perpendicular to the axis of the beam. A No. 32 covered copper wire is hitched to a pin in the middle of one of the bars and carried vertically downward around the yoke pulleys and up again to a pulley on the opposite side bar from which it is led to a dial X, also fastened to the bar. A weight W serves to keep the wire tight. The apparatus can be easily and quickly adjusted so that the wires on both sides of the beam are vertical. Thus a

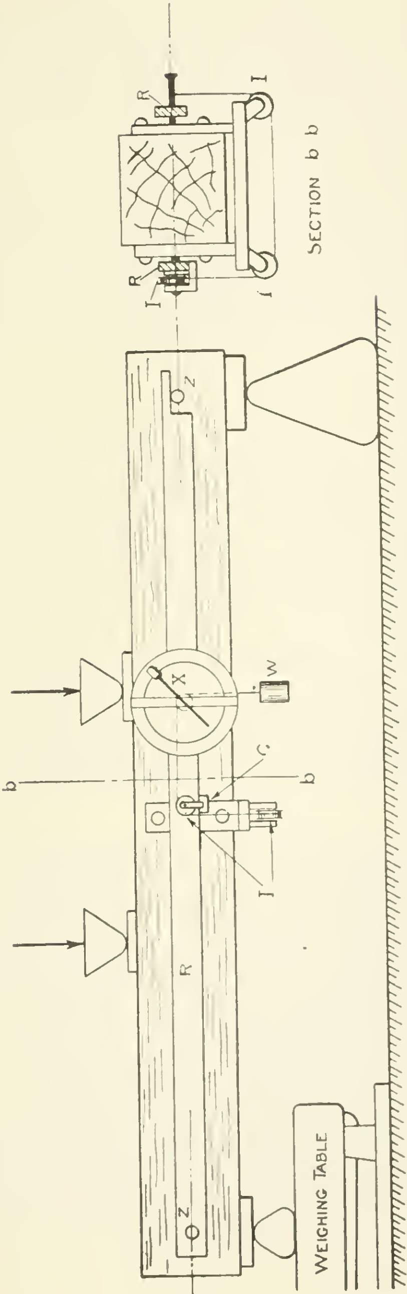

Fig. 7.—Deflectometer Apparatus.

means is furnished to measure the deflection of both sides of the beam with one reading of the dial. It is possible by this method to take readings to one ten-thousandth of an inch. For these tests the readings were taken to the nearest one-thousandth of an inch. Plate II shows the general arrangement of this apparatus on the overhanging beams..

Extensometer readings to determine the fibre deformations were taken in the tests made on simple beams. A general view of this apparatus is shown in Plate III. Covered copper wires were attached to the uprights at the left and carried around the dial drums on the right. One of the weights for keeping wires taut is shown just below the lower dials. For any one series of tests, a uniform position was adopted for the extensometer.

Computations:—In computing stresses in the steel and concrete in beams of Series A and B, the stress-deformation diagram for the concrete was assumed to be a full parabola. No value was placed upon the strength of the concrete in tension. The formulae used were:—

$$f_c = \frac{M}{\frac{2}{3}kbd^2\left(1 - \frac{3}{8}k\right)} \qquad (1)$$

$$f_s = \frac{M}{Ad\left(1 - \frac{3}{8}k\right)} \qquad (2)$$

M = maximum bending moment.
f_c = unit stress in concrete.
f_s = unit stress in steel.
b = breadth of beam.
d = distance from the top of beam to center of steel.
kd = distance from the top of beam to the neutral axis.
A = area of the steel in tension.

In the beams of Series B, the stress in the concrete was calculated from the following formula:—

$$f_c = \frac{f_s A - f'_s A'}{\frac{2}{3}kbd} \qquad (3)$$

f'_s = unit stress in the compression reinforcement. (Obtained from deformations.)
A' = area of the compression reinforcement.

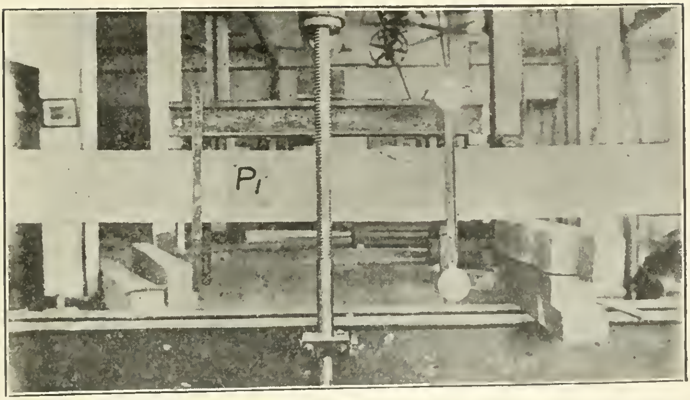

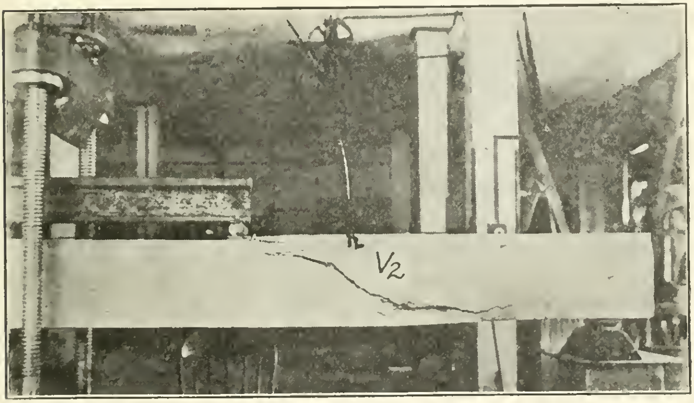

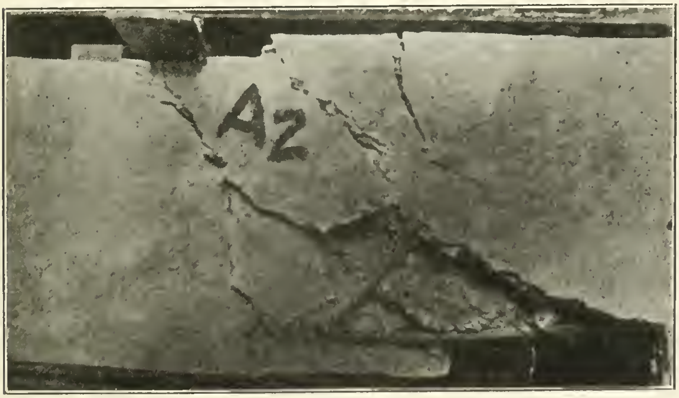

PLATE III.—FAILURE CRACKS IN BEAMS P_1, V_2 AND OVERHANGING BEAM A_2.

Stresses in the steel in the overhanging beams were computed from the following formula:—

$$f_s = -\tfrac{5}{6} E\Delta Ld + \left[(\tfrac{5}{6} E\Delta Ld)^2 + \tfrac{8}{3}\frac{ME\Delta L}{A}\right]^{\frac{1}{2}} \qquad (4)$$

M = bending moment.
E = modulus of elasticity of steel = 30,000,000 lbs./in.^{2}
Δ = deflection in the middle of the span.
L = constant depending upon the length of span and manner of loading.
d = effective depth of beam = distance from top to center of steel.

This formula depends upon the assumption that rods in a concrete beam obey the same laws as a portion of a steel beam similarly located with respect to the neutral surface. It was derived by combining equation (2) with $f_s = (1-k)\, d\, E\, \Delta\, L$. The latter equation is a form of the ordinary equation for stress in terms of the deflections, etc. To test the formula, stresses were computed for a number of beams made by different individuals. In Table X is given a comparison of the stresses in the steel obtained by moments, deformations and deflections. In figuring the stresses by moments, formula (2) was used. It will be seen that the stresses in the steel as figured from the deflections formula (4) are very nearly the same as those calculated by the other methods. The values of k as obtained from the above formula is in general larger than that computed from extensometer readings.

To obtain the stresses in the steel in tee beams, the assumption was made that centroid of the compressive stress was

$$f_s = \frac{M}{A(d - h/2)} \qquad (5)$$

at the center of the flange, and formula (5) was used. In this expression, h is the depth of the flange.

As the distribution of stress in beams with web reinforcement is very uncertain, it did not seem advisable to attempt to calculate values of the diagonal tension. The mean intensity of the vertical shear developed can be readily obtained and serves as a measure of the resistance of a beam against this inclined web stress. The formula used was:—

$$v = \frac{V}{bd}$$

v = the mean intensity of vertical shear.
V = the total maximum shear.
b = breadth of cross-section.
d = effective depth of cross section.

In the tee beams, the shear was assumed to be carried by the web.

TABLE X.

Stresses in Tensile Reinforcement Computed by Various Methods.

Modulus of Elasticity of Steel = 30,000.000 lbs /in.^{2}

Beam.	Area Steel (in sq. in.)	Span (in ft.)	Cross Sect. (in ins.)	k. Ext.	Stress in Steel in lbs in.^{2}		
					Mom.	Def.	Defl.
Talbot.							
1901							
No. 14	1.60	14	12x12	.458	29,900	30,200	31,000
No. 4	2.00	14	12x12	.469	29,800	33,800	30,800
No. 5	1.20	14	12x12	.417	30,000	30,600	30,400
No. 22	2.40	14	12x12	.656	28,400	33,800	28,900
No. 9	.75	12	12x12	.312	63,500	70,000	64,700
No. 21	.59	12	12x12	.333	36,000	32,900	33,300
No. 19	.59	12	12x12	.375	42,400	37,400	40,900
No. 28	2.19	12	12x12	.614	42,800	50,300	44,300
No. 27	2.25	12	12x12	.532	32,600	34,900	33,100
No. 7	.60	12	12x12	.312	57,300	58,300	56,900
No. 3	.60	12	12x12	.302	52,700	52,600	53,000
1905							
No. 5	.785	12	8x10	.450	45,000	39,600	44,000
No. 11	.785	12	8x10	.490	46,000	46,000	47,000
No. 48	.785	12	8x10	.440	37,800	37,800	38,800
Moritz.							
No. 13	1.57	12	$7\frac{3}{4}$x9.9	.575	40,000	50,400	43,000
No. 11	1.37	12	$7\frac{3}{4}$x9.9	.480	40,500	60,000	45,700
No. 15	1.57	12	$7\frac{3}{4}$x9.9	.580	39,000	45,000	40,600
No. 9	1 37	12	$7\frac{3}{4}$x9.9	600	42,800	47,400	44,200
U. W.							
1906							
P_1	2.20	12	$7\frac{3}{4}$x$9\frac{3}{4}$	.670	35,200	36,000	35,000
P_2	2.20	12	$7\frac{3}{4}$x$9\frac{3}{4}$	.680	31,600	33,000	32,400
R_1	2.20	12	$7\frac{3}{4}$x$9\frac{3}{4}$	.590	39,000	39,000	39,500
R_2	2.20	12	$7\frac{3}{4}$x$9\frac{3}{4}$	.600	39,100	39,000	39,600
S_1	2.20	12	$7\frac{3}{4}$x$9\frac{3}{4}$	.570	32,800	33,000	32,900
S_2	2.20	12	$7\frac{3}{4}$x$9\frac{3}{4}$	.560	35,700	33,800	35,800
T_1	2.20	12	$7\frac{3}{4}$x$9\frac{3}{4}$	.510	36,100	36,000	36,800
T_2	2 20	12	$7\frac{3}{4}$x$9\frac{3}{4}$	.550	42,500	42,000	43,400

1. BEAMS OF SERIES A.

In order to make a comparison between the compressive strength of concrete in a beam and that in a cube, four beams were made, reinforced and dimensioned as shown in Fig. 8. A large percentage of reinforcement was used to insure against tension failures. The beams, four cylinders and four cubes were made from one batch of concrete. After two days in the molds, S_3 and S_4 beams, cylinders and cubes were immersed in water for 26 days while the others were cured in air. Table XI contains the results of this series. The loads given include the weight of the beam. Beams cured in air weighed 235 pounds, while those cured in water weighed 260 pounds.

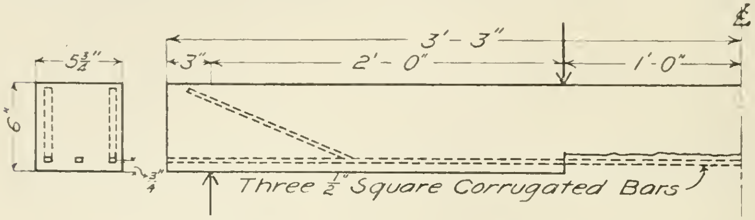

FIG. 8—BEAMS OF SERIES A—REINFORCEMENT.

The value of k was calculated from extensometer measurements. The stresses in column S are the averages for a cylinder and a cube.

TABLE XI.

SIMPLE BEAMS. SERIES A.

Span 6 ft. Loads at the ⅓ Points. 2½ per cent Reinforcement.

No. Beam.	Total Load (in lbs.)	Kind of Failure.	$\frac{M}{bd^2}$	Load Considered (in lbs.)	k = Proportionate Depth.	Stress in Steel (in lbs./in.^{2}) From Resisting Moment.	Stress in Steel (in lbs./in.^{2}) From Deformation.	Stress in Concrete in Beam (in lbs./in.^{2}) (B)	Stress in Compression Specimens (in lbs./in.^{2}) (S)	Ratio $\frac{B}{S}$
S_1	7,800	C	585	7,000	.580	27,100	36,000	1,740	1,285	1.22
S_2	7,000	C	523	6,000	.610	23,600	36,000	1,440	1,325	
S_3	8,000	DT	600	7,000	.560	26,800	31,500	1,780	1,360	1.17
S_4	8,760	C	657	7,000	.545	26,600	48,000	1,830	1,715	

C = Compression. DT = Diagonal Tension.

Beams S_1, S_2, and S_4 failed in compression, the concrete crushing at the top in the middle of the span. Beam S_3 failed in diagonal tension. The crack opened up from a tension crack about 6 inches outside the load, spread diagonally to the load and along the plane of the reinforcement. The values of $\frac{M}{bd^2}$ are low for such a high reinforcement. This fact is due largely to the low crushing strength of the concrete. In column B is given the unit compression developed as calculated by formula (1). In the last column of the table is given the ratio of the calculated strength of the concrete in the beam to that in the compression specimens. In all cases, the computed stress in the beam is greater than that developed in the cubes and cylinders. This difference is more marked in the specimens cured in air. Also a comparison of the stress-deformation curves for the concrete in the beams and for the cylinders shows that the concrete in the beams withstood a greater deformation. These facts seem to indicate that a higher compressive stress is developed in a beam. The stress on an elementary cube in a beam is more uniformly distributed owing to the perfect end conditions, consequently a greater strength and larger deformation may reasonably be expected. The action of the air has a greater effect upon the strength of a small specimen than upon a larger one, so that the compression specimens would suffer more when cured in air than the beams. It will be noted in Figs. 9 and 10 that the beams cured in water were both stiffer and stronger than those cured in air.

2. BEAMS OF SERIES B.

To determine the effect of reinforcement in the compression side of a beam, eight simple beams were reinforced and dimensioned as shown in Fig. 11. The amount of reinforcement used in the tension side was made high, 2.9 per cent, to balance the extra compression resistance afforded by the top reinforcement. Only one beam was made from a batch of concrete. The beams weighed about 1200 pounds each.

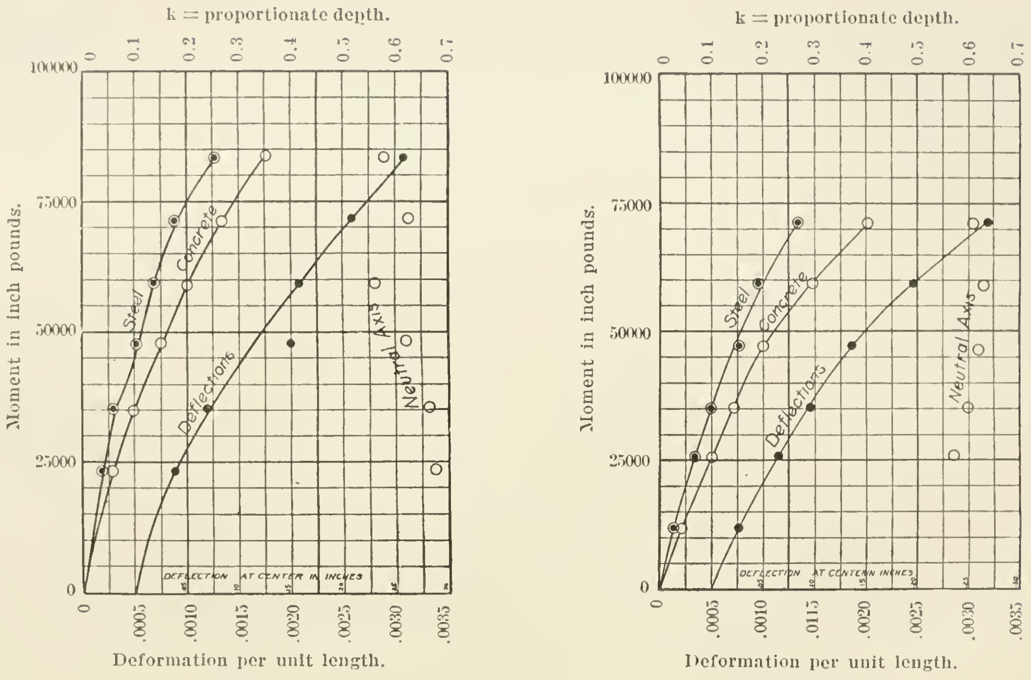

Beam S_1.

Beam S_2.

Deflection at center—1 square=0.1 inch.

FIG. 9.—BEAMS OF SERIES A—MOMENT-DEFORMATION CURVES, ETC.

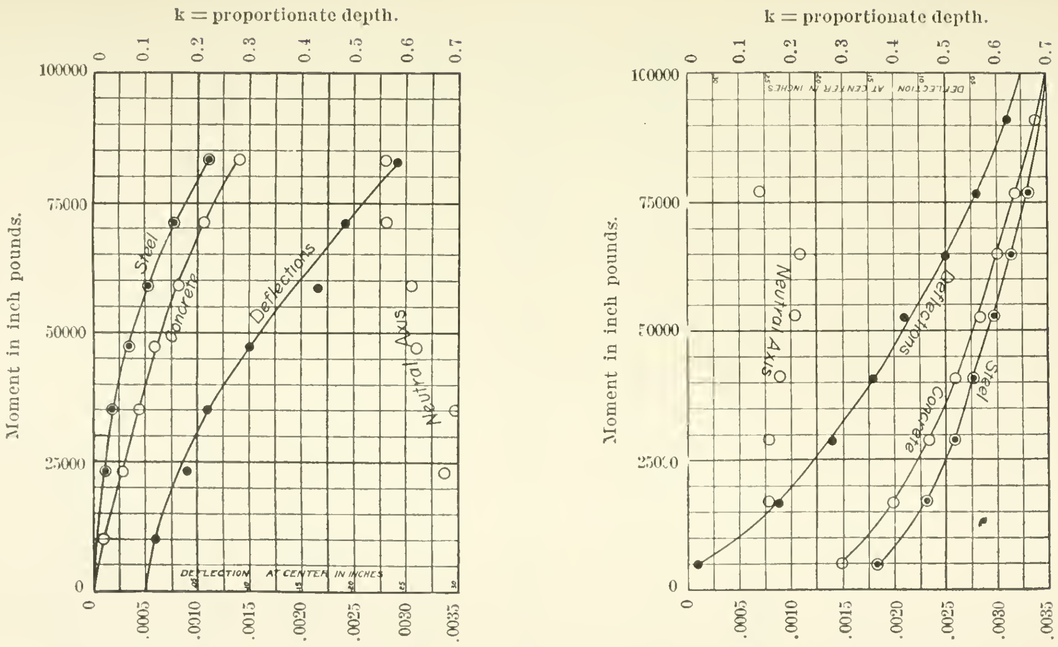

Beam S_3.

Beam S_1.

Deflection at center—1 square=0.1 inch.

FIG. 10.—BEAMS OF SERIES A—MOMENT-DEFORMATION CURVES, ETC.

The manner in which these beams failed can best be seen by a study of Fig. 11. The cracks are numbered in order of their appearance. It will be observed that tension cracks first appeared, as would be expected, in the middle portion of the span. In general, diagonal tension cracks started from tension cracks between the load and the support, spread toward the load and then out along the plane of the rods. Cracks 22 and 23 in beam T_1 illustrate the way in which these cracks developed. Plate III shows the compression failure in beam P_1 and the diagonal tension break in beam V_2.

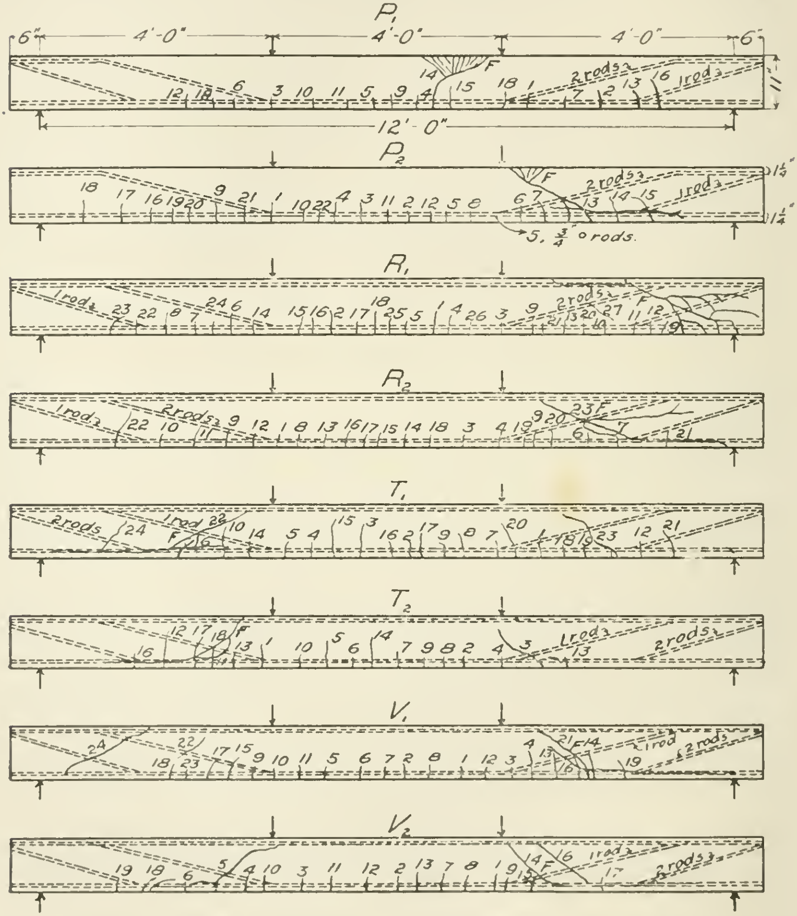

Fig 11.—Beams of Series B—Reinforcement and Cracks.

TABLE XII.

SIMPLE BEAMS. SERIES B.

Stresses in Steel and Concrete. 2.9 per cent Reinforcement in Tension

No. Beam.	No. $\frac{1}{2}$" Bars in Top.	Kind of Failure.	Load considered (in lbs.)	k— Proportionate Depth.	Stress in Steel. (inlbs. in.^{2})			Stress in Concrete in Beam (in lbs./in.^{2}) (B)	Stress in Compression Specimens. (in lbs./in.^{2} (S)	Ratio $\frac{B}{S}$
					From Resisting Moment.	From Deformation.	In Compression by Deformation.			
P_1		C	22,160	.670	35,200	36,000		2,260	1,290	1.75
P_2		C & D T	20,160	.675	31,600	33,000		2,050	1,275	1.61
R_1	2	DT	26,160	.590	39,000	39,000	40,000	2,370	1,715	1,43
R_2	2	DT	26,160	.600	39,100	39,000	45,000	2,260	1,580	1.46
T_1	4	DT	22,160	.570	32.800	33,000	33,000	1,610	1,715	0.94
T_2	4	DT	24,160	.565	35,700	33,800	36,000	1,760	1,385	1.27
V_1	6	DT	25,160	.510	36,100	36,000	28,500	1,780	2,240	0.79
V_2	6	DT	29,160	.555	42,500	42,000	39,000	1,670	1,770	0.94

Span 12 ft. Loads at the $\frac{1}{3}$ points.
C = Compression. DT = Diagonal Tension.

Computed data from these tests are contained in Tables XII and XIII. In these beams the stresses in the lower steel as computed by the two methods check very closely. The stress in the upper steel in beams R_1 and R_2 must have been beyond the elastic limit. The calculated strength of the concrete in the beams is considerably higher than that developed in the compression specimens. Even in beams V_1 and V_2, which were heavily reinforced in compression, a high compressive stress was borne by the concrete. The average ratio of the compressive stress in the top reinforcement to that in the concrete is about 19 to 1. The same value is also obtained by dividing the modulus of elasticity of steel by the average ultimate secant modulus of cylinders R_1, R_2, etc. Owing to diagonal tension failures, the increase in resisting moment supplied by the compression reinforcement cannot be accurately estimated. Table XIII shows that the value of $\frac{M}{bd^2}$ is increased roughly about 25 per cent by the addition of $\frac{1}{2}$ per cent or more steel in the compression area of the beam.

Figs. 12, 13, 14 and 15 show that the stiffness is also materially increased. With an efficient web reinforcement, beams T_1, T_2, V_1 and V_2 would probably have shown a more decided increase in strength over beams R_1 and R_2.

TABLE XIII.

BEAMS SERIES B.

Values of v and $\frac{M}{bd^2}$. Breadth $7\frac{3}{4}''$. Effective Depth $9\frac{3}{4}''$.

Beam.	Total Load Applied (in lbs.)	Kind of Failure.	Max. Moment (in lbs.)	$\frac{M}{bd^2}$.	v (in lbs./in².)	Stress on Cube and Cyl. in lbs./in².)
P_1	24,780	C	585,600	794	164	1,290
P_2	21,380	C & DT	504,500	683	141	1,275
R_1	28,740	DT	680,500	922	190	1,715
R_2	27,840	”	660,500	895	184	1,580
T_1	24,180	”	571,000	774	160	1,715
T_2	31,260	”	741,000	1,003	207	1,385
V_1	27,580	”	652,000	884	182	2,240
V_2	31,380	”	744,500	1,008	207	1,770

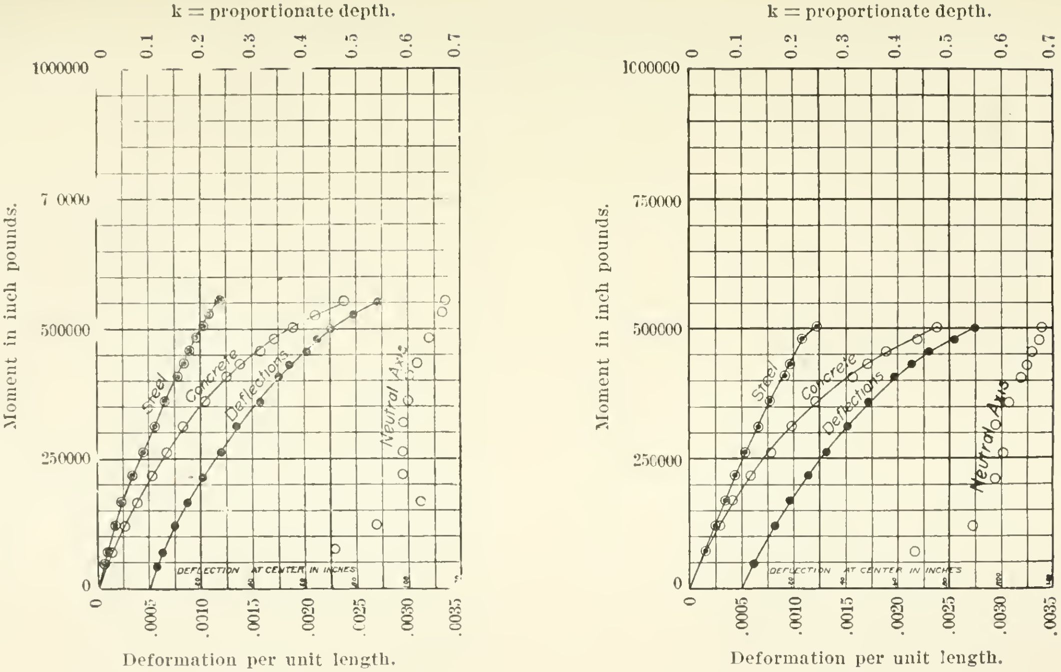

Beam P$_1$.

Beam P$_2$.

Deflection at center—1 square=0.1 inch.

Fig. 12.—Beams of Series B—Moment-Deformation Curves, Etc.

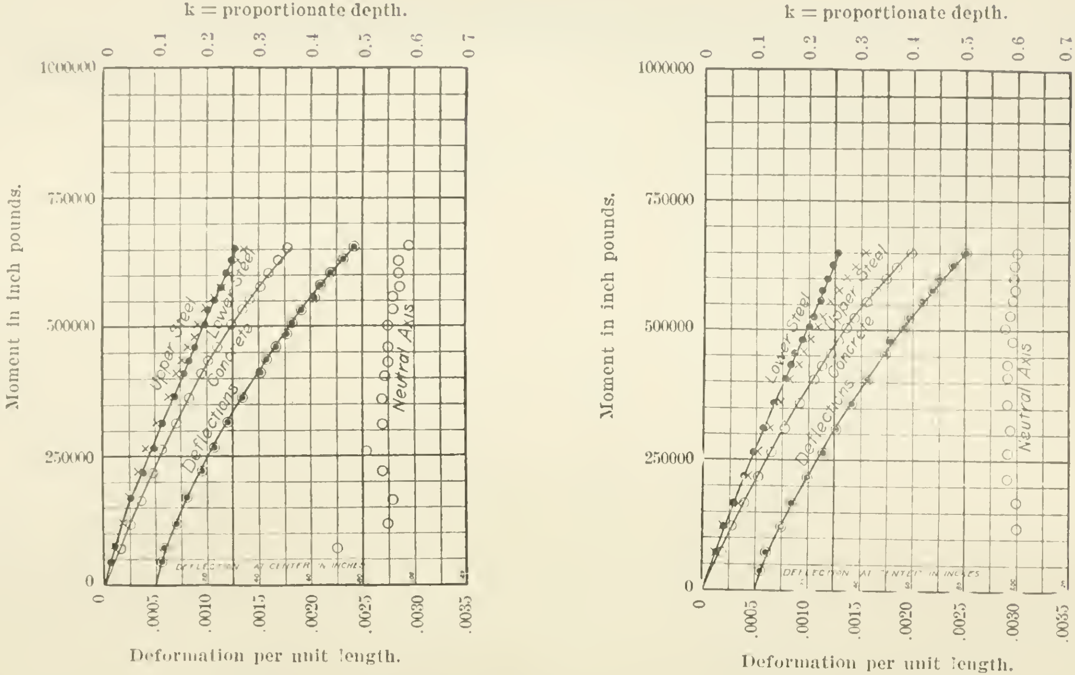

Beam R_1.

Beam R_2.

Deflection at center—1 square=0.1 inch.

FIG. 13.—BEAMS OF SERIES B—MOMENT-DEFORMATION CURVES, ETC.

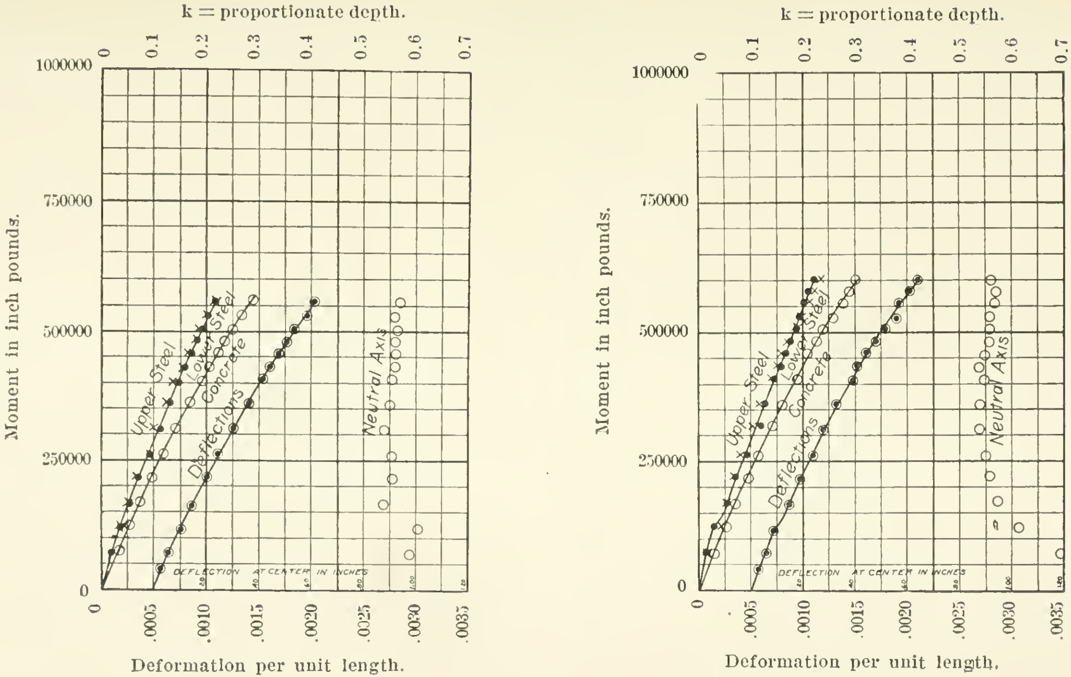

Beam T₁.

Beam T₂.

Deflection at center—1 square=0.1 inch.

FIG. 14.—BEAMS OF SERIES B—MOMENT-DEFORMATION CURVES, ETC.

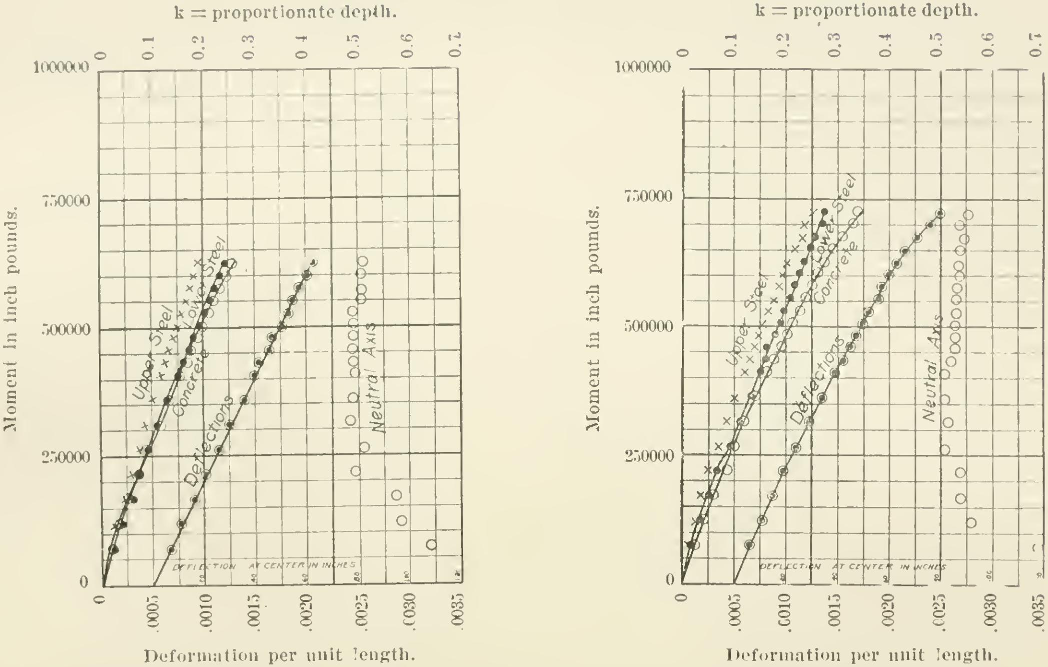

Beam V₁.

Beam V₂.

Deflection at center—1 square=0.1 inch.

FIG. 15.—BEAMS OF SERIES B—MOMENT-DEFORMATION CURVES, ETC.

OVERHANGING BEAMS.

These beams were made with two objects in view; first, to approach as nearly as possible the conditions of continuity over supports; second, to investigate the effects of different kinds of web reinforcement upon the strength of beams. The arrangement of the loads is shown for beams of Series C in Fig. 16, for those of Series D in Figs. 17, 18 and 19. In each case, the loads were so spaced that the tangent to the elastic curve over the support was practically horizontal. Two-tenths of the total load was applied on each of the cantilever portions of the beam and three-tenths at each point in the span.

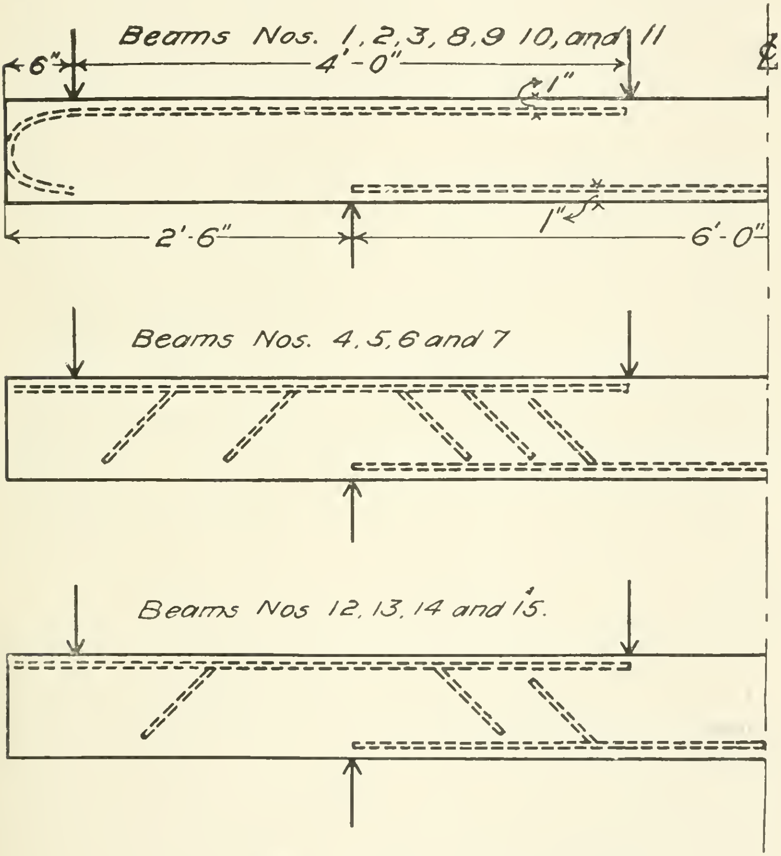

Beams Nos. 1, 2, 3, 8, 9 10, and 11
6"
4'-0"
1"
℄
1"
2'-6"
6'-0"
Beams Nos. 4, 5, 6 and 7
Beams Nos 12, 13, 14 and 15.

Fig. 16.—Beams of Series C—Reinforcement.

3. BEAMS OF SERIES C.

These beams were made two at a mixing. The sand and cement used in beams No. 2 and No. 3 stood mixed over night. Although no lumps were visible when the concrete was mixed, the strength of both beams and test cubes was greatly impaired. Table XIV gives the amounts of reinforcement used in beams of Series C. Fig. 16 shows the way in which these beams were reinforced. Rods were bent up in pairs, as many being bent up from the bottom as were bent down from the top. In beams Nos. 4, 5, 6 and 7, the middle upper rod was also bent down. The sizes of rod used and the effective cross-section of beams is given in the table. Number of rods bent refers to those turned up and down between middle of the span and the support. In testing beams Nos. 4, 6 and 7, the loads were applied 21 inches from the knife edges instead of 24 inches, as in the other beams of this series.

Tables XV and XVI contain data computed from these tests. All loads include the weight of the beam. Nos. 1 to 7 weighed about 420 pounds each and Nos. 8 to 15 about 550 pounds. The value L to be used in formula (4) is, for beams as. 4, 6 and 7, $\frac{1}{427.5}$ and for all others, $\frac{1}{360}$.

All of these beams failed in diagonal tension, but the manner in which this occurred was not always the same. In beams Nos. 1, 4, 5, 6, 7, 12, 13, 14 and 15, tension cracks first opened up either at the middle of the span or over the supports at loads given in Table XVI.. Next a diagonal crack would make its appearance in one of two ways. It would many times start from a tension crack in the top and run diagonally at an angle of 45° to the support while at the same time it would spread horizontally in the plane of the rods toward the load. In other cases, the crack would appear to start at the middle of the beam and spread diagonally downward to the support and upward in the direction of the load and then out along the rod. In beams Nos. 2, 3, 8, 9, 10 and 11, so far as could be detected by the naked eye, the diagonal crack was the first to make its appearance.

TABLE XIV.

Reinforcement of Beams. Series C.

Beam.	Effective Cross Section (in ins).	Per cent. Steel in Top.	Per cent. Steel in Bottom	Area Steel in Bottom.	Number Rods.	Elastic Limit. (in lbs. in.^{2})
1	$5\frac{3}{4}$″x5″	1.96	.... 1.10	.... .33	3, $\frac{1}{2}$″ 3, $\frac{3}{8}$″	44,000 51,000
2	$5\frac{3}{4}$″x5″	3.27	.... 1.50	.... .45	5, $\frac{1}{2}$″ 3, $\frac{7}{16}$″	44,000 47,000
3	$5\frac{3}{4}$″x5″	3.27	.... 1.50	.... .45	5, $\frac{1}{2}$″ 3, $\frac{7}{16}$″	44,000 47,000
4	$5\frac{3}{4}$″x5″	1.28	.... 0.65	.... .196	5, $\frac{5}{16}$″ 4, $\frac{1}{4}$″	48,500 52,000
5	$5\frac{3}{4}$″x5″	1.28	.... 0.65	.... .196	5, $\frac{5}{16}$″ 4, $\frac{1}{4}$″	48,500 52,000
6	$5\frac{3}{4}$″x5″	1.84	.... 1.02	.... .306	5, $\frac{3}{8}$″ 4, $\frac{5}{16}$″	51,000 48,500
7	,	1.84	.... 1.02	.... .306	5, $\frac{3}{8}$″ 4, $\frac{5}{16}$″	51,000 48,500
8	$5\frac{3}{4}$″x7″	2.04	.... 1.22	.... .590	5, $\frac{1}{2}$″ 3, $\frac{1}{2}$″	44,000 44,000
9	$5\frac{3}{4}$″x7″	2.04	.... 1.22	.... .590	5, $\frac{1}{2}$″ 3, $\frac{1}{2}$″	44,000 44,000
10	$5\frac{3}{4}$″x7″	3.10	.... 1.63	.... .785	4, $\frac{11}{16}$″ 4, $\frac{1}{2}$″	 44,000
11	$5\frac{3}{4}$″x7″	3.10	.... 1 63	.... .785	4, $\frac{11}{16}$″ 4, $\frac{1}{2}$″	 44,000
12	$5\frac{3}{4}$″x7″	1.28	.... 0 65	.... .306	4, $\frac{7}{16}$″ 4, $\frac{5}{16}$″	47,000 48,500
13	$5\frac{3}{4}$″x7″	1.28	.... 0.65	.... .306	4, $\frac{7}{16}$″ 4, $\frac{5}{16}$″	47,000 48,500
14	$5\frac{3}{4}$″x7″	1.63	.... 0.92	.... .442	4, $\frac{1}{2}$″ 4, $\frac{3}{8}$″	44,000 51,000
15	$5\frac{3}{4}$″x7″	1.63	.... 0.92	.... .442	4, $\frac{1}{2}$″ 4, $\frac{3}{8}$″	44,000 51,000

However, the high stress in the steel, at the time of this first visible crack, indicates that tension cracks too fine to be visible must have previously formed. The growth of the crack in these beams was similar to that already described, except that it was very much more rapid.

TABLE XV.

OVERHANGING BEAMS. SERIES C.

Values of v and $\frac{M}{bd^2}$.

No. Beam.	Total Load (in lbs.)	Web Reinforcement.	Maximum *Moment (in in. lbs.)	$\frac{M}{bd^2}$.	v (in lbs./in.^{2})	Stress in Cube (in lbs./in.^{2})
1	15,000	None..............	71,400	495	156	1,970
8	20,000	"	95,200	259	130	1,280
9	27,000	"	129,000	351	176	1,280
2	8,400	"	39,800	276	88	750
3	8,100	"	38,300	266	84	750
10	26,200	"	125,000	340	171	1,010
11	24,400	"	116,300	316	159	1,010
4	16,400	Five rods bent up..	68,300	474	171	1,785
5	13,000	"	61,700	429	136	1,785
12	35,200	Four rods bent up..	168,200	457	229	2,020
13	41,400	"	197,800	537	270	2,020
6	15,000	Five rods bent up .	62,400	433	156	1,610
7	17,000	"	70,700	491	177	1,610
14	41,400	Four rods bent up..	197,800	537	269	1,480
15	43,200	"	206,400	561	282	1,480

All beams failed in diagonal tension.
*Moment at the supports.

TABLE XVI.

OVERHANGING BEAMS. SERIES C.

Stresses in steel at center of span.

No. Beam.	Web Reinforcement.	Load at First Crack (in lbs.)	Load Considered (in lbs.)	*Moment at Load Considered (in in. lbs.)	Stress in Steel (in lbs./in.^{2})	Stress in Cube (in lbs./in.^{2})	Deflection at Load Considered (in ins.)
1	None.........	12,000	14,000	33,200	25,000	1,970	.125
2	"	6,100	7,140	16,700	9,300	750	.050
3	"	8,100	8,100	19,000	10,800	750	.060
4	Five rods bent up..........	11,000	16,000	33,200	40,200	1,785	.198
5	"	7,100	13,000	30,800	35,900	1,785	.128
6	"	11,000	15,000	31,100	25,300	1,610	.150
7	"	6,300	16,000	33,200	27,200	1,610	.166
8	None	20,000	19,200	45,600	11,600	1,280	.030
9	"	20,200	23,400	55,600	16,200	1,280	.083
10	"	17,200	26,200	62,400	14,500	1.010	.141
11	"	15,000	23,200	55,100	13,000	1,010	.132
12	Four rods bent up...........	20,300	35,200	84,000	42,300	2,020	.122
13	"	18,200	39,200	93,600	46,100	2,020	.126
14	"	22,200	40,200	96,000	34,000	1,480	.111
15	"	12,400	42,200	100,700	36,300	1,480	.133

All beams failed in diagonal tension.
* Moment at center of span.

The time of appearance of the first visible crack was about the same in all beams. In beams without inclined rods, failure soon followed the first crack. In beam No. 8, the first visible crack was the one which caused failure. Those beams which had a web reinforcement of bent rods stood higher loads and gave more indications of approaching collapse.

The average unit vertical shear developed in beams Nos. 1, 8, 9, 10 and 11 was 158 ibs./in^2., that developed in Nos. 4, 5, 6, 7, 12, 13, 14 and 15 averaged 211 lbs./in^2. an increase of about 30 per cent due to web reinforement. In the deeper beams this increase is still more marked.

For the 9-inch beams, without web reinforcement, the average vertical shear was 159 lbs./in^2. In beams of the same depth with bent rods, the average was 258 lbs./in^2., or a gain of over 60 per cent.

4. BEAMS OF SERIES D.

In order to make a further study of overhanging beams, 28 were dimensioned and reinforced as shown in Figs. 17, 18 and 19. The beams contained 1.97 per cent of steel in the top and half that amount in the bottom. The reinforcement was made large in order that the full strength of the concrete might be developed. Rods were turned up or down in pairs except as noted in beams A_1, A_2, H_1 and H_2. Those rods which were bent nearest the supports were continuous over the supports, the

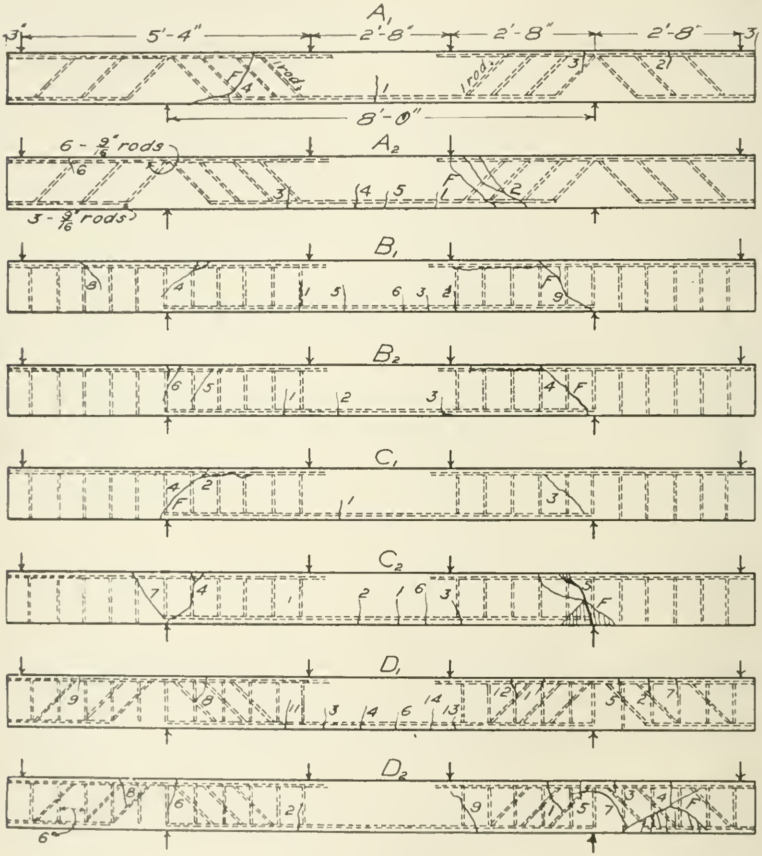

Fig. 17.—Beams of Series D—Reinforcement and Cracks.

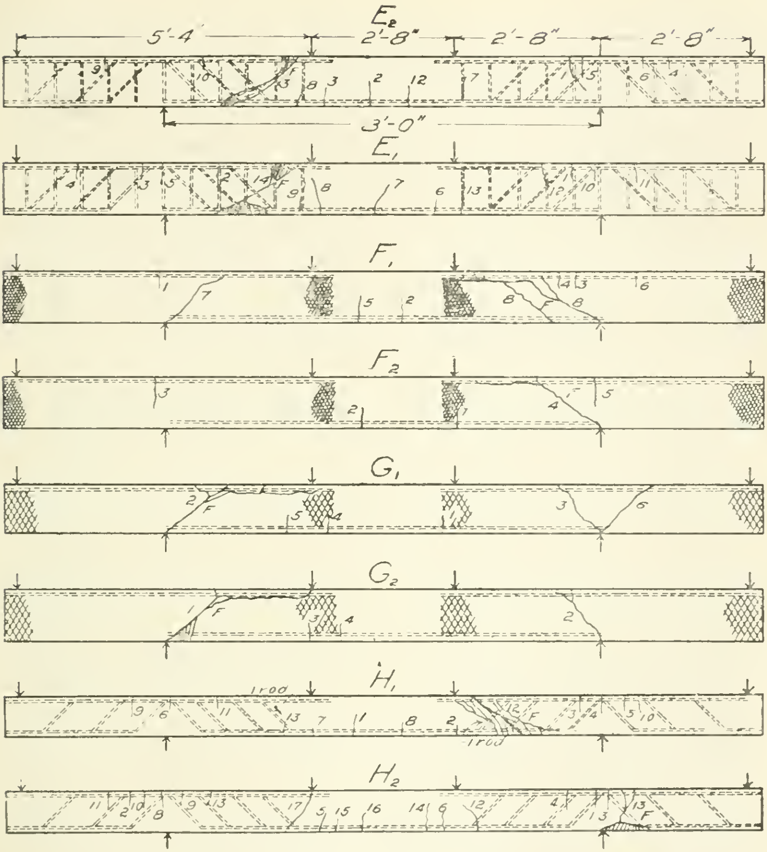

FIG. 18.—BEAMS OF SERIES D—REINFORCEMENT AND CRACKS.

others were bent up or down and stopped at the top or bottom of the beam. This arrangement would not be possible in practice as half of the bottom rods would have to be run through to provide against stresses which did not occur in these test pieces. The object here was to determine whether inclined members or some other form of reinforcement provided the best resistance against web stresses. The manner in which stirrups were placed is shown in Fig. 6. Duplicate beams were made, but only one was made from the same batch of concrete. Beams A to G weighed about 1,250 pounds each and beams H to N about 1,040

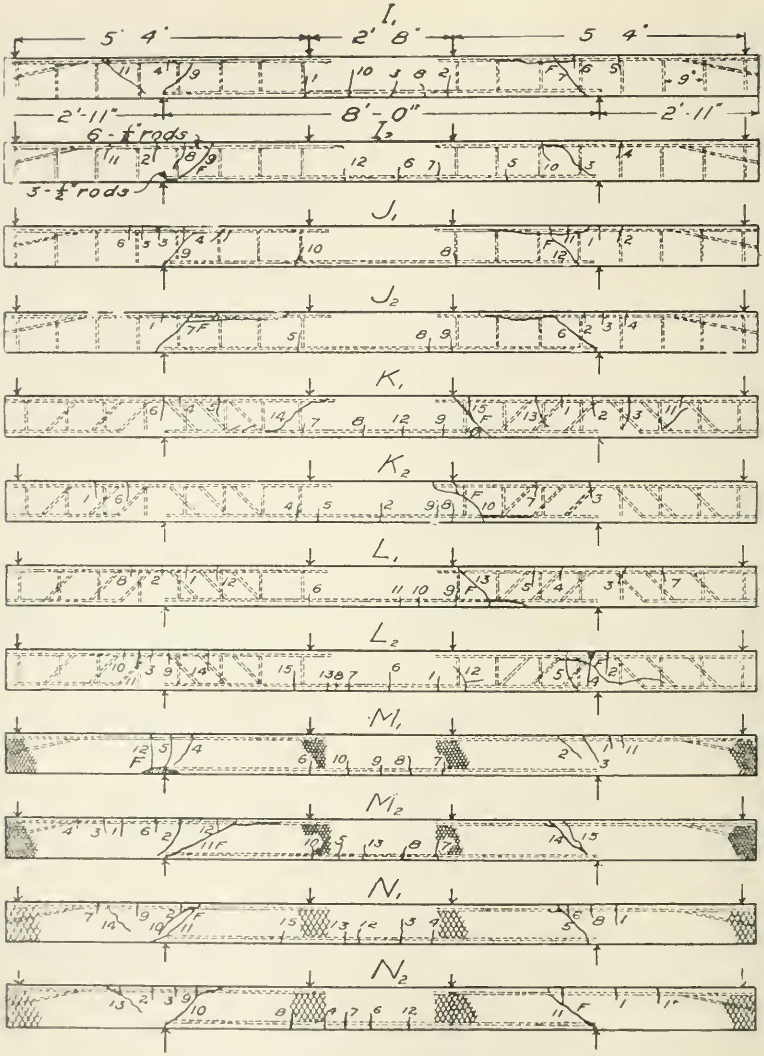

FIG. 19.—BEAMS OF SERIES D—REINFORCEMENT AND CRACKS.

pounds apiece. Tables XVII and XVIII contain the numerical results of these tests. The value of L for this series is 1-640. Load deflection curves for these beams will be found in Figs. 20, 21, 22 and 23.

TABLE XVII.

OVERHANGING BEAMS. SERIES D.

Values of v and $\frac{M}{bd^2}$.

Width of Beams $7\frac{3}{4}''$. 2 per cent Reinforcement.

Beam.	Total Load (in lbs.)	Web Reinforcement.	Kind of Failure.	Max. Moment at Support (in in. lbs.)	$\frac{M}{bd^2}$.	v (in lbs./in^2.)	Unit stress on Cyl. & Cubes (in lbs./in^2.)
A_1	76,000	Inclined Rods.	DT	482,000	655	302	1,990
A_2	69,500	”	”	441,000	600	276	2,120
H_1	50,540	”	”	321,000	690	253	2,010
H_2	53,800	”	T	341,000	733	269	1,255
B_1	55,000	$\frac{1}{4}''$ Stirrups.	DT	348,000	473	218	1,340
B_2	62,900	”	”	398,000	540	249	1,440
I_1	52,840	”	DT & T	335,000	720	264	2,185
I_2	42,800	”	DT	271,000	583	214	2,230
C_1	62,500	$\frac{3}{16}''$ Stirrups.	”	396,000	538	248	2,315
C_2	62,750	”	”	397,000	539	249	2,380
J_1	43,500	”	”	275,000	591	217	2,210
J_2	44,480	”	”	281,000	605	222	2,760
*D_1	84,000	Inclined Rods and	....	533,000	724	333	1,620
D_2	86,000	$\frac{1}{4}''$ Stirrups.	T	546,000	742	341	2,000
K_1	57,260	”	DT & T	363,000	780	286	1,475
K_2	36,400	”	DT	230,000	495	184	1,515
†E_1	66,000	Inclined Rods and	....	419,000	569	262	1,705
E_2	82,000	$\frac{3}{16}''$ Stirrup.	DT	521,000	709	325	1,845
L_1	46,860	”	DT	297,000	639	254	1,735
L_2	50,600	”	T	321,000	690	253	1,685
F_1	67,000	Expanded Metal	DT	425,000	577	266	2,110
F_2	55,600	No. 13 $\frac{3}{4}''$ Mesh.	DT	352,000	478	221	2,005
M_1	49,920	”	T	316,000	680	249	1,305
M_2	47,200	”	DT	299,000	643	236	1,485
G_1	65,600	Expanded Metal	”	416,000	565	260	1,505
G_2	53,200	No. 12 $2\frac{1}{2}''$ Mesh.	”	337,000	458	211	1,650
N_1	41,540	”	”	263,000	568	208	1,605
N_2	50,300	”	”	319,000	585	251	1,880

*=Broken as a simple beam.
T=Tension.
DT=Diagonal Tension.
t=Twisted off due to eccentric loading.

Table XVII shows that all beams which failed in tension had values of $\frac{M}{bd^2}$ greater than 680. Four out of seven of these beams were reinforced with inclined rods and stirrups. D_1 and D_2 were the only 11-inch beams which did not fail in diagonal tension. The $\frac{M}{bd^2}$ for these beams was 724 and 742 respectively. The average value of $\frac{M}{bd^2}$ for the 11-inch beams was 586 and for the 9-inch beams it was 650.

TABLE XVIII.

OVERHANGING BEAMS. SERIES D.

Stresses in Steel. 2 per cent Reinforcement.

Beam.	Web Reinforcement.	Kind of Failure.	Load at First Crack (in lbs.)	Load Considered (in lbs.)	Moment at Center (in lbs.)	Stress in Steel (in lbs./in.^{2})	Stress on Cyl. & Cubes (in lbs./in.^{2})
A_1	Inclined Rods.	DT	25,000	50,000	160,000	25,300	1,990
A_2	"	"	42,500	65,000	208,000	33,100	2,120
B_1	$\frac{1}{4}$" Stirrups.	"	40,000	52,500	168,000	25,200	1,340
B_2	$\frac{1}{4}$" "	"	42,500	52,500	168,000	27,000	1,440
C_1	$\frac{3}{16}$" "	"	40,000	60,000	192,000	32,200	2,315
C_2	$\frac{3}{16}$" "	"	30,000	47,000	150,000	24,200	2,380
*D_1	Inclined Rods and	....	40,000	76,000	243,000	38,600	1,620
D_2	$\frac{1}{4}$" Stirrups.	T	47,500	72,500	232,000	38,900	2,000
†E_1	Inclined Rods and	....	30,000	65,000	208,000	32,300	1,705
E_2	$\frac{3}{16}$" Stirrups.	DT	35,000	70,000	224,000	35,200	1,845
F_1	Expanded Metal	"	30,400	55,000	176,000	26,800	2,110
F_2	No. 13. $\frac{1}{4}$" Mesh.	"	40,000	50,000	160,000	25,000	2,005
G_1	Expanded Metal	"	40,000	50,000	160,000	25,600	1,505
G_2	No. 12. $2\frac{1}{2}$" Mesh.	"	35,000	50,000	160,000	25,400	1,650
H_1	Inclined Rods.	"	20,000	45,000	144,000	37,500	2,010
H_2	"	T	10,200	50,000	160,000	41,300	1,255
I_1	$\frac{1}{4}$" Stirrups.	DT & T	20,000	50,000	160,000	41,500	2,185
I_2	$\frac{1}{4}$" "	DT	20,200	40,000	128,000	31,600	2,230
J_1	$\frac{3}{16}$" "	"	20,000	40,000	128,000	32,300	2,210
J_2	$\frac{3}{16}$" "	"	15,000	40,000	128,000	33,300	2,760
K_1	Inclined Rods and	DT & T	20,000	55,000	176,000	47,000	1,475
K_2	$\frac{1}{4}$" Stirrups.	DT	20,200	35,000	112,000	29,300	1,515
L_1	Inclined Rods and	"	20,000	45,000	144,000	37,200	1,735
L_2	$\frac{3}{16}$" Stirrups.	T	20,400	40,000	128,000	33,200	1,685
M_1	Expanded Metal	T	20,000	45,000	144,000	37,900	1,305
M_2	No. 13. $\frac{3}{4}$" Mesh.	DT	20,000	45,000	144,000	37,300	1,485
N_1	Expanded Metal.	"	15,000	35,000	112,000	29,200	1,605
N_2	No. 12. $2\frac{1}{2}$" Mesh.	"	15,000	45,000	144,000	38,300	1,880

T = Tension. DT = Diagonal Tension.

* Broken as a simple beam.

† Twisted off due to eccentric loading.

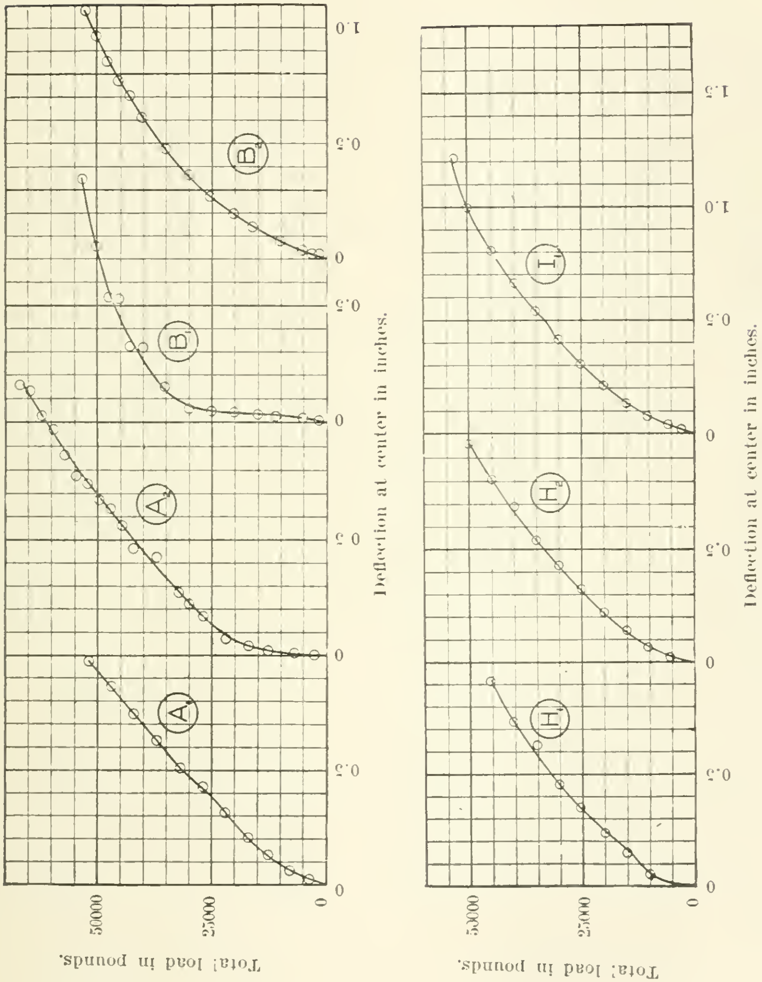

FIG. 20.—BEAMS OF SERIES D—LOAD-DEFLECTION CURVES.

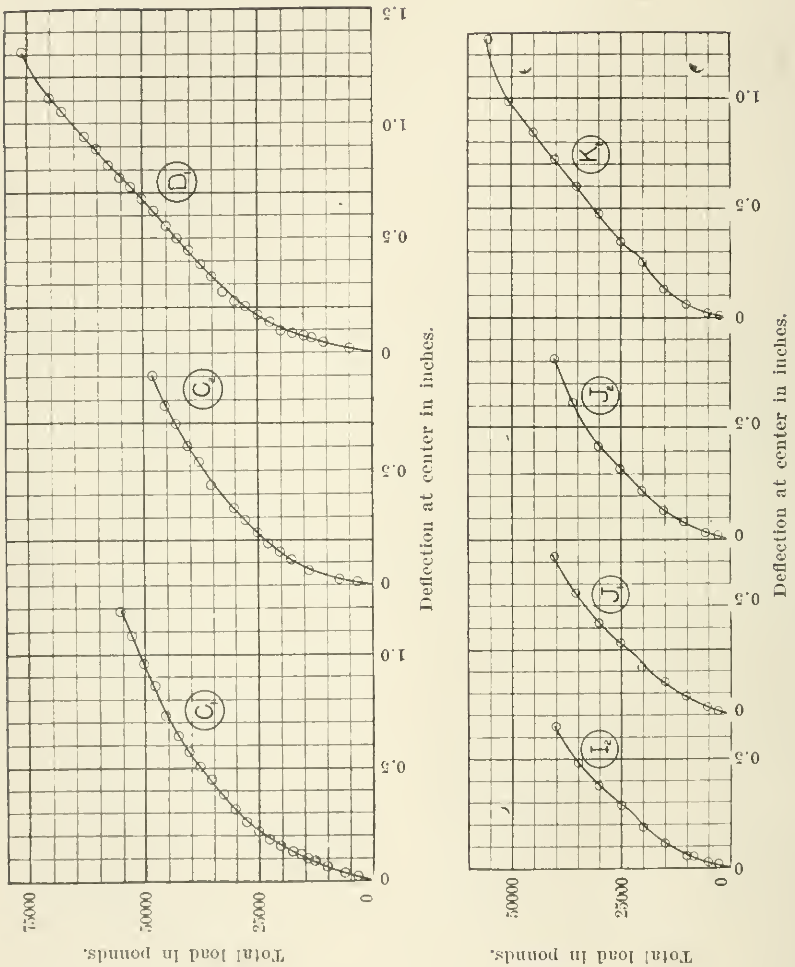

FIG. 21.—BEAMS OF SERIES D—LOAD-DEFLECTION CURVES.

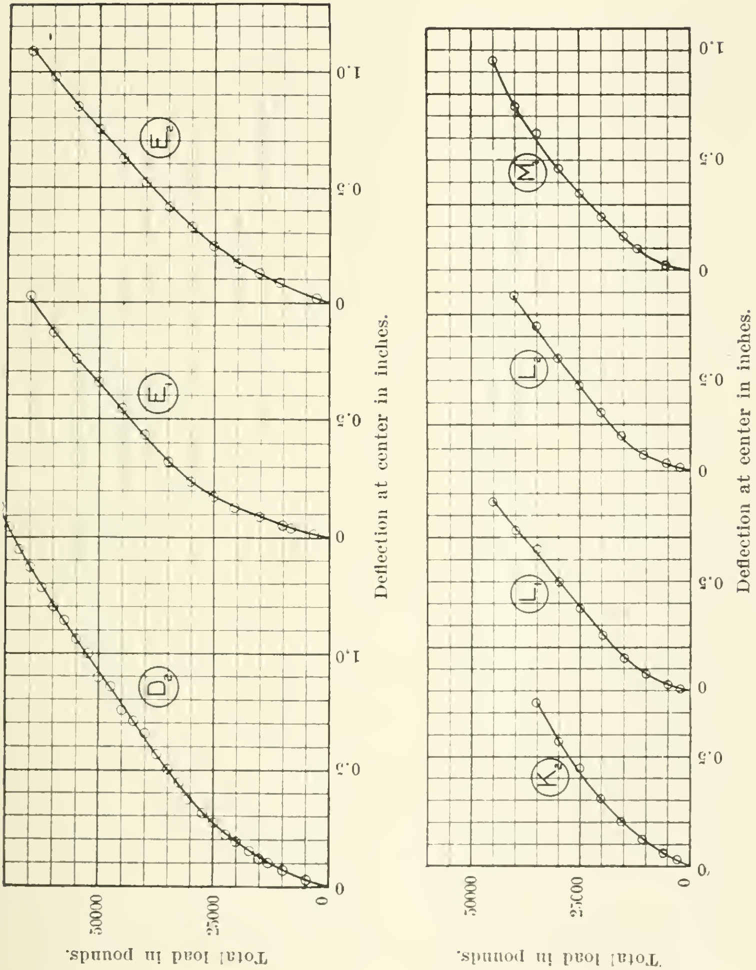

FIG. 22.—BEAMS OF SERIES D—LOAD-DEFLECTION CURVES.

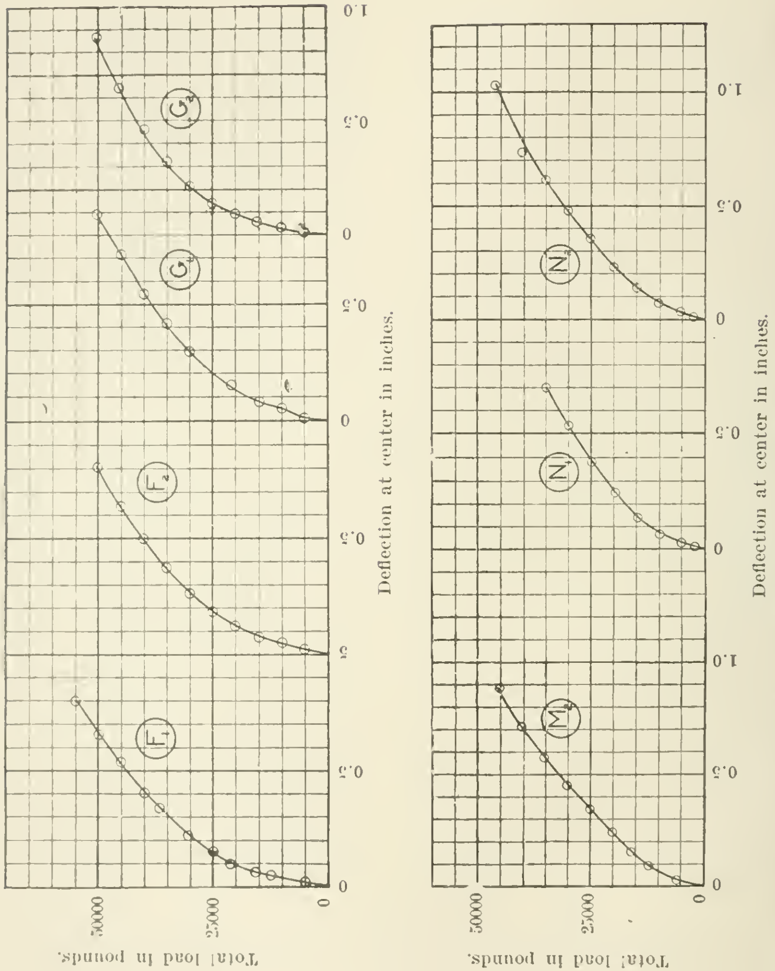

FIG. 23.—BEAMS OF SERIES D—LOAD-DEFLECTION CURVES.

The lowest value of vertical shear for the 11-inch beams was developed in G_2, 211 lbs./in^2., the highest in D_2, 341 lbs./in^2. The average value of v was, for this depth, 269 lbs./in^2. and for the 9-inch depth, it was 239 lbs./in^2.

The beams of this series failed either by tension in the steel or by diagonal tension in the concrete. The latter form of failure may be divided into two distinct classes, failures in which the crack spread horizontally along the plane of the reinforcement, generally followed by slipping of the rods, and those in which no splitting along the rods took place. Plate IV, beam B_2, is an illustration of the first type, while Plate V, beam K_1, shows the second class. Failures accompanied by stripping along the rods came about gradually while the other kind occurred suddenly, sometimes followed by a report.

In the following discussion, beams which were similarly reinforced will be grouped together. Figs. 17, 18 and 19 contain sketches of the cracks numbered in order of their appearance. Beams A_1, A_2, and H_2 failed suddenly by diagonal tension in the second manner described. Plate III shows how A_2 failed. Beam H_1 failed slowly in tension in crack No. 13. The diagonal tension failures in this set occurred near the load. It will be noted that but few visible cracks developed in beams A_1 and A_2, while in the shallower beams H_1 and H_2 a large number of tension cracks opened up.

Beams B_1, B_2 and I_2 all failed in diagonal tension with splitting at the rods. In I_1 the tension cracks in the middle of the span opened up so that it was impossible to tell whether failure was first caused by tension in the steel or by that in the web. A study of Plate IV shows how beam B_2 failed. The upper photograph, taken immediately after failure, shows crack No. 4 as it then appeared. The lower photograph was taken after the concrete had been chipped off at the end of the rods and stirrup. Evidently the diagonal crack brought an increasing stress upon the stirrup which started to slip. This caused the concrete to split along the reinforcement, weakening the bond so that the rods finally slipped and the beam failed. Beams B_2 and I_2 failed in a like manner. In beam I_1 no trace of slipping at the ends of the rods or stirrups could be discovered.

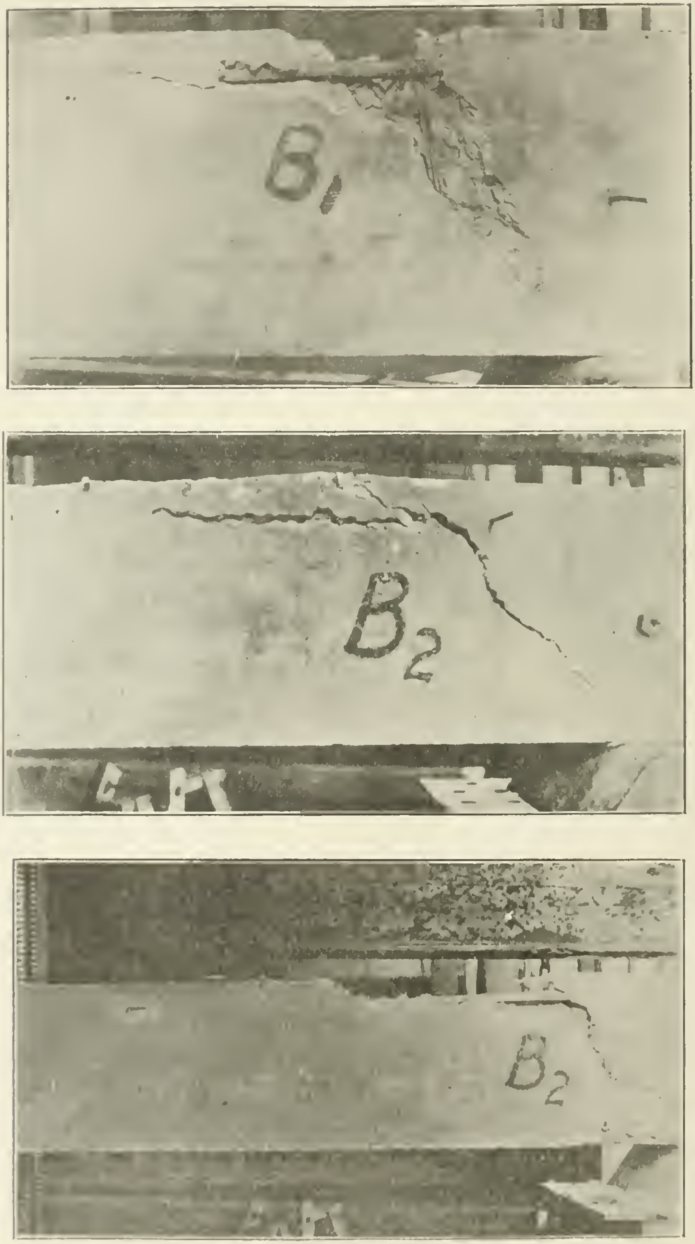

Plate IV.—Failure Cracks in Beams B_1 and B_2.

Beams C_1, C_2, J_1 and J_2 all failed in the same way as beam B_2. To make sure of the primary and secondary causes of failure, the concrete was chipped away from the ends of the rods in beam C_2 so that any slipping could be instantly detected. Plate VIII shows what happened. Diagonal cracks formed at both ends of the span at practically the same time. The one on the left, however, progressed more rapidly than that on the right, causing the rods to slip as shown in the photograph. On the right, not the slightest trace of any movement of the rod could be discerned, although the crack, as can be seen, had started along the plane of the reinforcement. Fig. 17 gives a sketch of the opposite side of beam C_2 from that shown in the photograph.

Beams D_1 and D_2 proved too strong for the loading apparatus. Beam D_2 was loaded up to 86,000 pounds, and then the load was released to repair the I beams of the loading apparatus which had been badly twisted. The load was again applied, and the beam failed at 84,000 pounds. Failure was primarily tension. Plate V shows view of the failure in crack No. 4. Beam D_1 was loaded twice up to a load of 82,000 pounds without any sign of failure other than the tension cracks shown in Fig. 17. It was then tested as a simple beam with an eight foot span loaded at the $\frac{1}{3}$ points, and broke in tension under a total load of 18,740 pounds. Beam K_1 stood the highest load of any of the 9-inch beams, finally failing as shown in Plate V. It will be noted that the failure crack came between two stirrups. On the other hand, beam K_2 failed at a lower load than any of the 9-inch beams. The break was sudden in both cases and occurred at the same place. The concrete around the crack in beam K_2 did not appear as sound as in beam K_1. No other reason for the difference in strength between these two beams was discovered.

Beam E_1 had so uneven a top that wedges were placed under the bearing points to level up the loading apparatus. This evidently produced an eccentric loading and caused the beam to twist off very suddenly at a much lower load than its mate, beam E_2. Plate VI shows how the crack extended diagonally across the top of the beam. Beam E_2 was loaded up to 82000

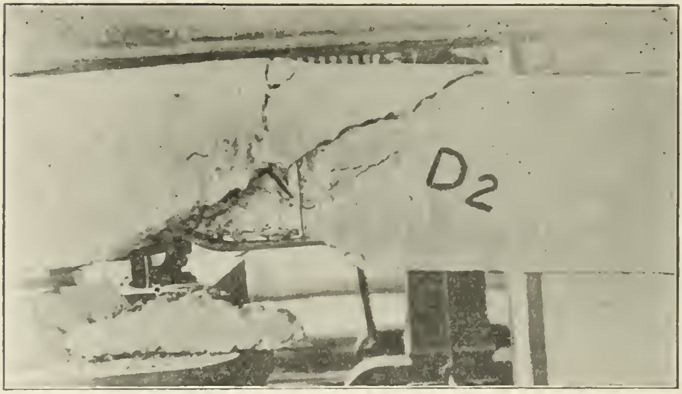

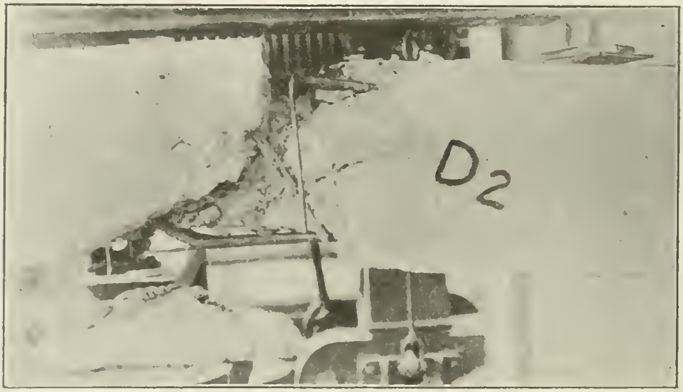

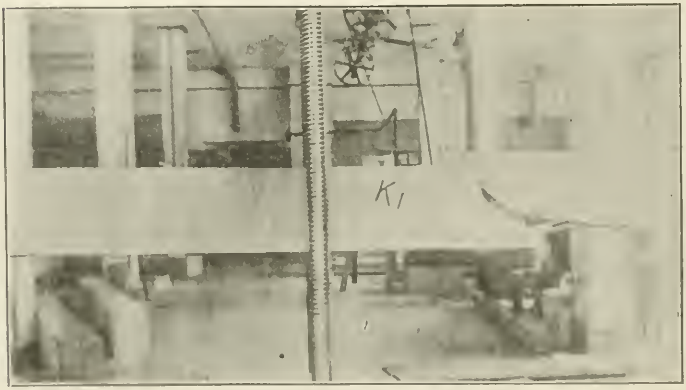

PLATE V.—FAILURE CRACKS IN BEAMS D_2 AND K_1.

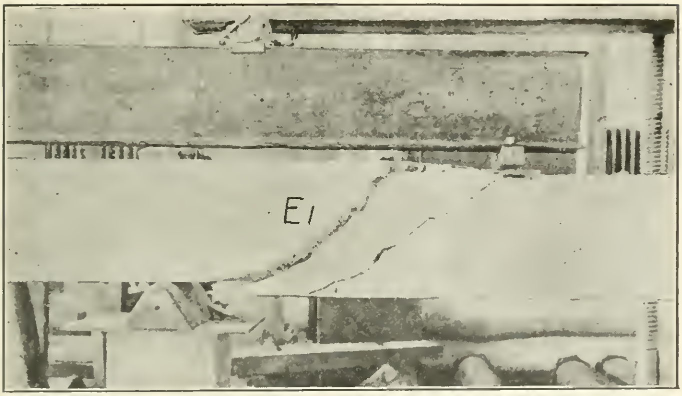

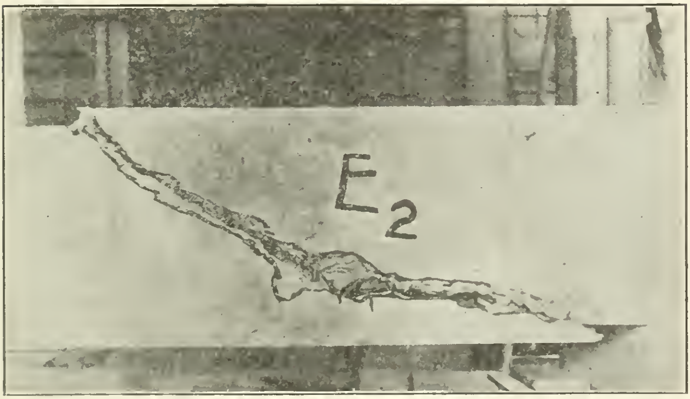

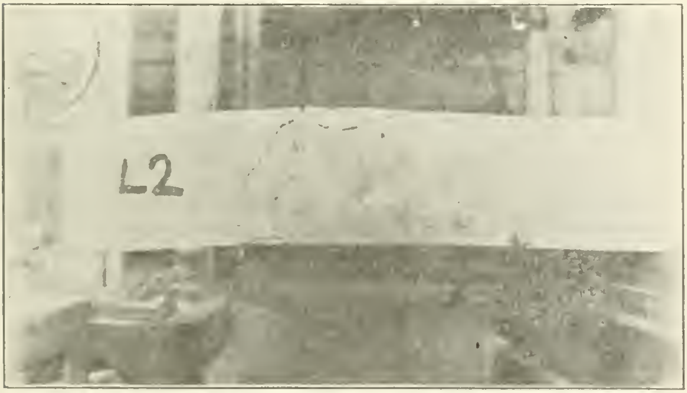

PLATE VI.—FAILURE CRACKS IN BEAMS E_1, E_2 AND L_2.

pounds and then released. The load was again applied up to 76000 pounds when failure took place. The break took place suddenly in crack No. 13, shown in Plate VI. The photograph was taken on the opposite side from that shown in the sketch in Fig. 18. Beam L_1 failed in a similar manner to beams K_1 and K_2. Beam L_2 failed slowly in tension, finally forcing a compression failure on the under side.

Beams F_1, F_2 and M_2 all failed in diagonal tension, accompanied by splitting at the rods. Beam M_1 failed in tension in crack No. 12, followed by compression at the support. Plate VII shows how the expanded metal pulled apart in beams F_1 and M_2.

Beams G_1, G_2, N_1 and N_2 all failed in a similar manner to beams F_1 and M_2. These beams were reinforced with a 2½-inch mesh expanded metal which seemed to pull apart more easily than the ¾-inch mesh used in the previous set.

A study of the crack sketches, Figs. 17, 18 and 19, shows that diagonal cracks developed closer to the supports in all beams which had no inclined rods than in those which contained them. In other words, beams with inclined rods developed diagonal cracks in the simple beam portion of the span. Practically all these beams which failed in diagonal tension failed in the second manner previously mentioned.

Those beams which depended upon inclined rods for resistance to web stresses showed greater strength than those which had stirrups or expanded metal. Inclined stirrups or vertical stirrups spaced more closely together would doubtless have given similar results.

There is no marked difference in strength in the beams reinforced with stirrups only. Judging from the way the cracks appeared in the 9-inch beams, a close spacing of 4 or 5 inches would have prevented many of the diagonal tension failures. The increased amount of metal in the ¼-inch stirrups did not seem to affect the resistance to web stress of the beams which contained them. In placing stirrups the problem seems to be to distribute the metal in small members rather than to concentrate it in large ones.

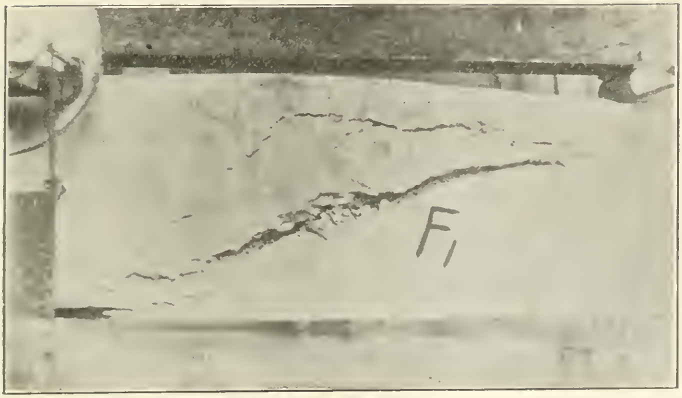

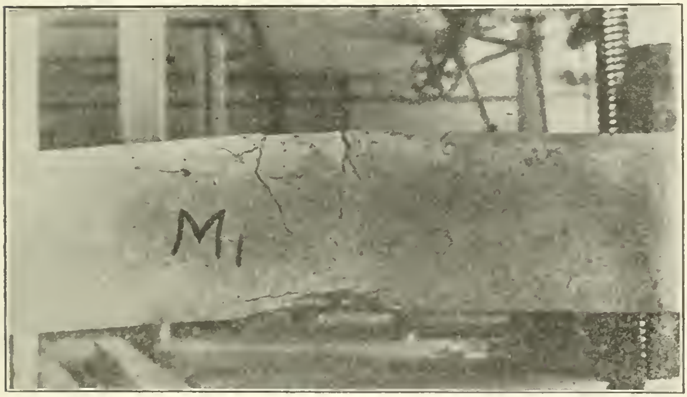

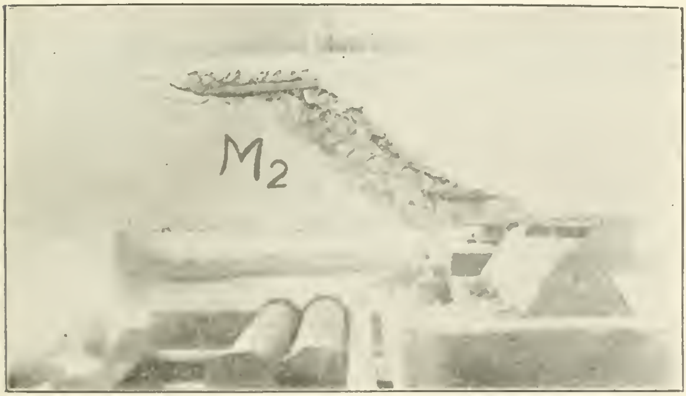

Plate VII.—Failure Cracks in Beams F_1, M_1 and M_2.

The chief difficulty experienced with expanded metal was its tendency to break off at the corners of the diamonds when under stress. This form of reinforcement is easily put in place. A stronger meshing would doubtless prove a very satisfactory web reinforcement. It is the opinion of those engaged in these tests that the tensile strength of concrete is a more important factor in deep beams than the compressive strength. The necessity for the exercise of great care in order to secure good concrete is decidedly essential if uniform results are to be obtained.

The resistance of a web reinforcement to diagonal stresses depends largely upon its being dispersed throughout the beam and not concentrated in large rods spaced at relatively wide intervals. Inclined members are in a better position to resist tensile web stresses than those which are vertical. In these tests stirrups and bent rods in combination made the strongest web reinforcement.

5. TEE BEAMS.

Sixteen tee beams were made as shown in Figs. 24 and 25. Stones larger than ½-inch were screened out of the aggregate so that the concrete might be easily placed around the reinforcement. In tee beams D_1, D_2, F_1, F_2, H_1 and H_2, the rods were placed in two layers and bent up in pairs. In the other beams rods were turned up at each of the points shown in the figures. It will be noted that the span for tee beams A_1, A_2, B_1 and B_2 was 6 feet while for all others it was reduced to 5 feet. Plate VIII gives a picture of apparatus. The extensometer readings taken were untrustworthy owing to lack of rigidity of the apparatus and are not given. Fig. 26 gives the moment-deflection curve for tee beams C_1 to H_2.

Tee beams A_1, A_2, B_1 and B_2 failed by slipping of the rods. In order to observe carefully the manner of failure the concrete was chipped away at the ends of rods so that the time at which slipping took place could be noted. In general, tension cracks first formed about half way between the load and support. These were due to the decreased tensile resistance caused

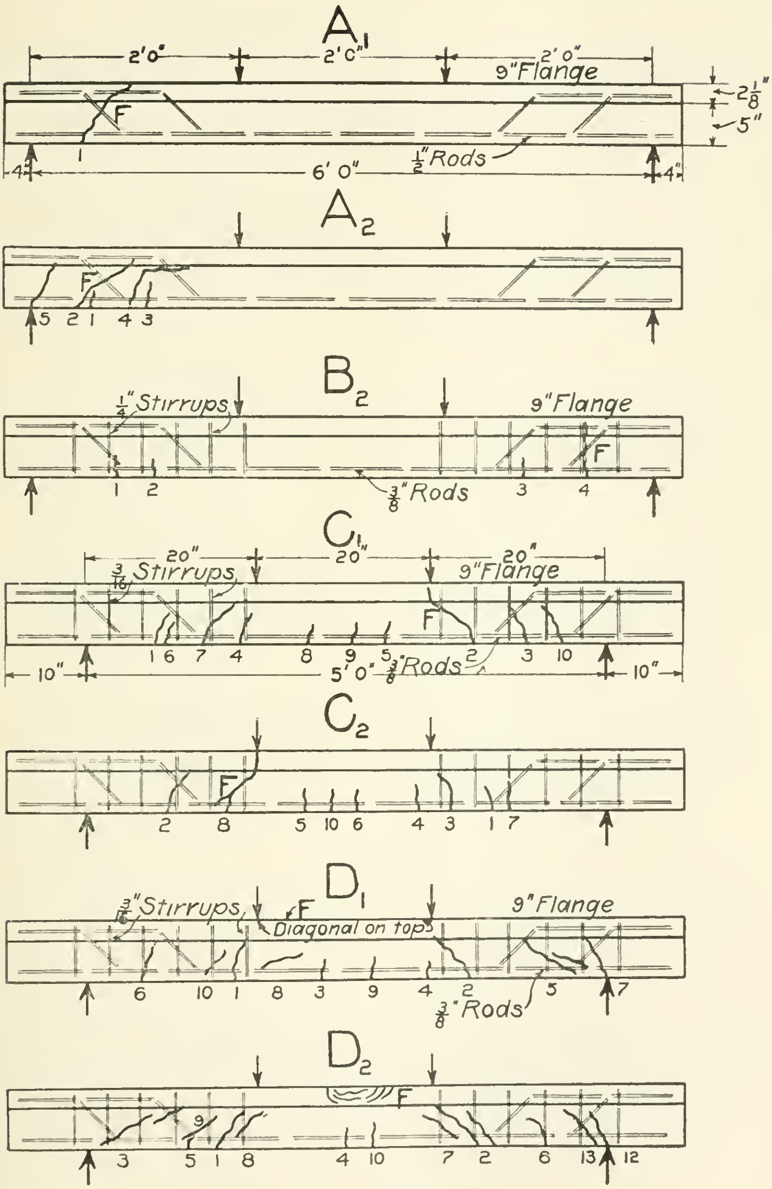

Fig. 24.—Tee Beams—Reinforcement and Cracks.

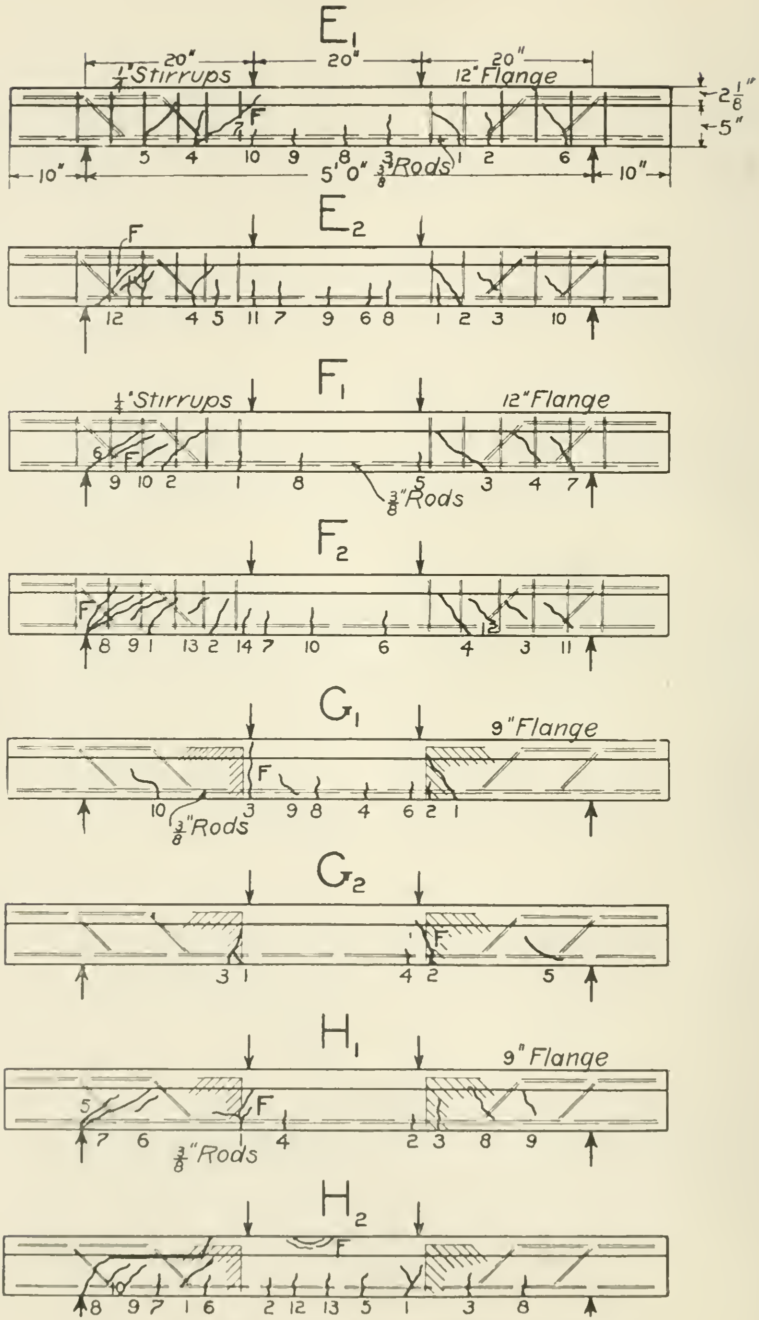

FIG. 25.—TEE BEAMS—REINFORCEMENT AND CRACKS.

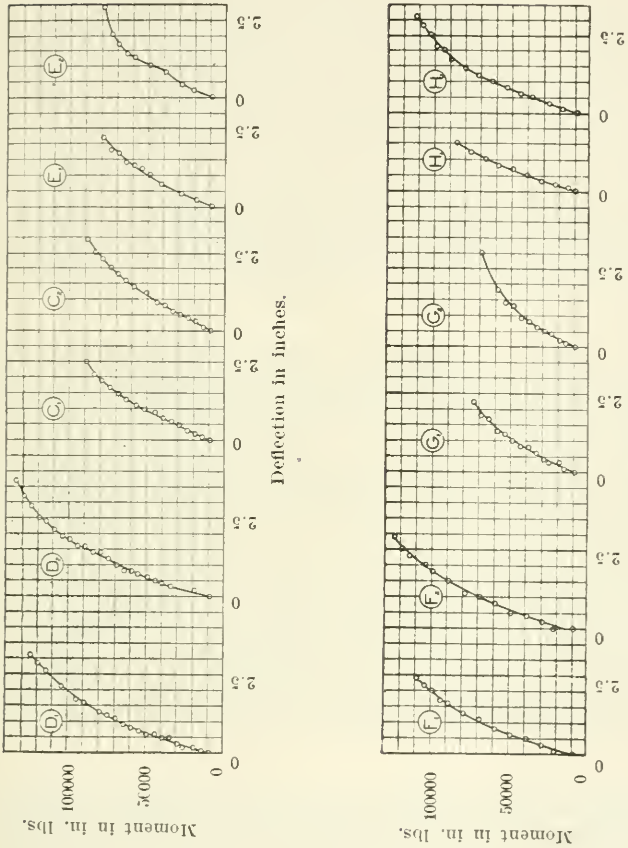

Fig. 26.—Tee Beams.—Moment-Deflection Curves.

by bending up the rods. Soon the lower rod, followed by the upper, would begin to slip, one of these cracks would widen and cause failure. Plate VII shows the failure crack in A_1. To avoid this sort of failure the span for the remaining tee beams was made 5 feet.

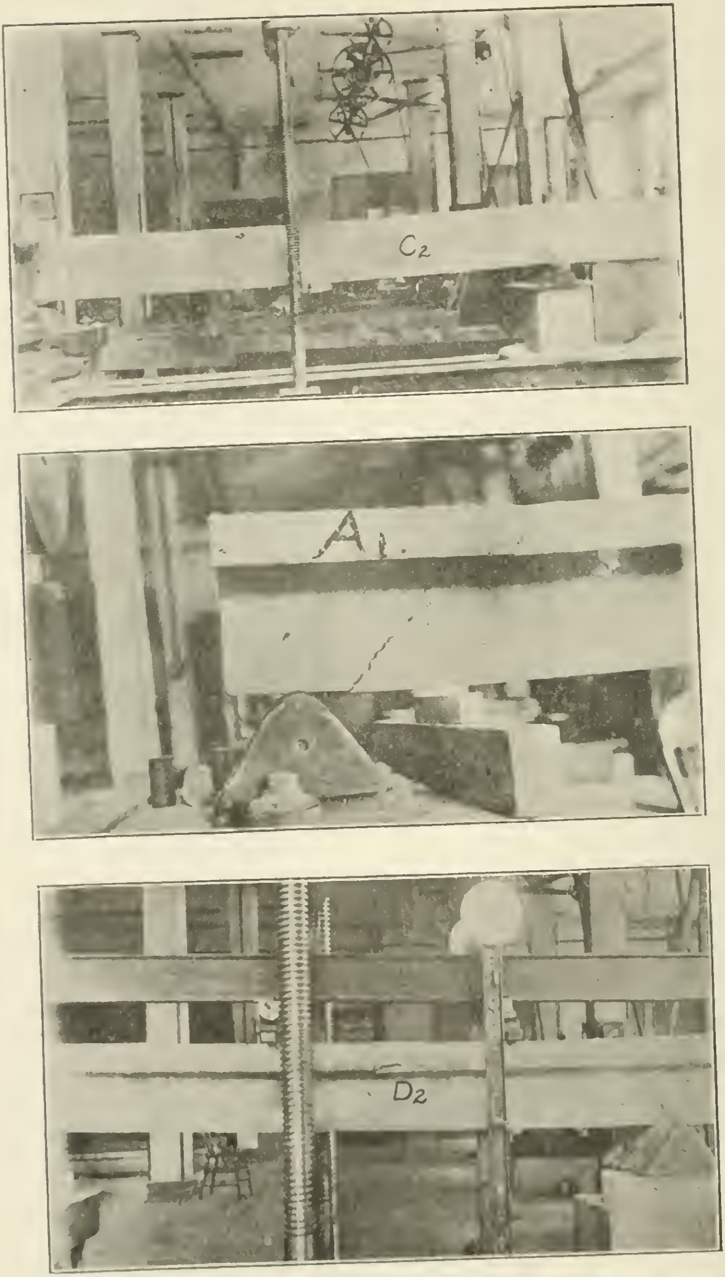

PLATE VIII.—FAILURE CRACKS IN BEAM C_2 AND TEE BEAMS A_1 AND D_2.

Tee beams C_1 and C_2 failed in tension primarily. Tee beam D_1 developed a compressive crack which extended diagonally across the top of the flange between the loads. At the same time crack 5 split open at the web. Tee beam D_2 failed as shown in Plate VIII by crushing of the concrete in the flange. Attention is called to the manner in which tee beams E_2, F_1 and F_2 failed near the support. Tee beams G_1 and G_2 failed through tension cracks which opened at the end of the expanded metal and spread directly upward to the load. Tee beam H_2 failed by compression in the flange and by diagonal tension and horizontal shear in crack No. 8. It will be noted that the diagonal tension cracks in many instances were first seen in the middle of the web without any connecting tensile crack running to the bottom of the beam. Tee beams E_2 and F_2 furnish illustrations of this kind of crack.

Table XIX gives values for v and the stress in the steel. It must be borne in mind that the shear was assumed to be carried by the web in computing v. The calculated stresses in the steel are based upon the assumption that the centroid of compression was at the center of the flange. For tee beams C_1 ,C_2, E_1, E_2, G_1 and G_2 the average intensity of vertical shear is 218 lbs./in^2. and for those with double the amount of reinforcement it is 344 lbs./in^2.

Tee beams E_1, E_2, F_1 and F_2 which had 12-inch flanges did not show any greater strength than those with 9-inch flange.

A further investigation of web reinforcement has been carried on in a later series of tests made at this institution, the results of which are now being prepared for publication.

TABLE XIX.

TEE BEAMS.

Compressive strength of concrete, 1,120 lbs./in.^{2}

No. Beam.	No. and Size of Rods.	Web Reinforcement.	Total Load (in lbs.)	Kind of Failure.	Effective Depth (in ins.)	v (in lbs./in.^{2})	Load Considered (in lbs.)	Stress in Steel. (in lbs./in.^{2})
A_1	3, $\frac{1}{2}$"	Rods bent up	4,000	B	6.25	107	4,000	15,400
A_2	3, $\frac{1}{2}$"	"	5,100	B	6.25	136	5,100	19,700
B_1	3, $\frac{3}{8}$"	$\frac{1}{4}$" stirrups and bent rods.	4,750	B	6.25	127	4,750	32,600
B_2	3, $\frac{3}{8}$"	"	4,000	B	6.25	107	4,000	27,400
C_1	3, $\frac{3}{8}$"	$\frac{3}{16}$" stirrups and bent rods.	9,380	T & DT	6.63	236	9,000	50,400
C_2	3, $\frac{3}{8}$"	"	9,400	"	6.38	246	9,000	52,900
D_1	6, $\frac{3}{8}$"	"	12,850	C&DT	6.50	330	12,500	35,300
D_2	6, $\frac{3}{8}$"	"	13,550	C	6.50	348	13,500	37,200
*E_1	3, $\frac{3}{8}$"	$\frac{1}{4}$" stirrups and bent rods.	8,400	DT	6.50	216	8,000	45,900
*E_2	3, $\frac{3}{8}$"	"	8,000	DT	6.50	205	8,000	43,700
*F_1	6, $\frac{3}{8}$"	"	11,400	DT	6.25	304	11,000	32,800
*F_2	6, $\frac{3}{8}$"	"	12,700	DT	6.13	346	12,500	37,400
G_1	3, $\frac{3}{8}$"	No. 13 Expanded Metal and bent rods.	7,800	T	6.00	217	7,500	47,000
G_2	3, $\frac{3}{8}$"	"	7,000	T	6.13	190	7,000	41,100
H_1	6, $\frac{3}{8}$"	"	13,800	T & DT	6.00	386	13,500	37,500
H_2	6, $\frac{3}{8}$"	"	12,600	C	6.00	350	11,000	34,300

B=Bond. C=Compression.
T=Tension. DT=Diagonal Tension.

BULLETIN OF THE UNIVERSITY OF WISCONSIN
NO. 197
ENGINEERING SERIES, VOL. 4, NO. 2, PP. 67–136

TESTS ON PLAIN AND REINFORCED CONCRETE
SERIES OF 1907

BY

MORTON OWEN WITHEY, C. E.
Instructor in Mechanics, University of Wisconsin

RESEARCHES IN APPLIED MECHANICS
EDWARD R. MAURER, PROFESSOR OF MECHANICS

*Published bi-monthly by authority of law with the approval of the Regents
of the University and entered at the post office at
Madison as second-class matter*

MADISON, WISCONSIN
FEBRUARY, 1908

CONTENTS

PAGE.
I. Introduction ... 71
II. Description of materials ... 72
III. Auxiliary tests ... 76
VI. Beams ... 80
  1. Series E. Reinforced in top and bottom ... 88
  2. Series F. Tee-beams ... 91
  3. Series N. Tee-beams ... 102
  4. Series G. Rectangular deep deams ... 127
  5. Web reinforcement ... 130

ILLUSTRATIONS

PLATES

I. Compressometer apparatus ... 78
II. Tee-beam E 2 ready to be tested ... 85
III. Failure cracks in tee-beam C 1 ... 96
IV. Failure crack in tee-beam D 2 ... 97
V. Cracks in tee-beam F 1 ... 126
VI. Failure crack in tee-beam G 1 ... 132
VII. Failure crack in tee-beam G 2 ... 133
VIII. Beam with stirrup deformation apparatus ... 135

FIGURES

1. Tension specimens (templates and apparatus for testing) ... 79
2. Tee-beam molds ... 81
3. Stirrups and dial socket ... 81
4. Beam extensometer apparatus ... 83
5. Diagram showing stress distribution in tee beams ... 86
6. Beams of series E—reinforcement and cracks ... 88
7. Beams of series E—moment-deformation curves, etc ... 92
8. Beams of series F—reinforcement and cracks ... 93
9. Beams of series F—reinforcement and cracks ... 94
10. Beams of series F—reinforcement and cracks ... 95
11. Beams of series F—moment-deformation curves, etc ... 103

PAGE
12. Beams of series F—moment-deformation curves. etc........... 104
13. Beams of series F—moment-deformation curves, etc............ 105
14. Beams of series F—moment-deformation curves, etc............ 106
15. Beams of series F—moment-deformation curves, etc 107
16. Beams of series F—moment-deformation curves, etc........... 108
17. Beams of series F—moment-deformation curves, etc............ 109
18. Beams of series N—reinforcement and cracks.................. 110
19. Beams of series N—reinforcement and cracks.................. 111
20. Beams of series N—reinforcement and cracks.................. 112
21. Beams of series N—reinforcement and cracks.................. 113
22. Beams of series N—moment-deflection curves, etc............. 118
23. Beams of series N—moment-deformation curves, etc........... 119
24. Beams of series N—moment-deformation curves, etc........... 120
25. Beams of series N—moment-deformation curves, etc........... 121
26. Beams of series N—moment-deformation curves, etc........... 122
27. Beams of series N—moment-deformation curves, etc........... 123
28. Beams of series G—reinforcement and cracks 124
29. Beams of series G—reinforcement and cracks............. 125
30. Beams M 1 and M 2—deformation in stirrups.................. 131

TABLES

I. Tension tests of steel.................................. 73
II. Analysis of Kankakee limestone......................... 74
III. Analysis of sand.. 74
IV. Tensile strengths of cements 75
V. Auxiliary tests 77
VI. Series B and E—stresses in steel and concrete............... 89
VII. Series B and E—values of v and $\frac{M}{b\,d^2}$ 90
VIII. Series F—stresses in steel and concrete.................... 99
IX. Series F—values of v and $\frac{M}{b'd^2}$ 101
X. Series N—stresses in steel and concrete..................... 115
XI. Series N—values of v and $\frac{M}{b'd^2}$ 117
XII. Series G—stresses in steel......... 128
XIII. Series G—values of v and bond.......................... 129
XIV. Computed stresses in stirrups 134

TESTS ON PLAIN AND REINFORCED CONCRETE

I. INTRODUCTION

In this bulletin are reported some of the tests on plain and reinforced concrete carried on in the laboratory for testing materials at the University of Wisconsin during the spring and summer of 1907. The investigations in plain concrete consisted of compression, tension and transverse tests made in conjunction with the other tests. The main work consisted of tests on rectangular beams reinforced in compression, tee-beams with both rigid and loose web reinforcement and tests on deep rectangular beams to determine the deformations of the stirrups. The tee-beams of Series N were made and tested as a thesis by G. C. Newton and W. L. Rowe of the Class of 1907. They are deserving of credit for the care with which they performed the tests and the concise summary which they reported in thesis form. The remainder of the tests were made during the summer by paid assistants.

The summer work on tee-beams was laid out with special reference to the investigation of stresses in the web of a reinforced concrete beam. Tension specimens were made with the beams so that a check upon the strength of the concrete in the web might be had. In the discussion of web reinforcement no attempt has been made to develop any formulae for design as these experiments do not cover a wide enough range to determine empirical constants for such formulae. It is hoped that further experiments may be made here in measuring deformations along stirrups and upon the amount of shearing reinforcement necessary; also further tests to show the relative values of loose and rigid web reinforcements, using high percentages of longitudinal reinforcement, would be interesting.

The beams with compression reinforcement give considerable information concerning methods for strengthening a beam without increasing the size. This is frequently necessary in building construction, both to permit uniformity in constructing the forms and also to conform to architectural features of the design. The shifting of the neutral axis in the beam subjected to a reversal of loading is of interest on account of its close application to the rib of a reinforced arch.

The crack sketches and drawings are made from measurements taken on the beams immediately after testing. The letter F indicates the failure crack in all cases where it occurs.

Due acknowledgment is made to Dean F. E. Turneaure for many suggestions received in this work. E. P. Abbott, of the class of 1908, deserves mention for efficient assistance in performing the tests and for the drawings of this bulletin.

II. DESCRIPTION OF MATERIALS

Steel:—All smooth rods used for reinforcement were purchased in the local market. The St. Louis Expanded Metal Company donated the corrugated bars, and the Trussed Concrete Steel Company of Detroit the Kahn bars. The wire meshing was obtained from the Clinton Wire Cloth Company. Table I gives data for tension tests of steel. At least two specimens of the same size were tested in all cases, and columns 5 and 6 are the averages for two specimens except in the case of the ¾-inch corrugated and the wire meshing where the individual results are given. It will be noted that the ¾-inch corrugated bars varied considerably in elastic limit and ultimate strength. This may have been the cause for the variation in strength of the tee-beams with the 24-inch flanges.

Stone:—Crushed limestone from Kankakee, Illinois, was used in making all specimens. Table II gives a mechanical analysis of a cubic foot of the material.

Sand:—The sand used was furnished by a local dealer. It was the best obtainable in this vicinity but too fine to make a strong concrete. An analysis of the sand is found in Table III.

TABLE I.

TENSION TESTS OF STEEL.

Size of Bar. ins.	Area. sq. in.	Load at Yield Point lbs.	Maximum Load. lbs.	Stress at Yield Point. lbs./in.^{2}	Ultimate Strength. lbs./in.^{2}
			Corrugated Bars.		
3/4"	.590	29,450	51,850	50,000	87,800
	.559	24,400	42,300	43,600	75,600
	.554	25,320	46,170	45,600	83,500
	.551	25,300	43,000	46,000	78,000
	.554	26,700	46,850	48,200	84,600
	.550	25,700	50,000	46,700	91,000
	.553	31,000	53,400	56,000	96,500
			Average	48,000	85,300
3/8"				41,300	64,500
1/4"				45,000	68,800
			Plain Round Bars.		
3/4"				41,000	61,100
5/8"				43,900	61,900
1/2"				46,100	66.800
3/8"				46,000	64,100
1/4"				47,400	62,000
			Wire Meshing.		
.120	.0113	850	850	75,100	75,100
.121	.0117	950	950	81,200	81.200
			Average	78,100	78,100
			Kahn Bars.		
1"				40,000	69,400
3/4"				39,300	65,400

TABLE II.

Analysis of Kankakee Limestone.

Beams.	Diameter of mesh. ins.	Amount retained. pounds.	Per cent passing.	Per cent voids.	Weight in pounds per cubic foot.
Series N N1—N6				48.5	83.0
N7—N19				44.5	91.5
Series E, F, and G.	1.5	0	100	43.0	94.0
	1.25	6.45	94.5		
	1.00	13.5	83.2		
	.75	24.7	62.5		
	.50	45.2	24.7		
	.33	9.5	16.7		
	.22	8.0	10.0		
	.14	5.4	5.5		
	.73	4.7	1.5		
	Dust.	1.8			

TABLE III.

Analysis of Sand.

Per cent Voids=37. Wt. per cu. ft.=105 lbs.

Sieve No.	Diameter of Mesh in ins.	Per cent Passing.
¼	.22	100
6	.131	94.0
10	.073	87.6
16	.042	81.6
20	.034	78.8
30	.022	68.9
40	.015	60.0
50	.011	34.9
74	.0078	16.5
100	.0045	8.6

Cement:—Alpena, Lehigh and Universal cements were used in these tests. Table IV contains the record of the tensile strengths of neat and 1:3 mortar briquettes tested at 7 and 28 days, and also indicates in which beams each brand was used. These cements were all purchased in the open market.

TABLE IV.

Tensile Strengths of Cements.

Briquette No.	Ultimate Strength in lbs./in.².				Brand.	Beams and Specimens.
	Age 7 days.		Age 28 days.			
	Neat.	1:3 Mortar.	Neat.	1:3 Mortar.		
1	580	192	712	275	Alpena	Series N N 1–N 15
2	654	147	694	294		
3	667	160	723	313		
4	710	183	670	256		
5	726	225	655	264		
6	638	181	595	298		
7	619	218	715	259		
8	647	183	693	251		
Av.	655	186	682	276		
1	550	182	590	298	Lehigh	Series F and G except Tee Beam C 1.
2	530	190	600	294		
3	550	172	760	258		
4	596	160	660	264		
Av.	556	176	652	278		
1	620	162	805	370	Universal	Series N N 15–N 19 Series E and Tee Beam C 1.
2	670	175	780	330		
3	723	158	800	350		
4	706	172	775	360		
Av.	680	167	790	352		

Concrete:—The mixture used in all tests was one part cement, two parts sand and four parts stone. Materials were proportioned by volume. Measurements of quantities required for a batch were made by weighing the number of cubic feet of each material on a platform scale. One hundred pounds of cement was considered a cubic foot. Weights of other materials are given in the tables. With the exception of the concrete for beams N 1 to N 6, which was mixed by hand, all concrete was mixed in a No. 0 Smith mixer (donated to the University by T. L. Smith & Company and the Contractors Supply and Equipment Company).

The same scheme of hand mixing was employed as is recorded in the bulletin of the series of 1906. In mixing by machine, four and one-half cubic feet of concrete was made in one batch. Sand was first thrown in and then the cement. After mixing about two minutes, the wetted stone and water were added. The whole batch was then allowed to turn for four or five minutes, the mixer making about 20 R. P. M. Concrete mixed by the machine was uniform in character and showed a higher average strength than the hand mixed. About 9 per cent. of water by weight was used to procure a wet concrete which could be easily worked around the reinforcement. A somewhat drier mix was used in making the tops of the beams.

III. AUXILIARY TESTS

In Table V are given the results of the compression, tension and transverse tests made in connection with beams of Series E, F and G. The specimens were from the same batch of concrete as the beams which are on the same line in the table. In many instances one batch of concrete went into two beams. In such cases, only one auxiliary specimen was made. For example, compression specimen No. 6 was made from a batch part of which went into the top of beam C 2 and the rest into the top of beam D 1.

Compression specimens were made from the same concrete that composed the tops of the corresponding beams. These specimens were cylinders 24 inches high and 10 inches in diameter. Cylinder E 2 was 18 inches high and 6 inches in diameter. The large cylinders were made in wrought iron pipe molds. The pipe was split longitudinally in halves and two small lugs were placed on the outside about ¼ of an inch from each edge so that when the halves were set up in form of a mold, the lugs on one half would be opposite to those on the other. Four-inch clamps were placed upon the lugs to hold the two parts together. This made an accurate mold which could be set up very quickly.

TABLE V.

AUXILIARY TESTS.

1:2:4 Concrete. Age of Specimens 28 days.

Beam.	Compression.			Tension.		Transverse.	
	Specimen.	Ultimate Strength lbs./in.^{2}	Modulus at one-third Ult. Str. lbs./in.^{2}	Specimen.	Ultimate Strength. lbs./in.^{2}	Specimen.	Modulus of Rupture. lbs./in.^{2}
A 1	1	2,460	3,500,000	1	256	1	320
A 2	2	1,640	....	2	167	......	....
B 1	3	1,970	....	3	260	2	398
B 2	4	1,930	3,600,000	4	157	3	248
C 1	5	1,950	....	5	197	4 5	359 410
C 2	6	1,650	....	6	216	6	339
D 1	6	1,650	....	7	182	7	325
D 2	......	....	....	......	....	......	....
E 1	4	1,930	3,600,000	8	148	8	374
E 2	7	1,730	....	9	184	9	416
F 1	8	1,770	2,800,000	10	142	10	288
F 2	9	2,290	3,800,000	11	174	11	276
G 1	......	....	....	12	184	......	....
G 2	10	2,290	....	13	164	......	....
H 1	11	1,900	3,500,000	14	208	12	333
H 2	11	1,900	....	14	208	12	333
I 1	12	1,900	....	10	142	10	288
I 2	12	1,900	....	10	142	10	288
J 1	13	1,960	3,800,000	4	157	3	248
J 2	14	2,170	....	4	157	3	248
K 1	15	1,650	3,700,000	15	201	13	320
K 2	15	1,650	....	15	201	13	320
L 1	16	1,910	3,600,000	......	....	14	372
L 2	16	1,910	....	......	....	14	372
M 1	......	....	....	16	172	......	....
M 2	......	....	....	17	180	......	....
W 1	17	2,600	....	18	208	15	377
W 2	17	2,600	....	19	217	16	418
X 1	18	1,500	....	20	150	17	367
X 2	19	1,530	3,100,000	20	150	18	350
Averages..........		1,940	3,500,000	......	189	......	352

The small cylinders were made in cast iron molds referred to in the bulletin of the series of 1906. The mold was set up on a horizontal iron plate and the concrete deposited in layers which were stirred with a rod. An excess of material was placed on top to allow for settling. After settling had ceased, the head of the cylinder was carefully smoothed off with a trowel.

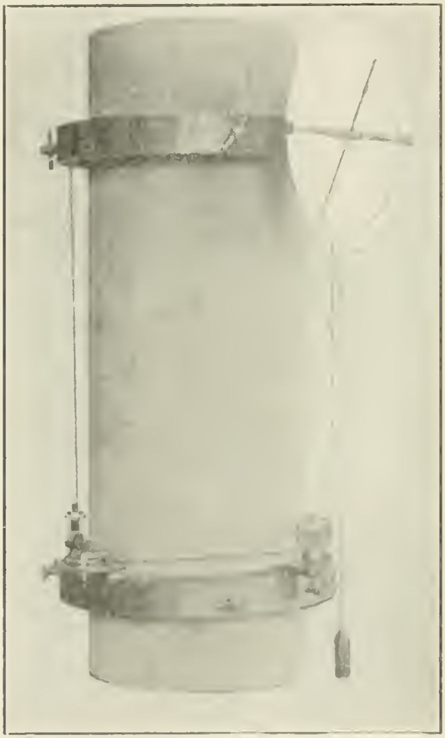

PLATE I.—COMPRESSOMETER APPARATUS.

In testing, two thicknesses of blotting paper were placed on the tops and underneath all compression specimens. The compressometer used is shown in Plate I and is described in the bulletin of the series of 1906.

The average compressive strength of the concrete in these tests was 1940 pounds per square inch. It will be noted that the modulus of elasticity is computed at one-third the ultimate strength instead of at a stress of 600 pounds per square inch, as was done in the bulletin of the series of 1906. This was done since the point on the stress deformation curve at which the modulus of elasticity is computed should be selected with reference to the ultimate strength of the concrete in each individual specimen. In this way a more reliable determination of an average working value for the modulus can be obtained than by selecting a fixed point for all specimens regardless of their strengths. The average value of the modulus of elasticity for this series of tests is 3,500,000 pounds per square inch.

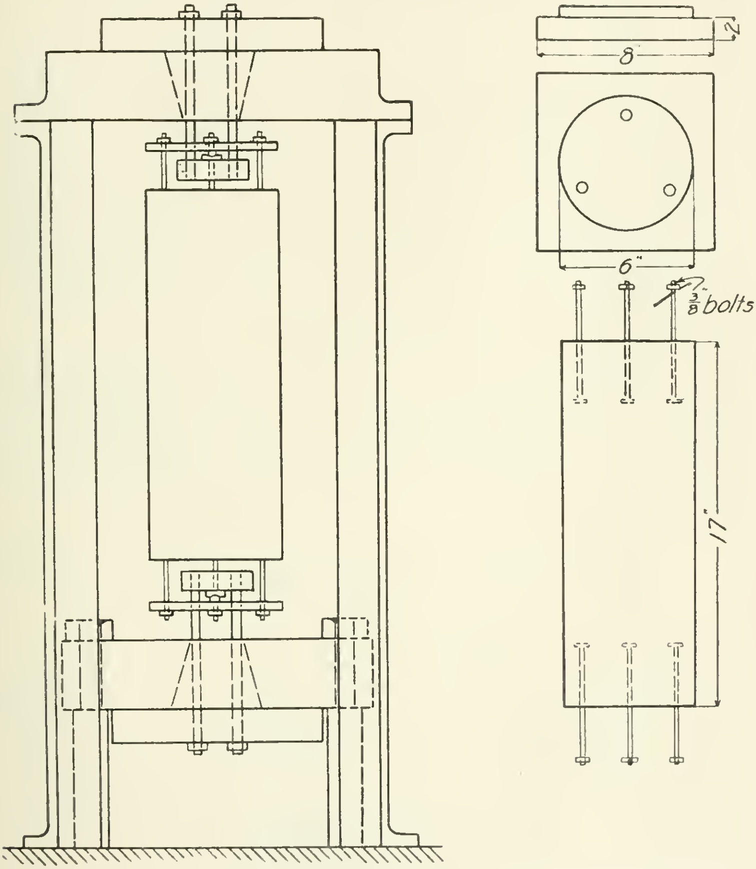

FIG. 1.—TENSION SPECIMENS—TEMPLATES AND APPARATUS FOR TESTING.

Tension specimens were made in the 6-inch cast iron molds from the concrete used in making the lower portions of the beams. Three $\frac{3}{8}$-inch bolts were placed in each end of the specimens as shown in Figure 1. While the concrete was setting, these were held in place by wooden templates shown in the figure. These templates were removed with the molds and used again. The left portion of the figure shows one of the specimens with the apparatus on it ready to be tested. An axial pull was secured through the two crossed knife edges shown just above and below the specimen in the machine.

A good many of these specimens broke in the plane of the bolt heads. In such cases, the net area was taken to find the ultimate strength. This could be obviated by making the specimens smaller in cross section in the middle. The ultimate tensile strength averaged 189 pounds per square inch or about one-tenth the ultimate compressive strength.

Plain concrete beams 3 feet 3 inches long and 6 inches by 6 inches cross-section were also made from the same batch of concrete as the tensile specimens. These were loaded at the middle over a 3-foot span. The modulus of rupture was computed from $S = \frac{6M}{bd^2}$.

M = bending moment at the break;
b = breadth of cross-section;
d = depth of cross-section;
S = modulus of rupture.

The average value of this quantity was 352 pounds per square inch or about 1.9 times the tensile strength.

All auxiliary specimens were cured in air. After 48 hours the molds were removed and the specimens were thoroughly sprinkled twice a day for about a week. They were then sprinkled every two or three days until tested.

IV. BEAMS

Method of Making:—The rectangular beams were made in the same kind of molds as shown in the bulletin of the series of 1906. The tee-beams were made in forms shown in Figure 2. They were made of 2-inch plank and braced every 4 feet by pieces of 2-inch plank b. These were cut to fit closely against the underside of the wing of the tee and held it securely in place. The wings of the tee w-w and the braces b-b were made in different breadths to permit increasing the width of flange of the beams. At the center and over the supports wires were stuck through the holes n and allowed to remain in the beams. These served to hold the deflection apparatus.

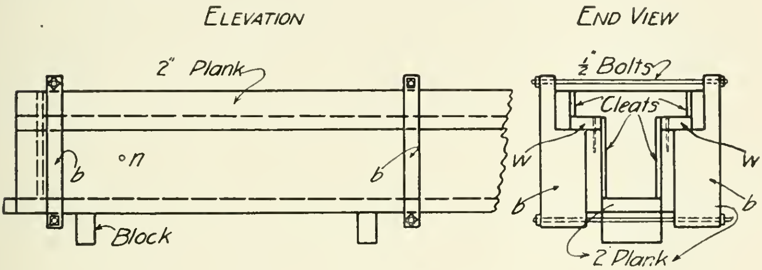

FIG. 2.—TEE-BEAM MOLDS.

In the beams of Series N, the loose stirrup reinforcement was held in position by $\frac{1}{4}$-inch rods placed in the tops of the beams to which the stirrups were securely wired. Figure 3, Nos. 1, 2 and 3 show how the stirrups were made in beams of Series E,

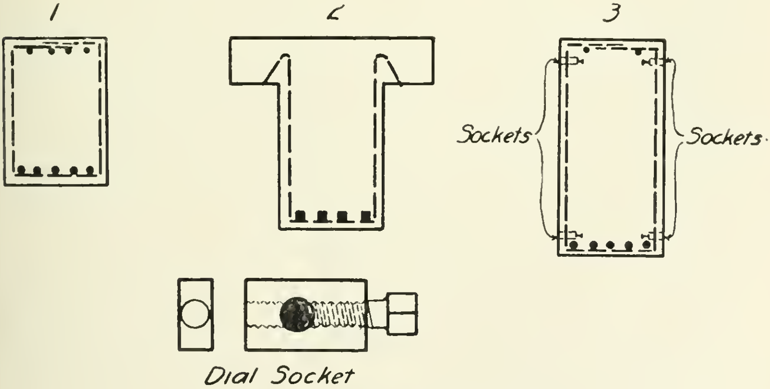

FIG. 3.—STIRRUPS AND DIAL SOCKET.

F and G, respectively. Rods in the tops of the beams were held in position by small wires run transversely through the forms. The upper rods in turn supported the stirrups and lower reinforcement. In the tee-beams of Series F the lower rods were supported by the stirrups. The distance of the rods from the bottom could easily be adjusted by bending the wing of the stirrup.

In beams of Series G, in order to measure the deformation over the length of a stirrup, it was necessary to devise some means of fastening a dial rigidly to the stirrup. This was accomplished by means of the dial socket shown in Figure 3. These sockets were securely clamped upon the stirrups and the dial end of the hole filled with oiled waste to keep out the concrete, water and dirt. The sides of the stirrups were sprung apart in the forms by a piece of wood placed near the top so that the dial holes were brought flush with the face of the beam. When the concrete had been put in the wooden brace was removed. No trouble was experienced in removing the waste or in putting on the dials for a test.

The concrete was placed in layers about four inches deep and spread around by bricklayers' trowels. The sides of the beams were surfaced by running a trowel around the edge of the mold and bringing the mortar to the surface. The top was floated with a mason's trowel.

Beams were cured in the same way as the auxiliary specimens.

Testing:—The beams of Series N were tested on an Olsen 100,000-pound hydraulic beam machine. The rest of the beams were tested on a new hydraulic universal machine which has a capacity of 200,000 pounds for transverse tests over a 20-foot span. The loads were applied through knife-edged bearings upon steel plates set in plaster of Paris. In beams of Series N the supports were a knife-edge resting against a steel plate 8 x 3 x $\frac{3}{8}$ inches at one end and a knife-edge and tipple at the other. In the rest of the beams, rocker bearings were employed at the supports. These rested upon 8 x 4 x $\frac{5}{8}$-inch steel plates set in plaster of Paris. All beams were loaded at the third points of the span by means of an I-beam. In the beams of Series N the loads were applied through a half roller and a pointed bearing block resting upon 10 x 2 x $\frac{3}{8}$-inch steel plates. These plates were too thin and cracks formed immediately below the loading points due to the concentration of pressure. In the later beams of this series, the loads were distributed over two bearing plates at each point.

In the beams of Series E, F and G, bearing plates 2½ inches wide and $\frac{7}{8}$ of an inch thick running across the full width of the beam were used to distribute the load from the I-beams. In the 24-inch flange tee-beams a 3½-inch steel roller was used above the bearing plate at each loading point.

In all beams deflections were taken at the middle of the span by means of the thread-scale-mirror device used in the tests of series of 1906.

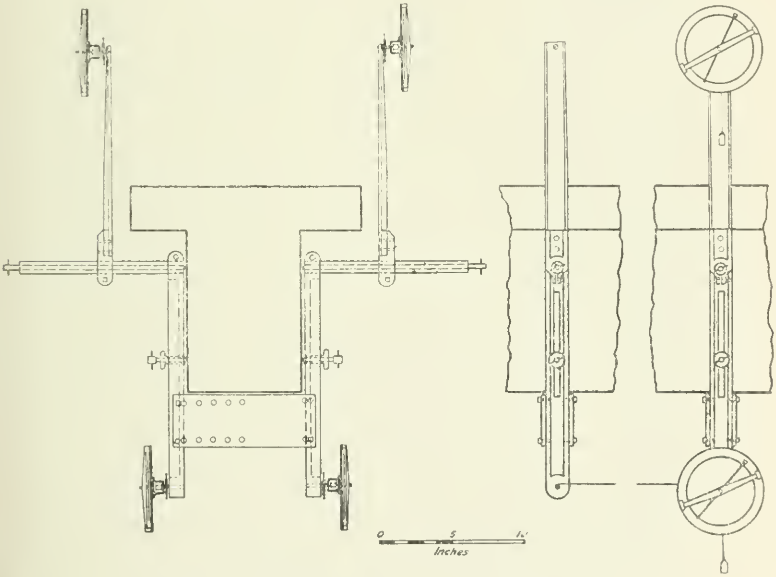

FIG. 4—BEAM EXTENSOMETER APPARATUS.

Extensometer readings were also taken on the beams of Series E and F and beams N 6 to N 19 inclusive by means of the apparatus shown in Figure 4. The upper arms of this apparatus can be adjusted to different flange widths by means of the split collar and set-screw at the lower end. The dials can be removed and placed on other apparatus if desired. This device was very rigid and gave trustworthy readings. The length over which deformations were measured varied from 30 inche for the 8-foot span to 45 inches for the 12-foot span. In al cases the extensometers were set just inside the points o loading.

Plate II shows beam E 2 ready to be tested. Plate V shows a beam similar to those of Series G with dials attached.

Computations:—The following symbols will be used in formulae applied to the results of tests in this bulletin:

A = area of steel in tension;
A' = area of steel in compression;
a = area of prong of a stirrup;
b = breadth of beam (web in tee-beams);
b' = breadth of flange in tee beams;
C = total compressive stress;
d = distance from top of beam to center of steel;
E_s = modulus of elasticity of steel;
E_c = modulus of elasticity of concrete;
ϵ = unit deformation in steel in compression;
f_c = unit stress in concrete on the extreme fibre;
f_s = unit stress in steel in tension;
f'_s = unit stress in steel in compression;
g = unit stress in stirrups;
jd = distance between centroids of tensile and compressive stresses;
kd = distance from top of beam to the neutral axis;
M = bending moment;
$n = \frac{E_s}{E_c}$;
p = ratio of longitudinal reinforcement;
$q = \frac{(kd - t)}{kd}$;
s = distance between stirrups;
t = thickness of flange in tee-beams;
u = number of prongs of a stirrup;
V = total shear on cross-section of a beam;
v = average unit shear on cross-section of a beam;
v' = maximum unit shear on cross-section of a beam;
z = distance from top of beam to centroid of compressive stresses.

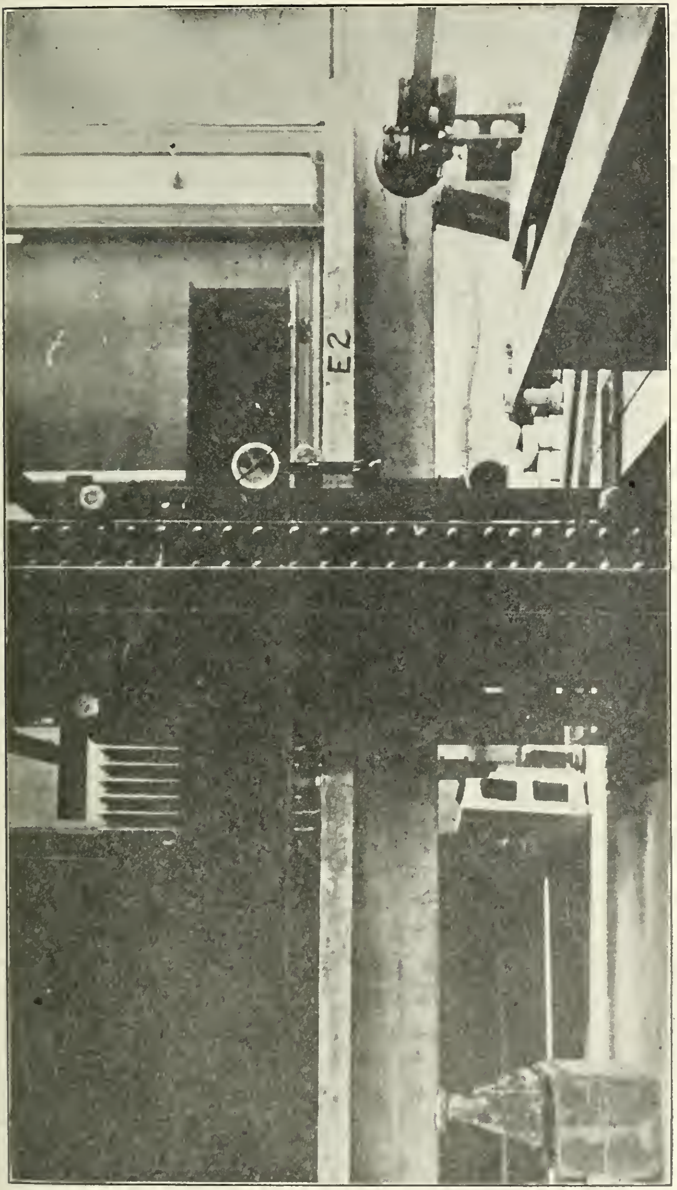

Plate II.—Tee-beam E2 Ready to be Tested.

The following well known formulae based upon a parabolic variation of stress were used:

$$f_c = \frac{M}{\frac{2}{3}kbd^2(1 - \frac{3}{8}k)} \qquad (1$$

$$f_s = \frac{M}{Ad(1 - \frac{3}{8}k)} \qquad (2$$

$$k = [3pn + \tfrac{9}{4}(pn)^2]^{\frac{1}{2}} - \tfrac{3}{2}pn \qquad (3$$

$$f'_s = \frac{f_s A - f'_s A'}{\frac{2}{3}kbd} \qquad (4$$

$$f'_s = \varepsilon E_s \qquad (5$$

$$v = \frac{V}{bd} \qquad (6$$

In computing the stresses in tee-beams of Series F where the neutral axis was below the bottom of the flange, a new formula was used based upon a parabolic stress deformation curve. This formula was derived for the sole purpose of computing stresses in the beams under discussion from experimental data and is not adapted to problems in design.

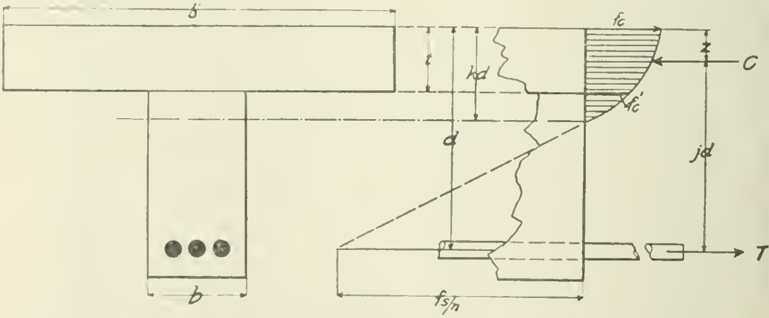

FIG. 5. DIAGRAM SHOWING STRESS DISTRIBUTION IN TEE-BEAMS.

As the neutral axis of the tee-beams discussed was never below the middle of the beam and the flange thickness was about one-fourth the depth of the beam, the error made by assuming the compressive stress lost, due to the decreased breadth below the flange, to be equal approximately to a triangular wedge of stress whose volume $= \frac{1}{2} f_c' \ (kd - t) \ (b' - b)$ will have but small effect upon the resulting formula.

$$C = \tfrac{2}{3} k\, b'\, d\, f_c - \tfrac{1}{2} (kd - t)(b' - b) f'_c$$

$$f'_c = (1 - \tfrac{1}{2} q)\, 2qf_c$$

$$kd - t = qkd$$

hence

$$C = \tfrac{2}{3} k\, b'\, d\, f_c - \tfrac{1}{2} (1 - \tfrac{1}{2} q)\, 2q^2 (b' - b)\, kdf_c$$

Taking moments of the compressive stresses about the top line of the section (Figure 5) there is found:

$$\Sigma M_a = zC = \tfrac{2}{3} kb'df_c \tfrac{3}{8} kd - \tfrac{1}{2} (1 - \tfrac{1}{2}q)\, 2q^2 (b' - b)\, kdf_c\, (kd - \tfrac{2}{3} qkd)$$

$$Z = \frac{\Sigma M_a}{C} = \frac{kd\, [\tfrac{1}{4} b' - (1 - \tfrac{7}{6} q + \tfrac{1}{3} q^2)\, q^2 (b' - b)]}{\tfrac{2}{3} b' - (1 - \tfrac{1}{2} q)\, q^2 (b' - b)}$$

$$jd = d - z; \qquad C = \Sigma f_c; \qquad M = jdC$$

Therefore

$$f_c = \frac{M}{jd\, [\tfrac{2}{3} kb'd - \tfrac{1}{2} (1 - \tfrac{1}{2} q)\, 2q^2 (b' - b)\, kd]} \tag{7}$$

$$f_s = \frac{M}{A\, j\, d} \tag{8}$$

Values of k were found experimentally.

For finding jd in order to compute v at the first diagonal crack, a formula similar to the above based upon a straight line variation of stress was employed.

$$C = \tfrac{1}{2} kdb'f_c - \tfrac{1}{2} (kd - t)(b' - b) f'_c$$

$$f'_c = qf_c$$

hence

$$C = \tfrac{1}{2} kdf_c\, [b' - q^2 (b' - b)]$$

$$z = \frac{\Sigma M_a}{C} = \frac{kd\, [\tfrac{1}{3} b' - q^2 (1 - \tfrac{2}{3} q)(b' - b)]}{b' - q^2 (b' - b)}$$

$$jd = d - z$$

The maximum unit shear was found by the formula

$$v' = \frac{V}{jdb} \tag{9}$$

In tee-beams $b =$ breadth of the web.

An attempt has been made to compute the stress in the stirrups. If no bars are turned up and the resistance to bending of the longitudinal bars be neglected, the stirrups will carry he full vertical component of the diagonal tensile stress when he concrete has cracked providing the distribution of stress is

unchanged. This component is equal in intensity to the maximum unit horizontal shear. Therefore with a constant shear from support to load each stirrup must carry a stress equal to the maximum unit horizontal shear multiplied by the area of the neutral surface between adjoining stirrups; this area's breadth is b and length s.
Therefore

$$g = \frac{v' \, sb}{u \, a} \tag{10}$$

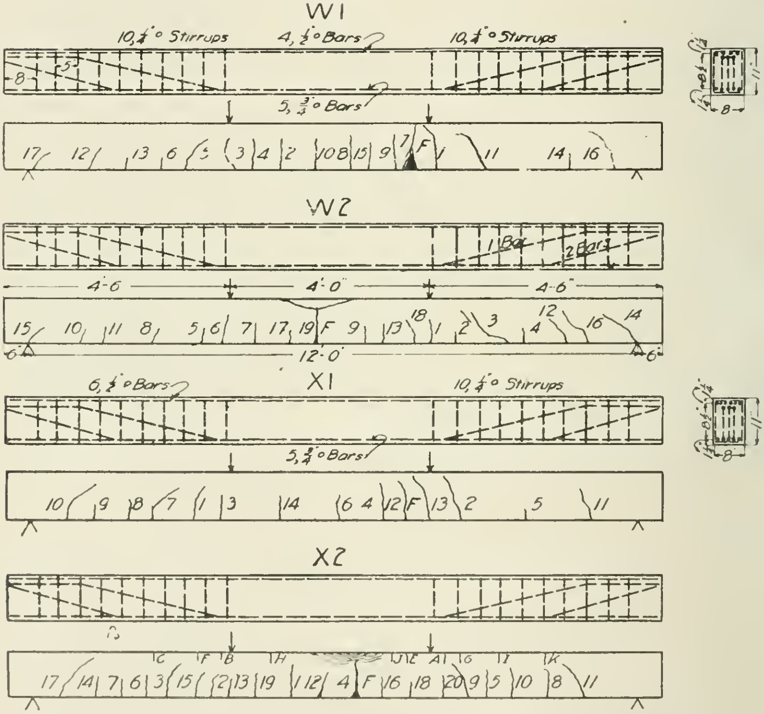

FIG. 6.—BEAMS OF SERIES E—REINFORCEMENT AND CRACKS.

1. BEAMS OF SERIES E

In order to secure more data concerning the effect of reinforcement in the compression side of a beam, four rectangular beams were reinforced and dimensioned as shown in Figure 6.

These beams were made like beams T_1, T_2, V_1 and V_2 of Series B in the bulletin of the series of 1906, with the exception that they had additional web reinforcement in the form of stirrups to prevent diagonal tension failures. In order to obtain a comparison of all the tests of this kind, Tables XII and XIII of the bulletin of the series of 1906 have been incorporated in Tables VI and VII of this bulletin.

TABLE VI.

SERIES B AND E: RECTANGULAR BEAMS.

Stresses in Steel and Concrete. 2.9 per cent Reinforcement in Tension.

No. Beam.	No. ½″ Bars in Top.	Kind of Failure.	Load considered lbs.	k = Proportionate Depth.	Stress in Steel. lbs./in.² From Resisting Moment.	From Deformation.	In Compression by Deformation.	Stress in Concrete in Beam lbs./in.² (B)	Stress in Compression Specimens. lbs./in.² (S)	Ratio $\frac{B}{S}$
P_1		C	22,160	.670	35,200	36,000		2,260	1,290	1.75
P_2		C & D T	20,160	.675	31,600	33,000		2,050	1,275	1.61
R_1	2	DT	26,160	.590	39,000	39,000	40,000	2,370	1,715	1.43
R_2	2	DT	26,160	.600	39,100	39,000	45,000	2,260	1,580	1.46
T_1	4	DT	22,160	.570	32,800	33,000	33,000	1,610	1,715	0.94
T_2	4	DT	24,160	.565	35,700	33,800	36,000	1,760	1,385	1.27
V_1	6	DT	25,160	.510	36,100	36,000	28,500	1,780	2,240	0.79
V_2	6	DT	29,160	.555	42,500	42,000	39,000	1,670	1,770	0.94
W 1	4	T	34,000	.503	46,100	43,500	34,000	2,880	2,600	1.11
W 2	4	T	34,000	.503	46,100	45,000	33,900	2,880	2,600	1.11
X 1	6	T	33,000	.511	45,000	48,000	39,000	2,000	1,500	1.33
X 2	6	T	34,000	.550	47,100	46,500	42,000	1,830	1,530	1.20

C = Compression. DT = Diagonal Tension. T = Tension.
Age of specimens 28 days.

As shown in Figure 6 these beams failed in tension followed rapidly by crushing at the top directly above the failure crack. The stirrups effectually prevented any diagonal tension failures.

The results given in the tables and the moment-deformation curves in Figure 7 show that lower steel was stressed beyond the elastic limit in the beams of Series E. The deflection curves show a more sudden failure in beams P_1 and P_2 than in those of Series E. The latter beams held the maximum load for some time before failure. It is of interest to note that the deflection curves for beams W 1. W 2, X 1 and X 2 are practically straight lines up to the maximum load. In beams W 1 and W 2 the concrete was much stronger than in beams X 1 and X 2 which accounts for the increased stress in the heavier compression reinforcement of the latter beams.

TABLE VII.

SERIES B AND E: RECTANGULAR BEAMS.

Values of v and $\frac{M}{bd^2}$. Breadth 7¾". Effective Depth 9¾".

Beam.	Total Load Applied lbs.	Kind of Failure.	Max. Moment in. lbs.	$\frac{M}{bd^2}$.	v lbs./in².	Stress on Cube and Cyl. lbs./in².
P_1	24,780	C	585,600	794	164	1,290
P_2	21,3[illegible]0	C & DT	504,500	683	141	1,275
R_1	28,740	DT	680,500	922	190	1,715
R_2	27,840	”	660,500	895	184	1,580
T_1	24,180	”	571,000	774	160	1,715
T_2	31,260	”	741,000	1,003	207	1,385
V_1	27,580	”	652,000	884	182	2,240
V_2	31,380	”	744,500	1,008	207	1,770
W 1	34,000	T	805,900	1,060	218	2,600
W 2	34,800	”	824,900	1,085	223	2,600
X 1	33,500	”	793,900	1,043	218	1,500
X 2	34,800	”	824,900	1,085	223	1,530

C = Compression. DT = Diagonal tension.
T = Tension. Age of specimens, 28 days.

Series B and E show conclusively that it is possible to greatly increase the strength of reinforced beams by placing reinforcement in the compression side and properly reinforcing against diagonal tension stresses. The average value of $\frac{M}{bd^2}$ for beams P_1 and P_2 is 739, and the same quantity for beams W 1, W 2. X 1 and X 2 is 1,068, or an increase of 44 per cent. Furthermore a steel reinforcement in the compression side provides an additional factor of safety against failure through poor concrete. This series of tests also shows the necessity of using stirrups in heavily reinforced beams, even where the ratio of span to depth is large, in order to provide against sudden failure due to excessive tensile web stresses.

An interesting experiment was performed on beam X 2. It was loaded up to 16,000 pounds and the load released. This was repeated four times. The stress developed in the lower steel was about 21,000 pounds per square inch and that in the upper about 17,000 pounds per square inch. The value of k for the first load was .524. After the first loading, there was a permanent deflection of .05 of an inch. This permanent deflection did not increase under the repetition of loads until the fifth load of 16,000 pounds was applied and released, when it became .055 of an inch. Cracks Nos. 1-8, Figure 6, appeared at the first loading, causing the first permanent deflection, and Nos. 9–18 causing the increase in permanent deflection, appeared at the fourth repetition. Cracks 1, 2 and 11 extended up to the middle of the beam at the last 16,000 pound load. The beam was then turned over so that the $\frac{1}{2}$-inch rods were in the tension side, and loads up to 9,000 pounds were applied and released. This load caused cracks A to L to appear and developed a permanent deflection after removal of load of .06 of an inch. The stress caused by this load in the $\frac{1}{2}$-inch rods, the lower reinforcement in this case, was about 20,000 pounds per square inch tension and in the upper $\frac{3}{4}$-inch rods, about 8,000 pounds per square inch compression. The value of k for this load was .366. The beam was then turned over and loads applied until failure occurred at 34,800 pounds. It will be noted that the ultimate strength of this beam could not have been greatly reduced by the repeated loadings as it withstood a somewhat higher load than its mate, X 1. In Figure 7, the permanent deformations and deflections for a set of loadings are shown by the position of the second set of points at the initial moment.

2. BEAMS OF SERIES F

This series consisted of fourteen beams dimensioned and reinforced as shown in Figures 8, 9 and 10. These beams were reinforced heavily, about one per cent. figured on the area of the

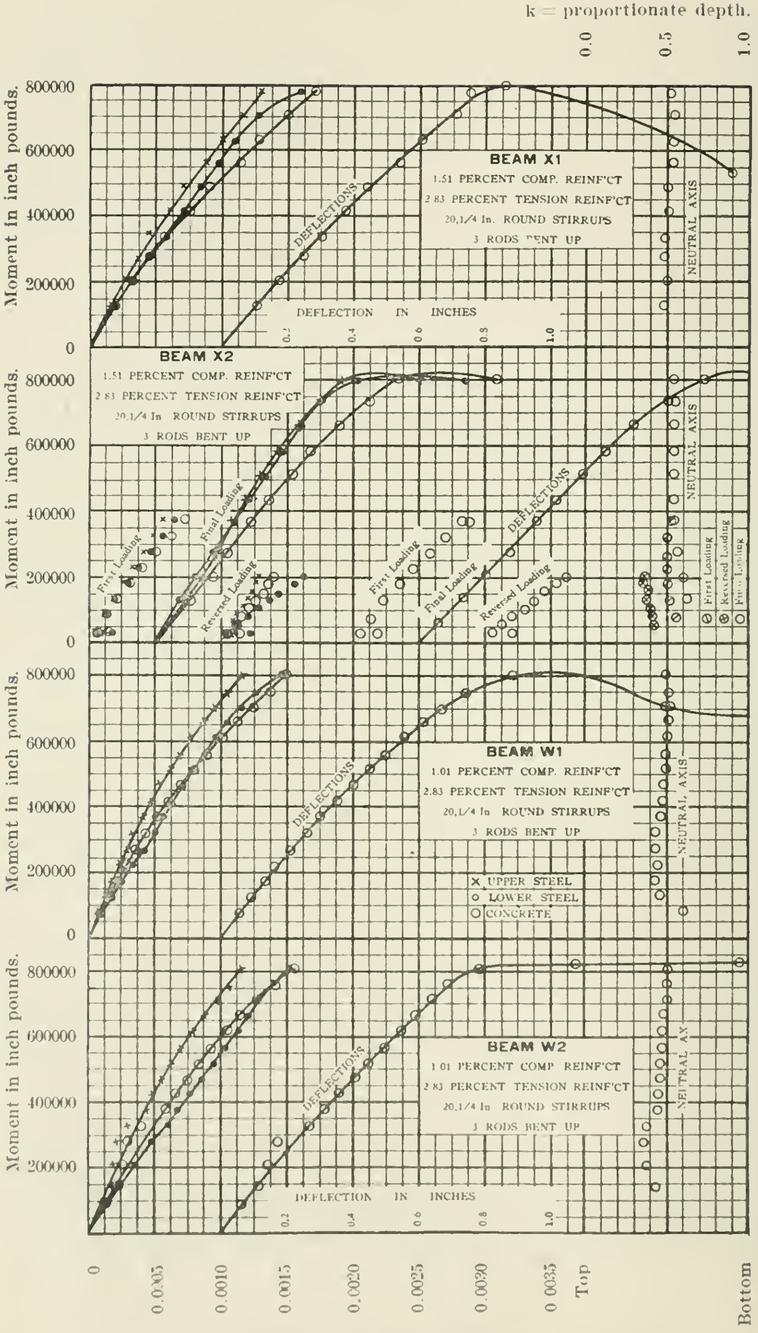

FIG. 7.—BEAMS OF SERIES E—MOMENT-DEFORMATION CURVES, ETC.

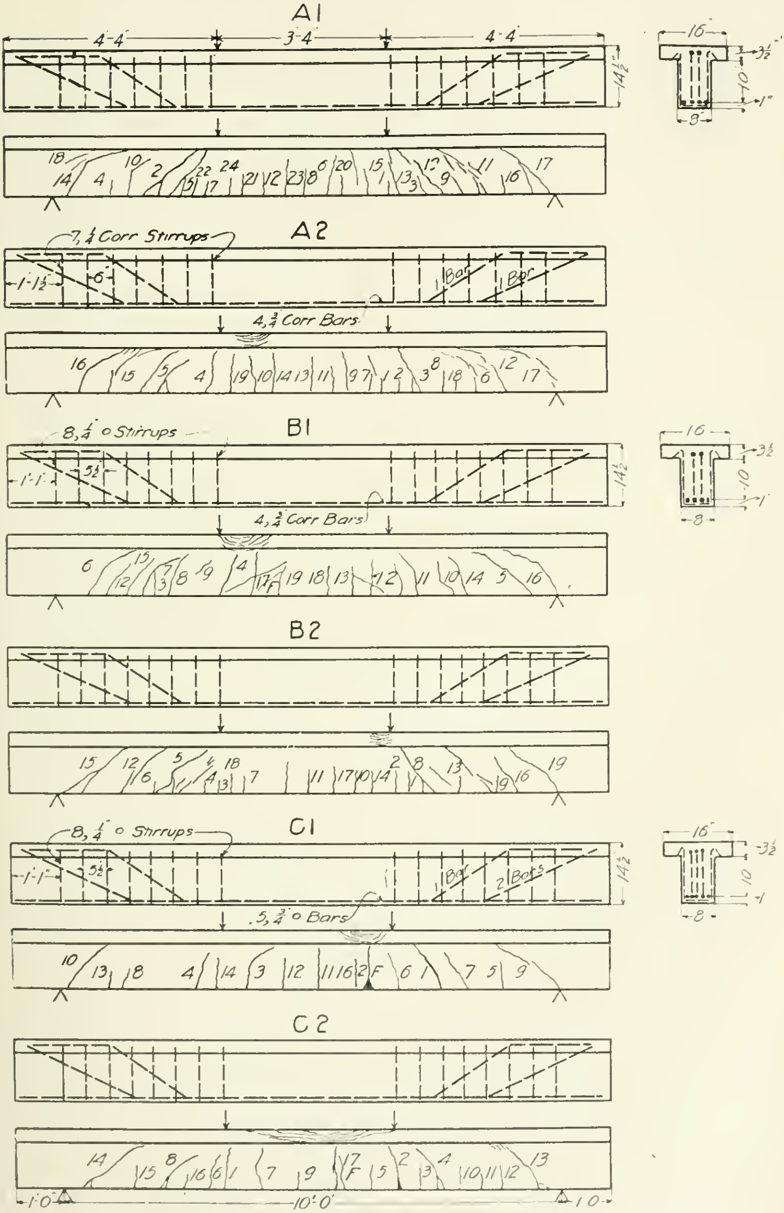

FIG. 8.—BEAMS OF SERIES F—REINFORCEMENT AND CRACKS.

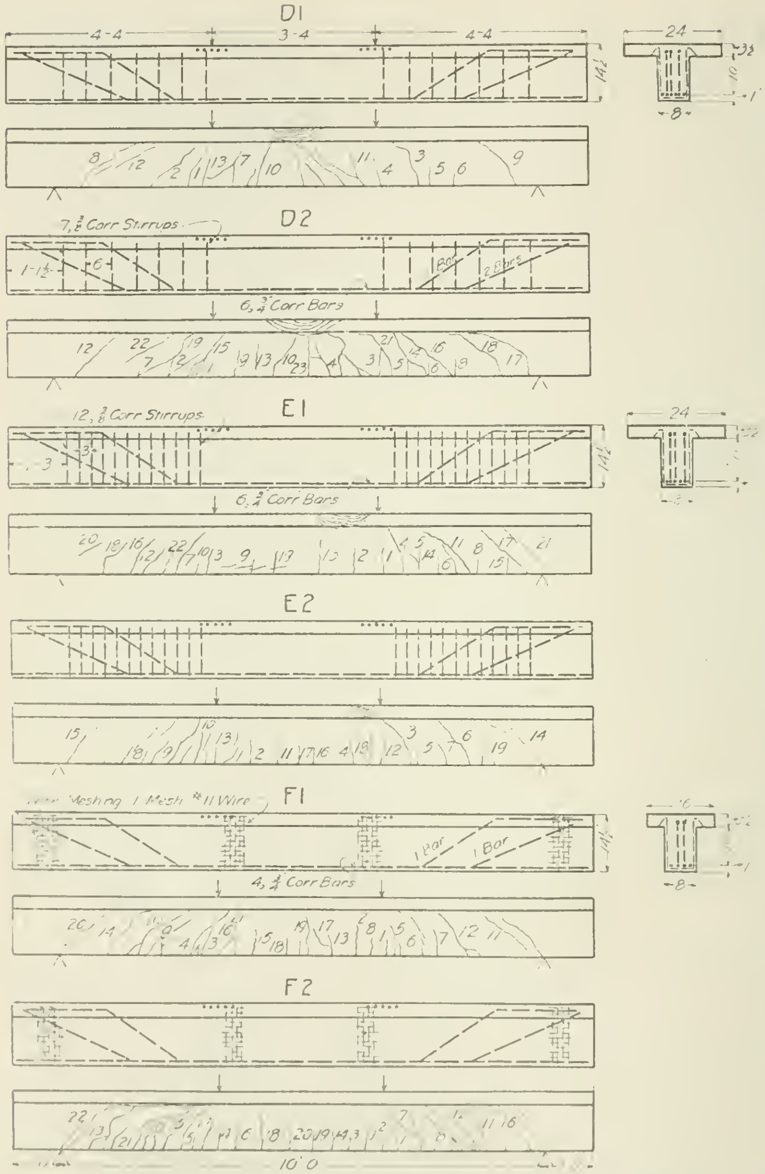

FIG. 9.—BEAMS OF SERIES F—REINFORCEMENT AND CRACKS.

enclosed rectangle b′ d, in order that high compressive stresses might be developed in the flange. This, together with the small ratio of span to depth, also caused large tensile stresses in the web. Stirrups, inclined rods and meshing were employed as web reinforcement. Figure 3 under 2 shows the kind of stirrups used in this series. The method of loading is shown in Plate II. The 16-inch flange beams weighed about 1,850 pounds and those with 24-inch flanges about 2,200 pounds each. Duplicate beams were made, the results of which show close agreement in all cases.

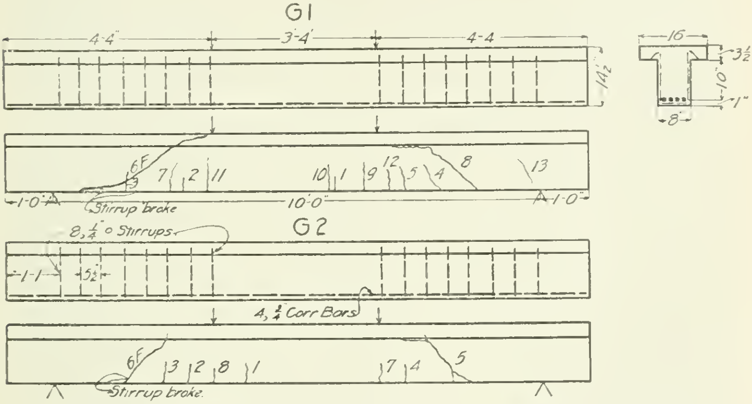

Fig. 10.—Beams of Series F—Reinforcement and Cracks.

Tables VIII and IX contain the computed data for this series of tests. Figures 11 to 17 give moment-deformation and deflection curves for this series. All beams of Series F, except beams G 1 and G 2, failed in tension followed by compression in the flange. In general, tension cracks were first visible in the middle and on the bottom of the span of the beam at a stress of 12,000 to 15,000 pounds per square inch in the steel. As soon as the diagonal tension became too great for the concrete in the web to transmit to the compression side, diagonal tension cracks would appear. These cracks sometimes started from tension cracks near stirrups, while at other times they opened up in the middle of the web between the stirrups. In nearly all cases they crept up to the flange and then horizontally along

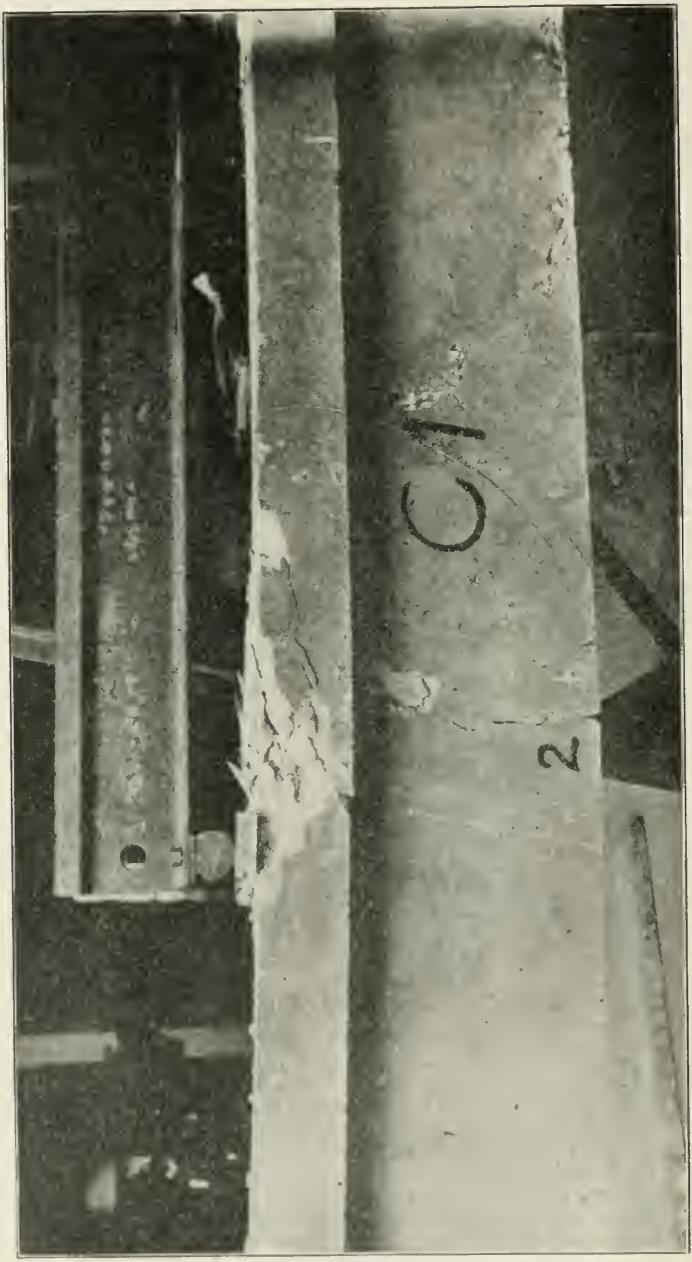

PLATE III.—FAILURE CRACKS IN TEE-BEAM C1.

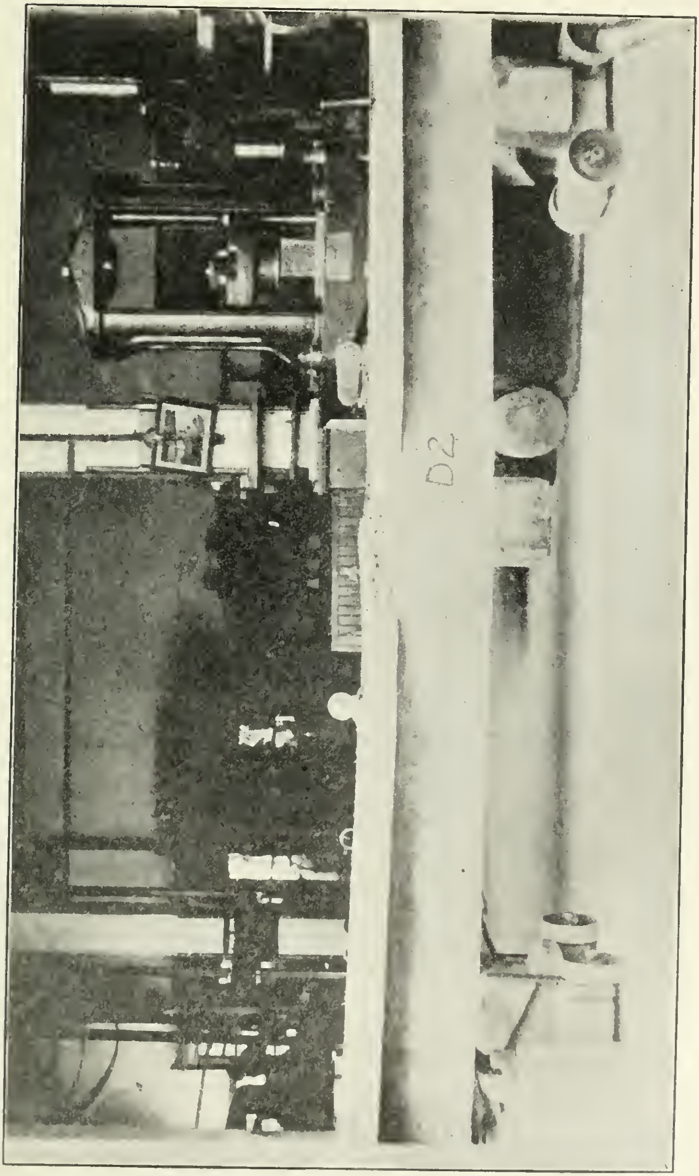

PLATE IV.—FAILURE CRACK IN TEE-BEAM D2.

the junction of flange and web. In the beams which had both stirrups and inclined rods for web reinforcement, these cracks did not produce failure. In these beams failure came through the weakening of the tension side of the beam when the steel passed the yield point; one of the previously observed tension cracks would widen considerably, owing to the increased stretch in the steel, and this caused a large amount of compressive stress to be thrown upon a small area in the flange which would finally crush. This general type of failure is well illustrated in Plate III, beam C 1, and Plate IV, beam D 2. In nearly all cases, upon removing the concrete from around the rods at the point of failure, the metal was found to have scaled, showing conclusively that it had passed the yield point. This was especially noticeable in beams A 1, A 2, C 1, C 2, D 1 and D 2.

Beams G 1 and G 2 failed through diagonal tension owing to insufficient web reinforcement. In both beams the ¼-inch stirrups were broken near the failure crack, indicating that the increased stress brought upon them by the failure of the concrete loaded them beyond their capacity. These two beams failed suddenly, accompanied by a sharp snap, due to the breaking of the stirrups. In Plates VI and VII just below the arrow tips are seen the broken stirrups.

In beams A 1 and A 2, corrugated bars and stirrups were employed to insure against a failure due to slipping of the stirrups. Beams B 1 and B 2 were similarly reinforced horizontally but had ¼-inch mild steel round rods for stirrups.

The tests of these four beams show there was no advantage gained in using the deformed bars as stirrups. In this series there was no evidence of slipping of the smooth rods either in the stirrups or horizontal reinforcement. Beam B 2 fell while being moved and was cracked in the middle, across the top and down through the flange. This injury did not materially affect its strength but accounts for the sag in the deflection curve and moment-deformation curve for concrete and the lower position of the neutral axis shown in Figure 12.

Beams C 1 and C 2 had smooth round mild steel rods for both web and main reinforcement. These two beams were not as strong as those whose main reinforcement consisted of corrugated bars owing to the lower yield point of the round rods.

The failure of both of these beams was slow as is shown by their deflection curve in Figure 13.

The beams reinforced with expanded metal, beams F 1 and F 2, showed a large number of cracks uniformly distributed along the beam. Beam F 1 stood the highest load of any of the 16 inch flange beams. Plate VIII and Figure 9 shows the cracks which appeared in this beam at the maximum load.

TABLE VIII.

SERIES F: TEE BEAMS A —1G 2.

Stresses in Steel and Position of the Neutral Axis. 1 per cent Reinforcement.

Tee Beam.	Load Considered. lbs	Moment at Load Considered. in. lbs.	Position of Neutral Axis. k.	Stress in Steel		Stress in Concrete		$\frac{B}{C}$
				by Moment lbs./in.^{2}	by Deformation. lbs./in.^{2}	by Moment lbs./in.^{2} B.	on Cylinder. lbs./in.^{2} C.	
A 1	64,000	1,265,000	.435	49,100	54,500	1,940	2,460	.79
A 2	64,000	1,265,000	.417	48,800	58.000	1,990	1,640	1 21
B 1	62,000	1,225,000	.449	47,600	48,000	1,840	1,970	.93
B 2	62,000	1,225,000	570	49,800	54,000	1,610	1,930	.83
C 1	58,000	1,145,000	.398	44,500	46,500	1,850	1,950	.95
C 2	54,000	1,065,000	481	42,600	42,000	1,550	1,650	.94
D 1	88,000	1,742,000	.489	45,500	47,500	1,740	1,650	1.05
D 2	96,000	1,902,000	.424	48,500	54,000	2,030	....	......
E 1	88,000	1,743,000	.478	45,200	50,500	1,750	1,930	.91
E 2	82.000	1,625,000	.516	42,600	46,000	1,570	1,730	.91
F 1	66,000	1,305,000	.448	50,800	57,500	1,970	1,770	1.11
F 2	64,000	1,265,000	.415	48,700	57,000	1,990	2,290	.87
*G 1	44,000	865,000	.394	33,100	32,200	1,400	. ....	......
*G 2	44,000	865,000	.421	33,400	27,900	1,360	2,290	.59

*Failed in diagonal tension: all others failed in tension.
Age of specimens 28 days.

Of the 24-inch flange beams, beam D 2 showed the greatest strength and held the maximum load from a deflection of .5 of an inch to 1.15 inches. Figure 9 shows that the web of this beam was covered with a large number of diagonal cracks caused by the high tensile web stress. Plate IV shows the beam after it was tested.

Beams E 1 and E 2 did not show as high strength as beam D 1 and D 2. As the kind of failure in all cases was practically the same and the deformation curves indicate that the yield point of the metal was reached, it seems evident that the steel in the former beams had a lower yield point than that in the latter.

Table VIII gives the position of the neutral axis and the stresses in the steel and concrete. The average position of the neutral axis for the 16-inch flange beams is about .43d. and for the 24-inch flange beams it is approximately .48d from the top of the beam. The value of k computed, on the basis of an enclosed rectangle, by formula (3) with $n = 10$ is .425.

The stresses in the concrete and steel were computed by formulae (7) and (8). The formulae for rectangular beams, formulae (1) and (2), if used in computing these stresses, would give results averaging two per cent. larger than those given by the formulae used for the stresses in the steel and about twenty per cent. smaller for those in the concrete for the narrower flanged beams and still larger discrepancies if applied to the wider flanged beams. The stresses in the steel obtained from deformations check quite closely those computed from resisting moment. The stresses in the concrete in general are somewhat lower than the ultimate compressive strength of the corresponding compression specimens. However, from the rapidity with which compression in the flange followed the tensile failures in the steel and from the large deformations in the concrete, it is quite evident that the compressive strength of the concrete was developed in these beams.

Table IX contains the values of tensile strength of the auxiliary specimens and v′ at the first diagonal crack, also values of v′ and $\frac{M}{b' d^2}$ at the maximum load. The quantity v′ was obtained by using formula (9) as previously explained. Considerable care was taken to note the load at the first appearance of a diagonal crack. The maximum unit shear v′ computed from these loads averages 179 pounds per square inch (excluding D 2) and the mean value of the tensile strength of the 6-inch cylinders is 187 pounds per square inch. There is, however, considerable difference between the strength of the specimen and v′ at the first crack in individual cases.

TABLE IX.

SERIES F: TEE BEAMS A 1--G 2.

Reinforcement—shearing stresses — $\frac{M}{b' d^2}$.

Tee Beam.	Reinforcement.	At First Diagonal Crack.		Ultimate tensile strength of cyl. lbs./in.².	At Maximum Load.			
		Load. lbs.	v′ Maximum shear. lbs./in.².		Maximum load. lbs.	v′ Average shear. lbs./in.².	v′ Maximum shear. lbs./in.².	$\frac{M}{b' d^2}$
A 1	4, $\frac{3}{4}$-in. cor. bars (2 bent).	24,000	128	256	66,600	308	361	452
A 2	14, $\frac{1}{4}$-in. cor. stirrups.	32,000	171	167	66,200	306	357	450
B 1	4, $\frac{3}{4}$-in. cor. bars (2 bent).	42,000	226	260	65,600	304	357	444
B 2	16, $\frac{1}{4}$-in. round stirrups.	26,000	150	157	62,400	289	354	425
C 1	5, $\frac{3}{4}$-in. round rods (3 bent).	34,000	181	197	60,000	278	322	407
C 2	16, $\frac{1}{4}$-in. round stirrups.	34,000	185	216	57,400	265	316	390
D 1	6, $\frac{3}{4}$-in. cor. bars (3 bent).	46,000	247	182	96,200	445	526	437
D 2	14, $\frac{3}{8}$-in. cor. stirrups.	58,000	306	......	101400	470	544	460
E 1	6, $\frac{3}{4}$-in. cor. bars (3 bent).	46,000	244	148	92,800	429	505	420
E 2	24, $\frac{3}{8}$-in. cor. stirrups.	40,000	215	184	88,000	407	485	400
F 1	4, $\frac{3}{4}$-in. cor. bars (2 bent).	30,000	158	142	67,600	313	368	459
F 2	1-in. wire mesh. No. 11 wire.	28,000	150	174	65,400	302	352	445
*G 1	4, $\frac{3}{4}$-in. cor. bars (straight).	24,000	126	184	48,000	222	259	323
*G 2	16, $\frac{1}{4}$-in. round stirrups.	28,000	149	164	48,200	223	260	324

*Failed in diagonal tension; all others failed in tension.
Age of specimens 28 days.

Beam D 2 developed the highest unit shearing stress of 544 pounds per square inch and also the highest value of $\frac{M}{b'd^2}$. (460). The high horizontal shearing stresses developed in these heavily reinforced beams of large depth in proportion to span length indicate that such stresses will not cause failure in the ordinary tee-beam if it is properly designed to resist diagonal tension stresses. In none of the beams tested did the flanges fail or separate from the web due to shearing stresses primarily. It is necessary, however, to guard against this form of failure by allowing the stirrups to extend well up into the flange of the beam.

3. BEAMS OF SERIES N

The beams of this series were made and tested as thesis work as previously stated in the introduction. The beams may be divided into two classes; those in which the web reinforcement was rigidly attached to the main bars, and those in which it was loosely attached. In the first twelve beams of this series, Kahn bars were used as reinforcement. In six of the twelve beams the flanges of the bars were entirely sheared off and the prongs replaced by loose stirrups. In the other six, the prongs were bent up either at 45° or 90° with the axis of the main bar. The last seven beams of this series had a variety of reinforcements. The amount of main reinforcement used in the first twelve beams was .6 of one per cent. of the area of the enclosing rectangle, b′d; beam N 14 had one per cent. and the rest of the series had approximately .66 of one per cent. Excepting beam N 14, the amount of web reinforcement was the same for all beams.

Figures 18, 19, 20 and 21, show how this series was dimensioned and reinforced. Tables X and XI contain the results of computations for this series. As the neutral axis for all these beams was in the flange, formulae (1) and (2) were used in computing stresses in the steel and concrete for all beams upon which extensometer readings were taken. Formula (3) was used to calculate the value of k for the first six beams, n being taken equal to 10.

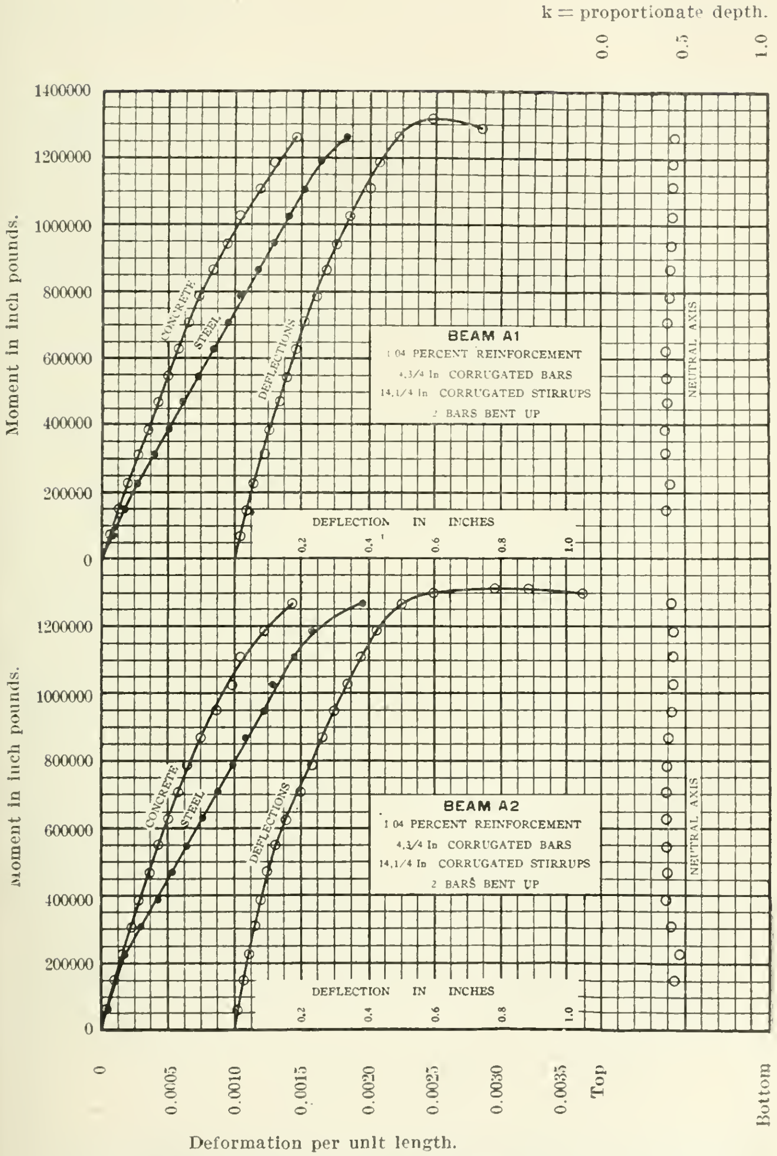

FIG. 11.—BEAMS OF SERIES F—MOMENT-DEFORMATION CURVES, ETC.

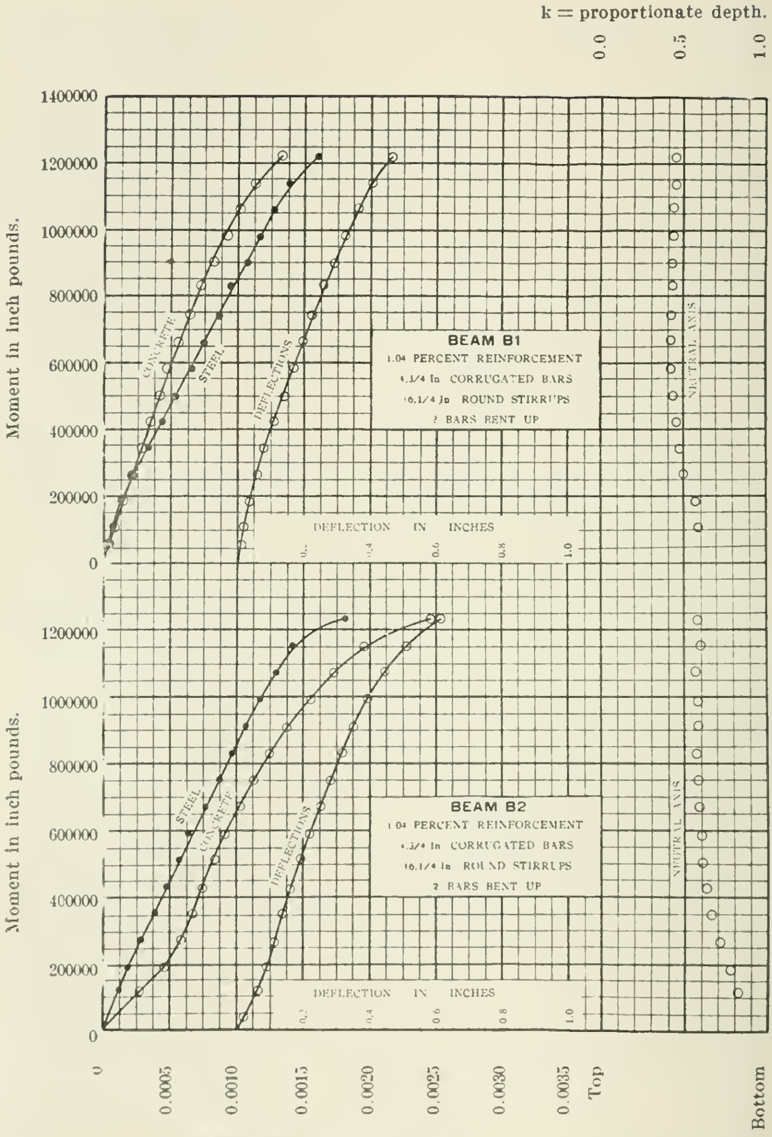

FIG. 12.—BEAMS OF SERIES F—MOMENT-DEFORMATION CURVES, ETC.

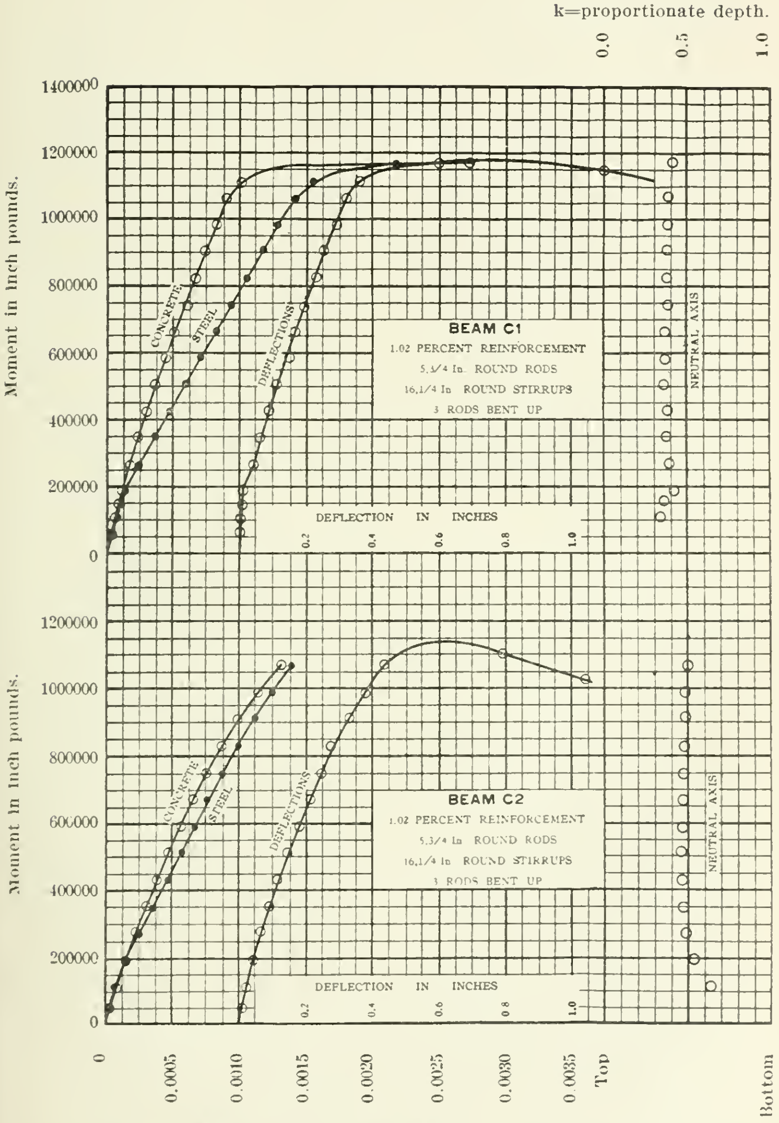

FIG. 13.—BEAMS OF SERIES F—MOMENT—DEFORMATION CURVES, ETC.

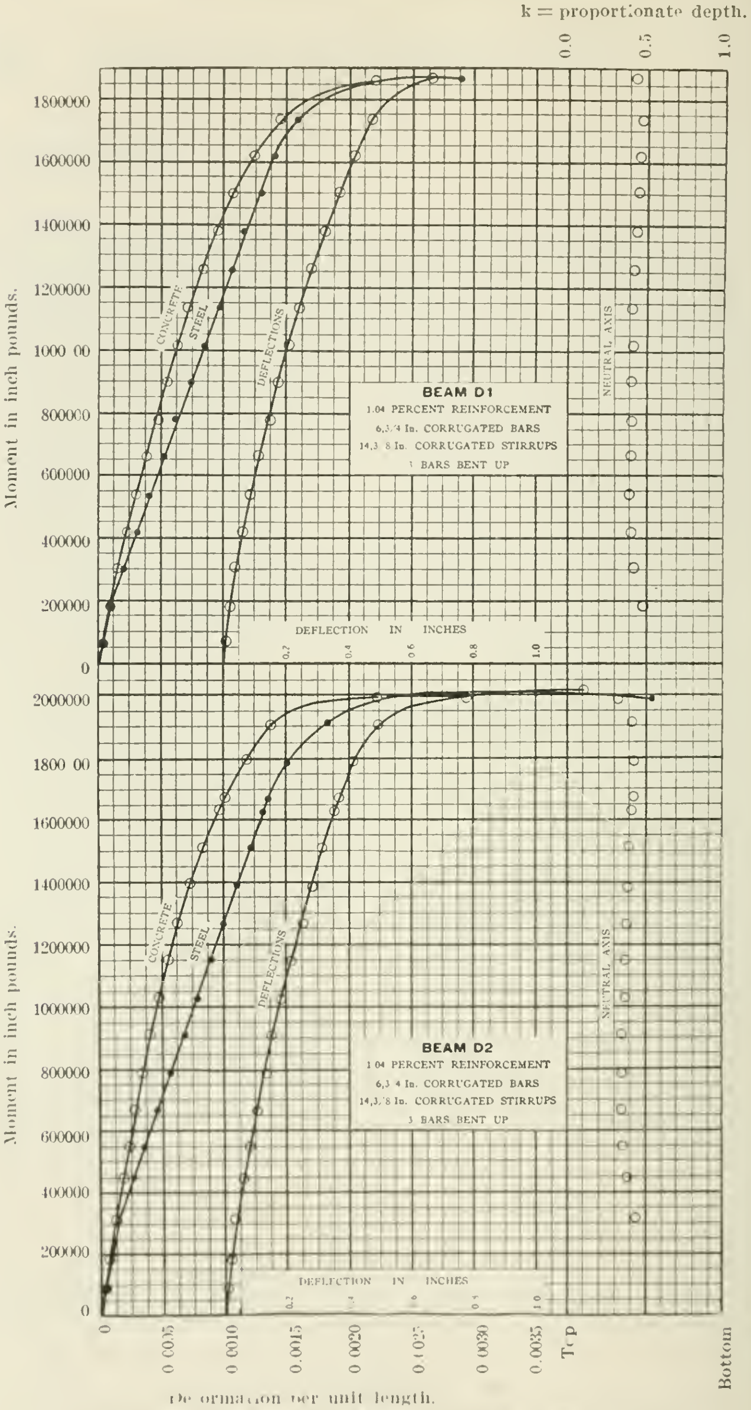

FIG. 14. BEAMS OF SERIES F—MOMENT-DEFORMATION CURVES, ETC.

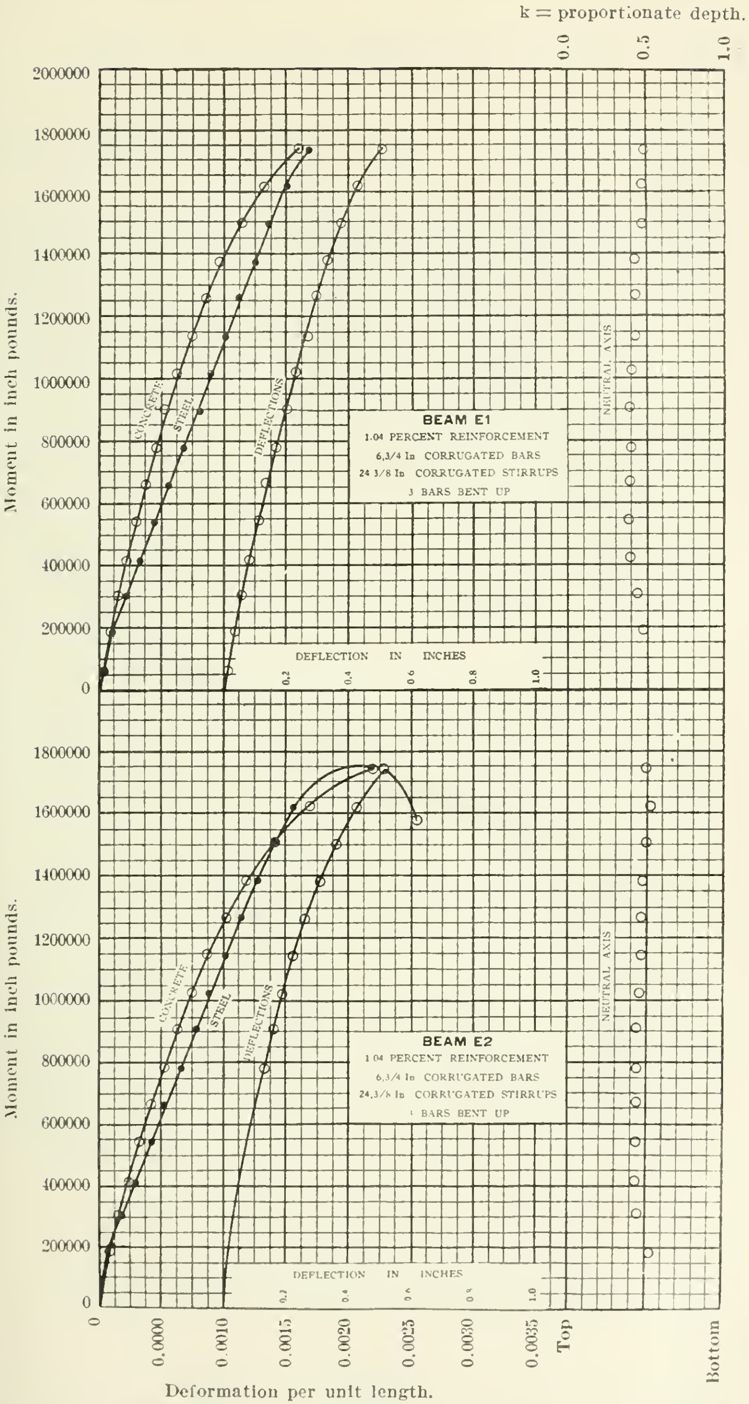

FIG. 15.—BEAMS OF SERIES F—MOMENT-DEFORMATION CURVES, ETC.

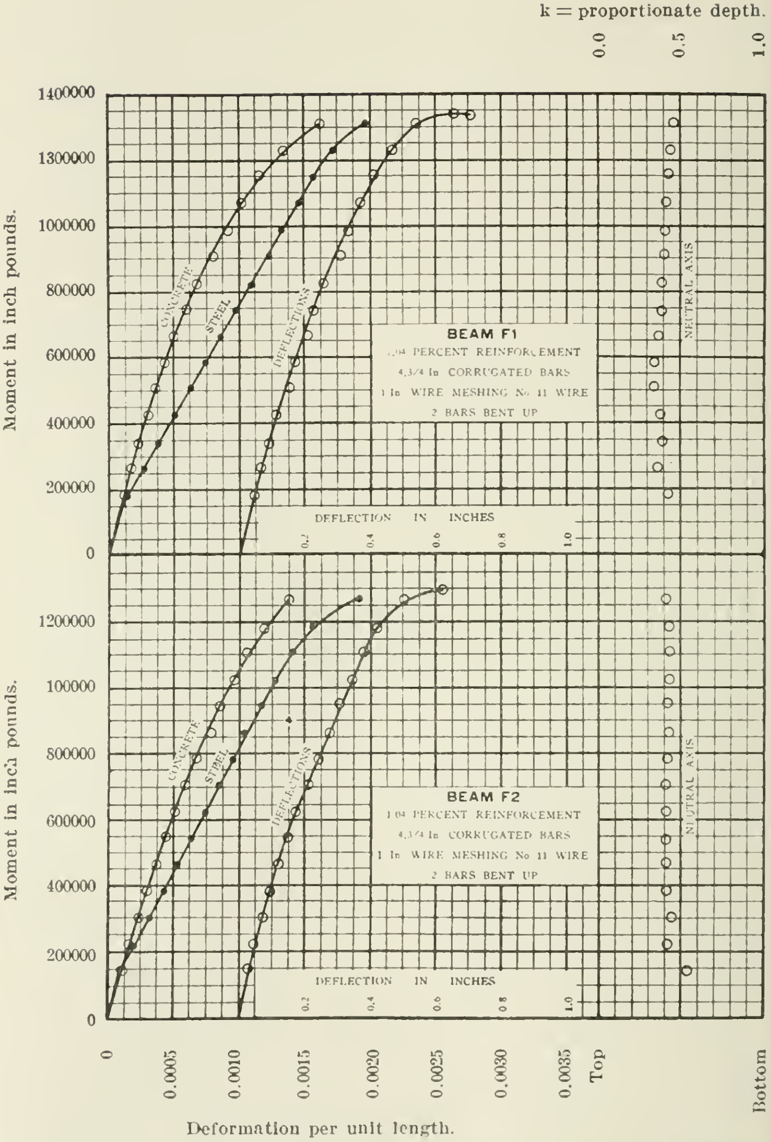

FIG. 16.—BEAMS OF SERIES F—MOMENT-DEFORMATION CURVES, ETC.

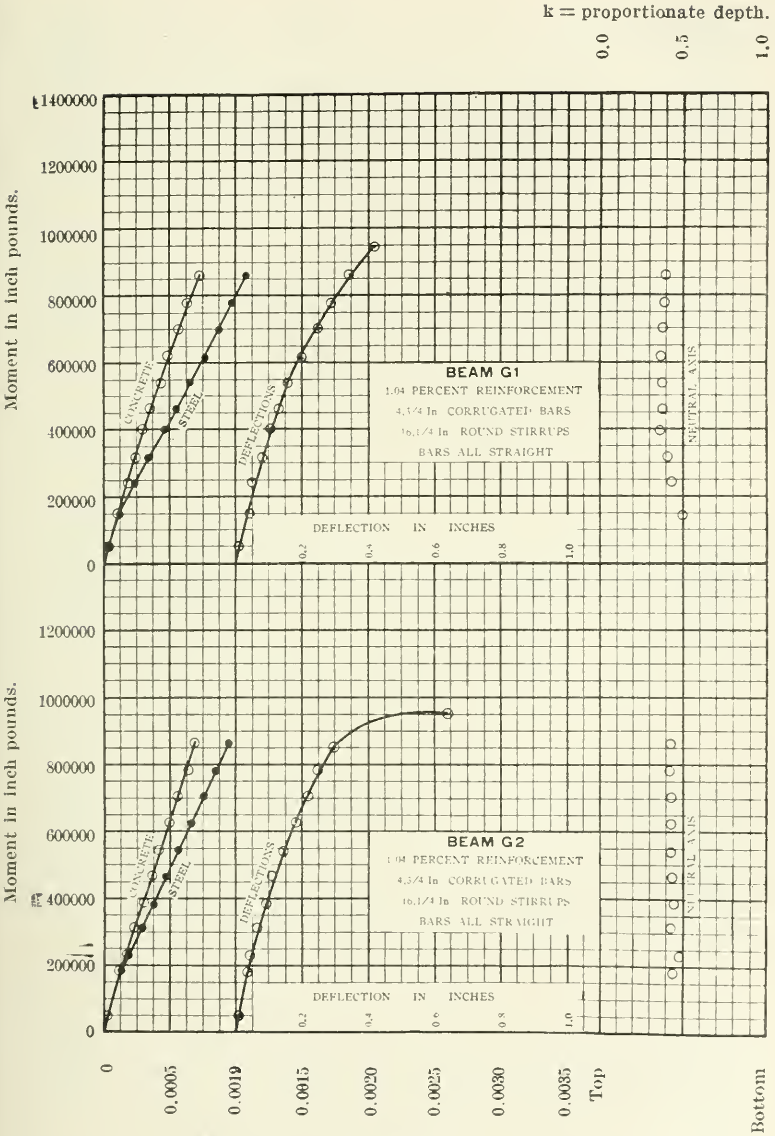

FIG. 17.—BEAMS OF SERIES F—MOMENT-DEFORMATION CURVES, ETC.

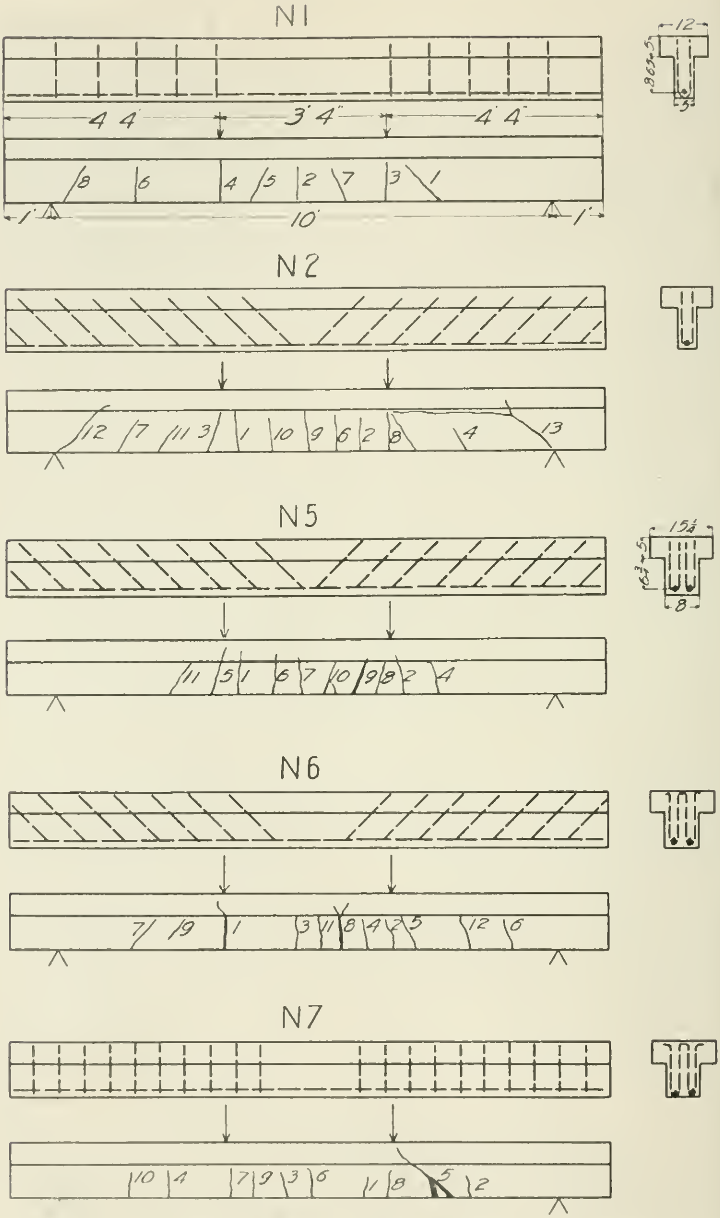

Fig. 18.—Beams of Series N—Reinforcement and Cracks.

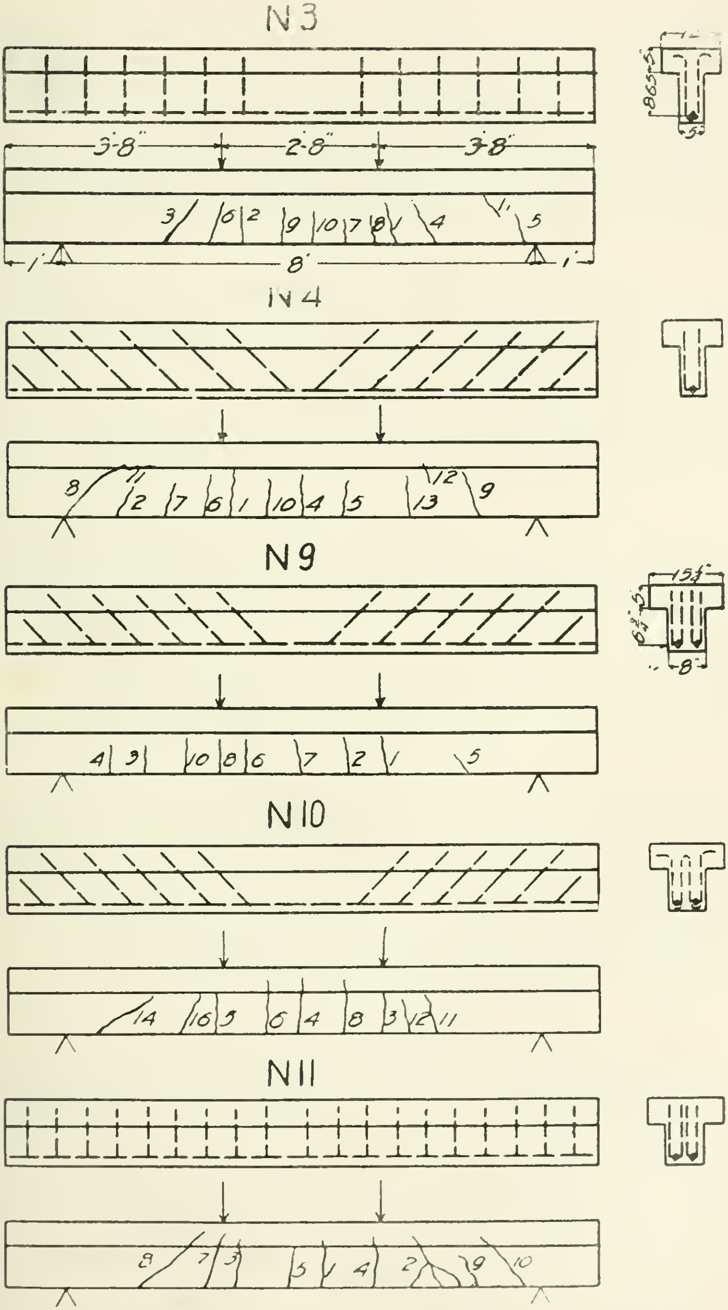

FIG. 19.—BEAMS OF SERIES N—REINFORCEMENT AND CRACKS.

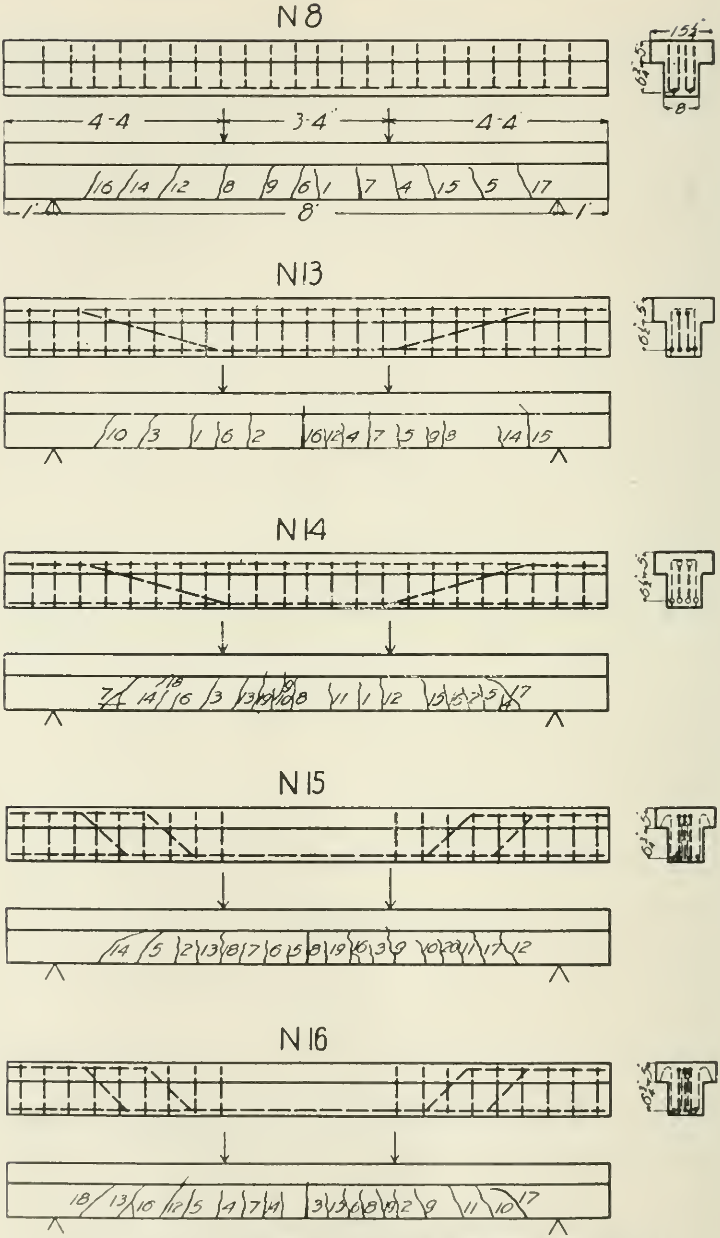

Fig. 20.—Beams of Series N—Reinforcement and Cracks.

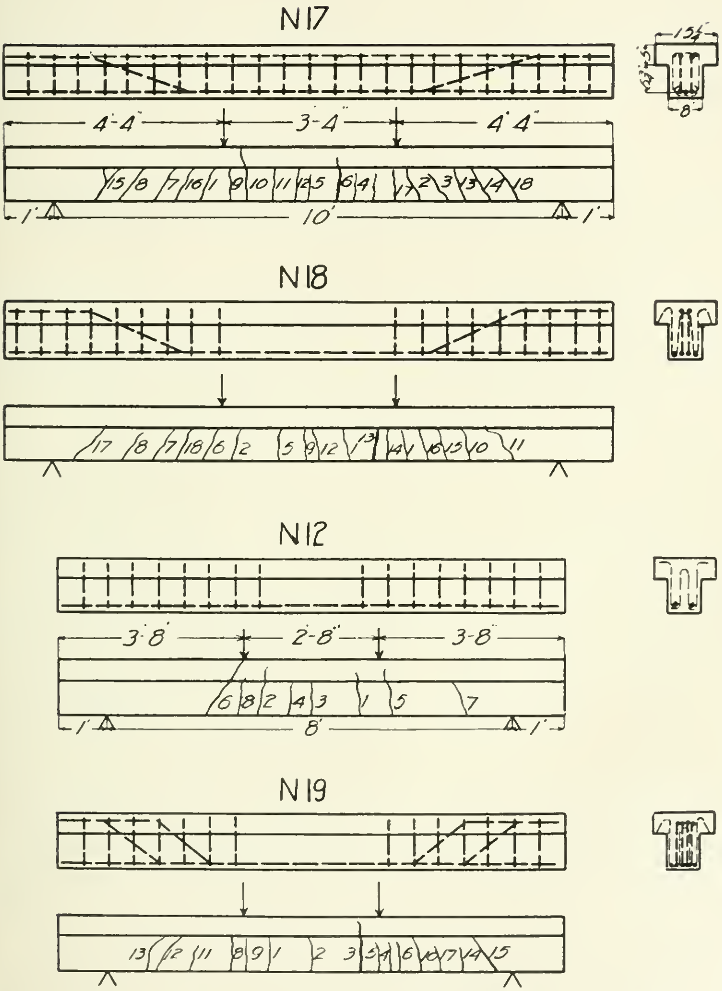

Fig. 21.—Beams of Series N—Reinforcement and Cracks.

In the beams with loosely attached web members and straight horizontal reinforcement, no rods bent up, the final failure occurred through slipping of the rods either before or just after the yield point of the metal was passed, when the load fell off rapidly. This did not occur in tests of the beams with rigidly attached web members. Beams N 1, N 3, N 6, N 7, N 10 and N 12 failed through slipping of the rods in the manner mentioned. Beams N 2, N 4, N 5, N 8, N 9 and N 11 failed in tension at the center. In these latter beams the steel was stressed considerably beyond the yield point, and failure was very slow as shown by the deflection curves.

In beams N 5 and N 9 the prongs of the Kahn bars were bent up at an angle of 45°, while in beams N 8 and N 11, they were bent up vertical. The former showed considerably greater strength than the latter beams. Beams reinforced with inclined loose stirrups showed a small increase in strength over those in which the stirrups were set vertically.

Beam N 13 was reinforced with four $\frac{5}{8}$-inch rods, the middle two being bent up as shown in Figure 20. Upon the other two rods were slipped twenty-three 1 x $\frac{1}{16}$-inch slitted band iron stirrups. These stirrups are shown in the end view of the beam. As can be seen, they were bent to form a rectangle open at the bottom. The slits were cut in the middle of the 1-inch sides near the ends and the iron pulled out so that the $\frac{5}{8}$-inch rods passed through parallel to the 1-inch sides. Beam N 14 was similarly reinforced with stirrups but had $\frac{3}{4}$-inch rods for main reinforcement and end plates to which these rods were attached to prevent any slipping. Beam N 17 was reinforced with two 1 x 1 x $\frac{1}{8}$-inch angles, one $\frac{1}{2}$-inch and two $\frac{5}{8}$-inch rods, the latter being bent up at the ends as shown in Figure 21. Twenty-three hoops of the band iron used in the above beam were spaced as shown and rigidly bolted to the angles at the lower corners of the hoops.

These three beams all failed slowly by tension at the center. In all three a large number of cracks were developed as shown in Figures 20 and 21. Beam N 13 failed in crack No. 16, which did not appear until the maximum load was almost reached. After beam N 14 had failed, the load was released, and it was again reloaded with the same maximum load but an increased deflection. This was followed by crushing of the concrete in the flange. The deflection curves for these beams indicate the slowness with which these beams failed.

Beams N 15, N 16, N 18 and N 19 were all reinforced with round rods, part of which were bent up, and loose W-stirrups set vertically. The manner in which these beams were reinforced is shown in Figures 20 and 21. These beams all failed by tension at the center. Beams N 15 and N 16 stood considerably higher loads than N 18, showing the advantage of distributing the metal in small rods. Beams N 15 and N 16 also show a

TABLE X.

SERIES N: TEE BEAMS N1–N19.
Stresses in Steel and Position of the Neutral Axis.

Tee Beam.	Load Considered. lbs.	Moment at Load Considered. in. lbs.	Position of Neutral Axis k.	Stress in Steel		Stress in Concrete		
				by Moment lbs./in.²	by Deformation. lbs/in.²	by Moment. lbs./in.² B.	on Cylinder. lbs./in.² C.	$\frac{B}{C}$
N 1	24,000	468,900	.345	39,400	....	1.050	1.540	.68
N 2	34,600	681.400	.345	57,400	....	1,530	1,310	1.17
N 3	26,000	407,900	.345	34,300	....	910	1,100	.83
N 4	37,400	591,000	.345	49,600	.... ..	1,320	1,450	.91
N 5	32,600	637,600	.344	62,100	....	1,510	2,140	.71
N 6	24,000	466,600	.344	45,500	.... ..	1,110	1,280	.87
N 7	22,000	426,600	.362	38,800	37,500	970	1,590	.61
N 8	24,200	470,000	405	43,700	42,000	970	1,640	.59
N 9	42,000	661,500	.360	60,200	36,000	1,500	1,390	1 08
N 10	26,000	405,000	.341	36,700	27,900	970	2,060	.42
N 11	34,000	535,000	.340	48,300	40,500	1,290	1,400	.97
N 12	32,000	505,000	.315	45,000	42,000	1,320	1,300	1 01
N 13	30,000	587,000	.313	47,100	46,500	1,540	2,030	.74
N 14	39,000	770,000	.425	45,000	33,000	1.600	1,520	1.05
N 15	32,000	625,000	330	51,600	40,500	1,540	1,200	1.28
N 16	32,500	635,000	.380	53.500	42,000	1,400	1,180	1.19
N 17	30,000	590,000	342	44,500	36,000	1,400	1,400	1.00
N 18	29,000	565,000	.324	44,400	40,500	1,420	1,320	1.08
N 19	38,000	595,000	.368	50.000	32,000	1,330	1,970	.67

Age of specimens 6 weeks.

large number of cracks distributed throughout the length of the beam.

It is of interest to compare these beams and beam N 13 with those having the rigidly attached reinforcement, beams N 5, N 8, N 9 and N 11. Figures 22 to 27 contain moment-deformation curves and deflection curves which will be of assistance in forming this comparison. It is very probable, in the tests of the beams with the round rod reinforcement, that the sudden decrease of loading after the maximum had been reached was due to the inability of the oil pump to supply pressure rapidly enough. The valves of this pump had become worn, and in the tests of the latter part of this series, considerable difficulty was encountered in holding the load long enough to take extensometer readings. This explanation seems all the more probable after the tests of Series E and F, in which the beams reinforced with smooth rods held the maximum load for some time. Outside of this, beams N 15 and N 16 compare well with beams having Kahn bars sheared up at 45°.

Table X shows the position of the neutral axis and the stresses in the steel and concrete for these beams. The average value of k corresponds very closely to the theoretical value computed from formula (3) when $n = 10$. The latter value is used in obtaining the stresses for beams N 1 to N 6. In beams N 5 and N 9, the steel was evidently loaded to its ultimate strength. Table XI gives values of the shearing stresses developed and $\frac{M}{b' d^2}$.

Not enough horizontal reinforcement was used in this series to fully test the value of the various reinforcements in preventing diagonal tension failures. It is quite evident that a rigidly attached web reinforcement is of decided advantage in preventing bond failures in short and relatively deep beams. How efficacious a reinforcement, which concentrates a large portion of its metal in single web members, would be in resisting high diagonal tensile stresses is a matter for further experiments to determine. Rigidly attached web members inclined at 45° are in a better position to resist diagonal tensile stresses than those which are bent up vertically.

In beams with smooth rods and loose web reinforcement, it is necessary, in short and relatively deep beams, to keep the

TABLE XI.

SERIES N: TEE BEAMS N1—N19.

Reinforcement—shearing stresses — $\frac{M}{b'd^2}$

Tee Beam.	Reinforcement.	At Maximum Load.			
		Maximum Load. lbs.	v Average shear. lbs./in.^{2}	v' Maximum shear lbs./in.^{2}	$\frac{M}{b'd^2}$
N 1	1, 1-inch square bar............. 10 $\frac{7}{8}$x$\frac{1}{4}$-inch stirrups.	24,000	176	202	209
N 2	1, 1-inch Kahn bar .... inclined alternate shearing	34,600	254	291	304
N 3	1, 1-inch square bar............ 12, $\frac{3}{8}$-inch stirrups	26,000	190	218	182
N 4	1, 1-inch Kahn bar .... inclined alternate shearing	37,400	274	314	264
N 5	2, $\frac{3}{4}$-inch Kahn bars .... inclined alternate shearing	32,600	174	200	302
N 6	2, $\frac{3}{4}$-inch square bars........... 14, $\frac{1}{4}$-inch inclined W-stirrups	24,000	128	147	221
N 7	2, $\frac{3}{4}$-inch square bars........... 20, $\frac{1}{4}$-inch W-stirrups	22,000	117	135	202
N 8	2, $\frac{3}{4}$-inch Kahn bars........... vertical alternate shearing	28,000	149	176	258
N 9	2, $\frac{3}{4}$-inch Kahn bars.... ...... inclined alternate shearing	47,200	251	290	352
N 10	2, $\frac{3}{4}$-inch square bars........... 12, $\frac{1}{4}$-inch inclined W-stirrups	34,000	181	207	253
N 11	2, $\frac{3}{4}$-inch Kahn bars........... vertical alternate shearing	39,000	207	238	290
N 12	2, $\frac{3}{4}$-inch square bars........... 16, $\frac{1}{4}$-inch W-stirrups	34,000	181	204	253
N 13	4, $\frac{5}{8}$-inch round rods (2 bent) ... 23, 1x$\frac{1}{12}$-inch slitted stirrups	32,000	174	197	312
N 14	4, $\frac{3}{4}$-inch round rods (2 bent)... 23, 1x$\frac{1}{12}$-inch slitted stirrups	44,000	239	274	431
N 15	6, $\frac{1}{2}$-nch round rods (4 bent).... 18, $\frac{1}{4}$-inch W-stirrups	34,200	182	207	317
N 16	Same as N 15..................	32,500	173	202	302
N 17	2, $\frac{5}{8}$ and 1, $\frac{1}{2}$-in. round rods (2 bent) 23, 1x$\frac{1}{8}$-inch hoops	32,400	172	197	302
N 18	4, $\frac{5}{8}$-inch round rods (2 bent) ... 18, $\frac{1}{4}$-inch W-stirrups	30,000	160	182	278
N 19	6, $\frac{1}{2}$-inch round rods (4 bent).... 14, $\frac{1}{4}$-inch W-stirrups	40,000	213	247	298

Age of specimens 6 weeks.

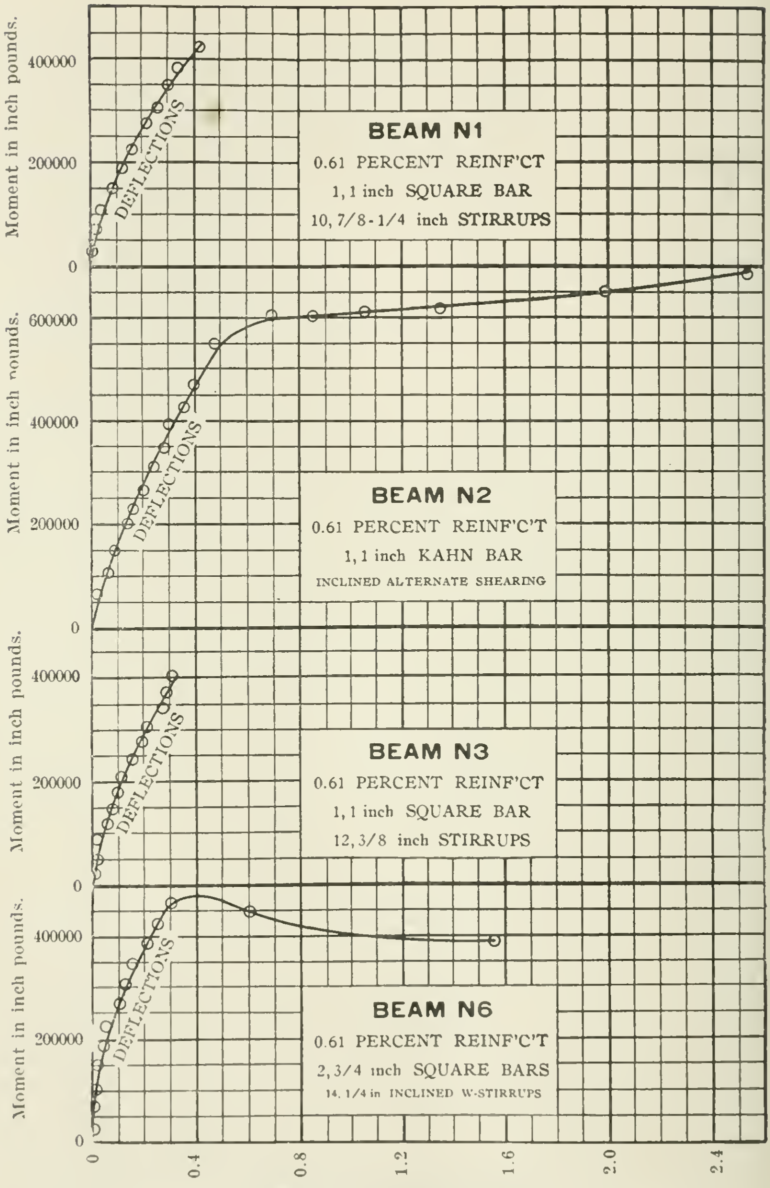

FIG. 22.—BEAMS OF SERIES N—MOMENT-DEFLECTION CURVES, ETC.

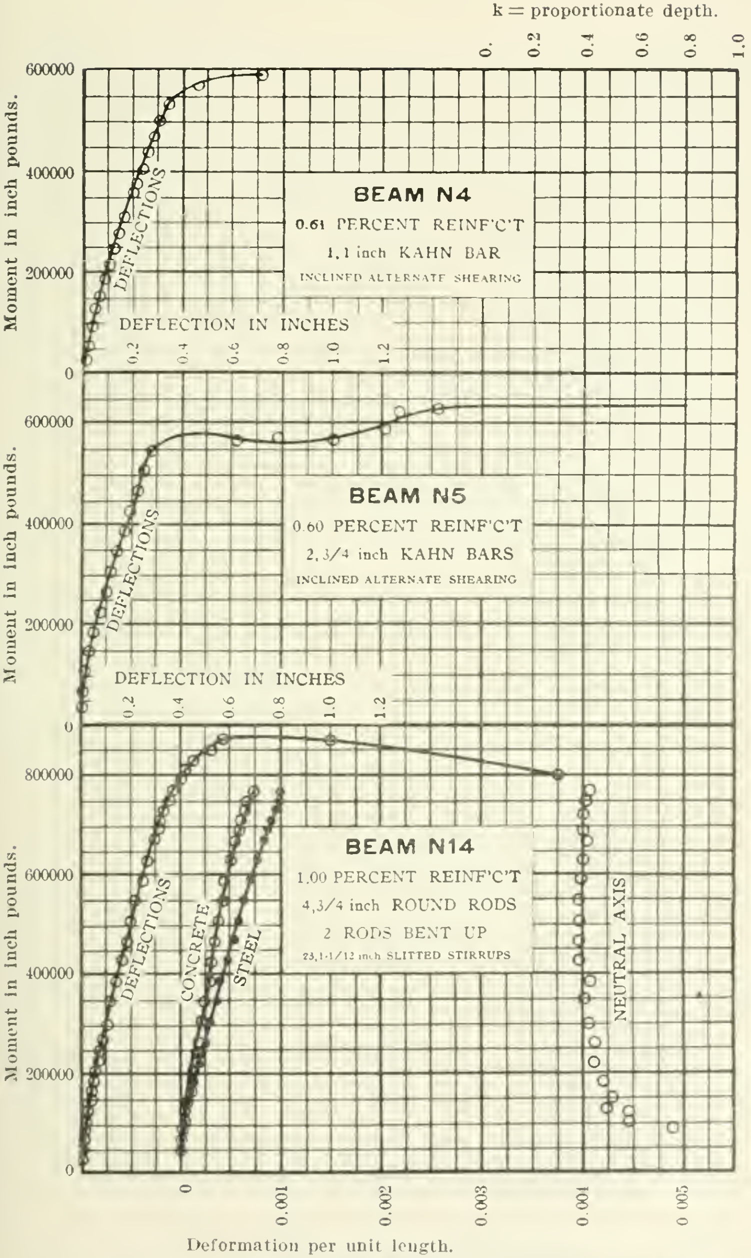

FIG. 23.—BEAMS OF SERIES N—MOMENT-DEFORMATION CURVES, ETC.

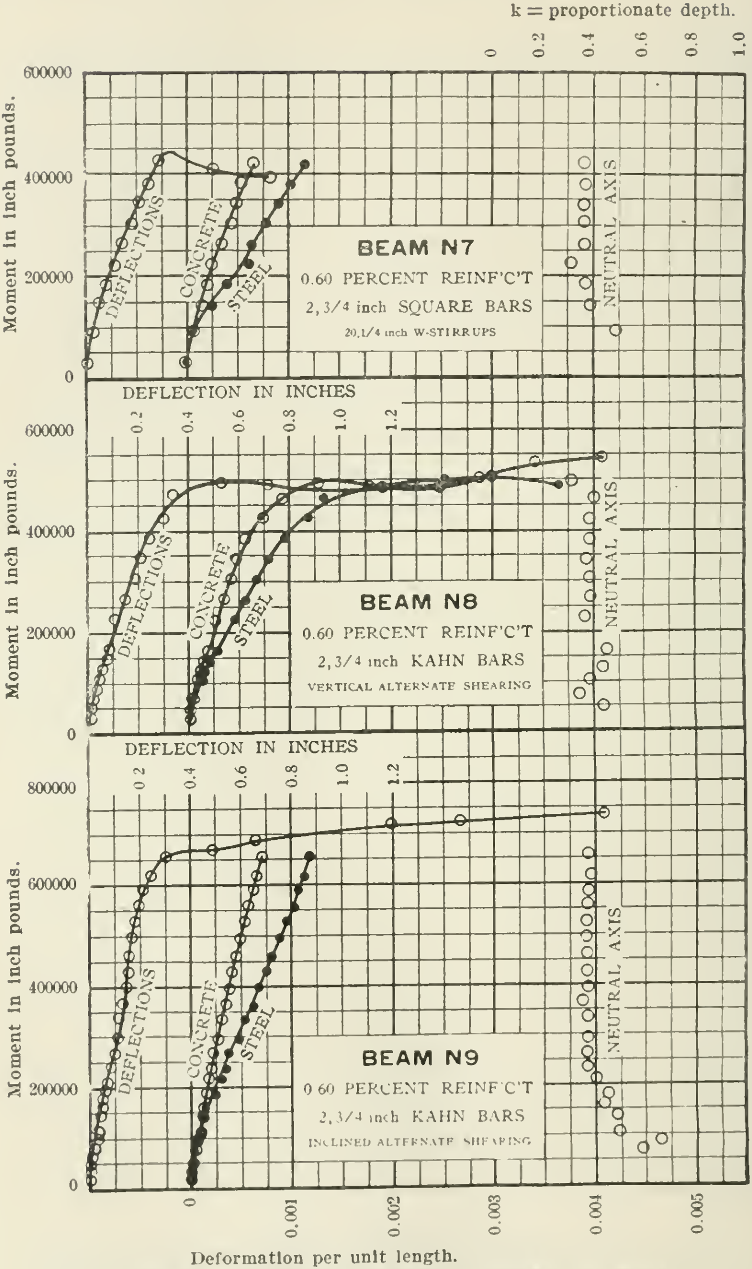

FIG. 24.—BEAMS OF SERIES N—MOMENT-DEFORMATION CURVES, ETC.

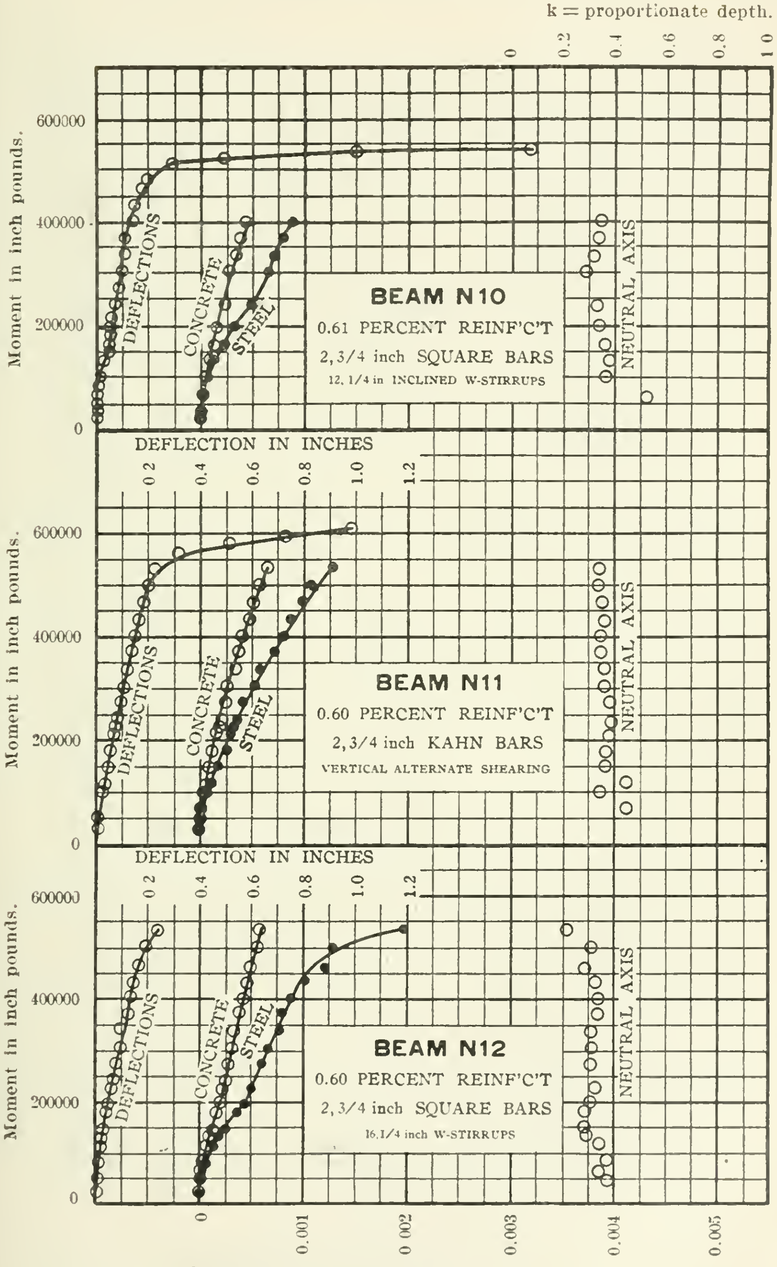

FIG. 25.—BEAMS OF SERIES N—MOMENT-DEFORMATION CURVES, ETC.

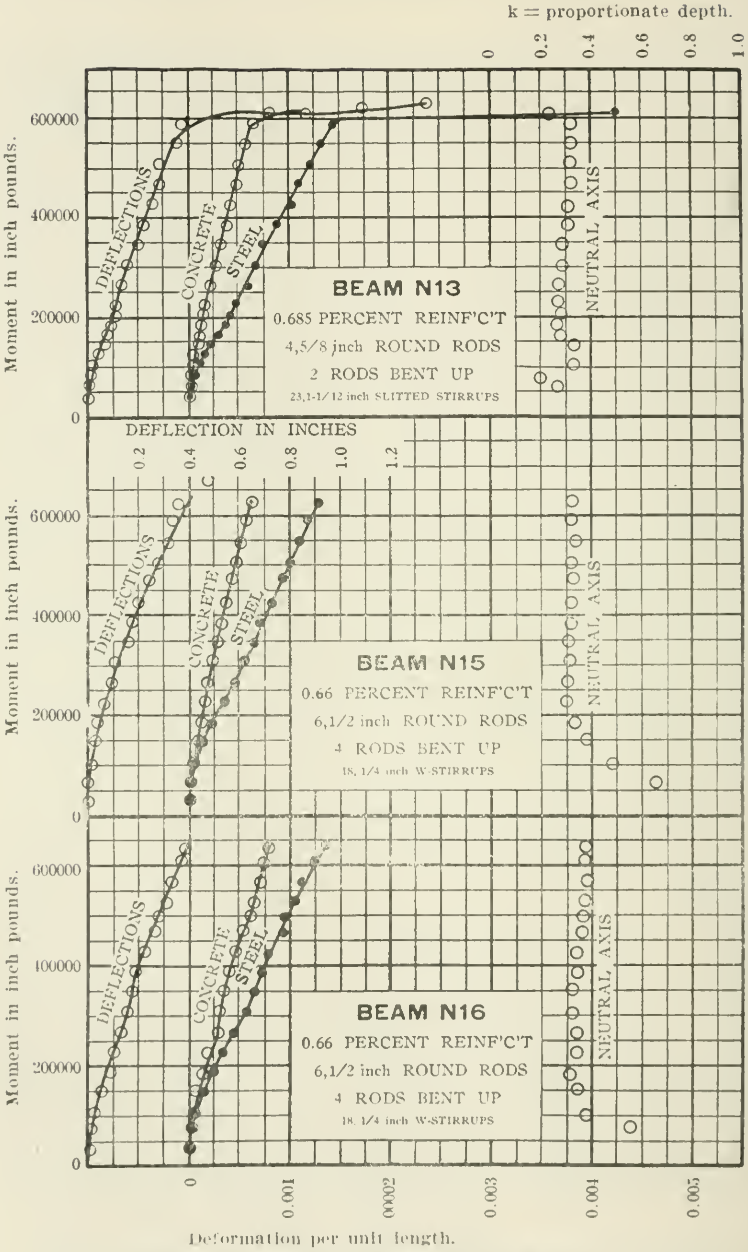

FIG. 26.—BEAMS OF SERIES N—MOMENT-DEFORMATION CURVES, ETC.

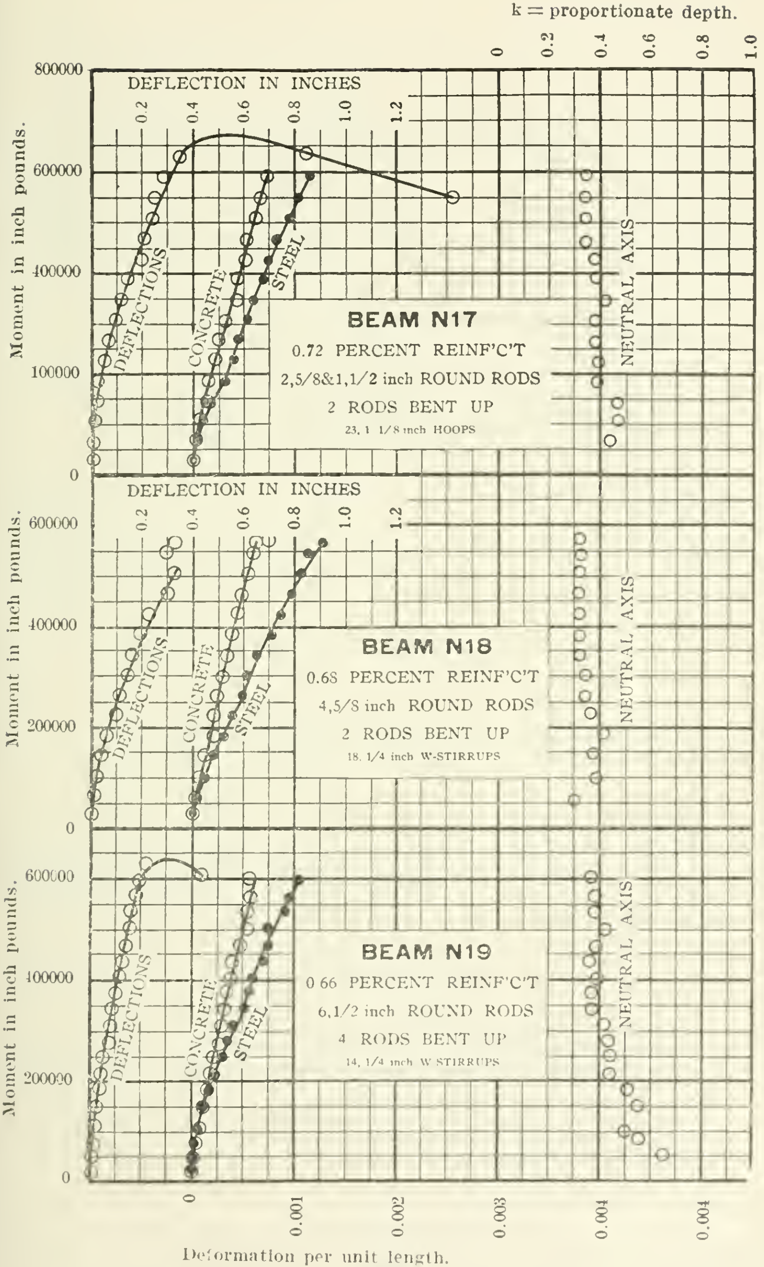

FIG. 27.—BEAMS OF SERIES N—MOMENT-DEFORMATION CURVES, ETC.

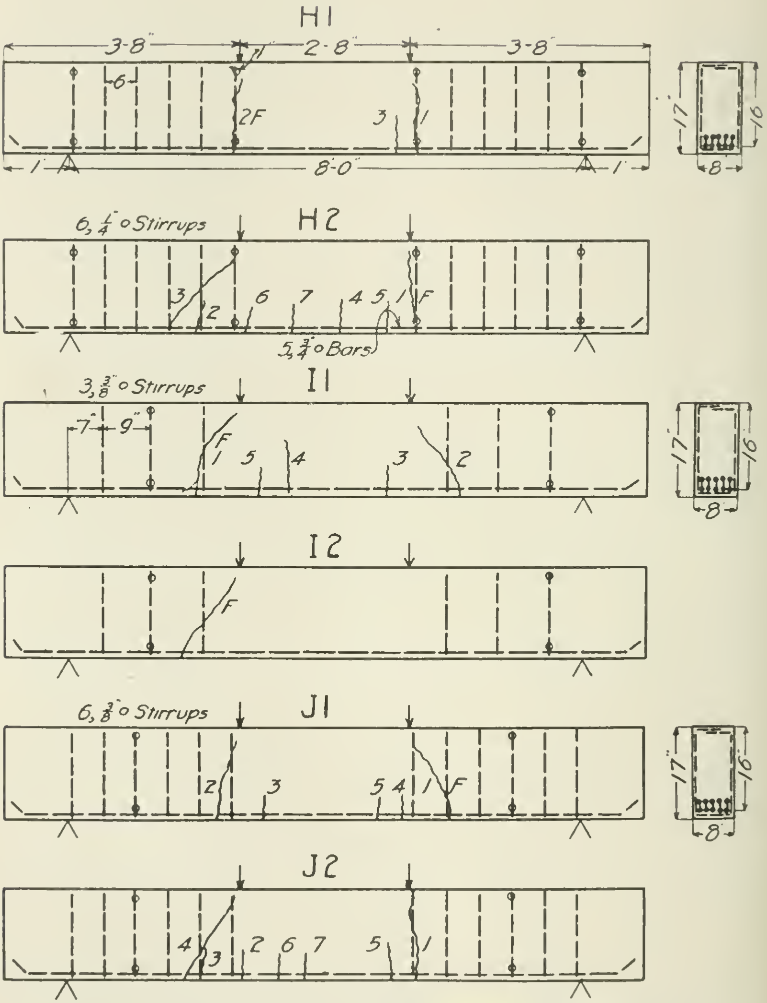

FIG. 28.—BEAMS OF SERIES G—REINFORCEMENT AND CRACKS.

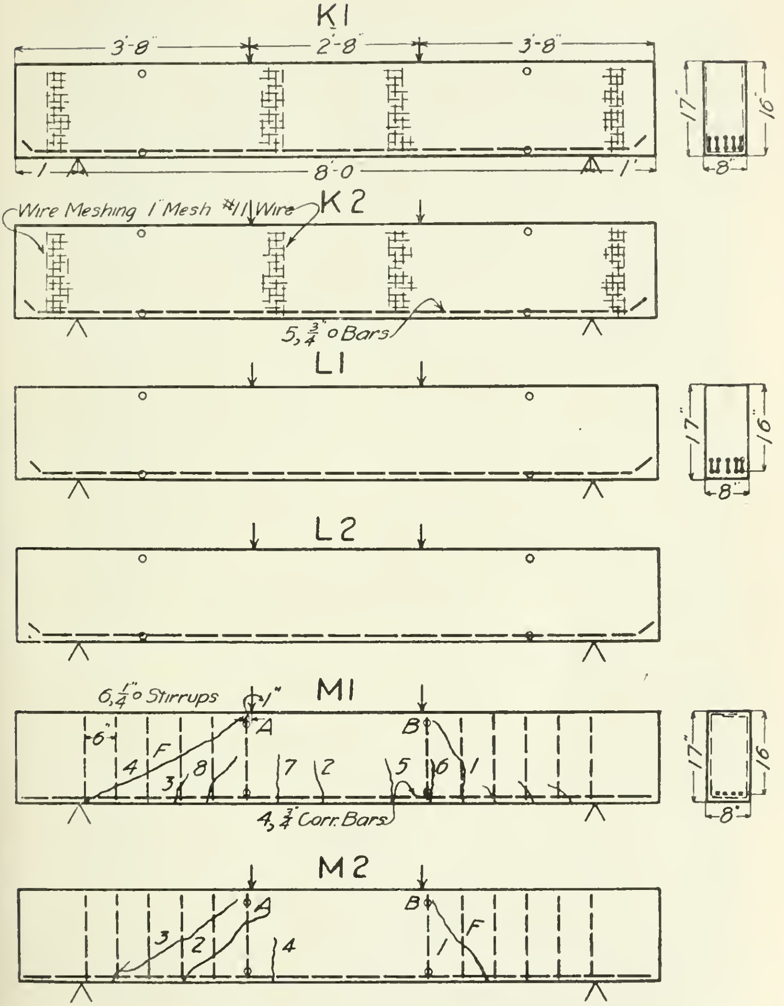

FIG. 29.—BEAMS OF SERIES G—REINFORCEMENT AND CRACKS.

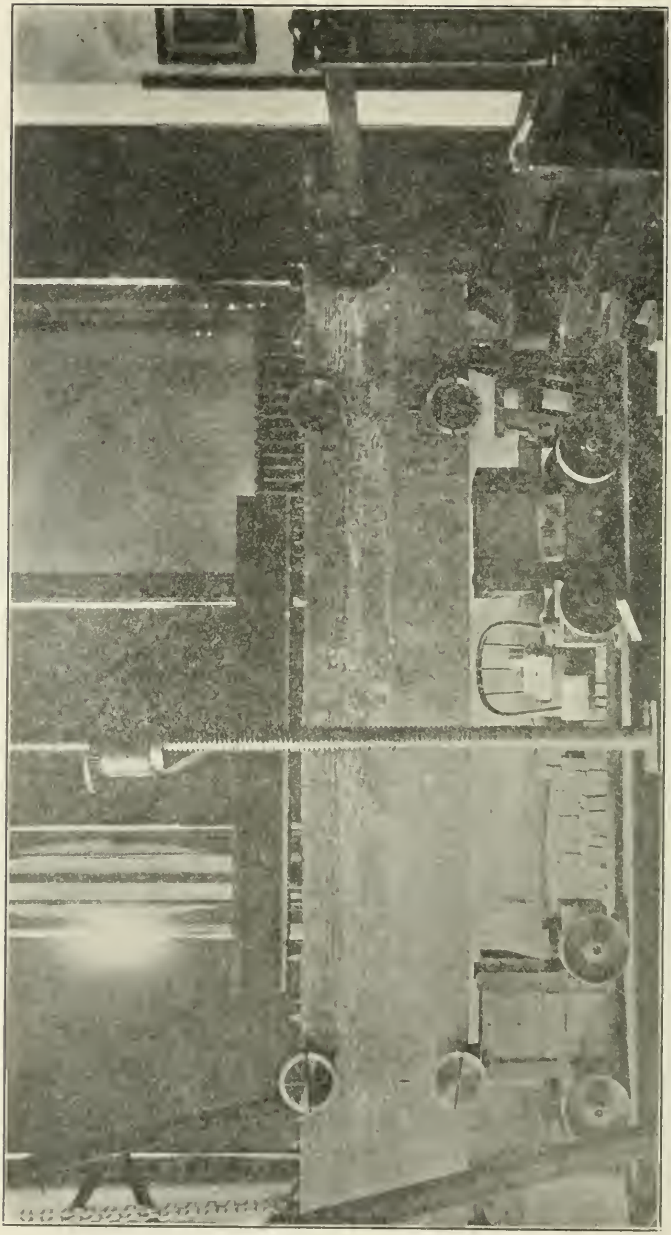

PLATE V.—BEAM WITH STIRRUP DEFORMATION APPARATUS.

main reinforcement distributed in small members to guard against failures due to insufficient bond. When a portion of the rods are bent up, the strength of the beam is increased against both bond and diagonal tension failures, and the bent up rods can be carried over the supports, if the span is continuous, furnishing resistance to the negative bending moment.

The subject of the amount of shearing reinforcement will be discussed further in this bulletin under the head of "Web Reinforcement." It is only necessary to say in passing that the stirrup bent rod combination, a strong meshing or a large number of small stirrups properly distributed with reference to the loading, such as was used in Series F and N appear to provide adequate resistance against these stresses.

4. Beams of Series G

This series of beams was designed to study the deformations along stirrups in reinforced concrete beams. The dial extensometer apparatus was used for measuring these deformations. The sockets shown in Figure 3 were placed on the stirrup when the beam was made, as previously explained, at the desired distance apart. When a beam was to be tested, dials were screwed into the upper sockets and metal plugs into the lower. To the plugs No. 32 covered copper wires were attached which were lead up around the drum of the dial and held taut by a weight; Figures 28 and 29 show how the beams were dimensioned and reinforced. The circles in the figures show where these plugs were placed in the beams. Plate V shows a beam with dials attached to both top and bottom sockets.

Unfortunately most of these tests failed to furnish trustworthy data owing to faults in mixing and in design. The stone used in making concrete for the bottom of these beams was too large to be worked around the rods and formed in pockets so that the bond between the concrete and smooth round rods was greatly impaired. As a consequence, slipping in the middle portion of the span occurred at a relatively small load, and a large part of the stress in the steel was carried to the hooks at the end of the rods in the overhanging end of the beam before it was transferred into the concrete. This brought about an entirely different distribution of web stress from that ordinarily encountered and caused tension cracks to appear in the tops of some of the beams over the supports. In most of these beams, failure occurred due to slipping of the rods accompanied by the breaking of the lower corner beneath the turned up portion of the rods. Stirrup deformation readings will not be given for beams H 1 to L 2. Tables XII and XIII contain the stresses in the steel, shearing stresses, and bond calculated for this series. The stress in the steel was computed by formulae (1), (2) and (3) with n = 10. The value of the bond is calculated by dividing the total stress in the steel by the product of the sum of the perimeters of the rods and the distance from load to end of beam. While the turned up bars affect this quantity materially, the results may be of empirical value.

TABLE XII.

SERIES G: RECTANGULAR BEAMS H 1–M 2.

Stress in Steel, 1.75 per cent. Reinforcement.

Beam.	Maximum Load. lbs.	Moment at Maximum Load. in. lbs.	Stress in Steel. lbs./in.^{2}
H 1.............. ...	51,400	811,000	28,400
H 2.................	59,400	940,000	32,800
I 1.................	58,000	918,000	32,000
I 2.................	57,700	914,000	31,900
J 1.................	60,000	950,000	33,200
J 2.................	68,200	1,080,000	37,800
K 1.................	57,700	914,000	31,900
K 2.................	55,200	873,000	30,500
L 1.................	52,000	822,000	28,700
L 2.................	37,700	593,000	20,700
M 1.................	69,800	1,107,000	38,100
M 2.................	60,200	954,000	32,800

Age of specimens 28 days.

Beams M 1 and M 2 were reinforced with straight corrugated bars and did not fail through bond but in diagonal tension. In testing these beams, dials were fastened on both sides of the beam at points A and B, Figure 29, and plugs placed directly below at a distance of 12 inches. In Figure 30 there are four curves showing deformations in stirrups for corresponding total loads. In beam M 1 crack No. 1 occurred at a load of 20,000 pounds, cracks Nos. 2, 3, 4 and 5 at 40,000 pounds, and cracks Nos. 6. 7 and 8 at 48.000 pounds. The metal in the third stirrup from the load scaled in crack No. 4. After crack No. 8 opened up, the dials on both sides of the beam at A showed a decreased reading for several loads.

TABLE XIII.

Series G: Rectangular Beams H 1—M 2.

Reinforcement—Shearing Stresses—Bond.

Beam.	Reinforcement.	At Maximum Load.			
		Load. lbs.	v Average Shear. lbs./in.^{2}	v' Maximum Shear. lbs./in.^{2}	Bond. lbs./in.^{2}
H 1	5, $\frac{3}{4}$-inch round rods..........	51,400	197	247	127
H 2	12, $\frac{1}{4}$-inch round stirrups........	59,400	232	285	146
I 1	5, $\frac{3}{4}$-inch round rods............	58,000	227	279	143
I 2	6, $\frac{3}{8}$-inch round stirrups	57,700	226	278	142
J 1	5, $\frac{3}{4}$-inch round rods............	60,000	234	288	148
J 2	12, $\frac{3}{8}$-inch round stirrups........	68,200	266	328	169
K 1	5, $\frac{3}{4}$-inch round rods........... ..	57,700	226	278	142
K 2	Wire Meshing 1-in. mesh No. 11 wire.........................	55,200	216	265	136
L 1	5, $\frac{3}{4}$-inch round bars...	52,000	203	250	128
L 2	5, $\frac{3}{4}$-inch round bars	37,700	148	181	123
*M 1	4, $\frac{3}{4}$-inch Cor. bars.............	69,800	272	335	170
*M 2	12, $\frac{1}{4}$-inch round stirrups........	60,200	235	290	146

*Failed in diagonal tension; all others failed in bond.
Age of specimens 28 days.

It will be noted in all the curves that there is a small amount of compression induced in these stirrups before the concrete cracks. This disappears, however, as soon as a crack appears in the vicinity of the stirrup. For example, in the test of M 2, there was a deformation of .00025 of an inch at a load of 17,100 pounds; at the next load, 25,300 pounds, crack No. 1 appeared and the deformation became zero. The deformation then became tensile as shown in the figure. Stirrup A in this beam, however, did not begin to stretch until crack No. 2 appeared on its side of the beam at a load of 36,000 pounds. Crack No. 3 came at a load of 44,000 pounds and crack No. 4 at 50,000 pounds. The total stretch at maximum load of stirrup A in beam M 1 was .0019 inches, in Beam M 2 .0027 inches. It would be interesting to see if similar results would be obtained from other stirrups further removed from the load.

5. Web Reinforcement

From the tests of Series G, especially beams M 1 and M 2, it seems quite evident that stirrups are not stressed with a tensile load until the adjacent concrete is cracked. The compression produced in the cases discussed at the first loadings may be due to the proximity of the stirrup to the point of application of the load. After the concrete is cracked, they carry a portion of the vertical shearing stresses depending upon the deformations produced in them by the opening crack. In general, then, stirrups are a factor of safety against rupture due to an overload.

Formula (10) $g = \frac{v'bs}{ua}$ (see page 88), is derived on the assumption that the shear is constant between loads and supports, that the concrete carries no diagonal stress after it is cracked, that no bars are turned up, that the rods' resistance to being bent be neglected and that the distribution of stress is unchanged after the crack appears. Whether these assumptions are correct or incorrect, for stresses in the stirrups below the yield point of the metal, is a matter for further investigation. In the tests of beams G1, G2, M1 and M2, the stresses in the stirrups ran beyond the yield point as indicated by the scaling and breaking which occurred; see Plates VI and VII. The results in Table XIV were computed from formula (10). It is quite evident from the computed stresses in the stirrups that the formula gives values which are too high. In the beams which had inclined rods a considerable portion of the diagonal

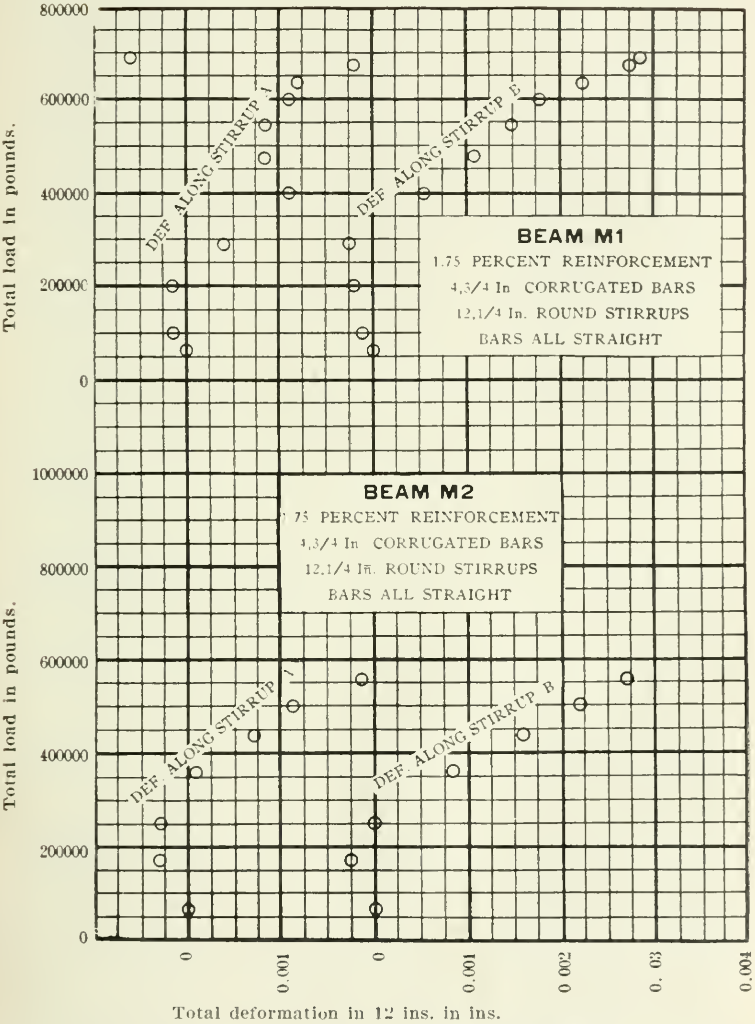

FIG. 30.—BEAMS M1 AND M2—DEFORMATION IN STIRRUPS.

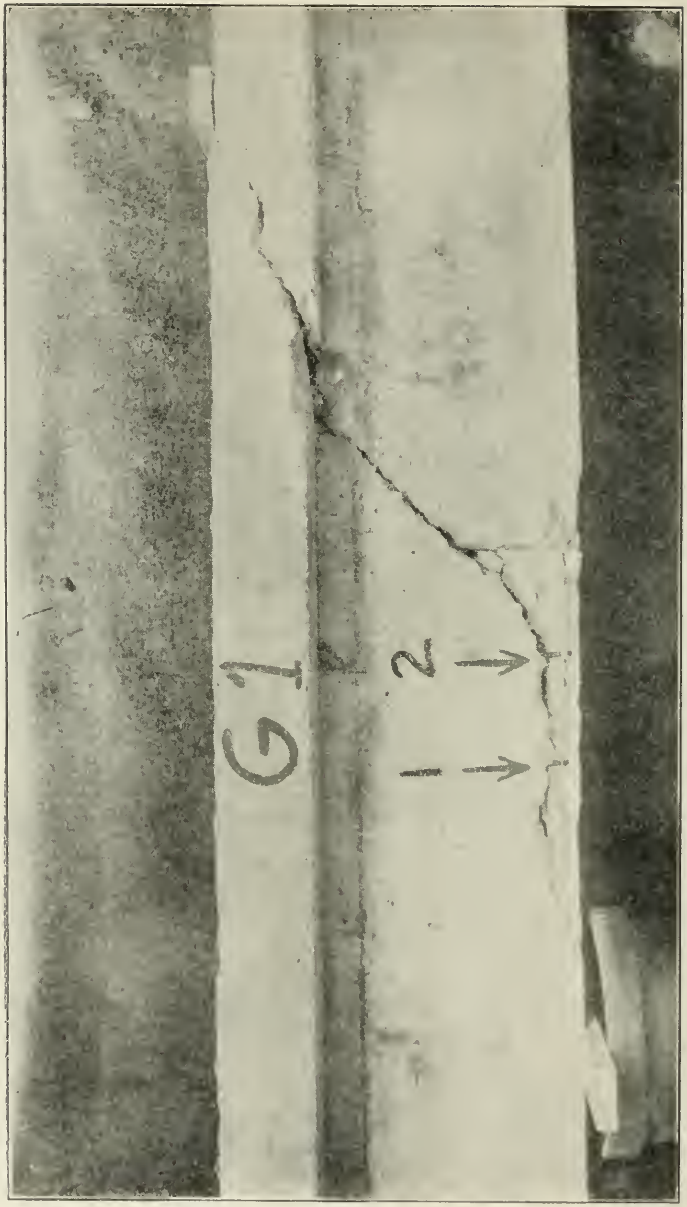

PLATE VI.—FAILURE CRACK IN TEE-BEAM G1.

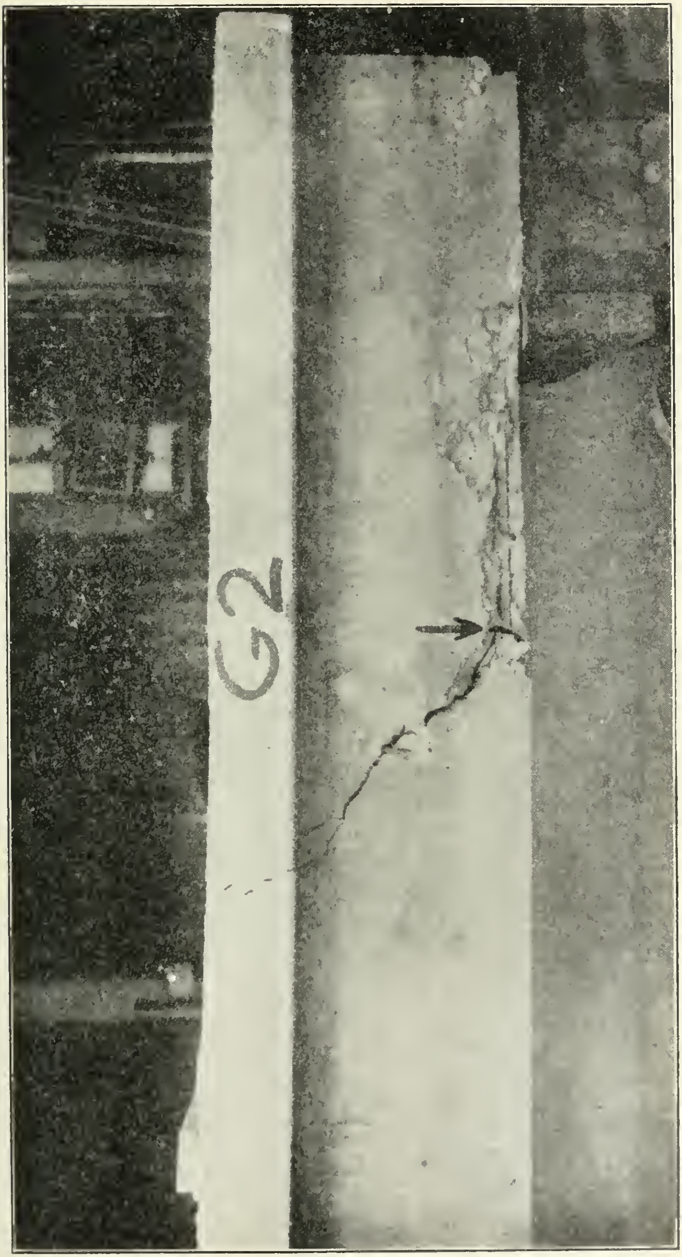

PLATE VII.—FAILURE CRACK IN TEE-BEAM G2.

tension was taken up by the rods. Perhaps in this series, where one-half of the rods were turned up, as much as one-half of the total diagonal tension was transmitted in this way.

Tests of the beams with straight rods demonstrate that there is a large error in the two assumptions that the concrete carries no web stress after it is cracked and that the resistance to bending of the reinforcing bars may be neglected.

TABLE XIV.

COMPUTED STRESSES IN STIRRUPS.

Beam.	Area of prong of stirrup. sq. in. (a)	Distance between stirrups. ins. (s)	Maximum shear. lbs./in.^{2} (v′)	v′ sb	Computed stress in stirrup. Max. load. lbs. in.^{2} $\left[g=\frac{v'sb}{ua}\right]$	Kind of failure.	Remarks.
A 1	.06	6	361	17,300	139,000	T	....
A 2	.06	6	357	17,150	137,000	T	....
B 1	.049	5½	357	15,700	160,000	T	....
B 2	.049	5½	354	15,600	159,000	T	....
C 1	.049	5½	322	14,200	145,000	T	....
C 2	.049	5½	316	13,900	142,000	T	....
D 1	.14	6	526	25,200	89,400	T	....
D 2	.14	6	544	26,100	92.900	T	....
E 1	.14	3	505	12,100	42,900	T	....
E 2	.14	3	485	11,600	41,300	T	....
F 1	.012	1	368	2,940	128,000	T	....
F 2	012	1	352	2,820	122,000	T	....
G 1	.049	5½	259	10,400	106,000	DT	2 stirrups broke.
G 2	.049	5½	260	10,500	107,000	DT	1 stirrup broke.
M 1	.049	6	335	16,100	164,000	DT	stirrups scaled.
M 2	.049	6	290	13,900	142,000	DT	....

T=tension. DT=diagonal tension.

The crack sketches Figures 8, 9, 10, 28, and 29 and the Plates VI, VII and VIII throw some light upon this problem. It will be noted in nearly all these sketches that the first diagonal cracks opened up near the loading points while those near the supports did not appear until sometime later. The cracks do not extend to the top of the beam until they produce failure. Then some of the web stress will be carried by the uncracked concrete and some by the stirrups going through the crack. As

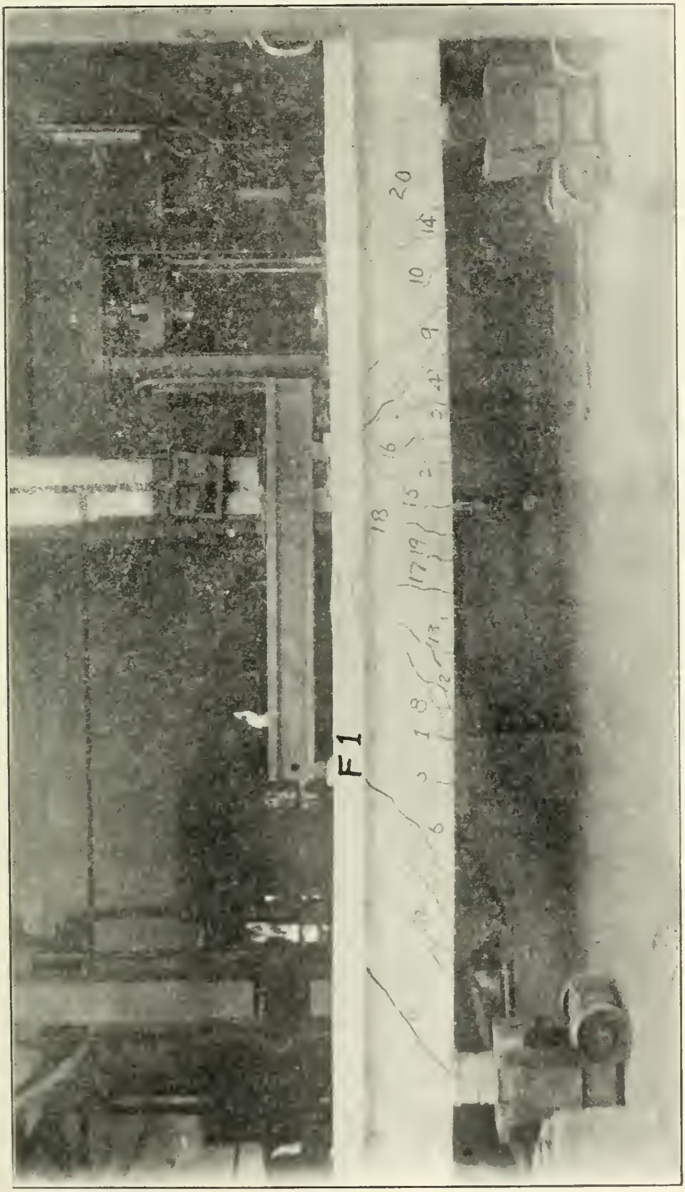

Plate VIII.—Cracks in Tee-beam F1.

the crack tends to spread, due to increased loads, the stirrup will take more and more stress. Now, if the amount of metal in the stirrups be small so that they alone cannot resist the vertical shear, they will be stressed beyond the yield point. Then, due to their increased deformation, there is a redistribution of stress in order to maintain equilibrium; the crack widens and more downward force is exerted upon the main rods which try to tear themselves free from the concrete. This results in producing the commonly observed crack running along the plane of the rods. Also some of the stress in the main rods, which would if the concrete were not cracked, be taken off as diagonal tension by the concrete, is transmitted along towards the end of the beam. This is followed by another diagonal crack nearer the support than the first, and the same sort of adjustment of stresses to preserve equilibrium again takes place. As a result the web stresses in the beam are partially taken care of by the concrete and the resistance to bending of the main rods, so that the assumptions underlying formula (10) must be considered when deformations in the web are sufficient to produce stresses in the stirrups beyond their yield point, if economy in stirrups be an object in design.

As was indicated in the tests of the series of 1906, distribution of web reinforcement is an important consideration in the design of reinforced concrete beams subjected to high shearing stresses. The manner in which the cracks appeared in the beams of the present series only serves to strengthen that assertion. It is noteworthy fact in this connection that the wire meshing used gave excellent results in the tests and was easily handled and kept in place while the beams were being made.

137

BULLETIN OF THE UNIVERSITY OF WISCONSIN

NO. 205

ENGINEERING SERIES, VOL. 4, NO. 3, PP. 137-247

AN INVESTIGATION OF THE HYDRAULIC RAM

BY

LEROY FRANCIS HARZA

Formerly Instructor in Hydraulic Engineering
University of Wisconsin

RESEARCHES IN HYDRAULICS

DANIEL W. MEAD, PROFESSOR OF HYDRAULIC AND SANITARY ENGINEERING

Published bi-monthly by authority of law with the approval of the Regents
of the University and entered at the post office at
Madison as second-class matter

MADISON, WISCONSIN
MARCH, 1908

139

CONTENTS

PAGE

INTRODUCTION 143
GENERAL DISCUSSION 145
  Description of the Typical Hydraulic Ram 145
  Choice of Formula for Efficiency 146
  Water Hammer 152
THEORETICAL ANALYSIS 157
  First or Acceleration Period 157
  Closure of Waste Valve 161
  Second Period, Retardation 164
    Case I 166
    Case II 168
    Case III 169
    Case IV 170
  Efficiency of the Machine or Total Efficiency 171
  Opening of the Waste Valve 171
  Closing of the Waste Valve 172
  Effect of the Assumptions 173
EXPERIMENTAL APPARATUS 176
  Results Desired 176
  The Ram 177
  Method of Varying the Conditions of Operation 180
    1. Supply head 180
    2. Pumping head 180
    3. Length of drive pipe 181
    4. Size of drive pipe 181
  5, 6 and 7. Valve motion 181
    8. Size of air chamber 184
    9. Amount of air in the air chamber 184
  Autographic Recording Instruments 186
EXPERIMENTAL VERIFICATION OF THEORY 192
  Observing 192
  Comparison of Theory and Experiment 207
    1. Acceleration period 208
    2. Retardation period 218
    3. Efficiency of the machine 224

PAGE
EFFECTS OF CHANGING THE CONDITIONS OF OPERATION............ 231
1. Supply head.. 231
2. Pumping head... 232
3. Length of drive pipe................................... 232
4. Size of drive pipe..................................... 234
5. Strokes per minute..................................... 236
6. Rate of waste valve closure............................ 238
7. Law of closure... 239
8. Volume of air in the air chamber....................... 239
9. Amount of water in the air chamber..................... 240
10. Amount of opening or range of movement of the waste valve.... 240
11. Type of waste valve................................... 240
12. Type and size of check valve.......................... 240
CONCLUSION.. 241
INDEX TO NOMENCLATURE USED IN FORMULAS..................... 242
BIBLIOGRAPHY.. 245
Hydraulic Rams.. 245
Water Hammer.. 247

LIST OF ILLUSTRATIONS

PLATES

PAGE
I—Sketch of Experimental Ram.................................. 178
II—Sketch of Waste Valve and Check Valve..................... 179
III—General Arrangement of all Apparatus..............(opposite) 180
IV—Sketch of Cams.. 183
V—General View of Ram and appurtenances..................... 184
VI—View of the machine for Valve control, Showing Cams in Place 185
VII—View of Autographic Recording Instruments 186

TABLES

I—Observed Data for l = 85.35 and H = about 8.2 feet 193
II—Observed Data for l = 51.5 feet and H = about 8.2 feet........ 199
III—Observed Data for l = 51.5 feet and H = about 6.2 feet........ 203
IV—Observed Data for l = 51.5 feet and H = about 4.2 feet........ 204
V—Observed Data for l = 51.5 feet and H = about 2.2 feet........ 205
VI—Table Showing Scheme for observing........................ 206

DIAGRAMS

I—Curve Showing the Stage During Closure of the Waste Valve at which the Velocity Ceases to Increase and begins to Decrease.. 162
II—Calibration Curves of the Velocity Recording Instrument 188
III—Curve showing Friction Loss in the Drive Pipe with Uniform Flow 190
IV—Sample Autographic Records........................ 207
V—Curve Showing Loss of Head through the Check Valve.. 209
VI to X incl.—Velocity Curves for Drive Pipe....... 210
XI to XV incl.—Efficiency Curves—Acceleration Period 216
XVI to XXV incl.—Efficiency Curves—Retardation Period ... 219

PAGE
XXVI to XXXV incl.—Curves Showing Total Efficiency of the Machine 225
XXXVI—Curves showing the Efficiency with which a Specified Velocity in the Drive Pipe can be obtained with a Given Supply Head 231
XXXVII—Assembly of the Retardation Efficiency Curves for the 51.5 foot Drive Pipe 232
XXXVIII—Curve Showing that there is a Pumping Head for which the Efficiency, with a Given Maximum Velocity, will be Maximum 233
XXXIX—Curve Showing the Effect of Length of Drive Pipe on the Efficiency during Acceleration Period 233
XL—Curve Showing the Effect of the Diameter of Drive Pipe upon the Efficiency during Acceleration Period .. 234
XLI—Efficiency Curves for 3 inch Drive Pipe—Retardation Period 235
XLII—Characteristic Operating Curves of the Experimental Ram under Assumed Conditions 237

INVESTIGATION OF THE HYDRAULIC RAM

INTRODUCTION

Although the "hydraulic ram" was invented over one hundred years ago, its design has never been put upon a rational basis. Because of this fact and the consequent inability of designers to forecast the performance of the machine, it has not received the attention from engineers which its usefulness, simplicity and cheapness should demand for it. Its use is mostly confined to small sizes, and it is still considered by many merely as a scientific novelty suitable for pumping only small amounts where efficiency is not of great importance.

Although the opportunities for using rams are limited, as compared with those for the use of steam pumping engines, nevertheless there are many cases where a ram could be employed for lifting water with a very material saving were its action better understood so that engineers and manufacturers might venture farther beyond the boundaries of precedent in their designs.[1]

Experimental data to be of general value must be accompanied by, and correlated with, a theoretical investigation. If not, the conclusions drawn can only be assumed to apply within the usually narrow range of the experiments and will not form a safe precedent for extending the size and range of usefulness of the machine.

Although the action of the ram is somewhat more complicated than that of other pumps, it is nevertheless controlled by absolute mathematical laws which can be derived with as great a degree of accuracy as that with which the original assumption can be made without obtaining irreducible equations.

---

[1] A notable example of a comparatively large hydraulic ram for municipal supply is that at West Dundee, Ill., which has supplied a town of 1,600 with water for about twelve years at a total operating cost of only a few dollars for the renewal of valves, and has required practically no attention. (See the description by the designer, Mr. D. W. Mead, member Am. Soc. C. E., *Eng. Rec.*, 44: 174.) Rams are also advertised for which the manufacturers claim deliveries as high as 1,000,000 gallons of water per day.

It has not been possible within the limited time at the disposal of the writer to cover the entire field of investigation which was originally planned, and the present paper should therefore be considered as a preliminary or progress report having the following objects in view:

1. To derive, in so far as possible, general mathematical laws which shall apply to all single-acting hydraulic rams under all conditions of use.

2. To show that these formulas are justified by experimental data in so far as the data thus far accumulated apply.

Acknowledgments are due Mr. A. H. Ayers and Mr. C. O. Brandel for valuable assistance in the work of observing and in the analysis of data; and to Mr. J. C. Steen for help in the detailing of apparatus.

GENERAL DISCUSSION

Description of the Typical Hydraulic Ram

A typical cross-section of a single acting hydraulic ram is shown in Figure 1.

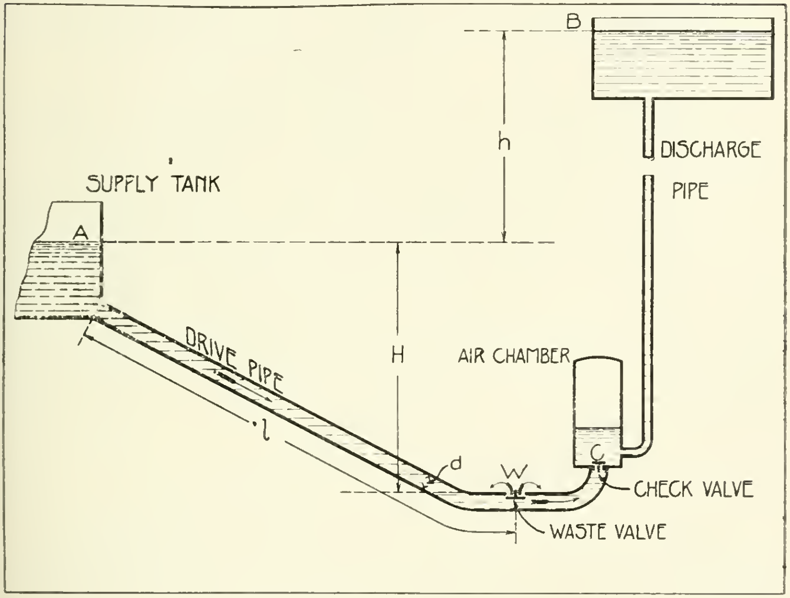

Fig. 1.—Typical Hydraulic Ram.

Without concerning ourselves at present with the cause for this action, let us assume the "waste-valve" W. to open while the water in the "drive-pipe" is at rest. Water will at once begin to flow down the drive pipe from A and escape at W. The rate of flow will increase until the forces acting upon the bottom of the valve, due to causes to be mentioned later, cause it to close. Thereupon the pressure will suddenly rise in the drive pipe due to the effect of the sudden retardation of the water, a phenomenon known as water hammer, and some water will be forced through the check valve into the air chamber even though the pressure in the air chamber greatly exceed that due to the head H. The cushioning effect of the air in the chamber serves nearly to equalize the pressure and therefore produce a nearly uniform flow from the ram to the discharge tank at elevation B. After the water in the drive pipe has been brought to rest. by the combined action of the opposing forces of pressure in the air chamber and friction, a reaction (the nature of which will be left for a later discussion) opens the waste valve and another cycle of events begins. A ram thus utilizes water power to pump water to an elevation greater than that of the supply.

Its action takes place in two entirely distinct stages. During one stage, kinetic energy is being stored in the drive pipe at the expense of the potential energy contained in the supply water. The drive pipe only is in action, and its function is that of an accumulator of energy. This will be called the "acceleration stage or period." During the second stage the water in the drive pipe, by virtue of its momentum acquired in the first stage, serves both as engine and pump piston to force water through the check valve into the air chamber. This will be called the "pumping or retardation stage."

CHOICE OF FORMULA FOR EFFICIENCY

For the presentation in this paper of a discussion of that already over-discussed subject of "the efficiency of the hydraulic ram," the writer feels that he owes an apology to the engineering public.

We would much prefer to assume a general understanding of the subject and to enter at once into a discussion of new theories and experiments, relating to the operation of the machine in question. Inasmuch, however, as there are now in use two formulas by which to express the efficiency, those of D'Aubuisson and Rankine, which give very discordant results, and as there are well known authorities upon hydraulics who still adhere to either formula, it is necessary for the writer to choose a formula for use in this paper, and to defend the one chosen.

The two formulas, the correctness of which have long been in dispute, are:

$$\text{Rankine, } E_m = \frac{qh}{QH}$$

$$\text{D'Aubuisson. } E_m = \frac{q\,(h + H)}{(Q + q)\,H}$$

where (see Figure 1):

Q=water wasted through valve W.

q = water pumped from the supply to the discharge reservoir,

H = elevation of water surface in supply tank above the level of the waste valve,

and h = elevation of water in the discharge tank above the level of water in the supply tank.

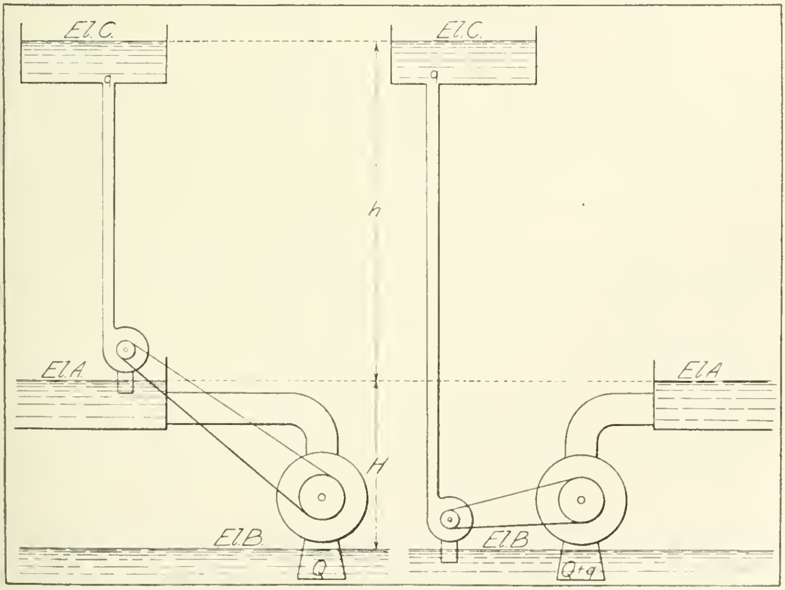

FIG. 2. FIG. 3.

For a clear understanding of the basis upon which the two formulas rest, consider Figures 2–7. Figure 2 represents a water turbine drawing water from the head-race A, and discharging it into the tail race B. The turbine is belted to a pump which draws water from the head race. The turbine uses an

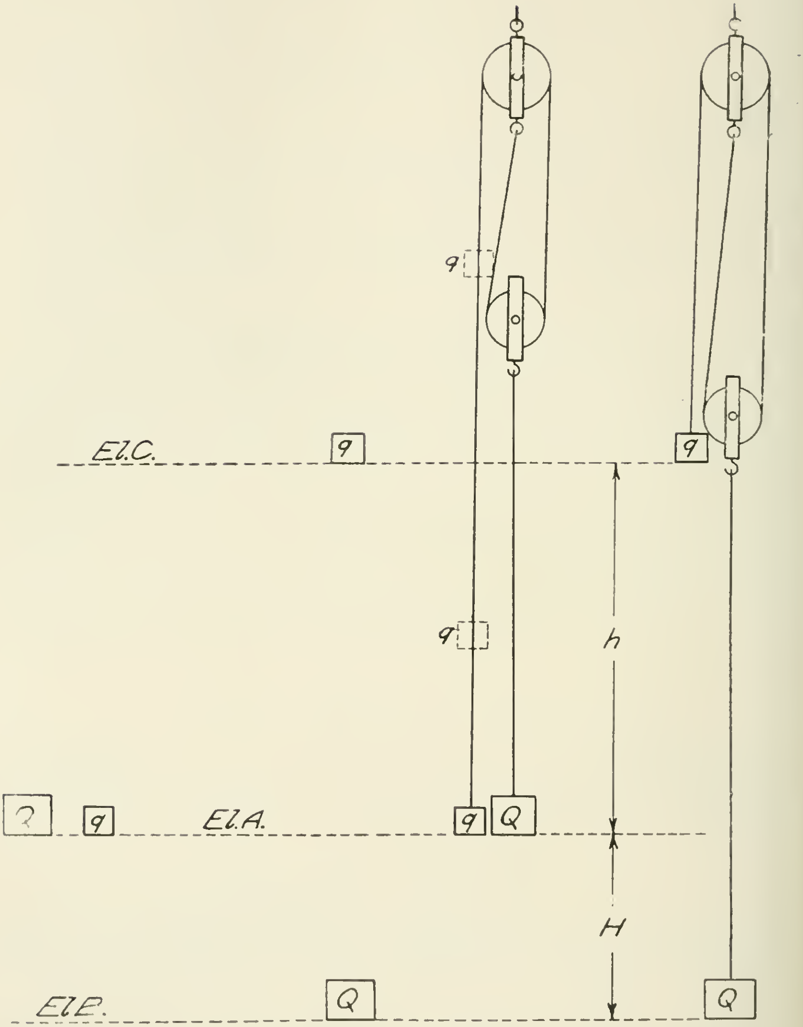

FIG. 4. FIG. 5. FIG. 6. FIG. 7.

amount of water Q per unit time, and the pump delivers an amount of water q into the higher reservoir C. The efficiency of the two machines considered as a unit is evidently $\frac{qh}{QH}$.

The condition represented in Figure 3 differs from that in Figure 2 in that the pump draws its water from the tail race B′, and the total flow, Q + q, must pass through the turbine. The efficiency of the combined machines, in this case, is $\frac{q(H+h)}{(Q+q)H}$.

Rankine's formula expresses the condition in Figure 2 and D'Aubuisson's that in Figure 3. In both cases, however, the initial and final conditions without regard to how they were brought about can be represented by Figures 4 and 5, respectively. If line B is datum level, then Q, in Figure 5, has lost all of its energy, and the ratio of the final to the initial energies is $\frac{q(h+H)}{(Q+q)H}$.

Figures 4 and 5 illustrate exactly the theory upon which D'Aubuisson's formula for the efficiency of the ram is based, and if this theory is correct, then the efficiencies of the machines shown in Figures 2 and 3 are equal, since the initial and final conditions are alike in both cases.

Again consider the condition represented in Figure 6. Suppose $Q = 100$ pounds and is just able to raise the weight of $q = 40$ pounds. Let $H = 10$ feet; then $h = 20$ feet, and the efficiency of the machine is unmistakably $\frac{qh}{QH} = 80$ per cent. The ratio of final to initial energy, however, is $\frac{q(h+H)}{(q+Q)H} = \frac{40 \times 30 =}{140 \times 10} = 85.8\%$. That this latter value of the efficiency of the pully system is inconsistent will be evident if we change the initial elevation of the weight q. Suppose, for example, that it starts from the elevation 20 feet (shown dotted); the ratio of final to initial energy is $\frac{40 \times 40}{100 \times 10 + 40 \times 20} = \frac{1600}{1800} =$ 89% instead of 85.8%. Thus, if we express the efficiency of the pully system by the ratio of final to initial energy, we might obtain an infinite number of values, depending upon the initial position of the load lifted, and each having as good a claim to truth as any other. It does not need to be argued that the efficiency of the pulley system is $\frac{qh}{QH} = 80\%$, which is the same regardless of the initial elevation of either Q or q and has no definite relation to the proportion of the total original potential energy which is conserved by the machine.

The principle illustrated by the pulleys is general and applicable to all machines. Applying it to the choice of formulas for the ram we must ask ourselves: (1) Which of the quantities, q or (q + Q), is utilized for power? (2) From what initial elevation is the quantity q raised? For answer let us follow the ram in its operation. The waste valve opens and water wastes until a certain velocity V is acquired. During this time an amount of water Q has been discharged, and the water q which is to be pumped by this stroke is still in its initial position in the supply tank. With the closure of the waste valve the machine changes its nature instantly from that of an accumulator of energy to a pumping engine. The forces tending to pump water are those due to the momentum of the water and to the supply head H. Resisting these forces we have those due to the head, H + h, and the frictional resistance of valve and pipe, or H + momentum = H + h + friction. Thus the head H cancels and the machine acts merely as an inverted syphon with the momentum of the water balanced against the resistances and the head alone. In fact the condition during the pumping period would be the same and the same amount of water would be pumped if the drive pipe, at the beginning of the pumping period, were raised to the upper position in Figure 8, provided both pipe lines offered the same resistance and the same mass of water were in motion in each with the initial velocity V.

It must therefore be conceded that:

(1) No energy is accumulated after the closing of the waste valve, and hence q, which is at rest in the supply tank at the time of closing, does not contribute to the work done upon the machine.

(2) q is raised from the elevation A and not from B, and hence the work given out by the machine is qh and not q(h+H).

(3. The efficiency of the ram is therefore $\frac{qh}{QH}$ as given by Rankine, and the condition is identical with that in Figure 2.

It is not to be assumed from this discussion that the writer intends to discard the use of the function $\frac{q(H+h)}{(Q+q)H}$ (by whatever name we may call it) as worthless. On the contrary it is a very useful expression for comparing the results obtained by alternative systems for disposing of the original energy

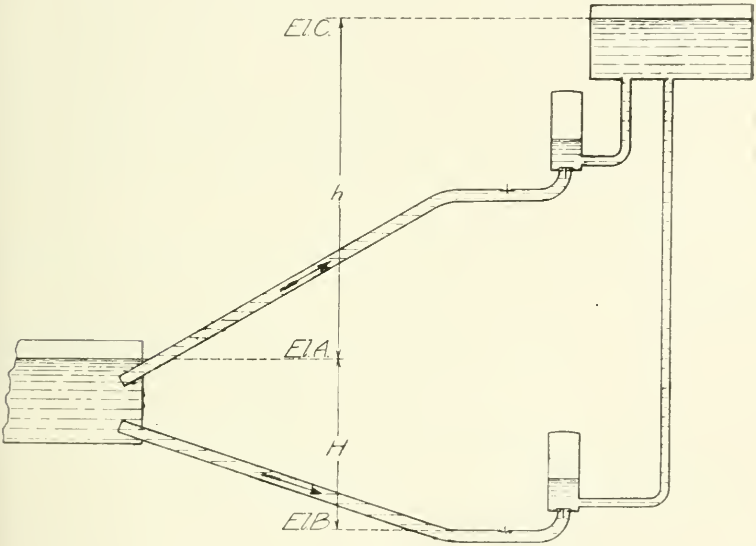

FIG. 8.

.(Q+q)H of the stream. On the other hand it does not form a fair basis for the comparison of the results obtained by the same or different machines under varying conditions, as it is a function not only of the mechanical efficiency of the machine but also of the conditions under which it operates.

Without agreeing entirely with the conclusions drawn, the writer would like to recommend the paper of A. J. Wood with discussions by William Kent and Theo. Woolsey Johnson as very instructive on this subject.[1]

---

[1] See the *Stevens Institute Indicator* for 1902, p. 144.

WATER HAMMER

In order to correctly understand the action of the hydraulic ram it will be necessary to review the laws of the phenomenon of "water hammer." Water hammer is the term commonly applied to the sudden rise in pressure which results when the flow in a pipe is quickly stopped by the sudden closure of a valve. It is closely related to the smaller rise in pressure due to a slow closure of the valve and to the fall in pressure as a valve is opened. In fact any change of velocity is accompanied by a change in pressure whose initial sign depends upon the sign of the velocity increment. Joukowsky in his admirable work of 1897–98[1] found the maximum water-hammer pressure which may be produced by the sudden closure of a valve to be given by the formula:

$$P = \frac{\lambda V w}{g} \qquad (1)$$

where

P = water hammer pressure (in excess of the static pressure) in pounds per square inch.
λ = the velocity of wave motion in the pipe.
V = the extinguished velocity of the water.
w = the weight of a cubic unit of water.
g = the acceleration due to gravity in feet per second per second.

If the pressure is converted into head, then

$$h = \frac{\lambda V}{g}. \qquad (2)$$

The value of λ as derived by Joukowsky is

$$\lambda = \frac{1}{\sqrt{\frac{w}{Kg} + \frac{d}{e}\frac{w}{Eg}}} \qquad (3)$$

---

[1] Joukowsky, N., *Über den Hydraulischen Stoss in Wasserleitungsröhren* in *Ann. Imp. Acad. Sci. of St. Petersburg*, 9: 5. (Published in Russian and German.) An excellent synopsis of this work, by O. Simin, may be found in the *Trans. of the Amer. Waterworks Assn. of 1904.*

where,

K = the volumnar modulus of elasticity of water (about 294,000–300.000 pounds per square inch).

d = diameter of the pipe.

e' = thickness of the pipe walls.

E = modulus of elasticity of the material of the pipe.

If W is expressed in pounds per cubic foot,

K in pounds per square inch,

g in feet per second per second,

d in inches,

e in inches,

E in pounds per square inch, and

λ in feet per second then (3) becomes

$$\lambda = \frac{12}{\sqrt{\frac{w}{g}\left(\frac{1}{K} + \frac{d}{e'E}\right)}} \qquad (4)$$

and varies from about 3.000 to 4.700 for ordinary sizes of pipe.

Joukowsky verifies these formulas both by deductive mathematical reasoning and by experiment.

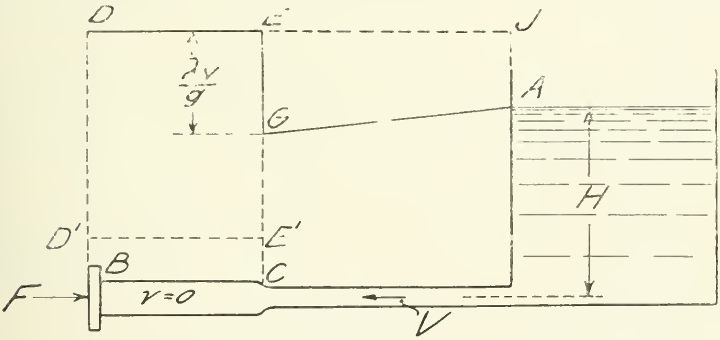

FIG. 9.

Let Figure 9 represent a pipe through which water was flowing only a moment ago with a velocity V. Suppose the gate B to be instantly closed as in the figure. The entire column of water will not be brought to rest at once. due to the elasticity of the pipe and water. The layer of water immediately adjacent to the valve B is first compressed and the pipe expanded. This process follows with each elementary layer in succession from the gate to the reservoir, thus having the nature of a pressure wave running along the pipe with velocity λ. The water to the right of C, the front of the wave, continues to flow toward the gate with its initial velocity V. The hydraulic gradient is shown by the line D E G A. When C finally reaches the supply reservoir the entire column of water is under a uniform pressure higher than the supply head, as shown by the hydraulic gradient D E J A, Figure 9, and is at rest. This condition evidently cannot continue. The result is that the layer adjacent to the reservoir expands at once to normal volume and the pipe surrounding it contracts, thus giving to this layer of water a velocity V toward the supply reservoir. The next layer follows and so on until the pressure is reduced to the original pressure throughout the pipe and the water all has a velocity V toward the reservoir. This flow of the water from the gate tends to vacate the pipe near the gate and thus rarefies the water here. This negative pressure wave then follows the same cycle as outlined for the higher pressure with a corresponding hydraulic gratient shown by line D′ E′ G A. This wave continues to traverse the pipe backward and forward until its energy is dissipated through friction.[2]

The writer will not review the derivation of formula (3) in this paper but would like to propose a new derivation for formula (1) based upon principles more directly applicable to the case in hand. Joukowsky derives this formula by two methods. One method is based upon the principle of the conservation of energy and the other upon the equality of the volumes of the flow in the pipe for a time $\triangle t$ and the space to be filled by this flow due to expansion of the pipe and compression of the water in a length $\triangle l$ of pipe.

The method the writer wishes to propose is based upon the principle of acceleration and retardation of masses by applied forces. Church[3] has studied from this standpoint the effect on the pressure in a pipe due to closing a valve very slowly at a uniform rate and also at variable rates. The equations are too complicated for a general solution, but he gives graphical solutions of particular cases. In his analysis he neglects the elasticity of the water. This can be safely done for slow closures only, as will be seen by the following analysis.

---

[2] For a further discussion of this process see the article by O. Simin in the *Trans. Am. W. W. Ass'n, 1904*. pp. 353-361.

[3] *Jour. Frank. Inst.*, **129**: 328, 374.

Let M equal the mass of water to be brought to rest from an initial velocity V by force F then (with a rate of retardation a) we have

$$F = Ma. \tag{5}$$

The force F which retards the water is equal to the excess of unit pressure in the pipe at the end over the static pressure, multiplied by the cross-sectional area of the pipe. When the valve is instantly closed, were it not for the elasticity of the water and pipe, the velocity V would be extinguished in zero time and therefore $a = \infty$ hence $F = \infty$ and also $P = \infty$. In reality the pressure P is limited, for the initial velocity V cannot be extinguished in less time than required for a wave to traverse the pipe $= \frac{l}{\lambda}$. Only one elementary layer of water is brought to rest at a time, and the maximum rate of retardation is therefore,

$$\frac{dv}{dt} = \text{acc.} = \frac{V}{\frac{l}{\lambda}} = \frac{\lambda V}{l}.$$

But

$$M = \frac{Alw}{g}$$

and

$$F = PA.$$

Substituting in (5)

$$PA = \frac{Alw}{g} \cdot \frac{\lambda V}{l},$$

or

$$P = \frac{\lambda Vw}{g},$$

the same [see equation (1)], as obtained by Joukowsky by other methods. Here l=length of pipe, and A=area of cross-section of pipe.

This pressure amounts, for ordinary pipes, to about 60 pounds per square inch for each foot of extinguished velocity.

Where the velocity is very slowly extinguished the elasticity of pipe and water has a very slight effect upon the pressure. The general formulas for all cases are,—

$$\text{acc.} = \frac{dv}{dt},$$

$$M = \frac{Alw}{g}.$$

$$F = PA,$$

$$P = \frac{lw}{g} \cdot \frac{dv}{dt}, \qquad (6)$$

$$h = \frac{l}{g} \cdot \frac{dv}{dt}, \quad \text{or}$$

$$\frac{dv}{dt} = \frac{g}{l} \times \text{(accelerating head)} \qquad (7)$$

where $\frac{dv}{dt}$ is (for any particular pipe) a function of the law and rate of closure of the valve, but can never be greater than λ, even though the valve close in zero time.

It will be seen as we proceed that the analysis of each stage of operation of the hydraulic ram is an application of formula (7).

THEORETICAL ANALYSIS

For convenience of reference, the meanings of the symbols used in this analysis are given in an Index to Nomenclature at the end of the paper, and are therefore omitted here.

The two principal periods of operation of the ram are:

1. The accumulation of kinetic energy at the expense of the potential energy of the supply-water while the waste valve remains open.

2. The transformation of this kinetic energy into potential energy in the form of water pumped while the waste valve is closed.

The former is a problem of acceleration under the influence of applied forces; the latter a problem of retardation.

FIRST OR ACCELERATION PERIOD

The condition during the first period is illustrated in Figure 10. The check valve is closed and water is flowing from the waste valve with increasing velocity. The head h_1 is that necessary to discharge the water through the waste valve, as through an orifice, and is therefore increasing as the water in the drive-pipe accelerates.

The velocity of discharge from the waste valve equals

$$v_1 = \sqrt{2gh_1} = \frac{A}{a_v} v.$$

Hence

$$q_1 = ca_v \sqrt{2gh_1} = Av,$$

and

$$h_1 = \frac{A^2}{c^2 a_v^2} \cdot \frac{v^2}{2g}. \qquad (8)$$

The entrance loss $= m_1 \frac{v^2}{2g}$.

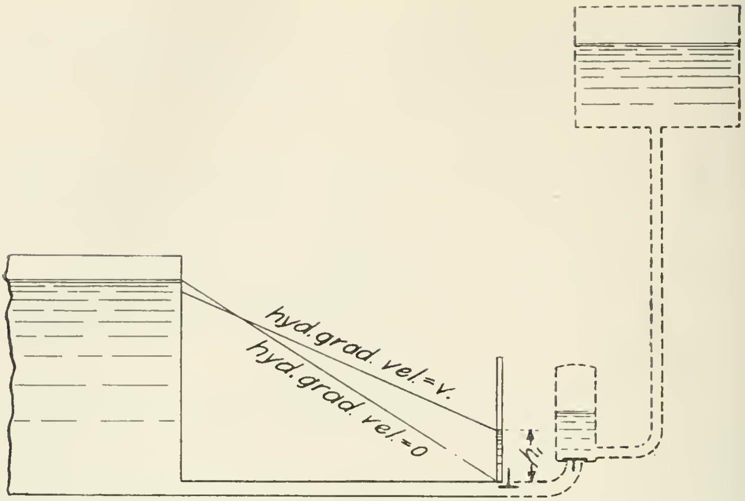

FIG. 10.—THE RAM DURING ACCELERATION.

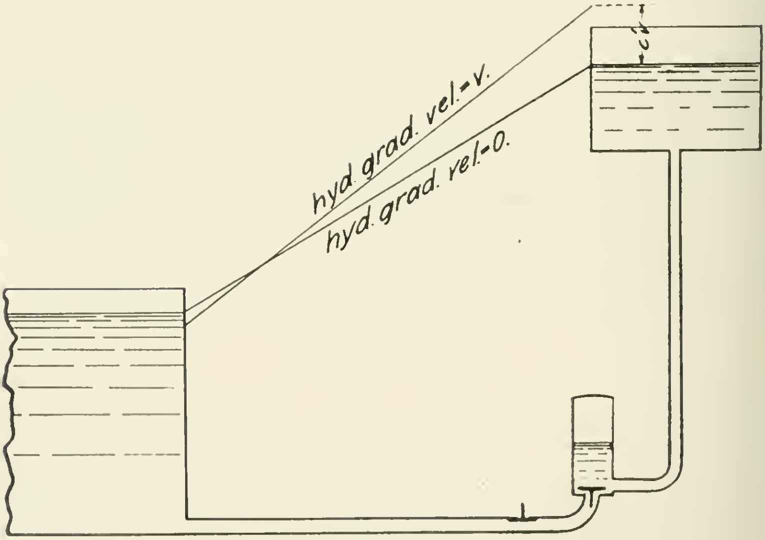

FIG. 11.—THE RAM DURING RETARDATION.

The loss of head due to friction[2] in the drive pipe is $f \frac{l}{d} \cdot \frac{v^2}{2g}$.

The loss due to elbows and other obstructions $= m_2 \frac{v^2}{2g}$.

The unbalanced head which is accelerating the water at any instant is therefore the difference between the supply head and the losses from all causes, or

$$H - \left(m_1 + f \frac{l}{d} + m_2 + \frac{A^2}{c^2 a_v} + \text{etc.} \right) \frac{v^2}{2g}.$$

Therefore,

$$\text{accelerating head} = H - mv^2$$

where

$$m = \left(m_1 + m_2 + f \frac{l}{d} + \frac{A^2}{c^2 a^2} + \text{etc.} \right) \frac{1}{2g}. \tag{8a}$$

The force produced by this head acting upon the area A is

$$F = Aw\,(H - mv^2).$$

The mass of water to be accelerated is

$$M = \frac{Alw}{g}.$$

The acceleration is

$$\frac{dv}{dt} = \frac{F}{M} = \frac{g}{l}\,(H - mv^2), \tag{9}$$

which may also be obtained from the general equation (7) directly. Separating the variables t and v, we have

$$dt = \frac{l}{g} \cdot \frac{dv}{H - mv^2},$$

$$t = \frac{l}{g} \int_0^v \frac{dv}{H - mv^2},$$

and

$$t = -\frac{l}{2g\sqrt{mH}} \log_e \frac{\sqrt{H} - v\sqrt{m}}{\sqrt{H} + v\sqrt{m}}. \tag{10}$$

Let

$$\frac{2g\sqrt{mH}}{l} = j.$$

Solving equation (10) for v, we have

$$v = \sqrt{\frac{H}{m}} \cdot \frac{e^{jt} - 1}{e^{jt} + 1}. \tag{11}$$

---

[2] See Merriman's *Treatise on Hydraulics*, p. 208.

It will be noticed that

$$v = \sqrt{\frac{H}{m}} \tag{11a}$$

is the equation for the maximum capacity of the pipe obtained by the ordinary method[3] and that $(e^{jt} - 1)/(e^{jt} + 1)$ approaches unity as t approaches infinity.

Thus the velocity continues to accelerate and approach $\sqrt{\frac{H}{m}}$ as a limit. Although the maximum value $\sqrt{\frac{H}{m}}$, is theoretically never reached, yet it is practically reached in a few seconds.

The water wasted in time t is proportional to the distance s moved by the water column in the drive pipe. To find s put

$$v = \frac{ds}{dt} = \sqrt{\frac{H}{m}} \cdot \frac{e^{jt} - 1}{e^{jt} + 1},$$

$$= \sqrt{\frac{H}{m}} \left(\frac{2e^{jt}}{1 + e^{jt}} - 1\right),$$

and

$$s = \sqrt{\frac{H}{m}} \left[\int_o^t \frac{2e^{jt}\,dt}{1 + e^{jt}} - \int_o^t dt\right].$$

Integrating

$$s = \sqrt{\frac{H}{m}} \left[\frac{2}{j} \log_e (1 + e^{jt}) - t - \frac{1}{j} \log_e 4\right],$$

or

$$s = \sqrt{\frac{H}{m}} \left[\frac{2}{j} \log_e \left(\frac{1 + e^{jt}}{2}\right) - t\right]. \tag{12}$$

Since

$$\log_e N = 2.3026 \log_{10} N,$$

then

$$s = \sqrt{\frac{H}{m}} \left[\frac{4.6052}{j} \log_{10} \left(\frac{1 + e^{jt}}{2}\right) - t\right]. \tag{13}$$

The kinetic energy which has been acquired by the water in the drive pipe at any time is

$$\frac{Wv^2}{2g} = \frac{\pi d^2}{4} \times 1 \times 62.5 \times \frac{v^2}{2g}.$$

---

[3] See Merriman's *Treatise on Hydraulics*, p. 241, formula (97).

The potential energy expended to produce this kinetic energy is

$$\frac{\pi d^2}{4} \times 62.5\, s \times H.$$

The efficiency is therefore the quotient, or

$$E = \frac{v^2 l}{2gsH}, \tag{14}$$

where v is obtained from (11) and s from (13). This expression may be called the *Efficiency during the Acceleration Period.*

CLOSURE OF WASTE VALVE

Strictly, the second period should begin at the instant that the velocity in the drive pipe ceases to accelerate and begins to retard. The instant at which this happens is, however, indefinite unless we first know the maximum velocity attained. It occurs some time during the closure of the waste valve but not at the beginning. Until the waste valve begins to close, m is constant. [See equation (8a)]. As a, the area of waste valve opening, begins to decrease in closing, m begins to increase. This causes the rate of acceleration to decrease (the velocity, however, continuing to increase) until it eventually becomes equal to zero.

Thus the maximum velocity is reached when

$$\frac{dv}{dt} = 0 \text{ in equation (9),}$$

or

$$\frac{dv}{dt} = \frac{g}{l}(H - mv^2) = 0.$$

Hence when

$$V = \sqrt{\frac{H}{m}} \tag{15}$$

and

$$m = \frac{H}{V^2}.$$

Thus the velocity v ceases to accelerate at the instant that the waste valve reaches a position such that the resistance of the pipe and waste valve together is sufficient to make V the maximum velocity attainable with conditions of uniform flow under head H. [See equation (11a)].

From (8a)

$$m = \left(m_1 + f\,\frac{l}{d} + m_2 + \frac{A^2}{c^2 a_v}\right)\frac{1}{2g},$$

hence

$$\frac{A^2}{c^2 a^2} = \frac{2gH}{V^2} - \left(m_1 + f\,\frac{l}{d} + m_2\right),$$

and

$$a_v = \frac{A}{c\sqrt{2g}} \cdot \frac{V}{\sqrt{H - \left(m_1 + f\,\frac{l}{d} + m_2\right)\frac{V^2}{2g}}} \cdot \qquad (16)$$

It will be observed that

$$\left(m_1 + f\,\frac{l}{d} + m_2\right)\frac{V^2}{2g}$$

represents the friction and other losses in the drive pipe. The quantity under the radical is therefore h_1 or the head on the

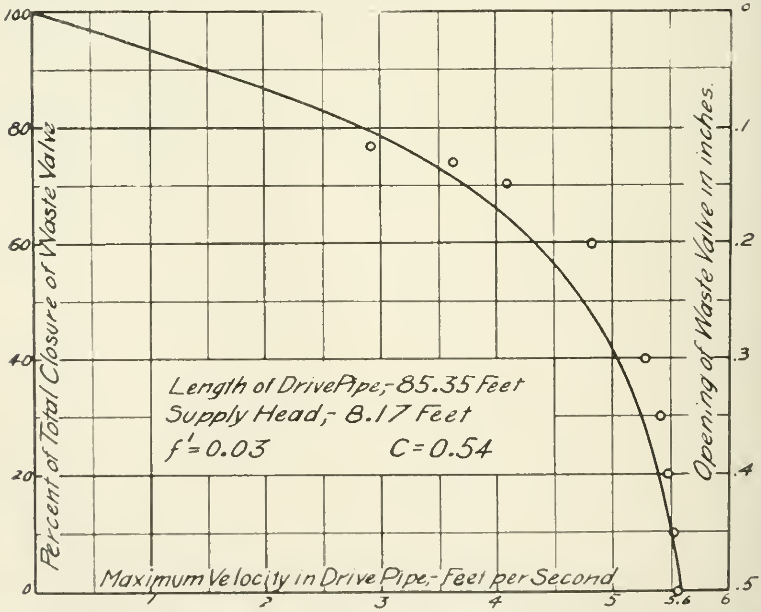

Diagram. I.—Showing the Stage During Closure of the Waste Valve at Which the Velocity Ceases to Increase and Begins to Decreases.

waste valve considered as an orifice. [See equation (8) and Figure 10.] Substituting we get

$$a = \frac{AV}{c\sqrt{2gh_1}}, \qquad (17)$$

which is the area of orifice required to discharge the maximum flow through the drive pipe. Therefore, where V is small, the waste valve is nearly closed before the velocity ceases to accelerate and begins to retard.

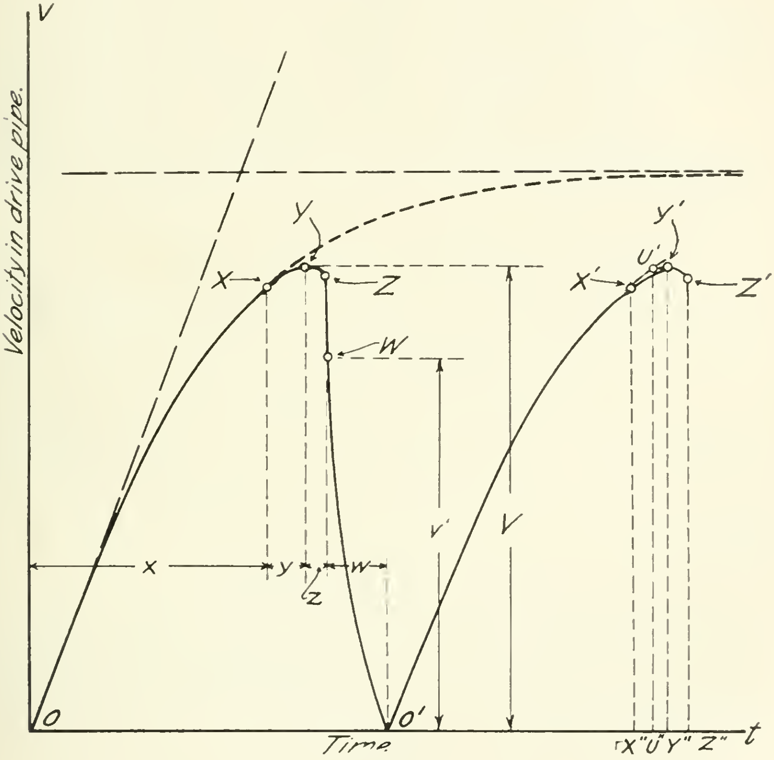

FIG. 12.

The curve in Diagram I was computed from equation (17) for the conditions given on the curve. The points shown were experimentally determined by measuring the maximum flow through the pipe with the waste valve fixed at various openings as shown.

The differential equation which represents the change in velocity during closure is rather complicated and depends upon the rate and law, $\left(R = \frac{da_v}{dt}\right)$, of valve closure. It may be expressed as follows; See equation (9).

$$\frac{dv}{dt} = \frac{g}{l}(H - mv^2)$$

where m, v and t are all variables.

Now

$$\frac{dv}{dt} = \frac{dv}{da_v} \times \frac{da_v}{dt} = \frac{dv}{da} \times R$$

and R is constant only when the valve closes with a uniform velocity.

Hence

$$R\frac{dv}{da_v} = \frac{g}{l}\left(H - \frac{1}{2g}\left[m_1 + m_2 + f\frac{l}{d} + \frac{A^2}{c^2 a_v^2}\right]v^2\right). \qquad (18)$$

The complete curve of v and t is about like that shown in Figure 12 where

X = point where waste valve begins to close,

Y = point where $v = V = \sqrt{\frac{H}{m}}$,

and

Z = point of complete closure of waste valve.

SECOND PERIOD, RETARDATION

Because of the complicated form of the equation which expresses the slope of the curve beyond the point X, it will be convenient to assume that the waste valve closes instantly without loss of velocity.

Now it will be necessary for the velocity in the drive pipe at the time of closure to exceed a certain fixed amount before any water will be pumped. This *critical velocity*, upon the assumption of instantaneous closure, will be that velocity which will produce a water-hammer head just equal to the pumping head. From equation (2) this velocity will be

$$v = \frac{gh}{\lambda},$$

which for the drive pipe in use amounts to one foot decrease in velocity for each 136.3 foot pumping head. (See page 208).

When V exceeds this critical value, it must be instantly retarded by an amount sufficient to overcome the pumping head and the initial friction head through the check valve and also the friction loss in the drive pipe for the initial velocity of flow in the drive pipe after closure of the check valve.

It was found by actual measurements, which will be described later, that the loss of head in the check valve varies as the first power of the rate of flow through it. This rate of flow is proportional to the velocity v in the drive pipe and hence

the check valve loss $= c'v$.

where c' is an experimental constant, the value depending upon the check valve used. Hence

$$\frac{\lambda}{g}(V - v') = h + c'v' + mv'^2. \qquad (19)$$[4]

Solving for v' we have

$$v' = \frac{-\left(c' + \frac{\lambda}{g}\right) + \sqrt{\left(c' + \frac{\lambda}{g}\right)^2 + 4m\left(\frac{\lambda}{g}V - h\right)}}{2m}. \qquad (20)$$

Expanding the radical into an infinite series to make the computation of v' more simple, we have

$$v' = \frac{\left(\frac{\lambda}{g}V - h\right)}{\left(c' + \frac{\lambda}{g}\right)} - m\frac{\left(\frac{\lambda}{g}V - h\right)^2}{\left(c' + \frac{\lambda}{g}\right)^3} + \text{etc.} \qquad (21)$$

Now it is found that in reality mv'^2 may be neglected in equation (19) without appreciably affecting the value of v'. Omitting this term and solving, we get

$$v' = \frac{\frac{\lambda}{g}V - h}{c' + \frac{\lambda}{g}}, \qquad (22)$$

which is identical with the first term in (21).

---

[4] The coefficient, m, for the retardation period is: $m = \left(1 + m_1 + m_2 + f\frac{l}{d}\right)\frac{1}{2g}$. The term, 1, is inserted because practically none of the velocity head would be recovered; it takes the place of $\frac{A^2}{c^2a^2}$ for the acceleration period.

Now

$$h' = c'v' = \frac{c}{c' + \frac{\lambda}{g}} \left(\frac{\lambda}{g} V - h \right). \tag{23}$$

This instantaneous drop $(V - v')$ in v is represented in Figure 12 by Z W.

Assuming now that the waste valve has closed and the velocity has been reduced from V to v' in order to create a pressure of $h + h'$, we will consider the forces acting upon the column of water in the drive pipe. The only head tending to accelerate the water is the head H. The heads opposing this acceleration are H, h, $c'v$ and mv^2. The H's cancel and leave a retarding head of $h + c'v + mv^2$. From the general equation of acceleration and using a negative sign to indicate retardation, we have

$$\frac{dv}{dt} = -\frac{g}{l}(h + c'v + mv^2), \tag{24}$$

or

$$dt = -\frac{l}{g} \cdot \frac{dv}{h + c'v + mv^2}. \tag{25}$$

This function has two integrals depending upon the value of the discriminant $(c'^2 - 4mh)$.

Case I:—(Low Heads), when $c'^2 > 4mh$

The integral of equation (25) gives

$$t = -\frac{l}{g\sqrt{c'^2 - 4mh}} \log_e \frac{2mv + c' - \sqrt{c'^2 - 4mh}}{2mv + c' + \sqrt{c'^2 - 4mh}} + C_1,$$

where C_1 is a constant of integration. To determine C_1 substitute the simultaneous values, $t = 0$ and $v = v'$, obtaining:

$$C_1 = \frac{l}{gD} \log_e \frac{2mv' + c' - D}{2mv' + c' + D}.$$

Substituting the value of C_1 thus found, we have:

$$t = \frac{l}{gD} \log_e \left(\frac{2mv' + c' - D}{2mv' + c' + D} \times \frac{2mv + c' + D}{2mv + c' - D} \right), \tag{26}$$

or

$$e^{\frac{gDt}{l}} = \left(\frac{2mv' + c' - D}{2mv' + c' + D} \times \frac{2mv + c' + D}{2mv + c' - D} \right). \tag{27}$$

Let

$$\frac{gD}{l} = r',$$

$$C' - D = a,$$

$$C' + D = b,$$

and

$$\frac{2mv' + b}{2mv' + a} = k.$$

Substituting in (27), we have

$$ke^{r't} = \frac{2mv + b}{2mv + a},$$

and solving

$$v = -\frac{1}{2m} \cdot \frac{ake^{r't} - b}{ke^{r't} - 1} = \frac{ds}{dt}. \tag{28}$$

Integrating again:

$$s = -\frac{1}{2m}\left[bt - \frac{2D}{r'}\log_e\left(1 - ke^{r't}\right)\right] + C_2.$$

Putting $s = 0$ when $t = 0$, we determine the constant of integration,

$$C_2 = -\frac{D}{mr'}\log_e(1 - k).$$

Simplifying,

$$s = \frac{D}{mr'}\log_e\frac{1 - ke^{r't}}{1 - k} - \frac{bt}{2m}. \tag{29}$$

The total water pumped into the air chamber will be proportional to the total distance S traversed by a cross-section of the water column in being brought to rest. To find this time T, required to bring water column to rest, put $v = 0$ in equation (26), obtaining after simplification:

$$T = \frac{l}{gD}\log_e\frac{b}{ka}. \tag{30}$$

Substituting this value of T in equation (29) we have:

$$S = \frac{l}{mg}\log_e\frac{2mv' + a}{a} - \frac{bl}{2mgD}\log_e\frac{b}{ka}. \tag{31}$$

The quantity of water pumped will be A S w and the energy recovered will be A S w h. The kinetic energy from which this was derived is $\frac{AlwV^2}{2g}$. The efficiency during the retardation period is therefore the quotient, or

$$E' = \frac{2gSh}{lV^2}. \tag{32}$$

Case II:—(High Heads), when $4mh > c'^2$

Assuming equation (25) which applies to both cases, we have

$$dt = -\frac{l}{g} \cdot \frac{dv}{h + c'v + mv^2}.$$

Integrating

$$t = -\frac{l}{g} \cdot \frac{2}{\sqrt{4mh - c'^2}} \tan^{-1} \frac{2mv + c}{\sqrt{4mh - c'^2}} + C_3.$$

Calling $\sqrt{4mh - c'^2} = D'$ and determining C_3 by the condition that $v = v'$ when $t = 0$, we get

$$t = \frac{2l}{gD'} \left[\tan^{-1} \frac{2mv' + c'}{D'} - \tan^{-1} \frac{2mv + c'}{D} \right]. \tag{33}$$

Let

$$\frac{gD'}{2l} = \beta,$$

and

$$\frac{2mv' + c'}{D'} = \alpha.$$

Take the tangent of both members of (33) and solve for v with the result that

$$v = \frac{D'}{2m} \left(\frac{\alpha - \tan \beta t}{1 + \alpha \tan \beta t} \right) - \frac{c'}{2m} = \frac{ds}{dt}. \tag{34}$$

Integrating and determining C_4 by the fact that $s = 0$ when $t = 0$ (hence $C_4 = 0$) we obtain

$$s = \frac{D'}{2m\beta} \log_e (\cos \beta t + \alpha \sin \beta t) - \frac{c't}{2m}. \tag{35}$$

To determine T, or the time required to bring the water column to rest, put $v = 0$ in (33) and simplify, obtaining:

$$T_c = \frac{1}{\beta} \tan^{-1} \frac{2mv'}{D' + c'\alpha}. \tag{36}$$

From (35)

$$S = \frac{l}{mg} \log_e (\cos \beta T + \alpha \sin \beta T) - \frac{c' T_c}{2m}. \tag{37}$$

This formula may be expressed thus:

$$S = \frac{l}{mg} \log_e \frac{(D' + c'\alpha) + 2mv'\alpha}{\sqrt{(D' + c'\alpha)^2 + 4m^2v'^2}} - \frac{c'T_c}{2m}, \qquad (38)$$

although nothing is gained by using this form of the expression. The efficiency, as for *Case I*, is

$$E' = \frac{2gSh}{lV^2}.$$

Case III:—(Neglecting mv^2)

An approximate formula, applying to all heads and giving results which differ for the economical velocities by only a few per cent. from those obtained by equations (31) and (37), (for S), may be obtained by neglecting the friction and other v^2 losses, thus obtaining from equation (25)

$$dt = -\frac{l}{g} \cdot \frac{dv}{h + c'v}, \qquad (39)$$

and

$$t = -\frac{l}{c'g} \log_e (h + c'v) + C_5.$$

When $t = 0$, $v = v'$,
hence

$$C_5 = \frac{l}{c'g} \log_e (h + h')$$

and

$$c'v' = h'.$$

Therefore

$$t = \frac{l}{c'g} \log_e \frac{h + h'}{h + c'v}. \qquad (40)$$

Solving (40) for v and letting $r = \frac{c'g}{l}$, we have:

$$v = \frac{h + h' - he^{rt}}{c'e^{rt}} = \frac{ds}{dt}, \qquad (41)$$

Integrating (41) we obtain:

$$s = -\frac{h + h'}{c'r} e^{-rt} - \frac{h}{c'} t + C_6.$$

When $t = 0$, $s = 0$, hence

$$C_6 = \frac{h + h'}{c'r}$$

and

$$s = \frac{(h + h')}{c\ r}(1 - e^{-rt}) - \frac{h}{c'}t. \qquad (42)$$

Putting $v = 0$ in (40), we get the time T required to extinguish the entire velocity:

$$T_c = \frac{1}{r} \log_e \frac{h + h'}{h}. \qquad (43)$$

Hence from (42), when $t = T$, may be readily derived:

$$S = \frac{1}{c\ r}\left(h' - h \log_e \frac{h + h'}{h}\right). \qquad (44)$$

Again

$$E' = \frac{2gSh}{lV^2} \text{ as for } \textit{Cases I} \text{ and } \textit{II}. \quad (32)$$

Case IV:—The fact that, in the experimental ram to be described later, the loss of head due to the check valve varies as the first power of v is probably due to the unusual construction of the valve. It is probable that it will more commonly vary as v^2, and we shall therefore derive equations for its condition. These equations may be obtained by assuming the original differential equation to be of the form

$$dt = -\frac{l}{g}\,\frac{dv}{h + Mv^2}, \qquad (45)$$

where

$$M = (1^* + f\frac{l}{d} + m_1 + m_2 + m')\frac{1}{2g}$$

and the new term m' represents the coefficient of loss through the check valve. The result desired may, however, be more easily obtained by making $c' = 0$ and $m = M$ in the previous equations for *Case II*, thus obtaining, after simplification: from (34)

$$v = \frac{v'\sqrt{\frac{M}{h}} - \tan\frac{g\sqrt{Mh}}{l}t}{\sqrt{\frac{M}{h}} + \frac{Mv'}{h}\tan\frac{g\sqrt{Mh}}{l}t}; \qquad (46)$$

---

[*] The coefficient, 1, is inserted because practically none of the velocity head is recovered when water is discharged through a valve into the air chamber.

from (36)

$$T_c = \frac{1}{g\sqrt{Mh}} \tan^{-1} v' \sqrt{\frac{M}{h}}; \qquad (47)$$

from (38)

$$S = \frac{1}{mg} \log_e \sqrt{1 + \frac{mv'^2}{h}}; \qquad (48)$$

and from (20)

$$v' = \frac{-\frac{\lambda}{g} + \sqrt{\left(\frac{\lambda}{g}\right)^2 + 4M\left(\frac{\lambda}{g} V - h\right)}}{2M}. \qquad (49)$$

The general form of the v-t curve during the second period, after the initial sudden decrease (Z W) in v, is shown in Figure 12 by line W O′.

EFFICIENCY OF THE MACHINE OR TOTAL EFFICIENCY

The efficiency E during the acceleration period expresses the proportion of the original potential energy of the waste water which is concerted into, and is therefore available as, kinetic energy for pumping water in the second period. The difference between this and the original energy is dissipated by friction in the drive pipe and converted into the useless kinetic energy of the water as it flows from the waste valve.

The efficiency E′ during the retardation period expresses the proportion of the useful kinetic energy acquired by the water in the first period which is conserved in the form of useful work done in raising water to the height h in the second period.

The efficiency of the machine is therefore equal to the product of the efficiencies obtained during the two periods, or

$$E_m = EE' \qquad (49a)$$

OPENING OF THE WASTE VALVE

Figure 11 shows the condition existing in the drive pipe during the retardation period. The waste valve is closed; the check valve is open and water is flowing through it into the air chamber. The hydrostatic pressure-head in the water below the check valve is equal to the sum of pumping head, supply head and friction head through the check valve. The hydraulic gradient when the velocity is v is shown in the figure by line A′ D. As the velocity is gradually extinguished. the point D falls toward C. and at the instant when the velocity becomes 0 the gradient is shown by the line AC. At this instant the water is in a compressed condition and the pipe is distended due to the excess of pressure, varying from 0 to h. above the supply pressure, and the condition is the same as during the compression wave discussed in connection with water hammer (see Figure 9) except that the excess of pressure above the supply pressure is not equal at all points along the pipe. This condition is obviously unstable and results in an expansion of the water together with a contraction of the pipe to normal size and a consequent slight flow of water back into the supply tank. Were the waste valve to remain shut. we should thus obtain alternate compression and rarefaction waves until the wave energy would be gradually dissipated by friction. The first rarefaction wave, however, opens the waste valve and starts a new cycle of events.

CLOSING OF WASTE VALVE

The waste valve closes due to three influences:

(1) The hydrostatic pressure against the bottom of the valve disk.

(2) Impact of the water against the valve disk in discharging.

(3) Frictional force exerted by the discharging water upon the valve.

The writer believes the first cause to be by far the most important at least in the case of this ram. Figure 10 shows the condition at the instant after the waste valve has opened. The hydraulic gradient has instantly fallen to the position AB[5], the pressure head being zero at the waste valve and increasing uniformly toward the supply tank. As the water in the drive pipe accelerates, the pressure must rise at B in order to discharge the increasing flow of water through the valve opening as though an orifice. The hydrostatic pressure thus produced on the under side of the valve is only partially balanced from above, and the result is an ultimate increase of pressure until the valve begins to close. Once started, the pressure increases more rapidly, due to the resulting water-hammer pressure, and the tendency is to rapidly accelerate the valve until it is stopped by impact against its seat. An autographic record of a waste valve action taken from the "Rife Hydraulic Engine No. 20" is shown below in Figure 13.

---

[5] Strictly the average head only for the first fraction of a second is represented by the gradient AB as the sudden change in pressure at B, due to opening, causes an oscillating water hammer wave in the drive pipe which, however, quickly subsides.

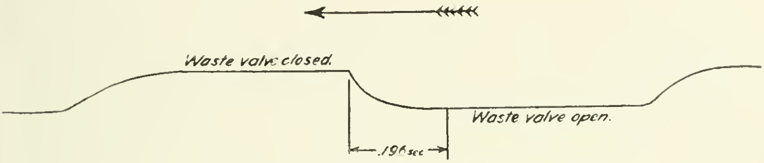

FIG. 13.

EFFECT OF THE ASSUMPTIONS

Several assumptions, only approximately true, were made in the foregoing analysis, the effects of which will now be considered.

In assuming that the waste valve closes instantly, thus conserving the entire kinetic energy resulting from the maximum velocity of water in the drive pipe, we are increasing the theoretical efficiency of both cycles above what could be obtained by experiment.

Referring again to Figure 12, we see that the velocity of the water accelerates during a part of the closure of the valve. It will be observed that $s = \int vdt$ and that this expression is also equivalent to the area bounded by the curve OX, the t axis and any ordinate at point t. The area of this figure is therefore proportional to s, which is again proportional to the water wasted.

At X and X′ the waste valve begins to close, and the rate of acceleration of the water begins to decrease more rapidly until the maximum velocity V is reached at Y and Y′. The energy expended in generating the increment of velocity from X to Y is proportional to the area of the figure X′ Y′ Y″ X″. Had the waste valve remained completely open, this increment of velocity would have been obtained by wasting an amount of water proportional to the area X′ U′ U″ X″. It is evident that this decrease in efficiency during the acceleration period, due to waste valve closure, can be made smaller by a more rapid closing of the waste valve because of the decrease that this will bring about in the ratio of the area U′ Y′ Y″ U″ to the total area of the curve O′ Y′ Y″.

During that part of the closure from Y to Z, a portion of the maximum velocity V is extinguished with some waste of water and without pumpage and hence reduces v′ below that given in the formula, thus affecting the result in the pumping period also.

In computing the instantaneous loss (ZW, Figure 12) of velocity necessary to raise the pressure up to the initial pumping pressure h′ no account was taken of the effect of this sudden rise in producing a vibratory pressure wave throughout the length of drive pipe, thus consuming energy and doubtless reducing the efficiency. This can not readily be expressed quantitatively from a theoretical standpoint, and more experiments are needed before conclusions can be drawn from them.

Another assumption which was made in the foregoing analysis and whose effect on the relative efficiencies is uncertain is that the pumping head h remains constant during the pumping, or retardation, period. Now, in reality, the water enters the air chamber only periodically. The air is compressed and the pressure rises during this pumping period, only to drop again during the acceleration period, for water is discharging from the air chamber but none is entering during this period. The writer has not been able to integrate the general equation involving the true variable h which is a function of the amount of air in the air chamber and of the rate at which water is entering and leaving. He is therefore not prepared to state quantitatively the effect of this omission in the theoretical formulas. It is, however, evident that if the head h, as recorded experimentally, were the initial or lowest head this would operate to decrease the experimentally determined efficiencies. In the experiments to be described later the head recorded was, in each case, the average head during the stroke and the effect of this on the comparison between experimental and theoretical data cannot be stated.

Again, the slip through the check valve at the conclusion of the retardation or pumping period has been neglected. Assuming the general equation (24) of retardation

$$\frac{dv}{dt} = -\frac{g}{l}(h + c\,v + mv^2)$$

and putting $v = 0$, we have

$$\frac{dv}{dt} = -\frac{gh}{l} \qquad (50)$$

as the expression for the rate of retardation at the end of the pumping period. The conditions under which the flow into the air chamber ceases are therefore always identical for equal values of h and will doubtless be succeeded by equal amounts of slip. The correction for slip will need to be determined experimentally, and the equation for efficiency corrected for slip will take the form of

$$E' = \frac{2g\,(S - s')\,h}{lV} \qquad (51)$$

where s′ is the slip.

The effect which slip has upon the efficiency is evidently proportionately greater for small velocities and hence tends to increase the efficient velocity above that obtained theoretically especially for low pumping heads.

EXPERIMENTAL APPARATUS

At the time the writer undertook this work the hydraulic laboratory at the University was equipped with a "Rife Hydraulic Engine No. 20," having a two-inch drive pipe and facilities for varying its length, as well as the supply head and pumping head. Since there are a number of other conditions effecting the operation of a ram in addition to those named, it was decided to construct a ram with more flexibility of adjustment and control than could be obtained in any commercial ram on the market.

Result Desired

In the design of apparatus for experimental work and in the design of the ram itself means were sought by which each of the following conditions could be varied independently:

1. Supply head,
2. Pumping head,
3. Length of drive pipe,
4. Size of drive pipe,
5. Time during which the waste valve remains open and hence the *maximum velocity* acquired,
6. Rate of closing the waste valve,
7. Law according to which the waste valve closes,
8. Size of the air chamber,
9. Proportion of the volume of the air chamber filled with air and with water,
10. Amount of opening of the waste valve during acceleration,
11. Type of waste valve,
12. Type and size of check valve.

Continuous autographic records were desired of:

1. Velocity of flow in the drive pipe,
2. Pressure in the drive pipe.

3. Motion of the waste valve,
4. Time.

In addition to a study of the ram the apparatus was to be suitable for experiments upon water hammer.

The Ram

The general make-up of the ram is shown in Plate I. F is the drive pipe leading from the supply tank shown in Plate III. T is a 2″ run, 4″ outlet cast iron tee. The waste valve W, thus far experimented with, and its enclosing chamber were borrowed from the Rife ram No. 20 and bolted, as shown, to the outlet flange A of the tee. G is a gate valve by which the air chamber is shut off when water hammer experiments are to be made but left completely open when the machine is operated as a ram. Its stem is placed horizontally to prevent the accumulation of air. E is a 2″ x 4″ expanding elbow with a special 16″ flange H at the 4″ end. B is a blind flange drilled and used as a valve seat or grid for the check valve. The air chamber is formed of two sections K and L, of 10″ standard wrought flanged pipe one foot and two feet long, respectively, and closed at the top by a blind flange C. Both sections of the air chamber provided with saddle flanges D for the connection of a 2″ discharge pipe, the intention being to vary the height of the air chamber through one, two and three feet. The check valve thus far used was also borrowed from the Rife ram and bolted to the upper side of flange B. The hole through the flange B reduces by means of a curve from the 4″ diameter of the elbow to the diameter of the valve opening.

Both check valve and waste valve are shown in detail in Plate II. A is the outlet flange of the tee T shown in Plate I. B is the casting which formed the valve seat on the Rife ram. C is a soft rubber valve disk held in place by a small washer above and a larger one and a cap screw below.

The check valve is shown at the left of Plate II. D is one of eighteen openings for the flow of water through the valve. The valve disk E is of soft rubber held securely against its seat in

Plate I.

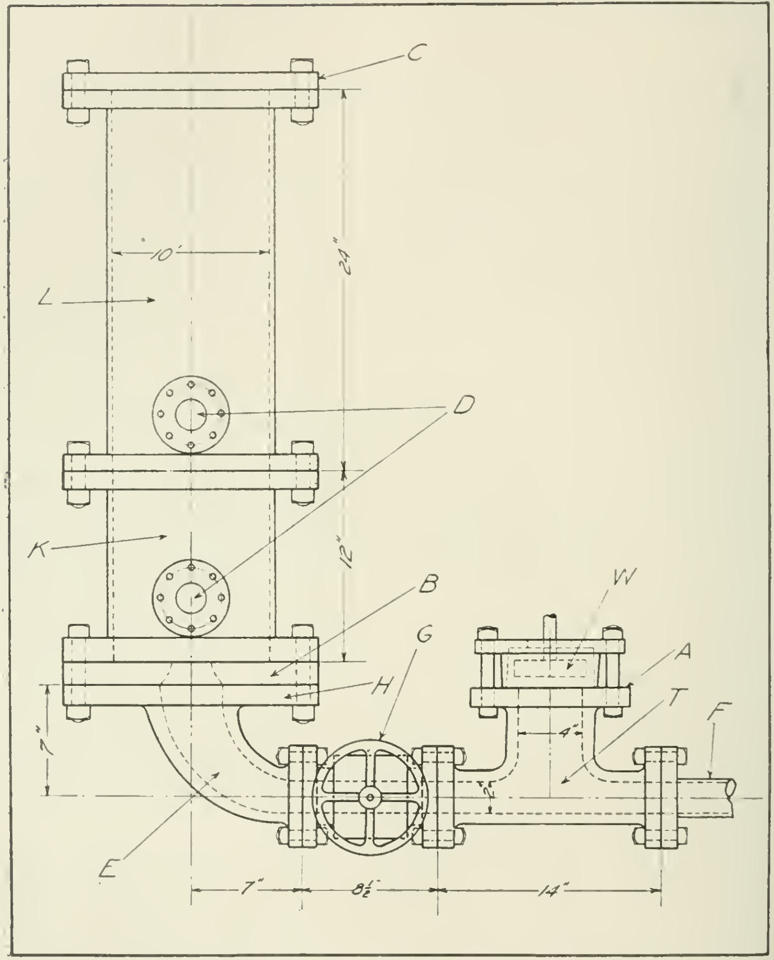

Plate II.

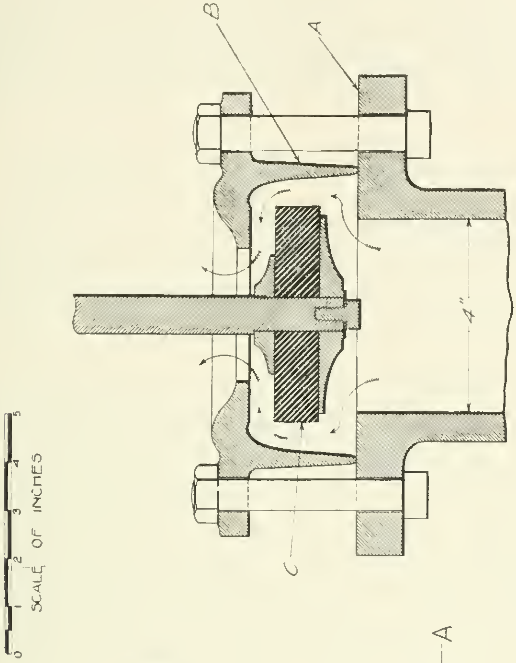

SCALE OF INCHES

VERTICAL SECTION OF WASTE VALVE

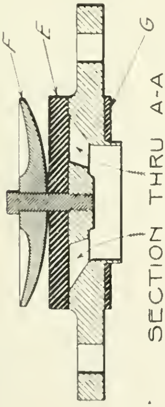

SECTION THRU A-A
OF CHECK VALVE COMPLETE

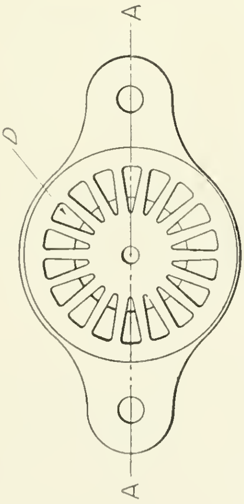

PLAN OF VALVE SEAT

the middle by a bolt but free to bend upward around the edge due to the pressure of the water from below. The amount which the valve can open is limited by the curved lower surface of the casting F. The valve is bolted to the blind flange B, (Plate I), by two bolts and made water-tight by the gasket G, (Plate II).

METHOD OF VARYING THE CONDITIONS OF OPERATION

Plate III shows the general arrangement of all apparatus. The method by which the various conditions outlined at the first of this chapter were, or are to be, varied will now be described by reference to this plate.

1. *Supply Head:*—The supply tank C is shown at the right of the figure. It is fed from the water main through a lead pipe which allows freedom of adjustment to any position. The inlet pipe is closed at the end by means of the float valve D, which automatically maintains the water at a nearly constant level in the supply tank C. The water level in the tank is read by means of the water-column E and the accompanying scale which is graduated to feet and tenths. Water enters the drive pipe F through a bell-mouth G which is provided with four guide plates to prevent eddying. The tank rests upon two rods H which are placed in slots cut in four strips of steel plate, which are in turn bolted to four vertical wooden posts. The slots in the steel plates are spaced 6″ on centers thus allowing the elevation of the tank to be varied by 6″ steps if desired. At each change of elevation the section F_1 of drive pipe F must be removed and replaced by another piece of the required length.

2. *Pumping Head:*—The head against which the water is delivered is created by means of the valve I shown toward the left of Plate III. A Bourbon and also a mercury pressure gage communicate with the air at the top of the air chamber. Since the supply head H (Fig. 1) is measured above the elevation K (Plate III) of the waste valve the total discharge head, $H + h$, must be taken as the pressure head existing in the water in the

Plate III. 160

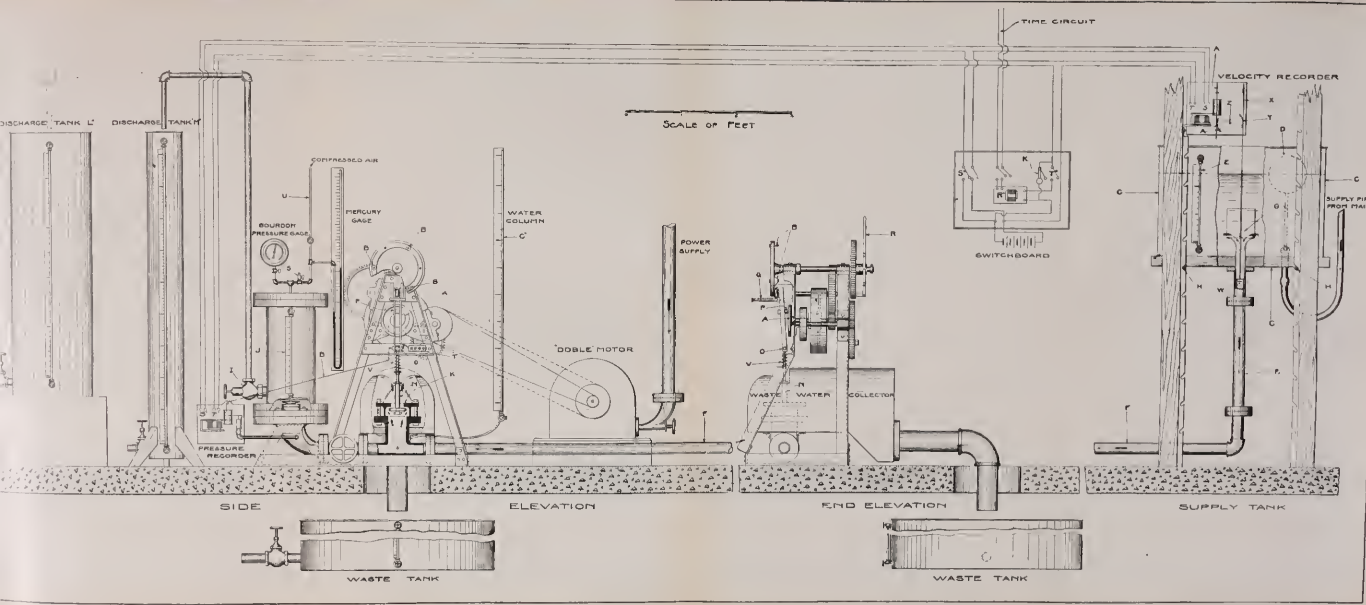

air chamber at the same elevation. This quantity might have been recorded directly by connecting the pressure gages to the air chamber at that elevation, i. e., 0.15 feet above the bottom of the chamber. They were, however, connected to the top so as to be filled with air instead of water, thus avoiding the difficulties which would otherwise have been encountered in keeping air bubbles out of the gage tubes.

The total head is therefore,—

$$H + h = \text{gage reading} + \text{height of water in air chamber} —0.15,$$

the height of water being read by means of the water-glass and graduated stick J.

The water pumped was measured either in tank L or M (depending upon the quantity to be measured) both graduated to read in pounds, and with capacities of 450 and 90 pounds respectively. The water wasted was collected as it discharged from the waste valve in an especially designed collector tank from which it was conveyed in a 4″ pipe through a manhole in the floor to a waste tank of 3,000 pound capacity in the basement.

3. *Length of Drive-Pipe:*—The method of changing the length of drive pipe is obvious. It required moving the ram, and accessories each time.

4. *The size of drive pipe:*—This has not yet been varied. It will require new pipe and fittings.

5, 6 & 7. *Valve Motion:*—For the control of the waste-valve motion a special machine was designed and built and run by a "Doble" water motor taking water from the main. Two views of this machine are shown in Plate III and details of the most essential parts, the cams, are shown in Plate IV.

Referring first to Plate III it will be observed that the rod N (which carries the waste valve at its lower end as shown in Plate II) passes upward through the top of a waste water collecting tank and through a guide in the frame work of the machine to a joint O. Above this joint a cam follower or roller P which rolls at intervals upon the cam A (see also Plate IV) is attached. This cam closes the valve. A compression spring V of adjustable strength acting downward upon the rod keeps the valve open until closed by the cam A. A tension spring Q holds the roller P free from cam A until one of the secondary cams B, by acting upon another roller attached to the same bar with P, forces roller P into position on its cam and the waste valve closes. The plate to which cams B are bolted rotates at a speed one-twelfth as great as the speed of cam A and contains holes so arranged that 1, 2, 3, 4 or 6 cams can be used at a time and be symmetrically spaced around the circumference of the plate. The bar carrying the cam roller P may also be locked into place and the cam plate B thrown out of gear by means of lever R thus obtaining the same result as would be accomplished with twelve B cams. Taking the number of B cams in use in the order given above, we would obtain one closure of the waste valve during every 12, 6, 4, 3, 2 and 1 revolutions respectively of the cam A, and thus be able to vary the number of strokes per minute through a wide range while maintaining a constant speed of the machine and therefore a constant rate of valve closure. On the other hand, by properly selecting the speeds and number of B cams we may vary the speed of rotation and therefore the rate of valve closure without affecting the number of strokes per minute.

The law of valve closure is determined by cam A of which there are three as shown in Plate IV. The diagram at the bottom of the plate shows the laws of closure obtained by each. The distance C is the time of closure. All three cams allow the same opening, one-half inch, of the valve. Cam A2 was designed to produce a law of closure as nearly as possible like that obtained in the automatic Rife ram which had previously been indicated autographically. Cam A1 reverses the law of A2, and A3 closes the valve with a uniform upward motion.

The time required to retard the water and therefore the time during which the waste valve remains closed is a function chiefly of the maximum velocity of water in the drive pipe, the head pumped against and the length of the drive pipe. Therefore no attempt was made to open the valve mechanically, but rather to allow it to open authomatically in order to determine the

Plate IV

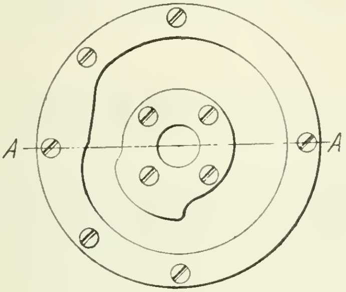

Cam A1

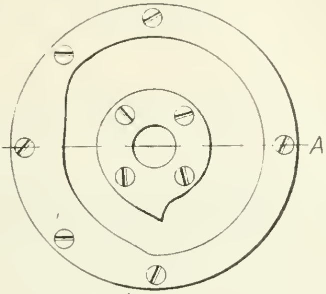

Cam A2

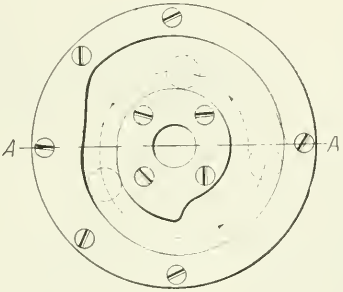

Cam A3

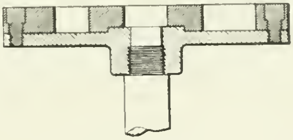

Section on A-A

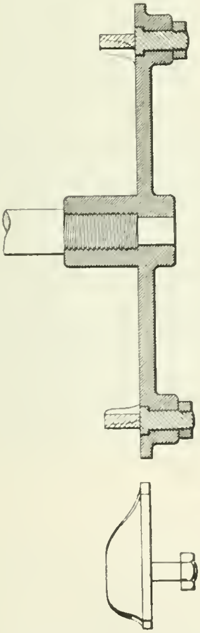

Cam B and Section of Plate

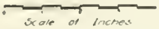

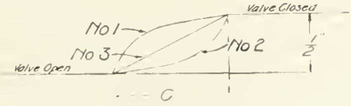

Law of Valve Closure

natural period of time required to retard the water. The A cams were therefore designed so that the valve could open automatically at any time after the closure. In cam A3, Plate IV, several positions of the cam roller are shown and also a path of its center.

The number of valve closures was registered directly by the tachometer T.

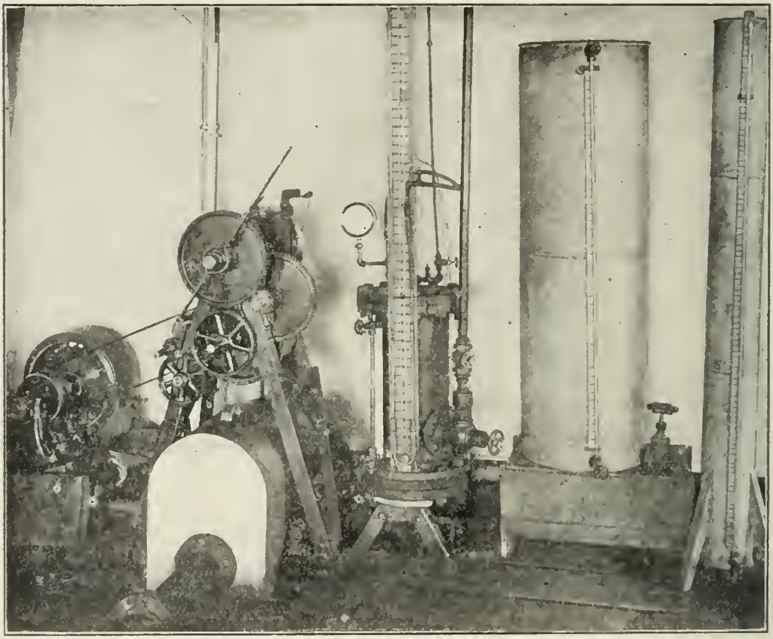

Plate V.

8. *The size of the air chamber:*—This is varied as explained in the description of the ram. Only the two foot height of chamber has been used thus far.

9. *Amount of air in the air chamber:*—To make possible a rapid adjustment of the amount of air in the air chamber a small pipe line U connects the air chamber of the ram with the large air tanks in the University pumping station which carry a pressure of 140 pounds per square inch. An escape

cock S is provided to decrease the amount of air when desirable. Items 10, 11 and 12 have not been investigated experimentally.

Plate V shows an assembly view of the ram discharge tanks, valve control machine and "Doble" motor. The view of the valve-control machine is from the opposite side from that shown in Plate III.

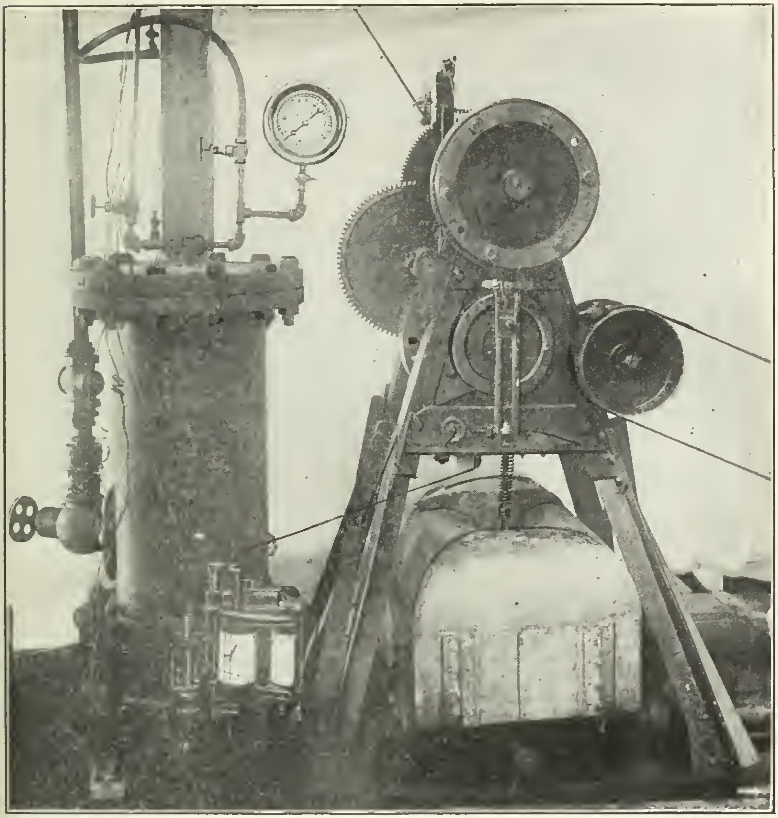

PLATE VI.

Plate VI shows the valve-control machine as in Plate III, together with the air chamber and, in the lower left-hand part of the view, is shown the pressure recorder.

Autographic Recording Instruments

From the theoretical discussion of the ram it is evident that for a comparison of the experimental results with the theoretical, a knowledge of the maximum velocity V of water in the drive pipe is absolutely essential. The measurement however, of this velocity proved to be the most difficult task encountered. Without discussing the relative merits of the various methods considered and experimented with, the adopted method will be described by reference to the diagrammatical sketch in the upper

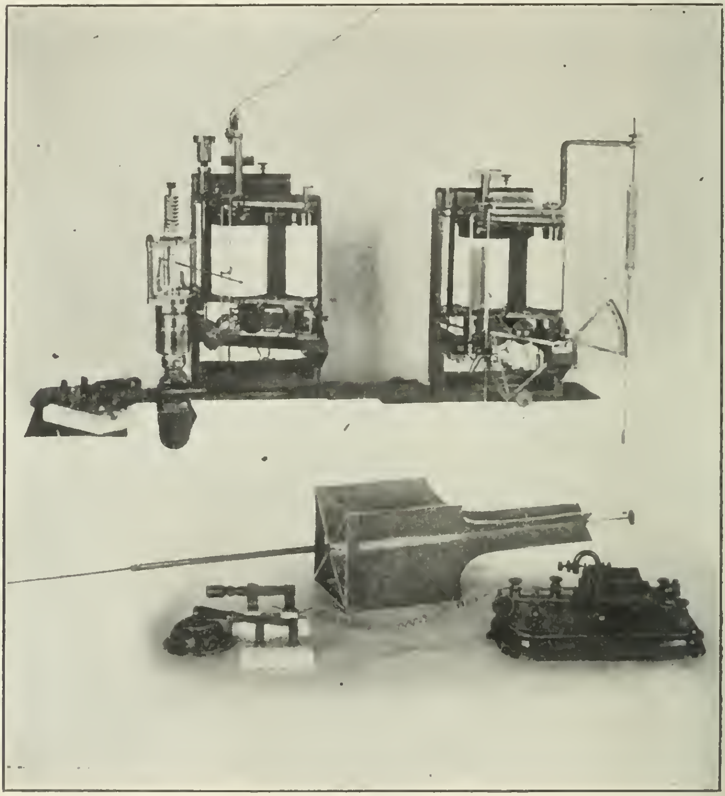

Plate VII.

right-hand corner of Plate III and also to Plate VII, which shows the velocity recording instrument at the right.

The guide vanes which steady the flow into the bell-mouth G radiate from a small central brass tube which extends from the bottom of the guide vanes within the drive pipe to a point a few inches above the water surface in the supply tank. The flow of water in the pipe produces a downward pressure upon a flat circular brass disk W. This pressure is conveyed upward by means of a small rod passing through the brass tube above mentioned and terminating in a fine copper wire fastened to, and passing over, the arc Y. Plate VII shows the guide vanes, disk and disk rod below the recording instruments. The upper end of the disk rod screws into the sleeve nut shown suspended from the arc by a fine wire. Another fine wire passing over the same arc is attached to a spiral spring X. A second arc, oppositely situated to arc Y and rigidly connected with it at knife edge Z moves, by means of two small steel ribbons, a vertical aluminum bar A′ to which is attached the recording pencil. Only one spring X was used, but disks of 5/8″, 3/4″, 1″, 1 1/4″ and 1 1/2″ diameters were used, the choice of disk for any particular observation depending upon the velocity to be measured. The drum upon which the record is made rotates by clockwork but is normally at rest due to the action of a friction brake which can be released magnetically, or by the hand operation of a small lever. A second pencil attached to the armature of a small electro-magnet makes a continuous line on the record with a notch for each second of time.

The frictional resistance offered by the small steel rollers which guide the aluminum bar and by the arc and knife edge arrangement is entirely negligible. The difficulty with the instrument is due to the friction of the disk rod in the tube and to pencil friction. Metallic surfaced record paper and indelible pencil were used in order to reduce the effect of the latter as much as possible.

The instrument was calibrated with each disk separately. The pencil was adjusted so that it just failed to touch the paper, and water was allowed to flow through the drive pipe at a uniform rate, which was determined by measuring, in the discharge tank, the water discharged by the pipe in the given time. The supply tank was lightly tapped meanwhile to eliminate the frictional resistance of the disk rod in the tube. The calibration curves are shown in Diagram II with an exaggerated vertical scale to show better the form of the curves. The scale at the right shows the loss of head in the pipe due to the disk as determined by assuming it equal to the height of a column of water whose cross section equals that of the drive pipe and whose weight is equal to the pressure on the disk.

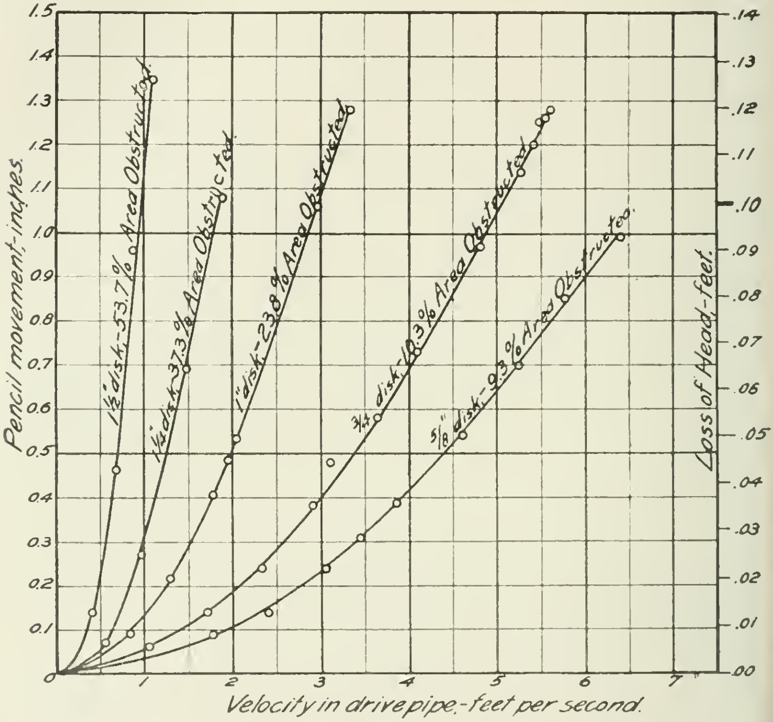

Diagram II.—Calibration Curves of the Velocity Recording Instrument.

The pressure is recorded, as shown to the left of the air chamber, (Plate III) upon a revolving drum by means of an ordinary steam indicator. The indicator cord B′ leads from the joint in the valve rod over two pulleys to the instrument and is opposed by a spring (not shown) thus giving a continuous record of the valve motion. This instrument is also equipped with an electro-magnetic time recorder in series with the one on the velocity instrument.

Both instruments were reconstructed from bridge extensometers of German manufacture which had been discarded for that purpose and were already equipped with the drums, clock work, time recording magnet and magnet for release of the friction brake (not shown in the figure).

In order to obtain simultaneous records from both instruments, the starting magnets were put in series with each other, with a switch S″ and with a battery. The time circuit has its origin in a clock contained in the physical laboratory of the University which breaks an electrical contact each second, thus actuating the relay R″. The secondary of the relay is in series with the battery, the switch T″ and the recording magnets on the two instruments. A telegraph key K′, for numbering records, is connected in parallel with the relay and the switch T″.

Diagram III, page 190, shows typical cards from both the velocity and pressure records, reduced about one-half. The paper moved to the right in both and the arrows show the order in which events occurred.

In all curves the points marked O represent the instant at which the waste valve opened. Points marked C represent the time at which the waste valve completed its closure. The run during which each record was taken is given below the record.

In the cards from the velocity recorder, it will be noticed that the curves fall suddenly below the line of zero velocity at the instant of closure. This is due to the inertia of the moving parts of the instrument and prevented measuring the velocity in the pipe during this retardation period.

In the cards from the pressure recorder, the points marked B indicate where the waste valve begins to close. The pressure in the drive pipe rises only slightly until the waste valve completes its closure.

The lower figure represents a theoretical curve of drive pipe pressure for conditions enumerated below the figure and shows

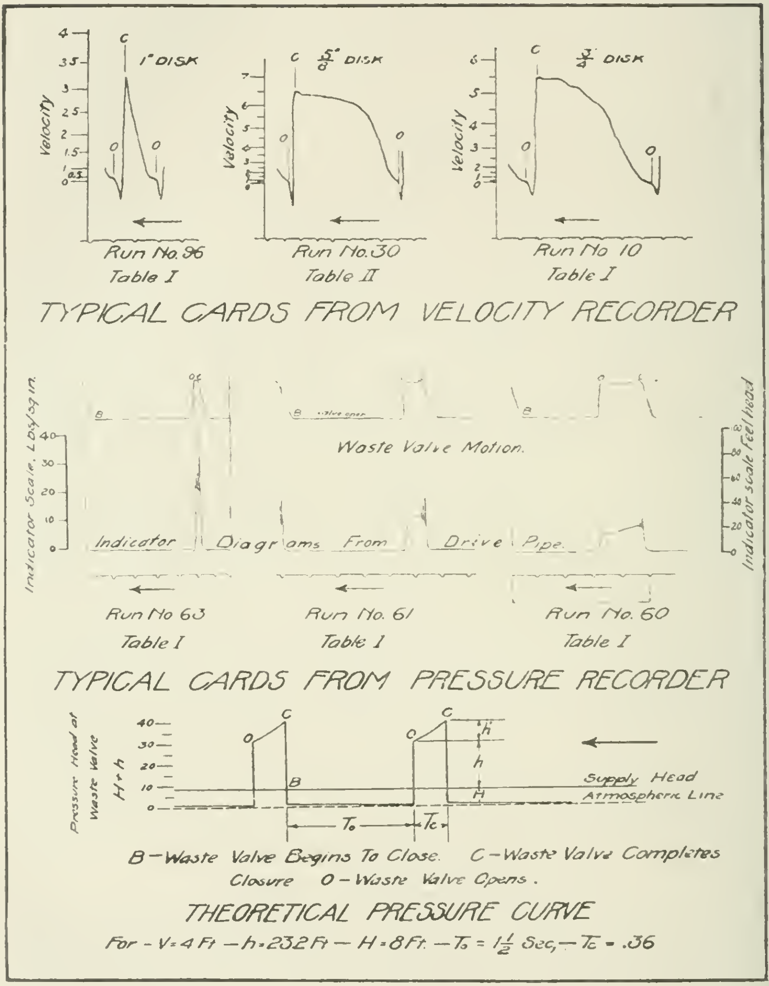

DIAGRAM III.—SAMPLE AUTOGRAPHIC RECORDS.

the same general form although the conditions are not the same as in the autographic records.

The curve of waste valve motion shows that the valve did not close at a uniform rate during the entire motion as was intended. When nearly closed, the water-hammer pressure became sufficient to overcome the spring V (Plate III) and raise the valve suddenly by taking up the play in the valve rod, in the cam roller on its journal and in the cam groove. It was found impossible to eliminate this play.

EXPERIMENTAL VERIFICATION OF THEORY

Observing

The scheme for observing shown in Table VI, was adopted.

The water motor was first regulated to a speed which would give any desired number of revolutions per minute of cam A as shown in the left column. This speed determined the time t required for valve closure, and together with the number of B cams, shown at the top of the columns, determined the number of valve closures or strokes per minute, n. With this speed kept as nearly constant as practicable, runs were then made with total heads, h + H, of 10, 20, 30, 50 and 70 feet. Thus with each (with a few exceptions) of the 36 possible combinations of speeds and cams shown in Table I, five runs were taken making in all 180 runs. Some of the low speeds with few cams were omitted and not many runs were taken with the 288 R. P. M., as this speed proved destructive to the cam rollers. One more or less complete set of runs, as shown by the table, were taken for each of the two lengths of drive pipe which were experimented with and for each supply head used.

The average conditions were:

Table I 85.35 ft. drive pipe. 8.17 supply head
Table II 51.5 ft. drive pipe. 8.16 supply head
Table III 51.5 ft. drive pipe, 6.17 supply head
Table IV 51.5 ft. drive pipe, 4.2 supply head
Table V 51.5 ft. drive pipe. 2.19 supply head

Lack of time prevented the use of any shorter lengths of drive pipe and of more than the one closing ram A3. The five tables mentioned above contain all the observed and computed data. The runs were numbered in the order taken beginning with one for each set of conditions but are grouped in the tables with pumping heads, which were intended to be equal, placed together.

TABLE No I.

LENGTH OF DRIVE PIPE 85.35 FT. HT. OF AIR CHAMBER 2 FT. UNIFORM VALVE CLOSURE SUPPLY HEAD ABOUT 8.2 FT.

Observed								Autographic			Computed					
1	2	3	4	5	6	7	8	9	10	11	12	13	14	15	16	17
Run	B Cams used	Length of Run	Strokes	Supply Head	Pumping Head	Water Wasted	Water Pumped	Maximum Velocity in Drive Pipe	Waste Valve Remains Open	Waste Valve Remains Closed	Valve Closure	Efficiency,—Acceleration Period	Efficiency.—Retardation Period	Efficiency of Machine	Total Water Q+q	Water Pumped q
No.	No.	Min. Sec.	No.	Ft	Ft.	Lbs.	Lbs.	Ft/sec.	Sec.	Sec.	Sec.	Percent	Percent	Percent	Gals/min.	Gals/min.
19	2	7 -36.6	87	8.18	4.9	840	384	4.20	1.78	2.98	.22	42.5	65.0	27.6	19.3	6.05
46	12	15-3.8	388	8.22	1.7	400	519	1.90			.58	80.9	34.0	27.5	22.0	4.13
50	12	21-13	986	8.20	1.5	540	916		0.10	0.85	.32			30.3	8.2	5.2
56	12	22-15.8	1528	8.24	1.3	580	1026		0.08	0.66	.22			27.7	8.7	5.5
60	6	13-28.5	169	8.14	2.2	2705	540	4.88	2.73	1.45	.60	34.8	15.4	5.4	28.9	4.8
65	6	18-14.3	422	8.20	1.9	1450	778	3.12	1.12	1.20	.32	65.5	18.8	12.3	14.7	5.1
70	6	28-7.8	992	8.22	3.3	1140	836	2.20	0.64	0.90	21	97.2	29.8	29.0	8.4	3.6
75	4	19-6.8	314	8.13	3.5	2620	901	4.38	1.97	1.46	.30	53.7	15.3	8.2	22.1	5.7
80	6	37-33.8	1813	8.28	3.7	665	692	1.48	0.35	0.76	.16	136.5 ?	34.3?	46.8	4.3	2.2
89	4	21-38.6	533	8.17	2.5	1280	900	2.44	0.89	1.39	.20	57.5	38.1	21.9	12.1	5.0
94	4	13-45.4	444	8.24	2.6	460	628		0.62	1.15	.15			43.1	9.5	5.5
103	3	22-37.4	566	8.20	3.1	1150	912	2.53	0.90	1.38	.16	73.1	41.3	30.2	11.0	1.3
A 103	3	13-50.6	169	8.07	2.6	2900	569	5.01	3.20	1.49	.31	34.4	18.0	6.2	30.1	4.9
112	3	18-4.6	342	8.20	3.2	1940	844	4.05	1.53	1.36	.20	67.0	25.2	16.9	18.5	5.6
121	2	11-43.2	143	8.18	1.2	2610	463.	5.04	3.40	1.42	.20	32.3	21.6	7.0	31.4	4.7
A 121	2	16-34.1	273	8.19	2.8	2440	806	4.23	2.16	1.42	.15	46.5	23.9	11.1	23.6	5.8
130	1	7-29.0	43	8.10	2.6	2680	126	5.19	8.48	1.38	.22	10.1	14.7	1.5	45.1	2.0
134	1	7-45.4	62	8.17	2.1	2600	277	5.22	6.28	1.01	.16	15.1	18.2	2.8	44 5	4.3

TABLE No I Continued

1 No.	2 No.	3 Min. Sec.	4 No.	5 Ft.	6 Ft.	7 Lbs.	8 Lbs.	9 Ft./sec.	10 Sec.	11 Sec.	12 Sec.	13 Percent	14 Percent	15 Percent	16 Gal./min	17 Gal./min.
138	1	10-3.8	127	8.20	2.0	2270	395	5.06	3.60	1.47	.10	33.2	12.9	4.3	31.8	4.1
14	2	10-51.7	105	8.16	11.8	3150	272	5.51	4.70	1.13	.26	23.6	53.0	12.5	37.8	3.0
18	2	11-55.4	167	8.20	9.2	2400	490	5.21	3.24	0.86	.18	43.7	52.8	23.1	29.1	4.9
47	12	15-13.0	377	8.18	9.7	1780	507	4.0	1.14	0.71	.61	78.5	43.0	33.8	18.1	4.0
49	12	14-17.0	362	8.20	11.0	1590	440	3.25			.42	55.7	66.6	37.1	17.1	3.7
51	12	19-27.2	1021	8.20	13.5	1200	417	2.07	0.58	0.48	.29	84.4	67.8	57.3	10.0	2.6
57	12	9-33.0	691	8.23	11.9	230	86	1.06	0.24	0.34	.21	78.2	69.6	54.4	4.0	1.1
61	6	9-38.2	109	8.15	11.2	2735	192	5.25	4.19	0.57	.66	25.6	37.9	9.7	36.5	2.4
66	6	20-0.6	502	8.21	12.2	2500	636	3.58	1.38	0.70	.30	59.4	63.8	37.9	18.2	3.8
71	6	29-15.7	1091	8.14	11.9	2500	698	2.68	1.01	0.50	.20	73.1	56.0	40.9	13.1	3.0
76	4	13-28.4	222	8.09	13.2	2870	370	4.86	2.70	0.68	.30	42.9	49.2	21.1	28.9	3.3
81	6	20-32.8	934	8.20	12.6	1050	398	2.05	0.70	0.48	16	86.6	67.4	58.3	8.5	2.3
85	6	29-11.4	1958	8.24	12.7	910	362	1.29	0.40	0.38	.12	82.5	68.7	56.7	5.2	1.5
90	4	18-24.2	431	8.14	12.5	2610	584	3.85	1.73	0.67	.21	57.1	60.1	34.3	20.8	3.8
95	4	15-38.6	508	8.13	12.6	1370	423	2.95	1.09	0.60	.15	75.4	63.5	47.9	13.8	3.2
99	4	18-26.4	890	8.23	12.5	930		1.86	0.66	0.50	.10	76.4			6.6	
B 103	3	9-35.4	122	8.06	13.3	2490	217	5.12	3.77	0.71	.30	30.3	47.5	14.4	34.9	2.7
104	3	13-4.2	330	8.14	12.5	1650	402	3.50	1.57	0.68	.15	57.2	65.5	37.5	18.8	3.7
108	3	14-34.4	542	8.16	12.7	1070	356	2.54	1.00	0.60	10	75.8	68.6	52.0	11.7	2.9
113	3	12-6	218	8.15	12.2	2200	365	4.64	2.27	0.69		49.75	49.8	24.8	25.4	3.6
120	2	9-23	119	8.15	13.2	2440	217	5.12	3.80	0.77	.20	29.8	48.3	14.4	34.0	2.8
122	2	11-13.4	173	8.14	13.4	2470	292	4.82	3.09	0.76	.16	38.0	51.3	19.5	29.6	3.1
129	2	13-3.8	317	8.15	13.0	1870	401		1.74	0.65	.10			34.3	20.9	3.7
131	1	7-24.6	46	8.12	12.9	2700	84	5.19	8.93	0.79	.20	10.7	46.3	5.0	45.1	1.4
135	1	8-2.0	67	8.16	13.6	2700	114		6.42	0.69	.15			7.0	42.1	1.[illegible]
139	1	10-32.4	129	8.18	11.5	2800	254	5.17	3.89	0.80	.10	28.6	44.8	12.8	34.8	2.9

TABLE No. I Continued

1	2	3	4	5	6	7	8	9	10	11	12	13	14	15	16	17
No.	No.	Min. Sec.	No.	Ft.	Ft.	Lbs.	Lbs.	Ft./sec.	Sec.	Sec	Sec.	Percent	Percent	Percent	Gal./min	Gal./min.
142	1	20-12	510	8.20	12.9	2640	648	3.66	1.70	0.68	.03	60.1	64.6	38.8	19.1	3.8
17	2	10-21.4	140	8.18	16.2	2550	282	5.28	3.45	0.86	18	35.6	61.5	21.9	32.8	3.3
12	2	5-32.2	61	8.18	15.3	1700	88	5.49	5.30	0.64	.23	25.2	38.1	9.6	38.9	1.9
13	2	9-15.4	96	8.20	16.1	2550	191	5.38	4.55	0.92	.24	25.3	58.5	14.8	35.5	2.5
3	2	5-42.8	67	8.14	24.6	1650	92	5.35			.21	27.1	62.0	16.8	36.6	1.9
16	2	9-13.2	128	8.18	27.5	2400	165	5.29	3.70	0.54	.18	34.7	66.6	23.1	33.4	2.2
48	12	18-17.1	466	8.19	21.0	2550	401	3.95	1.48	0.41	.43	66.2	60.9	40.3	19.4	2.6
52	12	18-16	1017	8.33	23.1	940	211				.27			64.4	7.6	1.4
58	12	22-51.8	1544	8.21	23.3	860	181	1.49	0.41	0.31	22	92.1	65.2	60.0	5.5	1.0
62	6	8-58.5	101	8.13	21.3	2710	124	5.23	4.44	0.57	.67	23.8	50.0	11.9	37.9	1.7
67	6	19-27.2	484	8.20	22.0	2810	412	3.82	167	0.44	30	58.2	67.5	39.3	19.9	2.5
72	6	22-26.3	865	8.12	23.1	2290	420	2.95	1.19	0.41	19	77.0	67.6	52.1	14.5	2.2
77	4	12-7	200	8.02	23.1	2800	228	4.96	2.92	0.49	.30	41.3	58.3	24.1	30.0	2.3
82	6	24-42.4	1108	8.18	23.7	1850	411	2.43	0.86	0.35	17	82.2	78.2	64.3	11.0	2.0
86	6	33-17.6	2342	8.23	22.8	1395	311	1.43	0.45	0.27	11	78.0	79.1	61.7	6.2	1.1
91	4	18-14	455	8.16	23.6	2840	401	4.02	1.85	0.48	.20	60.1	67.9	40.8	21.4	2.6
96	4	19-21.2	654	8.16	23.6	2050	370	3.20	1.24	0.42	.15	76.1	68.7	52.2	15.0	2.3
100	4	22-34.6	1099	8.20	23.0	1500	336	2.18	0.81	0.32	.10	80.7	77.7	62.8	9.8	1.8
C103	3	10-18.4	133	8.06	23.1	2810	161	5.14	3.93	0.52	.29	29.5	55.6	16.4	34.6	1.9
105	3	16-21.2	396	8.12	23.0	2570	360	3.94	1.84	0.49	.16	55.7	71.5	39.8	21.5	3.7
109	3	21-11.2	774	8.14	23.5	2070	387	2.87	1.10	0.31	.10	72.0	75.0	54.0	13.9	2.2
114	3	12-52.6	245	8.13	22.8	2550	282	4.72	2.51	0.48	.20	50.0	62.2	31.1	26.4	26
119	2	9-5.4	113	8.15	23.1	2530	142	5.12	4.15	0.54	.20	27.3	58.3	15.9	35.3	1.9
123	2	11-20.2	185	8.18	24.6	2580	211	4.86	3.11	0.52	15	39.2	62.8	24.6	29.6	2.2
128	2	15-34	377	8.18	22.4	2420	372		1.87	0.47	.10			37.6	21.2	26
132	1	7-30.2	44	8.15	22.7	2800	53	5.22	9.66	0.49	.21	100	52.8	5.3	45.6	0.8

TABLE No I Continued

1 No.	2 No.	3 Min. Sec.	4 No.	5 Ft.	6 Ft.	7 Lbs.	8 Lbs.	9 Ft./sec	10 Sec.	11 Sec.	12 Sec.	13 Percent	14 Percent	15 Percent	16 Gal./min	17 Gal./min.
136	1	7-30.4	60	8.16	22.4	2600	72		6.96	0.59	.17			7.6	42.7	1.2
140	1	9-23.0	112	8.18	21.2	2750	150	511	4.35	0.57	10	247	57.1	14.1	37.1	1.9
143	1	15-57	384	8.19	22.0	2500	370	4.03	1.95	0.50	.05	57.9	68.7	39.8	21.6	2.8
54	12	13-47.8	339	8.22	33.4	2200	215	4.14	1.68	0.35	.41	61.2	65.2	39.9	21.0	1.9
10	2	8-24.8	94	8.14	38.8	2700	82	5.51	5.10	0.39	.24	24.7	58.2	14.4	39.7	1.2
11	2	8-18.6	84	8.14	38.0	2700	81	5.46	5.40	0.47	.25	21.6	64.4	13.9	40.2	1.2
15	2	8-50.2	122	8.16	37.6	2400	116	5.25	3.70	0.34	.18	32.6	68.5	22.3	34.2	1.6
40	1	10-32.5	303	8.19	36.1	1730	96	3.83	1.62	0.36	.09	59.7	41.1	24.6	20.8	1.1
41	2	10-10.2	232	8.17	37.8	2060	100	4.42	2.15	0.41	.11	51.1	44.0	22.5	25.5	1.2
42	4	9-19.5	206	8.19	37.5	1950	90	4.54	2.22	0.38	.11	50.5	41.8	21.1	26.2	1.2
43	3	13-46	344	8.18	36.0	2570	134	4.24	2.0	0.38	.10	55.8	41.3	23.0	23.6	1.2
44	6	11-38.4	248	8.20	35.7	2450	116	4.44	2.21	0.37	.12	46.4	44.5	20.6	26.5	1.2
45	12	12-49.6	338	8.22	36.3	2400	116	4.01	1.67	0.32	.09	52.6	40.8	21.4	23.5	1.1
53	12	23-23	1163	8.22	45.2	1620	181	2.27	0.79	0.22	.30	85.8	71.8	61.6	9.2	0.9
59	12	31-30.6	2325	8.20	43.3	1060	104	1.43	0.45	0.18	.20	104.0?	49.8?	51.8	4.4	0.4
63	6	8-50.5	107	8.15	42.4	3035	76	5.29	4.70	0.25	.62	22.3	56.3	12.6	42.2	1.0
68	6	15-12.8	373	8.20	43.9	2430	190	4.05	1.82	0.33	.31	58.2	72.2	42.0	20.6	1.5
73	6	21-28.7	818	8.20	43.3	2470	248	3.10	1.31	0.30	.20	74.2	71.6	53.0	15.2	1.4
78	4	11-59.8	194	8.07	43.6	2950	142	4.96	2.99	0.30	.31	38.2	68.5	26.0	30.9	1.4
83	6	22-48.6	1036	8.23	43.3	1840	202	2.51	0.98	0.21	.17	82.0	71.7	57.8	10.7	1.1
87	6	41-32	2919	8.28	43.3	1420	147	1.33	0.54	0.22	.11	84.3	64.4	54.3	4.5	0.4
92	4	15-11	356	8.14	44.0	2560	195	4.18	2.01	0.35	.21	56.8	72.5	42.2	21.8	1.5
97	4	21-26	705	8.18	43.2	2470	248	3.45	1.41	0.28	.15	78.9	67.2	53.0	15.2	1.4
101	4	19-25.2	964	8.21	44.4	1420	169	2.32	0.92	0.24	.10	84.2	76.6	64.5	9.8	1.0
E 103	3	9-24.2	116	8.04	44.0	2660	84	5.13	4.25	0.35	.30	27.2	63.6	17.3	34.3	1.0
106	3	16-2.6	385	8.14	44.1	2580	205	4.02	2.05	0.34	.16	56.3	77.2	43.5	20.8	1.5

TABLE Nº I Continued

1	2	3	4	5	6	7	8	9	10	11	12	13	14	15	16	17
No.	No.	Min. Sec.	No.	Ft.	Ft.	Lbs.	Lbs.	Ft./sec.	Sec.	Sec.	Sec.	Percent	Percent	Percent	Gal./min.	Gal./min.
110	3	19-49.6	712	8.15	43.4	2070	214	2.95	1.24	0.31	.10	69.8	78.6	54.8	13.8	1.3
115	3	10-32	184	8.11	43.9	2430	131	4.90	2.91	0.35	.22	42.5	69.0	29.3	29.3	1.5
118	2	8-33.2	107	8.17	44.6	2440	78	5.12	4.28	0.39	.20	26.7	65.2	17.4	35.6	1.1
124	2	11-1	178	8.17	44.8	2660	125	4.93	3.21	0.35	.15	37.8	67.5	25.9	30.2	1.4
127	2	14-48.2	366	8.17	44.0	2430	189		2.05	0.32	.10			41.9	21.3	1.5
133	1	7-6.8	53	8.14	43.1	2700	30	5.24	9.85	0.29	.17	12.6	46.8	5.9	46.1	0.5
137	1	7-42.8	59	8.14	44.6	2750	44		7.40	0.39	.16			8.8	43.5	0.7
141	1	8-34.6	106	8.15	40.3	2550	85	5.16	4.87	0.36	.10	25.8	64.0	16.5	35.4	1.2
144	1	14-52	362	8.19	42.8	2600	216	4.20	2.06	0.34	.05	57.7	75.3	43.4	22.7	1.7
6	2	7-49.8	101	8.2	54.32	2300	69	5.39			.1934	29.0	68.2	19.8	36.3	1.06
20	2	7-30.8	108	8.18	56.79	2050	65	5.23	3.78	0.37	.1741	33.5	65.4	21.9	33.8	1.04
35	2	9-31.2	208	8.19	53.69	2100	61	4.40	2.30	0.393	.114	44.5	4.79	21.3	27.3	77
36	2	11-37.8	265	8.205	55.845	2470	67.8	4.58	2.113	0.345	.1098	52.15	40.15	20.9	26.2	70
39	2	10-44.8	238	8.18	58.4	2350	58.4	4.63	2.23	0.3715	.1127	50.5	37.75	19.05	26.9	.65
55	12	6-45.6	154	8.19	56.39	1120	68.	4.075	1.72	0.29	.38	53.0	78.8	41.8	21.1	1.21
38	2	10-56.4	250	8.205	56.40	2380	63.5	4.615	2.17	0.357	.1093	51.9	39.4	20.45	26.8	.69
7	2	9-6	107	8.148	65.28	2800	59.	5.39	4.67	0.273	.213	24.5	69.0	16.9	37.7	0.78
37	2	11-33	268	8.217	64.695	2450	63.3	4.575	2.13	0.355	.1077	53.0	37.4	19.8	26.1	0.66
64	6	7-29	83	8.14	63.12	2470	42.2	5.30			.68	22.1	59.8	13.2	40.2	0.68
69	6	16-19.7	375	8.18	63.04	2820	152.5	4.243	1.96	0.29	.327	55.5	75.3	41.7	21.8	1.12
74	6	26-4	945	8.20	63.17	2680	194.5	3.022	1.40	0.215	.2068	74.7	74.7	55.8	13.2	0.90
79	4	12-1.6	195	8.07	62.72	2970	101.0	4.940	3.15	0.24	.308	37.8	69.8	26.4	30.6	1.01
84	6	31-13.8	1539	8.24	63.14	2060	156	2.318	0.97	0.18	.1523	92.5	63.8	58.0	8.51	0.60
88	6	41-58.4	2978	8.286	62.94	1170	72	1.362	0.60	0.19	.1056			46.7	3.55	0.21
93	4	15-18.8	365	8.14	63.54	2580	143	4.11	2.03	0.30	.21	55.8	77.5	43.25	21.3	1.12
98	4	19-32.2	648	8.18	63.0	2390	172.5	3.166	1.54	0.27	.1508	63.3	88.0	55.7	15.73	1.06

TABLE No. 1 Continued

1	2	3	4	5	6	7	8	9	10	11	12	13	14	15	16	17
No.	No.	Min Sec.	No.	Ft.	Ft.	Lbs.	Lbs.	Ft/sec	Sec.	Sec.	Sec.	Percent.	Percent	Percent	Gal/min.	Gal/min.
102	4	29-32.8	1415	8.24	62.96	2020	156.3		0.945	0.188	.104			59.1	8.85	0.63
D 103	3	9 59.4		8.06	62.94	2690	69.5	5.17	4.17	0.31	.29			20.15	33.2	0.84
107	3	14 57	361	8.14	62.74	2470	142.2	4.02	2.11	0.31	.155	55.1	80.7	44.4	21.7	1.94
111	3	18-32.6	677	8.16	62.54	2000	152.	2.874	1.34	0.20	.1028	65.1	89.6	58.3	13.9	0.98
116	3	10 54	196	8.10	63.08	2450	90.8	4.78	2.88	0.33	.209	42.8	67.5	28.9	28.0	1.0
117	2	8 12	96	8.17	62.60	2460	53.	5.183	4.75	0.32	.2136	24.3	67.9	16.5	36.8	0.78
125	2	10 13.4	163	8.18	62.50	2500	90.7	4.91	3.327	0.323	.1565	36.5	76.0	27.7	30.4	1.07
126	2	15 9	374	8.20	62.71	2510	147	3.98	2.044	0.31	.1013	54.7	81.7	44.7	21.1	1.17
145	1	14-36.2	354	8.19	63.20	2500	147.5	4.16	2.17	0.23	.0516	56.9	80.1	45.6	21.8	1.22
21	2	7-49.	107	8.162	72.99	2300	26.3	5.24	3.85	0.34	.1825	29.8	34.2	10.2	35.6	0.34
8	2	9-1	110	8.163	73.813	2700	50.8	5.383	4.49	0.319	.205	25.9	65.7	17.0	36.7	0.68
22	2	7-3.2	102	8.175	90.12	2100	6.31	5.26	3.56	0.33	.173	31.2	10.6	3.3	35.9	0.11
9	2	8 55.6	117	8.18	102.3	2575	28.2	5.28	4.46	0.216	.1907	29.5	46.4	13.7	35.0	0.38

TABLE No II

LENGTH OF DRIVE PIPE 51.5 FT. HT. OF AIR CHAMBER 2 FT. UNIFORM VALVE CLOSURE SUPPLY HEAD ABOUT 8.16 FT

Observed								Autographic			Computed					
1	2	3	4	5	6	7	8	9	10	11	12	13	14	15	16	17
Run	B Cams used	Length of Run	Strokes	Supply Head	Pumping Head	Water Wasted	Water Pumped	Maximum Velocity in Drive Pipe	Waste Valve Remains Open	Waste Valve Remains Closed	Valve Closure	Efficiency,— Acceleration Period	Efficiency,— Retardation Period	Efficiency of Machine	Total Water Q+q	Water Pumped q
No.	No.	Min. Secs.	No.	Ft.	Ft.	Lbs.	Lbs.	Ft./sec.	Sec.	Sec.	Sec.	Percent.	Percent.	Percent.	Gals/min	Gals/min.
1	12	6 - 41.8	166	8.20	2.38	820	350	44.8	.192	1.107	.605		21.7	12.40	21.0	6.28
4	12	4 - 32.	216	8.27	2.125	130	147	1.92	.1275	.815	.315	85.2	34.2	29.1	7.33	3.89
9	12	7 - 26.2	748	8.21	2.79	210	264	1.325	.10	.394	.149	87.7	48.75	42.75	7.66	4.27
12	1	5 - 14	42	8.05	2.925		108	6.23	6.30	.975	.1551					2.48
17	1	3 - 57.2	51	8.13	3.755	1300	139	6.255	3.44	1.051	.097	21.7	22.75	4.94	43.7	4.22
22	1	4 - 46.6	114	8.17	3.415	720	256	5.10	1.368	1.00	.0524	57.9	25.65	14.85	24.5	6.43
26	2	4 - 54.6	39	8.08	3.56	1970	114	5.82	4.66	.30	.315	9.55	26.7	2.55	50.9	2.79
31	2	3 - 43.6	59	8.17	2.46	950	171	6.22	6.327	1.1	158	33.8	16.01	5.43	35.8	5.51
36	2	3 - 55.8	93	8.19	4.037	650	207.5	5.4	1.424	1.0	.1056	58.6	26.9	15.74	26.2	6.35
41	3	4 - 29.6	58	8.16	4.56	1550	144	6.33	3.57	.96	.29	21.1	24.6	5.19	45.3	3.85
46	3	3 - 18.8	79	8.20	3.83	530	175	5.2	1.4125	1.006	.1575	56.5	27.1	15.30	25.5	6.34
63	6	4 - 4.6	51	8.13	3.16	1300	147	6.13	3.16	1.062	.6	20.8	21.1	4.39	42.6	4.33
68	6	3 - 39.6	90	8.20	3.335	510	192	4.915	1.108	1.072	.305	59.6	25.66	15.30	23.1	6.50
2	12	5 - 35.8	132	8.12	12.48	1400	178	4.857	1.617	.405	.635	31.6	59.2	18.70	33.9	3.82
5	12	5 - 24.6	259	8.20	14.77	590	147	3.53	.5175	.375	.313	76.5	58.7	44.9	16.34	3.27
10	12	4 - 20	438	8.25	15.45	150	51	1.43	.146	.2685	.1484	83.3	76.5	63.7	5.57	1.41
13	1	4 - 56	36	8.03	14.52	2250	50	6.25	6.935	.44	.1714	89.5	41.4	3.7	56.00	1.22
18	1	4 - 59	60	8.08	12.07	1950	97	6.23	4.29	.581	.1038	16.96	43.75	7.42	49.3	2.34

TABLE No II Continued

1 No.	2 No.	3 Min Sec	4 No	5 Ft	6 Ft	7 Lbs.	8 Lbs	9 Ft/sec.	10 Sec.	11 Sec.	12 Sec.	13 Percent	14 Percent	15 Percent	16 Gal/min.	17 Gal/min.
23	1	4 - 45	111	8.15	13.925	1200	158	5.717	1.915	.507	.0535	42.65	52.75	22.5	34.3	3.99
27	2	4 - 42.4	39	8.07	14 14	2100	57	6.06	6.45	.535	.302	9.72	48.9	4.75	55.0	1.45
32	2	4 - 22.4	66	8 15	13.615	1500	106	6 33	3.02	.45	.1656	24.85	47.6	11.82	44.1	2.91
37	2	4 - 20.4	105	8.16	14.357	1100	134	5.884	1.827	.472	.1047	46.5	46.0	21.4	34.1	3.70
42	3	5 - 13.4	64	8.13	13.152	2050	100	6 25	4.04	.47	.3065	17.25	45.8	7.90	49.3	2.3
47	3	3 - 42.2	89	8.17	13.50	900	122	5.70	1.734	.49	.156	41.2	54.4	22.4	34.7	3.95
51	2	4 - 30.6	218	8.20	13.362	450	137	3.56	.73	.411	.0899	8.61	57.6	49.6	15.6	3.65
52	2	4 - 56.4	241	8.19	10.43	600	106	3.56	.82	.285	.084	71.5	30.2	21.6	17.1	2.58
55	3	5 - 15.8	195	8.22	12.805	750	190	4.285	1 01	.478	.1012	66.75	59.2	39.5	21.4	4.33
59	3	3 - 4	217	8.23	13.495	160	62	1 97	4145	.3445	.053	73.5	86.4	63.5	8.69	2.43
64	6	3 - 31.2	44	8 10	12.612	1360	68	6.10	3.772	.42	.60	17.08	45.7	7.8	48.7	2.32
69	6	2 - 59.6	72	8.15	13.82	720	100	5.812	1.632	.518	.312	47.6	49.4	23.5	32.9	4.01
73	6	3 - 11.8	158	8.21	13.332	310	95	3.1	592	.403	.1517	68.6	72.4	49.7	15.2	3.57
77	6	3 - 13.8	238	8.22	12.66	160	61	1.918	326	.3172	.1018	76.5	76.7	58.7	8.21	2.27
3	12	5 - 33.4	132	8 17	22.905	1540	119	4.93	1 68	.29	.632	29.35	68.0	19.95	35.8	2.57
6	12	4 - 15	202	8 17	22.595	540	95	3 6	.6475	.2975	315	68.3	71.25	40.6	17.93	2.68
11	12	4 26	450	8.24	26 10	180	31	1.557	.218	.224	.1478	84.0	65.0	54.6	5.71	0.84
14	1	4 - 45.8	40	8 05	23.825	2200	35	6.295	6.91	.363	.1487	10.28	44.3	4.55	56.4	0.88
19	1	3 - 42	46	8.10	25.58	1500	46 5	5.75	4.225	.323	.1006	14.4	67.9	9.78	50.1	1.51
24	1	3 - 4.6	71	8.12	24.6	850	68	5.83	2.147	.389	.0542	40.2	60.3	24.25	35.8	2.65
28	2	4 56.2	42	8.07	23.05	2240	43		6 66	.397	.294			5.48	55.6	1.05
33	2	4 - 46.6	76	8.14	24.602	1750	78	6.31	3.13	.373	.1573	24.45	55.25	13.50	45.9	2.72
38	2	4 - 11.8	116	8.17	23.21	1100	103	5.89	1.87	.3425	.0905	51.5	51.7	26.66	34.4	2.94
43	3	5 - 9.6	65	8 13	25.097	2100	65	6.36	4.225	.3275	.298	17.7	54.0	9.55	50.4	1.51
48	3	3 - 37.6	84	8.16	22.887	1000	86	5.77	2.115	.212	.162	34.25	70.5	24.13	35.9	2.85
56	3	3 - 51.2	146	8.20	23.462	630	96	4.41	1.08	.326	.099	63.2	69.0	43.6	22.6	2.99

TABLE No II Continued

1 No	2 No.	3 Min Sec.	4 No.	5 Ft.	6 Ft.	7 Lbs.	8 Lbs.	9 Ft/sec.	10 Sec.	11 Sec.	12 Sec.	13 Percent	14 Percent	15 Percent	16 Gal/min.	17 Gal/min.
60	3	3 - 4.6	213	8.20	25.142	230	47	2.34	505	.2327	.0542	71.1	88.2	62.7	10.8	1.83
65	6	4 - 10	55	8.04	22.355	1750	46.6	6.17	4.77	.3126	.568	17.1	44.45	7.6	51.8	1.34
70	6	3 - 24.6	83	8.17	23.07	900	80	5.57	1.842	.3555	.308	40.3	62.3	25.1	34.5	2.81
74	6	3 - 28.6	173	8.19	23.845	400	70	3.294	.686	.245	.1507	65.9	77.5	51.0	16.2	2.42
78	6	3 - 32.6	259	8.21	23.15	230	53	2.153	.401	.2082	.1026	73.0	89.0	65.0	9.58	1.80
7	12	3 - 42	176	8.17	47.11	500		3.4	79	.165	.315	57.3				
15	1	4 - 21	38	8.13	46.86	2000	18.5	6.31	6.48	.20	.143	10.7	49.8	5.33	55.7	0.51
20	1	4 - 9	54	8.10	45.02	1700	32.5	6.28	4.375	.2255	.0962	14.8	71.9	10.63	50.1	0.94
25	1	3 - 36	83	8.15	42.815	1050	56	5.55	2.203	.242	.0342	34.3	81.6	28.	36.9	1.87
29	2	6 - 7	50	8.10	42.845	2350	28	6.574	6.412	.237	.306	13.04	48.3	6.3	46.7	0.55
34	2	3 - 57.8	65	8.15	47.675	1460	40	6.27	3.16	.229	.1524	24.65	65.0	16.02	45.5	1.21
39	2	4 - 30.2	109	8.16	43.39	1300	69	6.025	2.07	.2467	.1034	42.9	65.8	28.20	36.5	1.84
44	3	4 - 0.2	50	8.14	47.205	1650	30	6.29	4.335	.174	.30	16.94	62.3	10.55	50.3	0.90
49	3	3 - 38.6	88	8.18	55.49	1050		5.64	2.15	.1683	.1554	37.5	37.4			
53	2	4 - 33.8	220	8.18	45.657	600	58	3.75	0.932	.183	.0897	72.5	74.5	54.0	17.3	1.53
57	3	4 - 40.4	170	8.17	43.295	900	76	4.81	1.267	.216	.125	61.5	72.8	44.75	25.0	1.95
61	3	3 - 18	225	8.16	42.257	270	32	2.50	0.587	.166	.054	73.3	83.8	61.4	11.0	1.16
66	6	4 - 30	59	8.12	43.57	1850	34.8	6.12	4.0	.222	.5725	16.9	59.8	10.1	50.3	0.93
71	6	3 - 27.6	88	8.20	43.022	930	51.7	5.43	1.826	.198	.295	39.1	74.7	29.2	34.1	1.7°
75	6	3 - 0.6	155	8.21	51.085	360	33	3.46	0.788	.1398	.1455	72.2	79.0	57.0	15.7	1.32
79	6	3 - 12	224	8.20	46.925	250	24.3	2.364	0.50	.127	.1071	70.25	79.25	55.65	10.3	0.91
8	12	6 - 57	339	8.21	63.38	980	66	4.7	0.7975	.156	.307	62.2	83.6	52.0	18.05	1.14
16	1	5 - 22.4	48	8.11	63.735	2480	20.6	6.3	6.655	.14	.14	10.89	60.0	6.53	55.8	0.46
21	1	3 - 46.2	50	8.13	64.26	1550	22.0	6.29	4.235	.1667	.094	18.04	62.3	11.22	50.0	0.70
30	2	4 - 33.4	41	8.07	70.135	2200	12.9	6.486	6.66	.175	.278	11.16	45.7	5.1	58.3	0.34
35	2	4 - 33.4	78	8.15	61.113	1650	38.4	6.35	3.19	.1805	.146	26.9	65.0	17.47	44.4	1.01

TABLE Nº II Continued

1	2	3	4	5	6	7	8	9	10	11	12	13	14	15	16	17
No.	No.	Min Sec.	No.	Ft.	Ft.	Lbs.	Lbs.	Ft/sec.	Sec.	Sec.	Sec.	Percent	Percent	Percent	Gal/min.	Gal/min.
40	2	4 - 15.2	103	8.15	66.61	1250	45	6.03	2.17	.196	.1032	42.25	69.85	29.5	36.6	1.27
45	3	4 - 20.2	55	8.14	64.582	1800	19.8	6.255	4.36	.1439	.291	16.93	51.60	6.74	50.3	.55
50	3	6 - 52.8	164	8.18	66.40	2010	69.4	5.87			.1575	39.5	68.0	26.8	36.2	1.21
54	2	4 - 45.2	232	8.20	66.035	650	46	4.00	.932	.157	.0872	80.0	71.4	57.1	17.6	1.16
58	3	3 - 35	127	8.20	64.68	680	38	4.84	1.33	.155	.1057	61.3	72.0	44.1	24.00	1.27
62	3	3 - 15.8	231	8.20	61.445	220	16.8	2.313	.588	.127	.053	78.7	72.7	57.2	8.72	.61
67	6	4 - 18.	60	8.18	64.95	1700	24	6.16	3.645	.1677	.538	18.85	59.4	11.2	48.2	.67
72	6	3 - 20.4	84	8.17	65.682	900	33	5.43	1.98	.1472	.299	38.7	76.25	29.5	33.5	1.10
76	6	3 - 21.6	164	8.20	66.657	440	29	3.54	.85	.122	.1535	65.5	81.9	53.6	16.8	1.24
80	6	3 - 34.2	247	8.21	64.10	240	16.3	2.335	.554	.1075	.1085	78.6	67.4	53.0	8.62	.53

TABLE No III

LENGTH OF DRIVE PIPE 51.5 FT. HT. OF AIR CHAMBER 2 FT. UNIFORM VALVE CLOSURE SUPPLY HEAD ABOUT 6.17 FT.

Observed								Autographic			Computed					
1	2	3	4	5	6	7	8	9	10	11	12	13	14	15	16	17
Run	B Cams used	Length of Run	Strokes	Supply Head	Pumping Head	Water Wasted	Water Pumped	Maximum Velocity in Drive Pipe	Waste Valve Remains Open	Waste Valve Remains Closed	Valve Closure	Efficiency,— Acceleration Period	Efficiency,— Retardation Period	Efficiency of Machine	Total Water Q+q	Water Pumped q
No.	No.	Min. Secs	No.	Ft.	Ft.	Lbs.	Lbs.	Ft/sec.	Sec.	Sec.	Sec.	Percent	Percent	Percent	Gals/min	Gals/min.
6	2	3 - 24.6	50	6.14	4.73	850	108	5.255	2.95	.9545	.1705	30.4	32.2	9.8	33.7	3.8
18	1	4 - 12.	42	6.15	5.39	1450	78	5.50	5.395	.9035	.125	16.38	28.7	4.71	43.7	2.23
11	3	3 - 48.8	88	6.19	5.957	610	138.5	4.506	1.584	.7795	.1625	54.25	40.25	21.85	23.6	4.36
1	6	4 - 27.6	229	6.25	6.117	190	98	1.763	.375	.538	.146	69.0	73.0	50.4	7.75	2.64
7	2	3 - 21.2	49	6.09	14.16	1000	59	5.35	3.33	.47	.1705	26.5	51.8	13.72	37.9	2.11
16	12	4 - 3.2	388	6.32	15.467	100	22.1	1.11	.181	.1994	.1568	87.0	62.2	54.1	3.62	.65
12	3	3 - 17.4	73	6.17	15.94	720	72.5	4.873	2.04	.447	.169	39.0	66.2	25.8	28.9	2.65
19	1	3 - 40.6	30	6.11	16.947	1400	31.4	5.483	6.45	.479	.153	12.1	51.5	6.23	46.7	1.03
2	6	4 - 30.4	218	6.16	15.827	370	75	2.62	.70	.326	.155	75.5	69.0	52.1	11.8	2.0
17	12	3 - 37.8	342	6.33	25.15	95	11.8		.242	.178	.159			49.5	3.86	.39
13	3	3 - 23.6	78	6.18	25.63	750	53.7	4.986	2.055	.325	.163	48.0	61.9	29.7	28.5	1.90
8	2	4 - 38.2	71	6.09	25.89	1400	55.2	5.26	3.42	.347	.164	26.5	63.3	16.75	37.7	1.43
20	1	4 - 8.2	34	6.12	26.52	1600	24.8	5.426	6.82	.3215	.152	11.7	57.5	6.72	47.1	.72
3	6	3 - 42.0	184	6.21	28.39	350	39	2.85	.8025	.224	.151	79.0	64.7	51.0	12.6	1.27
9	2	3 - 53.0	63	6.16	46.48		27.8	5.26	3.185	.252	.154					.86
4	6	3 - 20.6	156	6.24	47.39	270	16.5	2.74	.82	.133	.160	80.0	58.0	46.4	10.3	.59
21	1	4 - 18.0	34	6.11	48.48	1700	14.2	5.47	7.2	.239	.158	11.25	59.0	6.63	47.9	.36
14	3	3 - 20.8	77	6.15	48.52	760	29.2	4.99	2.19	.218	.162	47.8	63.6	30.4	28.3	1.05

TABLE No III Continued

1	2	3	4	5	6	7	8	9	10	11	12	13	14	15	16	17
No.	No.	Min. Sec.	No.	Ft.	Ft.	Lbs.	Lbs.	Ft./sec.	Sec.	Sec.	Sec.	Percent	Percent	Percent	Gal/min.	Gal/min.
5	6	3 - 19.6	154	6.20	63.37	295	14.3	2.963	.979	.125	.162	85.3	50.5	43.1	11.2	.52
15	3	3 - 23.8	82	6.16	63.5	750	22.7	4.85	2.12	.168	.155	48.0	65.0	31.2	27.3	.80
10	2	3 - 16.4	53	6.10	64.08	1000	17.8	5.253	3.575	.142	.154	32.9	56.9	18.7	37.4	.65

TABLE No IV

LENGTH OF DRIVE PIPE 51.5 FT. HT. OF AIR CHAMBER 2 FT. UNIFORM VALVE CLOSURE SUPPLY HEAD ABOUT 4.2 FT.

1	2	3	4	5	6	7	8	9	10	11	12	13	14	15	16	17
7	2	3 - 51.4	61	4.2	6.2	700	77.5	4.09	2.77	.742	.158	39.8	41.1	16.35	24.2	2.42
4	6	3 - 52.2	191	4.33	6.43	130	43.4	1.446	0.5	.49	.152	81.5	60.8	49.5	5.38	1.35
11	3	3 - 11.2	77	4.17	6.88	370	66.0	3.236	1.57	.664	.155	60.0	49.0	294	16.42	2.48
1	1	6 - 34.2	52	4.15	7.08		66.0	4.41	6.5	.725	.158					1.21
8	2	3 - 7.0	49	4.19	17.08	650	31.5	4.233	3.225	.40	.159	37.0	53.5	19.77	26.2	1.21
12	3	3 - 19.0	83	4.20	17.46	430	36.0	3.336	1.802	.367	.150	58.75	59.3	34.8	16.85	1.30
2	1	3 - 55.4	34	4.17	18.31	1150	19.8	4.46	6.415	.429	.144	16.2	46.7	7.57	35.8	0.61
5	6	3 - 56.0	191	4.28	19.65	200	20	1.75	0.731	.262	.155	78.5	58.5	45.95	6.71	0.61
13	3	4 - 1.8	105	4.22	27.4	500	25.5	3.31	1.805	.305	.144	62.7	52.8	33.1	15.55	0.759
3	1	3 - 36.4	31	4.16	28.96	1050	11.2	4.5	6.56	.262	.146	16.5	43.4	7.17	35.3	0.37
9	2	3 - 32.2	55	4.17	29.1	750	17.5	4.283	3.42	.277	.161	37.0	44.0	16.27	26.0	0.594
6	6	3 - 53.2	173	4.22	29.9	240	11.1	2.027	0.864	.212	.168	80.8	40.6	32.8	7.75	0.34
10	2	3 - 15.0	50	4.18	49.605	700		4.25	3.485	.189	.162	35.4				
14	3	3 - 50.6	93	4.21	50.165	500	9.5	3.485	2.07	.2105	.155	61.6	36.7	22.6	15.9	0.296

TABLE No V

LENGTH OF DRIVE PIPE 51.5 FT. HT. OF AIR CHAMBER 2 FT. UNIFORM VALVE CLOSURE SUPPLY HEAD ABOUT 2.19 FT.

1	2	3	4	5	6	7	8	9	10	11	12	13	14	15	16	17
No.	No.	Min. Sec.	No.	Ft.	Ft.	Lbs.	Lbs.	Ft/sec.	Sec.	Sec.	Sec.	Percent	Percent	Percent	Gal/min.	Gal/min.
5	6	5 - 38.6	282	2.24	4.93	100	13.1		0.559	.43	.15			28.8	2.41	.28
2	2	3 - 46.8	60	2.15	8.61	400	25.2	2.565	3.0	.558	.157	52.75	47.8	25.2	13.5	.80
1	1	4 - 38.2	36	2.13	9.39	850	15.8		6.95	.575	.171			8.2	22.4	.409
4	3	3 - 32.6	94	2.20	10.22	210	15.0	1.952	1.72	.432	.141	89.2	37.2	33.2	7.62	.51
6	3	5 - 55.2	130	2.22	19.67	450	10.7	2.107	2.20	.317	.171	67.0	31.5	21.4	9.33	.22
3	2	7 - 34.6	123	2.20	20.69	800	16.1	2.557	3.15	.361	.154	52.5	36.1	18.95	12.9	.255

TABLE Nº VI

n = STROKES PER MIN   t = TIME OF VALVE CLOSURE

			NUMBER OF B CAMS					
			1	2	3	4	6	12
R.P.M. OF CAM A	288	n	24	48	72	96	144	288
		t	052	052	052	052	052	052
	144	n	12	24	36	48	72	144
		t	104	104	104	104	104	.104
	96	n	8	16	24	32	48	96
		t	156	156	.156	.156	.156	.156
	72	n	6	12	18	24	36	72
		t	.208	.208	.208	.208	.208	.208
	48	n	4	8	12	16	24	48
		t	.313	.313	.313	.313	.313	.313
	24	n	2	4	6	8	12	24
		t	.625	.625	.625	.625	.625	.625

The term "strokes," column 4, refers to the total number of strokes or waste valve closures during the run.

The values given in columns 9, 10 and 11 are in each case the average of the values scaled from about ten autographic records taken during the run. See Diagram III.

The term "valve closure," column 12, indicates the time occupied by the waste valve in moving the one-half inch required to close it.

Columns 7 and 8 give the amount of water wasted and pumped, respectively, during the entire run, while these quantities are reduced to gallons per minute in columns 16 and 17.

Column 13 was computed by equation (53); E, column 15, was computed by Rankine's formula, p. 147; while the efficiency during the retardation period, or E′, is the quotient of the former by the latter (See equation [49a]).

Comparison of Theory and Experiment

In order to apply the theoretical formulas in a problem of design, it would be necessary to estimate the quantities f, m_1, m_2, c and c′. Where these coefficients are to be experimentally determined, however, it does not matter whether the several terms which constitute the quantity m are separately determined or not since m always enters (except in equation 16) in its complete form as given by equation (8a). The quantity m was therefore assumed to be of the form

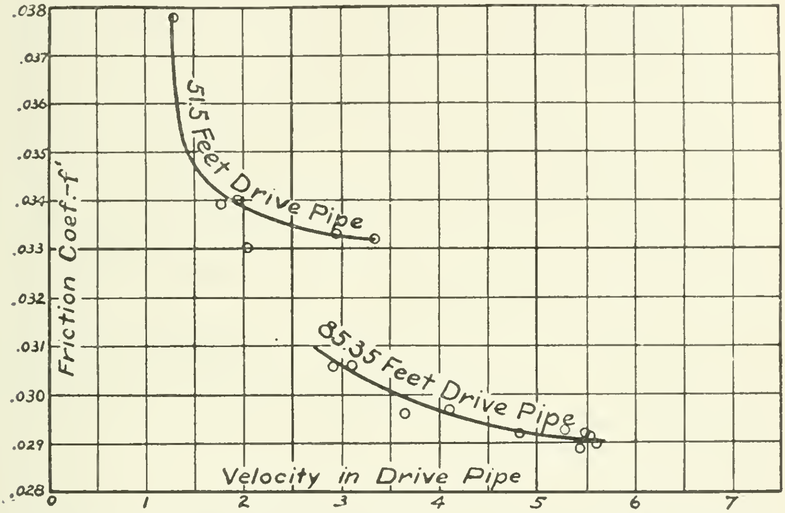

Diagram IV.—Showing Friction Loss in the Drive Pipe With Steady Flow.

$$m = \left(\frac{f'l}{d} + \frac{A^2}{c^2a^2} \right) \frac{1}{2g}$$

where f′ varies with the length of pipe, l, and f remains constant. Diagram IV shows the values obtained for the friction coefficient f′, as we may call it, for each of the two lengths of drive pipe. They were determined by measuring the discharge in a given time through the pipe and recording at the same time the readings of water columns C′ and E (Plate

III.) It was necessary to measure c only when the waste valve was completely open.

The values adopted for use in the theoretical formulas are:

f' (for the 85.35 ft. drive pipe) $= 0.03$
f' (for the 51.5 ft. drive pipe) $= 0.034$
$c = 0.54$

These values give:

m (for the 85.35 ft. drive pipe) $= 0.264$
m (for the 51.5 ft. drive pipe) $= 0.191$

To determine the loss through the check valve, and hence c', a differential mercury gage was used with one end connected to the elbow immediately below the check valve and the other end to the air chamber. The curve obtained in this way, (see Diagram V), shows that the loss of head varies as first power of the rate of flow through the valve and is equal to 1.76 feet per pound of water flowing through the valve in one second. For use in the formulas, this must be reduced to the loss per foot of velocity in the drive pipe which for a 2.05 inch pipe becomes equal to 2.52 feet.

λ is obtained from equation (4), for the drive pipe in use, by substituting: $w = 62.5$, $g = 32.15$, $K = 300.000$, $d = 2.05$, $e' = 0.151$, and $E = 24,000,000$. This gives: $\lambda = 4380$ feet per second, and $\frac{\lambda}{g} = 136.3$.

1. Acceleration Period:—The curves shown in Diagrams VI to X, inclusive, were computed from equation (11) for the average conditions obtained in the experiments.. The dashed lines tangent to the curves at the origin represent the equation

$$v = \frac{gH}{l} t \tag{52}$$

which would represent the velocity at any time were it not for the resistance of the pipe and the waste valve.

The horizontal dashed lines represent the maximum carrying capacity of the pipe under the several heads, or $\sqrt{\frac{H}{m}}$ and are asymptotes to the curves.

The experimental data which are plotted upon the same diagrams are to be found in Tables I to V respectively. A general

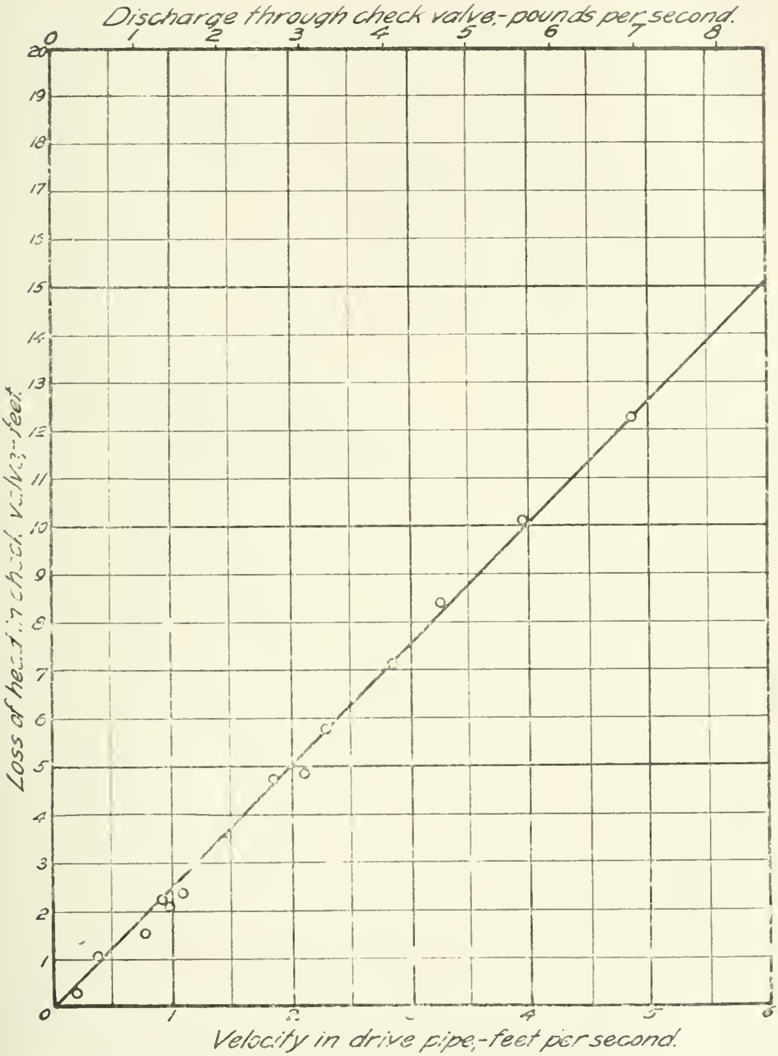

Diagram V.—Showing Loss of Head Through the Check Valve.

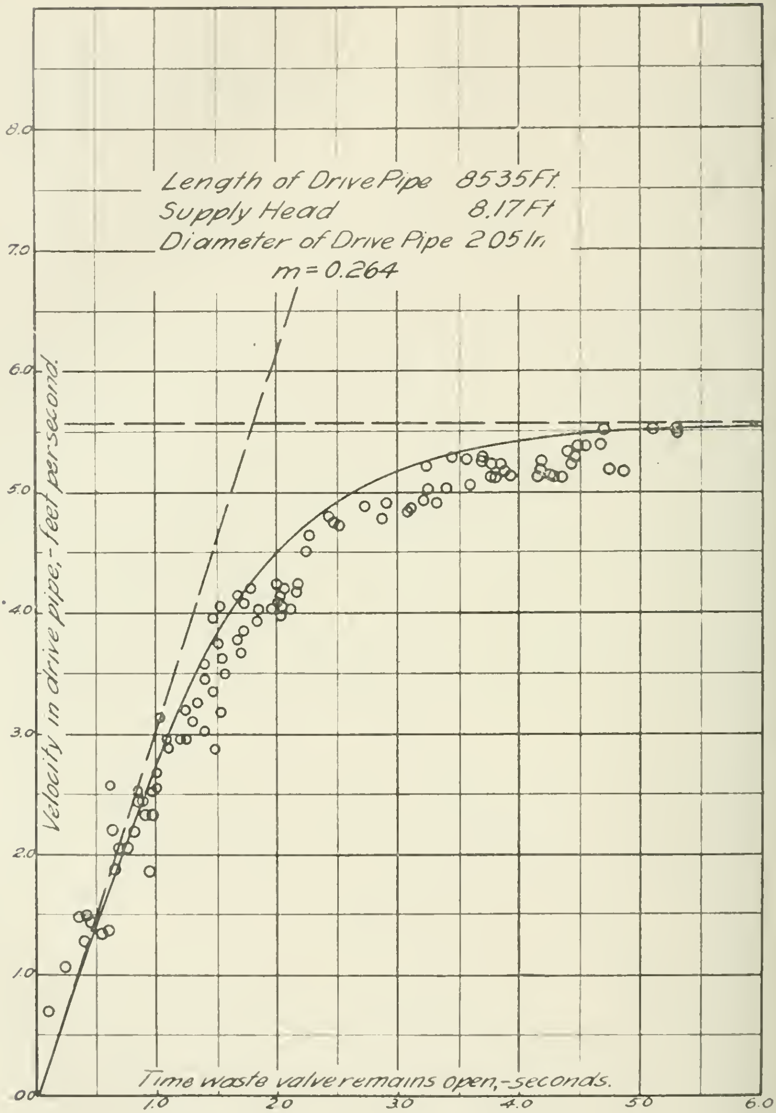

Diagram VI.—Velocity Curve for Drive Pipe.

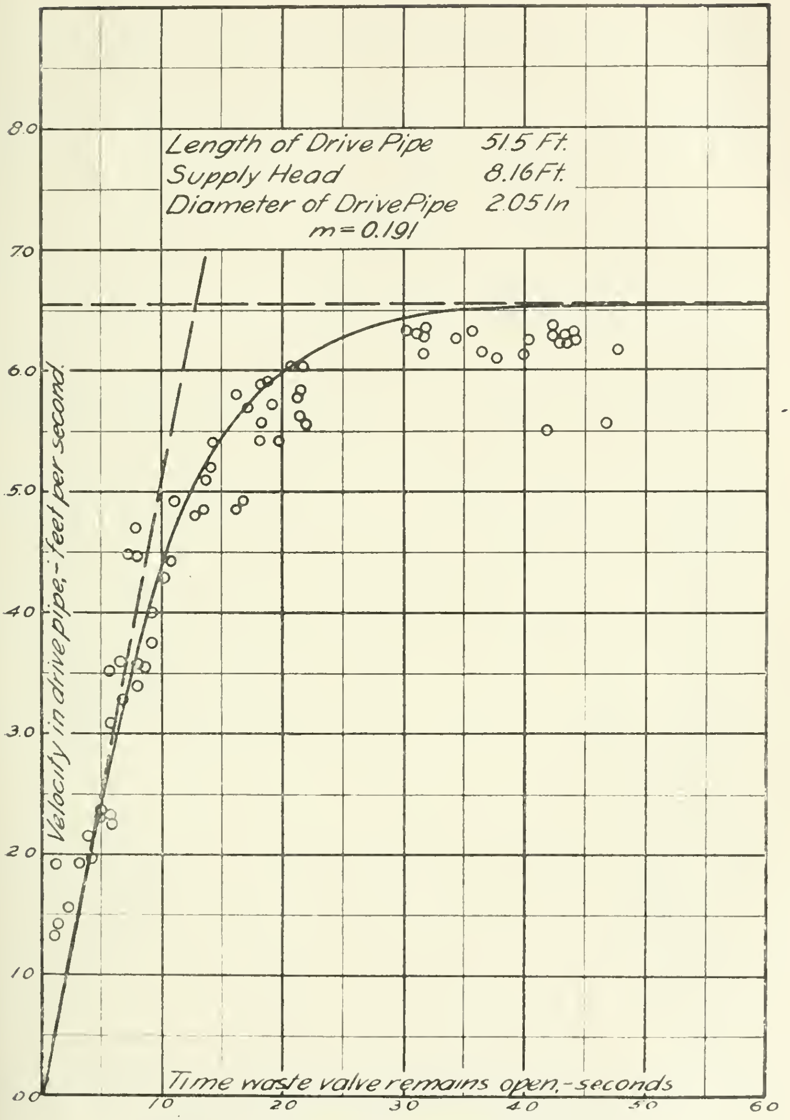

Diagram VII.—Velocity Curve for Drive Pipe.

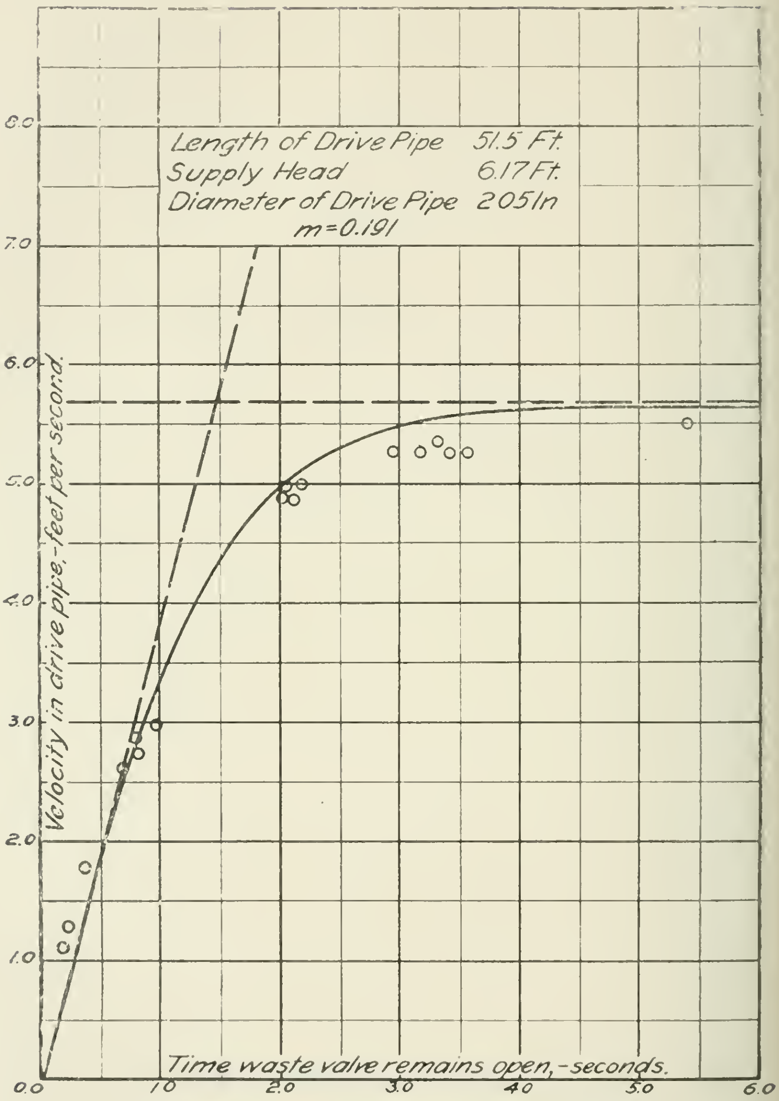

DIAGRAM VIII.—VELOCITY CURVE FOR DRIVE PIPE.

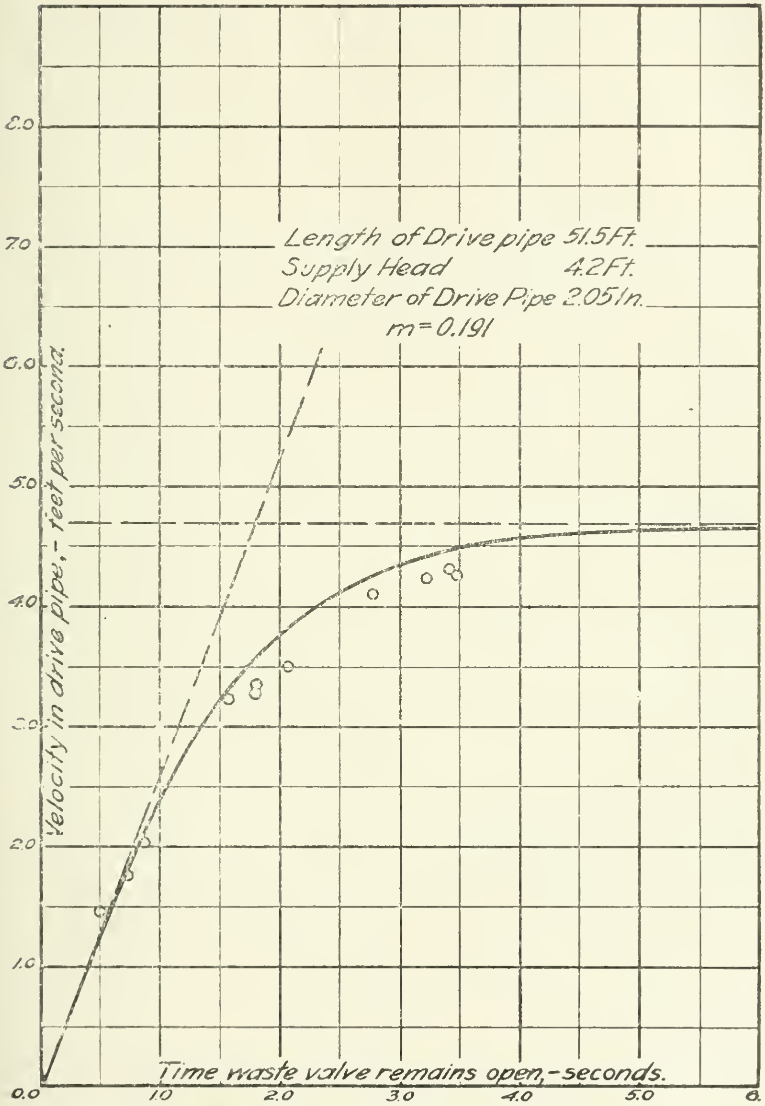

Diagram IX.—Velocity Curve for Drive Pipe.

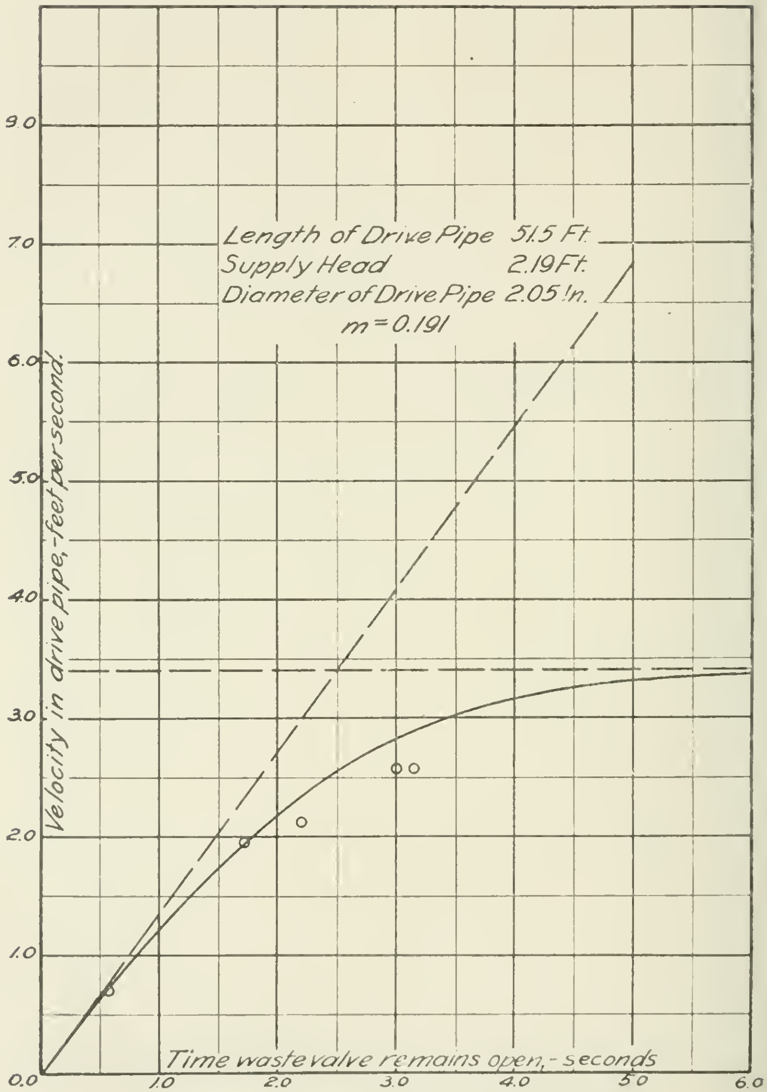

Diagram X.—Velocity Curve for Drive Pipe.

agreement is evident, although the experimental points seem to fall commonly below the theoretical curve. This is due without doubt to the fact that the recording pencil is always moving upward during this period, and the frictional resistances of the pencil, disk rod, and all other parts of the instrument combine to produce a reading below the true value.

The position of all asymptotes or $\sqrt{\frac{H}{m}}$ were accurately checked by allowing the water to flow continuously into the discharge tank for some time and then computing the limiting velocity from the cross-sectional area of the pipe, the discharge and the time. Notwithstanding this fact the points near the limiting velocity in Diagram VII are all below the true value, as experimentally proven, even though acceleration is known to have practically ceased; which fact shows conclusively that the disagreement is due to systematic errors in the instrument.

The fact that some points, for low velocities, fall above the curve results from using, for abscissas, the time during which the waste valve remains completely open, whereas Diagram I shows that the water continues to accelerate (although at a slower rate) for these low velocities until the waste valve is nearly closed. A further scattering of the points no doubt results from plotting on the same curve the results obtained from all rates of valve closure, although this cause is of minor importance except for low velocities.

The curves shown in Diagrams XI to XV inclusive were computed by the successive application of formulas (11), (13) and (14) for the average conditions existing during each set of runs. The experimental points plotted on the same diagrams were computed by the formula,

$$E = \frac{WV^2}{2g} \div \frac{QH}{N},$$

or

$$E = \frac{WV^2N}{2gQH} \tag{53}$$

where W = amount of water required to fill the drive pipe;
Q = total waste water during the run;
N = total strokes recorded by the tachometer during the run;
V was measured autographically.

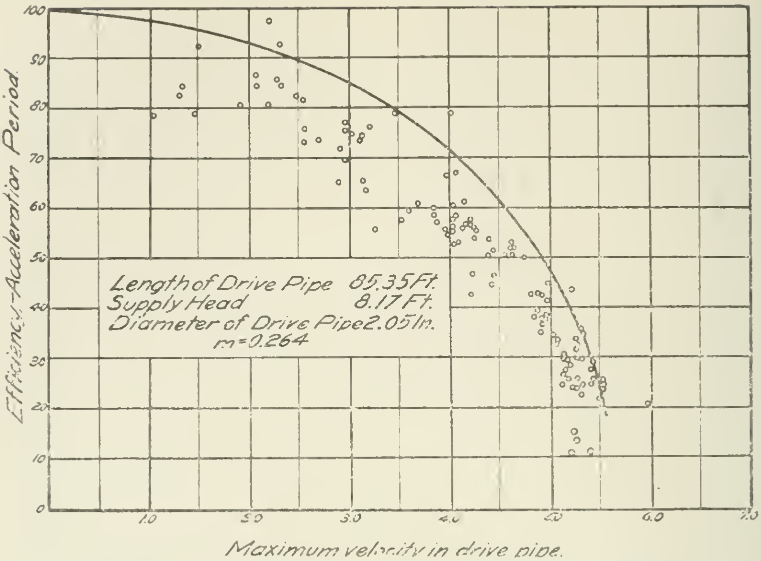

DIAGRAM XI.—EFFICIENCY CURVE—ACCELERATION PERIOD.

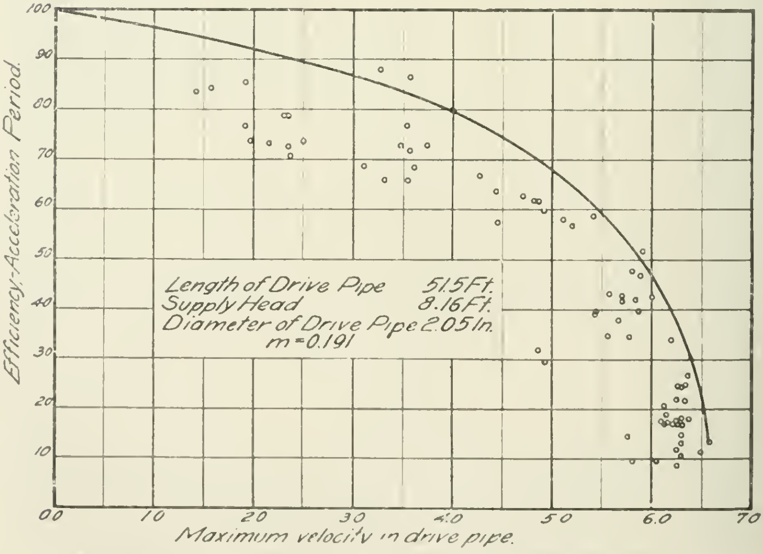

DIAGRAM XII.—EFFICIENCY CURVE—ACCELERATION PERIOD.

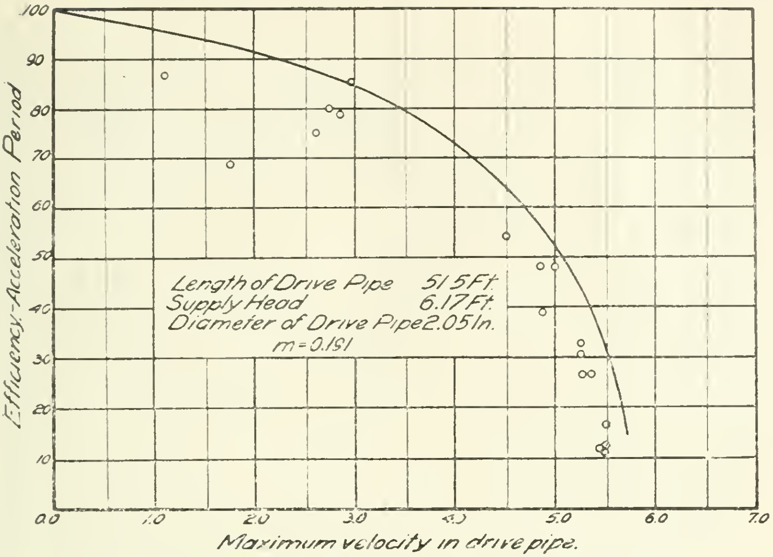

Diagram XIII.—Efficiency Curve—Acceleration Period.

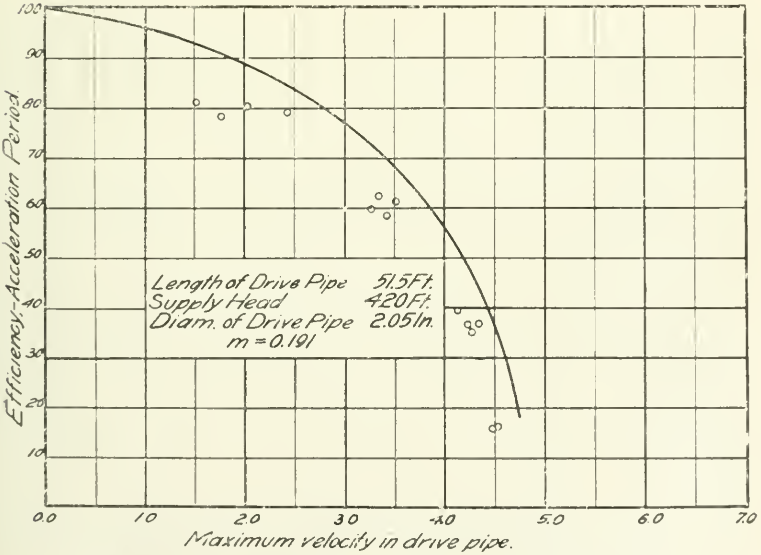

Diagram XIV.—Efficiency Curve—Acceleration Period.

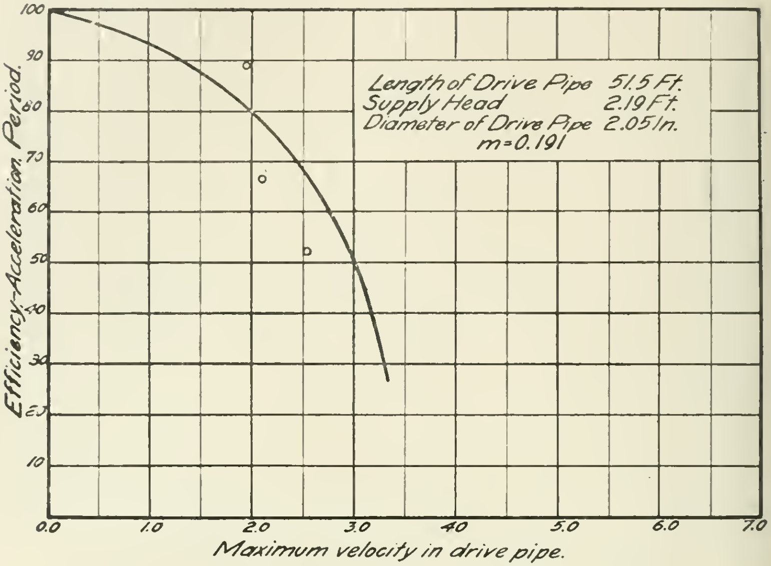

Diagram XV.—Efficiency Curve—Acceleration Period.

The experimental points in these curves do not show as close an agreement with the theoretical as in the other curves, due chiefly to the fact that V enters in equation (53) in the second degree, practically doubling the per cent. of error as may be readily shown algebraically. The efficiency is further decreased by the waste of water without proportionate increase in velocity during closure of the waste valve, although this effect is believed to be comparatively small.

2. *Retardation Period:*—A theoretical curve showing the effect of the maximum velocity V upon the efficiency during the pumping period can be obtained by assuming values of V and then applying equations (23), (44) and (32) successively for the particular value of h, or pumping head, under consideration. Diagrams XVIII, XX to XXV, inclusive, and the upper full-line curves in Diagrams XVI, XVII and XIX were computed in this way for the conditions given upon the respective diagrams which were average conditions existing during the experiments.

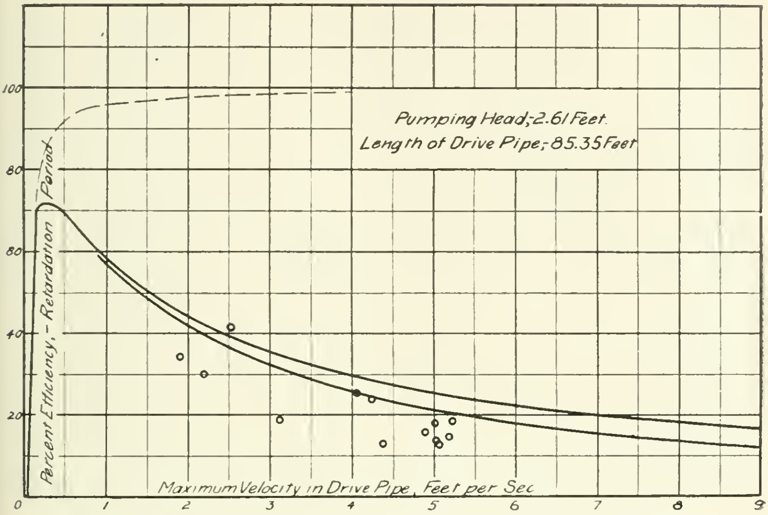

DIAGRAM XVI.—EFFICIENCY CURVES—RETARDATION PERIOD.

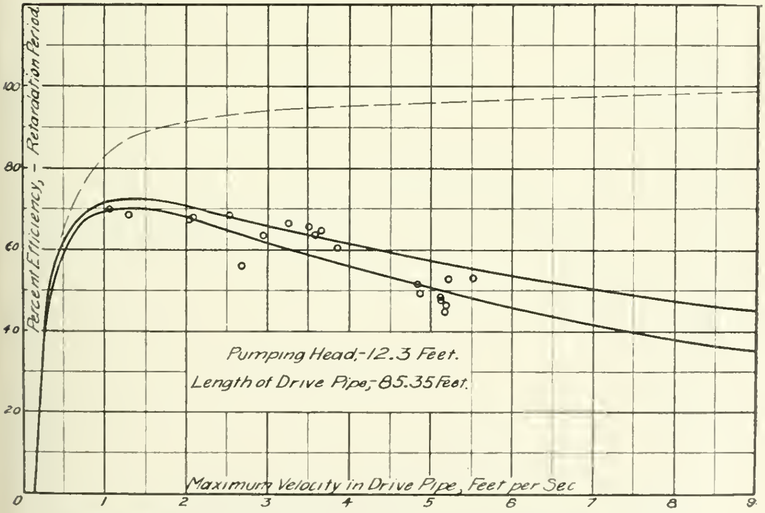

DIAGRAM XVII.—EFFICIENCY CURVES—RETARDATION PERIOD.

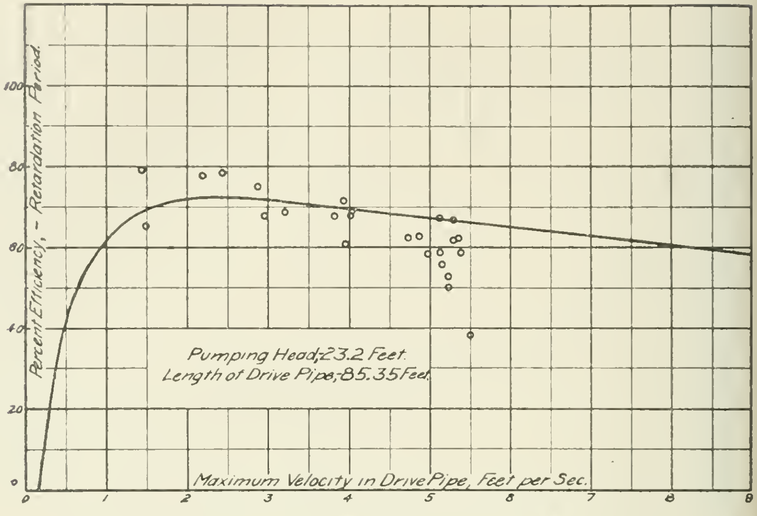

Diagram XVIII.—Efficiency Curve—Retardation Period.

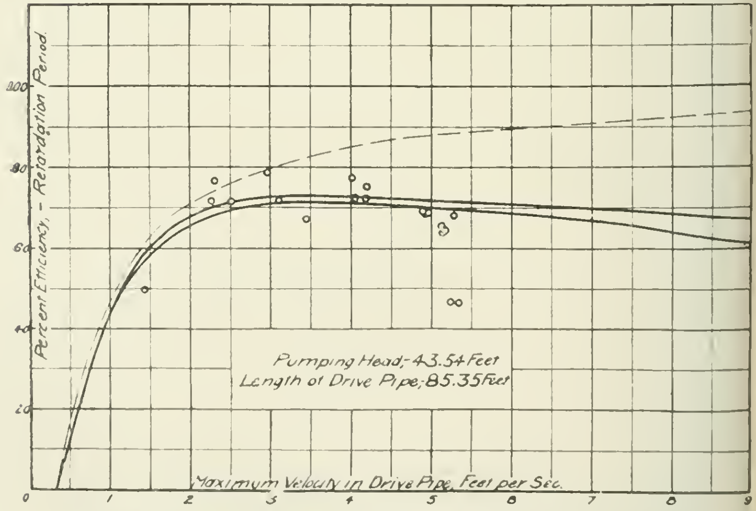

Diagram XIX.—Efficiency Curves—Retardation Period.

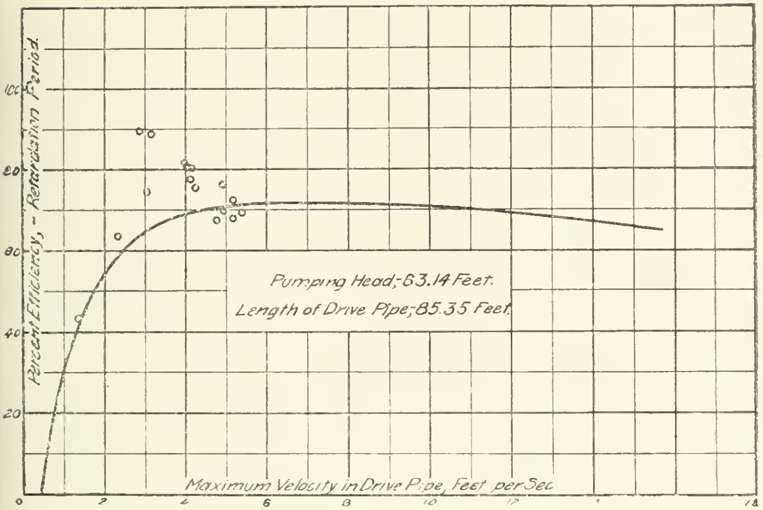

DIAGRAM XX.—EFFICIENCY CURVE—RETARDATION PERIOD.

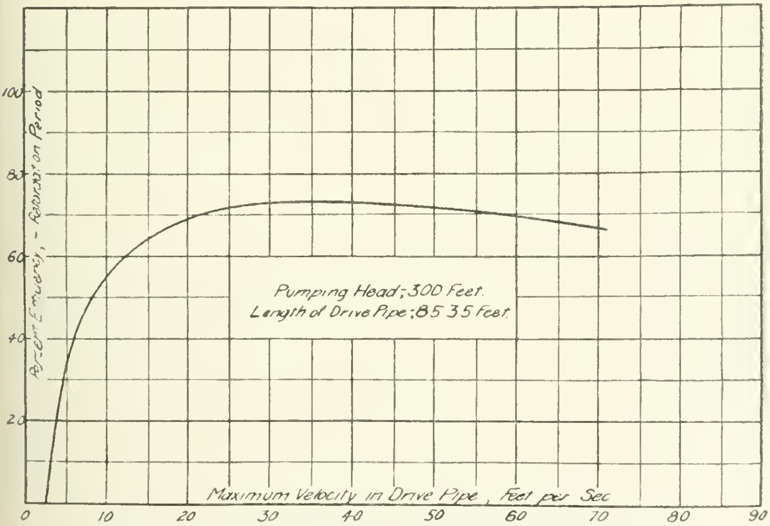

DIAGRAM XXI.—EFFICIENCY CURVE—RETARDATION PERIOD.

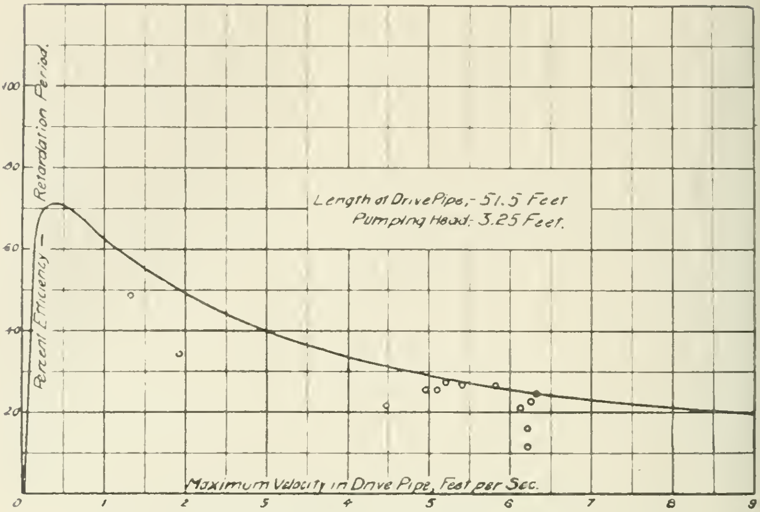

DIAGRAM XXII.—EFFICIENCY CURVE—RETARDATION PERIOD.

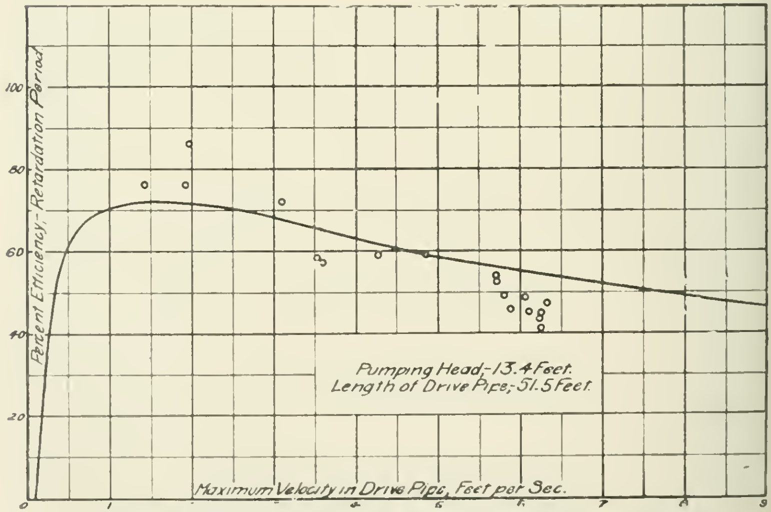

DIAGRAM XXIII.—EFFICIENCY CURVE—RETARDATION PERIOD.

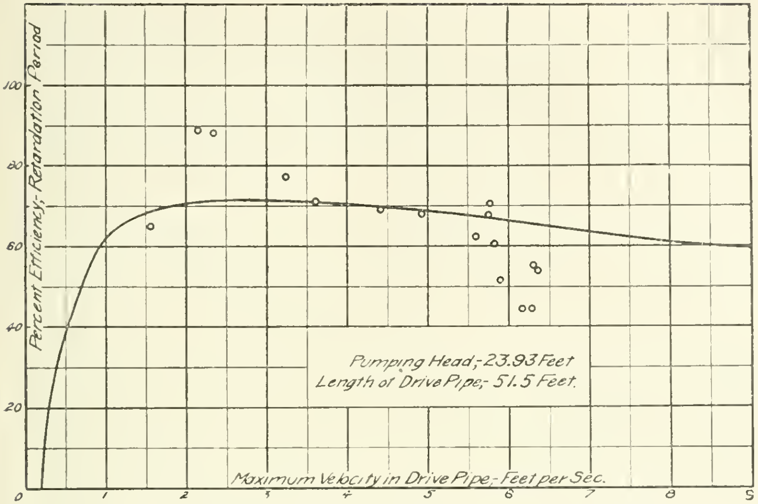

DIAGRAM XXIV.—EFFICIENCY CURVE—RETARDATION PERIOD.

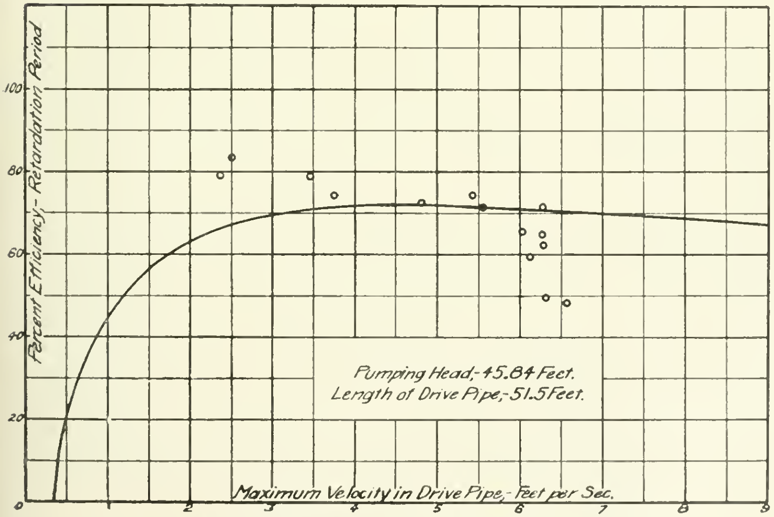

DIAGRAM XXV.—EFFICIENCY CURVE—RETARDATION PERIOD.

The lower curves in Diagrams XVI, XVII and XIX were obtained by the more exact formulas of cases I and II, pages 166 to 168, which take into account the retarding influences of the friction in the drive pipe. These formulas give lower efficiencies than the others, although the maximum efficiencies occur for practically the same velocities, and the curves do not differ much at the maximum points.

Since the values of efficiency, as shown by the experimental data plotted in these same curves, were obtained by the formula

$$E' = \frac{E_m}{E} \text{ (see equation [49a])}$$

they are affected by a systematic error (due to the velocity recording instrument) of the same size but opposite in sign to the errors which affect the efficiencies during the acceleration period, as shown in Diagrams XI to XV, inclusive. They are further subject to the accidental errors arising from observing Q, q, n, H, h, as well as V. The largest of such errors is probably that of h, as it was found to be quite impossible to maintain a constant head by means of the regulating valve. Furthermore, the value of the pumping heads as given on each diagram is the average pumping head for the points plotted and the values averaged commonly vary about two feet above and below the mean as may be seen by a study of the original data in Tables I and II. Another cause for lack of agreement between points is that data for all rates of valve closure are plotted on one curve.

Due to the systematic error in measuring V, we know that the plotted values of the efficiency during retardation are high. They do not, however, appear uniformly high in the curves. The two sets of efficiency curves are hence misleading in that they show the deficiency of experimental values to be due chiefly to causes operative in the acceleration period while in reality they are due very largely to losses in the retardation period, which were discussed in the theoretical analysis but could not be quantitatively expressed in the formulas. (See pages 173 to 175.)

3. *Efficiency of the Machine:*—The theoretical values are obtained by multiplying together the efficiencies, shown in the

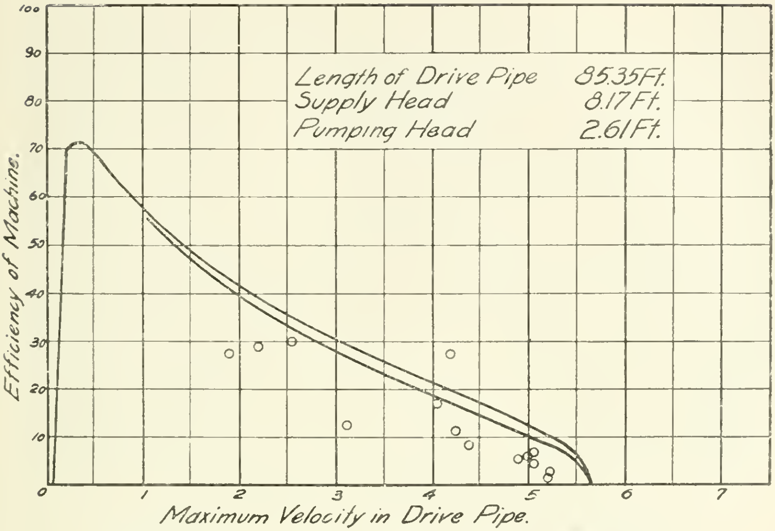

DIAGRAM XXVI.—TOTAL EFFICIENCY OF THE MACHINE.

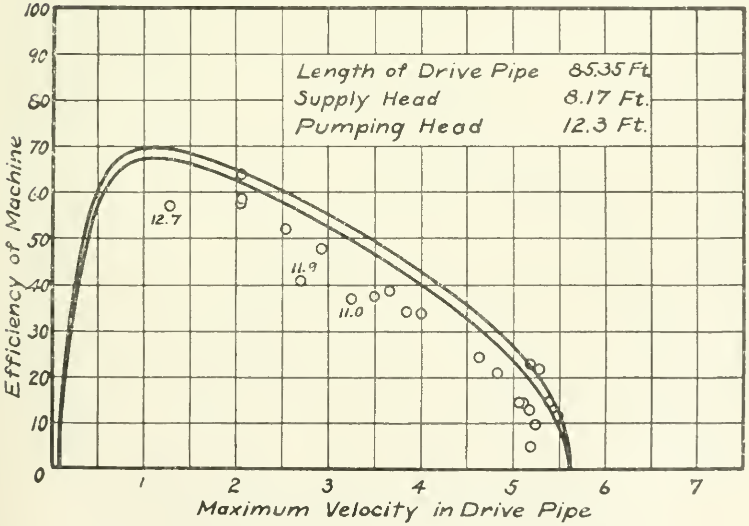

DIAGRAM XXVII.—TOTAL EFFICIENCY OF THE MACHINE.

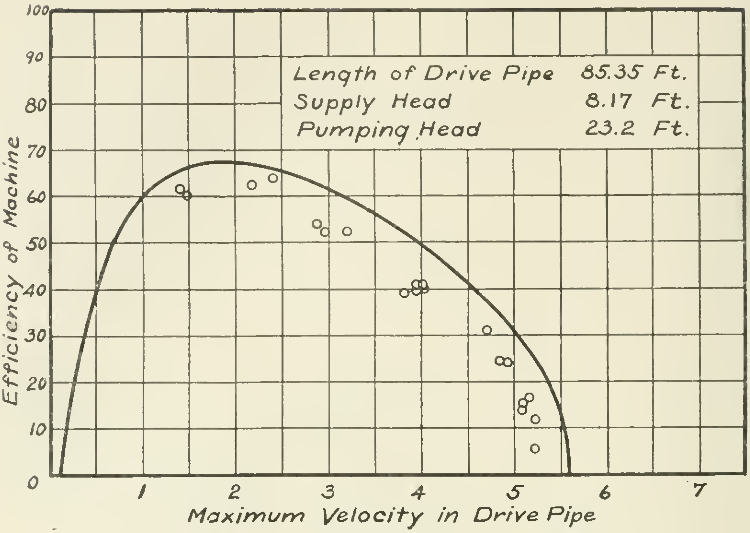

DIAGRAM XXVIII.—TOTAL EFFICIENCY OF THE MACHINE.

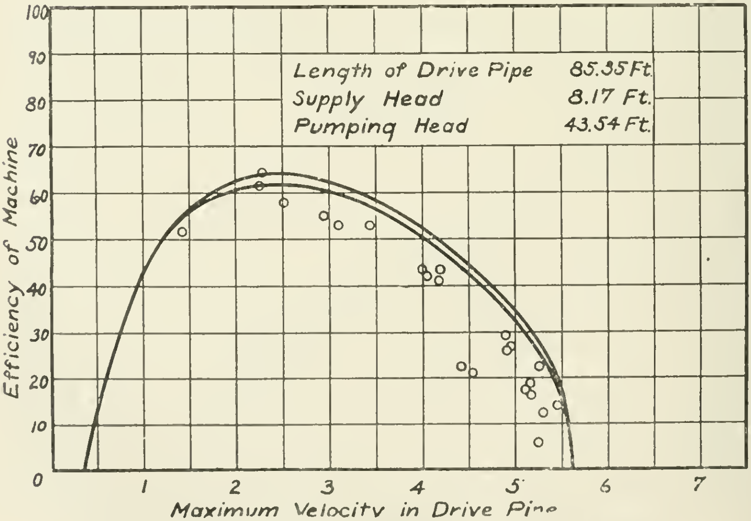

DIAGRAM XXIX.—TOTAL EFFICIENCY OF THE MACHINE.

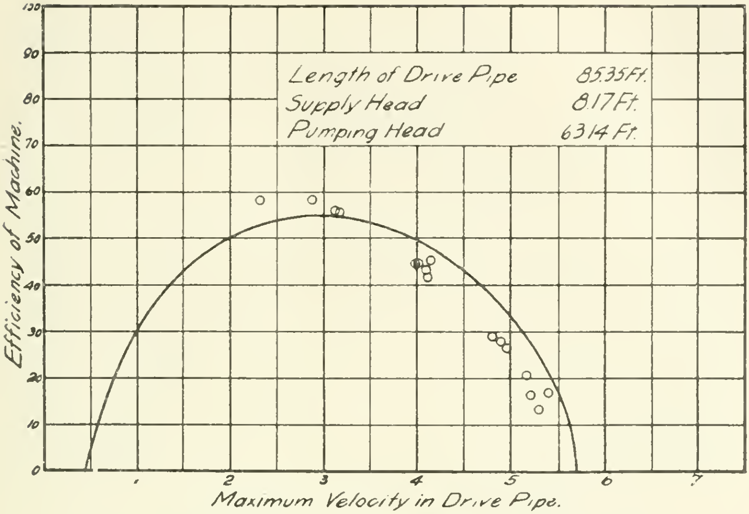

DIAGRAM XXX.—TOTAL EFFICIENCY OF THE MACHINE.

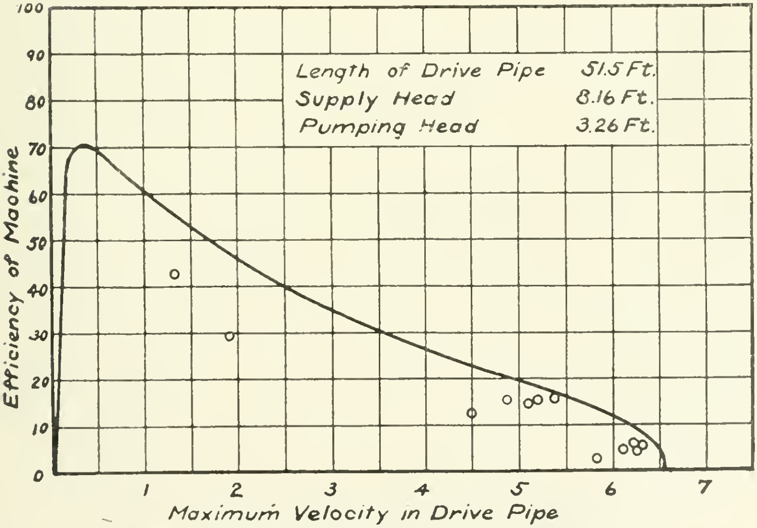

DIAGRAM XXXI.—TOTAL EFFICIENCY OF THE MACHINE.

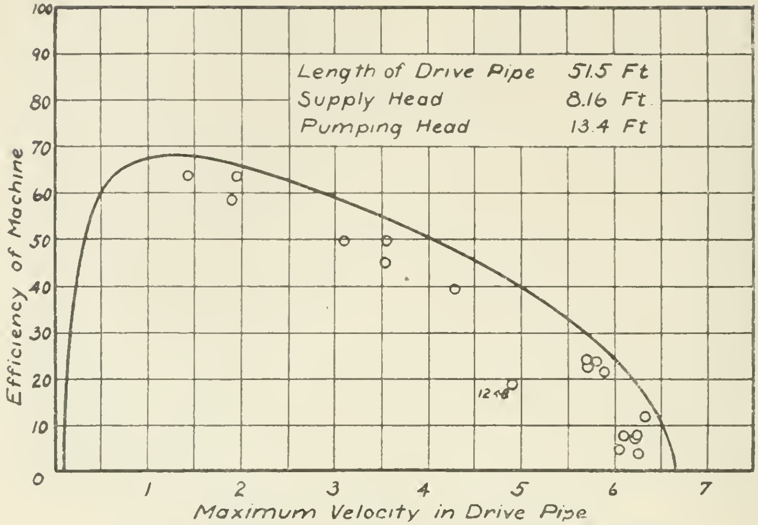

DIAGRAM XXXII.—TOTAL EFFICIENCY OF THE MACHINE.

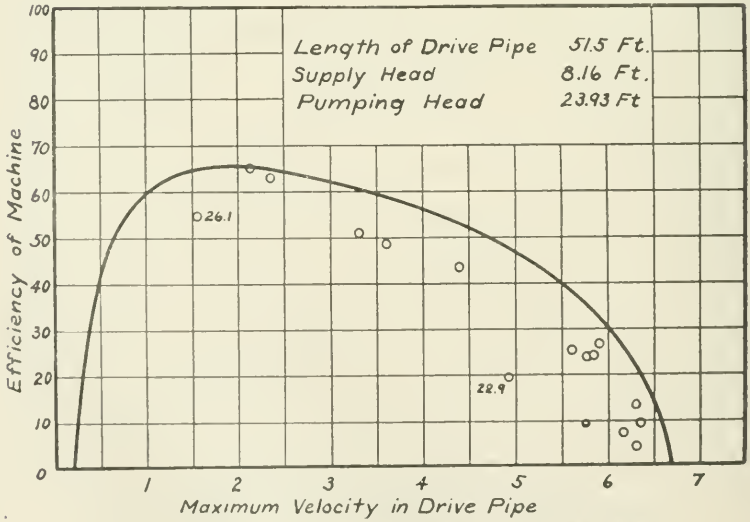

DIAGRAM XXXIII.—TOTAL EFFICIENCY OF THE MACHINE.

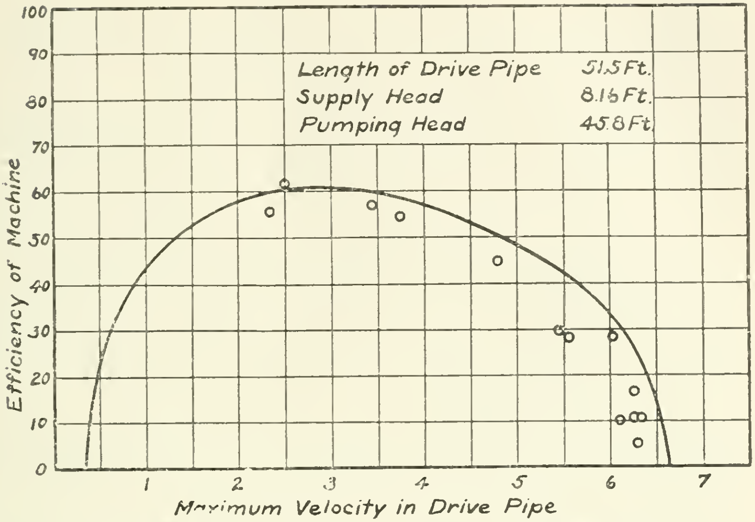

DIAGRAM XXXIV.—TOTAL EFFICIENCY OF THE MACHINE.

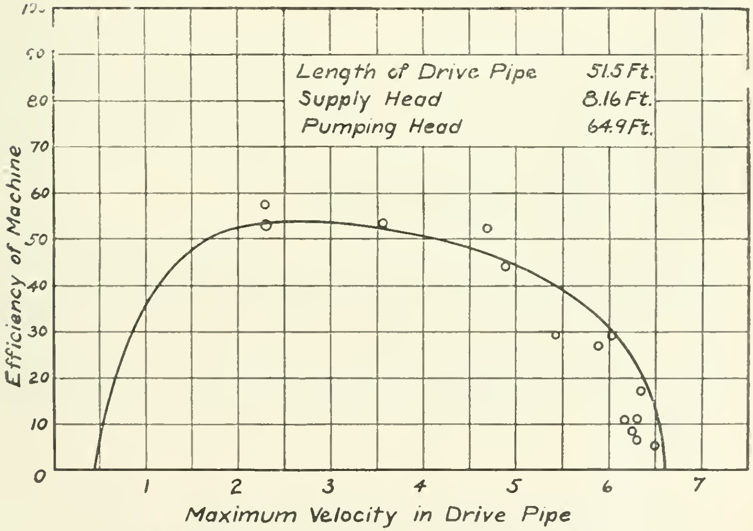

DIAGRAM XXXV.—TOTAL EFFICIENCY OF THE MACHINE.

preceding diagrams, during the two periods which compose the complete cycle. They are plotted in Diagrams XXVI to XXXV, inclusive, together with the experimental points.

The experimental values of this total efficiency are subject to much smaller errors than those of the two component periods since the errors of the velocity recorder do not enter. Since, however, values of V are used as abscissas in plotting the curves, the points are uniformly to the left of the position they would have taken, had the velocity been accurately recorded.

An important cause for the lack of agreement between points is that the curves are plotted for the average pumping heads. The true pumping head is shown on the curve opposite each point which differs greatly from the mean.

Another cause may be found in the fact that the plotted points include the readings taken with all rates of waste valve closure.

The general failure of experimental efficiencies to equal the theoretical is to be ascribed to losses not considered in the formulas and which occur chiefly during the retardation period. The general effect of these losses is discussed on pages 173 to 175.

It is to be regretted that lower velocities could not be obtained since the experimental points for low velocities are not sufficient to determine the economical velocity. The lack of the required data is due to the weight of the waste valve and valve rod which prevented rapid opening and closing.

In those diagrams which contain a double curve, the lower one results from using the more accurate formulas of Cases I and II, pages 166 to 168, in computing the efficiency during the retardation period. They differ but little from the more approximate curves immediately above them and serve no better for determining the economical velocity, for any given conditions.

EFFECTS OF CHANGING THE CONDITIONS OF OPERATION

1. *Supply Head:*—The effect of the supply head upon the operation of a ram is confined entirely to the acceleration period.

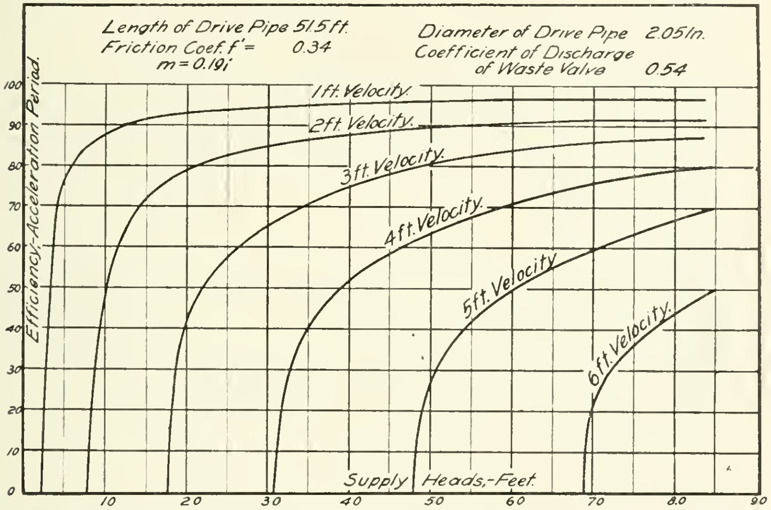

DIAGRAM XXXVI.—SHOWING THE EFFICIENCY WITH WHICH A SPECIFIED VELOCITY IN THE DRIVE PIPE CAN BE OBTAINED WITH A GIVEN SUPPLY HEAD.

Diagram XXXVI was computed by assuming values of v and H and then applying successively formulas (10), (13), and (14). It shows that any required velocity V can be more efficiently obtained the higher the supply head. We may therefore conclude that:

Other things remaining constant the efficiency during acceleration, and therefore of the ram itself, is increased by increasing the supply head.

2. Pumping Head:—The effect of the pumping head is confined to the retardation or pumping period.

Diagram XXXVII is an assembly of all the curves of efficiency during the retardation period for a 51.5′ drive pipe. These curves show that the same maximum efficiency during retardation can be obtained with any given pumping head, but that the velocity V required to obtain this maximum efficiency increases with the pumping head. The efficiency with which this required velocity can be produced in the drive pipe will, however, decrease and hence the combined efficiency will decrease with an increase in pumping head. This result is also evident from a comparison of the maximum points in Diagrams XXVI to XXXV, inclusive.

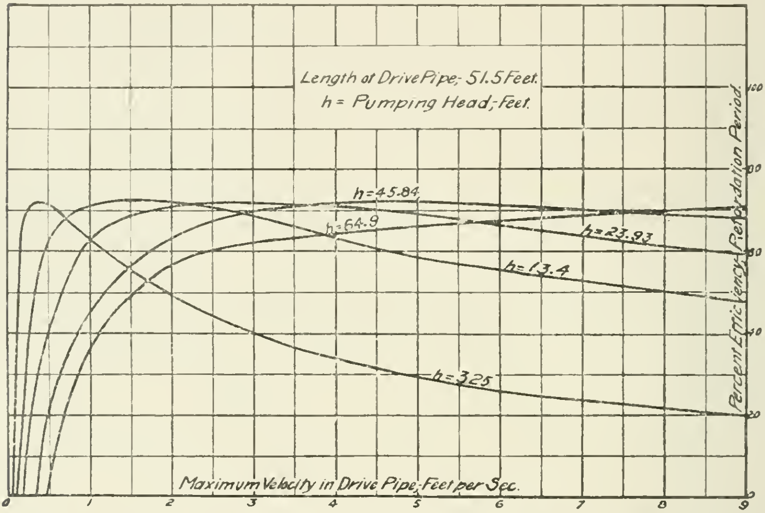

DIAGRAM XXXVII.—ASSEMBLY OF THE RETARDATION EFFICIENCY CURVES FOR THE 51.5 FT. DRIVE PIPE.

If, however, all conditions including the velocity V remain constant there is one pumping head for which the efficiency will be maximum, as shown by Diagram XXXVIII.

3. Length of Drive Pipe:—The efficiency with which a given velocity can be produced decreases as the length of drive pipe increases other things remaining constant. This is evident

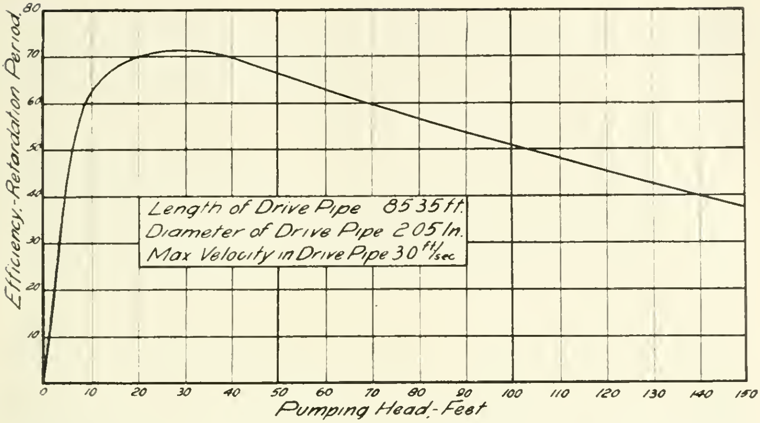

DIAGRAM XXXVIII.—SHOWING THAT THERE IS A PUMPING HEAD FOR WHICH THE EFFICIENCY, DURING RETARDATION WITH A GIVEN MAXIMUM VELOCITY, WILL BE MAXIMUM.

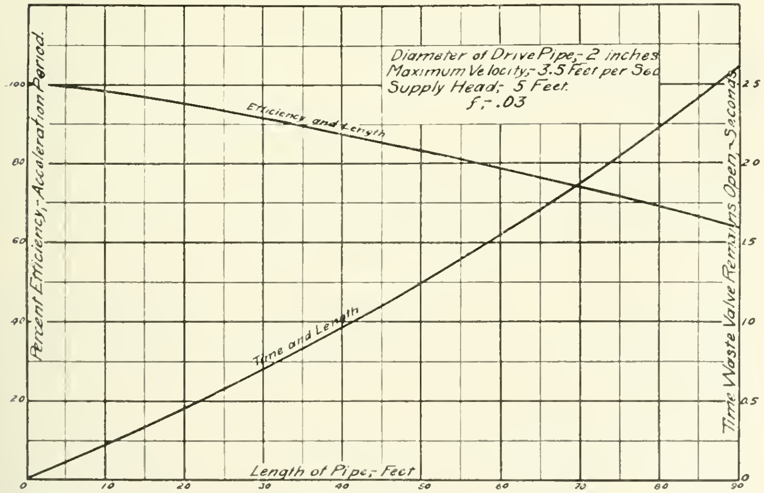

DIAGRAM XXXIX.—SHOWING THE EFFECT OF LENGTH OF DRIVE PIPE ON THE EFFICIENCY DURING ACCELERATION.

from a study of the formulas and by comparing Diagrams XI and XII. It is further shown by Diagram XXXIX, which also shows that the time necessary to develop a given velocity in the drive pipe increases with the length.

The efficiency during retardation according to the formulas is independent of the length I. However, both the slip and the loss in velocity during closure of the waste valve, which do not enter in the formulas, constitute a greater percentage of the total pumpage when the amount of water pumped during a stroke is small as with a short drive pipe. It is therefore safe to say that a decrease in efficiency during retardation results from shortening the drive pipe. Its importance, although small, is not determined.

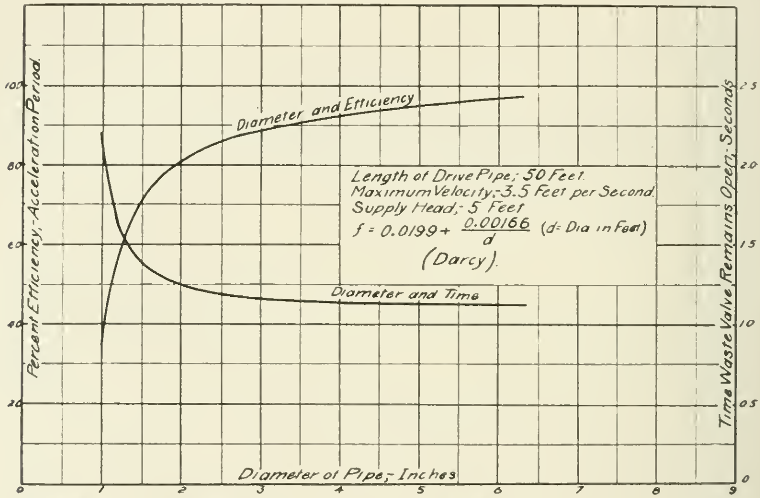

DIAGRAM XL.—SHOWING THE EFFECT OF DIAMETER OF DRIVE PIPE UPON THE EFFICIENCY DURING ACCELERATION.

The combined effect of lengthening the drive pipe is thus to decrease the efficiency except, perhaps, for short drive pipes and low velocities where the slip and loss due to closure become relatively more important.

4. Size of Drive Pipe:—Diagram XL shows, for a particular case, the effect of the diameter of the drive pipe upon the efficiency with which a given velocity may be acquired and the time required to produce this velocity. The conclusion that the efficiency increases with the diameter is obvious.

In the second or retardation period the problem of size of drive pipe is not very important, the efficiency being determined chiefly by the check valve. This is seen by a study of Diagrams XVI, XVII and XIX where the upper or dashed line is the efficiency which would be possible were there no loss in either the check valve or the drive pipe during this period; the upper full line is obtained by the approximate formula which takes account of the loss through the check valve only; the lower full line takes account of the losses in both the drive pipe and the check valve.

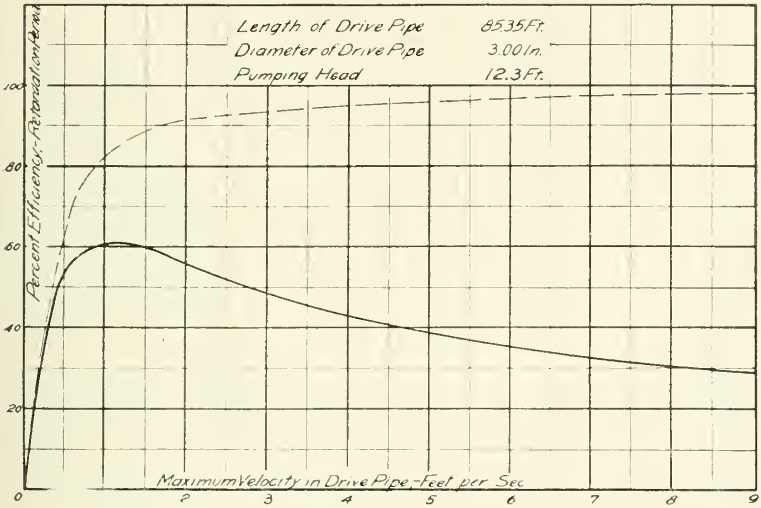

DIAGRAM XLI.—EFFICIENCY CURVES—RETARDATION PERIOD.

Diagram XLI was computed by means of the approximate formula and shows the result which would be obtained under the same conditions as shown in the upper full line of Diagram XVII except with a three-inch drive pipe. The efficiency is smaller for all velocities due, however, to the check valve. Were the check valve area increased to give the same loss per unit velocity in the drive pipe, the curve would coincide with the upper full line in Diagram XVII, while the loss in the drive pipe would be decreased thus raising the lower full line in Diagram XVII. This would increase somewhat the efficiency during this period and thus add to the beneficial effect obtained during acceleration.

5. *Strokes per Minute:*—Other things remaining constant the maximum velocity V in the drive pipe will decrease as the number of strokes per minute increases.

Diagrams XI to XV show that the efficiency during the acceleration period is 100 per cent. for a zero velocity and approaches zero as the velocity approaches its limiting value.

During the pumping or retardation period, however, there is an efficient velocity as shown in Diagram XVI to XXV.

The efficient velocity for the entire cycle or for the machine will be found at that point on the two curves where the slopes are opposite, i. e., for that velocity at which the efficiency during acceleration is decreasing, per unit increase in velocity, at the same rate at which the efficiency during retardation is increasing. This will always occur to the left of the maximum point in Diagrams XVI to XXV.

Diagrams XXVI to XXXV show the combined efficiency of both periods. There is a minimum velocity below which no water would be pumped. This critical value is: $v = hg/\lambda$. There is also a maximum velocity $\sqrt{\frac{H}{m}}$ which can be obtained under given conditions and this also with a zero efficiency.

Diagram XLII shows, for one set of given conditions, the effect of the number of strokes per minute upon: the maximum velocity V in the drive pipe; total gallons per minute $(Q + q)$ used by the machine; gallons per minute pumped q; and efficiency of the machine E. The velocity V was first assumed. The time required to generate this velocity was taken from Diagram VI. The time T, during which the waste valve remains closed, was computed from equations (22) and (36). The number of strokes per minute was then assumed to be

$$n = \frac{60}{T_o + T_c + 0.3} \qquad (54)$$

where the 0.3 seconds represents an estimated average value for

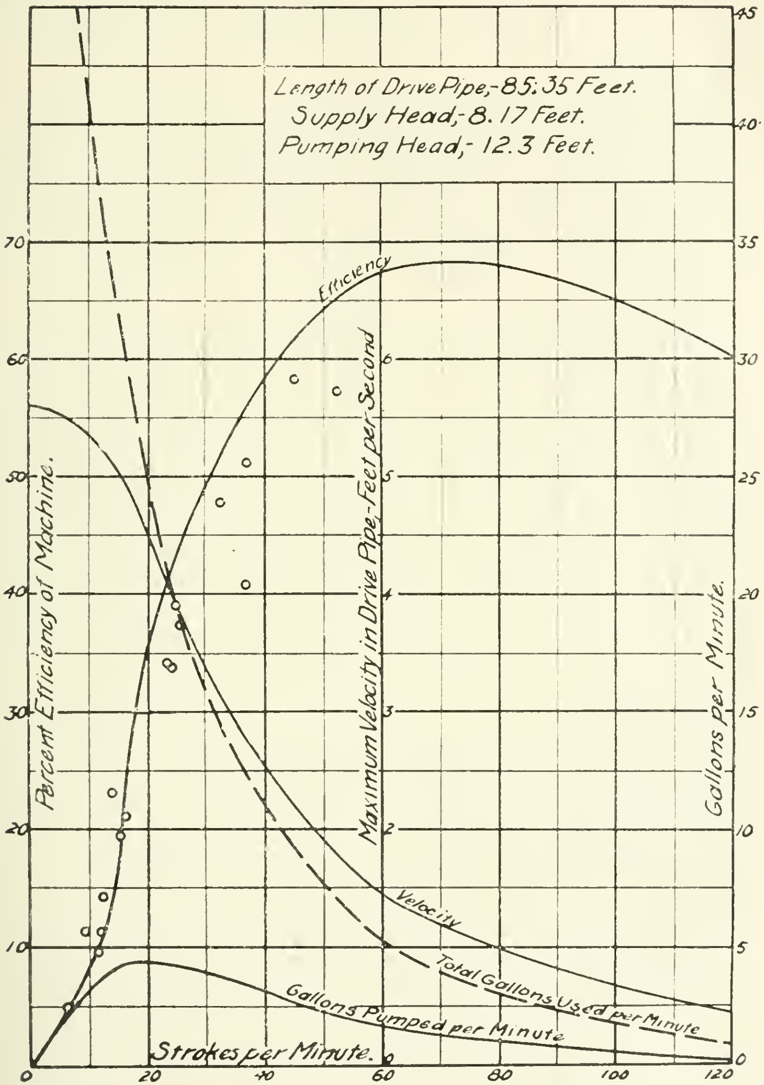

Diagram XLII.—Characteristic Operating Curves of the Experimental Ram Under the Conditions Assumed Above.

the time occupied by the waste valve in opening and closing. The method of obtaining Q, q and E_m from the formulas and previous curves is evident. Experimental points are shown for efficiency only.

These curves in Diagram XLII may be called the *characteristic operating curves* of this ram under the given conditions. It will be observed that the maximum efficiency is obtained for this case with about 70 strokes per minute; the maximum discharge at about 20 strokes per minute with only about 40 per cent. efficiency.

6. *Rate of Waste Valve Closure:*—Attempts were made to determine by means of the experimental data the effect of rate of closure. It was, however, in the experimental work, impossible to keep all other conditions constant. In addition the intended action of the closing cam A (Plate IV) was not fully realized. The increase in water pressure during closure became sufficient, before the valve had reached its seat, to overcome the action of the spring V (Plate III) and, by taking up the play in the joint O and the cam roller P on its journal as well as in the cam groove, to cause a sudden upward jump of the valve. This is readily seen in the sample cards shown in Fig. 14.

It was also found upon removing the valve at the completion of the experiment that the cap screw which fastened the valve to the lower end of the rod had loosened and this no doubt had operated to disguise the effect of valve closure in the experimental data. Results were discordant although a general tendency toward increased efficiencies with rapid closure was discernible.

A rapid closure of the valve reduces the time from X to Y (Fig. 12) during which the water is wasting with only a small proportionate increase in velocity. It also reduces the time from Y to Z during which velocity and water are both lost and, since the average pressure which is retarding this velocity and wasting the water during this period would be practically the same in any case of valve closure, we may reasonably conclude that it conserves more of the accumulated energy.

From the theoretical standpoint we may therefore safely say that a rapid valve closure conduces to greater efficiency of operation. Some manufacturers avoid a rapid closure in order to reduce the shock upon the machine.

7. *Law of Closure:*—From X to Y (Fig. 12) the efficiency with which each increment of velocity is obtained decreases (since the curve is concave downward). The less efficiently this gain in energy is obtained the less should be the length of time during which it is allowed to continue. From Y to Z the loss in velocity, per instant of time, will increase as the retarding head increases and therefore as the valve approaches its seat. The more rapid this loss the shorter should be its duration.

This reasoning leads to the conclusion that an accelerated movement of the valve gives greatest efficiency.

The magnitude of the effects of both shock pressure and loss during closure are unsettled questions. They should be corrected for by the introduction of an experimental coefficient C multiplied into the maximum velocity V in the retardation formulas. The present data is not sufficiently accurate or comprehensive to determine such a coefficient satisfactory.

8. *Volume of Air in the Air Chamber:*—As shown by the theoretical and experimental pressure curves in Fig. 14 the loss of head through the check valve is maximum and the efficiency of pumping therefore minimum at the first instant of the pumping period. The efficiency of the operation increases during the period until the loss of head becomes zero at the end. Now with a small volume of air the pressure increases greatly during the stroke, thus requiring the most efficient pumpage to take place (due to the increased pumping head) under the least favorable conditions.

A large volume of air thus increases the efficiency with which the water enters the air chamber besides conducing to a more uniform, and hence a more efficient discharge from the same.

It is desirable that future experimenters record, in order to prove this assertion, both the minimum pressure and the range of pressure during the pumping period instead of the average value only, as was done in these experiments.

9. Amount of Water in the Air Chamber:—If the amount of water were increased while at the same time the air chamber were extended upward so that the volume of air might remain constant, the effect would be negligible unless for a slender air chamber. In this case an appreciable effect might result from the necessity of starting this column of water upward at the beginning of each pumping period.

10. Amount of Opening or Range of Movement of the Waste Valve:—Increasing the opening of the waste valve decreases m (equation [8a]) and therefore increases the efficiency during acceleration. The loss of energy in closing is greater, however, and there is probably an economical opening for any given valve under each condition of operation.

11. Type of Waste Valve:—The waste valve should be as light as consistant with strength and durability. It should be held open with a long spring rather than by a weight in order that it close more quickly after starting. The necessary valve area should be obtained by a number of small valves with a small range of movement rather than by a large valve which would need to be built thicker and heavier to possess the required strength. They should be placed as close as practicable to the check valve.

12. Type and Size of Check Valve:—The efficiency during retardation is largely determined by the check valve, as explained in discussing the diameter of drive pipe (see 4). The great importance of reducing the loss through the check valve, or valves, should not be lost sight of in design. About the same principles no doubt apply as in the design of any pump valves.

CONCLUSION

It is the belief of the writer that the comparison of experiment and theory in the preceding pages has demonstrated the practicability of the logical design of a hydraulic ram for any given working conditions. There are, to be sure, certain constants entering in the formulas which require experimental determination. Most of these are, however, fairly well known already, such as f, m, m_2, etc. Some are as much needed for other classes of pumps as for the hydraulic ram, viz: c, c′, m′ and the slip s′. There is but one factor, C, which is useful to the ram only, and this can, by a properly designed waste valve, be reduced to nearly unity. Experiments are now in progress to determine C, and when determined equation (22) will take the form:

$$v' = \frac{\frac{\lambda}{g} CV - h}{c' + \frac{\lambda}{g} C} \qquad (55$$

Due to the fact that the formulas are perfectly general in their derivation, there is every reason to believe that they would agree as closely with the experimental results obtained with any other ram as with the one used in these experiments.

If there is any reason whatever tending to limit the size and capacity of the hydraulic ram, it is the practical difficulties which might be encountered in the design of valves. It is believed that these are no more insurmountable than those encountered in the design of valves for other pumping engines of large size.

We have made no attempt to discuss the basis for true economical design which involves first cost as well as operating efficiency. This is a problem to be separately investigated for each particular case.

INDEX TO NOMENCLATURE USED IN FORMULAS.

A = Cross-sectional area of the drive pipe.
a $= c' - D$
a_v = Area of the waste valve opening considered as an orifice.
b $= c' + D$
C = Proportion of the maximum velocity V which is conserved in closing the valve.
c = Coefficient of discharge of the waste valve.
c' = Loss of head through the check valve per unit rate of flow, (equals *2.52 feet* per foot of velocity in a two-inch drive pipe or 1.76 feet loss of head per pound of water flowing through the valve in one second, for the check valve used in these experiments).
D $= \sqrt{c'^2 - 4mh}$
D' $= \sqrt{4mh - c'^2}$
d = Diameter of the drive pipe in feet.
E = Efficiency during acceleration period.
E' = Efficiency during retardation period.
E_m = Efficiency of the machine, or total efficiency.
e = Base of natural system of logarithms = 2.71828.
e' = thickness of the pipe wall.
f = Friction factor for the drive pipe.
f' is defined by the equation:

$$m_1 + m_2 + f\frac{l}{d} = f'\frac{l}{d}$$

g = Acceleration due to gravity.
H = Supply head (Figure 1)
h = Head pumped against or pumping head (Figure 1)
h_1 = Head in drive pipe at waste valve during acceleration.
h' = loss of head through check valve.

$j = \frac{2g\sqrt{mH}}{l}$

K = Volumnar modulus of elasticity of water.

$k = \frac{2mv' + b}{2mv' + a}$

l = Length of drive pipe.

M $= \frac{1}{2g}$ (Summation of loss coefficients); where friction through check valve varies as v^2, or, loss of head in drive pipe and valve =

$$\left(1 + f\frac{l}{d} + m_1 + m_2 + m'\right)\frac{1}{2g}.$$

$m = \left(m_1 + m_2 + f\frac{l}{d} + \frac{A^2}{c^2a^2}\right)\frac{1}{2g}$ for acceleration period or = $\left(1 + m_1 + m_2 + f\frac{l}{d}\right)\frac{1}{2g}$ for the retardation period.

m′ = Coefficient of loss through the check valve where this loss varies as v^2, i. e., where lost head $= m'\frac{v^2}{2g}$

m_1 = Entrance loss coefficient.

m_2 = Coefficient of loss due to elbows and obstructions.

N = Number of strokes recorded by the tachometer during one run.

n = Strokes per minute.

P = Water hammer pressure in pounds per square inch.

Q = Water wasted.

q = Water pumped.

q_1 = Discharge per second through waste valve (and hence through drive pipe).

R = Rate of decrease of area a in square feet per second as the valve closes.

$r = \frac{c'g}{l}$

$r' = \frac{gD}{l}$

S = Total distance moved by a cross-section of the water column during a period.

s = Distance moved by the water column in the drive pipe in time t after opening or closing the waste valve.

s' = Slip through the check valve per stroke expressed in terms of number of feet of drive pipe filled by the water thus lost.

t = Time elapsed after beginning of the period under discussion.

T_c = Time waste valve remains closed.

T_o = Time waste valve remains open.

V = Maximum velocity of water in the drive pipe (equals velocity at time of closure of the waste valve).

v = Velocity of water in the drive pipe at time t.

v'' = Initial velocity in the drive pipe after closure of the waste valve.

v_v = Velocity of discharge from the waste valve.

W = Weight of water required to fill the drive pipe.

w = Weight of a cubic unit of water = 62.5 pounds per cubic foot.

$\alpha = \frac{2mv' + c'}{D'}$

$\beta = \frac{gD'}{2l}$

λ = Velocity of wave motion along the water in a pipe.

BIBLIOGRAPHY

Hydraulic Rams

Bentler, A. Jr., Brune, P. J. and Main, F. J., *Tests of a Rife Hydraulic Ram* in *Stevens Institute Indicator.* (April, 1898.)

Bjorling, P. R., *Water or Hydraulic Motors,* pps. 196–271, (Spon, London, 1894.)

Clark, J. Wright, *Hydraulic Rams, Their Principles and Construction.* (B. T. Batsford, London, 1900.)

Clay, H. H., *Design. Hydraulic Rams and Pumps* in *Plumber and Decorator.* (October 2, 1905.)

Chevillard, *Bélier Hydraulique Rife á Double Effet pour Service Public d'élevation d'Eau* in *Reveu Industrielle,* **30**: 21–2. (1899.)

Decoeur, *Bélier Hydraulique á Pulsations* in *Annales des Ponts et Chaussées Memories et Documents.* **2**:646. (1892.) Also *Portefinelle economique des machines de l'ontillage et des matériel.* **37**:93. (1892.)

Gelly, *Doppelt Wirkender Hydraulischer Widder* in *Gesundheits Ingenieur.* **22**:216–7. (1899.)

Hartmann, K. and Knobe, J. O., Revised by Berg, H., *Die Pumpen.* pps. 527–85. (Julius Springer, Berlin, 1906.)

Hillenbrand, *Hydraulic Ram* in *American Machinist,* **16**: No. 22, (1893.)

Josse, *Drucklust Wasserheber* in *Bohrtechniker,* **6**: No. 1, (1899.)

Krouse and Company, *Wasserhebung und Forderung mittelst Lustdruck* in *Die Metallarbeiter,* **25**:287, (1889.)

Kunz, *Wasserörderungsmachinen* in *Uhland's T. R. 1902.* Supplement, pps. 33–5. (1902.)

Masse, R., *Béliers Hydrauliques. Les Pompes,* pps. 363–88. Vve. Chc. Dunod, Paris, (1903.)

Mead, Daniel W., *Hydraulischer Widder* in *Uhland's T. R. 1902.* Supplement, p. 23. (1902.)
Engineering News, (February 1. 1890.)

Mead, Daniel W., *A Large Hydraulic Ram* in *Engineering Record,* (August 24, 1901.)

Mead, Daniel W., *The Hydraulic Ram for Use in Public Water Works System* in *Illinois Society of Engineers and Surveyors.* 11th Annual Report. (1896.)

Morin, Arthur. *Des Machine et Appareils Destinés à l'Elevation des Eaux.* pps. 180–235. Paris, (1863.)

Pixis, Carl, *Hydraulic Rams* in *Engineering and Mining Journal,* (April 2, 1896.)

Poillon, L., *Traite Théorique et Pratique des Pompes et Machines à Elever les Eaux.* **2**:137–212. E. Bernard & Co., Paris, 1888.)

Richards, J., *Hydraulic Rams* in *Journal of the Association of Engineering Societies.* (January, 1898.)

Sassmann, *Hydraulischer Widder* in *Der Gesundheits Ingenieur,* **22**: 122–3. (1899.)

Schuseil, *Wasserhebung und Wasserförderung mittelst Luftdruck* in *Sprechsaal,* **31**: 860–1. (1898.)

Simin, O., *Water Hammer* in *Proc. of Amer. Waterworks Assn.* (1904.)

Steen, *Hydraulischer Widder mit Selbsttätiger Inbetreibsetzung, System "Lön"* in *Metalische Arbeiter.* **27**: Pt. 1, 276. (1901.)

Wagner, *Hydraulischer Widder zur Förderung reinen quellwassers oder andere Flüssigkeiten, unabhängig von seinen Freibwasser* in *Polytechnisches Centralblatt.* **59**: 255–6. (1898.)

Webster, *Hydraulic Rams* in *The Engineer,* **74**: 509. (1892.)

Weisbach and Herrmann, *Mechanics of Pumping Machinery,* pp. 255–65. (MacMillan & Co. London and New York, 1897.)

Wood, A. J., With discussions by Kent, William, and Johnson, T. W., *The Determination of the Efficiency of Hydraulic Rams* in *Stevens Institute Indicator,* **19**: (1902.)

WATER HAMMER

Carpenter, R. C., *Some Experiments on the Effect of Water Hammer* in *Transactions of American Society of Mechanical Engineers.* **15**.

Church, Irving P., *Unsteady Flow of Water in Pipes* in *Transactions of Association of Civil Engineers of Cornell University.* (1898.)

Church, Irving P., *Water Hammer* in *Boston Journal of Commerce.* (November 21, 1896.)

Clark, J. Wright, *Water Hammer in Pipes.* Serial:—Pt. 1. in *Plumber and Decorator.* (May 1, 1905.)

Joukowsky, N., *Uber den Hydraulischen Stoss in Wasserleitungsröhren* in *Journal of the Imperial Academy of Sciences of St. Petersburg.* **9**: No. 5.

Walckenaer, M., *Chocs de l'Eau dans les Conduites de Vapeur* in *Ann. des Ponts et Chassées.* Trimestre. (1899.)

Williams, W. J., *Water Hammer in Steam Pipes* in *American Machinist.* (March 12, 1896.)

Winslow, G. E., *Experiences in Reducing Water Ram caused by Direct Acting Pumping Engines* in *Journal of New England Water Works Association.* (December, 1901.)

Weston, Edmund B., *Descriptions of Some Experiments made on the Providence, R. I., Water Works to Ascertain the Force of Water Ram Pipes* in *Transactions of Amer. Soc. of Civil. Engs.*, p. 308. (June, 1885.)

Lotta, G. T., *Water Ram Utilized* in *American Water Works Association.* (June, 1901.)

Church, Irving P., *"Water Ram" in Pipes* in *Journal of the Franklin Institute.* (April and May, 1890.)

BULLETIN OF THE UNIVERSITY OF WISCONSIN

NO. 216

ENGINEERING SERIES, VOL. 4, NO. 4, PP. 249–332

INVESTIGATION OF FLOW THROUGH LARGE SUBMERGED ORIFICES AND TUBES

PART I

EXPERIMENTS WITH SUBMERGED TUBES 4.0 FEET SQUARE

BY

CLINTON BROWN STEWART, C. E.

RESEARCHES IN HYDRAULICS
DANIEL W. MEAD, PROFESSOR OF HYDRAULIC AND SANITARY ENGINEERING

Published bi-monthly by authority of law with the approval of the Regents
of the University and entered as second-class matter at the
post office at Madison, Wisconsin

MADISON, WISCONSIN
APRIL, 1908

CONTENTS

PAGE
Introduction 255
Supply of water 256
Description of bulkhead and submerged tubes 257
Description of weirs 264
Description of hook gages and still water basins 270
Description of dial float gage 273
Calibration of sharp crested weir, 2.505 feet long 275
General method of making observations 284
Tabulated results of experiments with submerged tubes 285
Summary sheet showing results of experiments with submerged tubes 290
Curves showing average results of experiments with submerged tubes 301
  Effect of changing the length of tubes 301
  Effect of modifying entrance conditions to tubes 304
Conclusions and discussion of results of experiments 319

LIST OF ILLUSTRATIONS

PLATES

PAGE
I. Plan of hydraulic laboratory, showing arrangements for experiments with submerged tubes (opposite) 256
II. Longitudinal section of experimental channel, and details of bulkhead and weirs (opposite) 256
III. Sketch showing forms of entrance and length of tubes used (opposite) 256
IV. Photograph showing elliptical form of entrance to submerged tube ten feet long 258
V. Details of submerged tubes, Series Nos. 1-7 (opposite) ... 258
VI. Details of submerged tubes, Series Nos. 1a, 1b, 1c, and 1d 261
VII. Details of submerged tubes, Series Nos. 4a, 4b, 4c and 4d 262
VIII. Details of submerged tubes, Series Nos. 5a, 5b, 5c and 5d 263

PAGE
IX. Details of submerged tubes, Series Nos. 7a, 7b, 7c, 7d and 7c′ (opposite) 264
X. Photograph showing arrangement of three, two and one-half foot sharp crested weirs 265
XI. Photograph showing arrangement of still water basins for three, two and one-half foot weirs 266
XII. Details of adjustable hook gage and still water basins 271
XIII. Photograph showing adjustable hook gage 272
XIV. Details of dial float gage 274
XV. Discharge curve for sharp-crested weir 2.505 feet long (opposite) 280
XVI. Logarithmic discharge curve for a sharp crested weir 2.505 feet long 282
XVII. Curves showing fall in water surface between gage No. 3 and outlet end of tube 291
XVIII. Curves showing the effect on discharge of changing the length of tubes, Series Nos. 1–7 302
XIX. Curves showing the effect on coefficient of discharge of changing the length of tubes, Series Nos. 1–7 303
XX. Curves showing the effect on discharge of changing the length of tubes, Series Nos. 1d–7d 305
XXI. Curves showing the effect on coefficient of discharge of changing the length of tubes, Series Nos 1d–7d 306
XXII. Curves showing the effect on discharge of modifying entrance conditions of tube, length 0.31 feet 307
XXIII. Curves showing the effect on discharge of modifying entrance conditions of tubes, length 2.50 feet 308
XXIV. Curves showing the effect on discharge of modifying entrance conditions of tubes, length 5 00 feet 309
XXV. Curves showing the effect on discharge of modifying entrance conditions to tubes, length 10.0 feet 310
XXVI. Curves showing the effect on discharge of modifying entrance conditions of tubes, length 14 0 feet 311
XXVII. Curves showing the effect on coefficient of discharge of modifying entrance conditions of tubes, length 0 31 feet 312
XXVIII. Curves showing the effect on coefficient of discharge of modifying entrance conditions of tubes, length 2.50 feet 313
XXIX. Curves showing the effect on coefficient of discharge of modifying entrance conditions of tubes, length 5.00 feet 314

PAGE
XXX. Curves showing the effect on coefficient of discharge of modifying entrance conditions of tubes, length 10.0 feet 315
XXXI. Curves showing effect on coefficient of discharge of modifying entrance conditions of tubes, length 14.0 feet 316
XXXII. Summary of curves showing the effect on coefficient of discharge of modifying entrance conditions and changing the length of tubes (opposite) 322
XXXIII. Summary of curves showing the effect on coefficient of discharge of changing the length of tubes 325
XXXIV. Diagram of flow through submerged tube and orifices (opposite) 330

TABLES

I. Description of forms of entrance and outlet of submerged tubes 260
II. Lengths of tubes and forms of entrance and outlet used for submerged tubes 260
III. Cross-sections of submerged tubes 264
IV. Data for location of hook gages 273
V. Summary sheet showing results of experiments with sharp crested weir, 2.505 feet long 280
VI. Comparison of flow over sharp crested weir, 2.505 feet long by various formulae, and measurements of flow by C. B. Stewart 283
VII. Sample of tabulated results of experiments with submerged tube, 4 0 feet square 287
VIII. Summary sheet, showing results of experiments with submerged tubes 292
IX. Loss of head for flow through horizontal submerged tubes, for various rates of discharge 317
X. Preliminary values of the "Coefficient of Discharge," for flow through horizontal submerged tubes 318
XI. Final values of the "Coefficient of Discharge," for flow through horizontal submerged tubes 321
XII. Comparison of the results of partial suppression of contraction, for short and long tubes; head on tube =0.15 feet.. 326
XIII. Value of the "Coefficient of Loss" for flow through horizontal submerged tubes 329

INVESTIGATION OF FLOW THROUGH LARGE SUBMERGED ORIFICES AND TUBES

INTRODUCTION

The recent construction of large works in connection with the various lines of Hydraulic Engineering has emphasized the need of further experimental knowledge concerning the losses of head resulting from various forms of resistances interposed in flowing streams of considerable size. The loss of head resulting from the flow of water through submerged gates, tubes and orifices of considerable size, and with various forms of entrance and outlet is one of the most important divisions of the general subject which needs experimental investigation. Practically the only reliable experimental data available concerning the flow of water through large orifices is given in a valuable paper by Mr. Theodore G. Ellis, entitled "Description and Results of Hydraulic Experiments with large Apertures at Holyoke, Massachusetts," and printed in the Transactions of the American Society of Civil Engineers, Volume V, 1875. Mr. Ellis determined the loss of head for flow through apertures which were two feet square, and two feet by one foot, when discharging freely into the atmosphere. He also made a very few experiments on the loss of head for flow through submerged apertures one foot square and one foot in diameter under heads from two feet to fifteen feet. In nearly all the experiments of Mr. Ellis, the thickness of the edge of the apertures remained constant, about one-half inch for wood and one-fourth inch for iron, and perfect contractions of the emerging stream were supposed to take place on all sides of the aperture. In the single case of the aperture one foot square, the entrance was subsequently modified so as to have a curved approach on all four sides, and the resulting coefficients of discharge were determined.

In the experiments at the University of Wisconsin, described in the present paper, the cross-section of the orifice or tube has been kept constant. being four feet square, and the effects of changing the length of the tube and of modifying the entrance conditions by curved approaches on one, two, three and four sides respectively, for each of the various lengths, have been studied.

In future experiments on this subject at the University, it is planned to determine the coefficients of discharge for submerged tubes and orifices of various forms and areas of cross-section, with and without entrance and outlet modifications. It is intended that the experiments when completed will fairly covered the field of investigation laid out and it is hoped that the results will be of material aid to the Engineering Profession.

The writer desires to acknowledge the services of Mr. J. R. Sherman and Mr. W. A. Gattiker. who have aided him by careful work on the computations, and by suggestions in regard to the arrangement of the subject matter described in the bulletin.

SUPPLY OF WATER

The experiments were made at the new Hydraulic Laboratory of the University of Wisconsin, located on the shore of Lake Mendota, which furnished an abundant supply of fresh water. Exceptional facilities were afforded for experiments on a large scale. and care was taken that errors of observation should be reduced to as small a percentage as possible. Plate I is a plan of the Laboratory, showing the main features and arrangement for the experiments. The water was taken from the lake by a suitable inlet and raised about twelve feet by means of a 30 inch Morris Machine Works Centrifugal Pump, and delivered into a receiving basin which measures about fifteen feet by eighteen feet and ten feet deep. From the receiving basin the water flows through a flume ten feet wide. ten feet deep and about sixty-eight feet long. and may be used for operating a 30 inch turbine located at the end of the flume or may be wasted through gates underneath the turbine. after which the water flows back to the lake through a tail race ten feet wide, as shown.

[illegible] p. 2 & 6

PLATE I.

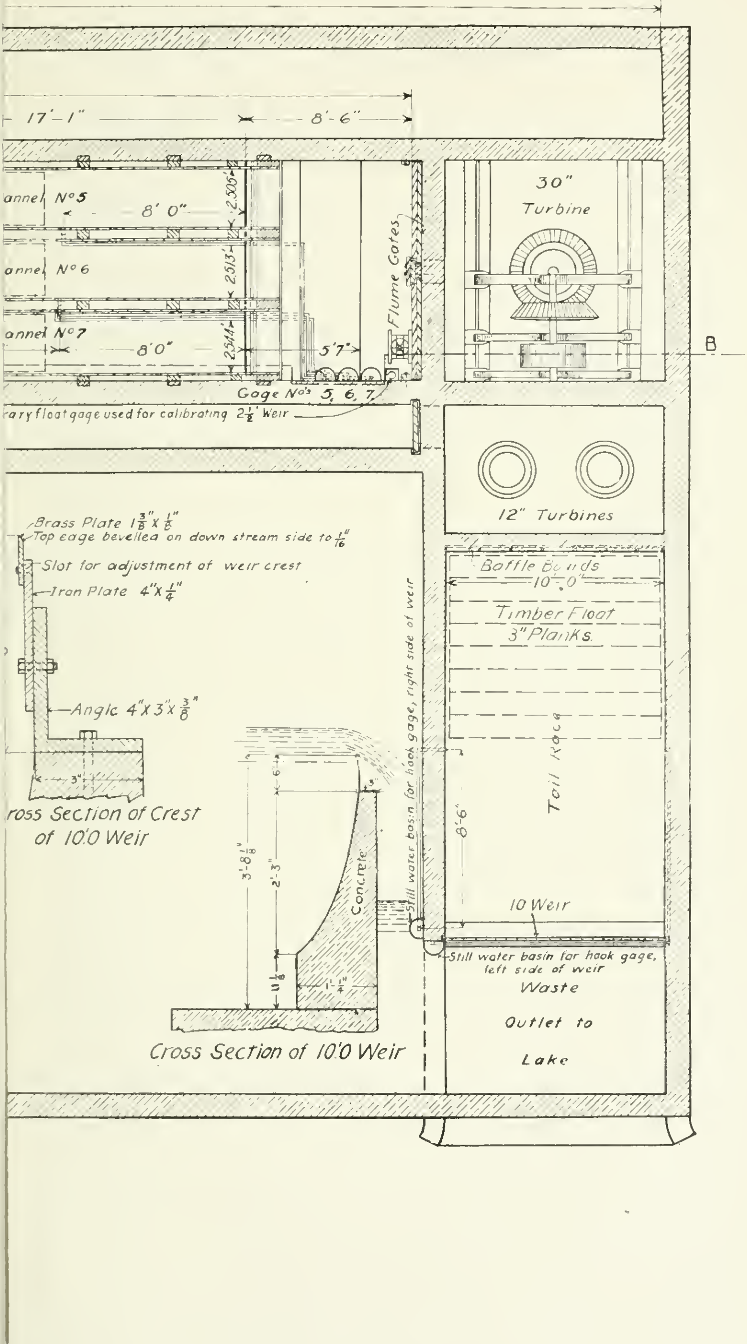
17'-1"
8'-6"
annel Nº 5
8' 0"
2.506'
annel Nº 6
2.513'
annel Nº 7
8'0"
2.514'
5'7"
Flume Gates
Gage Nᵒˢ 5, 6, 7
rary float gage used for calibrating 2½' Weir
30" Turbine
B
12" Turbines
Baffle Boards
10'-0"
Timber Float 3" Planks.
Tail Race
8'-6"
10 Weir
Still water basin for hook gage, right side of weir
Still water basin for hook gage, left side of weir
Waste Outlet to Lake
Brass Plate 1⅜" x ⅛"
Top edge bevelled on down stream side to 1/16"
Slot for adjustment of weir crest
Iron Plate 4" x ¼"
Angle 4" x 3" x ⅜"
3"
ross Section of Crest of 10.0 Weir
6"
3"
3'-8⅛"
2'-3"
11⅛"
1'-¼"
Concrete
Cross Section of 10.0 Weir

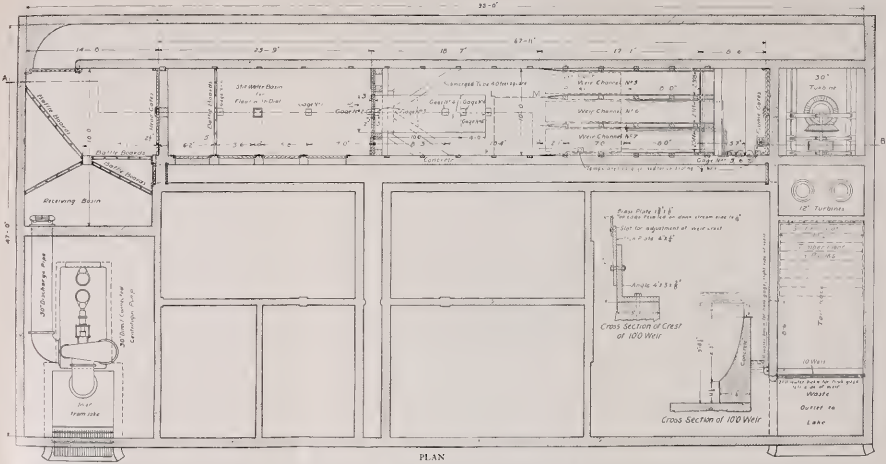

PLAN

OF

HYDRAULIC LABORATORY, UNIVERSITY OF WISCONSIN,

SHOWING

ARRANGEMENTS FOR EXPERIMENTS ON SUBMERGED TUBES.

[illegible]

SCALE

PLATE II.

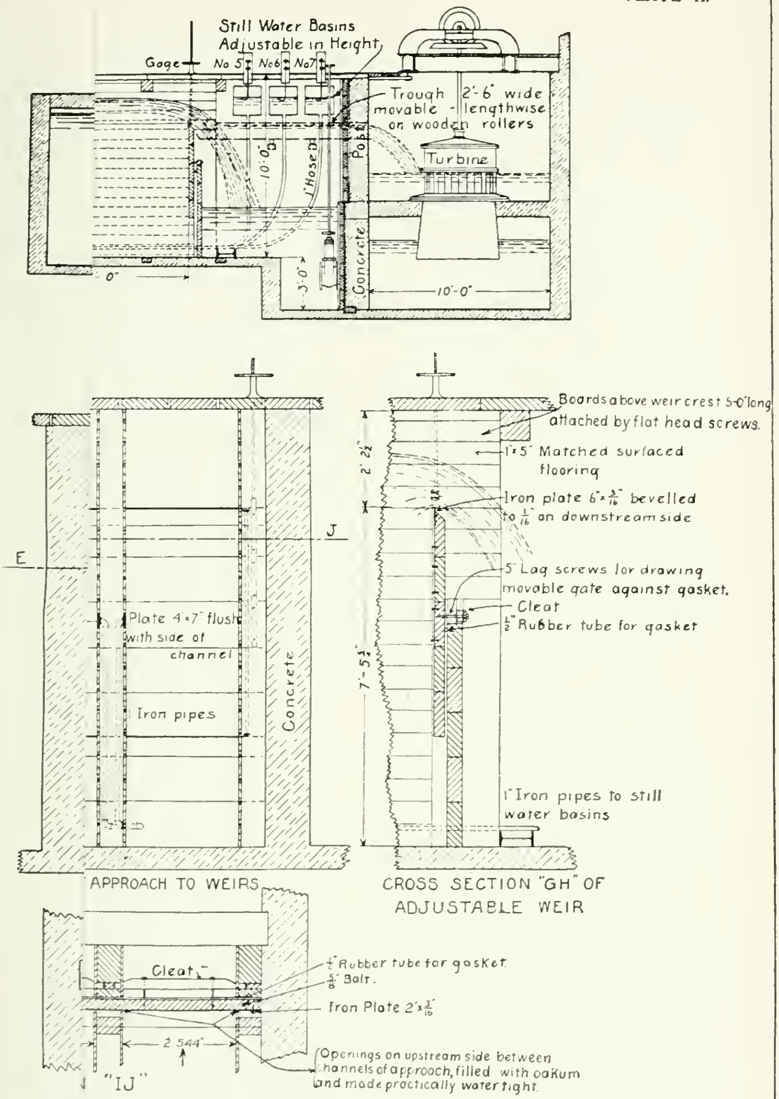
Still Water Basins
Adjustable in Height
Gage
No 5
No 6
No 7
Trough 2'-6" wide
movable - lengthwise
on wooden rollers
Turbine
Post
10'-0"
1" Hose
3'-0"
Concrete
0"
10'-0"
E
J
Plate 4"x7" flush with side of channel
Iron pipes
Concrete
2' 2½"
7'-5¼"
Boards above weir crest 5-0" long attached by flat head screws.
1"x5" Matched surfaced flooring
Iron plate 6"x3/16" bevelled to 1/16" on downstream side
5" Lag screws for drawing movable gate against gasket.
Cleat
½" Rubber tube for gasket
1" Iron pipes to still water basins
Cleat
½" Rubber tube for gasket.
5/8" Bolt.
Iron Plate 2"x3/16"
2.544'
Openings on upstream side between channels of approach, filled with oakum and made practically water tight.

APPROACH TO WEIRS

CROSS SECTION "GH" OF ADJUSTABLE WEIR

"IJ"

AILS OF ADJUSTABLE SHARP CRESTED WEIRS
USED FOR
MEASURING FLOW OF WATER.

SCALE 0' 1' 2' 3'

PLATE II.

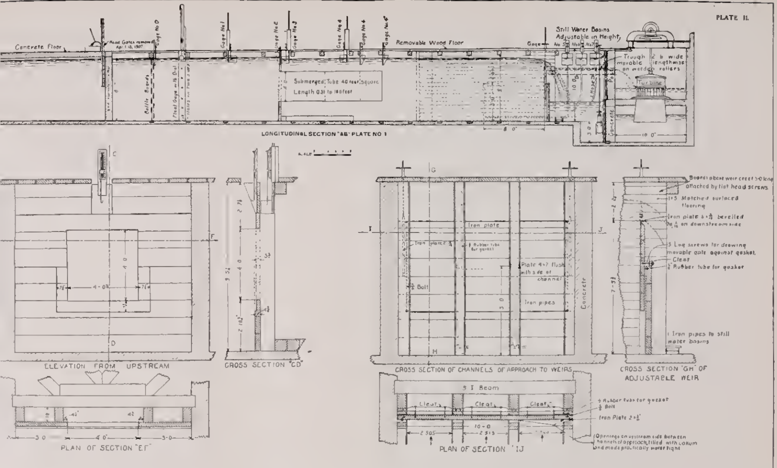
LONGITUDINAL SECTION "AB" PLATE NO 1

ELEVATION FROM UPSTREAM

CROSS SECTION "CD"

PLAN OF SECTION "EF"

CROSS SECTION OF CHANNELS OF APPROACH TO WEIRS

CROSS SECTION "GH" OF ADJUSTABLE WEIR

PLAN OF SECTION "IJ"

Concrete Floor
Head Gates removed Apr 18, 1907
Gage No 0
Gage No 1
Gage No 2
Gage No 3
Gage No 4
Gage No 4
Gage No 4'
Baffle Boards
Float Gage with Dial
Submerged Tube 4.0 feet square
Length 0.31 to 16.0 feet
Removable Wood Floor
Gage
Still Water Basins
Adjustable in Height
No 5
No 6
No 7
Trough 2 ft wide movable lengthwise on wooden rollers
Turbine
Concrete
8 0"
10 0"
3 0"
10 0"
SCALE
C
D
F
4 0
4 0"
2 7¾
3 5¼
2 10½
3 0
4 0
3 0
G
H
I
J
Iron plate
Iron plate 2 × ¼
¼ Rubber tube for gasket
Plate 4 × 7 flush with side of channel
⅝ Bolt
Iron pipes
Concrete
3 0
Boards above weir crest 5-0 long attached by flat head screws
1 × 5 Matched surfaced flooring
Iron plate 5 × ⅜ bevelled to 1/16 on downstream side
3 Lag screws for drawing movable gate against gasket
Cleat
¼ Rubber tube for gasket
Iron pipes to still water basins
2 2
7 5¼
5 I Beam
Cleat
Cleat
Cleat
¼ Rubber tube for gasket
⅝ Bolt
Iron Plate 2 × ½
10 0
2 505
2 515
Openings on upstream side between channels of approach filled with oakum and made practically water tight

DETAILS OF
BULKHEAD FOR SUBMERGED TUBES

SCALE

DETAILS OF ADJUSTABLE SHARP CRESTED WEIRS
USED FOR
MEASURING FLOW OF WATER.

SCALE

EXPERIMENTS
WITH
SUBMERGED TUBES 4.0 FEET SQUARE,
AT THE
UNIVERSITY OF WISCONSIN.

Sep. 11 1906 — May 10 1907

END VIEW

EXPERIMENTS WITH SUBMERGED TUBES 4.0 FT SQUARE

AT THE

UNIVERSITY OF WISCONSIN

PLATE III

SKETCH SHOWING FORMS OF ENTRANCE AND LENGHTS OF TUBES USED

Series Nos. 1–7— Entrance, square corners with full contraction
Series Nos. 1a–7a—Entrance, contraction suppressed on bottom
Series Nos. 1b–7b—Entrance, contraction suppressed on bottom and one side
Series Nos. 1c–7c—Entrance, contraction suppressed on bottom and two sides
Series No. 7c'— Entrance, contraction suppressed on bottom and two sides
Outlet, bulkhead to sides of channel
Series Nos. 1d–7d—Entrance, contraction suppressed on bottom, two sides and top

Sept. 11, 1906 — May 15, 1907

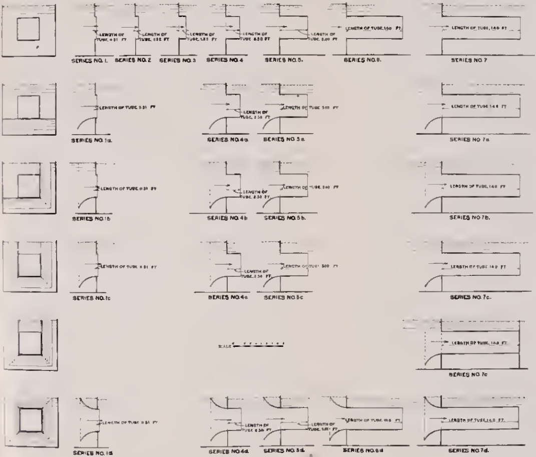

At the outlet end of the tail race is a sharp crested weir with end contractions suppressed and having a length of crest of ten feet.

Suitable baffle boards were inserted in the receiving basin and at the entrance to the flume until it was found by trial that the water flowed in lines practically parallel to the sides of the flume.

DESCRIPTION OF BULKHEAD AND SUBMERGED TUBES

The bulkhead containing the submerged tube was located about twenty-four feet from the entrance of the ten foot channel, the arrangement being shown in detail on Plates I and II. The planks near the bottom of the bulkhead containing the submerged tube were four and three-quarters inches thick in order to give the required strength, while those at or near the top were three and three-quarters inches thick. In order to have a uniform thickness of three and three-quarters inches at the entrance to the tube, it was necessary to diminish the thickness of the four and three-quarters inch planks around the entrance to the tube. A thickness of one inch and width of seven and one-half inches. was therefore cut from the up stream side of the thicker planks, around the entrance to the tube. The distance seven and one-half inches was arbitrary, and judged sufficient to prevent any influence of the one inch shoulder on the flow of water through the tube. The bulkhead was thoroughly caulked and tested for leakage previous and subsequent to the making of the experiments with the submerged tubes.

The plan followed was to study the simple forms of submerged tubes, four feet square with entrance having square corners, and of lengths varying from thirty-one hundredths feet to fourteen feet, finding the losses of head and coefficients of discharge for the various rates of flow through the tubes. The entrances to the tubes of various lengths were then modified by introducing curved approaches, elliptical in form, and thus suppressing the contraction first, on the bottom, second, on the bottom and one side, third, on the bottom and two sides, and fourth, on the bottom, two sides and top. Plate III is a sketch showing the various forms of entrance and lengths of tubes used. The elliptical form of the curved approach, see photograph Plate IV and details, Plate VI, was chosen to suppress the contraction because with the axes of the ellipse properly proportioned, it answered the purpose of gradually guiding the filaments of water into lines parallel with the axis of the tubes as well as would the more complicated transition curves. These curves of the ellipse with semi-axes, as shown, of three feet and two feet, were constructed by nailing wooden strips one inch by three inches to elliptical forms and planing the outer edges of the strips, until the surface became a smooth curve. These curved forms were held in place by bracing to the sides of the ten foot channel. No attempt was made to

PLATE IV—ELLIPTICAL FORM OF THE CURVED APPROACH

E

PLATE V

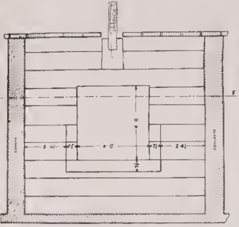

ELEVATION FROM UPSTREAM

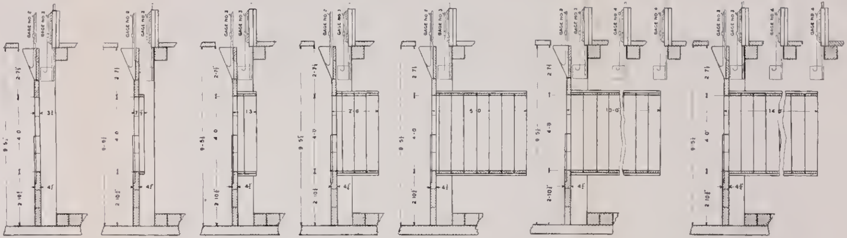

SERIES NO. 1

SERIES NO. 2

SERIES NO. 3

SERIES NO. 4

SERIES NO. 5

SERIES NO. 6

SERIES NO. 7

LONGITUDINAL SECTIONS

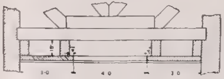

PLAN OF SECTION "EF"
SERIES NO. 1

EXPERIMENTS
WITH
SUBMERGED TUBES
AT THE
UNIVERSITY OF WISCONSIN

DETAILS OF SUBMERGED TUBES 4.0 FT. SQUARE
SERIES NOS. 1 - 7

[illegible]

SCALE

make the forms water tight but care was taken that they were sufficiently so, to prevent any cross currents from interfering with the flow along the surface of the curve as it entered the tube.

The experiments on the submerged tubes, with entrance having square corners and of lengths varying from thirty-one hundredths feet to fourteen feet, have been designated by series, (Numbers 1 to 7), the tubes being shown in detail on Plate V. In series Number 1, the length of the tube was three and three-quarters inches, equal to thirty-one hundredths feet, the same as the thickness of the bulkhead wall, the opening being cut through this wall at an angle as near ninety degrees as possible. The roughness from the effect of the saw was taken off with a smoothing plane, but sand paper was not used. The end of the wood was exposed at the sides of the tube as shown in the details. In Series Number 2, the length of the tube was made equal to sixty-two hundredths feet, double the length of Series Number 1, by adding wooden strips on the down-stream side. These wooden strips were surfaced and fitted closely to the down-stream edge of the previous tube so that the effect of the joint was practically eliminated. In Series Numbers 3, 4, 5 and 6, the length of the tube in each case was made double the length of the preceding series number, becoming respectively one and twenty-five hundredths feet, two and one-half feet, five feet and ten feet. In Series Number 7, the length of the tube was made fourteen feet, about the extreme length possible with the arrangement of bulkhead and weir channels at that time.

The outlet end of the submerged tube (with the single exception of the tube fourteen feet long, termed 7c′) projected into the water on the down stream side of the bulkhead and was firmly braced to the sides of the ten foot channel, the braces being arranged in such a way as not to interfere with the flow through the tube. In the case of the fourteen foot tube mentioned above, a light bulkhead of one inch boards was constructed at the outlet of the tube to the sides of the ten foot channel, in order to prevent the return currents along the sides of the tube.

The various forms of entrance and outlet of the submerged tubes used have been designated by the subscripts a, b, c, c′ and d, to the particular Series Number, by which the length is designated. Thus Series Number 7 refers to experiments on the submerged tube fourteen feet long with entrance having square corners and outlet projecting into the water on the down stream side of the bulkhead, while Series Number 7a refers to experiment on a tube of the same length but having the contraction suppressed on the bottom at entrance, the outlet condition remaining the same. The subscript, c′, has been used to designate the same entrance condition as the subscript, c, while the outlet condition has been varied by the construction of a bulkhead to the sides of the channel at the outlet of the tube. For convenience of reference the meaning of the subscripts, a, b, c, c′ and d are given in the following table:

TABLE I.

DESCRIPTION OF FORMS OF ENTRANCE AND OUTLET USED FOR EXPERIMENTS WITH SUBMERGED TUBES 4.0 FEET SQUARE.

Square Corners:—Entrance;	All corners 90°.
Outlet;	tube projecting into water on downstream side of bulkhead.
a:—Entrance;	contraction suppressed on bottom.
Outlet;	tube projecting into water on downstream side of bulkhead.
b:—Entrance;	contraction suppressed on bottom and one side.
Outlet;	tube projecting into water on downstream side of bulkhead.
c:—Entrance;	contraction suppressed on bottom and two sides.
Outlet;	tube projecting into water on downstream side of bulkhead.
c :—Entrance;	contraction suppressed on bottom and two sides.
Outlet;	square corners with bulkhead to sides of channel preventing the return current along the sides of the tube.
d:—Entrance;	contraction suppressed on bottom, two sides and top.
Outlet;	tube projecting into water on downstream side of bulkhead.

The following table is a summary giving the lengths and forms of entrance and outlet used in the experiments with submerged tubes.

TABLE II.

LENGTH OF TUBES AND FORMS OF ENTRANCE AND OUTLET USED FOR EXPERIMENTS WITH SUBMERGED TUBES 4.0 FEET SQUARE.

ILLUSTRATED BY PLATE III.

Series No.	Length in feet.	Form of Entrance and Outlet Used With Submerged Tube.					
1.........	0.31	Square corners............	a	b	c	....	d
2.	0.62	Square corners............	....	.... ..	....	....	....
3.........	1.25	Square corners........	....	.... ..	....	....	....
4.........	2.50	Square corners............	a	b	c	....	d
5.........	5.00	Square corners........ ..	a	b	c	....	d
6.........	10.00	Square corners........ ...	....	....	....	....	d
7.........	14.00	Square corners............	a	b	c	c′	d

Plates VI, VII, VIII and IX show respectively the details of the submerged tubes for the experiments of Series Number 1a, 1b, 1c, 1d; Series Numbers 4a, 4b, 4c, 4d; Series Numbers 5a, 5b, 5c, 5d and Series Numbers 7a, 7b, 7c, 7c′, 7d.

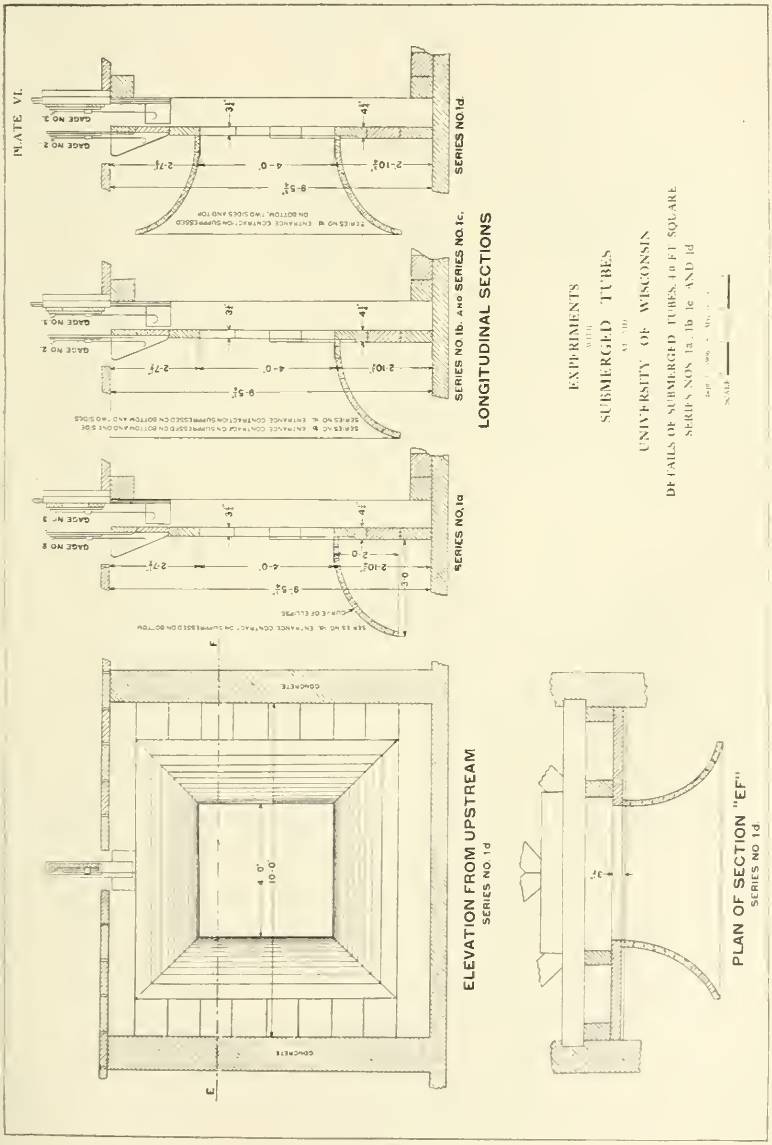
PLATE VI.
GAGE NO 3
GAGE NO 2
3¼"
4¼"
2-7¼"
4-0"
2-10¾"
9-5¼"
SERIES NO.1d
SERIES NO 1d ENTRANCE CONTRACTION SUPPRESSED ON BOTTOM, TWO SIDES AND TOP
SERIES NO.1b AND SERIES NO.1c
SERIES NO 1b ENTRANCE CONTRACTION SUPPRESSED ON BOTTOM AND ONE SIDE
SERIES NO 1c ENTRANCE CONTRACTION SUPPRESSED ON BOTTOM AND TWO SIDES
SERIES NO.1a
SERIES NO 1a ENTRANCE CONTRACTION SUPPRESSED ON BOTTOM
CURVE OF ELLIPSE
2-0
3-0
LONGITUDINAL SECTIONS
EXPERIMENTS
WITH
SUBMERGED TUBES
AT THE
UNIVERSITY OF WISCONSIN
DETAILS OF SUBMERGED TUBES 4.0 FT SQUARE
SERIES NOS 1a, 1b, 1c AND 1d
SCALE
CONCRETE
4-0"
10-0"
E
F
ELEVATION FROM UPSTREAM
SERIES NO 1d
3"
PLAN OF SECTION "EF"
SERIES NO 1d

PLATE VII.

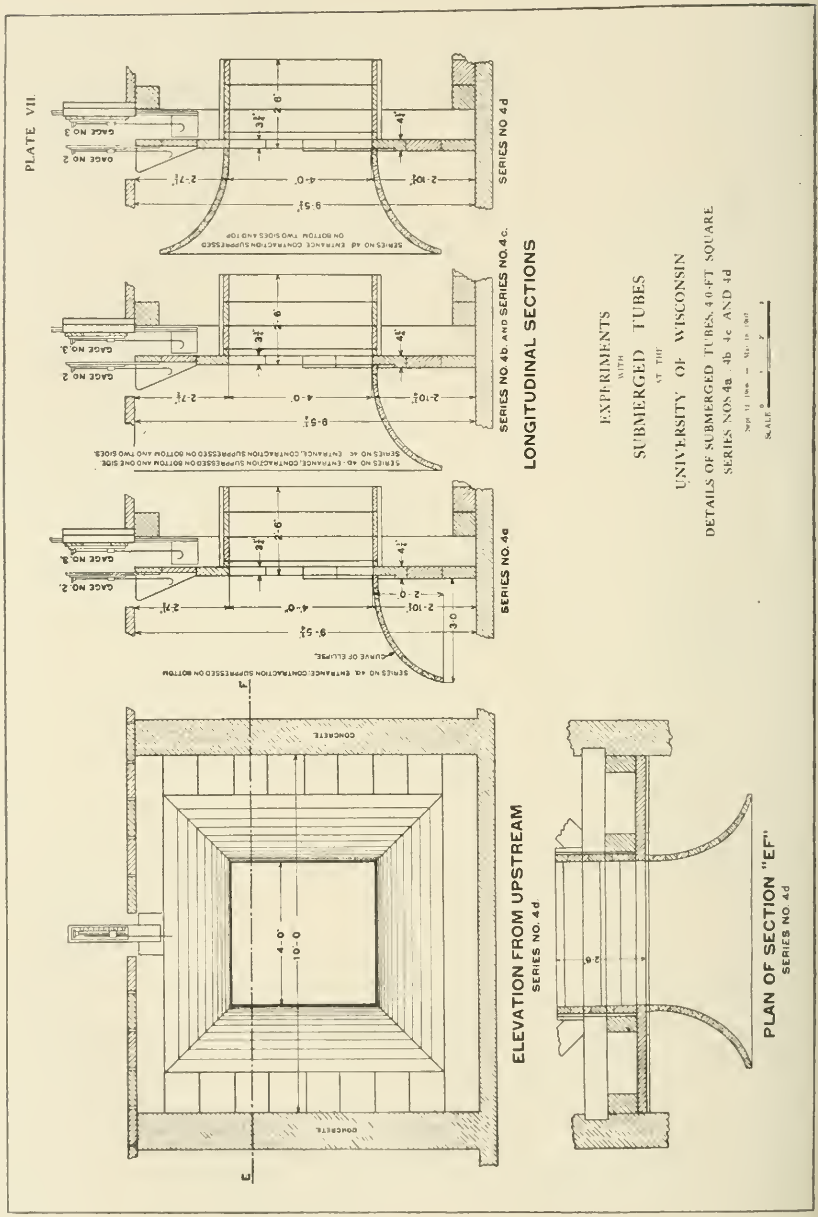
GAGE NO. 2
GAGE NO. 3
2'-7¼"
4'-0"
2'-10¾"
9'-5¼"
3¼"
2'-6"
4¼"
SERIES NO 4d
SERIES NO. 4d. ENTRANCE CONTRACTION SUPPRESSED ON BOTTOM, TWO SIDES AND TOP
SERIES NO. 4b. AND SERIES NO. 4c.
SERIES NO. 4b. ENTRANCE CONTRACTION SUPPRESSED ON BOTTOM AND ONE SIDE
SERIES NO. 4c. ENTRANCE CONTRACTION SUPPRESSED ON BOTTOM AND TWO SIDES.
SERIES NO. 4a
SERIES NO. 4a. ENTRANCE CONTRACTION SUPPRESSED ON BOTTOM
CURVE OF ELLIPSE
2'-0"
3'-0"
LONGITUDINAL SECTIONS
CONCRETE
4'-0"
10'-0"
E
F
ELEVATION FROM UPSTREAM
SERIES NO. 4d.
2'-6"
PLAN OF SECTION "EF"
SERIES NO. 4d
EXPERIMENTS
WITH
SUBMERGED TUBES
AT THE
UNIVERSITY OF WISCONSIN
DETAILS OF SUBMERGED TUBES, 4.0-FT SQUARE
SERIES NOS 4a, 4b, 4c AND 4d
SCALE

PLATE VIII.

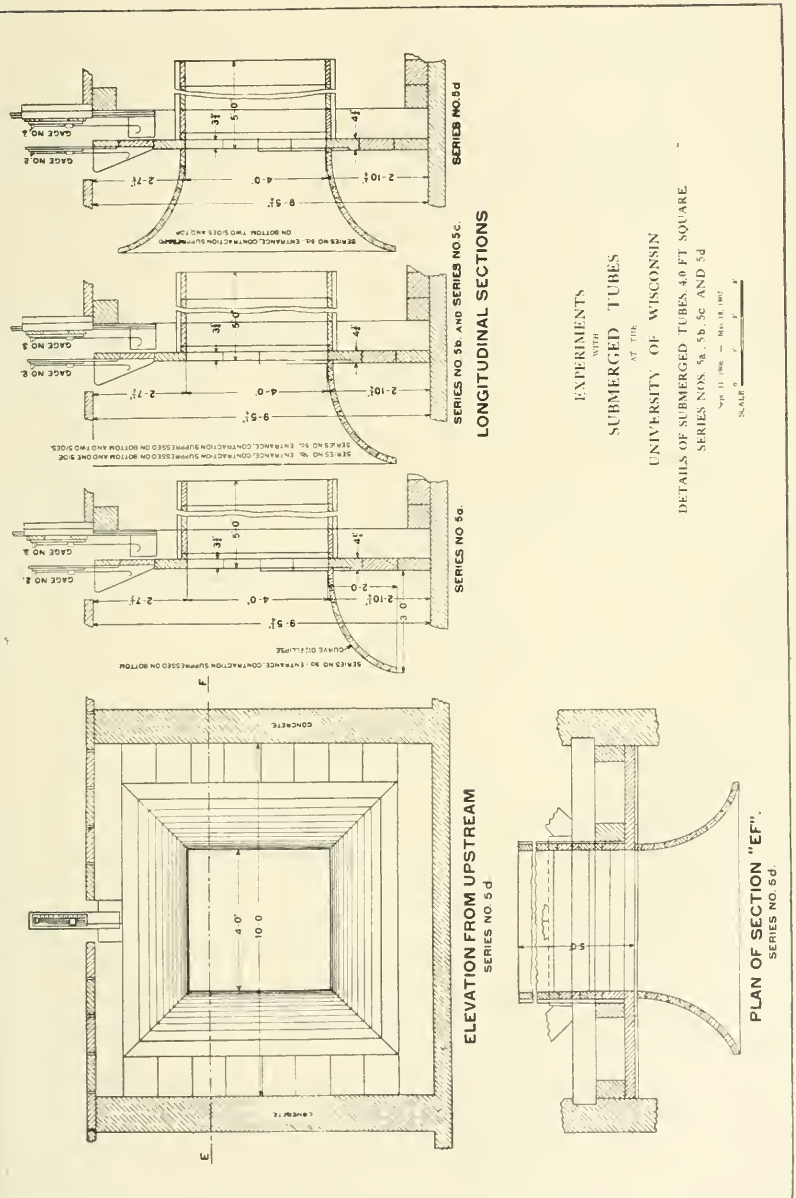
LONGITUDINAL SECTIONS
SERIES NO 5a.
SERIES NO 5a - ENTRANCE, CONTRACTION SUPPRESSED ON BOTTOM
CURVE OF ELLIPSE
SERIES NO 5b. AND SERIES NO 5c.
SERIES NO 5b. ENTRANCE, CONTRACTION SUPPRESSED ON BOTTOM AND ONE SIDE
SERIES NO 5c. ENTRANCE, CONTRACTION SUPPRESSED ON BOTTOM AND TWO SIDES.
SERIES NO 5d
SERIES NO 5d - ENTRANCE, CONTRACTION SUPPRESSED ON BOTTOM, TWO SIDES AND TOP
GAGE NO 2
GAGE NO 3
2-7¼"
4-0"
2-10¾"
9-5¼"
3¼"
5-0"
4¼"
2-0
3-0
ELEVATION FROM UPSTREAM
SERIES NO. 5d
CONCRETE
4-0"
10-0
E
F
PLAN OF SECTION "EF".
SERIES NO. 5d.
5-0
EXPERIMENTS
WITH
SUBMERGED TUBES
AT THE
UNIVERSITY OF WISCONSIN
DETAILS OF SUBMERGED TUBES, 4.0 FT SQUARE
SERIES NOS. 5a, 5b, 5c AND 5d
Sept. 11 1906 — May 18, 1907
SCALE 0 1' 2' 3'

The dimensions and areas of cross-sections of the submerged tubes experimented with are given in the following table.

TABLE III.
CROSS-SECTIONS OF SUBMERGED TUBES, 4.0 FEET SQUARE.

SERIES NO.	Length of tube.	DIMENSIONS OF TUBES.				Area of cross-section.
		Top.	Bottom.	Right side.	Left side.	
	Ft.	Ft.	Ft.	Ft.	Ft.	Sq. ft.
Inlet of all series............	... .	4.000	3.990	4.000	4.000	15.980
Outlet of series No. 1........	0.31	4.000	3.990	4.000	4.000	15.980
Outlet of series No. 2	0.62	3.990	3.980	4.002	4.002	15.948
Outlet of series No. 3........	1.25	3.980	3.970	4.005	4.005	15.920
Outlet of series No. 4........	2.50	3.960	3.960	3.980	3.980	15.761
Outlet of series No. 5........	5.00	3.955	3.953	3.986	3.986	15.721
Outlet of series No. 6.... ...	10.00	4.000	4.010	4.030	4.030	16.140
Outlet of series No. 7........	14.00	4.007	4.004	4.000	4.000	16.022

The slight variations from the four foot dimensions in the case of Series Numbers 3. 4 and 5 were accidental. In the computations of the coefficients of discharge (page 318), the area of the cross-section has been used as sixteen square feet in all cases.

DESCRIPTION OF WEIRS

THREE, TWO AND ONE-HALF FOOT SHARP CRESTED WEIRS

The facilities for making a volumetric calibration of a weir, whose length of crest is ten feet, were not available, so the expedient was used of dividing the ten foot channel into three similar channels, each having a length of about fifteen feet, and a sharp crested weir with end contractions suppressed at the end of each channel. Plates X and XI are photographs taken with a head on the weirs of about one and three-tenths feet and show very plainly the arrangement of the three channels of approach and sharp crested weirs. Plate XI shows the three adjustable still water basins used for measuring the heads on the weirs. In order to form a variable height of water surface on the down stream side of the bulkhead containing the submerged tube, the three sharp crested weirs were made adjustable in height, as shown on Plates I and II. The main feature of the weirs consisted of a fixed bulkhead, extending

PLATE IX.

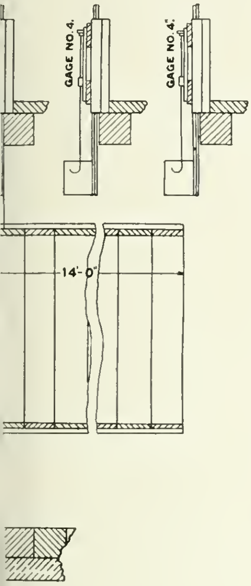

.7d.

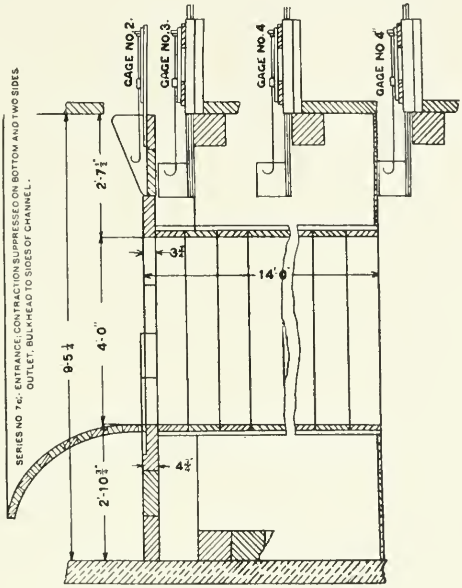
SERIES NO 7c':- ENTRANCE; CONTRACTION SUPPRESSED ON BOTTOM AND TWO SIDES
OUTLET, BULKHEAD TO SIDES OF CHANNEL.
GAGE NO.2.
GAGE NO.3.
GAGE NO.4
GAGE NO.4'
2'-7½"
3½"
14'-0"
9'-5¼
4'-0"
4¾"
2'-10¾"

SERIES NO.7c'.

PLATE IX.

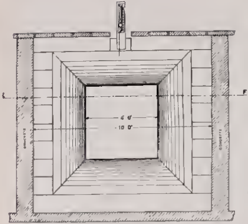

ELEVATION FROM UPSTREAM
SERIES NO 7d.

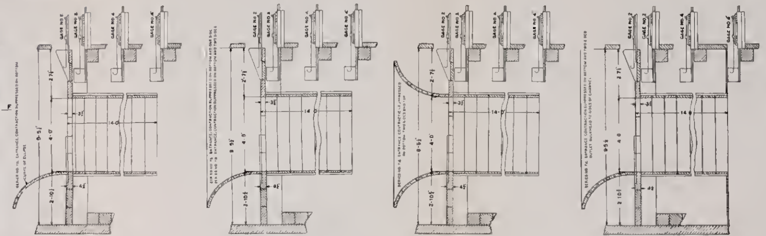

SERIES NO 7a.

SERIES NO 7b AND SERIES NO 7c.

SERIES NO 7d.

SERIES NO 7e'

LONGITUDINAL SECTIONS

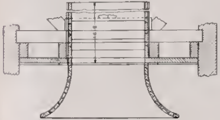

PLAN OF SECTION "EF"
SERIES NO 7d

EXPERIMENTS
WITH
SUBMERGED TUBES
AT THE
UNIVERSITY OF WISCONSIN

DETAILS OF SUBMERGED TUBES, 4.0 FT SQUARE
SERIES NOS 7a 7b, 7c 7d AND 7e
Sept 11 1906 — May 18 1907
SCALE 0 1 2 4

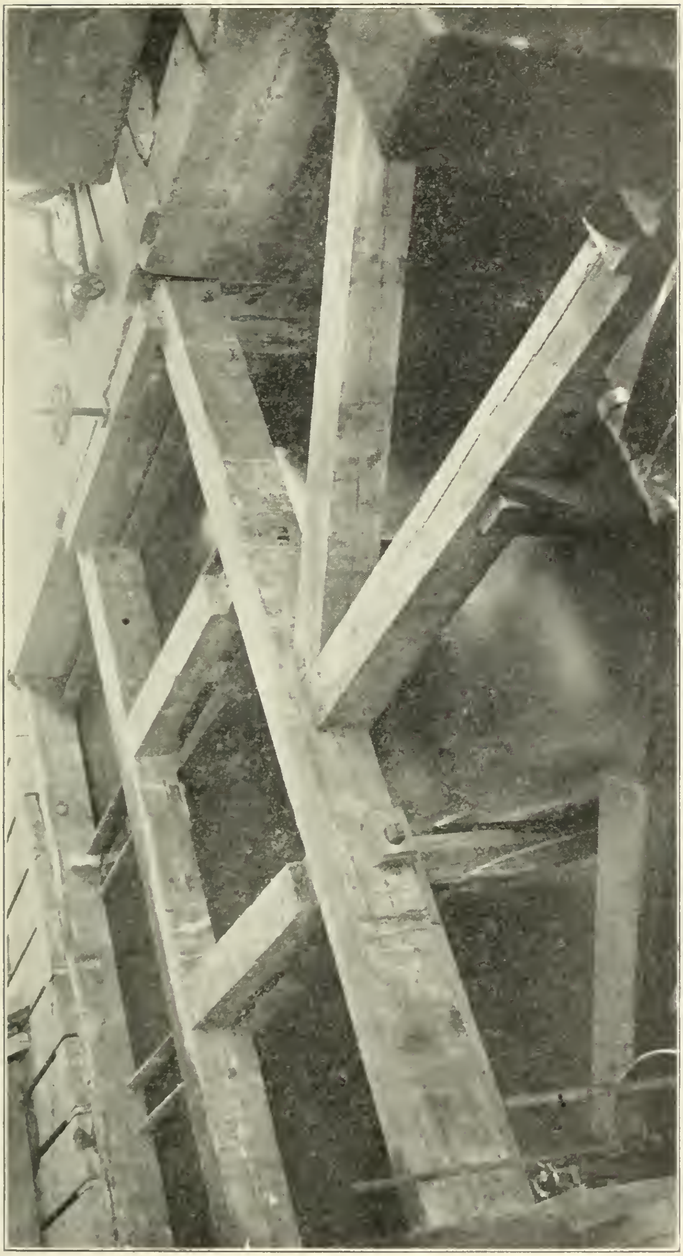

PLATE X. VIEW SHOWING ARRANGEMENT OF THREE, TWO AND ONE-HALF FOOT SHARP CRESTED WEIRS

Head on Weir=1.3 feet.

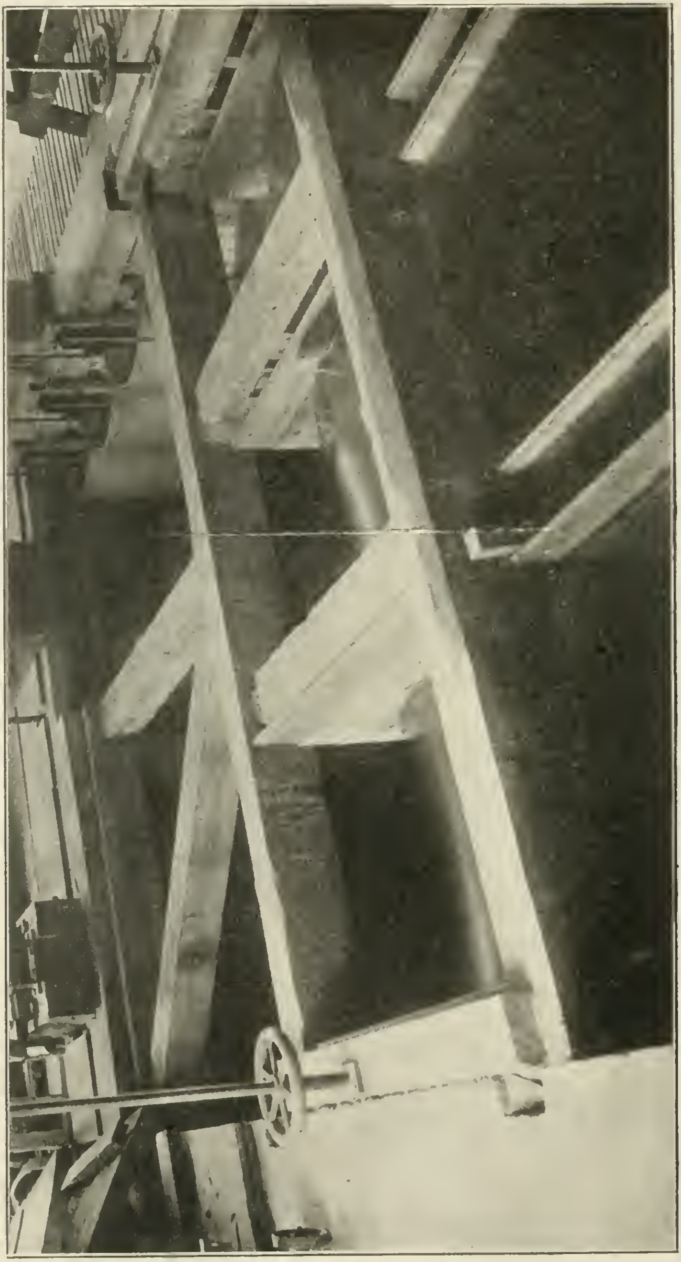

PLATE XI.—VIEW SHOWING ARRANGEMENT OF STILL WATER BASINS FOR THREE, TWO AND ONE-HALF FOOT SHARP CRESTED WEIRS

about five feet above the bottom of the channel and a movable gate above the bulkhead, extending the full width of the ten foot channel and capable of being raised or lowered by means of two hand wheels, one on each side of the channel. The crests of the three weirs were made of a single plate of wrought iron, six inches by three-sixteenths inches, bolted to the upper edge of the movable timber gate and beveled on the down stream side of the top edge to a thickness of about one-sixteenth of an inch. The joints around the weir openings were made water tight by means of gaskets which consisted of cloth insertion rubber tubing, one-half inch in diameter, the movable gate being drawn against the gaskets by means of lag screws passing through cleats adjustable vertically in the timber frame supporting the bulkhead and gate. These gaskets were horizontal at the top of the fixed bulkhead, and extended vertically upwards on each side of the weir openings to the maximum height of water in the channels of approach. Each of the three weirs had its own channel of approach, the channels being about fifteen feet long. The sides of the channels were lined with one inch pine surfaced flooring boards so that all three of the channels of approach and weirs were practically alike, the only variation being that of slight difference in width of about one-half inch in the case of one weir. The board linings of the channel were extended down stream from the crest of the weir a distance of one and one-half feet and also below the crest of the weir a distance of about two feet, so that the weirs had their end contractions suppressed and the filaments were guided in parallel planes after passing over the crest. The board linings around the crests of the adjustable weirs had to be removed each time the crests were adjusted. These boards, attached by counter-sunk flat headed screws, were five feet long just above the crest of the weir and extended up stream into the channels' approach so as to avoid making joints on the vertical lines above the crests of the weirs. The slight openings between the weir boards and the ends of the boards lining the channels were filled with oakum and make practically water tight, thus preventing cross-currents, which would interfere with the linear flow over the weir crest. A slight leakage between channels of approach was unavoidable. The arrangement of the weirs with the intervening spaces of about eight inches between the ends allowed free entrance of air beneath the nappes. The measurements of heads on the crest of the weirs were made by connecting the weir channels with still water basins located below the weirs, as shown on Plates I and II. Readings were taken of the elevations of water surfaces in the still water basins by means of accurate hook gages. The connections between the weir channels and still water basins were made by one inch wrought iron pipes and one inch rubber tubes as shown. The tubes were attached to the still water basins by means of malleable iron unions and were easily disconnected. By lowering the outlet end of a tube and allowing free circulation of the water, the air in the connecting pipe and rubber tube could be easily removed.

The connections with the weir channels were made at points eight feet up stream from the crest of the weirs, five feet above the floor of the channel and about two and one-half feet below the crest of the weirs. The iron pipes connecting with the weir channels were arranged so as to enter at right angles to the sides of the channels, provision being made that the inner ends of the pipes should be flush with the sides of the channels. In order to provide an even surface for the filaments of water adjoining the entrance to the pipes, to pass over, each entering pipe was screwed through the center of an iron plate, four inches by seven inches and one quarter inch thick, and the end of the pipe and surface of the plate made even by surfacing. The iron plates were then set into the wooden sides of the channels until the outer surfaces of the plates were flush with the wood, the seven inch dimensions of the plates being placed in the directions of the flow of water. In order to quiet the water in the channels of approach, timber floats two and one-half feet wide and eight feet long were constructed of three inch planks and floated in the up stream ends of the channels, as shown on Plate I.

The lengths of the crests of the weirs located at the outlets of channels, Number 5, 6, and 7, were 2.505 feet, 2.510 feet and 2.544 feet respectively.

In the series of experiments with submerged tubes, four feet square, the desired range of head on the tubes, zero to four-tenths feet, was found possible without adjusting the height of the crest of the weirs, which remained constant, being equal to seven and one-half feet.

Before using the weirs for purposes of measurement, they were tested for leakage by boarding above the crests of the weirs, to a height of about one and one-half feet and filled with water. The tubular gaskets were very satisfactory and very little additional caulking was found necessary to make the weir channels water tight.

TEN FOOT SHARP CRESTED WEIR

The details of the ten foot sharp crested weir, located at the outlet of the tail race, are shown on Plate I. The end contractions were suppressed, and the height of the crest of the weir above the bed of the channel of approach was equal to three and seven-tenths feet. The weir plate was perpendicular to the concrete side walls of the channel of approach. On the left side of the channel the concrete wall extended down stream from the crest of the weir and served to guide the filaments of water in parallel planes. On the right side of the channel the concrete wall ended at the crest of the weir, but the plane of the side wall was produced down stream about two feet and also below the crest of the weir a distance of about one foot by means of a galvanized iron plate. The space below this plate adjacent to the weir crest provided ample area for the admission of air underneath the nappe of the weir.

Heads on the crest of the weir were determined from the readings of accurate hook gages located in still water basins as shown on Plate I. These basins were connected with the channel of approach by one inch iron pipes at points eight and one-half feet up stream and three inches below the crest of the weir. These pipes entered the channel of approach at right angles and with ends flush with the surface of the concrete side walls. The hook gages were designated as "Right Side" and "Left Side" according as they were for readings of heads on the weir on the right and left sides respectively. In order to quiet the water, baffle boards were constructed at the entrance to the channel of approach and also a timber float nine feet square and three inches thick was held in position near the entrance to the tail race, as shown on Plate I. Simultaneous readings were made of heads on the two and one-half foot weirs and on the ten foot weir during a portion of the observations for the purpose of comparison of individual measurements of flow with computed results, and for calibration of the ten foot weir.

DESCRIPTION OF HOOK GAGES AND STILL WATER BASINS

The form of hook gages used is shown in detail on Plate XII and by photograph, Plate XIII. The hook was fastened on one end of a brass tube about three and one-half feet long, on which were accurately marked one-half foot spaces. The principal scale on the hook gage was one foot long and divided into tenths and hundredths of a foot. A micrometer screw with its head divided into one hundred parts made it possible to obtain readings of the elevation of the water surface to thousandths of a foot. A very convenient feature of the hook gage was the arrangement of an adjustable frame which carried the principal scale, micrometer screw and hook with its tube. This frame was adjustable vertically by means of a screw on the fixed frame which served to adjust the point of the hook to any desired elevation, as, level with the crest of the weir when the readings of the principal scale and micrometer were zero. The brass tube with its hook could be made of any length desired, and thus any change of elevation of the water surface within the length of the tube accurately noted.

The hook gages were designed by Professor D. W. Mead and made in the Mechanician Department of the College of Engineering of the University, under the direction of Mr. E. H. J. Lorenz, to whom credit is also due for the perfecting of the details of the instruments.

Still water basins twelve inches by twelve inches and twelve inches deep were constructed of galvanized iron and arranged to be adjustable vertically as shown on Plate XII. Holes one-

PLATE XII.

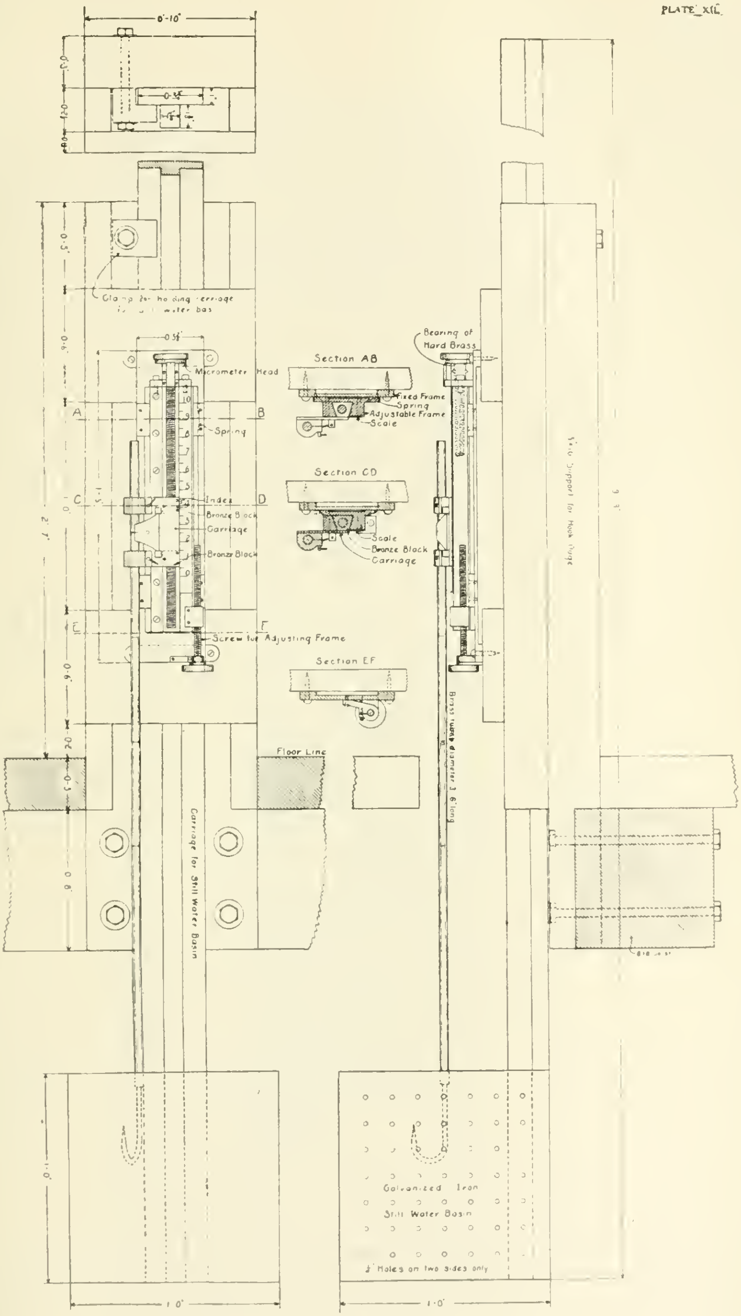

DETAILS OF ADJUSTABLE HOOK GAGE

AND

STILL WATER BASIN

USED FOR

EXPERIMENTS WITH SUBMERGED TUBES

SCALE

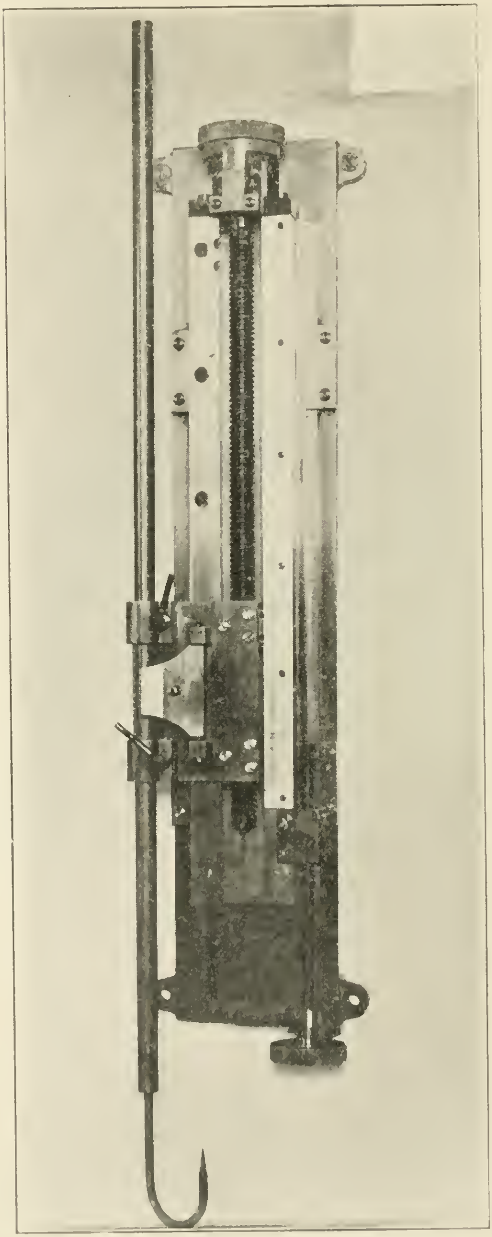

PLATE XIII—VIEW SHOWING ADJUSTABLE HOOK GAGE.

quarter inch in diameter and about one and one-half inches apart were made in the sides of these basins, while the ends and bottom were left closed.

The gages in the channel, ten feet wide, were located on the center line of the channel and at points selected with the object of determining the head on the submerged tube and the slope of the water surface, both up stream and down stream, from the bulkhead containing the submerged tube. The locations of the various hook gages are shown on Plate I, and for convenience of reference the various distances of the gages from the bulkhead and the locations of the gages used for given heads on the two and one-half foot weirs and the ten foot weir are arranged in the form of a table.

TABLE IV

DATA FOR THE LOCATION OF THE HOOK GAGES USED.

Hook Gage No.	Location.
	For Heads on the Submerged Tube and Slope of Water Surface in the Ten Foot Channel.
0	17 feet 0 inches upstream from the bulkhead containing tube.
1	7 feet 0 inches upstream from the bulkhead containing tube.
2	0 feet 2 inches upstream from the bulkhead containing tube.
3	0 feet 3 inches downstream from bulkhead containing tube.
4	8 feet 3 inches downstream from bulkhead containing tube.
4′	10 feet 0 inches downstream from bulkhead containing tube.
4″	14 feet 0 inches downstream from bulkhead containing tube.
	For Heads on the Two and One-Half Foot Weirs.
5	In still water basin connected with weir channel No. 5.
6	In still water basin connected with weir channel No. 6.
7	In still water basin connected with weir channel No. 7.
	For Heads on the Ten Foot Weir.
"Right side"	In still water basin connected with right side of tail race.
"Left side"	In still water basin connected with left side of tail race.

DESCRIPTION OF DIAL FLOAT GAGE

For maintaining a constant elevation of water surface in the canal leading to the submerged tube, a dial float gage was constructed, see Plate XIV. The float was made of galvanized iron, cylindrical in form, seven and one-half inches in diameter

PLATE XIV.

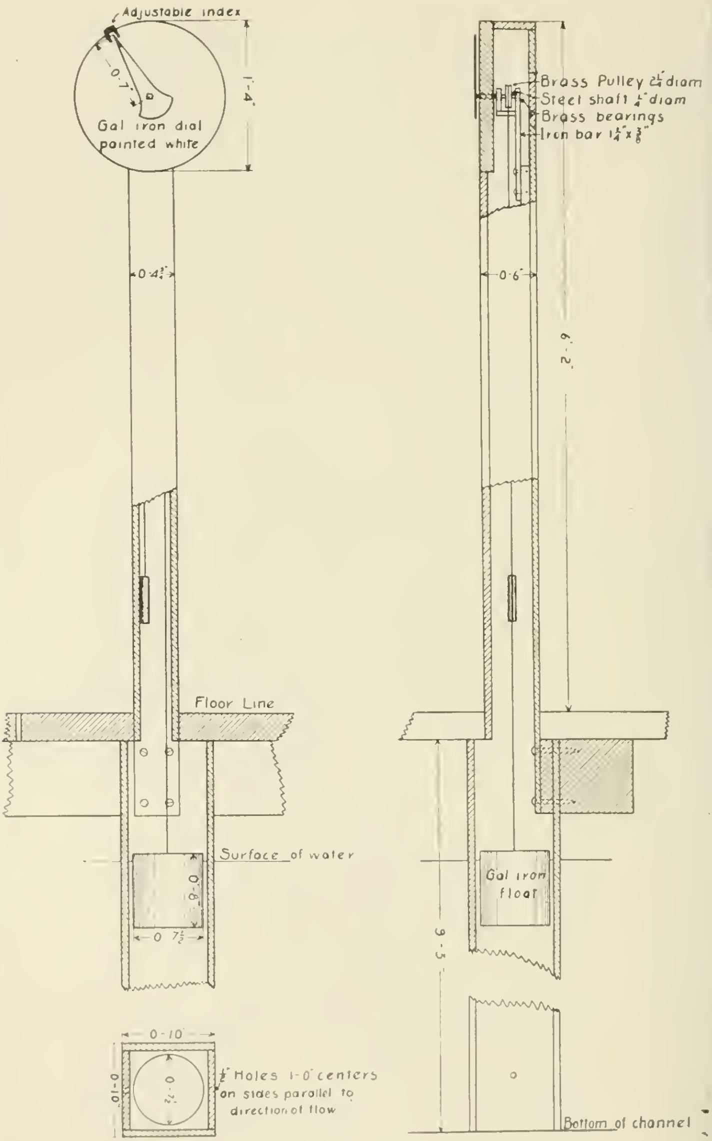

DETAILS
OF
DIAL FLOAT GAGE
USED FOR
EXPERIMENTS WITH SUBMERGED TUBES
SCALE

and eight inches high. It was guided vertically by being placed in a wooden tube, eight inches by eight inches inside measurements and ten feet long, the water being admitted through holes one-quarter inch in diameter and spaced one foot center to center along the center line of the side parallel to the direction of flow. A cord from the float was passed over a brass pulley of one and one-eighth inch radius and was connected to a counterweight. An index hand seven inches long was attached to the axle of the pulley and revolved in front of a galvanized iron circular plate of eight inches radius. The displacement of the outer end of the hand was thus about five and one-half times the change in elevation of the water surface. The gage was located in the ten foot channel, about thirteen feet up stream from the bulkhead containing the submerged tube, and placed so as to be easily seen from the centrifugal pump. It was the duty of the man operating the pump to keep constant watch of the index hand and by regulation of the throttle valve in the pipe supplying the stream to the pump, to maintain the index hand at any given position. It will be noticed that the gage did not indicate actual elevations of the water surface but simply made it possible to observe the fluctuations in elevation so that they could be kept within desirable limits. The method was very satisfactory. The maximum variation in elevation of water surface with careful work did not exceed three one-hundredths of a foot during an experiment lasting from one-half hour to one hour.

CALIBRATION OF SHARP CRESTED WEIR, 2.505 FEET LONG

End Contractions Suppressed; Height of Crest Above the Bed of Channel, 7.5 Feet

In order to determine with accuracy the quantity of water flowing through the submerged tube, it was considered necessary to determine the coefficients of discharge of the three sharp crested weirs for the same conditions of flow as existed during the experiments.

The three weirs being practically the same with respect to form, length and height of crest, the channels of approach being the same in all respects and of sufficient length to insure flow parallel to the sides of the channel, the three weirs would then have the same coefficient of discharge for any one head.

The weir chosen for calibration was at the outlet of weir channel Number 5, adjoining the left side of the ten foot channel, as shown on Plates I and II. For the measurement of the volume of water flowing in a given time, a suitable measuring basin practically water tight was provided. This measuring basin consisted of the space about eight feet by ten feet just below the weirs and extending to the head gates for the 30 inch turbine, and also of a space about seven feet by twenty-five feet, occupied by the two weir channels, Numbers 6 and 7, which were made water tight by means of a bulkhead built along the dotted line, KLM, Plate I. The former space has been termed measuring basin Number 1, and the latter, measuring basin Number 2. An aperture about two feet by six feet was made in the walls between the two measuring basins, so the two basins were practically the same as one. The maximum depth of water allowable in the measuring basin was about six feet, the water above this depth preventing the free entrance of air underneath the nappe of the weir.

These two measuring basins were carefully calibrated by the writer previous to the cutting of the large aperture which made them practically one basin. For this purpose the weight of a cubic foot of water was assumed as sixty-two and four-tenths pounds, and measured quantities of water of about fifty cubic feet successively emptied into the basins until they were filled. A record of time was also kept so that allowance could be made for infiltration and leakage. The infiltration was into measuring basin Number 2, and resulted from having water in the adjoining ten foot channel so as to reproduce the same conditions as existed during the calibration of the weir. During the calibration of the weir the surface of the water in the ten foot channel varied from level with the crest of the weir to one and one-half feet head on the crest of the weir. The height of the crest of the weir above the bed of the channel being seven and one-half feet, the depth of the water in the ten foot channel varied from seven and one-half feet to nine feet. Corresponding to each of the depths, seven and one-half, eight, eight and one-half and nine feet in the ten foot channel, measurements of infiltration into measuring basin Number 2 were made for the depths of water in this basin varying from zero to six feet. From the results of these measurements, curves representing infiltration were platted for the various depths of water in the ten foot channel. These curves were checked by measurements subsequent to the calibrations of the measuring basins and weir, and indicated practically constant conditions of infiltration. The amount of infiltration varied from zero to a maximum of three-quarters of a cubic foot per minute, depending on the difference of level between the water surfaces in the ten foot channel and basin Number 2.

Measurements of leakage from basin Number 1 through the gates underneath the turbine pit were also carefully made previous and subsequent to the calibrations of the measuring basins and weir. The leakage from basin Number 1 varied from zero to a maximum of one-half cubic foot per minute, depending on the difference of level between the water surfaces in basin Number 1 and the tail race. As the time interval required for calibrating each of the measuring basins was about one and one-half hours, the corrections for infiltration and leakage were very necessary. The results of the calibration of the measuring basins showed an average of 81.4 cubic feet for each foot of rise in basin Number 1, and an average of 142.9 cubic feet for each foot of rise in basin Number 2.

To indicate the depths of water in the measuring basins, two float gages were used, one located in each compartment, as shown on Plate I. These floats were made of galvanized iron cylindrical in form, seven and one-half inches in diameter and eight inches high, each having a rising stem about ten feet long made of one-eighth inch iron pipe. Fastened to the upper end of each stem was an index which enabled readings to be accurately made on a graduated stationary scale behind the stem. The floats were guided vertically by being placed in wooden boxes eight inches by eight inches inside measurements and having vertical slot openings one inch wide at each corner and extending throughout their length. The object was to prevent, as much as possible, the fluctuations of the floats from wave motion, and still have sufficient openings for the water to enter the boxes so that the elevation of the water surface in the boxes would not lag behind that outside.

In order to empty the measuring basins while the water was flowing over the weir, a ten inch gate valve was placed in the timber waste gate leading underneath the turbine as shown on Plates I and II. This valve not being of sufficient capacity to take the entire flow of the two and one-half foot weir, it was necessary to provide some further means of wasting the water. For this purpose a trough two and one-half feet wide and one and one-half feet high (Plate II) was arranged to be easily and quickly moved lengthwise on rollers by means of a lever, and to intercept the sheet of water flowing over the weir and carry it to the turbine pit. In placing the trough to intercept the nappe of the weir, the inner end was kept about four inches from the face of the weir so as to allow space for the admission of air underneath the nappe of the weir.

A set of careful observations were made to determine if there was any sudden or gradual change of head on the weir resulting from removing the trough from the position intercepting the nappe of the weir. For this purpose, an additional hook gage was placed in a still water basin in the center of the channel and eight feet up stream from the crest of the weir. Simultaneous readings of this hook gage and hook gage Number 5 were made at intervals of one-half minute during a period of one hour, the trough remaining for at least fifteen minutes in each of the two positions, intercepting or clearing the nappe of the weir. The comparison of the averages of the observed heads on the weir for the two positions showed that there was no measureable change of head on the weir resulting from the change of position of the trough. The comparison of the averages of the readings of the two hook gages also showed the correctness of the method of measuring the head on the crest of the weir by means of the still water basin located below the crest of the weir.

In making the observations for calibration of the weir, a running start was made. The head on the weir was maintained as nearly constant as possible, the readings of the hook gage, Number 5, taken at intervals of one-half minute, furnished an indication of when conditions were suitable for starting an observation. The water was lowered as much as possible in the measuring basin, the ten inch waste valve closed, and the trough for carrying the waste water rolled back so as to be clear from the nappe of the weir. The readings of the float gages were then taken simultaneously with the starting of the stop watch. When the measuring basins were filled to a depth of about six feet, readings of the float gages were again taken simultaneously with the stopping of the watch. The hook gage giving the reading of the head on the crest of the weir was read at intervals of one-half minute for at least five minutes previous to the experiment and then at intervals of one-half minute during the experiment. The following table is a summary of the results of the observations for calibration of the weir. The values in columns Number 5 and 6 are the rise of water in the meauring basins Number 1 and 2, respectively. Column Number 7 gives the volume of water flowing into the basins in the given time interval. Columns Number 8 and 9 give the necessary data for the calibration of the weir.

TABLE V.

RESULTS OF OBSERVATIONS FOR CALIBRATION OF SHARP CRESTED WEIR 2.505 FEET LONG. END CONTRACTIONS SURPRESSED; HEIGHT OF CREST ABOVE THE BED OF CHANNEL, 7.5 FEET.

Date. 1907.	Time.	Reference No.	Time interval filling measuring basins.	Rise of water in measuring basins.		Total volume.	Discharge cubic ft. per sec.	Average observed head on weir during observations.
				No. 1	No. 2			
	H. M.		M. S.	Feet.	Feet.	Cubic ft.		Feet.
1	2	3	4	5	6	7	8	9
April 4......	3 55	1	1 44.0	4.40	4.44	1008	9.69	1.0980
	4 06	2	1 36.2	3.98	4.00	910	9.44	1.0886
	4 17	3	1 42.3	4.23	4.20	958	9.37	1.0835
	4 25	4	1 39.8	4.06	4.02	915	9 26	1.0784
	4 38	5	1 40.0	4.10	4.15	940	9.40	1.0798
	5 14	6	3 29.0	4.28	4.28	960	4.59	0.6821
	5 25	7	3 22.3	4.18	4.19	950	4.69	0.6783
	5 34	8	3 36.8	4.36	4.36	985	4.56	0.6682
	5 43	9	3 36.5	4.40	4.39	993	4.58	0.6745
	5 51	10	3 31.4	4.19	4.19	954	4.51	0.6703
April 5.......	3 16	11	3 38.2	4.40	4.44	1000	4.58	0.6645
	3 29	12	3 44.5	4.40	4.40	996	4.44	0.6492
	3 41	13	3 48.0	4.40	4.44	1004	4.39	0.6453
	3 51	14	3 34.5	4.20	4.23	959	4.47	0.6470
	4 00	15	3 44.5	4.35	4.40	994	4.42	0.6459
	4 14	16	2 58.0	4.30	4.33	985	5.53	0.7462
	4 27	17	3 03.0	4.30	4.33	980	5.36	0.7389
	4 40	18	2 58.3	4.35	4.27	966	5.42	0.7414
	4 50	19	3 01.3	4.30	4.33	980	5.41	0.7416
	4 54	20	2 24.0	4.25	4.27	968	6.71	0.8563
	5 12	21	2 24.5	4.20	4.21	956	6.66	0.8568
	5 21	22	2 26.5	4.25	4.28	970	6.63	0.8523
	5 28	23	2 26.5	4.20	4.23	958	6.57	0.8423
April 6.......	9 14	24	30 00.0	4.57	4.57	1030	0.57	0.1608
	10 52	25	14 26.3	4.37	4.35	984	1.11	0.2552
	11 25	26	9 03.0	4.57	4.56	1029	1.90	0.3702
	11 39	27	5 49.7	4.20	4.20	954	2.73	0 4702
	12 07	28	4 38.3	4.50	4.50	1016	3.65	9.5706
	3 12	29	2 09.2	4.33	4.38	988	7.61	0.9433
	3 36	30	2 14.0	4.36	4.37	990	7.37	0.9184
	3 47	31	1 52.5	4.30	4.33	980	8.70	1.0234
	4 04	32	1 28.8	4.22	4.25	964	10.97	1.1983
	4 10	33	1 30.5	4.35	4.35	986	11.02	1.2019
	4 19	34	1 19.5	4.22	4.21	963	12.27	1.2936
	4 32	35	1 19.0	4.26	4.23	954	12.15	1.2910
	4 41	36	1 19.3	4.29	4.27	972	12.22	1.2934
	4 48	†37	1 9.3	4.10	4.11	937	13.52	1.3720
	4 54	†38	1 9.1	4.06	4.09	930	13.46	1.3515
	5 01	†39	1 9.0	4.08	4.13	938	13.60	1.3738
	5 07	†40	0 59.3	3 60	3.53	819	13.58	1.3738
	5 14	†41	0 56.0	3.80	3.77	868	15.49	1.4785
	5 21	†42	1 1.0	4.00	4.06	922	15.10	1.4582
April 8.......	4 20	43	1 25.4	4.20	4.23	960	11.24	1.2128
	4 29	44	1 27.2	4.20	4.22	960	11.01	1 1944
	4 41	45	1 22.5	4.20	4.20	956	11.73	1.2515
	4 49	46	1 22.0	4.14	4.22	954	11.63	1.2465
	5 01	†47	1 13.5	4 10	4.17	944	12.85	1.3177
	5 08	†48	1 9.3	3.93	3.97	904	13.03	1.3204
	5 14	†49	1 6.2	3.80	3.71	855	12.91	1.3179
	5 27	†50	1 12.0	4.07	4.13	936	13.00	1.3207
	5 38	†51	0 51.5	3.50	3.47	796	11.60	1.4149
	5 50	†52	0 59.2	3.82	3.83	875	14.77	1 4252
	5 59	†53	0 52.0	3.65	3.61	834	16.02	1.5177
April 10.	4 25	†54	0 50.1	3.70	3.58	828	16.52	1.5417
	4 33	†55	0 48.5	3 60	3.51	811	16.72	1.5495
	4 40	†56	0 50.9	3.70	3.61	831	16.32	1.5418
	4 54	†57	0 50.5	3.67	3 65	836	16.55	1.5395
	5 10	†58	0 46.6	3.55	3.45	798	17.12	1.5778
	5 18	†59	0 47.0	3.60	3.48	808	17.17	1.5757
	5 27	†60	0 44.2	3.47	3.40	786	17.78	1 6063
	5 34	†61	0 44.0	3.40	3.35	768	17.45	1.8176

†Observations rejected.

To face p. 280

PLATE XV.

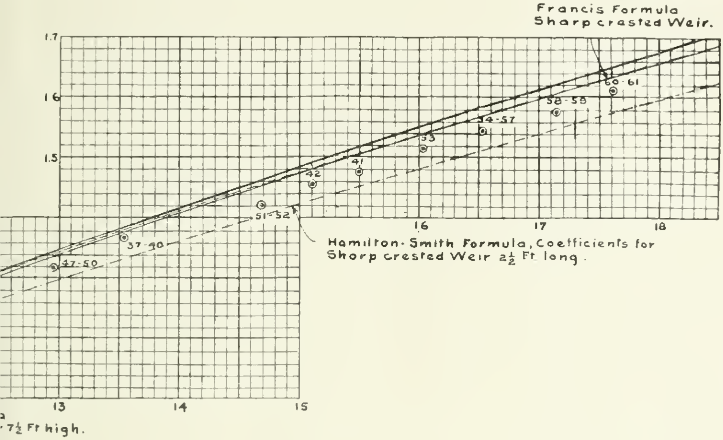

DISCHARGE CURVE

FOR A

SHARP CRESTED WEIR 2.505 FT. LONG.

END CONTRACTIONS SUPPRESSED;
HEIGHT OF CREST ABOVE BED OF CHANNEL, 7.5 FT.
AND

COMPARATIVE DISCHARGE OVER WEIR BY DIFFERENT FORMULÆ.

BAZIN FORMULA $Q=mLH\sqrt{2gH}$

Q = Discharge in cubic feet per second.
L = Length of crest in feet
H = Head on crest in feet measured from surface of water 8.0 feet upstream
m = Coefficient of discharge derived by experiment for each form of weir.
g = Acceleration due to gravity.

HAMILTON SMITH FORMULA $Q=C\frac{2}{3}\sqrt{2g}\ Lh^{\frac{3}{2}}$

C = Coefficient of discharge taken from curves showing relation of C and L.
h = Observed head on crest H plus correction due to velocity of approach.

FRANCIS FORMULA $Q=3.33L[(H+h_a)^{\frac{3}{2}}-h_a^{\frac{3}{2}}]$

H = Observed head on weir in feet
h_a = Head due to velocity of approach

DISCHARGE CURVE FROM RESULTS OF OBSERVATIONS
BY C. B. STEWART

○ Represents observations accepted
⊙ Represents observations rejected

Equation of Curve, $Q=8.38\ H^{1.491}$
$Q=3.35LH^{1.491}$

PLATE XV

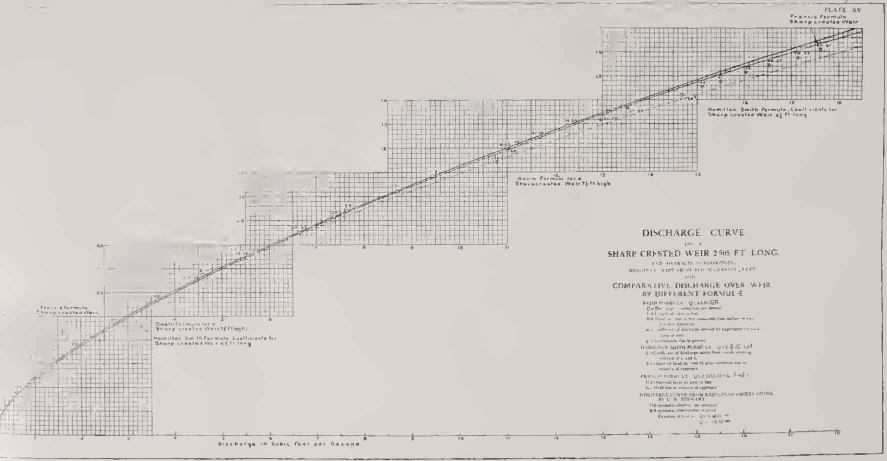

DISCHARGE CURVE

FOR A

SHARP CRESTED WEIR 2.505 FT. LONG.

END CONTRACTIONS SUPPRESSED,
HEIGHT OF CREST ABOVE BED OF CHANNEL, 7.5 FT.
AND

COMPARATIVE DISCHARGE OVER WEIR BY DIFFERENT FORMULÆ

BAZIN FORMULA $Q = mLH\sqrt{2gH}$
Q = Discharge in cubic feet per second
L = Length of weir in feet
H = Head on weir in feet measured from surface of water [illegible] feet upstream
m = coefficient of discharge derived by experiments for each form of weir
g = Acceleration due to gravity

HAMILTON SMITH FORMULA $Q = C\frac{2}{3}\sqrt{2g}\,Lh^{\frac{3}{2}}$
C = Coefficient of discharge taken from curves showing relation of h and L
h = Observed head on weir H plus correction due to velocity of approach

FRANCIS FORMULA Q = [illegible]
H = Observed head on weir in feet
h = Head due to velocity of approach

DISCHARGE CURVE FROM RESULTS OF OBSERVATIONS BY C. B. STEWART
○ Represents observations accepted
● Represents observations rejected
Equation of curve Q = [illegible]
Q = [illegible]

The total rise of water in the measuring basin being about four feet in each case, and the measurement of this rise being correct within about ±.02 feet, the percentage error of a single measurement of the volume probably did not exceed about one-half of one per cent. The measurement of the time interval was probably correct within about one-quarter of one per cent.

The range of head on the weir, covered by the experiments varied from sixteen hundredths feet to one and six-tenths feet; but it was observed that above one and three-tenths feet head on the weir air was drawn into the water in the measuring basin by the falling sheet of water, and it was necessary to reject observations for heads on the weir above this value.

The results of the observations have been platted on Plate XV as a discharge curve, the abscissae being equal to the discharge in cubic feet per second and the ordinates equal to the observed head in feet on the crest of the weir. On Plate XVI a logarithmic discharge curve has been drawn, the abscissae being equal to the logarithm of the discharge in cubic feet per second, and the ordinates being equal to the logarithm of the observed head in feet on the crest of the weir. The center of co-ordinates of the logarithmic curve corresponds to the discharge of one cubic foot per second, and to the observed head of one foot on the crest of the weir. Below the logarithmic value corresponding to one and three-tenths feet head on the weir, the results of the observations as platted lie on a straight line, while, above this value the platted points lie slightly below the straight line. It is possible that there may be a gradual change in the law of flow over the weir as the head increases above one and three-tenths feet, yet the observed fact that air was drawn into the water in the measuring basin for the higher heads is partial evidence that the law of flow remains practically the same for heads above one and three-tenths feet as for heads below one and three-tenths feet. Assuming the straight line as representing the law of flow over the weir as expressed by logarithmic co-ordinates, the equation of the line as platted on Plate XVI is:

$$\text{Log } Q = 0.923 + 1.481 \log H$$

where Q represents the discharge in cubic feet per second and H represents the observed head on the crest of the weir. The

PLATE XVI

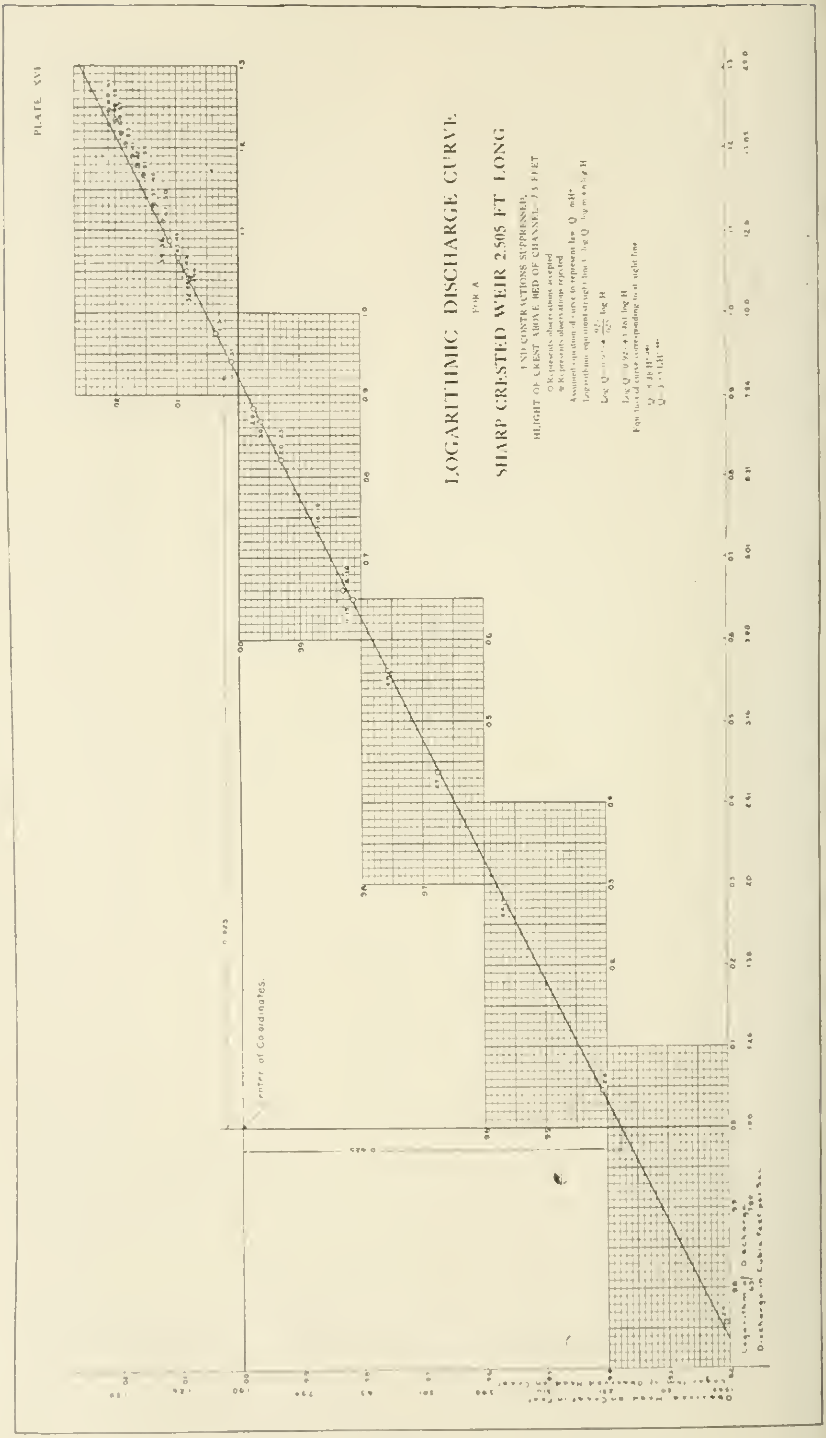
LOGARITHMIC DISCHARGE CURVE
FOR A
SHARP CRESTED WEIR 2.505 FT LONG
END CONTRACTIONS SUPPRESSED,
HEIGHT OF CREST ABOVE BED OF CHANNEL—7.5 FEET
○ Represents observations accepted
Represents observations rejected
Center of Coordinates.
Logarithms of Discharge
Discharge in Cubic Feet per Sec.

equation of the corresponding curve using natural co-ordinates as platted on Plate XV is:

$$Q = 8.38\ H^{1.481}$$

or

$$Q = 3.35\ L\ H^{1.481}$$

where L represents the length of the crest of the weir in feet.

For the purpose of comparison of the results of this calibration with the results obtained by using the formulae of Francis, Bazin and Hamilton Smith, curves have been drawn on Plate XV. In addition Table VI has been arranged, giving the discharge for each tenth of a foot head on the weir from the results obtained by using the calibration curve and by using the various formulae.

TABLE VI.

COMPARISON OF FLOW OVER SHARP CRESTED WEIR, 2.505 FEET LONG BY VARIOUS FORMULAE, AND MEASUREMENTS OF FLOW BY C. B. STEWART.

Observed Head on Weir. Ft.	Discharge in Cubic Feet Per Second.				Percentage Variation of Discharge.		
	Francis.	Bazin.	Hamilton Smith.	C. B. Stewart.	Columns 2 and 5.	Columns 3 and 5.	Columns 4 and 5.
1	2	3	4	5	6	7	8
.1	0.26	0.29	0.28	0.28	−7.1	+6.4	+ 0.0
.2	.75	0.79	0.78	0.77	−2.8	+2.8	+ 1.0
.3........	1.37	1.43	1.42	1.41	−1.7	+1.4	+ 0.7
.4........	2.11	2.18	2.16	2.16	−1.0	+0.9	+ 0.0
.5........	2.95	3.03	3.02	3.00	−1.7	+1.0	+ 0.7
.6.......	3.88	3.96	3.97	3.93	−1.3	+0.8	+ 1.5
.7........	4.89	4.96	5.02	4.94	−1.0	+0.4	+ 1.6
.8........	5.98	6.05	6.16	6.02	−0.7	+0.5	+ 2.3
.9..	7.14	7.20	7.38	7.16	−0.3	+0.6	+ 3.1
1.0........	8.37	8.44	8.68	8.38	−0.1	+0.7	+ 3.6
1.1.	9.66	9.71	10.08	9.64	+0.2	+0.7	+ 4.6
1.2.......	11.02	11.06	11.51	10.98	+0.4	+0.9	+ 4.8
1.3........	12.43	12.45	13.05	12.35	+0.6	+0.8	+ 5.7
1.4	13.91	13.91	14.64	*13.78	+0.9	+0.9	+ 6.3
1.5........	15.43	15.46	16.30	*15.27	+1.0	+1.2	+ 6.8
1.6	17.02	17.04	18.04	*16.80	+1.3	+1.4	+ 7.4
1.7..	18.69	18.68	19.83	*18.38	+1.6	+1.6	+ 7.9
2.0........	....	....	25.60	*23.38	....	....	+ 9.5
3.0........	....	....	48.91	*42.62	....	....	+14.7

*Computed from formula $Q = 3.35\ L\ H^{1.481}$

Columns Numbers 6, 7 and 8 give the percentage variation of the results, by using the various formulae, from the results of the writer's calibration curve. It will be observed that the results obtained by using the formulae of Francis, Bazin and the writer's calibration curve practically agree, while the results by using the formula of Hamilton Smith are considerably larger. The percentage excess resulting from using the formula of Hamilton Smith, for heads on the weir of one, two and three feet, amounts respectively to about five, ten and fifteen per cent. The cause of this comparatively large variation by using the formula of Hamilton Smith will be considered in a future Bulletin on "Experiments on Flow of Water over Weirs" which is in course of preparation. The close agreement of the experimental results with the results from using the formulae of Francis and Bazin is evidence that the measurements of flow were carefully made.

As a further test of the accuracy of the measurements of flow, a careful calibration was made of the ten foot weir by taking simultaneous readings of heads on the two and one-half foot weirs and on the ten foot weir. These readings were taken during a portion of the regular observations on the submerged tubes. The comparisons of the individual measurements of flow with the computed results, and of the resulting calibration curve with the theoretical curves of flow over the weir by using the formulae of Francis, Bazin and Hamilton Smith, furnished an approximate check on the measured flow and a basis for judging of the accuracy of the results of the experiment. The results of the calibration of the ten foot weir show very close agreement with the computed results using the formulae of Francis, Bazin and Hamilton Smith, and will be considered in the future bulletin on weirs.

GENERAL METHOD OF MAKING OBSERVATIONS

The program for observing was to take the readings of the important hook gages, giving data for head on the submerged tube and heads on the two and one-half foot weirs, simultaneous, and the others as nearly simultaneous with these as necessary to give the desired data as to slopes of water surfaces. Gages Nos 2 and 3, immediately above and below the bulkhead respectively, and giving data for head on the tube, were arranged so that one person could take practically simultaneous readings, the eye glancing from one water surface to the other while both hands were free to make the final adjustments with the micrometer heads. Gages Nos. 5, 6 and 7, giving data for heads on weirs, were read in succession by one observer in the order named, as rapidly as possible without sacrificing accuracy, the time of reading the three gages not exceeding about ten seconds. Gages Nos. 1 and 4 were read alternately by one observer.

The head on the tube being adjusted to the desired amount, a marker was placed on the rim of the dial of the dial float gage, and the desired elevation of water surface in the channel leading to the submerged tube maintained as nearly constant as possible. For the experiments with the submerged tubes with lengths varying from thirty-one hundredths feet to five feet, simultaneous readings of gages Nos. 2, 3, 5, 6, and 7 were made at intervals of two minutes, see table, page 287, while gages Nos. 1 and 4 were read alternately with these gages. For the experiments with the submerged tubes of ten feet and fourteen feet lengths, an additional hook gage was placed at the lower end of each tube and designated as gage No. 4′ and gage No. 4″ respectively: readings were made with these gages at the two minute intervals, simultaneous with readings of gages Nos. 2, 3, 4, 5, 6 and 7, while gages Nos. 1 and 4 were read alternately with these gages. The observations were continued for a period of from one-half hour to one hour, or until certain that the average of the observed readings was within the desired degree of accuracy.

TABULATED RESULTS OF EXPERIMENTS WITH SUBMERGED TUBES 4.0 FEET SQUARE

The results of the experiments were recorded in tabular form, the experiments of each series being accompanied by a sketch showing the principal dimensions of the tube, distances from the sides and bottom of the channel, and the maximum and minimum distances from the top of the tube to the surface of the water. These tabulated results giving the details of the experiments with observations at the two minute intervals, and lasting about one-half hour, cover about one hundred pages, and were considered too voluminous to be published. They have, however, been filed in the office of the Department of Hydraulic Engineering of the University, and are accessible to any one who desires to refer to the original data.

In order to show the character of the original data, and especially the amount of the individual fluctuations in the water surface, Table VII is given. Figure A shows the sketch to accompany experiments Nos. 1 and 6 of series No. 5, experiment No. 1, being for a small discharge, and experiment No. 6 for one of the larger discharges.

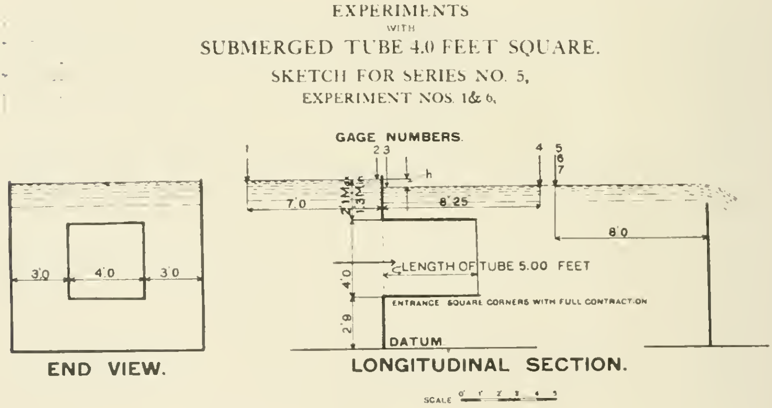

FIGURE A

TABLE VII.

RESULTS OF EXPERIMENTS WITH SUBMERGED TUBE 4.0 FEET SQUARE. LENGTH OF TUBE, 5.00 FEET. ENTRANCE: SQUARE CORNERS WITH FULL CONTRACTION.

All readings in feet.

SERIES NO. 5, EXPERIMENT NO. 1.

	Time. H. M.	No. of reading.	Readings for Heads on Submerged Tubes. Gage No. 1.	Gage No. 2.	Gage No. 3.	Gage No. 4.	Readings for Heads on 2.5 Feet Weirs. Gage No. 5.	Gage No. 6.	Gage No. 7.	Fall (gage No. 1, —gage No. 2).	Observed head h′ (gage No. 2. —gag, No. 3).	Fall (gage No. 3, —gage No. 4.)
April 19, 1907	3:00	1	1.5673	1.5731	1.5281	......	......	......	......	—.0055	.0447	......
	02	2	......	1.5655	1.5190	1.5159	.9124	.9309	.9158	......	.0465	+.0031
	04	3	1.5616	1.5680	1.5215	......	.9102	.9217	.9109	—.0064	.0465	......
	06	4	......	1.5567	1.5124	1.5082	.8981	.9160	.8999	......	.0443	+.0042
	08	5	1.5335	1.5553	1.5133	......	.9005	.9137	.9005	—.0218	.0420	......
	10	6	......	1.5661	1.5115	1.5100	.8935	.9089	.8959	......	.0546	+.0015
	12	7	1.5420	1.5465	1.5034	......	.8910	.9115	.8958	—.0045	.0431	......
	14	8	......	1.5173	1.5060	1.5012	.9121	.9276	.9135	......	.0413	+.0048
	16	9	1.5479	1.5496	1.5084	......	.9105	.9310	.9164	—.0017	.0412	......
	18	10	......	1.5452	1.5045	1.5017	.9014	.9241	.9099	......	.0407	+.0028
	20	11	1.5620	1.5640	1.5210	......	.9104	.9309	.9134	—.0020	.0430	......
	22	12	......	1.5435	1.5012	1.5000	.8957	.9156	.9032	......	.0423	+.0012
	24	13	1.5495	1.5515	1.5100	......	.8969	.9176	.9045	—.0020	.0415	......
	26	14	......	1.5550	1.5120	1.5065	.8986	.9090	.9010	......	.0430	+.0055
	28	15	1.5415	1.5450	1.5035	......	.9042	.9254	.9072	—.0035	.0415	......
	30	16	......	1.5392	1.4966	1.4941	.9006	.9106	.8992	......	.0426	+.0025
	32	17	1.5458	1.5510	1.5052	......	.8979	.9157	.8980	—.0062	.0458	......
	34	18	......	1.5503	1.5093	1.5053	.9149	.9338	.9213	......	.0410	+.0040
	36	19	1.5380	1.5696	1.5270	......	.9040	.9259	.9182	—.0016	.0426	......
	38	20	......	1.5460	1.5035	1.4976	.9013	.9215	.9090	......	.0425	+.0059
Average of readings (Nos. 1, 3, 5, etc)			......	1.5574	......	......	......	......	......	......	......	......
Average of readings (Nos. 2, 4, 6, etc)			......	......	1.5076	......	......	......	......	......	......	......
Average of all readings			1.5519	1.5544	1.5109	1.5040	.9028	.9206	.9070	—.0055	.0435	+.0036
Correction to gage reading			......	+6.7	+6.7	......	+7.31	+7.31	+7.31	......	......	......
Average elevation of water surface			......	8.2544	8.2109	......	8.2128	8.2306	8.2170	......	......	......
Discharge of weirs Nos. 5, 6 and 7, cubic feet per second			......	......	......	......	7.17	7.42	7.35	......	......	......
Total discharge cubic feet per sec			......	......	......	......	......	......	21.94	......	......	......
Average observed head h′, on tube			......	......	......	......	......	......	.0435	......	......	......
Value of C, in formula $Q=Ca\sqrt{2gh'}$			......	......	......	......	......	......	.8195	......	......	......

TABLE VII—Continued.

RESULTS OF EXPERIMENTS WITH SUBMERGED TUBE 4.0 FEET SQUARE. LENGTH OF TUBE, 5.00 FEET. ENTRANCE: SQUARE CORNERS WITH FULL CONTRACTION.

All readings in feet.

SERIES NO. 5, EXPERIMENT NO. 6.

	Time. H. M.	No. of reading.	Readings for Heads on Submerged Tubes.				Readings for Heads on 2.5 Feet Weirs.			Fall (gage No. 1, —gage No. 2).	Observed head h' (gage No. 2, —gage No. 3).	Fall (gage No. 3, —gage No 4).
			Gage No. 1.	Gage No. 2.	Gage No. 3.	Gage No. 4.	Gage No. 5.	Gage No. 6.	Gage No. 7.			
April 20, 1907	11:08	1	2.1942	2.2205	2.0293		1.4262	1.4968	1.4293	—.0263	.1912	
	10	2		2.2477	2.0315	2.0257	1.4435	1.5026	1.4367		.2032	
	12	3	2.2033	2.2310	2.0320		1.4428	1.5145	1.4366	—.0277	.1990	
	14	4		2.2290	2.0318	2.0255	1.4431	1.4981	1.4367		.1972	+.0063
	16	5	2.2067	2.2285	2.0332		1.4427	1.5160	1.4304	—.0218	.1953	
	18	6		2.2295	2.0303	2.0216	1.4452	1.5125	1.4371		.1962	+.0087
	20	7	2.2013	2.2380	2.0392		1.4315	1.5023	1.4258	—.0367	.1988	
	22	8		2.2265	2.0276	2.0257	1.4328	1.5031	1.4262		.1989	+.0019
	24	9	2.2066	2.2380	2.0363		1.4257	1.5148	1.4312	—.0314	.2017	
	26	10		2.2400	2.0367	2.0308	1.4363	1.5018	1.4237		.2033	+.0059
	28	11	2.2152	2.2385	2.0310		1.4358	1.4900	1.4261	—.0233	.2015	
	30	12		2.2325	2.0357	2.0300	1.4446	1.5178	1.4430		.1988	+.0057
	32	13	2.2070	2.2285	2.0275		1.4354	1.5084	1.4285	—.0215	.2010	
	34	14		2.2430	2.0395	2.0310	1.4365	1.5092	1.4301		.2035	+.0085
	36	15	2.2055	2.2300	2.0320		1.4437	1.5143	1.4395	—.0245	.1980	
	38	16		2.2330	2.0350	2.0323	1.4305	1.5081	1.4316		.1980	+.0027
Average of readings (Nos. 1, 3, 5, etc.)				2.2316								
Average of readings (Nos. 2, 4, 6, etc.)					2.0338							
Average of all readings			2.2049	2.2334	2.0311	2.0285	1.4373	1.5069	1.4320	—.0265	.1993	+.0051
Correction to gage reading				+6.7	+6.7		+7.31	+7.31	+7.31			
Average elevation of water surface				8.9331	8.7341		8.7173	8.8169	8.7425			
Discharge of weirs, Nos. 5. 6 and 7, cubic ft per second							1 433	15.42	11.47			
Total discharge, Q, cubic ft. per sec									14.22			
Average observed head, h' on tube									.1993			
Value of C, in formula $Q=Ca\sqrt{2gh'}$									.7716			

The readings from hook gages Nos. 1, 2, 3, and 4, 4′ and 4″, gave, when the proper corrections were applied, the elevations of the water surfaces at the respective gages above an assumed datum. This reference plane of zero elevation was the bottom of the ten foot channel just above the bulkhead containing the tube. The readings from hook gages Nos. 5, 6 and 7 gave the heads on crests of the respective weirs located in the weir channels Nos. 5, 6, and 7. These readings when corrected by a certain constant, gave the elevation above the reference plane of the surface of the water at the points of measuring the heads on the weirs. In order to obtain the fall in the water surface between the points of the respective gages, it was necessary to use simultaneous observations taken at the respective points considered. Thus to obtain the fall in the water surface between gages Nos. 1 and 2 (see Table VII), it will be observed that the readings of gage No. 1 were taken simultaneous with those of gage No. 2, which correspond with the odd numbers 1, 3, 5, etc. The fall, computed from each individual pair of observations, has been tabulated under the column "Fall, (gage No. 1—gage No. 2.)" The average fall between gages Nos. 1 and 2 during the set of readings corresponding to any experiment number was obtained by taking the average of the individual values in this column. The average of the observations at gage Number 2 which were taken simultaneously with the observations at gage Number 1 have been designated in the summary below the table as "Average of readings Nos. 1, 3, 5, etc." The difference of the average of the simultaneous readings at the two gages should agree with the average of the individual differences of gage readings and furnished a check on the arithmetical work.

For the fall in the water surface between gages Nos. 2 and 3, each of the pairs of observations were simultaneous, and the differences of the readings have been recorded; for the short tubes, Series Nos. 1 to 5 inclusive, as "Observed head, h′, on tube." The average elevations of water surfaces at these gages were determined from the values designated in the summary below the table as "Average of all readings."

For the fall in the water surfaces between gages Nos. 3 and

4, the readings of gage No. 3, which were simultaneous with the readings of gage No. 4, correspond with the even numbers 2, 4, 6, etc. For determining the average of the readings of gage No. 3 to be used in connection with the average of the readings of gage No. 4, the term "Average of readings Nos. 2, 4, 6, etc." was used.

SUMMARY SHEET, SHOWING RESULTS OF EXPERIMENTS WITH SUBMERGED TUBES 4.0 FEET SQUARE

In the preliminary computations of the results of the experiments, the head due to velocity of approach to the tube was neglected, and the observed head on the tube, termed h′, was taken as the difference of level between the surface of the water just above the bulkhead containing the submerged tube and the surface of the water at the outlet of the tube. (See discussion, page 319). For the tubes of lengths from thirty-one hundredths feet to five feet, the observed head, h′, has been taken as the fall in water surface from gage No. 2 to gage No. 3. While for the tubes of ten and fourteen feet lengths, the observed head, h′, has been taken as the "Fall, (gage No. 2—gage No. 3)," plus the fall of the water surface from gage No. 3 to the end of the tube.

In some of the experiments the gage at the lower end of the tube was not read, and in order to determine the fall of water surface from gage No. 3 to the lower end of the tube, curves of fall were platted from the data taken. The observations giving the fall of the water surface from gage No. 3 to the end of the tube, or "Fall (gage No. 3—gage No. 4′)" and "Fall, (gage No. 3—gage No. 4″)" have been platted on Plate XVII and curves drawn which showed the relation of fall in water surface to discharge. In determining the fall in the water surface from gage No. 3 to the end of the tube, *to be used in the computations*, values from these curves were used in preference to observed fall, as it was considered that the results would be more uniform. The observed head obtained by adding these values to the "Fall, (gage No. 2—gage No. 3)" was termed h″.

PLATE XVII.

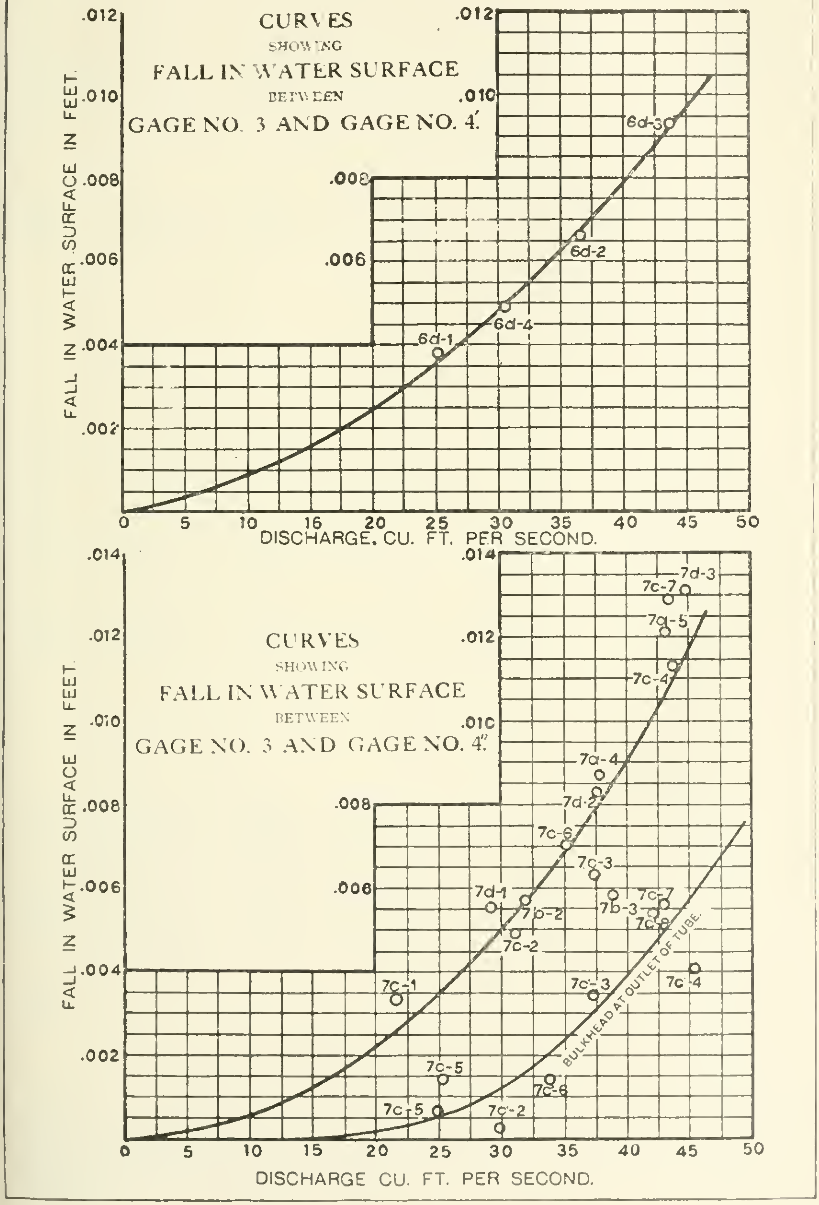
CURVES
SHOWING
FALL IN WATER SURFACE
BETWEEN
GAGE NO. 3 AND GAGE NO. 4'.
FALL IN WATER SURFACE IN FEET.
.012
.010
.008
.006
.004
.002
0
5
10
16
20
25
30
35
40
45
50
DISCHARGE, CU. FT. PER SECOND.
6d-1
6d-4
6d-2
6d-3
CURVES
SHOWING
FALL IN WATER SURFACE
BETWEEN
GAGE NO. 3 AND GAGE NO. 4".
FALL IN WATER SURFACE IN FEET.
.014
.012
.010
.008
.006
.004
.002
0
5
10
15
20
25
30
35
40
45
50
DISCHARGE CU. FT. PER SECOND.
7d-3
7c-7
7a-5
7c-4
7a-4
7d-2
7c-6
7c-3
7d-1
7b-2
7c-2
7b-3
7c-7
7c-8
7c-1
7c-3
7c-4
BULKHEAD AT OUTLET OF TUBE.
7c-5
7c-5
7c-2
7c-6

TABLE VIII.

SUMMARY SHEET, SHOWING RESULTS OF EXPERIMENTS WITH SUBMERGED TUBES, 1.0 FEET SQUARE.

Time.	Series No.	Experiment No.	No. of Reading.	Average Elevation of Water Surface.				Average Fall Between Gages.						Average Observed Head, h', on Tube. (Cols. 9—(11 or 12)).	Average Observed Head, h'', on Tube. (Cols. 9+13.)	Discharge cubic feet per second.	Coefficient of Disc., C, in formula (Q=Ca $\sqrt{2gh'}$.)	Value of Coefficient of Discharge C. (Q=Ca $\sqrt{2gh''}$.)
				Gage No. 2.	Gage No. 3.	Gage No. 4'.	Gage No. 4''.	(Gage No. 1—gage No. 2.)	(Gage No. 2—gage No. 3.)	(Gage No. 3—gage No. 4.)	(Gage No. 3—gage No. 4'.)	(Gage No. 3—gage No. 4''.)	(Gage No. 3—gage (No. 4' or No. 4'')). (From Curve of Fall, Plate XVII.)					
	1	2	3	4	5	6	7	8	9	10	11	12	13	14	15	16	17	18
		Feet.	Feet.	Feet.	Feet.	Feet.	Feet.	Feet.	Feet.	Feet.	Feet.	Feet.	Feet.	Feet.	Feet.			
Sept. 11, 1906	1 Length 0.31 feet.																	
11:22—12:08		1	36	8.7094	8.5120	.....	.....	—.0252	.1971	+.0169	....	......	....	.1974	....	35.08	.6151	....
3:01—3:59		2	56	8.4745	8.3139	......	......	—.0170	.1305	+.0095	..	......	.... ..	.1305	....	28.20	.6081	....
4:00—4:43		3	44	8.4678	8.3117	......	......	—.0161	.1260	+.0085	......	......	....	.1260	.. ....	28.68	.6160	......
Sept. 12, 1906																		
9:53—11:12		4	80	8.2835	8.2081	......	......	—.0058	.0751	+.0063	......	......	....	.0751	....	21.96	.6230	....
11:30—11:57		5	28	8.2294	8.1669	....	......	—.0051	.0626	+.0074	......	.. ..	....	.0626	....	20.01	.6231	....
3:50—4:31		6	22	8.1198	8.0753	......	......	—.0051	.0445	+.0061	....	......	....	.0445	....	17.10	.6315	....
Sept. 17, 1906																		
9:16—11:30		7	53	8.1326	8.0962	......	......	—.0050	.0364	+.0038	...	......	....	.0364	. ...	15.36	.6369	....
3:06—4:36		8	46	8.1006	8.0779	.....	......	—.0025	.0227	+.0031	......	......	......	.0227	.	12.62	.6525	....
Sept. 18, 1906																		
10:54—11:10		9	4	8.7201	8.5168	......	.... .	—.0295	.2032	+.0016	......	......	.. ....	.2032	....	35.86	.6202	....
11:28—11:31		10	4	8.7236	8.5163	. ....	......	—.0298	.2073	+.0164	......	......	....	.2073	....	35.36	.6050	....
May 15, 1907																		
3:48—4:12		11	13	8.4364	8.3194	......	......	—.0061	.1171	—.0002	......	......	.. ....	.1171	....	26.82	.6105	....
4:20—4:42		12	12	8.6055	8.4378	......	....	—.0102	.1677	—.0006	.....	...	....	.1677	....	31.64	.6019	..
4:50—5:16		13	11	8.8217	8.5855	......	......	—.0145	.2362	+.0051	......	....	....	.2362	.. ...	38.07	.6102	....
5:22—5:48		14		9.0394	8.7184	... .	......	—.0100	.3210	+.0107	......	......	....	.3210	....	41.90	6174	....

May 16, 1907																		
9:46—10:30		15	23	8.5377	8.2926	......	......	—.0083	.1451	+.0012	.....	......	....	.1451	....	29.71	.6076	....
10:46—11:12		16	11	8.9423	8.6636	......	......	—.0102	.2787	+.0077	......	......	....	.2787	....	42.00	.6198	....
11:31—11:41		17	6	9.1773	8.7957	......	......	....	.3816	+.0059	.....	.....	....	.3816	....	49 09	.6191	....
May 16, 1907	1a																	
2:40—3:04	Length 0.31 feet.	1	13	8.2954	8.2221	......	......	+.0001	.0733	+.0012	...	......	....	.0733	....	22.83	.6569	....
3:12—3:38		2	14	8.5111	8.3806	..	......	—.0065	.1301	+.0006	......	......	....	.1304	....	28 97	.6250	....
3:52—4:22		3	16	8.7373	8.5378	......	.....	—.0131	.1995	+.0012	.....	......	....	.1995	....	36.13	.6301	....
4:32—5:02		4	16	8.8981	8.6447	..	.....	—.0121	.2537	+.00.3	.....	.....	....	.2537	....	41.00	.6341	....
5:10—5:40		5	16	9.0113	8.7349	......	......	.0063	.3061	+.0078	......	.....	....	.3061	....	45.35	.6482	....
May 17, 1907	1b																	
9:54—10:24	Length 0.31 feet.	1	16	8.5153	8.3986	......	......	—.0048	.1168	—.0004	......	......	....	.1168	....	29.75	.6781	....
10:30—11:00		2	16	8.7131	8.5406	......	.....	—.0142	.1728	+.0057	......	......	....	.1728	....	36.21	.6786	....
11:10—11:36		3	14	8.8981	8.6670	......	..	—.0077	.2311	+.0055	.....	......	....	.2311	....	42.01	.6807	....
11:40—11:58		4	10	9.0371	8.7602	......	......	—.0061	.2768	+.0004	......	......	....	.2768	... .	46.55	.6892	......
May 17, 1907	1c																	
2:42—3:02	Length 0.31 feet.	1	11	8.2772	8.2316	......	....	+.0001	.0456	+.0038	.....	...	....	.0456	....	22.71	.8296	....
3:18—3:48		2	16	8.5511	8.4497	......	......	.0074	.1018	+.0120	.....	..	.....	.1018	....	31.50	.7691	....
4:00—4:34		3	18	8.8055	8.6368	.....	.....	.0130	.1687	+.0173	...	......	....	.1687	....	39.92	.7571	....
4:41—5:11		4	16	8.9380	8.7399	.....	.....	—.0072	.1980	+.0245	.....	.....	....	.1980	....	44.61	.7815	....
5:22—5:50		5	15	9.0400	8.8113	.....	......	—.0052	.2287	+.0278	......	.....	....	.2287	.....	48.20	.7852	....
May 18, 1907	1d																	
9:32—10:02	Length 0.31 feet.	1	31	8.3700	8.3266	.....	......	—.0022	.0431	—.0003	.....	......	....	.0431	..... .	26.58	.9939	......
10:20—10:50		2	31	8.6142	8.5308	.....	......	.0061	.0833	+.0027	.....	......	......	.0833	.....	35.08	.9468	...
11:08—11:38		3	31	8.8116	8.7117	.....	......	—.0125	.1299	+.0035	.. ..	......	....	.1299	....	43 28	.9355	......
11:56—12:26		4	31	8.9891	8.8291	....	......	—.0103	.1603	+.0060	......	......	....	.1603	....	48.92	.9519	....
Sept. 18, 1906	2																	
3:20—4:22	Length 0.625 feet.	1	32	8.3989	8.2975	......	.....	—.01.7	.1013	+.0024	......	.....	....	.1013	....	26.24	.6122	....
4:32—5:22		2	26	8.4886	8.3628	......	......	—.0167	.1258	+.0036	......	......	....	.1258	.....	28.77	.6319	......
Sept. 20, 1906																		
9:08—10:20		3	37	8.2408	8.1739	.....	...	.0053	.0669	+.0009	......	....	....	.0669	....	21.36	.6433	....
10:34—11:54		4	41	8.5882	8.4332	......	......	—.0198	.1551	+.0015	.....	.....	....	.1551	....	31.72	.6274	....
3:52—5:20		5	45	8.7050	8.5119	......	.....	—.0271	.1931	+.0068	......	......	....	.1931	....	35.25	.6249	....
Sept. 21, 1906																		
10:30—11:36		6	49	8.1190	8.0725	......	......	—.0033	.0461	+.0027	......	.....	....	.0461	....	17.84	.6452	....

TABLE VIII—Continued.

SUMMARY SHEET, SHOWING RESULTS OF EXPERIMENTS WITH SUBMERGED TUBES, 4.0 FEET SQUARE.

Time.	Series No.	Experiment No.	No. of Reading.	Average Elevation of Water Surface.				Average Fall Between Gages.						Average Observed Head, h', on Tube. (Cols. 9+(11 or 12)).	Average Observed Head, h", on Tube (Cols. 9+13.)	Discharge cubic feet per second.	Coefficient of Disc., C., in formula ($Q=Ca\sqrt{2gh'}$.)	Value of Coefficient of Discharge C. ($Q=Ca\sqrt{2gh"}$.)
				Gage No. 2.	Gage No. 3.	Gage No. 4'.	Gage No. 4".	(Gage No. 1—gage No. 2.)	(Gage No. 2—gage No. 3.)	(Gage No. 3—gage No. 4.)	(Gage No. 3—gage No. 4'.)	(Gage No. 3—gage No. 4".)	(Gage No. 3—gage (No. 4 or No. 4")). (From Curve of Fall. Plate XVII.)					
	1	2	3	4	5	6	7	8	9	10	11	12	13	14	15	16	17	18
			Feet.	Feet.	Feet.	Feet.	Feet.	Feet.	Feet.	Feet.	Feet.	Feet	Feet.	Feet.	Feet.			
Sept 22, 1906	3																	
9:32—10:41		1	37	8.3109	8.2328	.....	.....	—.0116	.0781	+.0024	.....	.....	.....	.0781	.....	23.67	.6581	.....
10:51—11:44		2	26	8.4426	8.3335	.....	.....	—.0163	.1091	+.0046	.....	.....	.....	.1091	.....	27.48	.6481	.....
2:10— 3:24		3	38	8.0921	8.0529	.....	.....	— 0019	.0392	+.0033	.....	.....	.....	.0392	.....	16.99	.6693	.....
3:40— 4:18		4	20	8.5950	8.4439	.....	.....	—.0249	.1510	+.0 82	.....	.....	.....	.1510	.....	32.04	.6410	.....
Sept. 24, 1906																		
10:52—12:04		5	37	8.7160	8.5470	.....	.....	—.0342	.1990	+.0105	.....	.....	.....	.1990	.....	36.69	.6107	.....
May 15, 1907	Length 1.25 feet.																	
11:38—11:56		6	10	8.5023	8.3816	.....	.....	.....	.1212	.....	.....	.....	.....	.1212	.....	29.01	.6191	.....
12:02—12:24		7	12	8.6745	8.5024	.....	.....	.....	.1722	.....	.....	.....	.....	.1722	.....	31.20	.6420	.....
12:30—12:52		8	12	8.8908	8.6499	.....	.....	.....	.2409	.....	.....	.....	.....	.2409	.....	41.14	.6529	.....
Sept. 25, 1906	4																	
11:10—12:04		1	28	8.4178	8.3322	.....	.....	—.0159	.0856	+.0029	.....	.....	.....	.0856	.....	27.37	.7287	.....
2:50— 3:50		2	31	8.6209	8.4824	.....	.....	—.0296	.1386	+.0018	.....	.....	.....	.1386	.....	33.70	.7052	.....
4:14— 5:14		3	31	8.7968	8.6030	.....	.....	—.0440	.1938	+.0017	.....	.....	.....	.1938	.....	39.02	.6905	.....
April 16, 1907																		
5:16—5:46		4	16	8.6636	8.5188	.....	.....	—.0276	.1448	+.0074	.....	.....	.....	.1448	.....	35.22	.7210	....

April 18, 1907																		
9:50 – 10:28	Length 2.50 feet.	5	20	8.5813	8.4592	......	......	—.0172	.1220	+.0093	......	......	......	.1220	....	31.97	.7127	....
10:48 – 11:30		6	22	8.3408	8 2722	......	......	—.0041	.0686	+.0022	......	......	....	.0686	....	21.47	.7278	....
11:48 – 12:26		7	20	8.2371	8.1894	......	......	—.0022	.0477	+.0071	......	......	....	.0477	....	21.29	.7596	....
3:46 – 4:28		8	22	8.6846	8.5370	......	......	—.0197	.1476	+.0012	......	......	....	.1476	....	35.41	.7180	....
4:46 – 5:12		9	14	8.8952	8.6914	......	......	—.0148	.2041	+.0073	......	......	....	.2041	....	42.53	.7331	....
5:24 – 5:52		10	15	8.0208	8.7784	......	......	—.0020	.2424	+.0025	......	......	....	.2424	....	47.07	.7448	....
May 14, 1907																		
2:46 – 3:14		11	15	8.3752	8.2990	......	......	—.0066	.0762	+.0021	......	......	....	.0762	....	25.57	.7216	....
3:24 – 3:54		12	16	8.5528	8.4363	......	......	—.0105	.1165	+.0057	......	......	....	.1165	....	31 03	.7082	....
4:10 – 4:42		13	17	8.7283	8 5636	......	......	—.0179	.1647	+.0043	......	......	....	.1647	....	36.75	.7051	....
4:56 – 5:22		14	14	8.9544	8.7293	......	......	+.0160	.2251	+.0051	......	......	....	.2254	....	44.36	.7283	....
5:26 – 5:46		15	14	9.0276	8.7792	......	......	—.0127	.2184	+.0052	......	......	....	.2484	....	46.92	.7331	....
May 10, 1907	4a																	
10:36 – 11:08	Length 2.50 feet.	1	17	8.3214	8.2559	......	..	—.0029	.0655	+.0032	......	......	....	.0655	....	23.72	.7220	....
11:13 – 11:46		2	15	8.5213	8.4077	......	......	—.0095	.1136	+.0066	......	......	....	.1136	....	29.96	.6924	....
11:52 – 12:22		3	16	8.8195	8.6168	......	...	—.0169	.2027	+.0099	......	......	....	.2027	....	39.64	.6854	....
2:54 – 3:24		4	16	8.2949	8.2344	......	......	—.0045	.0605	+.0007	......	......	....	.0605	....	23.37	.7402	....
3:32 – 4:00		5	15	8.4766	8.3749	..	......	—.0073	.1017	+.0026	......	......	....	.1017	....	28.81	.7038	....
4:06 – 4:36		6	16	8.6798	8.5229	......	......	—.0149	.1569	+.0039	......	......	....	.1569	....	35.07	.6897	....
4:48 – 5:20		7	17	8 8323	8.6269	......	......	— 0152	.2051	+.0075	......	......	....	.2054	....	39.69	6821	....
May 14, 1907	4b																	
10:08 – 10:30	Length 2.50 feet.	1	12	8.2725	8.2189	......	......	—.0029	.0536	+.0039	......	......	....	.0536	....	22.44	.7551	....
10:40 – 11:06		2	14	8.4738	8.3764	......	....	—.0032	.0973	+.0015	......	......	....	0973	....	28.70	.7168	....
11:16 – 11:44		3	15	8.6711	8.5211	......	......	—.0115	.1498	+.0078	......	......	....	.1498	....	34.87	.7018	....
11:54 – 12:24		4	16	8.83 3	8.6371	......	......	—.0149	.1961	+.0127	......	......	....	.1961	....	40.10	.7054	....
May 14, 1907	4c																	
2:48-3:18	Length 2.50 feet.	1	16	8.3005	8.2502	......	......	+.0029	.0503	+.0038	......	......	....	.0503	....	23.88	.8294	....
3:26-3:56		2	16	8.4662	8:3758	......	......	—.0011	.0904	+.0056	......	......	....	.0904	....	28 35	.7345	....
4:02-4:32		3	16	8.6801	8.5299	......	......	—.0108	.1502	+.0132	......	......	....	.1502	....	35.19	.7073	....
4:40-5:14		4	18	8.8548	8.6529	......	......	—.0095	.2019	+.0196	......	......	....	.2019	....	40.93	.7096	....
May 13, 1907																		
11:40-12:12		5	17	8.9146	8.6932	......	......	......	.2164	......	......	......	....	.2184	....	43.14	.7194	....
12:22-12:42		6	11	9.0459	8.7889	......	......	....	.2570	....	......	......	....	.2570	....	47.73	.7335	....
May 14, 1907																		
10:08-10:22		7		8.8514	8.6455	......	......	....	.2059	....	......	......	....	.2059	....	41.03	70.44	....

TABLE VIII—Continued.

SUMMARY SHEET SHOWING RESULTS OF EXPERIMENTS WITH SUBMERGED TUBES, 4.0 FEET SQUARE.

Time.	Series No.	Experiment No.	No. of Reading.	Average Elevation of Water Surface.				Average Fall Between Gages.						Average Observed Head, h', on Tube. (Cols. 9+(11 or 12.))	Average Observed Head, h'', on Tube (Cols. 9+13.)	Discharge, cubic feet per second.	Coefficient of Disc., C., in formula (Q = Ca $\sqrt{2gh'}$.)	Value of Coefficient of Discharge, C, (Q = Ca $\sqrt{2gh''}$.)
				Gage No. 2.	Gage No. 3.	Gage No. 4'.	Gage No. 4''.	(Gage No. 1—gage No. 2.)	(Gage No. 2—gage No. 3.)	(Gage No. 3—gage No. 4.	(Gage No. 3—gage No. 4'.)	(Gage No. 3—gage No. 4''.)	(Gage No. 3—gage (No. 4' or No. 4''.)) (From Curve of Fall Plate XVII.)					
	1	2	3	4	5	6	7	8	9	10	11	12	13	14	15	16	17	18
			Ft.	Feet.	Feet.	Feet.	Feet.	Feet.	Feet.	Feet.	Feet.	Feet.	Feet.	Feet.	Feet.			
May 13, 1907	4d																	
3:08-3:38	Length 2.50 feet.	1	16	8.3782	8.3272	......	......	—.0058	.0460	+.0036	......	......	......	.0460	......	26.50	9625	......
3:50-4:20		2	16	8.7605	8.5931	......	......	.0182	.1074	+.0037	......	......	......	.1074	......	37.71	.8961	......
4:36-5:06		3	16	8.7831	8.6604	......	......	—.0181	.1227	+.0070	......	......	......	.1227	......	41.09	.9138	......
5:10-5:18		4	5	8.7317	8.6210	......	......	—.0162	.1107	+.0030	......	......	......	.1107	......	39.14	.9161	......
5:26-5:50		5	13	8.9071	8.7584	......	......	—.0186	1487	+.0042	......	......	......	.1487	......	45.48	.9188	......
Apr. 19, 1907	5																	
3:00-3:38		1	20	8.2544	8.2109	......	......	—.0055	.0455	+.0036	......	......	......	.0435	......	21.94	.8195	......
3:46-4:16		2	16	8.4144	8.3642	......	......	—.0130	.0802	+.0038	......	......	......	.0802	......	27.91	.7678	......
4:24-4:54		3	16	8.6145	8.4969	......	......	—.0190	.1176	+.0073	......	......	......	.1176	......	33.50	.7610	......
5:02-5:32	Length 5.00 feet.	4	16	8.7551	8.6010	......	......	—.0278	.1541	+.0079	......	......	......	.1541	......	38.16	.7573	......
Apr. 20, 1907																		
10:02-10:41		5	22	8.8158	8.6681	......	......	—.0284	.1777	+.0055	......	......	......	.1777	......	41.32	.7634	......
11:08-11:38		6	16	8.9334	8.7341	......	......	—.0265	.1993	+.0054	......	......	......	.1993	......	44.22	.7716	......
12:08-12:34		7	14	8.7725	8.6136	......	......	—.0271	.1589	+.0059	......	......	......	.1589	......	38.69	.7561	......
3:28- 4:04		8	19	9.0176	8.7917	......	......	—.0214	.2249	+.0070	......	......	......	.2249	......	47.32	.7756	......
May 9, 1907	5a																	
2:34-:304		1	16	8.2709	8.2241	......	......	—.0019	.0468	+.0015	......	......	......	.0468	......	22.65	.8156	......
3:12-3:42	Length 5.00 feet.	2	16	8.5378	8.4398	......	......	—.0106	.0980	+.0035	......	......	......	.0980	......	31.08	.7734	......
3:50-4:20		3	16	8.7269	8.5814	......	......	—.0177	.1455	+.0056	......	......	......	.1455	......	37.41	.7640	......
4:26-4:56		4	16	8.8898	8.7025	......	......	—.0170	.1873	+.0075	......	......	......	.1878	......	43.00	.7740	......

May 9, 1907	5b																	
9:58-10:24	Length 5.00 feet.	1	14	8.2591	8.2173	......	......	-.0032	.0417	+.0040	......	......	......	.0417	......	22.40	.8545	......
10:30-10:58		2	15	8.4812	8.3996	......	......	-.0069	.0815	+.0071	......	......	......	.0815	......	29.52	.8055	......
11:01-11:31		3	16	8.7164	8.5795	......	......	-.0141	.1369	+.0071	......	......	......	.1369	......	37.30	.7853	......
11:40-12:12		4	17	8.8677	8.6924	......	......	-.0148	.1752	+.0063	......	......	......	.1752	......	42.48	.7906	......
May 8, 1907	5c																	
3:16-3:46	Length 5.00 feet.	1	16	8.2619	8.2247	......	......	-.0016	.0378	+.0009	......	......	......	.0378	......	23.02	.9224	......
3:58-4:28		2	16	8.5151	8.4313	......	......	-.0099	.0841	+.0026	......	......	......	.0841	......	30.63	.8228	......
4:36-5:06		3	16	8.6701	8.5501	......	......	-.0160	.1197	+.0066	......	......	......	.1197	......	35.98	.8101	......
5:14-5:44		4	16	8.9287	8.7525	......	......	-.0063	.1762	+.0086	......	......	......	.1762	......	45.46	.8437	......
May 7, 1907	5d																	
2:54-3:20	Length 5.00 feet.	1	14	8.2486	8.2172	......	......	-.0017	.0314	+.0027	......	......	......	.0314	......	22.29	.9799	......
3:34-4:04		2	16	8.4980	8.4307	......	......	-.0080	.0673	+.0038	......	......	......	.0673	......	30.76	.9258	......
4:14-4:44		3	16	8.7019	8.5874	......	......	-.0181	.1076	+.0034	......	......	......	.1076	......	38.13	.9056	......
4:50-5:20		4	16	8.8602	8.7159	......	......	-.0249	.1443	+.0066	......	......	......	.1443	......	43.51	.8923	......
Apr. 23, 1907	6																	
3:56-4:18	Lenght 10.0 feet.	1	12	8.2582	8.2176	......	......	-.0009	.0406	+.0018	......	......	.0029	......	.0135	22.36	......	.8352
4:28-4:54		2	14	8.5821	8.4778	......	......	-.0146	.1043	+.0005	......	......	.0056	......	.1099	33.05	......	.7766
5:01-5:34		3	16	3.7819	8.6307	......	......	-.0213	.1512	+.0000	......	......	.0079	......	.1591	39.65	......	.7741
Apr. 24, 1907																		
2:56-3:26		4	16	8.8547	8.6871	......	......	-.0219	.1677	+.0037	......	......	.0088	......	.1765	42.31	......	.7845
3:56-4:26		5	16	8.0075	8.8029	......	......	-.0111	.2045	+.0029	......	......	.0110	......	.2155	48.07	......	.8067
May 6, 1907	6d																	
3:30-3:52	Length 10.0 feet.	1	12	8.3368	8.2955	8.2917	...	-.0013	.0443	+.0006	+.0038	......	.0038	.0451	.0451	25.17	.9233	.9233
4:04-4:34		2	16	8.6607	8.5660	8.5594	......	-.0149	.0947	+.0016	+.0066	......	.0066	.1013	.1013	36.51	.8914	.8944
4:44-5:14		3	16	8.8535	8.7161	8.7068	......	-.0237	.1474	+.0017	+.0093	......	.0093	.1467	.1467	43.69	.8886	.8886
5:20-5:46		4	14	8.4980	8.4335	8.4286	...	-.0079	.0645	+.0000	+.0049	......	.0049	.0694	.0694	30.63	.9058	.9058
Apr. 25, 1907	7																	
3:34-4:04	Length 14.0 feet.	1	16	8.2657	8.2252	......	......	+.0006	.0405	-.0001	......	......	.0030	......	.0435	22.97	......	.8579
4:14-4:44		2	16	8.4760	8.3987	......	......	-.0079	.0773	+.0008	......	......	.0048	......	.0821	29.52	......	.8026
4:54-5:24		3	16	8.7046	8.5796	......	......	-.0179	.1250	+.0033	......	......	.0078	......	.1328	37.24	......	.7961
5:32-5:50		4	10	8.8118	8.6608	......	......	-.0218	.1510	+.0038	......	......	.0095	......	.1605	40.82	......	.7937
Apr. 26, 1907																		
2:52-3:26		5	18	8.8998	8.7291	......	......	-.0180	.1708	+.0016	......	......	.0111	......	.1822	44.01	......	.8037
3:48-4:12		6	14	9.0443	8.8316	......	......	-.0107	.2097	-.0015	......	......	.0147	......	.2244	49.34	......	.8114

TABLE VIII—Continued.

SUMMARY SHEET SHOWING RESULTS OF EXPERIMENTS WITH SUBMERGED TUBES, 4.0 FEET SQUARE.

Time.	Series No.	Experiment No.	No. of Reading.	AVERAGE ELEVATION OF WATER SURFACE.				AVERAGE FALL BETWEEN GAGES.						Average Observed Head, h′, on Tube. (Cols. 9+(11 or 12)).	Average Observed Head, h″, on Tube. (Cols. 9+13.)	Discharge, cubic feet per second.	Coefficient of Disc., C., in formula (Q=Ca √2g h′.)	Value of Coefficient of Discharge, C. (Q=Ca √2g h″.)
				Gage No. 2.	Gage No. 3.	Gage No. 4′.	Gage No. 4″.	(Gage No. 1—gage No. 2.)	(Gage No. 2—gage No. 3.)	(Gage No. 3—gage No. 4.)	(Gage No. 3—gage No. 4′.)	(Gage No. 3—gage No. 4″.)	(Gage No. 3—gage (No. 4′ or No. 4″.)) (From Curve of Fall, Plate XVII.)					
	1	2	3	4	5	6	7	8	9	10	11	12	13	14	15	16	17	18
			Ft	Feet.	Feet.	Feet.	Feet.	Feet.	Feet.	Feet.	Feet.	Feet.	Feet.	Feet.	Feet.			
Apr. 27, 1907	7a Length 14.0 feet.																	
10:38-11:14		1	19	8.2361	8.1993	....	......	—.0005	.0368	—.0002	....	....	.0027	....	.0395	21.92	....	.8592
11:26-11:56		2	16	8.4432	8.3749	....	....	—.0049	.0683	—.0018	....	....	.0045	....	.0728	28.47	....	.8220
12:06-12:36		3	16	8.6306	8.5238	......	....	—.0151	.1068	—.0008	....	......	.0067	....	.1135	34.86	....	.8061
3:18- 3:48		4	16	8.7275	8.5952	....	8.5865	—.0183	.1322	—.0002	....	+.0088	.0081	.1410	.1403	37.89	.7861	.7880
4.08- 4:42		5	18	8.8733	8.7082	....	8.6960	—.0183	.1651	+.0033	....	+.0122	.0109	.1773	.1760	43.19	.7990	.8020
Apr. 29, 1907	7b Length 14.0 feet.																	
3:50-4:20		1	16	8.2729	8.2329	......	....	—.0006	.0100	—.0005	....	.....	.0030	....	.0430	23.02	.....	.8648
4:36-5:06		2	16	8.5490	8.4619	......	8.4560	—.0117	.0870	+.0021	....	+.0058	.0056	.0928	.0925	31.94	.8168	.8181
5:18-5:48		3	16	8.7429	8.6118	....	8.6060	—.0161	.1311	+.0031	....	+.0058	.0086	.1869	.1397	38.90	.8190	.8108
Apr. 30, 1907	7c Length 14.0 feet.																	
2:55 3:32		1	18	8.2341	8.2017	......	8.1984	—.0016	.0324	—.0012	......	+.0033	.0026	.0357	.0350	21.63	.8918	.8981
3:40-4:26		2	24	8.5166	8.4381	....	8.4331	—.0096	.0785	—.0012	....	+.0049	.0053	.0831	.0838	31.16	.8405	.8405
4:31-5:12		3	20	8.6992	8.5845	....	8.5782	—.0162	.1147	+.0015	.....	+.0063	.0079	.1210	.1226	37.41	.8385	.8370
5:30-5:52		4	12	8.8733	8.7189	......	8.7075	—.0146	.1543	—.0030	....	+.0113	.0112	.1656	.1655	43.81	.8387	.8389
May 4, 1907																		
8:54- 9:24		5	16	8.3450	8.2978	....	8.2961	—.0020	.0472	—.0016	....	+.0014	.0036	.0486	.0508	25.35	.8956	.8762
9:34-10:08		6	18	8.6259	8.5268	....	8.5198	—.0098	.0991	—.0003	.....	+.0070	.0068	.1061	.1059	35.10	.8394	.8402
10:18-10:48		7	16	8.8594	8.7116	....	8.6988	—.0120	.1477	+.0047	....	+.0129	.0110	.1606	.1587	43.41	.8438	.8489

May 1, 1907	7c																	
2:58–3:28	Length 14.0 feet.	1	16	8.2328	8.1986	......	8.2000	—.0015	.0312	—.0021	......	—.0015	.0003	.0327	.0315	21.59	.9301	.9055
3:38–4:08		2	16	8.4760	8.4031	....	8.4030	—.0088	.0726	—.0008	....	+.0002	.0012	.0729	.0738	29.72	.8575	.8522
4:18–4:48		3	16	8.6991	8.5783	....	8.5750	—.0157	.1208	—.0013	....	+.0034	.0030	.1242	.1238	37.28	.8241	.8251
4:58–5:36		4	20	8.9012	8.7444	....	8.7103	—.0080	.1598	—.0002	.....	+.0011	.0060	.1639	.1658	45.17	.8692	.8612
May 3, 1907																		
2:38–3:12	Length 14.0 feet.	5	18	8.3307	8.2823	......	8.2815	—.0051	.0181	—.0008	....	+.0007	.0005	.0491	.0489	24.79	.8720	.8733
3:21–3:58		6	18	8.5951	8.4969	......	8.4951	—.0114	.0985	—.0010	......	+.0015	.0020	.1000	.1005	33.69	.8299	.8279
4:28–5:02		7	18	8.8695	8.7106	....	8.7050	—.0111	.1589	—.0010	....	+.0056	.0053	.1645	.1642	43.43	.8242	.8319
5:10–5:16		8	4	8.8167	8.6932	....	8.6877	—.0161	.1535	—.0007	....	+.0055	.0047	.1590	.1582	42.04	.8213	.8231
May 4, 1907	7d																	
2:56–3:26	Length 14.0 feet.	1	16	8.4492	8.3937	.....	8.3882	—.0032	.0555	+.0001	...	+.0055	.0047	.0610	.0602	29.29	.9210	.8299
3:46–4:20		2	18	8.6941	8.5941	....	8.5860	—.0151	.1060	+.0031	....	+.0083	.0080	.1083	.1080	37.71	.8934	.8916
4:32–5:06		3	18	8.8848	8.7471	....	8.7031	—.0171	.1376	+.0073	....	+.0131	.0118	.1507	.1494	44.82	.8994	.9033

Table VIII, preceding, is a summary sheet, showing the results of the experiments collected for reference. The greater portion of the table will be intelligible from the headings of the several columns without further explanation. The elevations of the water surfaces at the various gages is referred to a common datum. The plane of zero elevation being the bottom of the channel just above the bulkhead containing the submerged tube. The average fall in the water surface between the various gages is given in columns 8 to 13 inclusive. Negative values for fall represent a rise or increase of elevation of the water surface. Column 13 gives the fall in water surface from gage No. 3 to the lower end of the tube, the values being taken from Plate XVII. Columns 14 and 15 give values of the average observed head, h′ or h″, on the tube. Column 16 gives the discharge through the tube and was determined from readings of heads on the three, two and one-half foot weirs. Columns 17 and 18 give values of the coefficient of discharge, C, computed by using the heads, h′ and h″, respectively. For the tubes of length from thirty-one hundredths to five feet inclusive, values of the observed head, h′, column 9 to 14, have been used for computing the values of C. For the tubes of ten and fourteen feet length, values of C have been computed by using values of both h′ and h″, (columns 14 and 15 respectively,) where data are available, for purposes of comparison. For the platting of curves preference has been given to the values of C as computed by using values of h″. These values of the coefficient of discharge represent the ratio of the average velocity in the cross-sectional area of the tube to the velocity due the head on the tube.

CURVES SHOWING AVERAGE RESULTS OF EXPERIMENTS WITH SUBMERGED TUBES 4.0 FEET SQUARE

Effect of Changing the Length of Tubes

1. *Entrance, Square Corners with full Contraction*:—The results of the experiments on the submerged tubes of various lengths and having entrance square corners are illustrated by Plates XVIII and XIX. Plate XVIII shows the relation of discharge through the tubes to the loss of head, the maximum discharge being about fifty cubic feet per second and the corresponding maximum loss of head about four-tenths of a foot. Each point as platted represents the result of an experiment lasting about one-half hour, the data being taken directly from the Summary Sheet, Table VIII. For a given discharge the loss of head decreases as the length of tube increases, this law continuing until the length of the tube equals about fourteen feet or about three and one-half times the length of the side of the square cross-section of the tube. The curve representing the velocity head, $\frac{v^2}{2g}$ for various rates of discharge has also been drawn for the purpose of comparison. Plate XIX shows the relation of the coefficient of discharge to the loss of head for the various lengths of tubes. Each of the platted points represented by a circle is the result of a single experiment lasting about one-half hour, while the points represented by heavy dots "●", three for each curve, represent computed values of the coefficient of discharge obtained by taking discharge and loss of head from the average curves of Plate XVIII. These latter points were given considerable weight in adjusting the curves as they represented average conditions with observational errors reduced to a minimum.

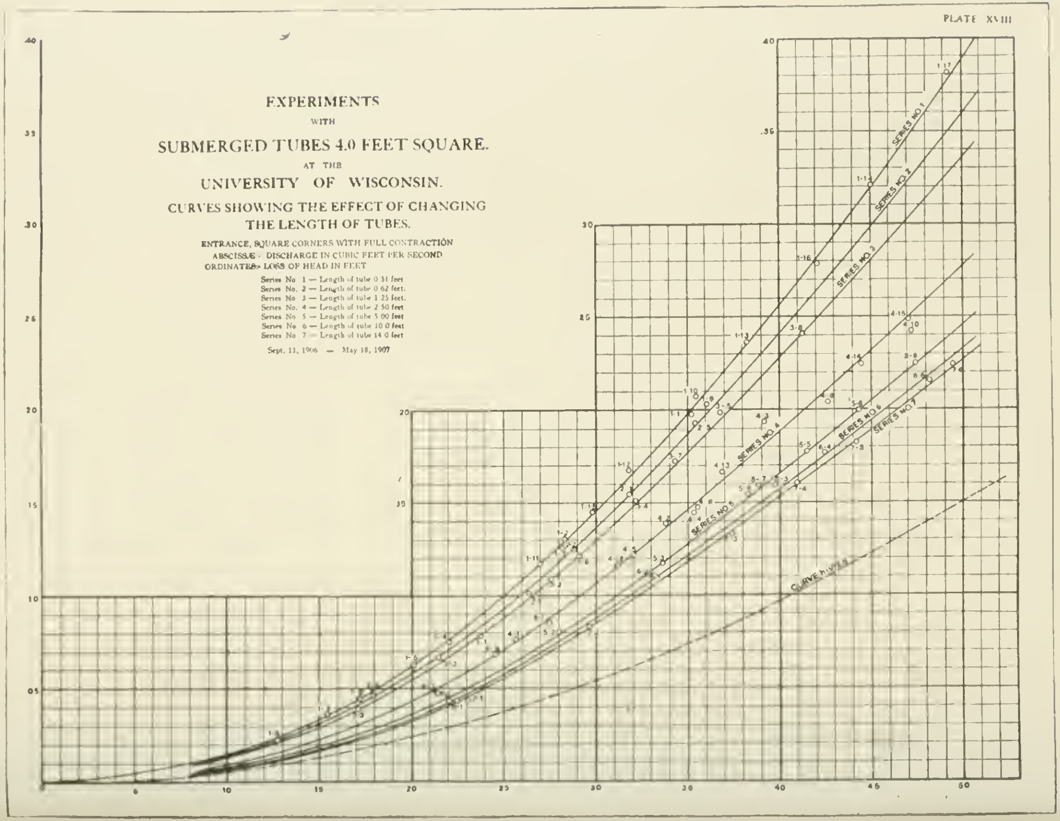
PLATE XVIII
EXPERIMENTS
WITH
SUBMERGED TUBES 4.0 FEET SQUARE.
AT THE
UNIVERSITY OF WISCONSIN.
CURVES SHOWING THE EFFECT OF CHANGING THE LENGTH OF TUBES.
ENTRANCE, SQUARE CORNERS WITH FULL CONTRACTION
ABSCISSÆ - DISCHARGE IN CUBIC FEET PER SECOND
ORDINATES - LOSS OF HEAD IN FEET
Series No 1 — Length of tube 0 31 feet
Series No. 2 — Length of tube 0 62 feet.
Series No 3 — Length of tube 1 25 feet.
Series No. 4 — Length of tube 2 50 feet
Series No 5 — Length of tube 5 00 feet
Series No 6 — Length of tube 10 0 feet
Series No 7 — Length of tube 14 0 feet
Sept. 11, 1906 — May 18, 1907
SERIES NO 1
SERIES NO 2
SERIES NO 3
SERIES NO 4
SERIES NO 5
SERIES NO 6
SERIES NO 7
CURVE hv
.40
.35
.30
.25
.20
.15
.10
.05
5
10
15
20
25
30
35
40
45
50

PLATE XIX.

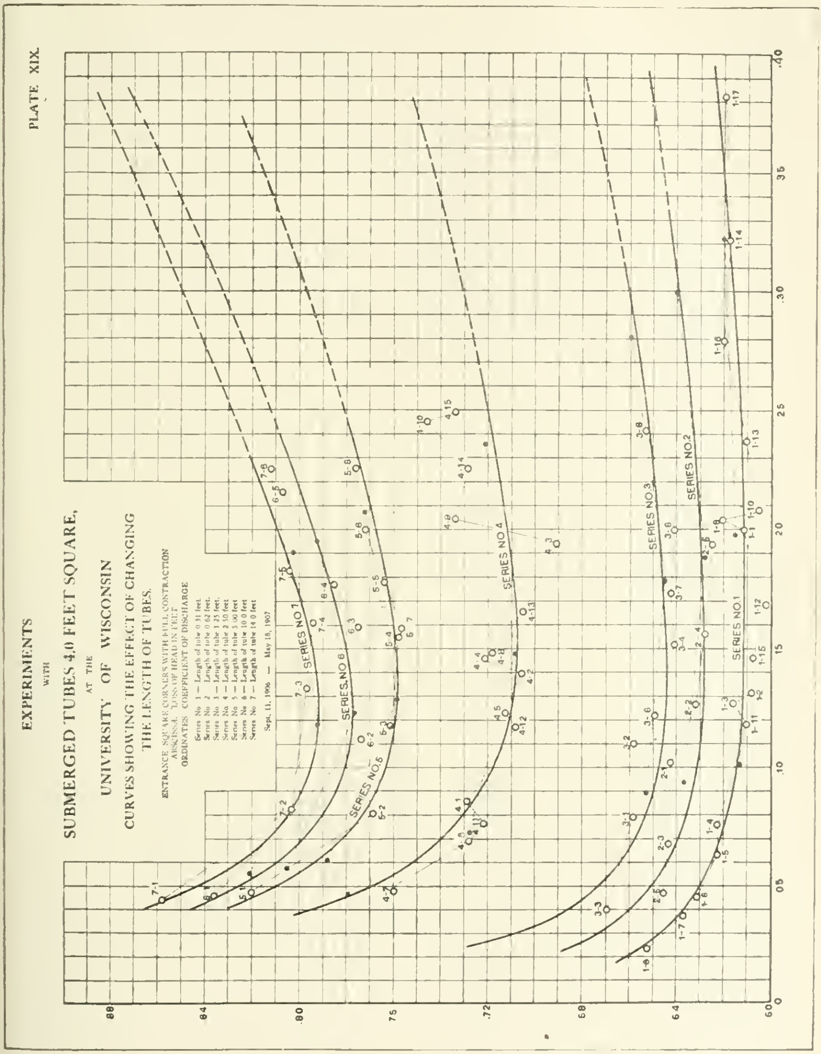
EXPERIMENTS
WITH
SUBMERGED TUBES 4.0 FEET SQUARE,
AT THE
UNIVERSITY OF WISCONSIN
CURVES SHOWING THE EFFECT OF CHANGING
THE LENGTH OF TUBES.
ENTRANCE SQUARE CORNERS WITH FULL CONTRACTION
ABSCISSA: LOSS OF HEAD IN FEET
ORDINATES: COEFFICIENT OF DISCHARGE
Series No 1 — Length of tube 0.31 feet.
Series No 2 — Length of tube 0.62 feet.
Series No 3 — Length of tube 1.25 feet.
Series No 4 — Length of tube 2.50 feet
Series No 5 — Length of tube 5.00 feet
Series No 6 — Length of tube 10.0 feet
Series No 7 — Length of tube 14.0 feet
Sept. 11, 1906 — May 18, 1907
SERIES NO 1
SERIES NO 2
SERIES NO 3
SERIES NO 4
SERIES NO 5
SERIES NO 6
SERIES NO 7
.88
.84
.80
.76
.72
.68
.64
.60
0
.05
.10
.15
.20
.25
.30
.35
.40

2. *Entrance, Contraction Suppressed on Bottom, Two Sides and Top*:—The results of the experiments under the conditions stated and having the various lengths of tubes are shown on Plates XX and XXI. Plate XX shows the relation of discharge through the tubes to the loss of head. For a given discharge the loss of head increases with the length of tube. This evidently results from the stream entering the tube without contraction and the friction on the sides of the tube producing the increase in loss of head as the length of tube increases. Plate XXI shows the relation of the coefficient of discharge to the loss of head for the various lengths of tubes. In general the coefficient of discharge decreases as the length of the tube increases.

EFFECT OF MODIFYING ENTRANCE CONDITIONS OF TUBES

Plates XXII, XXIII, XIV, XXV, and XXVI show the relation of discharge to loss of head for the length of tubes 0.31, 2.50, 5.00, 10.00 and 14.00 feet, respectively, each length having the various entrance conditions specified by the subscripts a, b, c and d as explained on each plate. Corresponding to each of these plates showing the loss of head for the various lengths and under various entrance conditions, Plates XXVII to XXXI, inclusive, have been drawn showing the relation of the coefficient of discharge to loss of head. The data for the platting of the curves has been taken directly from the summary sheet, Table VIII. From the results of the experiments as represented by the average curves, Tables IX and X have been arranged giving the results in more convenient form. Table IX gives the loss of head in feet for the various lengths of tubes, rates of discharge and forms of entrance and outlet used. The coefficients of discharge, termed "Preliminary value of coefficient of discharge," Table X, are results from using the observed head on the tube, no corrections being made for velocity of approach.

PLATE XX

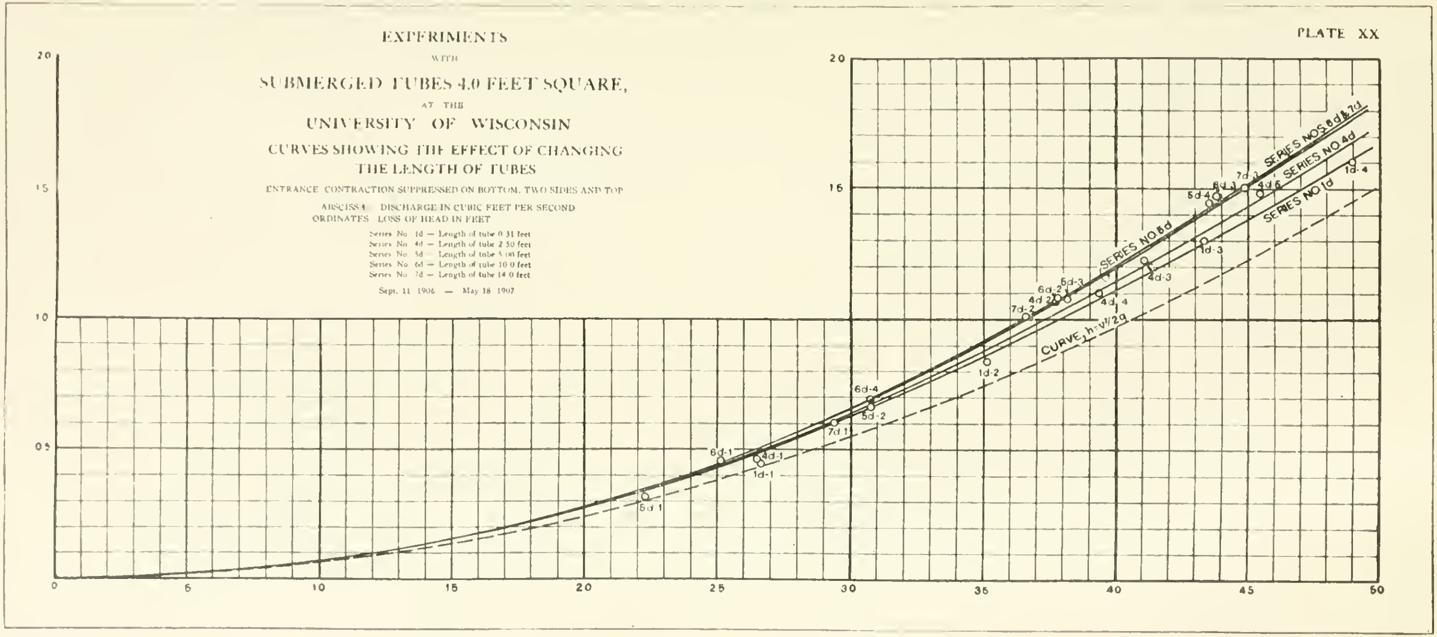

EXPERIMENTS

WITH

SUBMERGED TUBES 4.0 FEET SQUARE,

AT THE

UNIVERSITY OF WISCONSIN

CURVES SHOWING THE EFFECT OF CHANGING
THE LENGTH OF TUBES

ENTRANCE CONTRACTION SUPPRESSED ON BOTTOM, TWO SIDES AND TOP

ABSCISSÆ DISCHARGE IN CUBIC FEET PER SECOND
ORDINATES LOSS OF HEAD IN FEET

Series No 1d — Length of tube 0 31 feet
Series No 4d — Length of tube 2 50 feet
Series No 5d — Length of tube 5 00 feet
Series No 6d — Length of tube 10 0 feet
Series No 7d — Length of tube 14 0 feet

Sept. 11 1906 — May 18 1907

PLATE XXI.

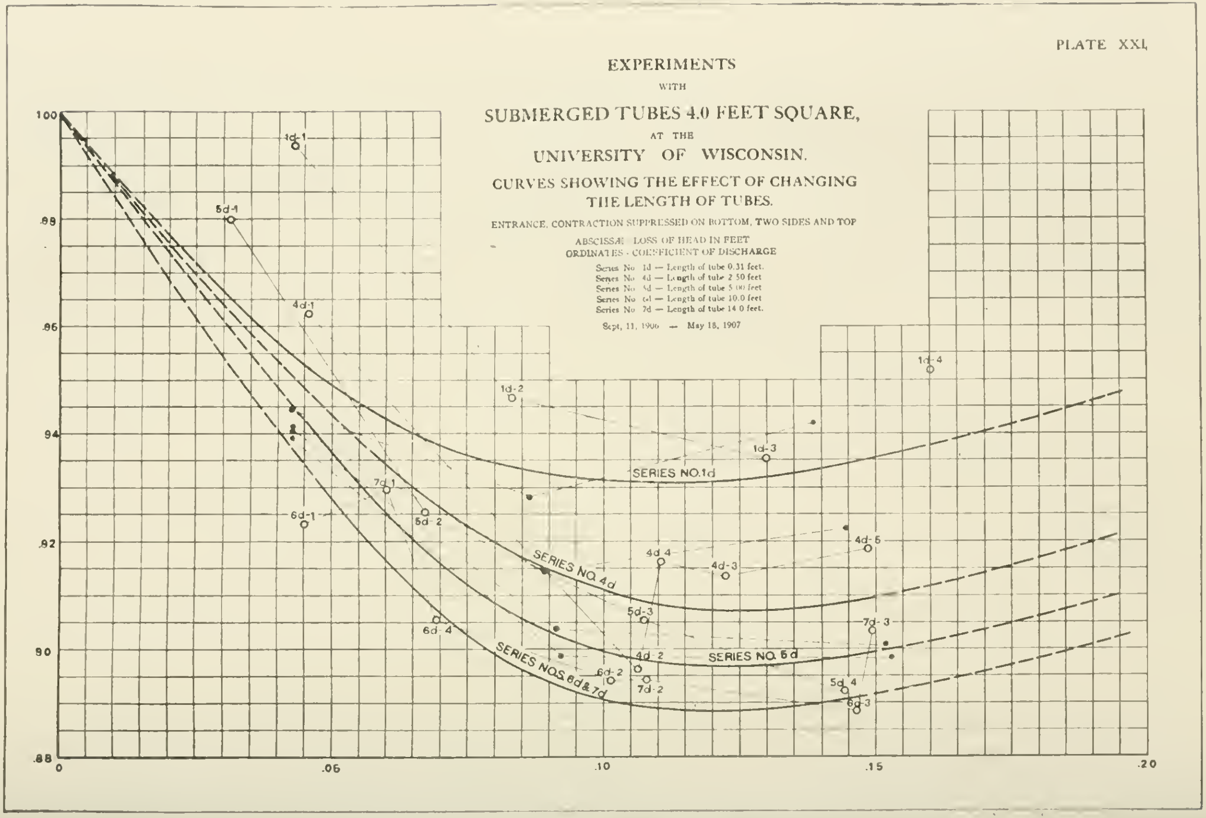

EXPERIMENTS
WITH
SUBMERGED TUBES 4.0 FEET SQUARE,
AT THE
UNIVERSITY OF WISCONSIN.
CURVES SHOWING THE EFFECT OF CHANGING
THE LENGTH OF TUBES.

ENTRANCE, CONTRACTION SUPPRESSED ON BOTTOM, TWO SIDES AND TOP

ABSCISSÆ LOSS OF HEAD IN FEET
ORDINATES - COEFFICIENT OF DISCHARGE

Series No 1d — Length of tube 0.31 feet.
Series No 4d — Length of tube 2.50 feet
Series No 5d — Length of tube 5.00 feet
Series No 6d — Length of tube 10.0 feet
Series No 7d — Length of tube 14.0 feet.

Sept, 11, 1906 — May 18, 1907

PLATE XXII.

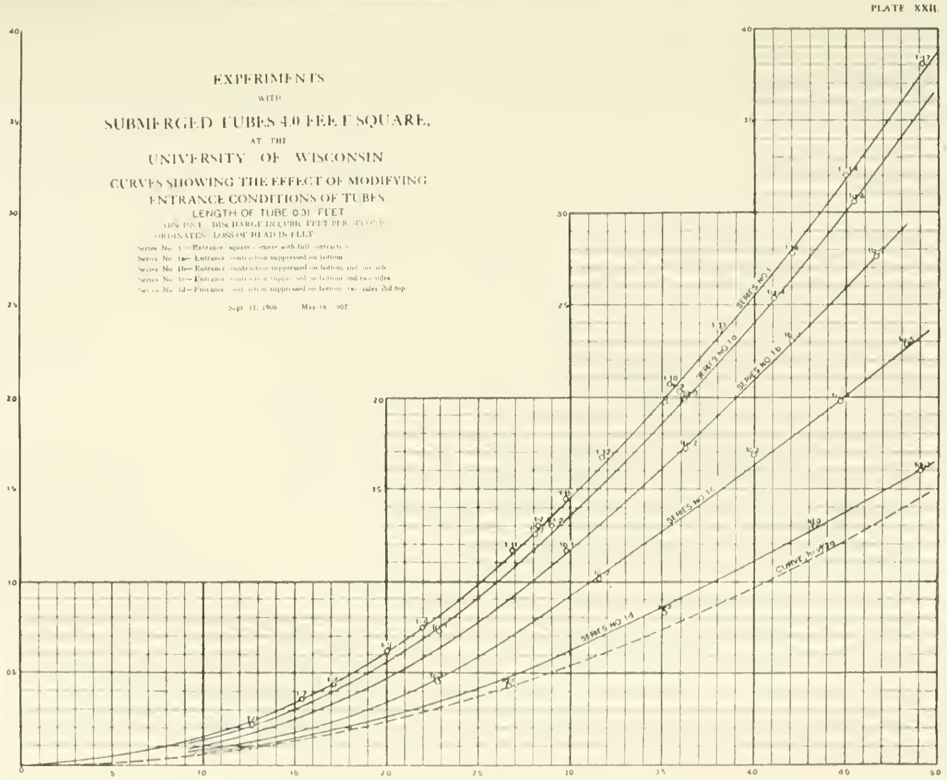
EXPERIMENTS
WITH
SUBMERGED TUBES 4.0 FEET SQUARE,
AT THE
UNIVERSITY OF WISCONSIN
CURVES SHOWING THE EFFECT OF MODIFYING
ENTRANCE CONDITIONS OF TUBES
LENGTH OF TUBE 0.31 FEET
ABSCISSAE—DISCHARGE IN CUBIC FEET PER SECOND
ORDINATES—LOSS OF HEAD IN FEET
Series No. 1—Entrance square corners with full contraction
Series No. 1a—Entrance contraction suppressed on bottom
Series No. 1b—Entrance contraction suppressed on bottom and one side
Series No. 1c—Entrance contraction suppressed on bottom and two sides
Series No. 1d—Entrance contraction suppressed on bottom, two sides and top
Sept. 11, 1906   May 18, 1907
SERIES NO 1
SERIES NO 1a
SERIES NO 1b
SERIES NO 1c
SERIES NO 1d
CURVE h=V²/2g
0
5
10
15
20
25
30
35
40
45
50
05
10
15
20
25
30
35
40

PLATE XXIII.

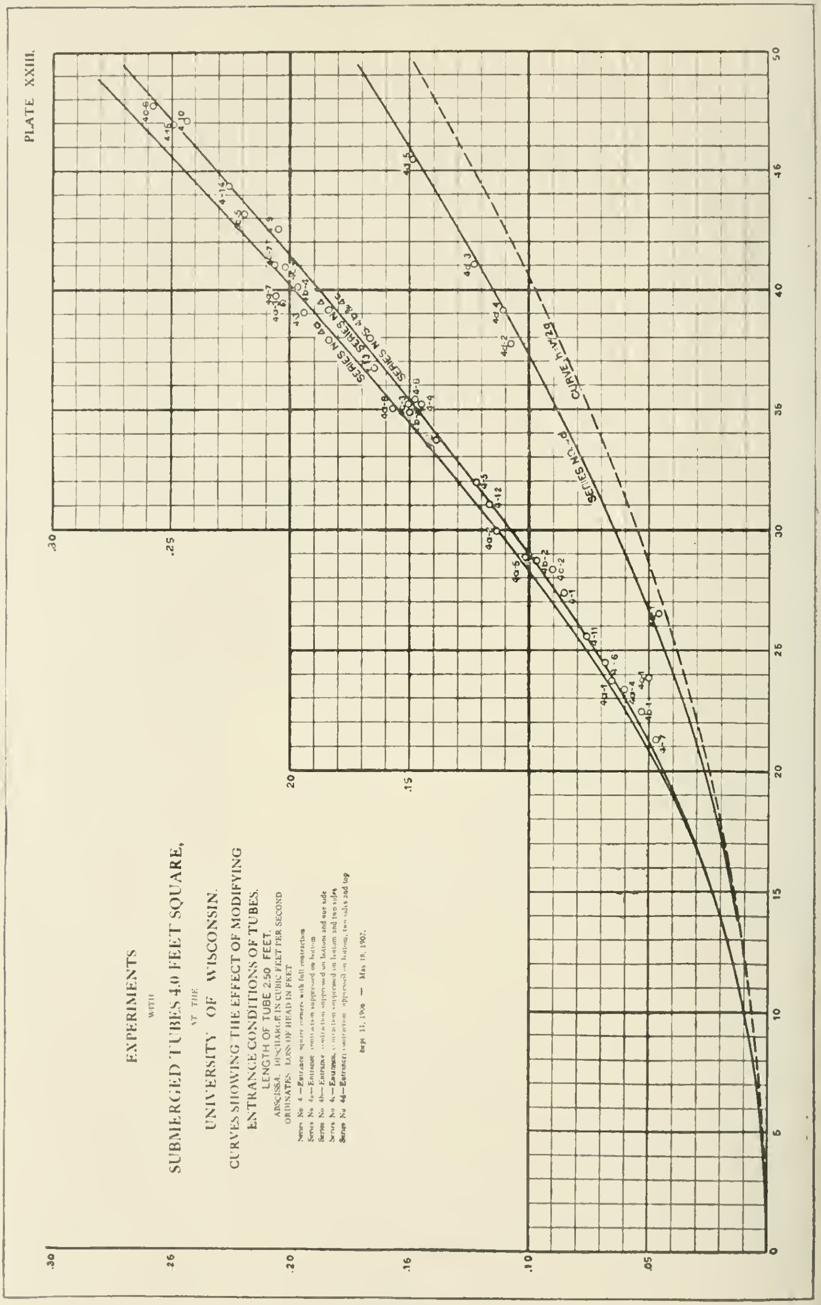
EXPERIMENTS
WITH
SUBMERGED TUBES 4.0 FEET SQUARE,
AT THE
UNIVERSITY OF WISCONSIN.
CURVES SHOWING THE EFFECT OF MODIFYING
ENTRANCE CONDITIONS OF TUBES.
LENGTH OF TUBE 2.50 FEET.
ABSCISSA. DISCHARGE IN CUBIC FEET PER SECOND
ORDINATES. LOSS OF HEAD IN FEET
Series No. 4 —Entrance square corners with full contraction
Series No. 4a—Entrance contraction suppressed on bottom
Series No. 4b—Entrance contraction suppressed on bottom and one side
Series No. 4c—Entrance contraction suppressed on bottom and two sides
Series No. 4d—Entrance contraction suppressed on bottom, two sides and top
Sept. 11, 1906 — May 18, 1907.
SERIES NO 4
SERIES NO 4a
SERIES NOS 4b & 4c
SERIES NO 4d
CURVE h=V²/2g
0
5
10
15
20
25
30
35
40
45
50
.05
.10
.15
.20
.25
.30

PLATE XXIV.

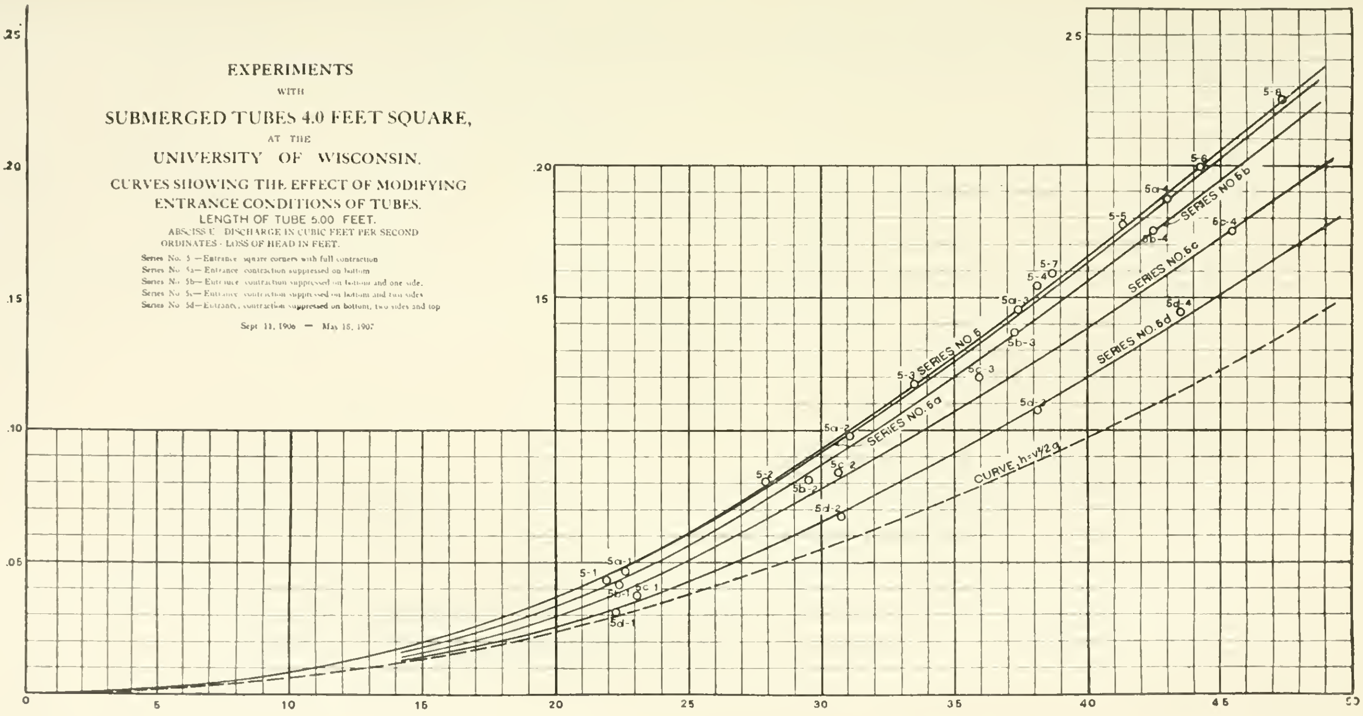
EXPERIMENTS
WITH
SUBMERGED TUBES 4.0 FEET SQUARE,
AT THE
UNIVERSITY OF WISCONSIN.

CURVES SHOWING THE EFFECT OF MODIFYING ENTRANCE CONDITIONS OF TUBES.
LENGTH OF TUBE 5.00 FEET.
ABSCISSÆ - DISCHARGE IN CUBIC FEET PER SECOND
ORDINATES - LOSS OF HEAD IN FEET.

Series No. 5 —Entrance square corners with full contraction
Series No 5a—Entrance contraction suppressed on bottom
Series No 5b—Entrance contraction suppressed on bottom and one side.
Series No 5c—Entrance contraction suppressed on bottom and two sides
Series No 5d—Entrance, contraction suppressed on bottom, two sides and top

Sept 11, 1906 — May 18, 1907

PLATE XXV

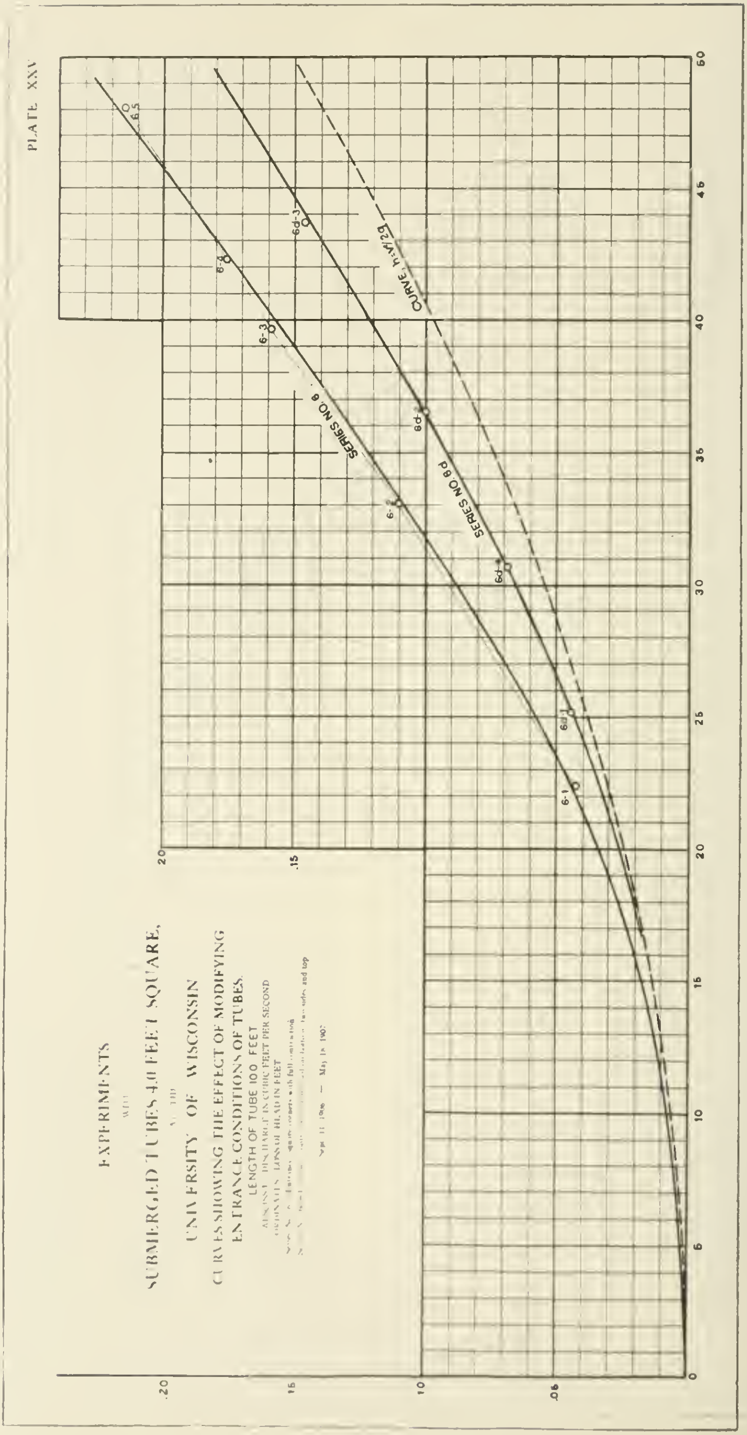
EXPERIMENTS
WITH
SUBMERGED TUBES 4.0 FEET SQUARE,
AT THE
UNIVERSITY OF WISCONSIN
CURVES SHOWING THE EFFECT OF MODIFYING
ENTRANCE CONDITIONS OF TUBES.
LENGTH OF TUBE 100 FEET
ABSCISSAE DISCHARGE IN CUBIC FEET PER SECOND
ORDINATES LOSS OF HEAD IN FEET
SERIES NO. 6
SERIES NO. 6d
CURVE, h=V²/2g
6-1
6-2
6-3
6-4
6-5
6d-1
6d-2
6d-3
6d-4
0
5
10
15
20
25
30
35
40
45
50
.05
.10
.15
.20

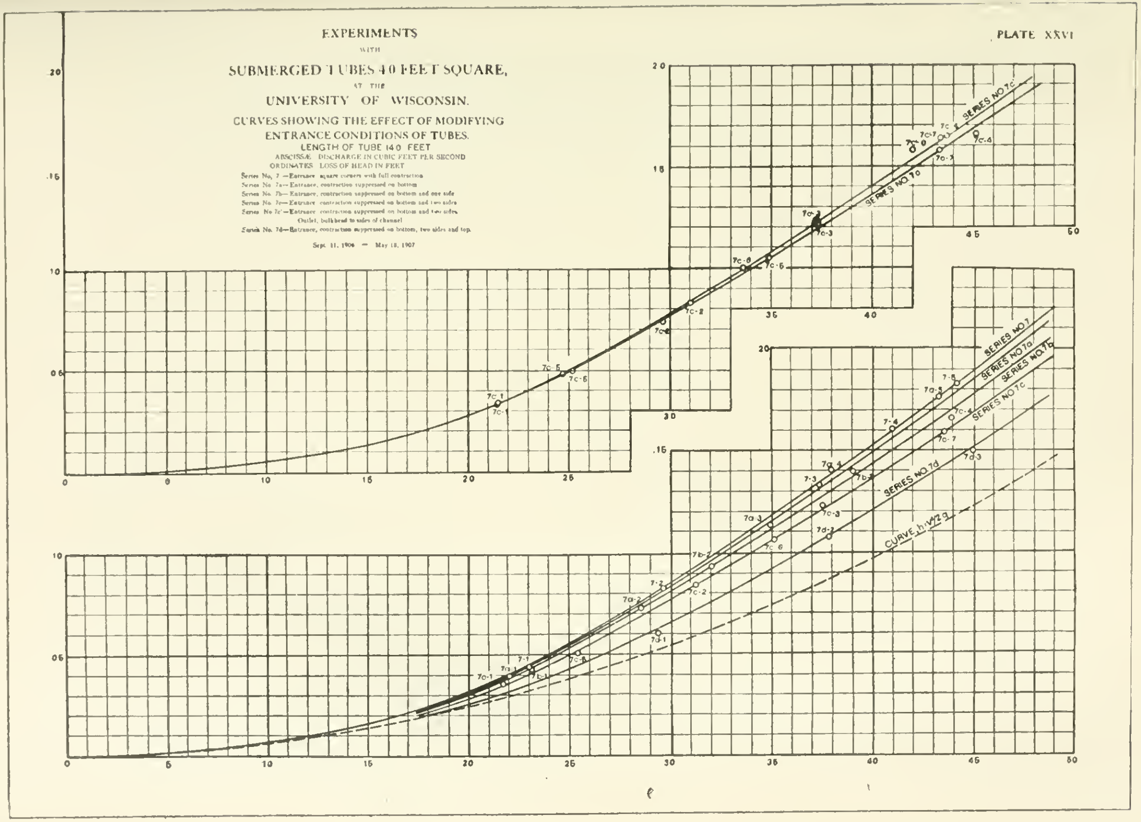
EXPERIMENTS
WITH
SUBMERGED TUBES 4.0 FEET SQUARE,
AT THE
UNIVERSITY OF WISCONSIN.
CURVES SHOWING THE EFFECT OF MODIFYING
ENTRANCE CONDITIONS OF TUBES.
LENGTH OF TUBE 140 FEET
ABSCISSÆ DISCHARGE IN CUBIC FEET PER SECOND
ORDINATES LOSS OF HEAD IN FEET
Series No. 7 —Entrance square corners with full contraction
Series No. 7a—Entrance, contraction suppressed on bottom
Series No. 7b—Entrance, contraction suppressed on bottom and one side
Series No. 7c—Entrance contraction suppressed on bottom and two sides
Series No 7c'—Entrance contraction suppressed on bottom and two sides
Outlet, bulkhead to sides of channel
Series No. 7d—Entrance, contraction suppressed on bottom, two sides and top.
Sept. 11, 1906 — May 18, 1907
PLATE XXVI
SERIES NO 7c
SERIES NO 7c
SERIES NO 7
SERIES NO 7a
SERIES NO 7b
SERIES NO 7c
SERIES NO 7d
CURVE h=V²/2g
7c-1
7c-2
7c-3
7c-4
7c-5
7c-6
7c-7
7c-8
7-1
7-2
7-3
7-4
7-5
7a-1
7a-2
7a-3
7a-4
7a-5
7b-1
7b-2
7b-3
7d-1
7d-2
7d-3
.20
.15
.10
.05
0
5
10
15
20
25
30
35
40
45
50

PLATE XXVII

EXPERIMENTS
WITH
SUBMERGED TUBES 4.0 FEET SQUARE,
AT THE
UNIVERSITY OF WISCONSIN.

CURVES SHOWING THE EFFECT OF MODIFYING
ENTRANCE CONDITIONS OF TUBES.
LENGTH OF TUBE 0.31 FEET.
ABSCISSÆ - LOSS OF HEAD IN FEET
ORDINATES - COEFFICIENT OF DISCHARGE.

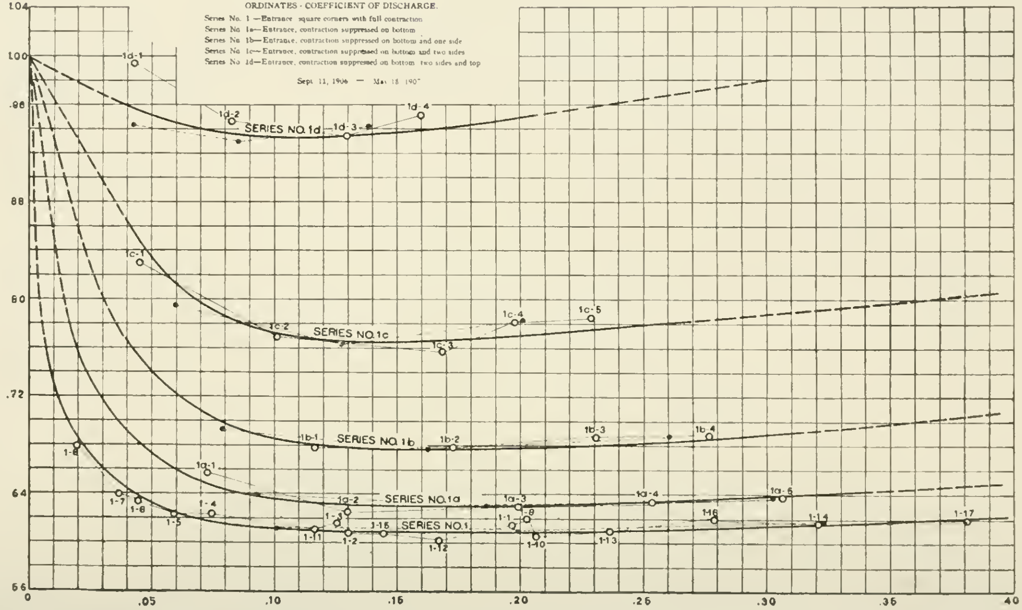

Series No. 1 —Entrance square corners with full contraction
Series No 1a—Entrance, contraction suppressed on bottom
Series No 1b—Entrance, contraction suppressed on bottom and one side
Series No 1c—Entrance, contraction suppressed on bottom and two sides
Series No 1d—Entrance, contraction suppressed on bottom two sides and top

Sept 11, 1906 — May 18 1907

PLATE XXVIII.

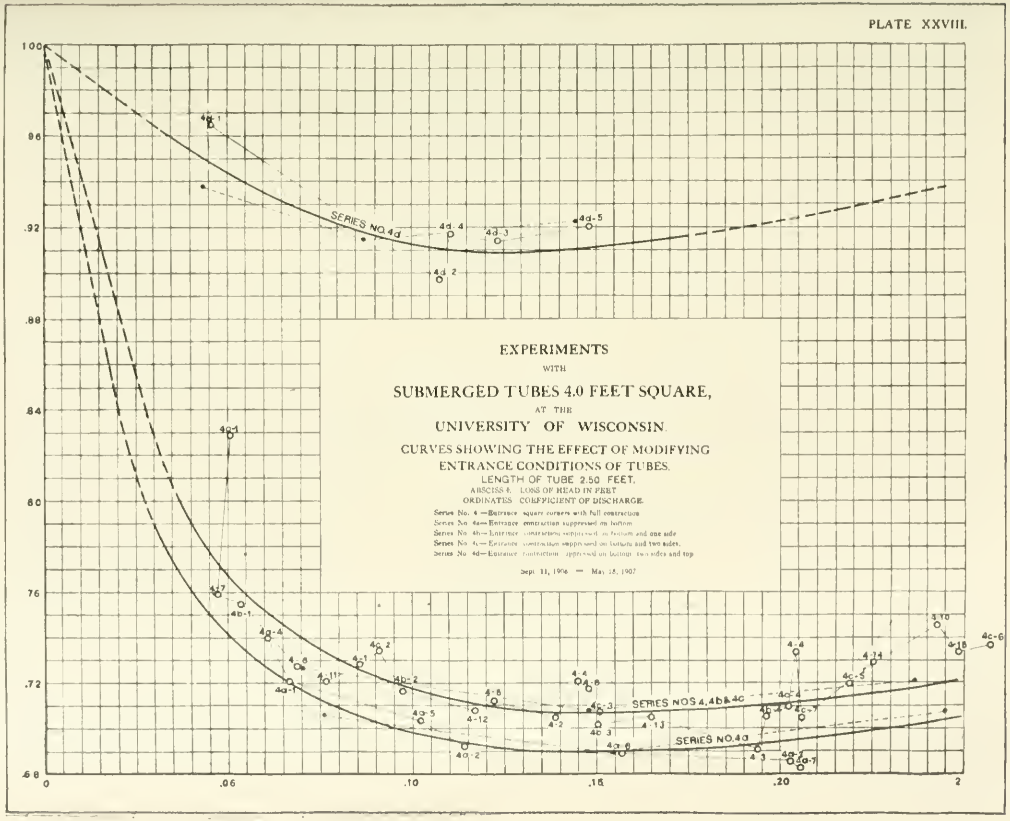

EXPERIMENTS
WITH
SUBMERGED TUBES 4.0 FEET SQUARE,
AT THE
UNIVERSITY OF WISCONSIN.
CURVES SHOWING THE EFFECT OF MODIFYING
ENTRANCE CONDITIONS OF TUBES.
LENGTH OF TUBE 2.50 FEET.
ABSCISSÆ LOSS OF HEAD IN FEET
ORDINATES COEFFICIENT OF DISCHARGE.

Series No. 4 —Entrance square corners with full contraction
Series No 4a—Entrance contraction suppressed on bottom
Series No 4b—Entrance contraction suppressed on bottom and one side
Series No 4c—Entrance contraction suppressed on bottom and two sides.
Series No 4d—Entrance contraction suppressed on bottom two sides and top

Sept 11, 1906 — May 18, 1907

PLATE XXIX.

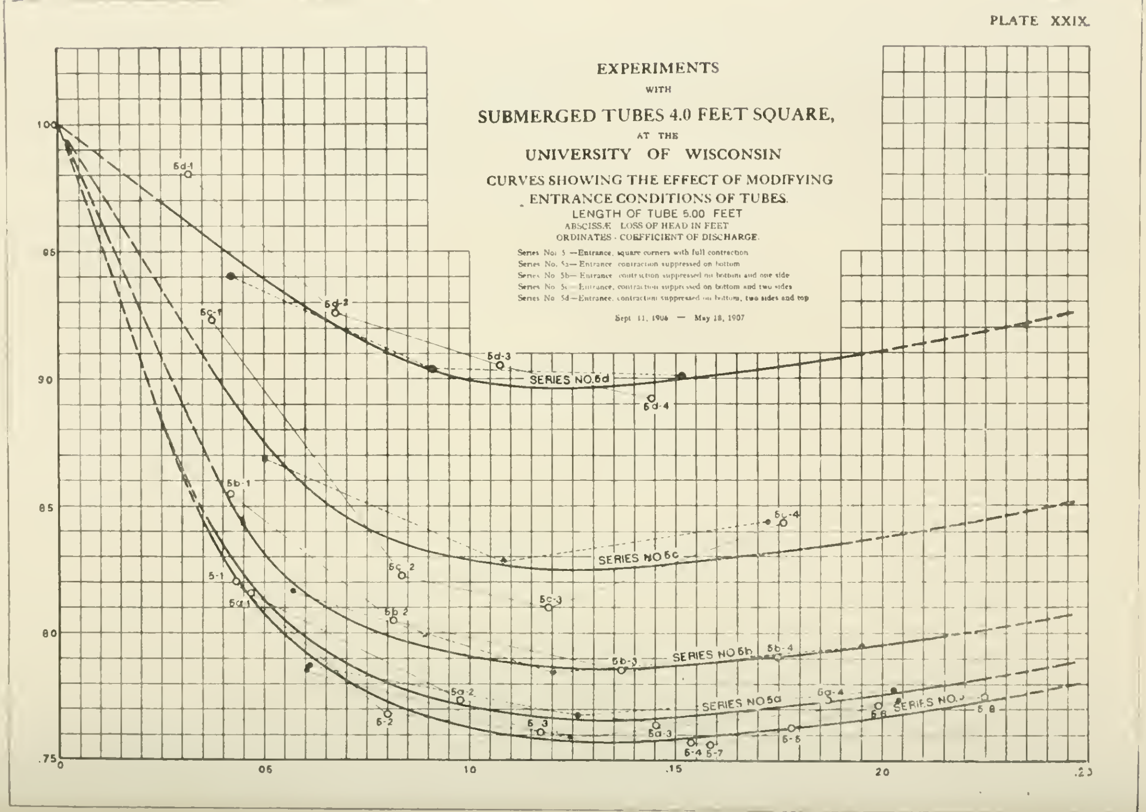

EXPERIMENTS
WITH
SUBMERGED TUBES 4.0 FEET SQUARE,
AT THE
UNIVERSITY OF WISCONSIN
CURVES SHOWING THE EFFECT OF MODIFYING
ENTRANCE CONDITIONS OF TUBES.
LENGTH OF TUBE 5.00 FEET
ABSCISSÆ LOSS OF HEAD IN FEET
ORDINATES · COEFFICIENT OF DISCHARGE.

Series No. 5 —Entrance, square corners with full contraction
Series No. 5a—Entrance contraction suppressed on bottom
Series No 5b—Entrance contraction suppressed on bottom and one side
Series No 5c—Entrance, contraction suppressed on bottom and two sides
Series No 5d—Entrance, contraction suppressed on bottom, two sides and top

Sept 11, 1906 — May 18, 1907

PLATE XXX.

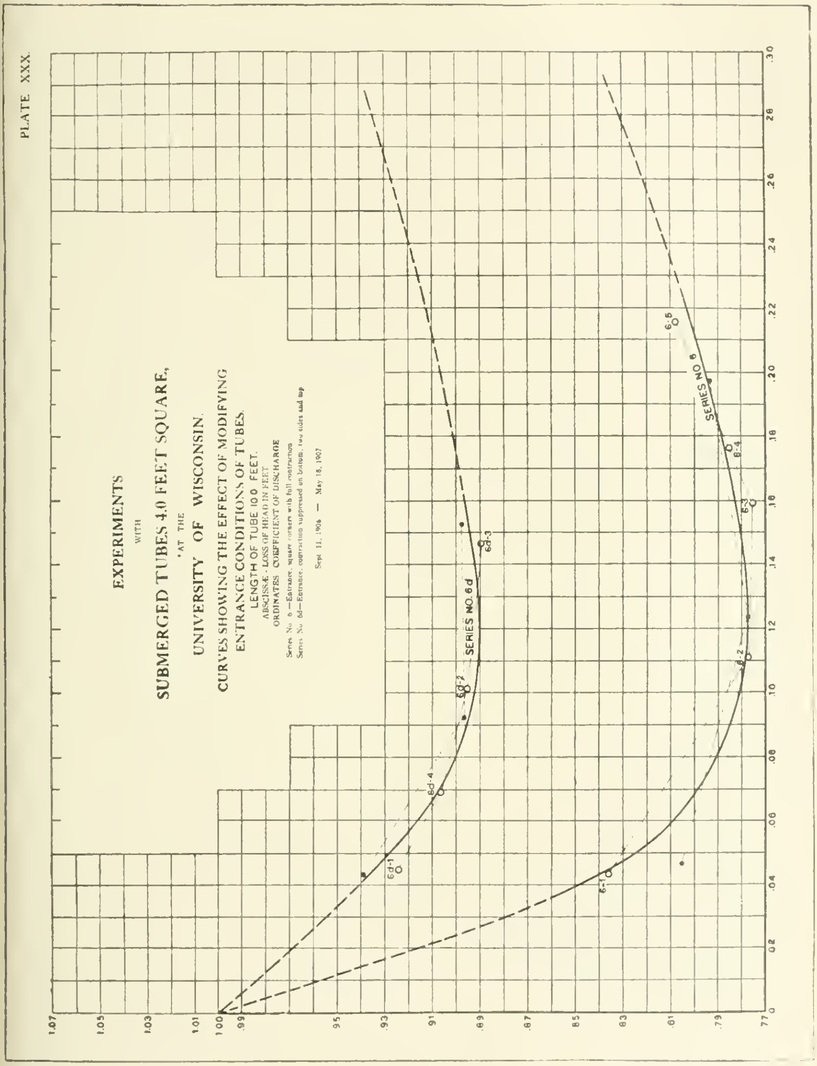
EXPERIMENTS
WITH
SUBMERGED TUBES 4.0 FEET SQUARE,
AT THE
UNIVERSITY OF WISCONSIN.
CURVES SHOWING THE EFFECT OF MODIFYING
ENTRANCE CONDITIONS OF TUBES.
LENGTH OF TUBE 100 FEET.
ABSCISSÆ - LOSS OF HEAD IN FEET
ORDINATES COEFFICIENT OF DISCHARGE
Series No 6 —Entrance, square corners with full contraction
Series No 6d—Entrance, contraction suppressed on bottom, two sides and top
Sept 11, 1906 — May 18, 1907
SERIES NO. 6d
SERIES NO 6
6d-1
6d-4
6d-2
6d-3
6-1
6-2
6-3
6-4
6-5
1.07
1.05
1.03
1.01
1.00
.99
.95
.93
.91
.89
.87
.85
.83
.81
.79
.77
0
.02
.04
.06
.08
.10
.12
.14
.16
.18
.20
.22
.24
.26
.28
.30

PLATE XXXI.

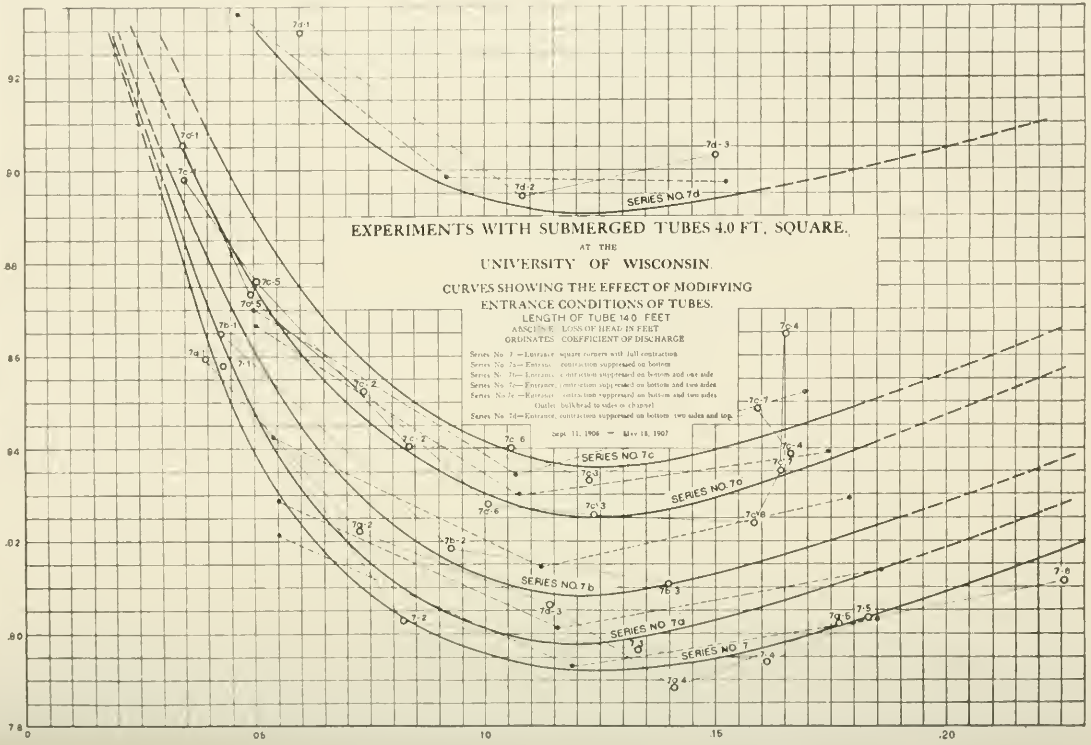

EXPERIMENTS WITH SUBMERGED TUBES 4.0 FT. SQUARE,
AT THE
UNIVERSITY OF WISCONSIN.

CURVES SHOWING THE EFFECT OF MODIFYING
ENTRANCE CONDITIONS OF TUBES.
LENGTH OF TUBE 140 FEET
ABSCISSÆ LOSS OF HEAD IN FEET
ORDINATES COEFFICIENT OF DISCHARGE

Series No 7 —Entrance square corners with full contraction
Series No 7a—Entrance contraction suppressed on bottom
Series No 7b—Entrance contraction suppressed on bottom and one side
Series No 7c—Entrance, contraction suppressed on bottom and two sides
Series No 7e —Entrance contraction suppressed on bottom and two sides
Outlet bulkhead to sides of channel
Series No 7d—Entrance, contraction suppressed on bottom two sides and top.

Sept 11, 1906 — May 18, 1907

TABLE IX.

LOSS OF HEAD FOR FLOW THROUGH HORIZONTAL SUBMERGED TUBE. 4.0 FEET SQUARE, FOR VARIOUS LENGTHS, RATES OF DISCHARGE AND FORMS OF ENTRANCE AND OUTLET.

Rate of discharge, cu. ft. per sec.	Forms of entrance and outlet.	Length of Tube in Feet.						
		.31	0.62	1.25	2.50	5.00	10.0	14.0
		Loss of Head in Feet.						
10	Square corners	.017	.014	.013	.010	.008	.008	.007
	a	.015	....	....	.010	.008	....	.007
	b	.011	....	....	.010	.008	....	.007
	c	.009	......	....	.010	.007	......	.007
	c′	....	....	....	....	....	....	.007
	d	.007	....	....	.007	.007	.007	.007
20	Square corners.	.063	.058	0.55	.044	.038	.034	.032
	a	.057	....	....	.045	.037	....	.031
	b	.048	......	....	.044	.033	....	.030
	c	.035	....	....	.044	.029	....	.029
	c′	....	....	....	....	....	....	.029
	d	.027	....	....	.027	.025	.026	.026
30	Square corners.	.146	.137	.130	.108	.093	.088	.085
	a	.136	....	....	.114	.092	....	.084
	b	.117	....	....	.108	.087	....	.082
	c	.092	....	....	.108	.079	....	.077
	c′	....	....	....	....	....	....	.082
	d	.062	....	....	.064	.065	0.65	.065
40	Square corners	.257	.241	.228	.189	.166	.158	.155
	a	.239	....	....	.200	.164	....	.150
	b	.210	....	....	.189	.157	....	.145
	c	.164	....	....	.189	.140	....	.138
	c′	....	....	....	....	....	....	.140
	d	.112	....	....	.115	.121	.122	.122
50	Square corners.	.389	.359	.335	.277	.247	.233	.227
	a	.370	....	....	.292	.244	....	.221
	b	.312	....	....	.277	.234	....	.213
	c	241	....	....	.277	.210	....	.201
	c′	....	....	....	....	....	....	.217
	d	.166	....	....	.176	.184	.184	.184

TABLE X.

PRELIMINARY VALUES OF THE "COEFFICIENT OF DISCHARGE" FOR FLOW THROUGH HORIZONTAL SUBMERGED TUBE, 4.0 FEET SQUARE, FOR VARIOUS LENGTHS, LOSSES OF HEAD, AND FORMS OF ENTRANCE AND OUTLET; (RESULTS TAKEN FROM CURVES PLATTED ON PLATES XXVII – XXXI) HEAD DUE TO VELOCITY OF APPROACH TO TUBE NEGLECTED IN COMPUTATION.

Loss of head, h, in feet.	Forms of entrance and outlet.	Length of Tube in Feet.						
		0.31	0.62	1.25	2.50	5.00	10.0	14.0
		Values of the Coefficient, C.						
.05	Square corners.	.631	.650	.672	.769	.807	.824	.838
	a	.672	....	....	.742	.810	....	.848
	b	.740	....	....	.769	.832	....	.862
	c	.834	....	....	.769	.875	....	.890
	c′	....	....	....	....	....	....	.875
	d	.948	....	....	.943	.910	.927	.931
.10	Square corners.	.611	.631	.647	.718	.763	.780	.795
	a	.636	....	....	.698	.771	....	.801
	b	.685	....	....	.718	.791	....	.813
	c	.772	....	....	.718	.828	....	.841
	c′	....	....	....	....	....	....	.830
	d	.932	....	....	.911	.899	.892	.893
.15	Square corners.	.609	.628	.644	.708	.758	.779	.794
	a	.630	....	....	.689	.767	....	.803
	b	.677	....	....	.708	.787	....	.814
	c	.765	....	....	.708	.828	....	.839
	c	....	....	....	....	....	....	.829
	d	.936	....	....	.910	.899	.893	.894
.20	Square corners.	.609	.630	.647	.711	.768	.794	.809
	a	.632	....	....	.694	.777	....	.819
	b	.678	....	....	.711	.796	....	.833
	c	.771	....	....	.711	.838	....	.856
	c′	....	....	....	....	....	....	.846
	d	.948	....	....	.923	.911	.906	.905
.25	Square corners.	.610	.634	.652	.720	.782	.812	.828
	a	.634	....	....	.705	.790	....	....
	b	.683	....	....	.720	.809	....	....
	c	.779	....	....	.720	.854	....	....
	c	....	....	....	....	....	....	......
	d	.965	....	....	.938	.928	....	....
.30	Square corners.	.614	.639	.660	.731	.796	.832	.850
	a	.639	....	....	....	....	....	....
	b	.689	....	....	....	....	....	....
	c	.788	....	....	....	....	....	....
	c	....	....	....	....	....	....	....
	d	.980	....	....	....	....	....	....

CONCLUSIONS AND DISCUSSION OF RESULTS OF EXPERIMENTS WITH SUBMERGED TUBES 4.0 FEET SQUARE

For convenience of reference the symbols used in the discussion. are collected and explained.

A =Cross-sectional area of stream in channel of approach.

a = Cross-sectional area of submerged tube.

L =Length of tube.

D =Length of side of square cross-section of tube.

g =Acceleration due to gravity.

Q =Discharge in unit time.

v =Average velocity in cross-sectional area, "a."

h =Effective head on the submerged tube, equal to observed head plus head due to velocity of approach.

h' = Observed head, equal to fall, (gage No. 2–gage No. 3) plus observed fall, gage No. 3 to lower end of tube. (See remarks, page 290.)

h'' =Observed head, equal to fall, (gage No. 2–gage No. 3) plus fall, gage No. 3, to lower end of tube, (as estimated from curve of fall, Plate XVII).

C =Coefficient of Discharge, as computed from the general formula $Q = Ca\sqrt{2gh}$, being equal to the ratio of the average velocity in the cross-sectional area of the tube, to the velocity due the head.

$m = \frac{1}{C^2}$ =Coefficient of loss, in formula, $h = m\frac{v^2}{2g}$.

In the preliminary computations of results of the experiments it was thought best to neglect the head due to the velocity of approach to the tube, for the reason that the cross-sections of the stream in the channel of approach immediately above the entrance and just below the outlet of the tube were practically the same. The observed head, h' or h'', was taken as the difference of level between the surface of water just above the bulkhead containing the submerged tube and the surface of the water at the outlet of the tube. In the computation and platting of curves for determining the results of the experiments, the coefficients of discharge have been computed by using this observed head. Subsequently it was thought best to include the head due to the velocity of approach to the tube, as a part of the actual head on the tube. The water surrounding the outlet of the tube was nearly quiet, there being only slight currents up stream near the surface of the water and near the sides of the channel, and slight currents down stream along the side of the tube. The velocity head from these currents was practically zero. The including of the head resulting from the velocity in the channel of approach seems necessary, therefore, in order to give the effective head or the actual difference of hydrostatic pressure in feet of water between the inlet and outlet of the tube. The velocity of approach varied from about one-quarter of a foot to one-half foot per second and the resulting velocity head from about one thousandth to five thousandths of a foot. The effect on the coefficient of discharge was a variation of from one-third of one per cent. to about one and one-half per cent. The corrected or final values of the coefficients of discharge are given in Table XI, determined by using the formula:

C (computed by using the effective head, h) equals C (computed by using the observed head, h′ or h″) multiplied by

$$\frac{1}{\sqrt{1+\cfrac{1}{\cfrac{C^2\,a^2}{A^2}}}}.$$

TABLE XI.

FINAL VALUE OF THE "COEFFICIENT OF DISCHARGE" FOR FLOW THROUGH HORIZONTAL SUBMERGED TUBE 4.0 FEET SQUARE, FOR VARIOUS LENGTHS, LOSSES OF HEAD AND FORMS OF ENTRANCE AND OUTLET; HEAD DUE TO VELOCITY OF APPROACH TO TUBE CONSIDERED IN COMPUTATION.

Loss of head, h, in feet.	[1]Forms of entrance and outlet.	Length of Tube in Feet.						
		0.31	0.62	1.25	2.50	5.00	10.0	14.0
		Values of the Coefficient, C.						
.05	Square corners	.626	.645	666	.761	.797	.814	.828
	a	.666	......	......	.735	.801	......	.837
	b	.733	......	......	.761	.822	......	.851
	c	.823	......	......	.761	863	......	.877
	e	...	......	......	......	......	......	.873
	d	.934	......	......	.928	.925	.913	917
.10	Square corners.	.608	6.26	.642	.712	.755	.772	.786
	a	631	......	......	.692	.763	......	.792
	b	.679	......	......	.712	.783	......	.804
	c	.764	......	......	.712	.818	...	.831
	e	....	......	......	......	......	......	.820
	d	.919	......	......	.899	.887	.880	.881
.15	Square corners	.605	.624	.639	.702	.751	.771	.786
	a	.626	......	....	.653	.760	......	.795
	b	.672	......	......	.702	.779	......	805
	c	.758	....	......	.702	.8 9	......	.830
	e	......	......	......	......	......	......	.820
	d	.924	......	......	.898	.888	.882	.883
.20	Square corners.	.605	.626	.642	.705	.761	.786	.801
	a	.628	......	......	.689	.770	......	.811
	b	.673	......	......	.705	.788	......	.824
	c	.764	......	......	.705	.829	......	.846
	e	......	......	......	......	......	......	.837
	d	.936	......	......	.911	.900	.895	.894
.25	Square corners.	.606	.630	.648	.714	.775	.804	.820
	a	630	......	......	.709	.783	......	......
	b	.678	......	......	.714	.801	......	......
	c	.772	......	......	.714	.845	......	......
	e	......	......	......	......	......	......	......
	d	.953	...	......	.926	.917	......	......
.30	Square corners.	.610	.635	.656	.725	.789	.824	.841
	a	.635	......	......	......	......	......	......
	b	.684	......	......	......	......	......	......
	c	.781	......	...	......	......	......	......
	e	......	......	......	......	......	......	......
	d	.968	......	......	......	......	......	......

---

[1] See page 322 for explanation of forms of entrance and outlet.

FORMS OF ENTRANCE AND OUTLET USED FOR TUBES.

Square corners:—Entrance: all corners, 90°.
Outlet: tube projecting into water on down stream side of bulkhead.
a:—Entrance: contraction suppressed on bottom.
Outlet: tube projecting into water on down stream side of bulkhead.
b:—Entrance: contraction suppressed on bottom and one side.
Outlet: tube projecting into water on down stream side of bulkhead.
c:—Entrance: contraction suppressed on bottom and two sides.
Outlet: tube projecting into water on down stream side of bulkhead.
c:—Entrance: contraction suppressed on bottom and two sides.
Outlet: square corners with bulkhead to sides of channel preventing the return current along the sides of the tube.
d:—Entrance: contraction suppressed on bottom, two sides and top.
Outlet: tube projecting into water on downstream side of bulkhead.

In order to show more plainly the results of the successive modifications of length of tube and form of entrance and outlet used, Plates XXXII and XXXIII have been arranged from the data given in Table X. Plate XXXII shows the relation of the coefficient of discharge to head for each of the lengths of tube used and for the various entrance conditions. For each length of tube, it is seen that the coefficient of discharge first decreases and then increases as the head increases. The minimum values of C occur for a head on the tube of from 0.10 to 0.15 feet, while the corresponding average velocity through the tube, given by the formula, $v=C\sqrt{2gh}$, varies from 2.0 to 2.5 feet per second, the smaller value being for the entrance condition square corners (see values of v marked on Plate XXXII). The experimental evidence (see also Plates XXVII to XXXI) seems to be that the coefficient of discharge equals unity for a zero head for each of the lengths of tube and forms of entrance used. For the short tube, Series No. 1, length thirty-one hundredths feet with entrance square corners, the coefficient of discharge was very nearly constant for the range of heads five hundredths feet to four-tenths feet, (See Plate XXVII), while for the same tube with the contraction at entrance partially and wholly suppressed, there was a marked increase in the coefficient of discharge as the head increased above fifteen-hundredths feet. The range of head obtainable, however, was not sufficient to determine the slope of the curve for to face p. 322

PLATE XXXII.

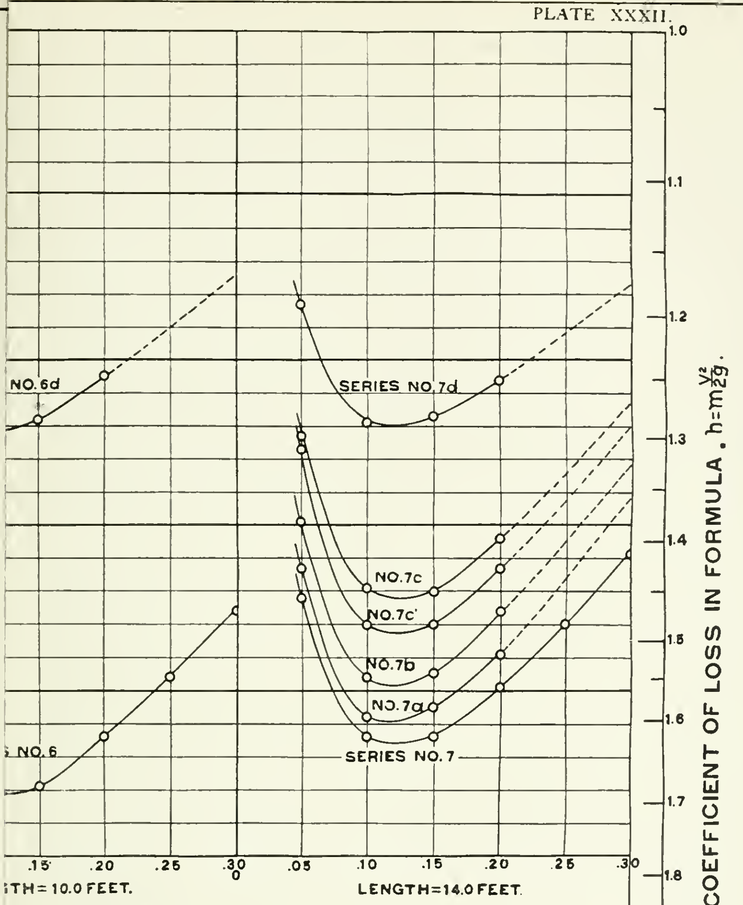

ENTS WITH SUBMERGED TUBES 4.0 FT. SQUARE.

AT THE

UNIVERSITY OF WISCONSIN.

CURVES SHOWING THE EFFECT OF MODIFYING
ENTRANCE CONDITIONS AND OF
CHANGING THE LENGTH OF TUBES.

FORMS OF ENTRANCE AND OUTLET:

SQUARE CORNERS; ENTRANCE, ALL CORNERS 90°.

a ; ENTRANCE, CONTRACTION SUPPRESSED ON BOTTOM.

b ; ENTRANCE, CONTRACTION SUPPRESSED ON BOTTOM AND ONE SIDE.

c ; ENTRANCE, CONTRACTION SUPPRESSED ON BOTTOM AND TWO SIDE.

c' ; ENTRANCE, CONTRACTION SUPPRESSED ON BOTTOM AND TWO SIDES.
OUTLET, SQUARE CORNERS WITH BULKHEAD TO SIDES OF CHANNEL.

d ; ENTRANCE, CONTRACTION SUPPRESSED ON BOTTOM TWO SIDES AND TOP.

Opp. p 322

PLATE XXXII

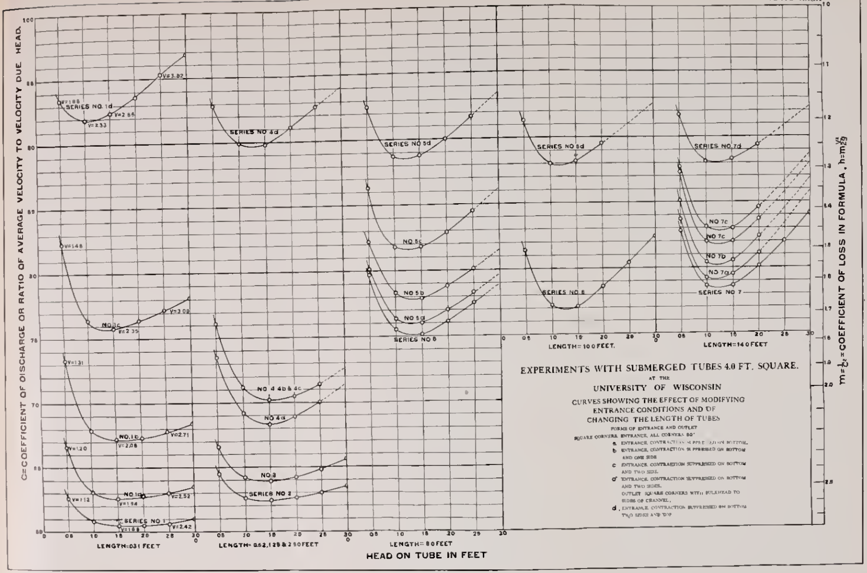

EXPERIMENTS WITH SUBMERGED TUBES 4.0 FT. SQUARE.
AT THE
UNIVERSITY OF WISCONSIN

CURVES SHOWING THE EFFECT OF MODIFYING
ENTRANCE CONDITIONS AND OF
CHANGING THE LENGTH OF TUBES

FORMS OF ENTRANCE AND OUTLET
SQUARE CORNERS. ENTRANCE, ALL CORNERS 90°
a. ENTRANCE, CONTRACTION SUPPRESSED ON BOTTOM.
b. ENTRANCE, CONTRACTION SUPPRESSED ON BOTTOM AND ONE SIDE
c. ENTRANCE, CONTRACTION SUPPRESSED ON BOTTOM AND TWO SIDES.
c′ ENTRANCE, CONTRACTION SUPPRESSED ON BOTTOM AND TWO SIDES.
OUTLET SQUARE CORNERS WITH BULKHEAD TO SIDES OF CHANNEL.
d. ENTRANCE, CONTRACTION SUPPRESSED ON BOTTOM TWO SIDES AND TOP

heads above about three-tenths feet, but it is probable that for heads above this value the curve reverses slightly and gradually becomes horizontal.[1]

The effect of modifying the entrance condition of the tube for the various lengths is shown by the curves marked by the subscripts, a, b, c, c′ and d. Each of the respective forms of approach for the lengths of tubes used, has a minimum value of the coefficient of discharge corresponding to a head on the tube of from one-tenth to fifteen-hundredths of a foot.

Plate XXXIII has been arranged to show the relation of the minimum coefficient of discharge, assumed as occurring at the head of fifteen-hundredths feet, to the length of tube for each of the forms of entrance. For the tubes having entrance square corners, the coefficient of discharge increases at first almost directly as the length of the tube increases, then at a gradually decreasing rate until a length of tube of about three to three and one-half times the side of the square cross-section has been reached. This increase of coefficient of discharge, as the length of tube increases, evidently results from the stream inside the tube acting somewhat as a stream inside of a diverging tube. For a submerged orifice having entrance square corners, the cross-sectional area of the stream gradually decreases, after leaving the plane of the orifice, until some minimum area has been reached. This stream flowing through quiet water tends to communicate motion to the adjoining water and to cause it to move in the same direction. When the submerged orifice takes the form of a submerged tube with the stream flowing through it, the results of the transmission of motion to the adjoining water is to cause a current up stream inside of the tube at its edges, to take the place of the quiet water removed. Figure I shows the results of observations made to locate the up stream currents, with the tubes one and one-quarter and two and one-half feet long. A white string about five inches long was tied to the end of a stick and placed at the outet of the tube; then by means of an incandescent electric light, which was lowered under the water, it was observed that the current was up stream in the portions of the outlet end of the tube, as shown in the figure. The influence of the force of gravity on the shape of the stream was shown by the current being up stream only at the top of the tube. With the tube one and one-quarter feet long and having entrance square corners, the current was up stream throughout the entire width at the top of the tube. The depth in the tube to which the current up stream extended was about one inch at the center and four inches at the corners. As the length of the tube was increased to two and one-half feet, entrance having square corners, the tube became more nearly filled, the current up stream only occurring at the upper corners as shown. The distance marked S, Figure I, decreased from five inches to three inches as the discharge increased from twenty-five to forty-four cubic feet per second. The effective area for discharge at the outlet end of the tube was therefore increased by increasing the length of the tube, and also for any one length by increasing the head on the tube. When the length of the tube became about five feet, the entire outlet end of the tube became filled by the emerging stream and conditions existed for the forming of a region inside the tube having a less hydrostatic pressure than the normal pressure due the depth of water. No readings of this pressure

---

[1] The result of an increase in coefficient of discharge as the head increases and the curve becomes horizontal was obtained by Mr. J. B. Francis in his experiments with submerged tubes and orifices, the orifice having a diameter of one-tenth foot with a curved approach of the cycloidal form. See "Lowell Hydraulic Experiments," page 218, Experiment Nos. 1–18.

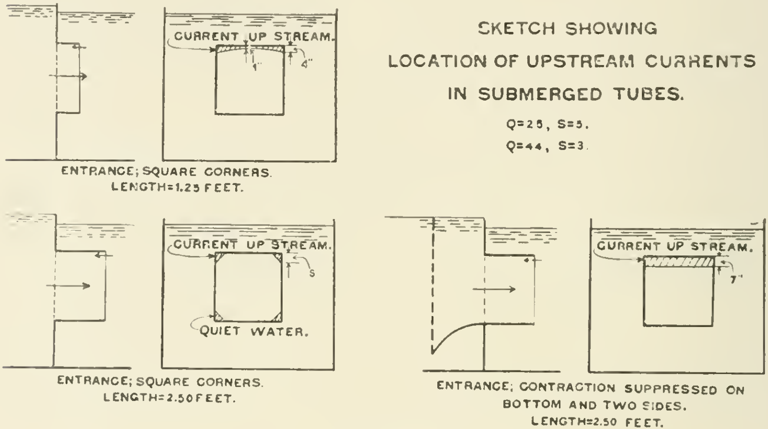

ENTRANCE; SQUARE CORNERS.
LENGTH=1.25 FEET.

ENTRANCE; SQUARE CORNERS.
LENGTH=2.50 FEET.

ENTRANCE; CONTRACTION SUPPRESSED ON BOTTOM AND TWO SIDES.
LENGTH=2.50 FEET.

FIGURE I.

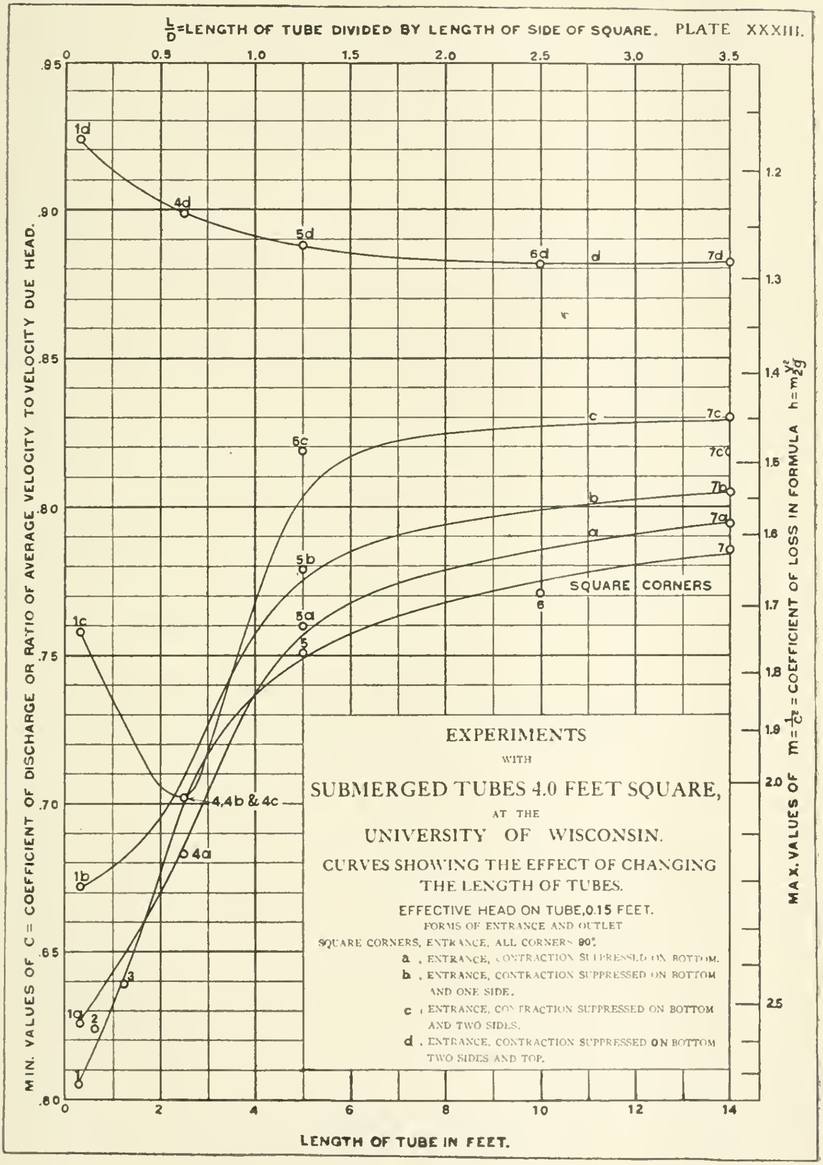
$\frac{L}{D}$=LENGTH OF TUBE DIVIDED BY LENGTH OF SIDE OF SQUARE.
PLATE XXXIII.
0
0.5
1.0
1.5
2.0
2.5
3.0
3.5
.95
.90
.85
.80
.75
.70
.65
.60
1.2
1.3
1.4
1.5
1.6
1.7
1.8
1.9
2.0
2.5
MIN. VALUES OF C = COEFFICIENT OF DISCHARGE OR RATIO OF AVERAGE VELOCITY TO VELOCITY DUE HEAD.
MAX. VALUES OF $m=\frac{1}{c^2}$ = COEFFICIENT OF LOSS IN FORMULA $h=m\frac{v^2}{2g}$
1d
4d
5d
6d
d
7d
c
7c
5c
7c
b
7b
a
7a
7
5b
SQUARE CORNERS
6
1c
5a
5
4,4b & 4c
4a
1b
3
1a
2
1
EXPERIMENTS
WITH
SUBMERGED TUBES 4.0 FEET SQUARE,
AT THE
UNIVERSITY OF WISCONSIN.
CURVES SHOWING THE EFFECT OF CHANGING THE LENGTH OF TUBES.
EFFECTIVE HEAD ON TUBE, 0.15 FEET.
FORMS OF ENTRANCE AND OUTLET
SQUARE CORNERS, ENTRANCE, ALL CORNERS 90°.
a. ENTRANCE, CONTRACTION SUPPRESSED ON BOTTOM.
b. ENTRANCE, CONTRACTION SUPPRESSED ON BOTTOM AND ONE SIDE.
c. ENTRANCE, CONTRACTION SUPPRESSED ON BOTTOM AND TWO SIDES.
d. ENTRANCE, CONTRACTION SUPPRESSED ON BOTTOM TWO SIDES AND TOP.
0
2
4
6
8
10
12
14
LENGTH OF TUBE IN FEET.

inside the tube were taken, but it is intended to do so before completing the final experimental data on submerged tubes. As the length of tube increased to fourteen feet, a point was finally reached where the advantage from the decrease of pressure inside the tube was balanced by the loss from friction along the side of the tube.

For the tubes having the contraction at entrance entirely suppressed (Series Nos. 1d to 7d, Plate XXXIII), the coefficient of discharge decreases gradually as the length of tube increases. This evidently results from the stream entering the tube without contraction, and the friction on the sides of the tube producing an increase in loss of head as the length of the tube increases.

The effect on the coefficient of discharge of the partial suppression of contraction at entrance, Plate XXXIII, was very similar for the short tubes having a length of thirty-one hundredths feet, $\left(\frac{L}{D} = .07\right)$ and for tubes whose length exceeds about five feet $\left(\frac{L}{D} = 1.25\right)$. Table XII shows a comparison of results of the partial suppression of contraction for the tubes

TABLE XII.

COMPARISON OF THE RESULTS OF PARTIAL SUPPRESSION OF CONTRACTION, FOR SHORT AND LONG TUBES; HEAD ON TUBE =0.15 FT.

Forms of entrance.	Length of Tube in Feet.								
	0.31				11.0				
	Value of C. 1	Increase of C. 2	Per cent increase of C. 3	Increase of C. / Max. increase of C. 4	Value of C. 5	Increase of C. 6	Per cent increase of C. 7	Increase of C / Max. increase of C. 8	Col. No. 2 / Col. No. 6. 9
Square corners	.605	....	.....	....	.786	...	..	...	......
a	.626	.021	3	.07	.795	.009	1.7	.09	(2.34)
b	.672	.067	11	.21	.805	.019	2.4	.20	3.52
c	.758	.153	25	.48	.830	.044	5.6	.45	3.47
d	.924	.319	53	1.00	.883	.097	12.0	1.00	3.29
Average of Col. No. 9									3.43

of lengths thirty-one hundredths and fourteen feet. The table shows that for corresponding entrance conditions, the increase of C for the short tubes is about 3.43 times greater than the increase of C for the long tubes. The results of using the entrance conditions, a, b, c and d for these lengths of tubes amount respectively to an increase in the coefficient of discharge of about 8, 21, 46 and 100 per cent. of the increase which would result from having complete suppression of contraction. The numbers, 5.5, 22, 49.5 and 88, vary directly as the square of the number of sides, 1, 2, 3 and 4, on which the contraction was suppressed. The effect of the suppression of contraction, thus varied practically as the square of the number of sides corresponding to the entrance conditions a, b, c and d, on which the suppression of contraction occurred. Taking x as representing the number of sides on which the suppression of contraction occurs, and noting that the order in which the suppression was made is represented by the entrance conditions, a, b, c and d: the following equations give the minimum values of C, corresponding to a head of about 0.15 feet, within about two per cent.:

$$\text{For } \frac{L}{D} \leqq 0.1;\ C = .605 + .019x^2$$

$$\text{For } \frac{L}{D} \geqq 3.0;\ C = 786 + .0055x^2$$

For the tubes having a length of two and one-half feet, the result of partial suppression was to make practically no change in the coefficient of discharge. The results of the experiments showed the coefficient of discharge for Series No. 4a (Plate XXXIII) to be slightly less than the coefficient for Series No. 4. While for Series Nos. 4b and 4c the value remained the same as for Series No. 4. By suppressing the contraction on the remaining side, (Series No. 4d) the coefficient of discharge was greatly increased to the value shown. Figure 1 shows the portion of the outlet end of the tube which was utilized for discharge in the case of Series No. 4c. It seems evident therefore that by suppressing the contraction at the entrance on the bottom edge of the tube, the emerging stream was allowed to fall more rapidly, from the influence of the force of gravity, than when the entrance conditions were square corners, the result being a slight decrease in discharge for a given head.

As yet no experiments have been made with the contraction suppressed on the top, or top and two sides, while the bottom remains square corners, but it is planned to do so before the completion of the experiments with submerged tubes.

In order to determine the loss of head, h, for flow through the submerged tube or orifice, it is necessary to know the coefficient of discharge and solve for h, in the general formula;

$$Q = Ca\sqrt{2gh},$$

then

$$h = \frac{1}{C^2} \cdot \frac{Q^2}{a^2} \cdot \frac{1}{2g}$$

or

$$h = \frac{1}{C^2} \cdot \frac{v^2}{2g} = m \cdot \frac{v^2}{2g}$$

The value of $\frac{1}{C^2}$, termed m, has been called the "Coefficient of Loss." Table XIII gives the values of this coefficient as computed from the values of the coefficient of discharge given in Table XI.

The average values of m. for heads on the tube of from 0.05 to 0.20 feet, are given at the foot of the table. The maximum values of m, occur for a head on the tube of about 0.15 feet. The values of m for the various lengths of tubes, entrance conditions and heads are shown in Plate XXXII; while the maximum values of m for the various lengths of tube and assumed as occurring at the head of fifteen hundredths feet, are shown in Plate XXXIII.

When the submerged tube forms the entrance to a pipe or tube of greater length than $\frac{L}{D}$ = about 3.5, and it is desired to determine the entrance loss from the total loss as given; the outlet loss for the experiments with $\frac{L}{D} = 3.5$, may be safely assumed as $\frac{v^2}{2g}$, and the value of the entrance loss determined from:

$$\text{entrance loss} = \left(\frac{1}{C^2} - 1\right)\frac{v^2}{2g}$$

$$= (m - 1)\frac{v^2}{2g}$$

TABLE XIII.

VALUE OF THE "COEFFICIENT OF LOSS," REPRESENTED BY "m," IN THE FORMULA $h=m\frac{v^2}{2g}$, FOR FLOW THROUGH HORIZONTAL SUBMERGED TUBE, 4.0 FEET SQUARE, FOR VARIOUS LENGTHS, LOSSES OF HEAD AND FORMS OF ENTRANCE AND OUTLET.

Loss of head, h, in feet.	Forms of entrance and outlet.	LENGTH OF TUBE IN FEET.						
		0.31	0.62	1.25	2.50	5.00	10.0	14.0
		Values of the Coefficient, m.						
.05	Square corners.	2.55	2.40	2 25	1.73	1.58	1.51	1.46
	a	2.25	....	....	1.85	1.56	....	1.43
	b	1.86	....	....	1.73	1.48	....	1.38
	c	1.48	....	....	1.73	1.34	....	1.30
	c′	....	....	....	....	....	....	1.31
	d	1.15	....	....	1.16	1.17	1.20	1.19
.10	Square corners.	2.70	2.55	2.42	1.97	1.76	1.68	1.62
	a	2.51	....	....	2.09	1.72	....	1.60
	b	2.17	....	....	1.97	1.63	....	1.55
	c	1.71	....	....	1.97	1.50	....	1.45
	c′	....	....	....	....	....	....	1.49
	d	1.19	....	....	1.24	1.27	1.29	1.29
.15	Square corners.	2.73	2.57	2.45	2.03	1.77	1.68	1.62
	a	2.55	....	....	2.14	1.73	....	1.58
	b	2.22	....	....	2.03	1.65	....	1.54
	c	1.74	....	....	2.03	1.49	....	1.45
	c′	....	....	....	....	....	....	1.49
	d	1.17	....	....	1.24	1.27	1.29	1.28
.20	Square corners.	2.73	2.55	2.42	2.01	1.73	1.62	1.56
	a	2.54	....	....	2.11	1 69	....	1.52
	b	2.21	....	....	2.01	1.61	....	1.47
	c	1.71	....	....	2,01	1.45	....	1.40
	c′	....	....	....	....	....	....	1.43
	d	1.14	....	....	1.21	1.24	1.25	1.25
.25	Square corners.	2.72	2.52	2.38	1.96	1.66	1.55	1.49
	a	2.52	....	....	2.04	1.63	....	....
	b	2.18	....	....	1.96	1.56	....	....
	c	1.68	....	....	1.96	1.40	....	....
	c′	....	....	....	....	....	....	....
	d	1.10	....	....	1.17	1.19	....	....
.30	Square corners.	2.69	2.48	2.38	1.90	1.61	1.47	1.41
	a	2.48	....	....	....	....	....	....
	b	2.14	....	....	....	....	....	....
	c	1.64	....	....	....	....	....	....
	c′	....	....	....	....	....	....	....
	d	1.06	....	....	....	....	....	....
Average for heads .05 to .20	Square corners.	2.68	2.52	2.38	1 94	1.71	1.62	1.56
	a	2.46	....	....	2.05	1.68	....	1.53
	b	2.12	....	....	1.91	1.59	....	1.48
	c	1.66	....	....	1.94	1.44	....	1.40
	c′	....	....	....	....	....	....	1.43
	d	1.16	....	....	1.21	1.24	1.26	1.25

Using the maximum values of m, for length of tube 14.0 feet, corresponding to the head on the tube of 0.15 feet, and noting that m for outlet condition, c′, was greater than m for inlet and outlet condition. c, by the amount of 0.04, the following values for the entrance loss are obtained:

Entrance loss; square corners ....0.66 $\frac{v^2}{2g}$

Entrance loss; contraction suppressed on bottom..0.62 $\frac{v^2}{2g}$

Entrance loss; contraction suppressed on bottom and one side ....0.58 $\frac{v^2}{2g}$

Entrance loss; contraction suppressed on bottom and two sides ....0.49 $\frac{v^2}{2g}$

Entrance loss; contraction suppressed on bottom, two sides and top..........................0.32 $\frac{v^2}{2g}$

The values given above for the entrance loss include the frictional loss in a length of tube equal to 3.5D. This frictional loss cannot be stated in the case of the tubes with entrance conditions a, b and c. In the case of the tube, with entrance condition d, contraction fully suppressed, the data show the frictional loss to be about 0.11 $\frac{v^2}{2g}$, leaving the entrance loss alone as equal to 0.21 $\frac{v^2}{2g}$.

As the head on the tube increases above fifteen hundredths feet, the coefficient of loss decreases. For a head of about three-tenths feet, the entrance loss (including friction in length equal to 3.5 D) for condition square corners, equals about 0.45 $\frac{v^2}{2g}$. For the tube having contraction at entrance entirely suppressed, the entrance loss alone equals about 0.10 $\frac{v^2}{2g}$.

The longitudinal profile of the water surface may be approximately traced from the data giving elevations of water surface at the various gages (see Table VII). At the outlet end of the tubes of ten and fourteen feet length, there was a noticeable lowering of the water surface below the normal level, the amount

PLATE XXXIV.

DIAGRAM

FOR THE

GRAPHICAL SOLUTION OF THE EQUATIONS

$Q = Ca\sqrt{2gh}$ & $Q = av$.

FOR

SUBMERGED ORIFICES AND TUBES.

Q = Discharge in cubic feet per second.
C = Coefficient of discharge.
a = Area of cross-section of orifice or tube in square feet.
g = Acceleration due to gravity in feet per second per second
h = Head on orifice or tube in feet.
v = Average velocity in feet per second in cross-sectional area "a"

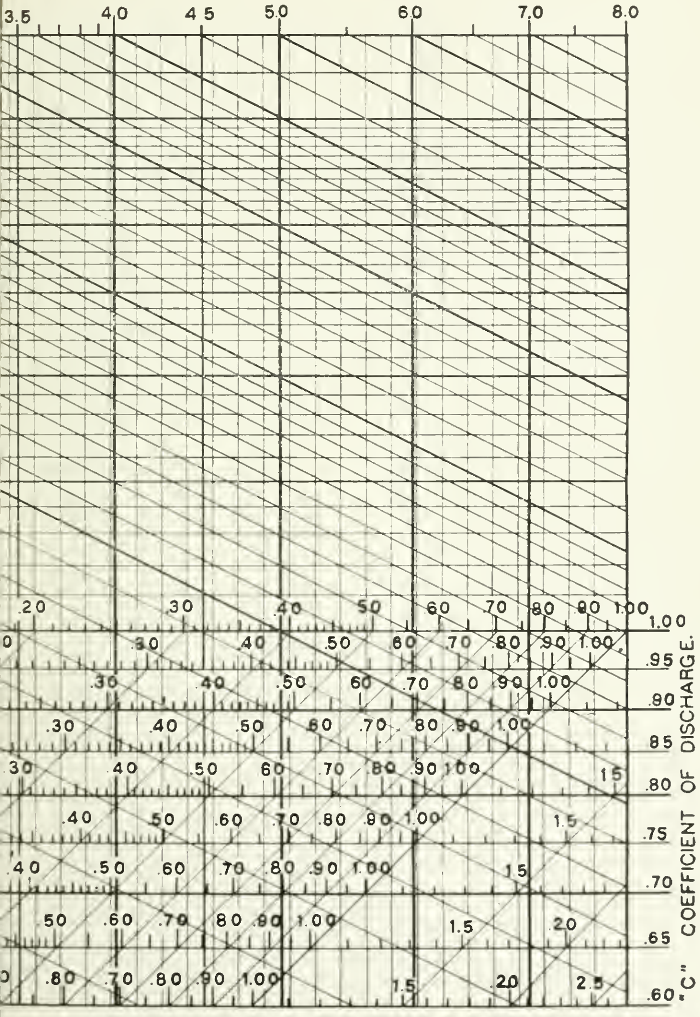

PLATE XXXIV.

DIAGRAM
FOR THE
GRAPHICAL SOLUTION OF THE EQUATIONS
$Q=Ca\sqrt{2gh}$ & $Q=av$
FOR
SUBMERGED ORIFICES AND TUBES

Q = Discharge in cubic feet per second
C = Coefficient of discharge
a = Area of cross-section of orifice or tube in square feet
g = Acceleration due to gravity in feet per sec. per second
h = Head on orifice or tube in feet
v = Average velocity in feet per second in cross-sectional area "a"

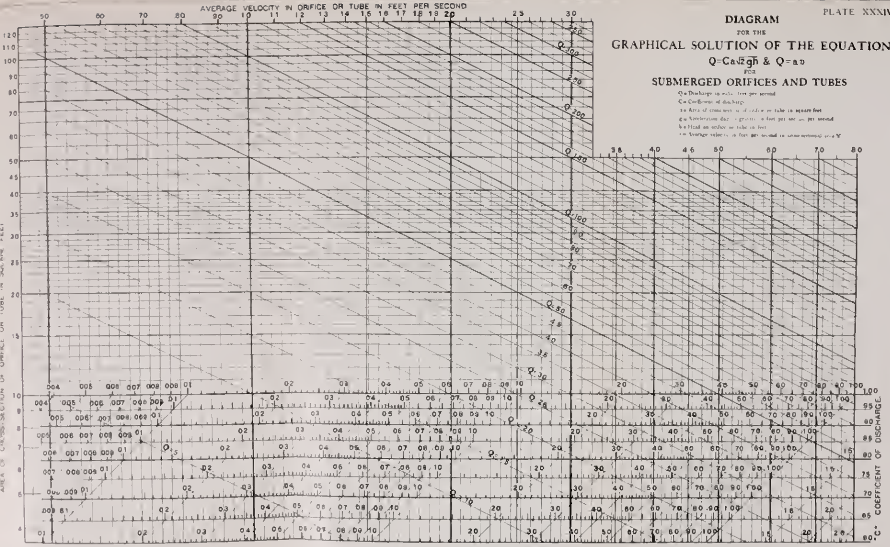

depending on the discharge (see Plate XVII). About fifteen feet below the outlet end of the tube, there was a rise in elevation of the water surface. The average rise as determined from the readings of gages Nos. 5, 6 and 7 varied from zero to a maximum of about five-hundredths of a foot. With the tubes ten and fourteen feet long and a discharge of about fifty cubic feet per second, there was a surface current up stream above the outlet end of the tube of about one foot per second, the current gradually decreasing after passing the end of the tube. The rise in water surface below the outlet end of the tube evidently resulted from partial recovery of the velocity head of the emerging stream. The amount of velocity head recovered depends on the form and size of channel into which the tube discharges. The effective head on the tube, as used for determining C, depended on the elevations of water surfaces at the inlet and outlet ends of the tube, and thus gave a true measure of the difference of pressure producing the flow through the tube.

DIAGRAM FOR FLOW THROUGH SUBMERGED TUBES AND ORIFICES

For convenience in using the coefficients of discharge for determining the loss of head under various conditions the writer has arranged the diagram Plate XXXIV, which is a graphical solution of the equations $Q=Ca\sqrt{2gh}$ and $Q=av$.

The diagram is not connected with the experimental results, but as stated, is simply a graphical solution of the equations given, by means of which values of h may be determined for various assumed values of Q and C.

The ordinates on the left side of the diagram represent values of the cross-sectional areas, a, and vary from four square feet to one hundred and twenty square feet. The abscissae marked on the lower part of the diagram represent values of the head, h, on the submerged tube or orifice. These values of, h, have been plotted on horizontal lines, each line representing values corresponding to a certain value of the coefficient of discharge, C, as shown on the lower right hand part of the diagram. The abscissae marked on the upper horizontal line of the diagram represent values of the average velocity, v, in the cross-sectional area, a, of the orifice or tube. The oblique lines on the upper part of the diagram represent values of the discharge, Q. The diagram is used like an ordinary diagram, having rectangular coordinates, except that the line on which the abscissae, h, are to be read varies in position and depends on the value C.

The diagram may be used in a variety of ways; values of C and h may be assumed, as $C=.75$ and $h=0.10$, the vertical line through $h=0.10$ will intersect lines representing Q, any value of which may be selected, and the corresponding value of, a, determined by the horizontal line through the point of intersection of the vertical line and the line representing Q, as, for $Q=50$, $a=26.3$. By producing the vertical lines to the horizontal line on the upper part of the diagram, values of, v, may be determined, thus for the above example, $v=1.91$. The diagram may also be used by assuming values of, a, and Q, or, v, and Q, and the resultant values of, h, read on the horizontal lines corresponding to some value of C, as shown on the lower right-hand part of the diagram.

The diagram will be found of special service in preliminary study, where it is desired to study the relative effects of changes in a portion of the equation $Q=Ca\sqrt{2gh}$, as the effects on, h, of certain changes in, C, for a given area of cross-section and discharge.

BULLETIN OF THE UNIVERSITY OF WISCONSIN
NO. 252
ENGINEERING SERIES, VOL. 4, NO. 5, PP. 333-412

CURRENT PRACTICE IN STEAM ENGINE DESIGN

BY

OLE N. TROOIEN

WITH FOREWORD BY PROF. H. J. THORKELSON

A THESIS SUBMITTED FOR THE DEGREE OF MECHANICAL ENGINEER,
UNIVERSITY OF WISCONSIN
1907

*Published bi-monthly by authority of law with the approval of the Regents
of the University and entered as second-class matter
at the post office at Madison, Wisconsin*

MADISON, WISCONSIN
OCTOBER, 1908

CONTENTS

PAGE
FOREWORD 337
INTRODUCTION 339
METHOD OF PROCEDURE 340
PISTON ROD 341
CYLINDER 345
  Thickness of cylinder wall 345
  Stud bolts for cylinder covers 347
  Clearance volume of cylinders 347
  Ratio of stroke to cylinder diameter 347
PISTON 350
  Face of piston 350
  Piston rings 355
  Piston speed 355
CROSS HEAD 355
  Crosshead shoes 355
  Crosshead pin 358
CONNECTING RODS 361
CRANK PIN 366
MAIN JOURNALS OF CRANK SHAFT 373
THE FLY WHEEL 376
  Relation of diameter and width to face 384
  Belt surface per I. H. P. 389
  Velocity of wheel rim 394
WEIGHT OF RECIPROCATING PARTS 394
WEIGHT OF ENGINE PER I. H. P 396
RELATION OF AREA OF BED AND I. H. P. 396
CONCLUSION 401
LETTER OF INQUIRY 406

TABLES

Page
FIG. 1.—Piston Rod High Speed Engines 343
FIG. 2.—Piston Rod Corliss Engines 344
Fig. 3.—Thickness of Cylinder Wall 346
FIG. 4.—Diameter of Stud Bolts 348
FIG. 5.—Ratio of Length of Stroke to Diameter of Cylinder in Engines having a speed greater than 200 R. P. M. 349

Page
FIG. 6.—Ratio of Length of Stroke to Diameter of Cylinder in Engines having a speed between 110 and 200 R. P. M. 351
FIG. 7.—Ratio of Length of Stroke to Diameter of Cylinder in Corliss Engines 352
FIG. 8.—Width of Face of Piston High Speed Engines 353
FIG. 9.—Width of Face of Piston Corliss Engines 354
FIG. 10.—Area of Crosshead Shoes 356
FIG. 11.—Crosshead Pin High Speed Engines 359
FIG. 12.—Crosshead Pin Corliss Engines 360
FIG. 13.—Diameter of Crosshead Pin 361
FIG. 14.—Ratio of Height to Breadth in Rectangular Connecting Rods . . . 364
FIG. 15.—Connecting Rods High Speed Engines 365
FIG. 16.—Connecting Rod Corliss Engines 367
FIG. 17.—Crank Pin High Speed Engines 368
FIG. 18.—Crank Pin Corliss Engines 369
FIG. 19.—Relation between Length from Center to Center of Main Journals and Diameter of Crank Pin 371
FIG. 20.—Diameter of Crank Pin High Speed Center Crank Engines 372
FIG. 21.—Diameter of Crank Pin Corliss Engines 374
FIG. 22.—Diameter of Main Journals High Speed Engines 375
FIG. 23.—Diameter of Main Bearing Corliss Engines 377
FIG. 24.—Ratio of Length to Diameter Main Journals High Speed Engines 378
FIG. 25.—Ratio of Length to Diameter of Main Bearing Corliss Engines 379
FIG. 26.—Relation between Projected Area of Main Journals and Area of Cylinder High Speed Engines 380
FIG. 27.—Relation between Projected Area of Main Bearing and Area of Cylinder Corliss Engines 381
FIG. 28.—Weight of Flywheel High Speed Engines having a Capacity less than 175 H. P. 383
FIG. 29.—Weight of Flywheel High Speed Engines Including Capacities up to 400 H. P. 385
FIG. 30.—Weight of Flywheel Corliss Engines 386
FIG. 31.—Relation between Length of Stroke and Diameter of Flywheel High Speed Engines 387
FIG. 32.—Relation between Length of Stroke and Diameter of Flywheel Corliss Engines 388
FIG. 33.—Relation between Face and Diameter of Flywheel High Speed Engines 390
FIG. 34.—Relation between Face and Diameter of Flywheel Corliss Engines 391
FIG. 35.—Sq. Ft. of Belt Surface per I. H. P. High Speed Engines 392
FIG. 36.—Sq. Ft. of Belt Surface per I. H. P. Corliss Engines 393
FIG. 37.—Weight of Reciprocating Parts High Speed Engines 395
FIG. 38.—Weight of Engine per I. H. P. High Speed Engines 397
FIG. 39.—Weight of Engine per I. H. P. Corliss Engines 398
FIG. 40.—Area of Engine bed per I. H. P. High Speed Engines 399
FIG. 41.—Area of Engine Bed per I. H. P. Corliss Engines 400
FIG. 42.—Length of Crank Pin High Speed Engines 404

537

FOREWORD

A rational basis for the design of an implement, tool, engine, or structure of any kind is to be desired above all things. Such a basis is readily secured when the forces acting on all the parts are easily analyzed. There are, however, many structures for which it is difficult to make an analysis complete enough to separate all the forces and determine the effects of each. In such cases many costly and sometimes disastrous experiments form the chief guide in determining a basis for design. These two methods are naturally quite opposed to each other, and in an endeavor to place steam engine design on a better footing and to assist in bringing theoretical analysis and actual practice in closer harmony, the investigation outlined in the thesis here given was undertaken.

Many of the parts of an engine are quite simple. The forces exerted on them can be analyzed and their value and line of action determined with little difficulty. When this is done, a formula for the proper proportion of the parts can be made which will agree very closely with practice. In other cases it is quite evident that the analysis made is not correct as its results differ materially from actual practice. Strictly speaking, there is no conflict between theory and practice. A difference such as indicated shows either a wrong application of theory or theories based on false assumptions. It is hoped that in the near future we may have more satisfactory formulas than those outlined in the discussion following. For example, there is little justification in applying Euler's formula to the piston rod, as the length is so great in proportion to its diameter as to exceed limits for which this formula can be correctly applied.

The charts given should be of assistance to the designer as a check on his calculations, showing when his results are near the minimum, average or maximum values as found from an inspection of a number of designs.

It must be borne in mind that conditions of practice often require duplication of parts in different engines, for example the use of one size of pin or bearing on engines of several different sizes in order to decrease the cost of manufacture. These commercial requirements will account for many of the apparent differences among engine manufacturers.

It is hoped that this little contribution which was prepared under the direction of the late Professor Storm Bull, by Mr. O. N. Trooien as a thesis for the degree of M. E. will prove of assistance to engineers engaged in the design of reciprocating steam engines. If it results in a stimulation of an investigation into modern methods of design and in a more rational basis for proportioning the many intricate parts of a reciprocating steam engine, its purpose will have been accomplished.

H. J. Thorkelson.

CURRENT PRACTICE IN STEAM ENGINE DESIGN

INTRODUCTION

This investigation was undertaken for the purpose of adding a little information to the present knowledge of current practice in proportioning steam engine parts.

A similar investigation was undertaken at Cornell University ten years ago, and by comparing the two results, the trend of progress in the design of steam engines during the last decade may be observed.

Practice in proportioning standard steam engine parts has settled down to certain definite values, which have by long usage in actual operation been found to give good and satisfactory results. This general agreement is found to exist not only in different engines made by one manufacturer but also in engines made by different manufacturers as well. These values are of such a nature that they can readily be expressed in a formula, showing the relation between the more important factors entering the problem of design.

Although these formulas are not always mathematically exact, still they show in an approximate way the relation between the more important variables to be considered in proportioning engine parts. They may be considered as partly rational and partly empirical; rational in the sense that the variables enter in the same manner as in a strictly analytical analysis and empirical in the sense that the constants, instead of being obtained from assumed working strength, bearing pressures, etc., are derived from actual practice and include elements whose values are not accurately known but require consideration which is given by assigning values that have been found to be safe and economical.

The formulas here given at least show the general trend of practice and in some cases will serve as a check upon the "engineering sense" and good judgment of the designers.

METHOD OF PROCEDURE

In order to successfully carry out an examination of this nature, it was first necessary to secure data as to dimensions and weights in actual use which had proven satisfactory in practice. This required a cooperation of the builders of the engines examined, and in order to better secure this cooperation, printed forms (see page 406), containing about 150 questions concerning the different engine parts were sent to the builders of the classes of engines examined. A printed circular stating the plan and object of the undertaking was also included as well as a personal letter.

As was expected the matter of collecting this data presented some difficulty and although all the engine builders communicated with did not see fit to furnish the desired information, still data covering a large number of engines and representing many different builders were secured. This information represented sizes varying from 20 to 400 rated Horse Power and the data secured were first tabulated and separated into classes and subclasses, the two main classes being high speed or quick revolution engines and low speed or slow revolution engines (the latter class being principally the Corliss). Divisions into subclasses were made in the treatment of such parts as the crank pin for center crank and side crank engines, while in dealing with such parts as the piston rod or crosshead pin, no such division was thought necessary.

The following symbols of notation are used in the formulas given:

D = diameter of piston.

A = area of piston.

L = length of stroke.

p = unit steam pressure, taken as 125 lbs. per sq. in. above exhaust as a standard pressure.

H. P.=rated Horse Power.
N=revolutions per minute.
C=a constant.
K=a constant.
d=diameter of unit under consideration..
l=length of unit under consideration.

The commercial point of cut-off taken at 1/4 of the stroke.

All dimensions are given in inches unless otherwise indicated.

Other notation than the above is explained as used.

The general method employed in deriving the various expressions and in plotting the curves shown in the cuts (usually straight lines) may be illustrated by referring to the method used in obtaining the formula for the piston rod diameter and in deriving values of the constants used.

PISTON ROD

It was deemed best in this case to treat the piston rod as a long strut, to be designed for rigidity, inasmuch as any considerable buckling or flexure would be very objectionable, and a slight increase in diameter, due to this method of treatment, would only add to the factor of safety. Euler's formula for long columns was used. It has the form

$$P = K\pi^2 \frac{EI}{L^2}$$

in which E=modulus of elasticity; I=moment of inertia for the section; L=the length of the strut (in this case the free length of the piston rod); and P=the greatest load consistent with stability. The value of the constant K depends upon the end conditions of the strut, as to whether they are fixed or pivoted, free or guided. In this case the piston rod was considered as fixed at one end and free at the other, because some forms of guides are poorly adapted to resist lateral flexure. Here

$$K = 1/4$$

$$\text{or } P = \frac{\pi^2}{4}\frac{EI}{L_1^2}$$

$$L_1 = \text{length of rod}$$

$P=p\frac{\pi}{4}D^2$; $I=\frac{1}{64}\pi d^4$; L_1 (in plotting) was taken equal to the length of the stroke L. This will merely change the constant in the final result. In plotting it was found that

$L_1 = 1.8$ L for high speed engines and $L^2{}_1 = 3.2\ L^2$
$L_1 = 1.4$ L for low speed engines and $L^2{}_1 = 1.96\ L^2$

Assuming p as a standard steam pressure of 125 pounds per square inch and that $E = 30{,}000{,}000$, the Euler formula will take the following form for high speed engines (with $L^2{}_1 = 3.2\ L^2$).

$$125\ \frac{\pi D^2}{4} = \frac{\pi^2 \times 30{,}000{,}000 \times \pi \times d^4}{4 \times 3.2\ L^2 \times 64}$$

$$\text{or } d^4 = \frac{125 \times 64 \times 3.2}{\pi^2 \times 30{,}000{,}000}\ D^2L^2$$

therefore $d = .95\sqrt{DL}$

In a similar manner for low speed engines (taking $L^2{}_1 = 1.96\ L^2$)

$$d = .085\sqrt{DL}.$$

Both of these expressions are for a factor of safety of unity. The equation used in plotting is

$$d = C\sqrt{DL}$$

In plotting the curves for the diameter of the piston rod for these two classes of engines, values of d were used as ordinates and values for $\sqrt{DL}$ for the same engine were used as abscissas.

Points located in this way are indicated by small circles in Figs. 1 and 2, and where two or more points derived from different engines coincide, a double circle is used. All points obtained from the engines of one maker are connected by a conventional line. The broken character of most of these lines is largely accounted for by the fact that sizes usually run in even fractional increments not less than 1/16 in. and are usually more, and it is also due to such commercial considerations as using the same size of frame, pins and rods for different sized cylinders and speeds.

A heavy full line is drawn to represent the average of the observations. Lines are also drawn to embrace the extreme points. From the equations of these lines different values of C are obtained which represent the average, maximum and minimum values of practice, as shown by the engines examined.

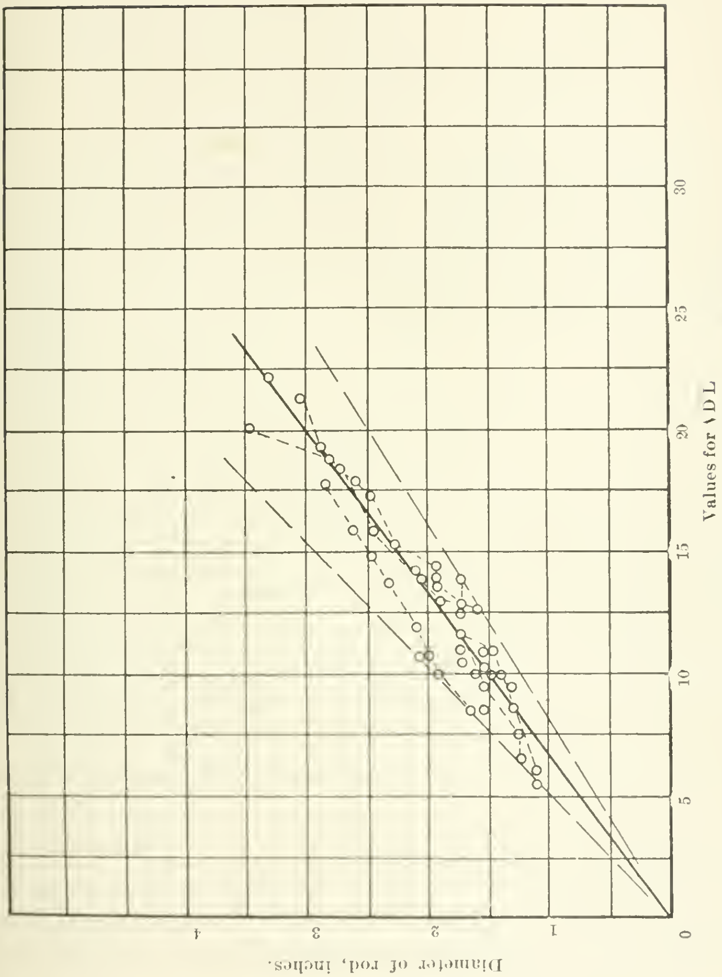

FIG. 1.—PISTON ROD HIGH SPEED ENGINES.

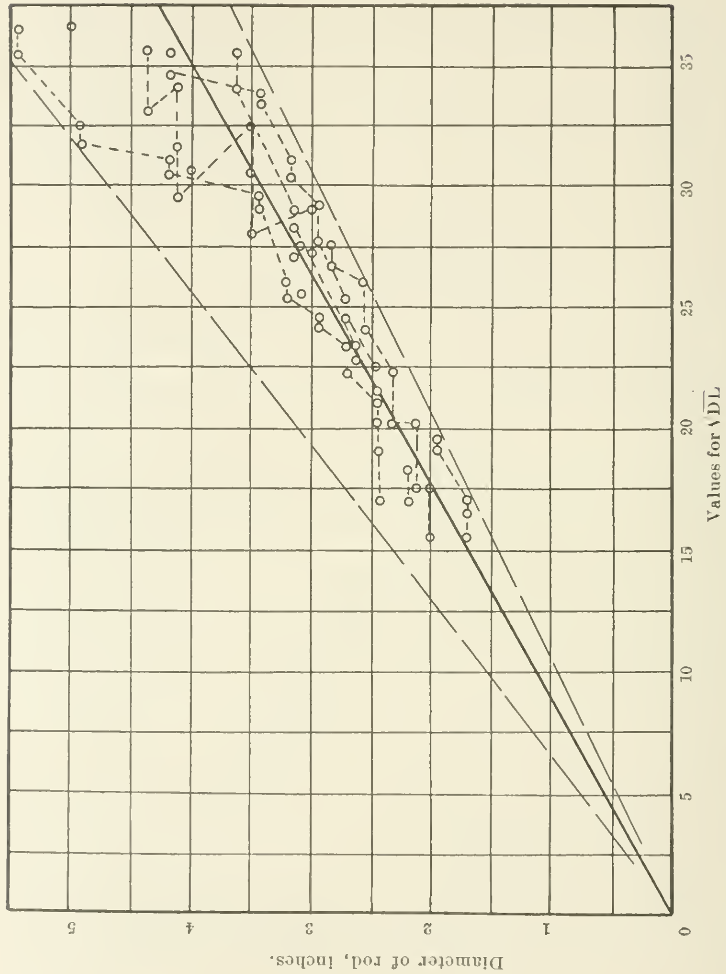

Fig. 2.—Piston Rod Corliss Engines.

Piston rods of high speed engines, Fig. 1:
mean value of $C = .15$
maximum value of $C = .187$
minimum value of $C = .125$
Piston rods of low speed engines, Fig. 2:
mean value of $C = .114$
maximum value of $C = .156$
minimum value of $C = .1$

As the strength of a long strut varies as the fourth power of the diameter, it is necessary to compare the mean value of C, here obtained, with that obtained with a factor of safety of unity in order to get the true factor of safety. This is found to be $\left(\frac{.15}{.096}\right)^4 = 6$ for high speed engines, and $\left(\frac{.114}{.085}\right)^4 = 3.25$ for low speed engines.

CYLINDER

The Thickness of Cylinder Wall, Fig. 3.

Theoretically the thickness of a thin cylindrical shell is proportional only to the pressure which it has to sustain, and the internal diameter of the shell. In the case of the cylinder wall of a steam engine, this thickness is modified somewhat in order to allow for reboring, and in small engines it is increased still more in order to insure good castings.

Several methods of expressing this thickness were tried but none give any better satisfaction than the empirical formula used by Unwin. It has the form

$$t = CD + B$$

where $t =$ the thickness of the cylinder wall; $D =$ diameter of piston; and C and B are constants.

From the engines examined it was found that $B = .28$ in.
and mean value of $C = .054$
maximum value of $C = .072$
minimum value of $C = .035$

No characteristic difference was found to exist between high speed and low speed engines.

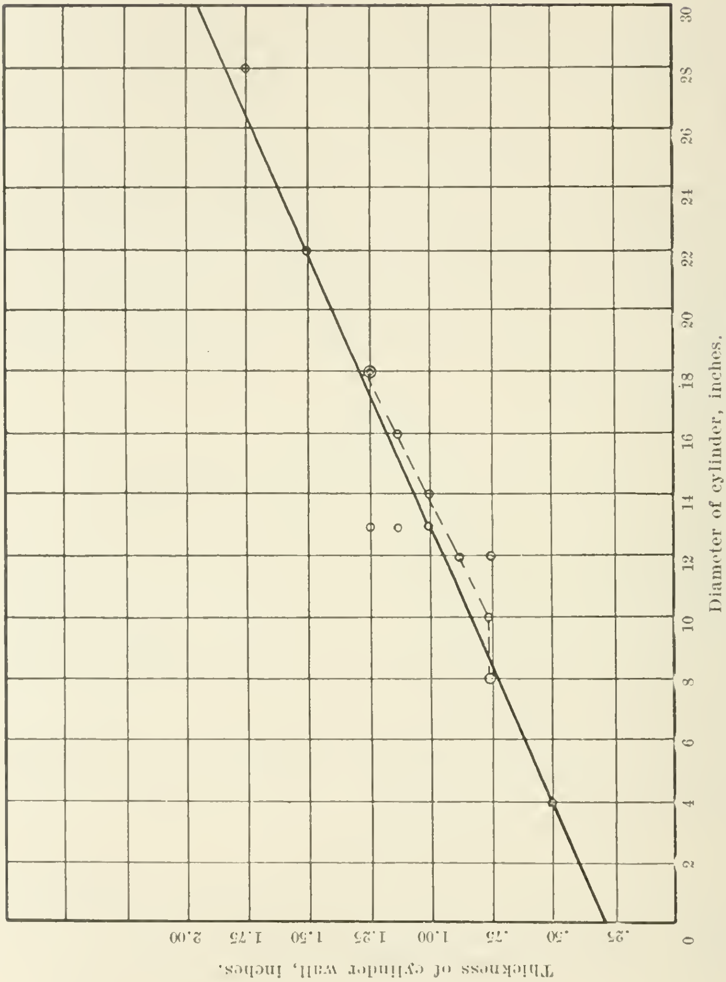

FIG. 3.—THICKNESS OF CYLINDER WALL.

DIAMETER OF STUD BOLTS, FIG. 4.

The diameter of stud bolts used for the cylinder cover may be expressed by the formula

$$d = CD + B$$

when d = diameter of bolts; D = diameter of cylinder; and C and B are constants.

mean value of C = .04 and B = 3/8 in.

With only one exception the smallest diameter of bolts used in the high speed engines was 3/4 in. and in the Corliss engine the smallest value was 1 in.

The mean thickness of cylinder flanges for holding cylinder covers, where these were bolted to cylinder flanges, was found to be 1.12 times the thickness of cylinder wall, for both high speed and Corliss engines.

The thickness of cylinder cover at center seems to vary a great deal, but for the engines examined it may be taken as 2.75 times the thickness of the cylinder wall for high speed engines and 1.12 times the thickness of cylinder wall for Corliss engines.

The number of stud bolts used for cylinder covers may roughly be expressed by N = CD

where N = the number of bolts
mean value of C = .72 for high speed engines
mean value of C = .65 for Corliss engines

The least number of bolts used for any engine was found to be 6.

CLEARANCE VOLUME OF CYLINDER

The clearance volume was found to vary from 5 to 11% in high speed engines and from 2 to 5% in Corliss engines.

RATIO OF STROKE TO CYLINDER DIAMETER

Ratio of length of stroke to diameter of cylinder in engines having a speed greater than 200 revolutions per minute, Fig. 5:

$$L = CD$$

mean value of C = 1.07
maximum value of C = 1.55
minimum value of C = .82

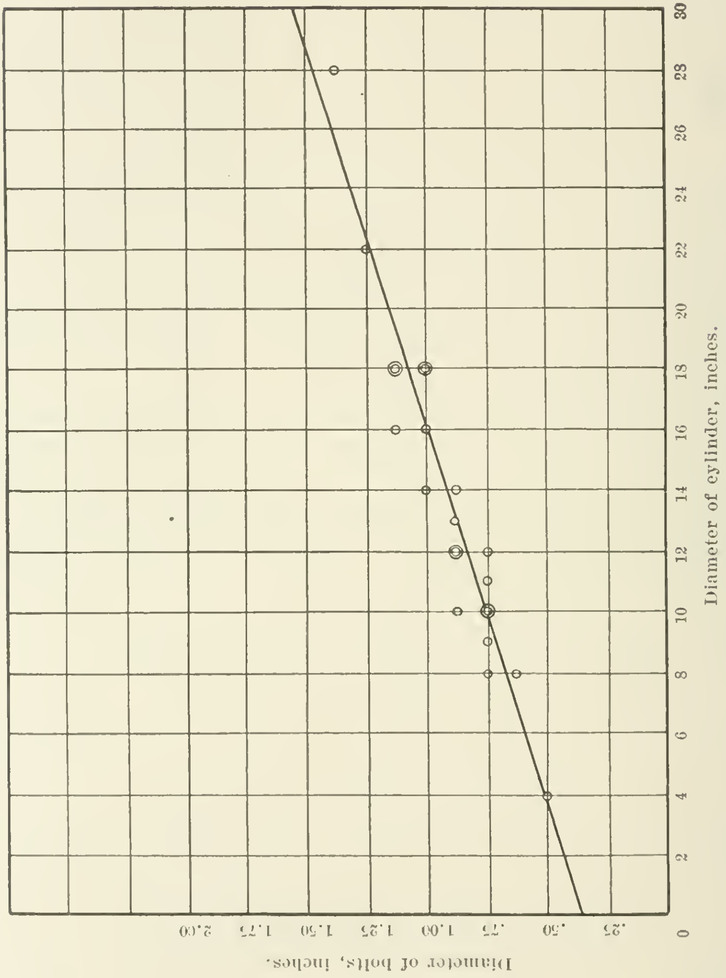

FIG. 4.—DIAMETER OF STUD BOLTS.

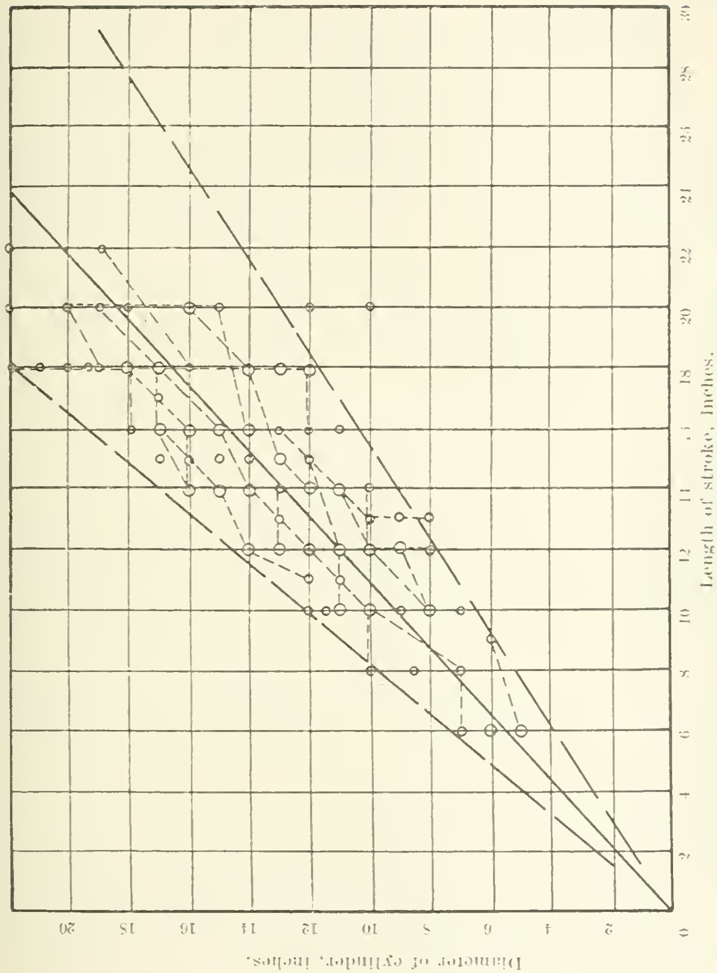

FIG. 5.—RATIO OF LENGTH OF STROKE TO DIAMETER OF CYLINDER IN ENGINES HAVING A SPEED GREATER THAN 200 R. P. M.

Ratio of length of stroke to diameter of cylinder in engines having a speed between 110 and 200 revolutions per minute, Fig. 6:

$$L = CD$$

mean value of $C = 1.36$
maximum value of $C = 1.88$
minimum value of $C = 1.03$

Ratio of length of stroke to diameter of cylinder in engines having a speed less than 110 revolutions per minute. (Corliss engines.) Fig. 7:

$$L = CD + B$$

$$B = 8 \text{ in.}$$

mean value of $C = 1.63$
maximum value of $C = 2.40$
minimum value of $C = 1.15$

PISTON

Face of Piston

The relation existing between the width of the face of piston and the diameter of the piston can be expressed equally well in two ways:

by $w = CD$
or by $w = CD + B$

where w = width of piston; D = diameter of piston; and C and B are constants.

Using $w = CD$

gives for high speed engines, Fig. 8:

mean value of $C = .40$
maximum value of $C = .47$
minimum value of $C = .30$

For Corliss engines, Fig. 9:

mean value of $C = .32$

Using the equation $w = CD + B$

gives for high speed engines, Fig. 8:

$$B = 1 \text{ in.}$$

mean value of $C = .32$
maximum value of $C = .40$
minimum value of $C = .24$

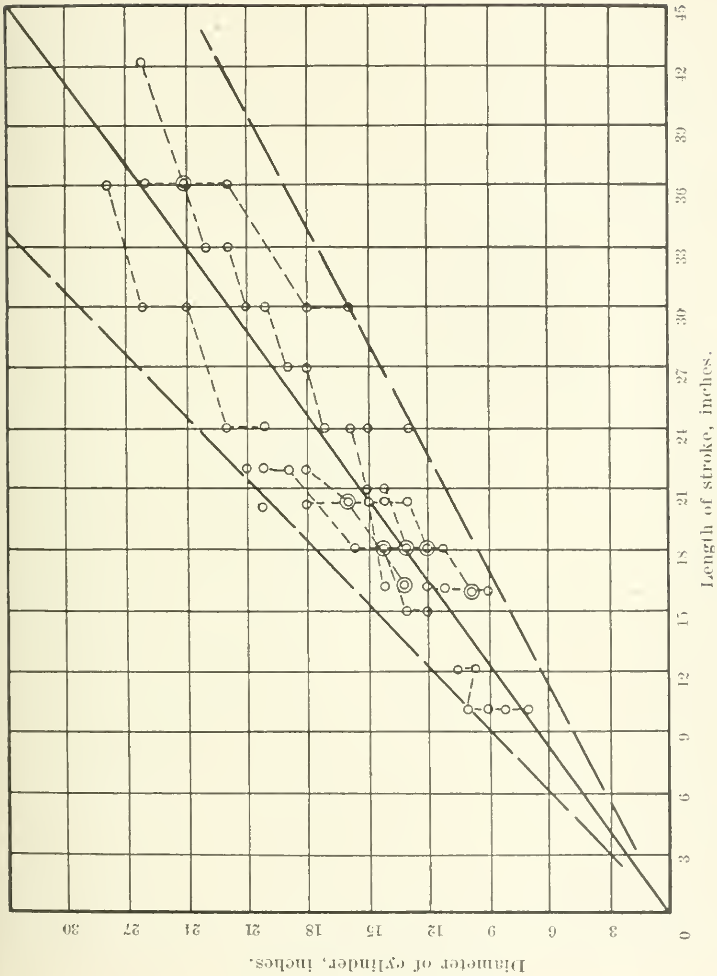

FIG. 6.—RATIO OF LENGTH OF STROKE TO DIAMETER OF CYLINDER IN ENGINES HAVING A SPEED BETWEEN 110 AND 200 R. P. M.

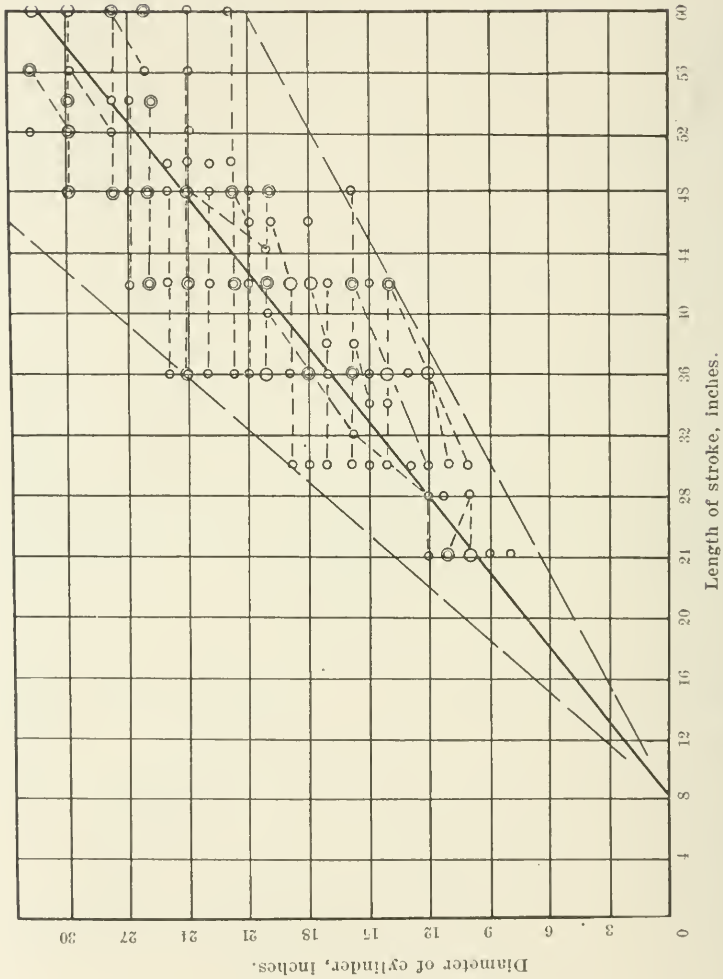

FIG. 7.—RATIO OF LENGTH OF STROKE TO DIAMETER OF CYLINDER IN CORLISS ENGINES.

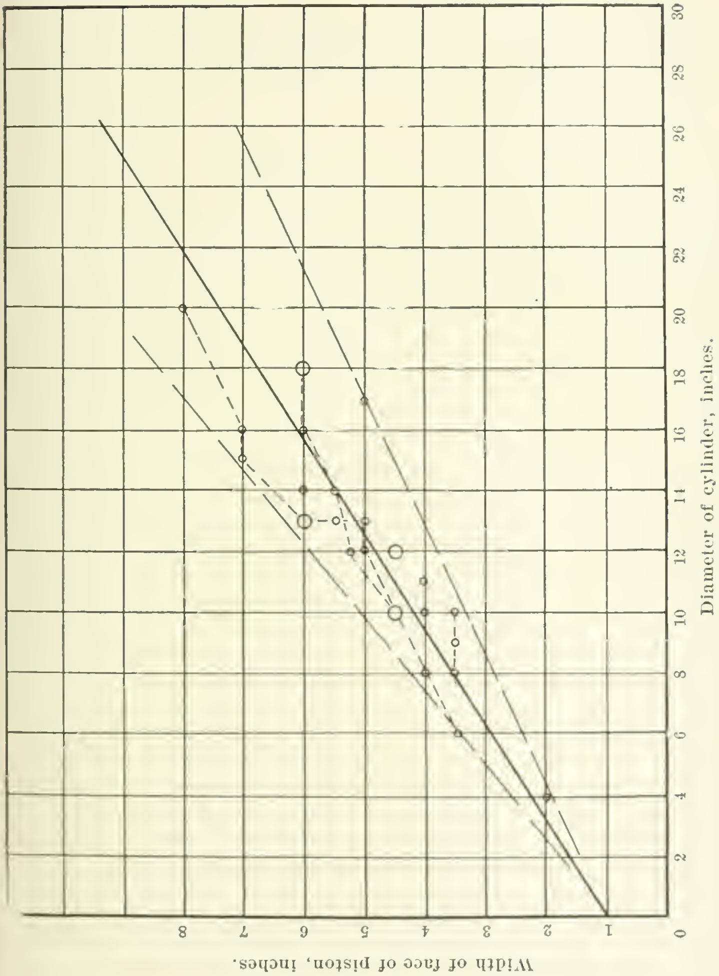

Fig. 8.—Width of Face of Piston High Speed Engines.

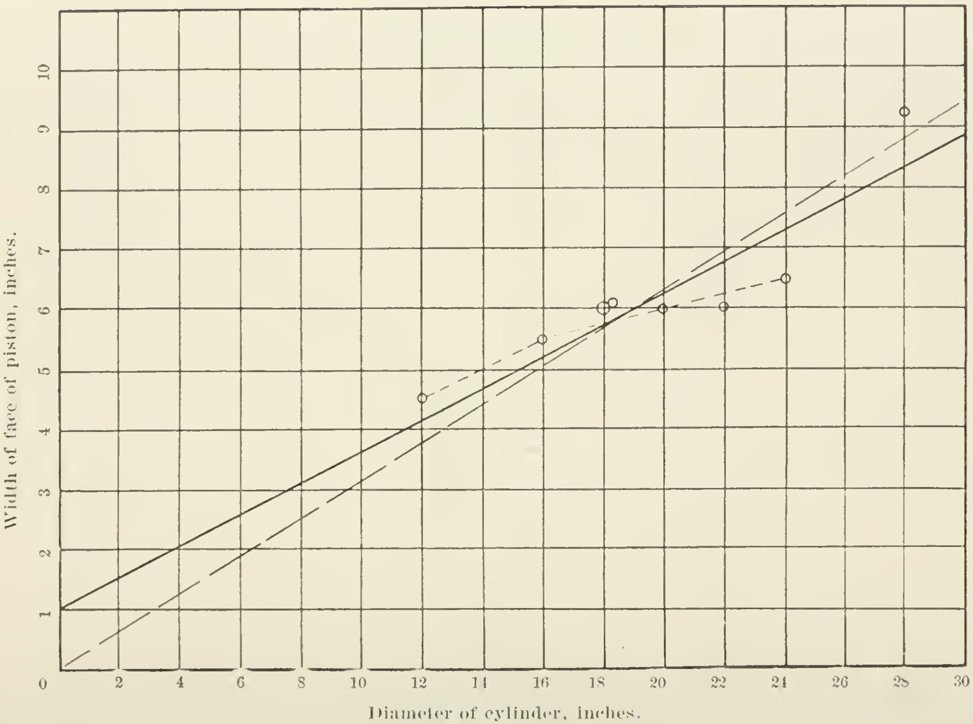

FIG. 9.—WIDTH OF FACE OF PISTON CORLISS ENGINES.

For Corliss engines, Fig. 9:

$$B = 1 \text{ in.}$$

and mean value of $C = .26$

The box type seems to be the prevailing form of piston. The thickness of shell of piston in high speed engines is about .6 of the thickness of cylinder wall, and for Corliss engines this ratio is about .7.

PISTON RINGS

The prevailing number of rings used for the piston is two, and the rings are usually turned to a diameter 1/4 in. larger than the bore of the cylinder.

PISTON SPEED

HIGH SPEED ENGINES

mean piston speed = 605 feet per minute
maximum piston speed = 900 feet per minute
minimum piston speed = 320 feet per minute

CORLISS ENGINES

mean piston speed = 592 feet per minute
maximum piston speed = 800 feet per minute
minimum piston speed = 400 feet per minute.

CROSS HEAD

CROSSHEAD SHOES, FIG. 10

The crosshead shoes are usually designed to withstand a certain unit bearing pressure, and this pressure is necessarily proportional to the pressure on the piston. The area of the crosshead shoes which sustains the vertical component of the force transmitted through the connecting rod may be expressed by the equation

$$a = CA$$

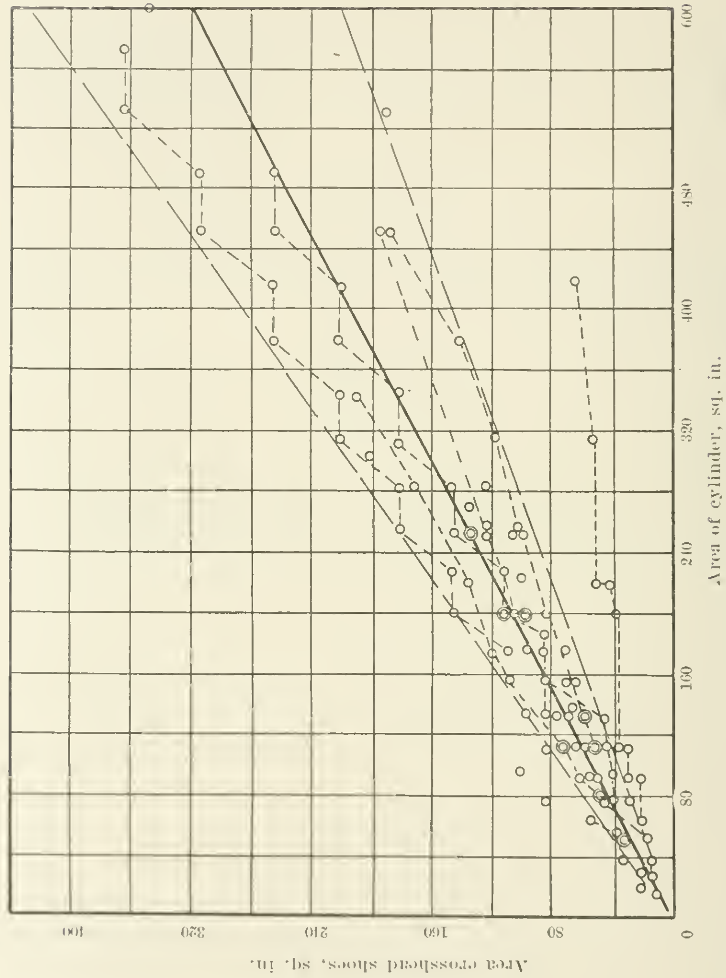

FIG. 10.—AREA OF CROSSHEAD SHOES.

The maximum pressure S on cross head (if the steam follows up for half stroke) is nearly equal to

$$\frac{r}{L_c} \times P = S = sa$$

$$sa = \frac{1}{n} \times pA$$

$$a = \frac{p}{ns} A = CA$$

where S = total pressure on crosshead shoes; s = unit pressure on crosshead shoes; a = area of crosshead shoes; r = length of crank; L_c = length of connecting rod.

The unit pressure on crosshead shoes may be found as follows:

$$sa = \frac{pA}{n}$$

$$s = \frac{pA}{na} = \frac{pA}{nCA} = \frac{125}{nC}$$

$n = \frac{L}{r}$ may be taken as 6 for high speed engines and 5.5 for Corliss engines. The value of C was found to be the same for both the high speed and Corliss engines.

mean value of C = .53, Fig. 10
maximum value of C = .72
minimum value of C = .37

For high speed engines:

mean value of s = 39.5
maximum value of s = 57
minimum value of s = 28

For Corliss engines:

mean value of s = 43
maximum value of s = 61
minimum value of s = 32

While these pressures may seem high, it will be noted that cut-off usually takes place before mid-stroke is reached. If cut-off takes place at 1/4 stroke (which is considered as the commercial point of cut-off in this examination) the steam pressure when at mid-stroke will be about 1/2 of its former value at this point. The earlier point of cut-off will reduce the unit pressures to safe working conditions under actual operation.

CROSSHEAD PIN

Ratio of diameter to length of bearing part of crosshead pin in high speed engines, Fig. 11:

$$l = Cd$$

mean value of $C = 1.25$
maximum value of $C = 1.5$
minimum value of $C = 1.0$

For Corliss engines, Fig. 12:

$$l = Cd$$

mean value of $C = 1.43$
maximum value of $C = 1.9$
minimum value of $C = 1.0$

The crosshead pin may be designed either for strength or for a definite unit bearing pressure on the projected area. For strength the crosshead pin may be treated as a fixed beam, in which case we will have

resisting moment = bending moment or

$$\pi/32\ fd^3 = 1/8\ Pl$$

For high speed engines, mean value of $l = 1.25$ d, then

$$\pi/32\ fd^3 = 1/8\ P \times 5/4\ d$$

$$\text{or } C_1 d^2 = P = pA = p\pi/4\ D^2$$

$$\text{and } d = CD.$$

In treating the crosshead pin for a definite unit bearing pressure on projected area, the following relation may be used.

$$dl = KA$$

as before take $l = 1.25$ d, then

$$1.25\ d^2 = KA = K\pi/4D^2$$

and $d = CD$ as before.

This gives the same final expression for both cases and the equation $d = CD$ is used in plotting. As should be expected no difference was found in the value of C for high speed and Corliss engines.

mean value of $C = .25$, Fig. 13
maximum value of $C = .28$
minimum value of $C = .17$

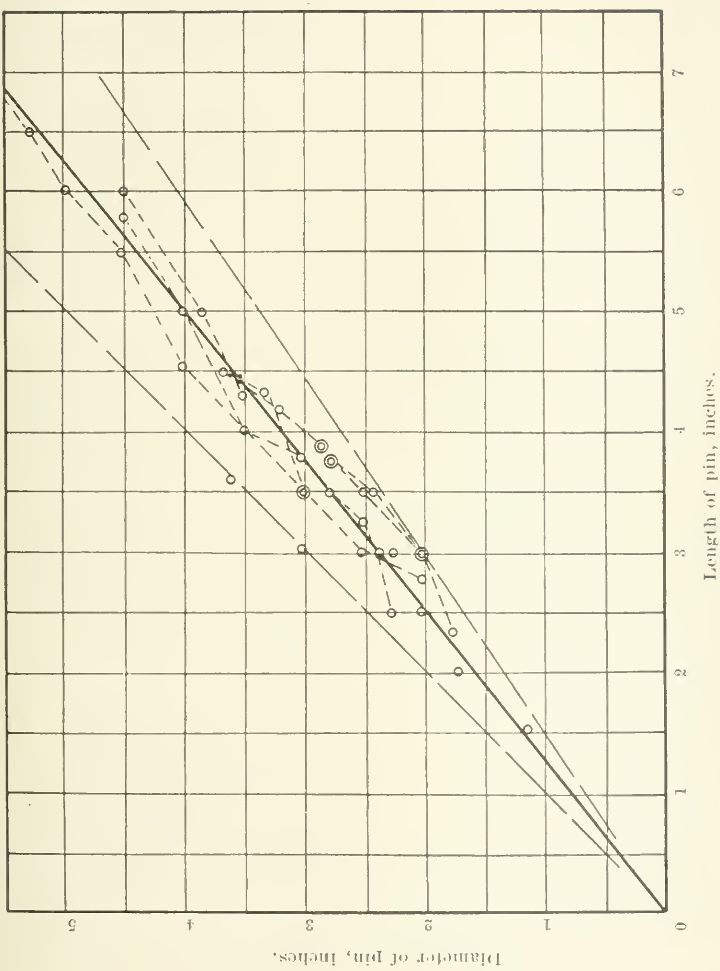

Fig. 11.—Crosshead Pin High Speed Engines.

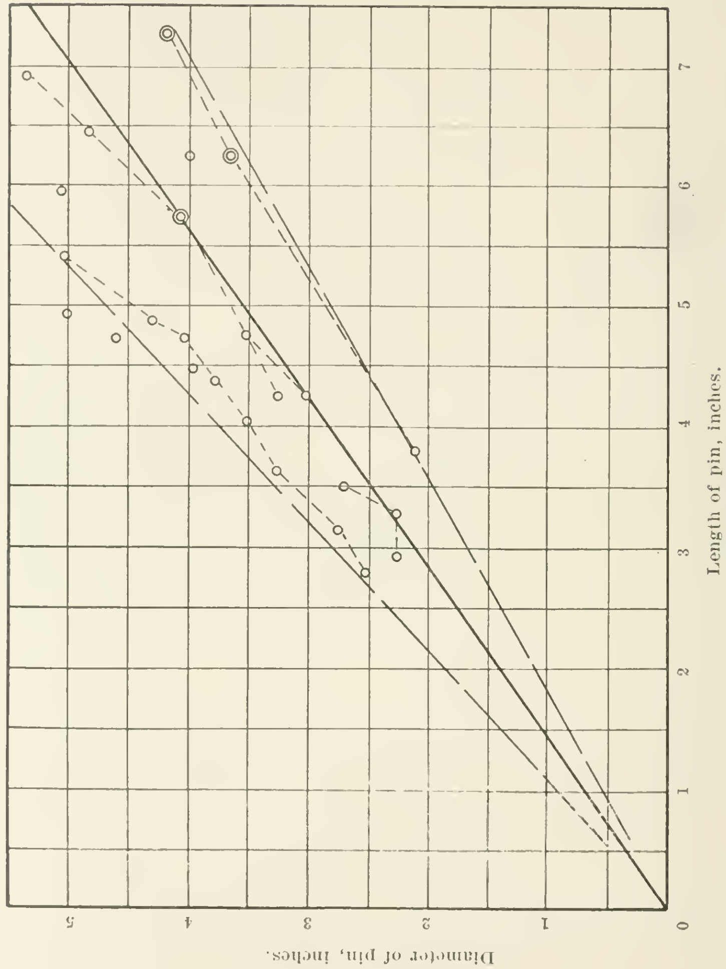

FIG. 12.—CROSSHEAD PIN CORLISS ENGINES.

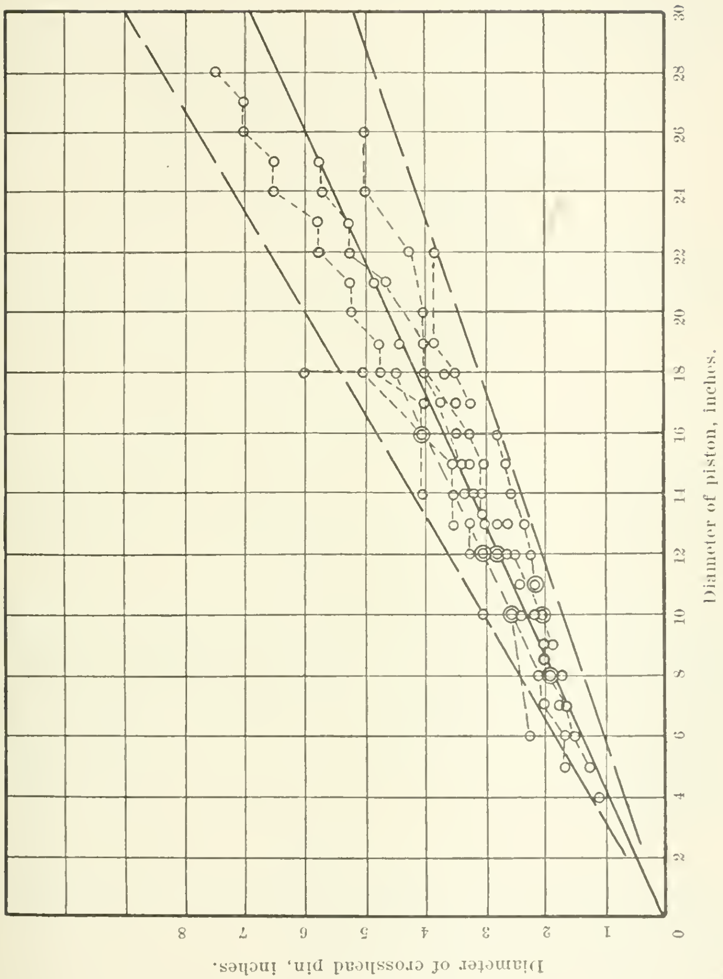

FIG. 13.—DIAMETER OF CROSSHEAD PIN.

Using the mean value of $l = 1.25d$ for the high speed engines and $l = 1.43d$ for the Corliss engines, the following are the values of K and f respectively:

For high speed engines:

mean value of K = .10
maximum value of K = .15
minimum value of K = .037
mean value of f = 2,500
maximum value of f = 5,400
minimum value of f = 2,000.

For Corliss engines:

mean value of K = .115
maximum value of K = .19
minimum value of K = .037
mean value of f = 2,870
maximum value of f = 6,450
minimum value of f = 2,300.

CONNECTING RODS

The method of treating the connecting rods is similar to the method employed for the piston rods. The Euler formula for long columns is used and the constants modified for end conditions. As regards buckling in the plane of its motion, the connecting rod may be treated as having both ends free but guided in the direction of the plane of the motion, and the formula becomes

$$P = \pi^2 \frac{EI}{L^2_c}$$

For lateral deflection the rod may be considered as having both ends fixed, and the formula becomes

$$P = 4\pi^2 \frac{EI}{L^2_c}$$

where P is the greatest safe load for stability; E is the modulus of elasticity; I is the moment of inertia of mid-section; and L_c is the length of strut (center to center of connecting rod).

From a comparison of the above equations it is seen that the resistance of a rod of circular cross section to lateral deflection is four times as great as its resistance to buckling in the plane of its motion and hence it need only be considered for the latter condition. A rod of rectangular cross section may buckle in either plane depending upon the ratio of the height h to the breadth or thickness b, at center. For the engines examined the mean ratio of h to b at center of rods was found to be 2.28.

The relation of $h = Cb$ was used in plotting Fig. 14.

$$\text{mean value of } C = 2.28$$
$$\text{maximum value of } C = 3.0$$
$$\text{minimum value of } C = 1.85$$

By comparing the above formula for the resistance of a rod of rectangular cross section, to buckling in either plane for a given load, the following relation holds true.

$$\frac{\pi^2 E}{L^2_c} I_b = \frac{4\pi^2 E}{L^2_c} I_h$$
$$\text{or } I_b = 4 I_h$$

where I_b is the moment of inertia of mid-section of rod about the b or shorter axis through center of section, and I_h is the moment of inertia about the h or longer axis through center of section

$$\text{or } 1/12\ bh^3 = 4/12\ b^3h$$
$$\text{and } h = 2b.$$

This shows that when $h = 2b$ at center for a rod of rectangular cross section, it will have equal rigidity against buckling in either plane. For the engines examined the mean value of $h = 2.28\ b$, and hence these rods need be considered for lateral deflection only.

Connecting rods of high speed engines, Fig. 15 (rectangular sections only).

These are treated for lateral deflection and

$$P = 4\pi^2 \frac{EI}{L^2_c}$$

If the rigidity of the rod is considered as determined by the breadth b and height 2b, the error will only be on the side of safety, and then

$$I = 1/12\ b^3h = 1/12\ b^3 \times 2b = \frac{b^4}{6}$$

$$\text{then } P = p\pi/4\ D^2 = 4\pi^2 \times \frac{30{,}000{,}000}{L^2_c} \times \frac{b^4}{6}$$

$$\text{and } b = .026\sqrt{DL_c} \text{ (for factor of safety of unity)}$$

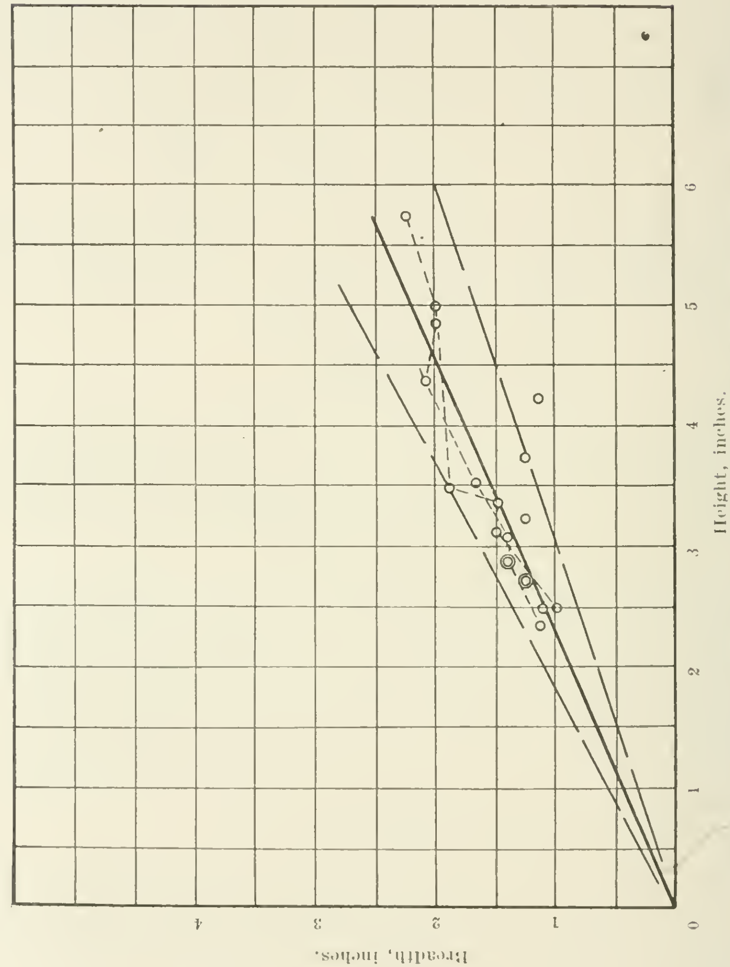

FIG. 14.—RATIO OF HEIGHT TO BREADTH IN RECTANGULAR CONNECTING RODS.

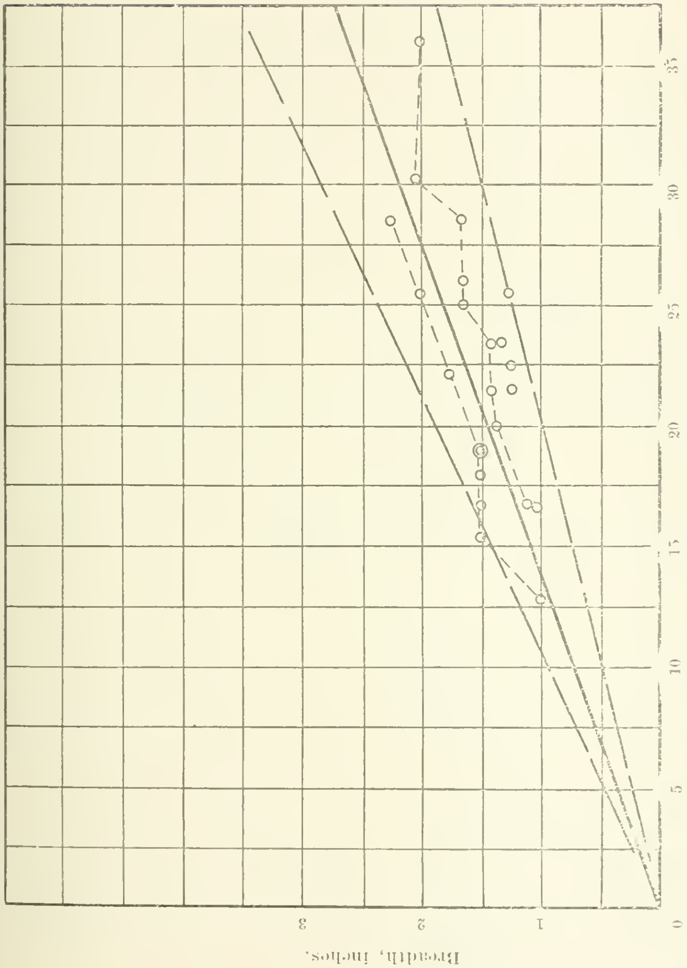

FIG. 15.—CONNECTING RODS HIGH SPEED ENGINES.

The expression $b = C\sqrt{DL_c}$ was used in plotting

mean value of $C = .073$
maximum value of $C = .094$
minimum value of $C = .05$

This gives a factor of safety of $\left(\frac{.073}{.026}\right)^4 = 60$

Connecting rods of low speed engines, Fig. 16 (circular sections only).

These are treated for flexure in the plane of their motion and

$$P = \pi^2 \frac{EI}{L^2_c}$$

$$\text{or } 125 \times \pi/4D^2 = \pi^2 \times \frac{30.000.000}{L^2_c} \times \frac{\pi d^4}{64}$$

and $d = .051\sqrt{DL_c}$ (for factor of safety of unity)

The expression $d = C\sqrt{DL_c}$ was used in plotting.

mean value of $C = .092$
maximum value of $C = .104$
minimum value of $C = .081$

This gives a factor of safety of $\left(\frac{.092}{.051}\right)^4 = 11.$

CRANK PIN

The ratio of length to diameter of crank pin may be expressed by

$$l = Cd$$

For high speed engines, Fig. 17:

mean value of $C = .87$
maximum value of $C = 1.25$
minimum value of $C = .66$

For Corliss engines, Fig. 18:

mean value of $C = 1.14$
maximum value of $C = 1.30$
minimum value of $C = 1.0$

In treating the crank pin for strength it was, in the case of center crank engines, taken as a simple beam having a length

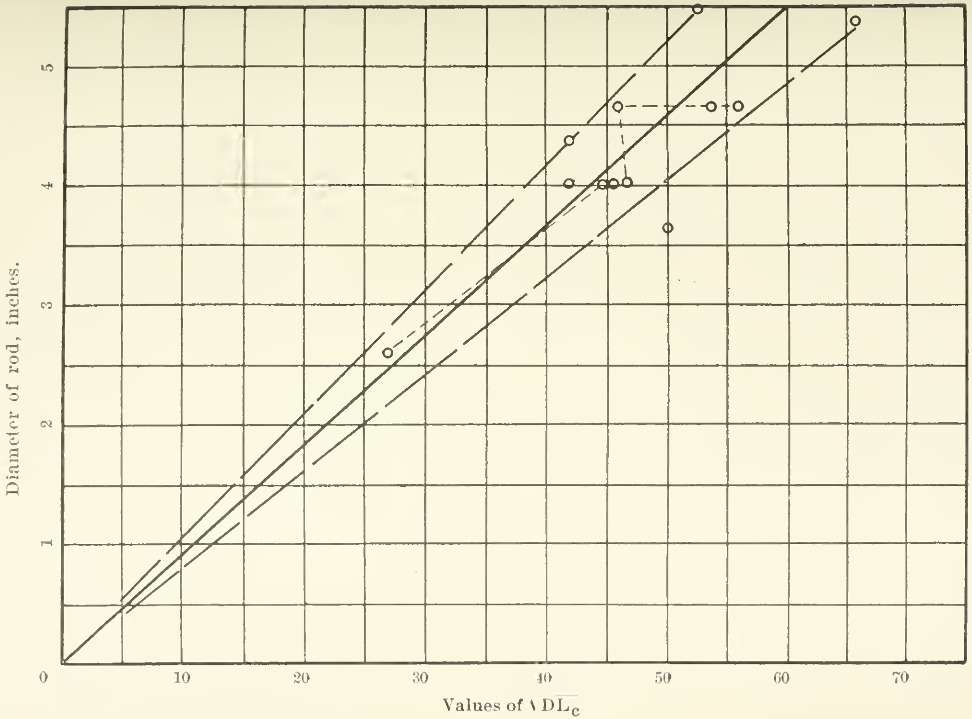

FIG. 16.—CONNECTING ROD CORLISS ENGINES.

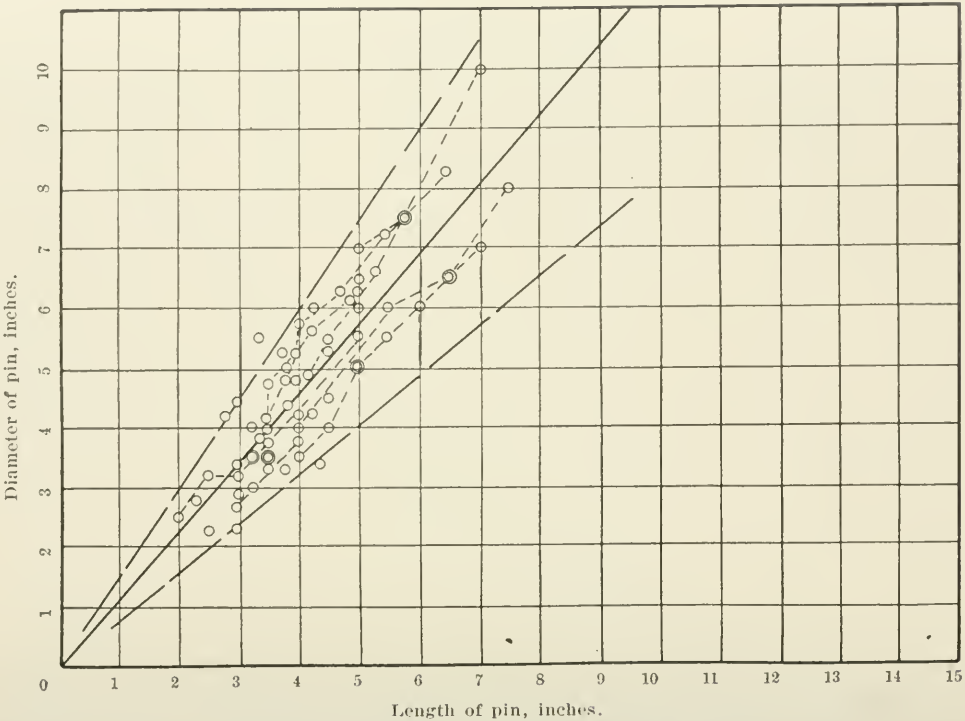

Fig. 17.—Crank Pin High Speed Engines.

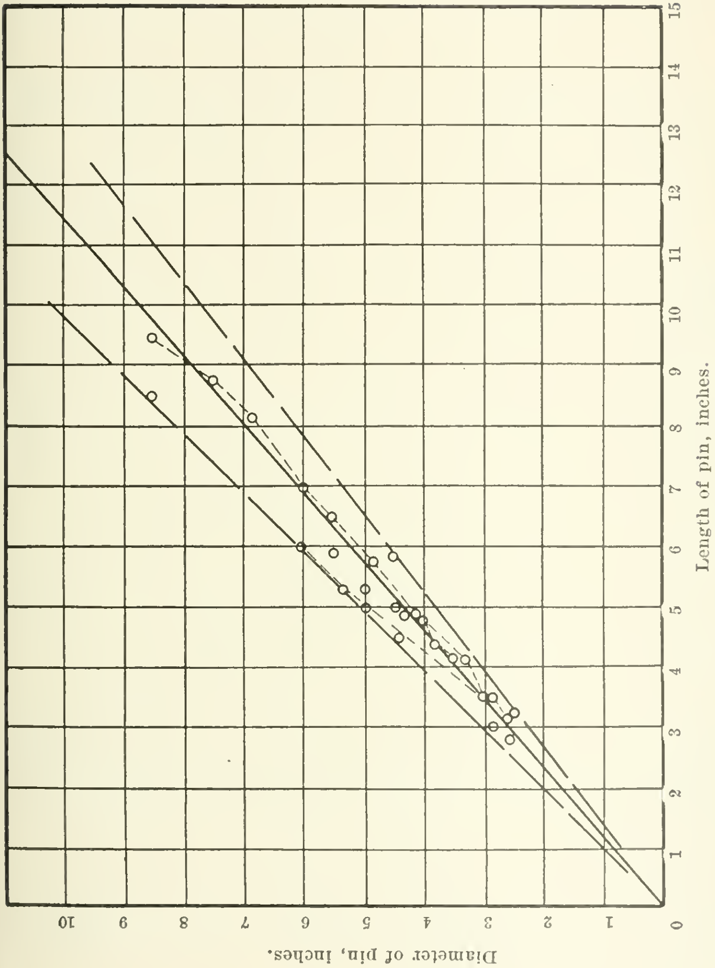

Fig. 18.—Crank Pin Corliss Engines.

equal to the distance between the center lines of main journals of the engine, and for strength

resisting moment = bending moment, or

$$\pi/32\ \mathrm{fd}^3 = \frac{\mathrm{PL_b}}{4}$$

where d is the diameter of the pin and L_b is the distance from center to center of main bearings. The relation between the diameter d and the length L_b may be expressed by

$$L_b = Cd.$$

mean value of C = 4.2, Fig. 19

$$\text{then } \pi/32\ \mathrm{fd}^3 = \frac{4.2\ \mathrm{Pd}}{4} = 1.05\ \mathrm{d} \times \mathrm{p}\ \pi/4\ \mathrm{D}^2$$

$$C_1 d^2 = 1.05 \times 125 \times .78\ D^2 \text{ and}$$

$$d = CD$$

which is the expression used in plotting.

For high speed center crank engines. Fig. 20:

mean value of C = .40
maximum value of C = .526
minimum value of C = .28
mean value of f = 6,600
maximum value of f = 13,400
minimum value of f = 3,800

The crank pin for side crank Corliss engines was treated as a single cantilever beam having a length equal to the bearing length of the crank pin, and in the same manner as before

$$\pi/32\ \mathrm{fd}^3 = \frac{\mathrm{P}l}{2}$$

where d is the diameter and l is the length of the crank pin.

The mean relation between the length and the diameter of the crank pin as already found is

$$l = 1.14\ d$$

and as before, the following final expression is obtained:

$$d = CD.$$

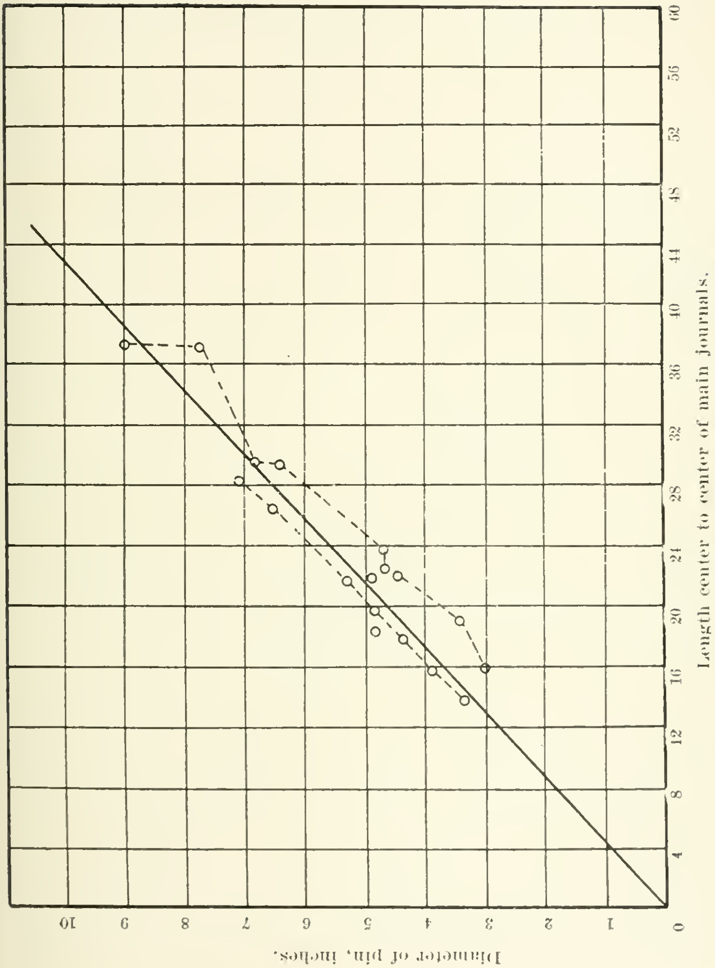

FIG. 19.—THE RELATION BETWEEN LENGTH FROM CENTER TO CENTER OF MAIN JOURNALS AND DIAMETER OF CRANK PIN.

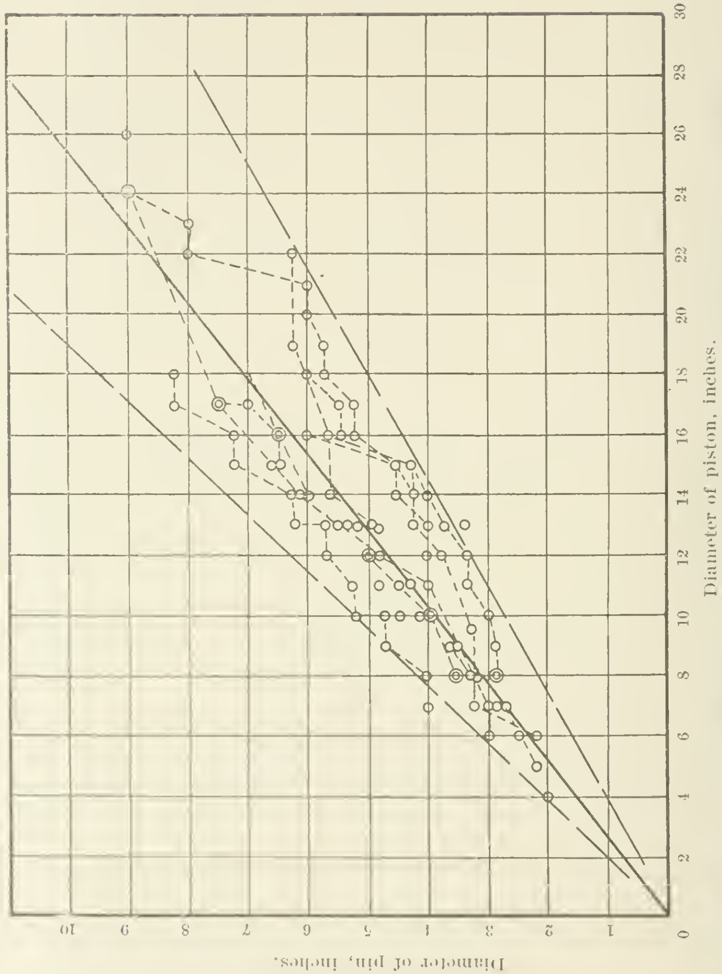

FIG. 20.—DIAMETER OF CRANK PIN HIGH SPEED CENTER CRANK ENGINES.

For side crank Corliss engines, Fig. 21:

mean value of $C = .27$
maximum value of $C = .32$
minimum value of $C = .21$
mean value of $f = 7{,}800$
maximum value of $f = 13{,}000$
minimum value of $f = 5{,}500$

MAIN JOURNALS OF CRANK SHAFT

Crank shafts are subject to variable combined bending and twisting moments, but these moments, when their magnitude and direction are known, can be reduced to an equivalent twisting moment by the formula

$$M_t = M + \sqrt{M^2 + T^2}$$

where M_t is the equivalent twisting moment; M the simple bending moment; and T the simple twisting moment for the point. If now the ratios of bending and twisting moments and of maximum to mean moments are constant, the above transformation will retain the same general form and change only in the numerical coefficient. In the engines examined there is a general agreement as to the above ratios of moments among engines of the same class.

For maximum fibre stress the main journals of the crank shaft may be treated as subjected to this equivalent twisting moment. A common expression for twisting moment is,

$$d = C \sqrt[3]{\frac{H.\ P.}{N}}$$

where d is the diameter of main journal; H. P. is the Horse Power of the engine; and N is the number of revolutions per minute.

For high speed center crank engines, Fig. 22:

mean value of $C = 6.6$
maximum value of $C = 8.2$
minimum value of $C = 5.4$

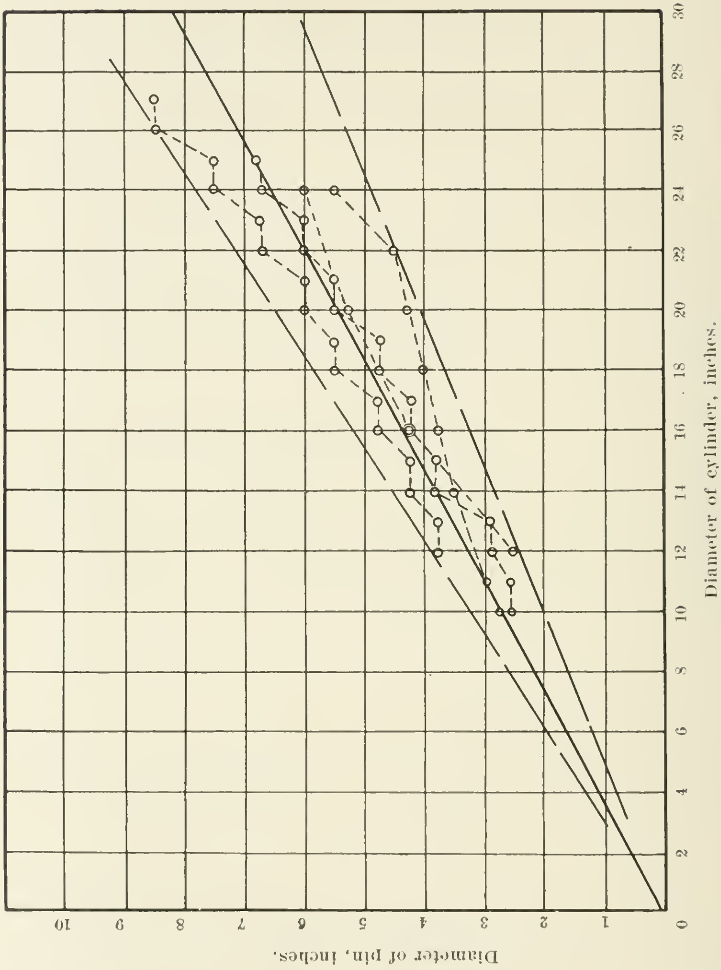

Fig. 21.—Diameter of Crank Pin Corliss Engines.

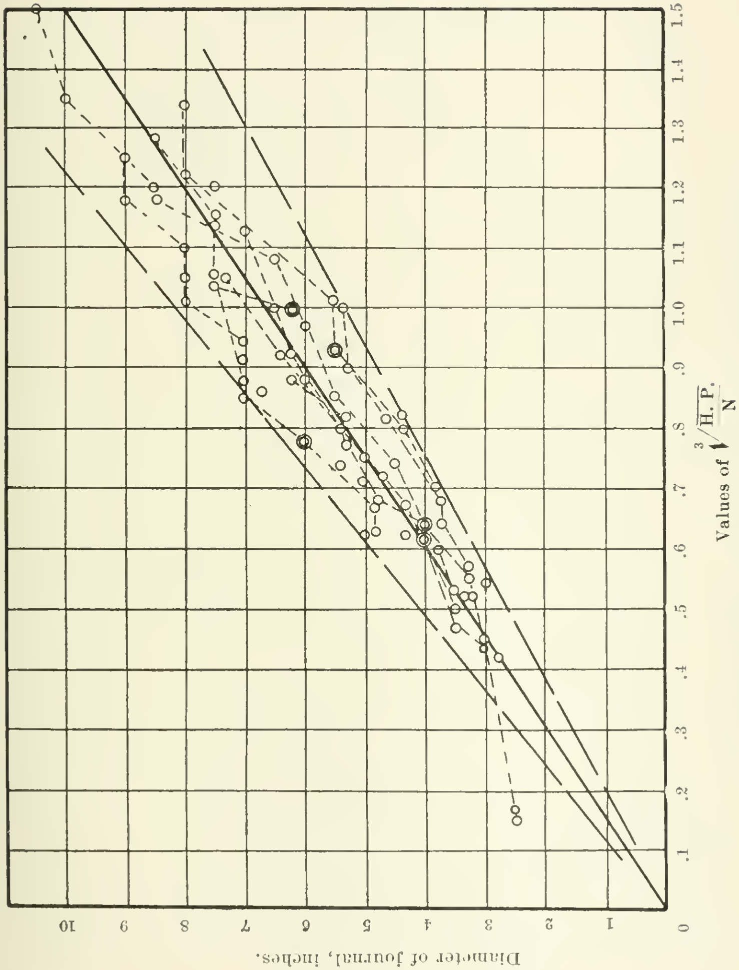

FIG. 22.—DIAMETER OF MAIN JOURNALS HIGH SPEED ENGINES.

For Corliss engines, Fig. 23, this relation seems best expressed by the form

$$d = C\left(\sqrt[3]{\frac{H.P.}{N}} - B\right)$$

$$B = .30$$

mean value of $C = 7.2$
maximum value of $C = 8.0$
minimum value of $C = 6.4$

The relation between the length and diameter of the main journals of crank shafts may be expressed by

$$l = K\,d.$$

For high speed center crank engines, Fig. 24:

mean value of $K = 2.1$
maximum value of $K = 2.9$
minimum value of $K = 1.6$

For Corliss side crank engines, Fig. 25:

mean value of $K = 1.90$
maximum value of $K = 2.20$
minimum value of $K = 1.62$.

The relation between the projected area of the main journals and the area of the piston may be expressed by

$$d\,l = a = FA.$$

For high speed center crank engines, Fig. 26:

mean value of $F = .48$
maximum value of $F = .78$
minimum value of $F = .32$

For Corliss side crank engines, Fig. 27:

mean value of $F = .6$
maximum value of $F = .66$
minimum value of $F = .5$.

THE FLY WHEEL

The weight of fly wheel rim was found to be almost too uncertain a value to lend itself to any satisfactory comparative treatment. There is a marked difference in opinion among the different engine builders, not only as to what would constitute

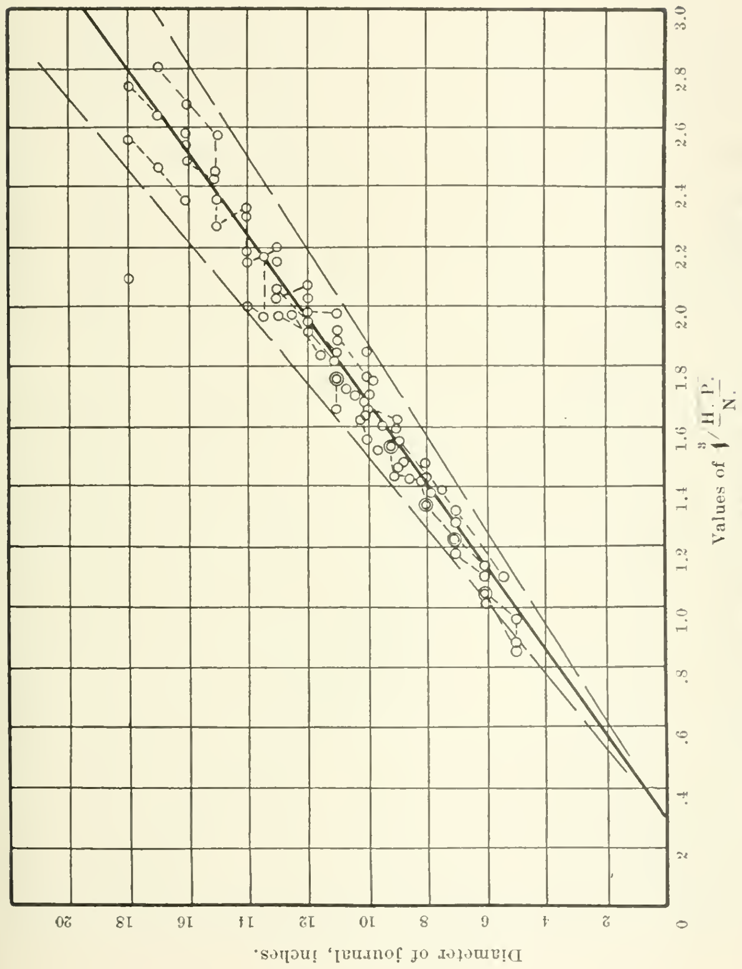

FIG. 23.—DIAMETER OF MAIN BEARING CORLISS ENGINES.

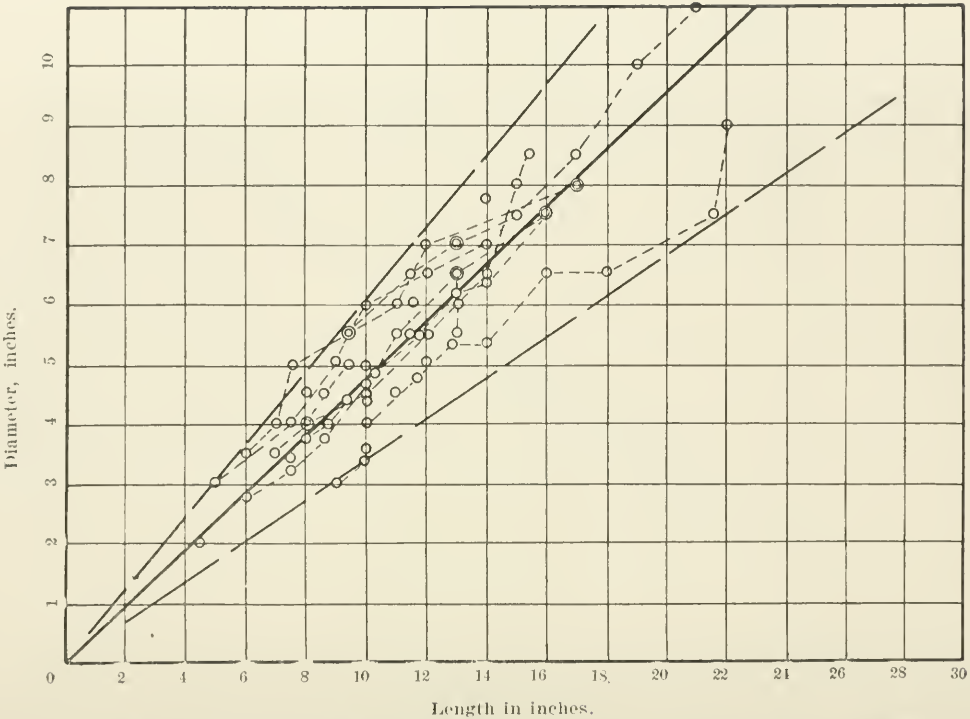

FIG. 24.—THE RATIO OF LENGTH TO DIAMETER MAIN JOURNALS HIGH SPEED ENGINES.

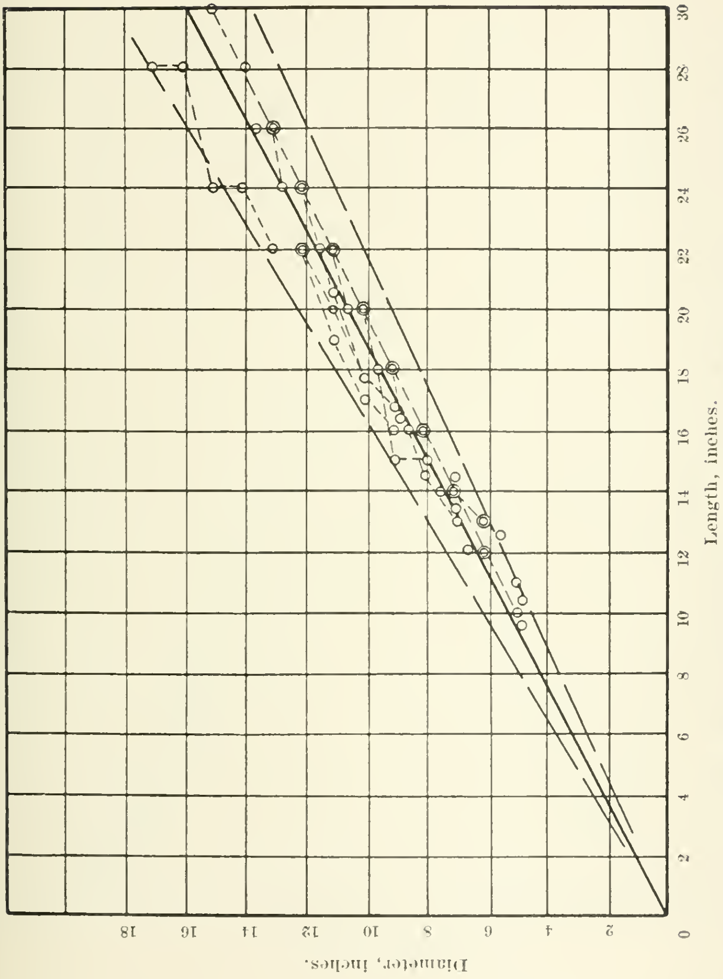

FIG. 25.—THE RATIO OF LENGTH TO DIAMETER OF MAIN BEARING CORLISS ENGINES.

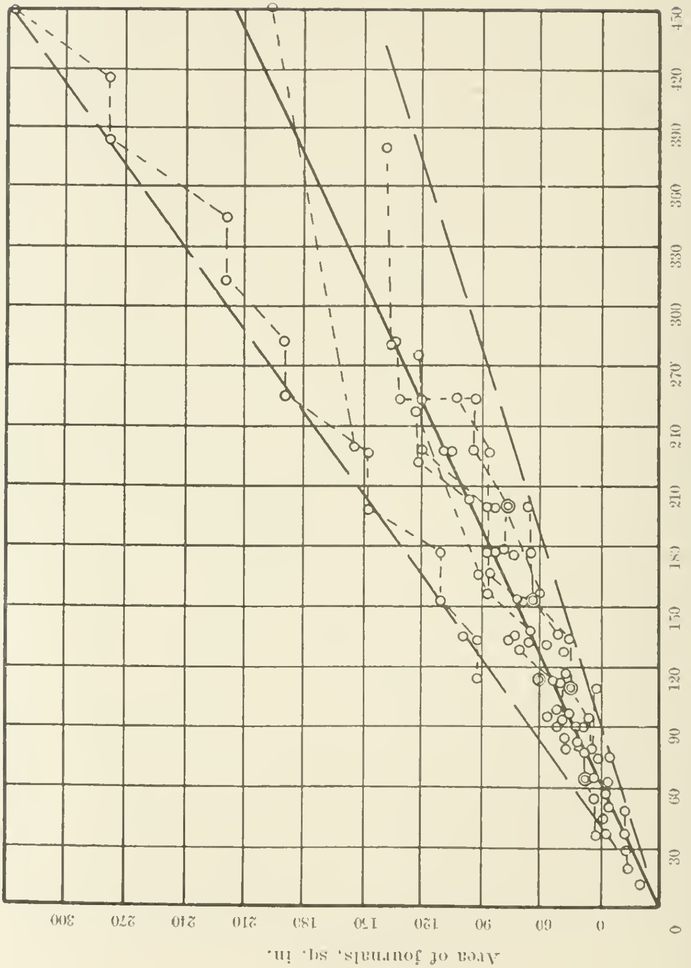

FIG. 26.—THE RELATION BETWEEN PROJECTED AREA OF MAIN JOURNALS AND AREA OF CYLINDER HIGH SPEED ENGINES.

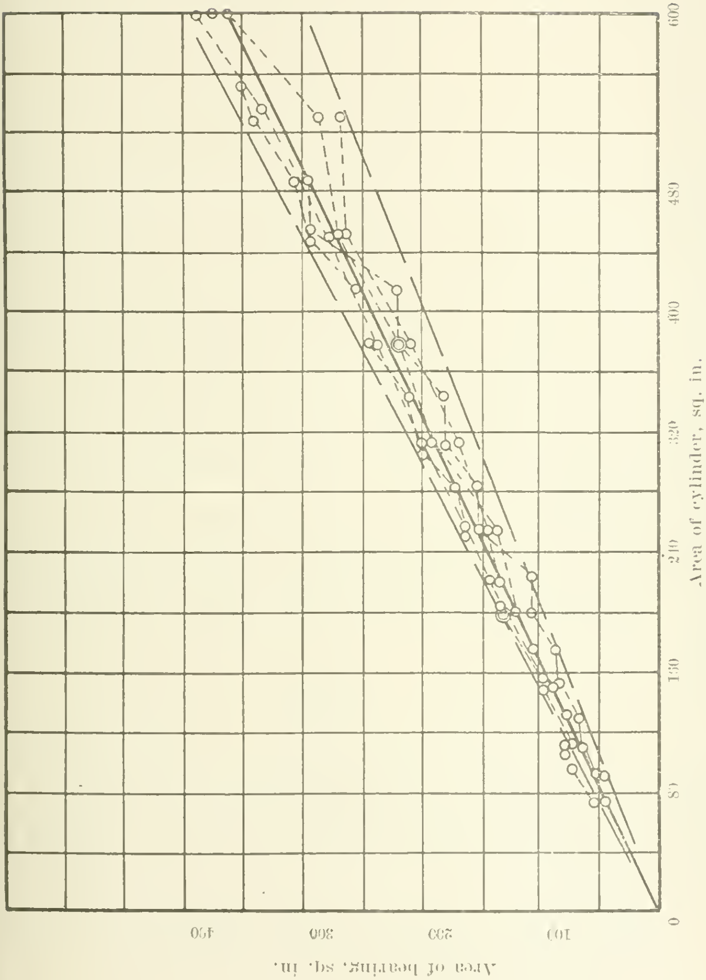

FIG. 27.—THE RELATION BETWEEN PROJECTED AREA OF MAIN BEARING AND AREA OF CYLINDER CORLISS ENGINES.

a proper total weight of fly wheel for an engine of certain Horse Power, but there is an equally marked difference in opinion as to how much of the total weight should be considered as acting at the center of the fly wheel rim in producing inertia effect.

Some manufacturers consider the total weight of the wheel as acting at the rim in producing inertia effect; others consider the weight of the rim, spokes and hub as all acting at their respective centers of gravity, the weight of the spokes being considered as about 1/3 of the total weight of the wheel; still others consider the weight of the rim and 1/3 of the weight of the spokes acting at their respective centers of gravity; and finally some consider the weight of the fly wheel rim only and disregard the weight of the remaining parts of the wheel.

From the engines examined it was found that the weight of the rim of the wheel varied from 44 to 75% of the total weight of wheel in high speed engines and from 52 to 68% in Corliss engines.

In view of these variations it was deemed best to use the total weight of the wheel in plotting. And the formula that is most commonly used for finding the weight of fly wheel was used.

It has the form

$$W = C \times \frac{H.P.}{D^2_1 N^3}$$

where $W =$ total weight of wheel; $D_1 =$ the diameter of wheel in inches; and $N =$ the number of revolutions per minute.

This relation gives fairly satisfactory results for high speed engines up to about 175 Horse Power, and for this range, Fig. 28:

mean value of $C = 1{,}300{,}000{,}000{,}000$
maximum value of $C = 2{,}800{,}000{,}000{,}000$
minimum value of $C = 660{,}000{,}000{,}000$

But when high speed engines of larger size are considered, the relation seems better expressed by

$$W = C \times \frac{H.P.}{D^2_1 N^3} + B$$

$$B = 1{,}000$$

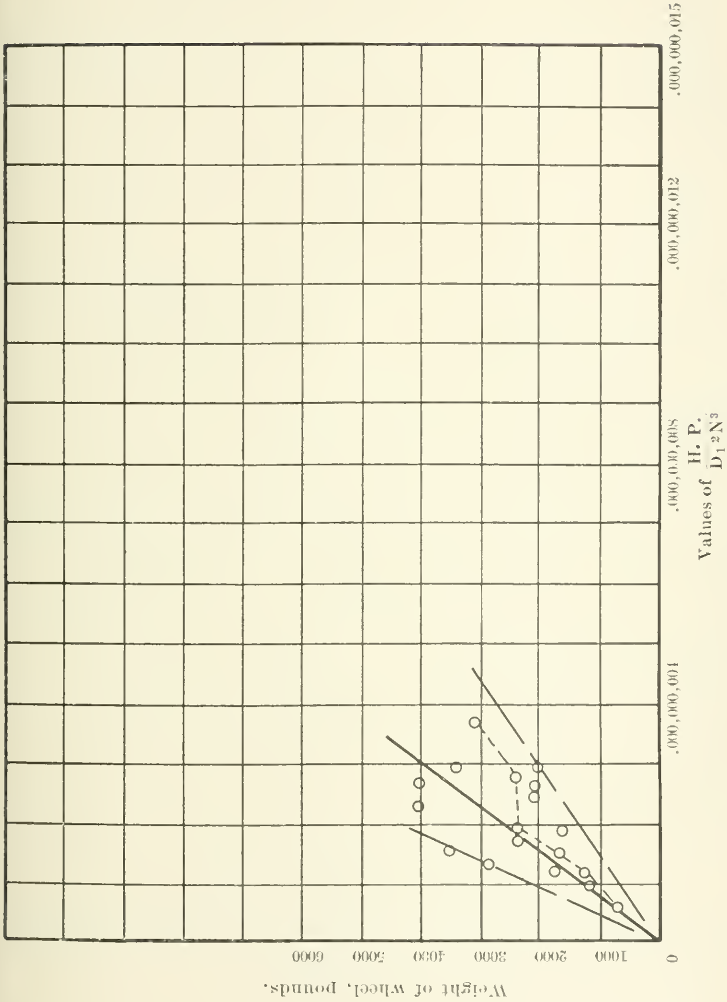

FIG. 28.—WEIGHT OF FLYWHEEL HIGH SPEED ENGINES HAVING A CAPACITY LESS THAN 175 HORSE POWER.

mean value of $C = 720,000,000,000$, Fig. 29
maximum value of $C = 1,140,000,000,000$
minimum value of $C = 330,000,000,000$.

A somewhat greater uniformity seems to exist among the builders of standard Corliss engines. In these engines the relation seems best expressed by

$$W = C\left(\frac{H.\,P.}{D^2_1 N^3} - B\right)$$

$$\text{or } W = C\frac{H.\,P.}{D^2_1 N^3} - K$$

$$B = .000,000,004,5.$$

mean value of $C = 890,000,000,000$, Fig. 30
maximum value of $C = 1,330,000,000,000$
minimum value of $C = 625,000,000,000$

The corresponding values of K are
mean value of $K = 4,000$
maximum value of $K = 6,000$
minimum value of $K = 2,800$

The relation between the length of the stroke and diameter of fly wheel in high speed engines may be expressed by

$$D_1 = CL$$

where D_1 = outside diameter of wheel in inches; and L = length of stroke in inches.

mean value of $C = 4.4$, Fig. 31
maximum value of $C = 5.0$
minimum value of $C = 3.4$

For Corliss engines, Fig. 32:
mean value of $C = 4.40$
maximum value of $C = 5.25$
minimum value of $C = 3.25$

The relation between the width of the face and the outside diameter of the fly wheel may be expressed by

$$w = C\ (D_1 - B)$$

$$\text{or } w = CD_1 - K$$

where w = the width of face of fly wheel; and D_1 the diameter in inches.

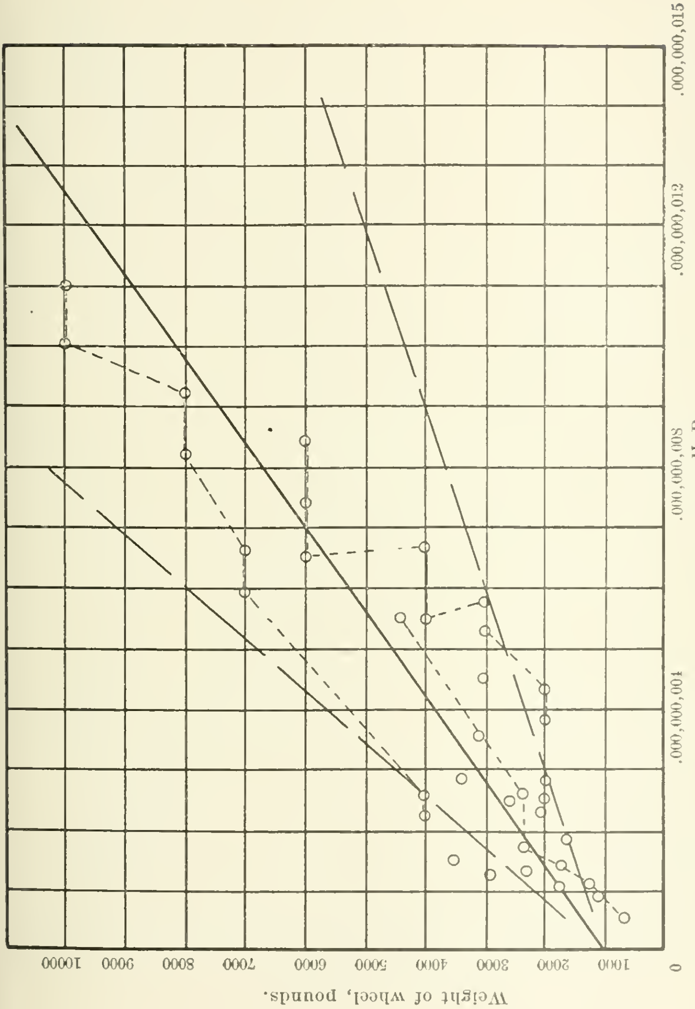

FIG. 29.—WEIGHT OF FLYWHEEL HIGH SPEED ENGINES INCLUDING CAPACITIES UP TO 400 HORSE POWER.

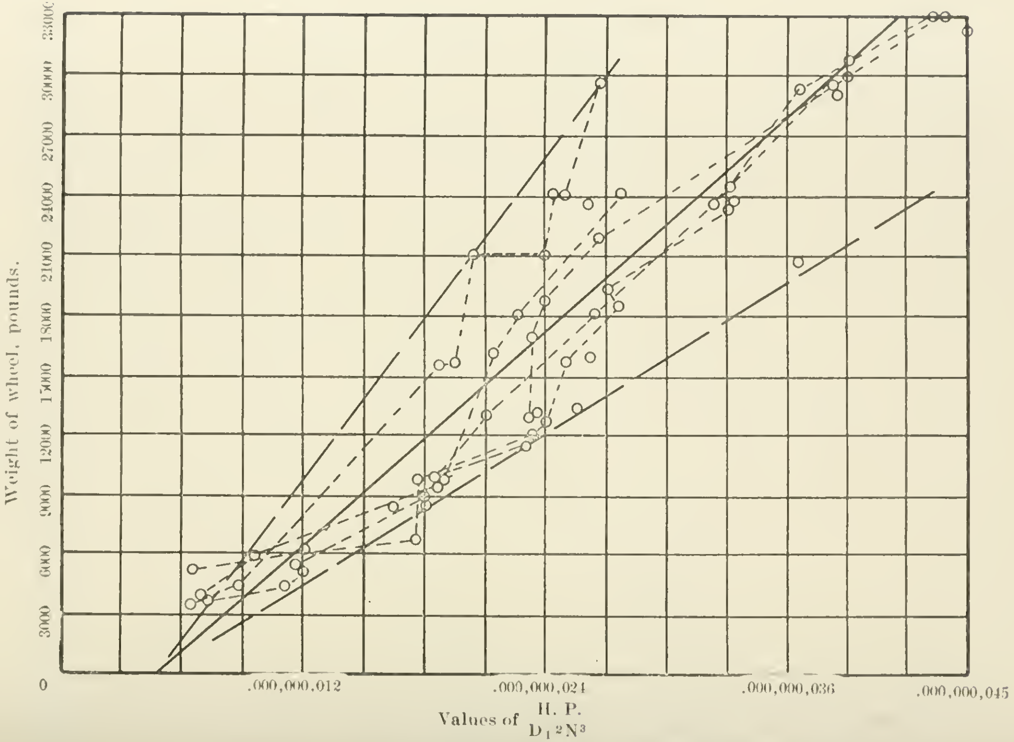

FIG. 30.—WEIGHT OF FLYWHEEL CORLISS ENGINES.

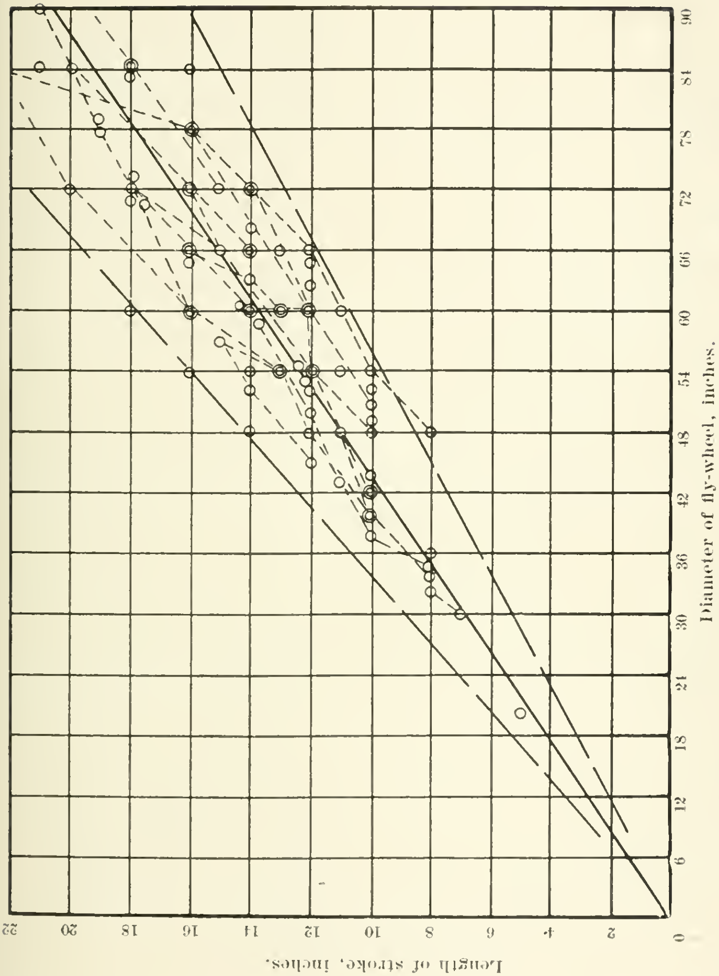

Fig. 31.—Relation Between Length of Stroke and Diameter of Fly-Wheel High Speed Engines.

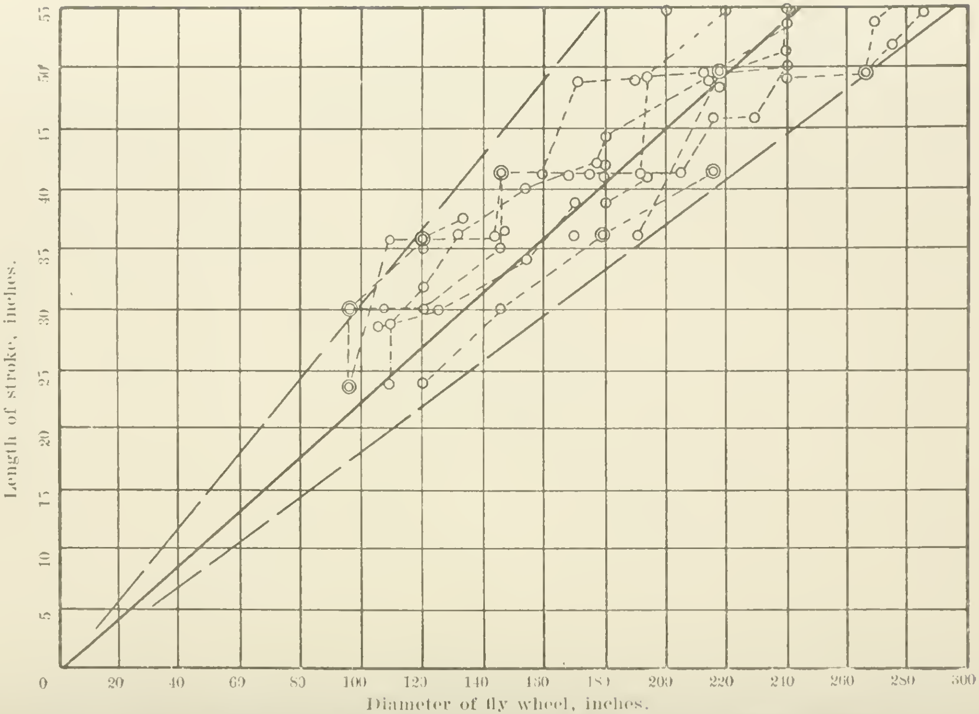

FIG. 32.—RELATION BETWEEN LENGTH OF STROKE AND DIAMETER OF FLY-WHEEL CORLISS ENGINES.

For high speed engines, Fig. 33:

$$B = 18$$

mean value of $C = .31$
maximum value of $C = .46$
minimum value of $C = .24$

The corresponding values of K are

mean value of $K = 5.6$
maximum value of $K = 8.3$
minimum value of $K = 4.3$

For Corliss engines, Fig. 34:

$$w = C\ (D_1 - B)$$

$$\text{or } w = CD_1 - K$$

$$B = 50$$

mean value of $C = .22$
maximum value of $C = .30$
minimum value of $C = .18$

The corresponding values of K are

mean value of $K = 13$
maximum value of $K = 15$
minimum value of $K = 9$

BELT SURFACE PER I. H. P.

The relation between the number of square feet of belt surface per minute and the Horse Power of an engine may be expressed by

$$S = C \times \text{H. P.}$$

where S = the velocity of fly wheel rim in feet per minute multiplied by the width of belt in feet.

For high speed engines, Fig. 35:

mean value of $C = 26.5$
maximum value of $C = 55.$
minimum value of $C = 10.$

For Corliss engines, Fig. 36. This relation seems better expressed by

$$S = C \times \text{H. P.} + B$$

$$B = 1{,}000$$

mean value of $C = 21$
maximum value of $C = 35$
minimum value of $C = 18.2$

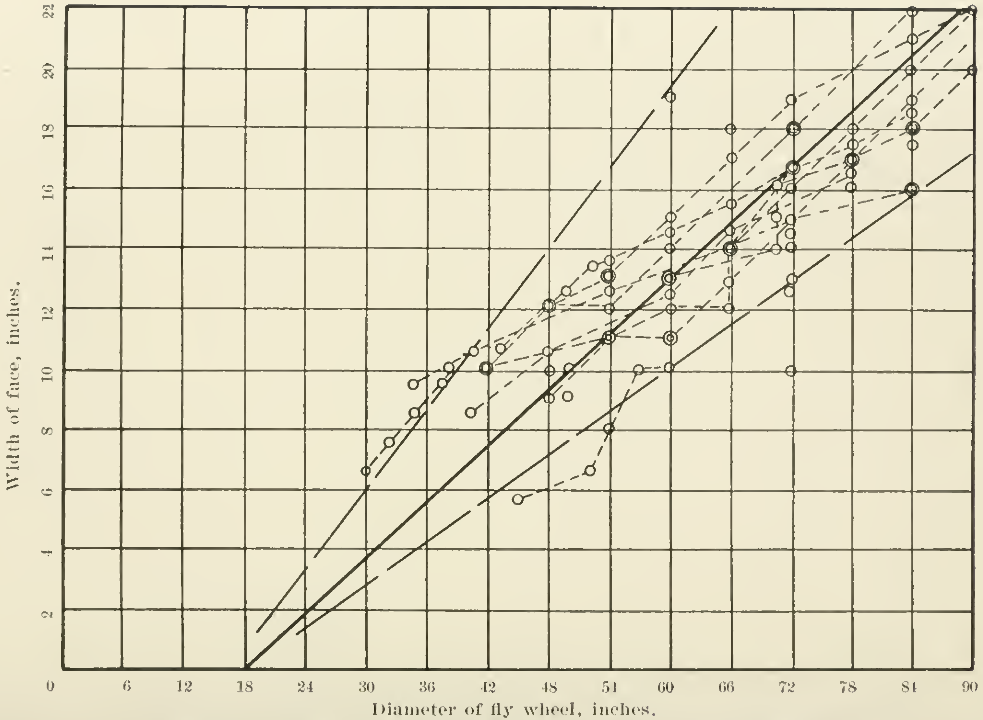

FIG. 33.—RELATION BETWEEN FACE AND DIAMETER OF FLYWHEEL HIGH SPEED ENGINES.

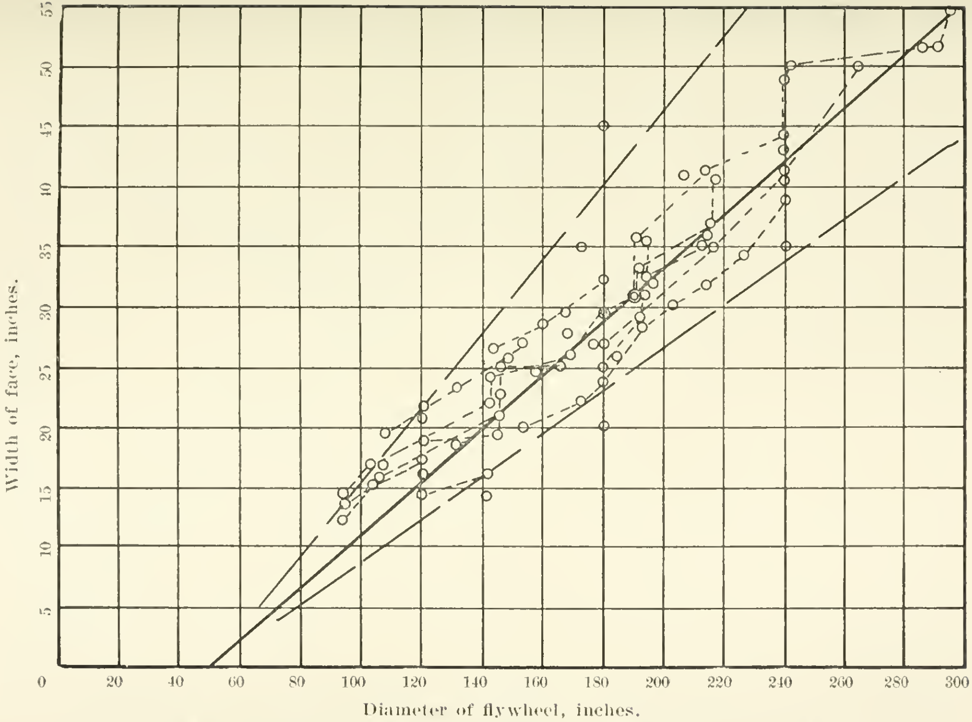

Fig. 34.—Relation Between Face and Diameter of Flywheel Corliss Engines.

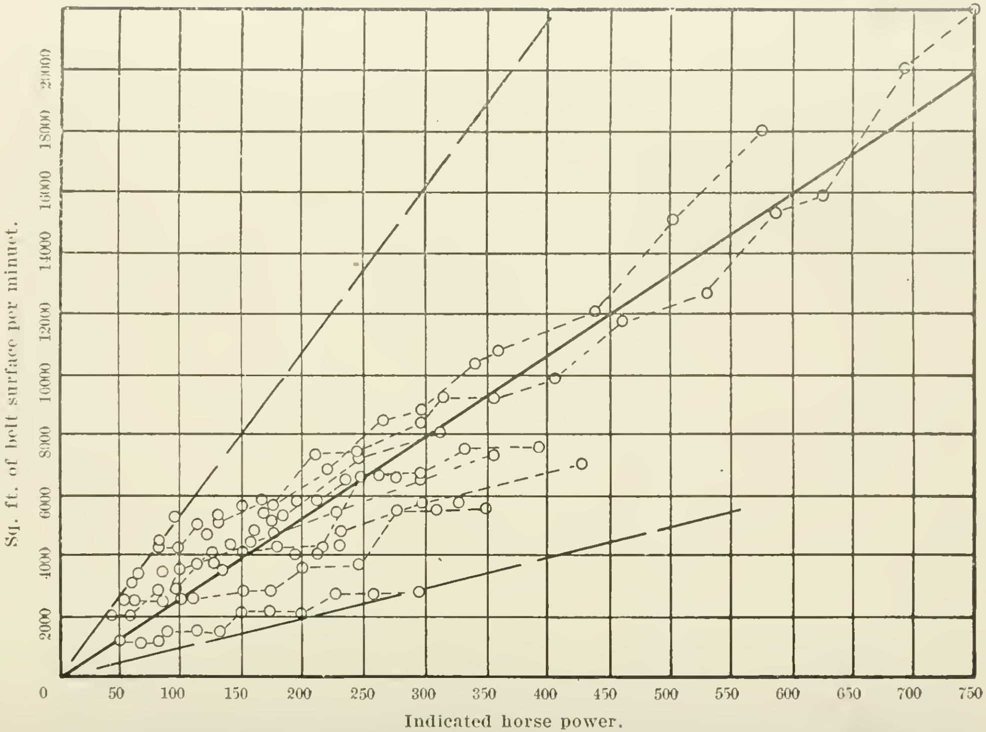

FIG. 35.—SQ. FT. OF BELT SURFACE PER I. H. P. HIGH SPEED ENGINES.

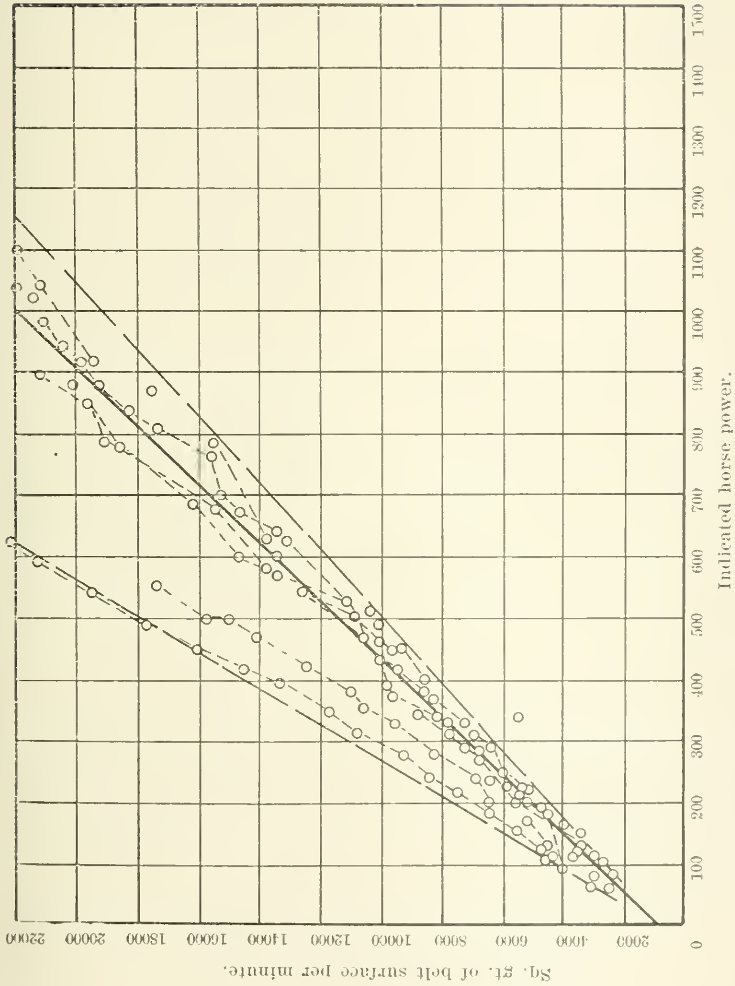

FIG. 36.—SQ. FT. OF BELT SURFACE PER I. H. P. CORLISS ENGINES.

Velocity of Wheel Rim

Velocity of fly wheel rim in feet per second.

For high speed engines:

mean velocity = 70 feet per sec.
maximum velocity = 82 feet per sec.
minimum velocity = 48 feet per sec.

For Corliss engines:

mean velocity = 68 feet per sec.
maximum velocity = 82 feet per sec.
minimum velocity = 40 feet per sec.

WEIGHT OF RECIPROCATING PARTS

In this investigation the weight of the reciprocating parts was assumed to be directly proportional to the pressure on the piston and inversely proportional to the length of the stroke and to the square of the number of revolutions. Putting this in the form of a formula and remembering that the total pressure on the piston varies as D^2, the above relation gives the expression

$$W = C \times \frac{D^2}{LN^2}$$

where W = the weight of the reciprocating parts, composed of the weight of the piston, piston rod, crosshead, and 1/2 the weight of the connecting rod; D = diameter of piston; L = the length of stroke in inches; and N = the number of revolutions per minute.

Data for plotting was obtained for high speed engines only.

mean value of C = 2,000,000. Fig. 37
maximum value of C = 3,400,000
minimum value of C = 1,370,000.

For the cases where the information was obtainable, the balance weight opposite crank pin was found to be about 75% of the weight of the reciprocating parts.

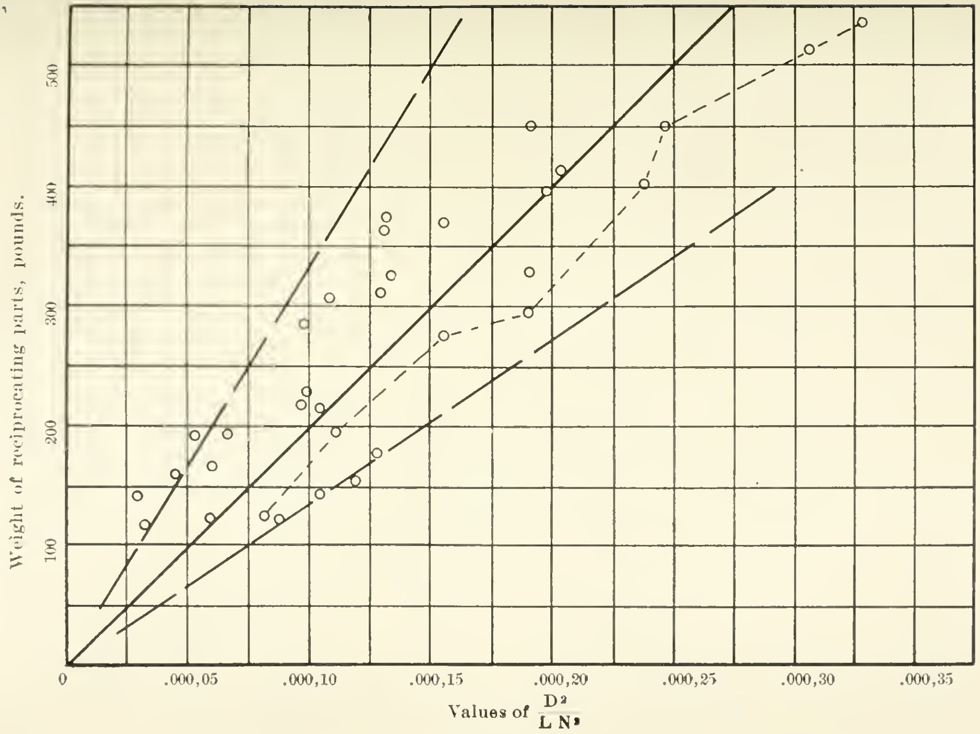

FIG. 37.—WEIGHT OF RECIPROCATING PARTS HIGH SPEED ENGINES.

WEIGHT OF ENGINE PER I. H. P.

The relation between the total weight of the engine and the number of Horse Power may be expressed by

$$W = C \times \text{H. P.}$$

where W = the total weight of the engine.

For belt connected high speed engines, Fig. 38:

mean value of C = 82
maximum value of C = 120
minimum value of C = 52

For direct connected engines, the weight of the engine without the generator was found to be from 10 to 25% greater than the weight of belt connected engines of the same capacity.

For Corliss engines, Fig. 39:

$$W = C \times \text{H. P.}$$

mean value of C = 132
maximum value of C = 164
minimum value of C = 102

RELATION BETWEEN AREA OF BED AND I. H. P.

The relation between the number of square feet of area occupied by the bed of engine and the Horse Power may be expressed by

$$A = C \times \text{H. P.} + B$$

For high speed engines, Fig. 40:

B = 10
mean value of C = .32
maximum value of C = .44
minimum value of C = .20

This area may be increased by from 15 to 25% for direct connected engines.

For Corliss engines, Fig. 41:

B = 80
mean value of C = .6.

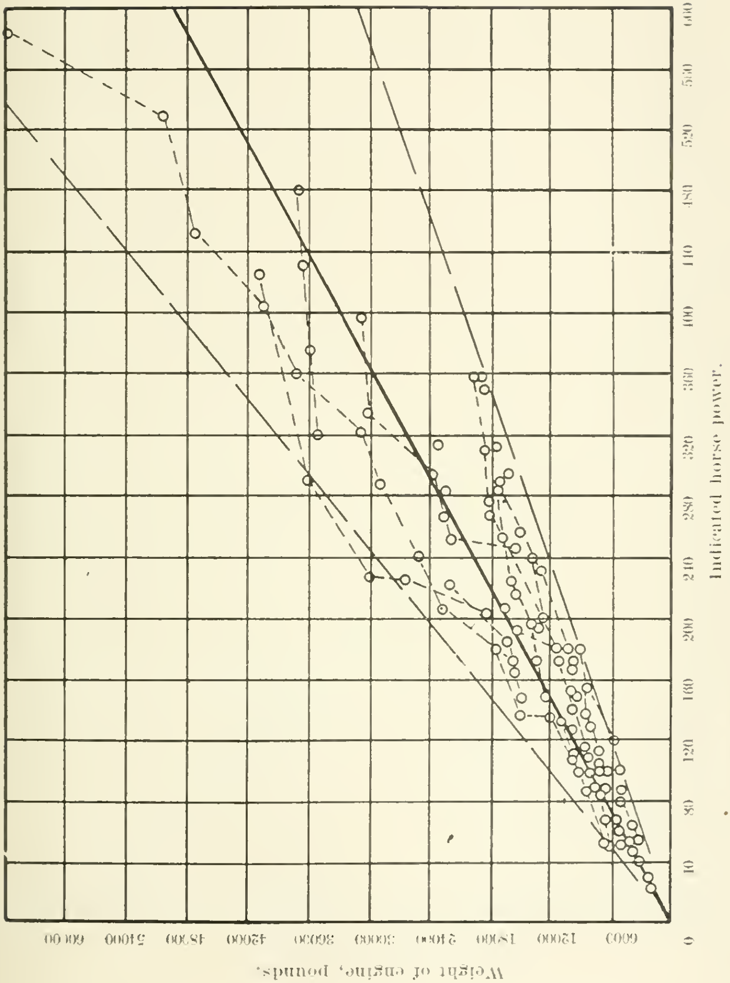

FIG. 38.—WEIGHT OF ENGINE PER I. H. P. HIGH SPEED ENGINES.

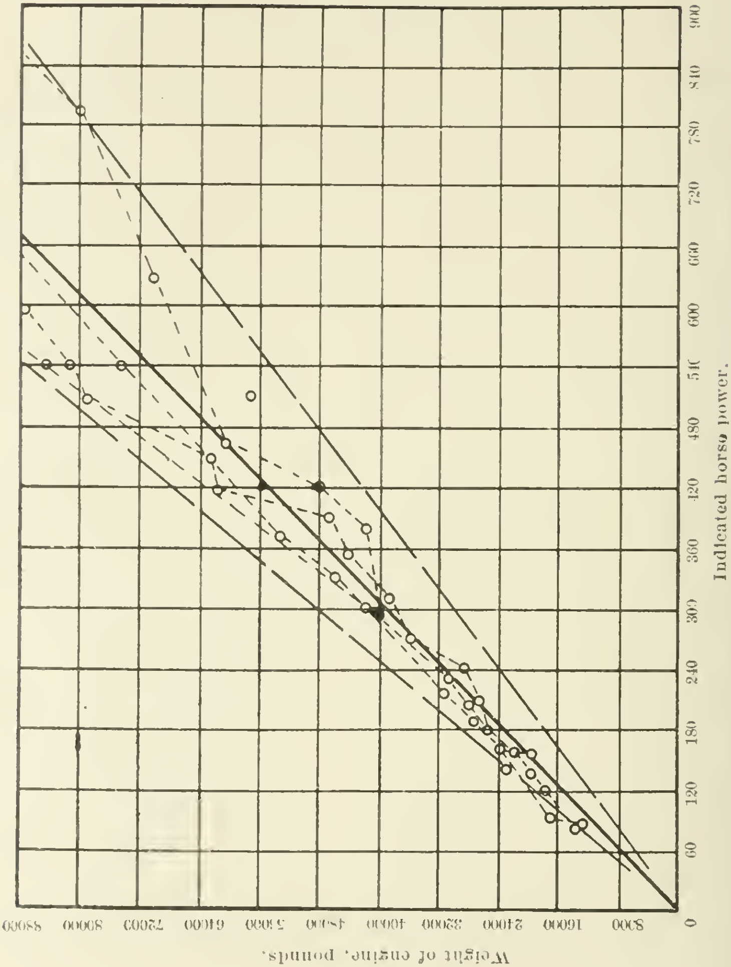

FIG. 39.—WEIGHT OF ENGINE PER I. H. P. CORLISS ENGINES.

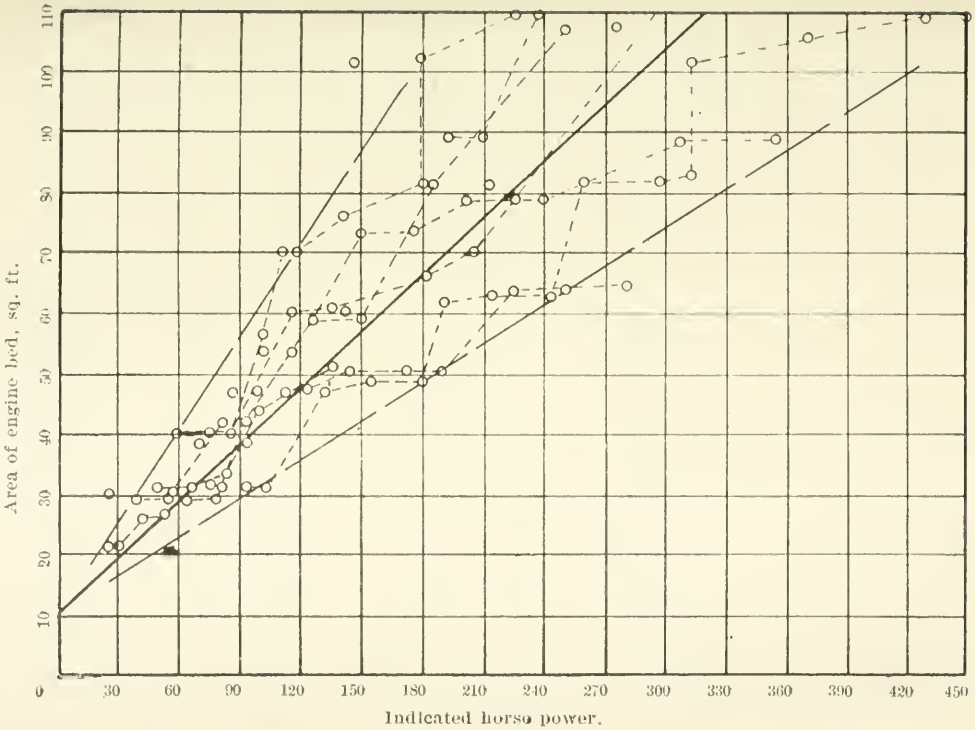

Fig. 40.—Area of Engine Bed Per I. H. P. High Speed Engines.

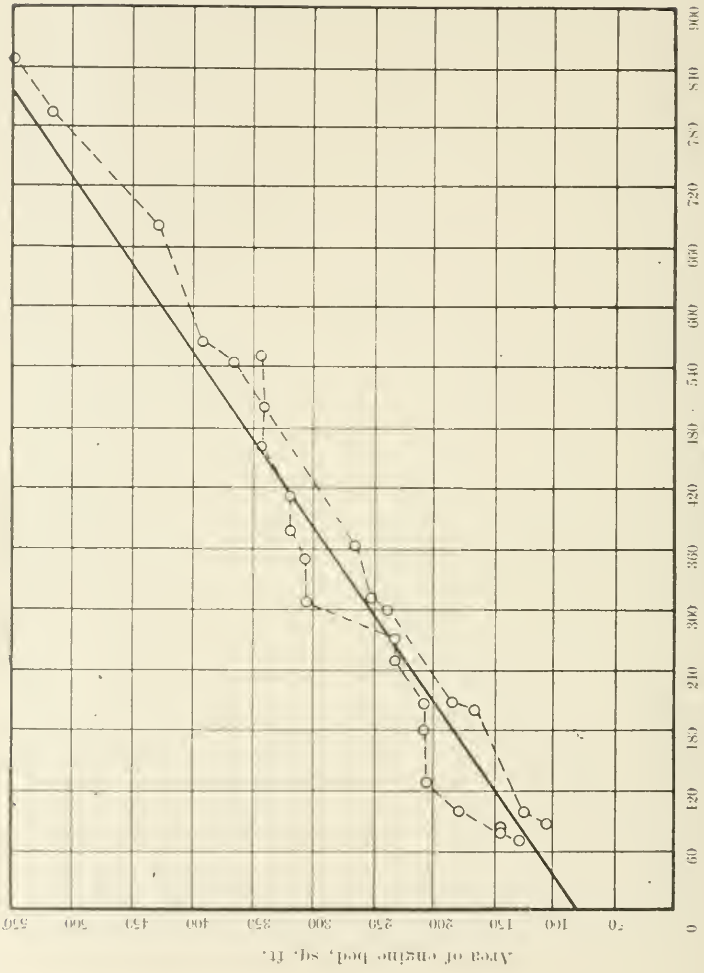

Fig. 41.—Area of Engine Bed Per I. H. P., Corliss Engines.

CONCLUSION

A comparison of the results obtained from this investigation and those obtained from a similar investigation carried out at Cornell University ten years ago,[1] reveals several interesting features. It shows that there has been a gradual change during the last decade, in the coefficients and factors of safety used in the design of the steam engine. It also shows how these coefficients and constants have been modified to meet existing conditions, and although there is still a great variation as to the practice among the different builders, in proportioning the different parts, there appears, however, on the whole to be a somewhat greater uniformity in this respect now than formerly.

The steam pressure used and assumed constant in this examination is 125 pounds per square inch as against 100 pounds in the former discussion. Notwithstanding this, the constants obtained in the two different discussions show in many instances a remarkably close similarity. The changes that have taken place seem to have been in direct accordance with the increase in pressure and speed.

In such parts as the piston rod, which can be based on rational treatment and designed for strength and rigidity, the results agree very closely. The results also agree very closely in the case of the connecting rods of the low speed engines. In the case of the connecting rods of the high speed engines there is an increase in the mean value of the factor C in the expression $b = C \sqrt{DL_c}$ from .057 as found by Professor Barr to .073 as found in the present discussion. This, since the factor of safety varies as the fourth power of the factor C, more than doubles the factor of safety. It increases from 27 to 60. While a factor of safety of 60 seems unnecessarily large and uncalled for, it may partly be accounted for by the increased steam pressure and speed used in recent years.

The relation between the thickness of the cylinder walls and diameter of cylinder is practically the same now as formerly.

---

[1] *Trans. A. S. M. E.*, 18:737.

The area of the crosshead shoes presents some differences. The present investigation shows the relation between the area of the crosshead shoes and the area of the piston to be the same for both high speed and Corliss engines and gives a value which is about half way between what was found to be current practice for high speed and low speed engines ten years ago. The present value of C in the relation $a = CA$ gives $C = .53$ for both high speed and low speed engines as against $C = .63$ for high speed and $C = .46$ for low speed engines in the previous examination. This gives an increase of about 45% in the unit bearing pressure on crosshead shoes in the case of high speed engines and an increase of about 8% in Corliss engines over what was formerly found to exist. Improved methods of lubrication probably account for this in part.

In treating the crank pin and crosshead pin in the present discussion it was deemed more satisfactory to consider them on the basis of strength rather than on the basis of bearing pressures and friction alone as was done in the former discussion. The ratio of length to diameter of the crosshead pin is found to be practically the same now as formerly. Owing to the difference in the method of treatment of the crosshead pin, the result obtained in the two cases can not be compared directly, but by substituting the mean values as found in this present investigation, the mean value for an expression similar to the one used by Professor Barr can be obtained. Knowing that

$$l = 1.25\,\mathrm{d}$$

$$\text{and that } \mathrm{d} = .25\,\mathrm{D}$$

these values can be substituted in the expression $a = l\,\mathrm{d} = CA$ as used by Professor Barr and the corresponding value of C found. From the above expression

$$C = \frac{l\mathrm{d}}{A} = \frac{1.25\,\mathrm{d} \times \mathrm{d}}{\pi/4\,\mathrm{D}^2} \quad \frac{1.25 \times .25\,\mathrm{D} \times .25\,\mathrm{D}}{.78\,\mathrm{D}^2} = .10$$

The mean value of C as found by Professor Barr was .08. This shows a slight increase in the ratio between the projected area of the crosshead pin and the area of the piston.

In order to obtain a comparison for the crank pin, values for high speed engines were plotted for the equation $l = C \times \frac{H.P.}{L} + B$ as used by Professor Barr. where l = length of crank pin; and L = length of stroke. The results are shown in Fig. 42.

B = 1.6 in.
mean value of C = .28
maximum value of C = .35
minimum value of C = .14

The corresponding values obtained by Professor Barr are

B = 2.5 in.
mean value of C = .30
maximum value of C = .46
minimum value of C = .13.

These values show that for the same Horse Power and length of stroke there is a considerable reduction in the length of the crank pin. This figure also shows that there exists, among the different engine builders, a much greater uniformity in proportioning the crank pin now than formerly. In treating the crank pin for strength, however, as was done in the present investigation, there is, as shown by Fig. 20, even a greater uniformity exhibited than is shown by Fig. 42.

The ratio of length to diameter of main journals is almost identical in the two cases. And so also is the ratio of projected area of journals to the area of the piston. In the expression $d = C \sqrt[3]{\frac{H.P.}{N}}$ there is in the case of the high speed engines a decrease in the coefficient C from 7.3 to 6.6 which gives a corresponding decrease in the diameter. In the case of the Corliss engines a comparison of the diagrams shows that there has not been much change in the value of the diameter of main journals although the above relation seems to be better expressed in a slightly different manner at the present time.

In the case of the weight of fly wheel, if Professor Barr in his examination used the weight of rim of fly wheel only, then there is no comparison between the results obtained then and now. But if the total weight of wheel was used in plotting, in the former case, then for engines up to about 175 Horse

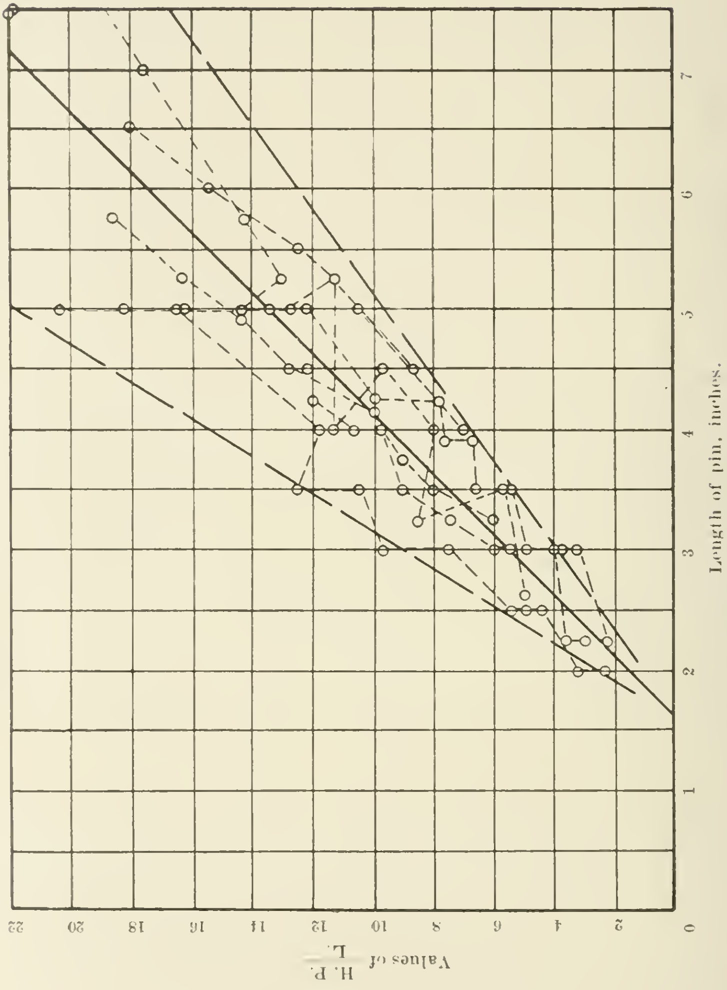

Fig. 42.—Length of Crank Pin High Speed Engines.

Power there is a fairly close similarity in the two cases, the present tendency showing an increase in the weight of fly wheels, a condition resulting no doubt from the exacting requirements of speed regulation of recent years.

The velocity of fly wheel rim is practically the same now as formerly. In the case of the number of square feet of belt surface per Horse Power, there is a great reduction in the factor C in the relation $S = C \times H.P.$ In the case of the high speed engines, C has a value of 26.5 now as against 55 in the former discussion. This, seeing that the velocity of the fly wheel rim is the same now as formerly, must mean a decrease in width and a corresponding increase in thickness of belts used for the same amount of power transmitted, at the present time.

In the expression $w = C \frac{D^2}{NL^2}$ for the weight of the reciprocating parts, C shows an increase from a value of 1,860,000 ten years ago to a value of 2,000,000 at the present time.

The weight of the engine per Horse Power shows a decrease of 29% in the case of the high speed engines and a decrease of 25% in the Corliss engines below what it formerly was. The constants in the relation $w = C \times H.P.$ are 82 and 132 now as against 115 and 175 in the former discussion, for the high speed and Corliss engines, respectively. In fact, lightness of construction, good workmanship and materials of the greatest strength and durability are among the factors which have brought about the improvement of the steam engine and made possible the fulfillment of the present day requirements.

UNIVERSITY OF WISCONSIN

MADISON

DEPARTMENT OF STEAM ENGINEERING

Storm Bull, Professor.

Thesis Investigating on the Current Practice in Proportioning Steam Engine Parts, by O. N. Troolen.

(Manufacturer)
(Address)

Gentlemen:—In view of the fact that there is very little data published regarding current practice in proportioning steam engines, we are attempting to compile such information as may be available and wish to secure your cooperation in the matter.

Other objects in view are to add, if possible, some information which may assist in establishing a uniform basis for design, to obtain safe values from acknowledged successful practice, and to express the constants that are thus derived in mathemathical form, and in this way make data available for use, which will bring theory and practice into closer and more intimate contact.

In order to handle a problem of this nature in a satisfactory manner, a knowledge of the details of the various engine parts is essential. For this reason we are asking a series of questions, which are enclosed, and also desire blue prints of such parts as the piston, crosshead, connecting rod, governor, etc.

If you will kindly enclose as many such prints as possible and give the information requested regarding the various engine parts, as well as such formulas and constants as you are accustomed to use in your design, we shall appreciate this assistance very highly.

Yours respectfully,

Kind of engine, horizontal or vertical ....
Used for electric lighting? ....
Direct connected? ....
Center crank or side crank? ....
Length of stroke ....
Diameter of cylinder ....
Initial pressure ....
Most economical point of cut-off ....
I. H. P. of engine ....
B. H. P. of engine ....
R. P. M. of engine ....
Size of steam pipe ....
Size of exhaust pipe ....
Total length of engine frame ....
Total width of engine frame ....
Total weight of engine complete ....

CYLINDER

Material used ....
Ultimate strength of material used ....
Thickness of cylinder walls ....
Separate liner used for cylinder? If so, thickness of same....
....
Thickness of cylinder flange for holding cylinder covers .....
Thickness of cylinder head at center ....
Thickness of cylinder head where bolted to cylinder..........
Distance between piston and cylinder head when piston is at end of stroke ....
Total clearance in per cent. of cylinder volume ....
Diameter of bolt circle in cylinder head ....
No. of bolts ....
Diameter of bolts ....
If steam jacket is used, width of steam space ....
Thickness of steam jacket wall ....
Diameter of cylinder drain pipes ....
Size of relief valves, if any ....

PISTON

Type of piston used ....
Material used ....
Thickness of shell if box type piston is used ....
Least thickness of piston if solid type is used................
Width of face of piston ....
Depth of slots for rings ....
No. of rings ....
Width of rings ....
Outside diameter of rings before being cut ....
Greatest thickness of rings ....
Least thickness of rings ....

PISTON ROD

Material used ....
Diameter ... .
Total length, end to end ....
Length between piston and crosshead ....
Piston rod end, how fastened to piston ....
Piston rod end, how fastened to crosshead ....

CROSSHEAD

Material used in main part ....
Material used in bearing part ....
Length of crosshead shoes ....
Width of crosshead shoes ....

GUIDES

Material used in main part ....
Material used in bearing part ....

CROSSHEAD PIN

Material used ....
Total length ....
Length of bearing part ....
Diameter of bearing part ....

CONNECTING ROD

Material used ....
Total length ....
If of circular section, diameter near crosshead ....
Diameter near crank pin ....
Diameter at middle ....
If of rectangular section, height of section near crosshead....
Breadth of section near crosshead...........................
Height of section near crank pin ....
Breadth of section near crank pin ....
If strap connection is used, width of strap ....
Thickness of strap ....
Material used for strap ....
Wearing material used for boxes ....

CRANK PIN

Material used ....
Total length ....
Length of bearing part ....
Diameter of bearing part ....
How fastened to crank arms ....

CRANK ARMS OR DISCS

Material used ....
If crank arms are used, dimensions of least cross-section......
....
If crank discs are used, width of same ....
Total amount of balance weight for each disc if center crank
....
Total amount of balance weight if side crank ....
Distance of center of gravity of balance weight from center of crank shaft ....

CRANK SHAFT

Material used ....
Total length ....
Length of both journals ....
Diameter of both journals ....
Diameter of shaft where fly wheel is attached ....
Distance from center to center of journals ....
Wearing materials used in boxes ....

FLY WHEELS

Outside diameter ....
Width of face ....
Thickness of rim ....
Thickness of flanges of rim, if any.........................
Thickness of metal of hub ....
Length of hub ....
No. of spokes ....
Taper of spokes ....
Least cross-sectional area of spoke ....
Greatest dimension of this area ....
Least dimension of this area ....
One or two fly wheels used? ....
Total weight of one wheel ....
Horizontal distances between centers of fly wheels and center line of engine ....

VALVE ROD

Material used ....
Length of rod ....
Diameter of rod ....
Le[illegible]th of rocker arm if used ....

ECCENTRIC ROD

Material used ....
Length of rod ....
Diameter of rod ....

ECCENTRIC SHEAVE

Material used ....
Diameter ....
Thickness ....
Eccentricity of eccentric ....
Diameter of crank shaft where eccentric is attached ....

ECCENTRIC STRAP

Material used ....
Thickness of maximum cross-section ....
Thickness of minimum cross-section ....
Width of flanges ....
Thickness of flanges ....

PENDULUM GOVERNOR

(See accompanying diagram)

Kind of governor used ....
No. of balls ....
Weight of one ball ....
Weight of central load on spindle ....
At what speed will governor begin to act?..................
Give values for (r) and (h) at this point ....
At what speed will governor reach its upper limit? ....
Give values for R and H at this point ....

SHAFT GOVERNOR

(See accompanying diagram)

Weight (A) suspended in each arm ....
Total weight (including arm and weights A) ....
Distance of point of suspension of arm from center of crank shaft (O B) ....
Distance of center of gravity of weights (A) from center of crank shaft ....

Length (h) of lever arm of spring ....

Angle that spring makes with normal to lever arm ....

Diameter of wire used for helical springs ....

Outside diameter of coil used ....

No. of turns of wire used ....

Movement of arm—is it caused by centrifugal force? ....

or angular acceleration? ....

or tangential acceleration? ....

Angle of advance (△) of the eccentric ....

Area of steam port ....

Width of steam port ....

Area of exhaust port when separate from steam port ....

Width of same ....

Volume of steam chest ....

Thickness of steam chest wall ....

Type of valve used ....

Total travel of valve ....

Inside lap ....

Outside lap ....

Amount of lead used ....

Angle of advance of eccentric ....

413

BULLETIN OF THE UNIVERSITY OF WISCONSIN

NO. 264

ENGINEERING SERIES, VOL. 4, NO. 6, PP. 413-500

SELF-EXCITED POLYPHASE ASYNCHRONOUS GENERATORS

BY

LEWIS FUSSELL, M. S.

A THESIS SUBMITTED FOR THE DEGREE OF DOCTOR OF PHILOSOPHY
UNIVERSITY OF WISCONSIN
1907

*Published bi-monthly by authority of law with the approval of the Regents
of the University and entered as second-class matter at the
post office at Madison, Wisconsin*

MADISON, WIS.
DECEMBER, 1908

415

CONTENTS

PAGE
CHAPTER I.—Historical 5
  Heyland's Diagrams 7
  Heubach's Improvement 12
  Ossanna's Diagram 14
    Torque 16
    Mechanical power 17
    Efficiency 17
    Slip 18
  Grob's Diagram 19
    Generator 22
    Motor 22
    Sink of energy 22
  Grob's 1904 diagram 22
    Torque 24
    Mechanical power 25
    Slip 25
  Oerlikon Three Phase 20-Horse Power Motor 26
  General Electric Co.'s Motor, No. 71602 30
  General Electric Co.'s Motor, No. 2577 33
  Westeras Motor 35
  Brown, Boveri Motor, No. 193913 38
  Slip Scale for hypersynchronism 45
APPENDIX TO CHAPTER I 54
  Kuhlmann's Diagram 54
CHAPTER II.—Self-exciting Asynchronous Generators 58
  Heyland's Diagram for Compensated Motors 59
  Oscillograms 64
  The Machines 76
BIBLIOGRAPHY 85

PLATES

PAGE
Plate I. The Heyland Diagram........................... 8
Plate II. Heyland's Improved Diagram....................... 10
Plate III. Heubach's Diagram........................... 12
Plate IV. Diagram of Ossanna........................... 16
Plate V. Hugo Grob's Diagram........................... 21
Plate VI. Diagram of Hugo Grob. 1904....................... 23
Plate VII. Oerlikon 20 Horse Power 3 Phase Induction Motor.. 27
Plate VIII. Oerlikon 20 Horse Power 3 Phase Induction Motor.. 29
Plate IX. Five Horse Power Induction Motor. G. E. No. 71602 31
Plate X. Five Horse Power Induction Motor. G. E. No. 71602 32
Plate XI. Five Horse Power Induction Motor. G. E. No. 2577 34
Plate XII. Five Horse Power Induction Motor. G. E. No. 2577 36
Plate XIII. Westeras 100 Horse Power 3 Phase Induction Motor 37
Plate XIV. Westeras 100 Horse Power Induction Motor........ 39
Plate XV. Westeras 3 Phase Induction Motor................ 40
Plate XVI. Grob Diagram of Brown Boveri 3-Phase Induction Motor 41
Plate XVIIa. Brown Boveri 5 Horse Power 3 Phase Induction Motor 42
Plate XVIIb. Brown Boveri Induction Motor................ 43
Plate XVIII. Connections 46
Plate XIX. Condenser Excitation and Pump. Back Connections 47
Plate XX. Curve I From Motor Slip Line Continued. Curve II From Corrected Slip Line........................... 50
Plate XXI. Comparison of Slip Scales...................... 51
Plate XXII. Karl Kuhlmann's Diagram...................... 55
Plate XXIII. Diagram Compensated Machine................ 60
Plate XXIV. Heyland, July 23, 1903........................ 63
Plate XXV. Oscillograms 66
Plate XXVI. Voltage Determined by Capacity............... 69
Plate XXVII. Brown Boveri Induction Generator............. 71
Plate XXVIII. Brown Boveri Induction Generator........... 72
Plate XXIX. Winding Diagrams............................ 82
Plate XXX. Heyland's Connections......................... 83

SELF-EXCITED POLYPHASE ASYNCHRONOUS GENERATORS

CHAPTER I

HISTORICAL

The science of electromagnetism received its inception when Hans Christian Oersted, a Danish physicist, discovered on July 21, 1820, the effect produced upon a magnetic needle by the passage near it of an electric current. This discovery stimulated Andre Marie Ampere, who made public, in 1822, his laws of parallel currents: and Michael Faraday, who described first the revolution of a magnet around an electric current, and later his famous "Faraday disc" experiment.

Dominique Francois Arago[1] in 1825, made a magnetic needle follow the revolutions of a copper disc beneath it.

Then follows a long unfruitful period, until in 1879, Walter Baily[2] by the progressive shifting of the poles of two two-pole electro-magnets caused the rotation of a copper disc suspended above them. He employed two battery circuits commutated at regular intervals although he mentions that polyphase currents could well be used.

Marcel Deprez[3] in 1883 published a theorem on the true rotary magnetic field produced by two alternating fields with a quarter period phase difference.

Then follows the bitter discussion of the Tesla-Ferraris controversy, the fundamental features of which appear to be the following: Galileo Ferraris,[4] having by 1885 independently evolved the ideas of Baily and Deprez, built a motor but failed to publish until 1888. His machine was two-phase, the second one being produced by an inductance in one circuit, the "Phase-splitter" from which Tesla obtained much credit. The model used by Ferraris developed only a watt output of 2.77 watts, and of it he says: "It is at once evident and it also results from considerations which I shall go into later on that a motor thus constructed [he used a copper cylinder] would not be of any importance as a means of transforming electrical energy." Though he regarded it as a toy, he suggested its use as a meter, and gave the idea of slip, showing also that the current in the rotating secondary varies with the slip.

---

[1] *Annales de chemie et de physique,* **24:** 363 (1824); **28:** 375 (1825).

[2] *Phil. Mag.,* vol. 8, No. 49, p. 286.

[3] *Comptes Rendus,* 1883, p. 1193.

Nicola Tesla applied for in 1887, and received in 1888, a great number of patents on polyphase motors, underlying which, however, was but the one idea of rotating magnetic fields. Thus, in spite of the great advance in the commercial development which is largely due to Tesla, the invention cannot be claimed for him.

Charles S. Bradley's patents of 1887, 1888 and 1889, described generators and motors of two and (1889) three phases, the rotary field being described in October, 1888. His machines were Gramme rings with equidistant taps brought out to slip rings.

The three phase Lauffen-Frankfort transmission in 1891 of about 100 H. P. over 110 miles of millimeter wire, at a frequency of 30 to 40 cycles per second and a pressure of 8,500 volts, had an average efficiency of 74 per cent. It was a very bold attempt and awakened great interest not only in the possibilities of long distance transmission but in those of polyphase motors as well, since induction motors were used to develop power at the point of delivery.

In 1895, Alexander Heyland[5] published an account of a simplified relation between the vectors of an induction motor which gave an approximation only but which tallied very satisfactorily with the experiments he made on motors up to ten horse power. He offered no complete mathematical proof.

---

[4] *Atti di Torino*, Mar. 18, 1888.

[5] *Elektrotechnische Zeitschrift*, 1895, p. 649.

B. A. Behrend[6] gave independently a more rigorous proof of the relations of the vectors to a circle. Since, however, he very gracefully withdraws his claims to priority and since development has followed more particularly the lines laid down by Heyland, this discussion will take up more particularly Heyland's figures.

Julius Heubach, Karl Kuhlmann, Ossanna, Adolph Thomälin, and Hugo Grob have further developed the circle diagrams and their work will be shown later.

HEYLAND'S DIAGRAMS

Heyland realized the accurate relations of primary to secondary current. (See Plate I.) Here AC′ represents the primary current, I_1; AC represents the magnetizing current, I_m: and c′C′ represents the secondary current, I_2. For accuracy the length c′C′ must be determined as the length of a line through C between its intersections with the semi-circles CC′D and Cc′A. The pressure line is AE.

Heyland neglects primary resistance in his electrical calculations and sets $I_1 = I_2$. This is for purposes of simplification and is not such a violent assumption as might appear at first sight, since CD is always very large as compared with AC.

"This gives us the law: In induction motors the relations between pressure and phase displacement may be represented by a vector diagram in which the vector, changing with the load which represents the current, is defined, in that its free terminus moves upon a circle whose position is defined through the relation

$$\frac{AD}{AC} = \frac{\text{Magnetic Resistance Strayfield}}{\text{Magnetic Resistance Rotorfield}}.$$

Plate I, shows AB the pressure line; AC the magnetizing current; CC° the energy component, their resultant AC° being the no-load current. The length CC° represents "The constant

---

[6] *Ibid.*, Feb. 1896.

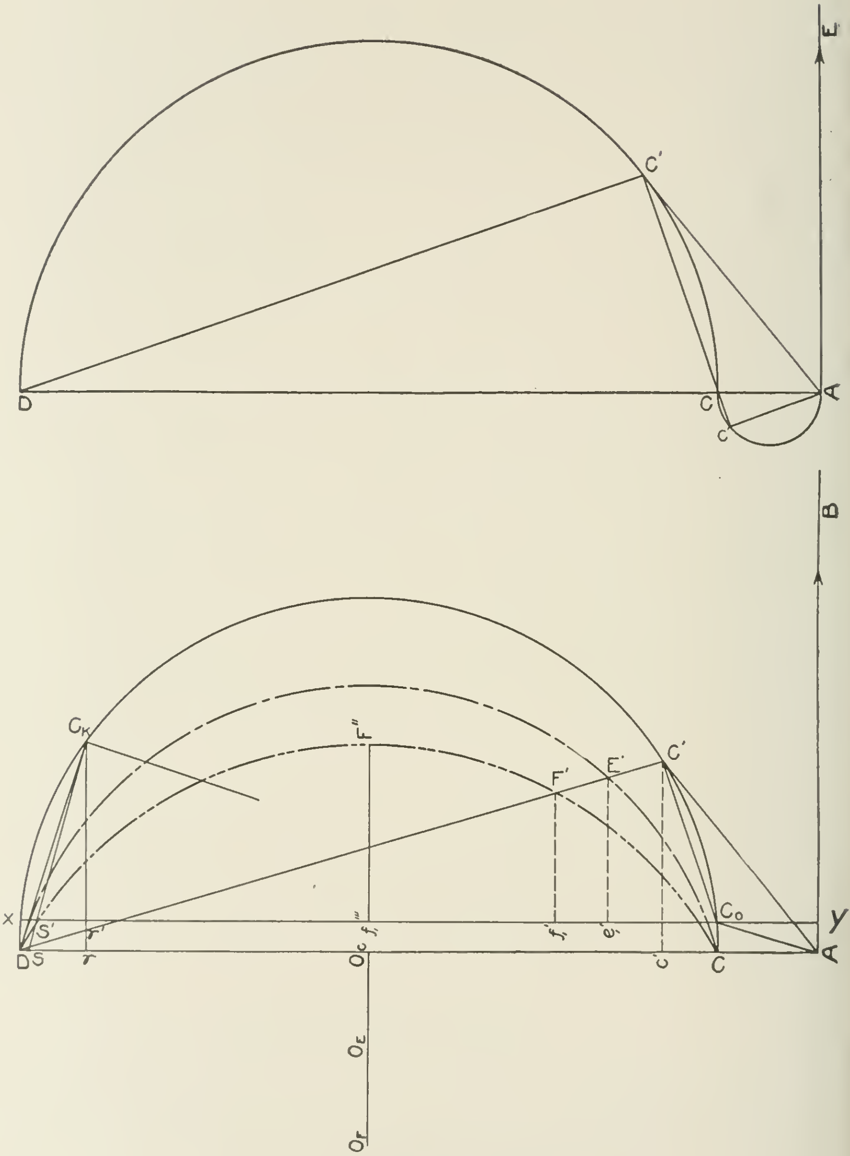

Plate I.—The Heyland Diagram.

friction and iron losses, and the copper loss of the magnetizing current.'' $I_1 = AC'$: $I_2 = C^{\circ}C'$; the angle of phase displacement is the angle BAC′.

Draw DC′, subtract along this line a length proportional to I_1R_1, giving the point E′; and from DE′ subtract I_2R_2 giving F′. Draw circles through DE′C and DF′C with centers on a perpendicular dropped from O_c.

A perpendicular let fall from C′ at any load represents electrical input, since in any triangle with constant base the area is proportional to the altitude.

Primary stray flux really C′A is assumed by Heyland to be equal to CC′ which is the case when AC becomes zero. In the triangle DCC′, therefore, the electric input varies as the area, since it is equal to rotor flux times primary stray flux. Since the base CD is constant, the electric input varies as the altitude of the triangle DCC′.

Similarly, perpendiculars dropped from E′ and F′ represent torque and power output, but the constant losses CC° must be subtracted, giving torque equal to E′e′; power equal to F′f.′

The maximum power output does not coincide with the maximum power input nor with the maximum current in primary nor secondary.

As C″ swings around counter-clockwise E′ and F′ also revolve and the maximum power output occurs when F′ reaches the perpendicular through O_c. Further increase in current decreases the output until the output becomes zero, when F′ and D coincide, the motor comes to a standstill, E′ and C′ assume the positions E^k and C^k such that DC^k is perpendicular to O_fD, that is, tangent to the power circle. The perpendicular from E^k represents starting torque, that from C^k power input while AC^k and C_oC^k represent I_1, and I_2 respectively .

Slip is the ratio $S = \frac{\omega_1 - \omega_2}{\omega_1}$ where ω_1 is 2π times the primary frequency in cycles per second, and ω_2 corresponds for the secondary frequency. Since the frequency of the secondary depends upon its speed of rotation, at standstill $\omega_2 = 0$ and $S = 100$ per cent.

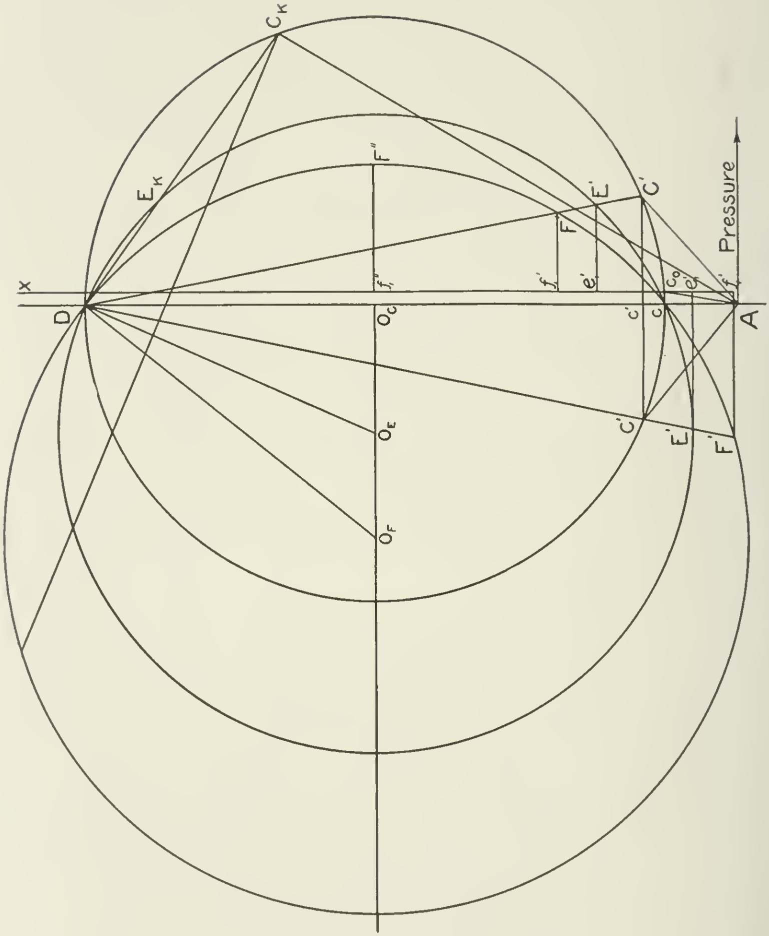

PLATE II.—HEYLAND'S IMPROVED DIAGRAM.

If we lay off SC^k perpendicular to O_eD, we may divide SC^k into 100 alloquot parts, each of which represents 1% slip, which may therefore be read off directly for any load as the distance sS′ along sC^k from the base line AD to the intersection with the line DC′ for that load. Approximately $Y'C^k$ represents the efficiency at the same load since YY′ represents the losses.

This figure is the one commonly intended when Heyland's diagram is mentioned.

The power factor cos ϕ is of course a maximum when AC′ comes nearest to AB, that is when it is tangent to the circle O_c

"The characteristic of the induction motor is known that, if driven above synchronism, it works as a generator[7] and delivers current in a manner analogous to the direct current shunt machine. It is interesting that the diagram gives explanation of these relations simply by completing the circles to the left of AD—." Plate II. "The electric energy delivered by the generator at the same phase angle is exactly equal to the electric energy delivered to the motor, [This is not accurate] The mechanical power becomes naturally considerably higher and indeed as is easily seen by twice the losses since now all losses are added to the electric power which were formerly subtracted from it."[8]

He plots curves of all quantities with respect to mechanical power, but since all later writers plot with respect to slip the consideration of his curves is not of the highest importance. He makes no explanation of the phenomena from + 100% to ∞ nor from ∞ to — 100% simply saying that from o to + 100% slip the machine functions as a motor and everywhere else as a generator. Some power could conceivably be abstracted from the rotating secondary, electrically, but the better conception is that from + 100% to — 100% slip through ∞ the machine acts merely as a sink of energy requiring both mechanical and electrical input and giving no output except heat.

---

[7] See Danielson, *Elec. World,* 1893, **21:** 44.

[8] Ernst Danielson, Westeras, Sweden, gave in *Electrical World* for Jan. 21, 1893, a description of experiments performed by him. Having a three phase induction motor on a synchronous generator, he reversed the power and the synchronous machine ran as a motor. "This field is capable of maintaining the current, provided the conditions in the external circuit are such that the current comes in advance of the induced E. M. F. These conditions can be fulfilled by having a regular three phase generator in circuit, or by condensors. It would be impossible to have the motor act as a generator on a regular lamp circuit or on a circuit with self induction." He took no quantitative observations.

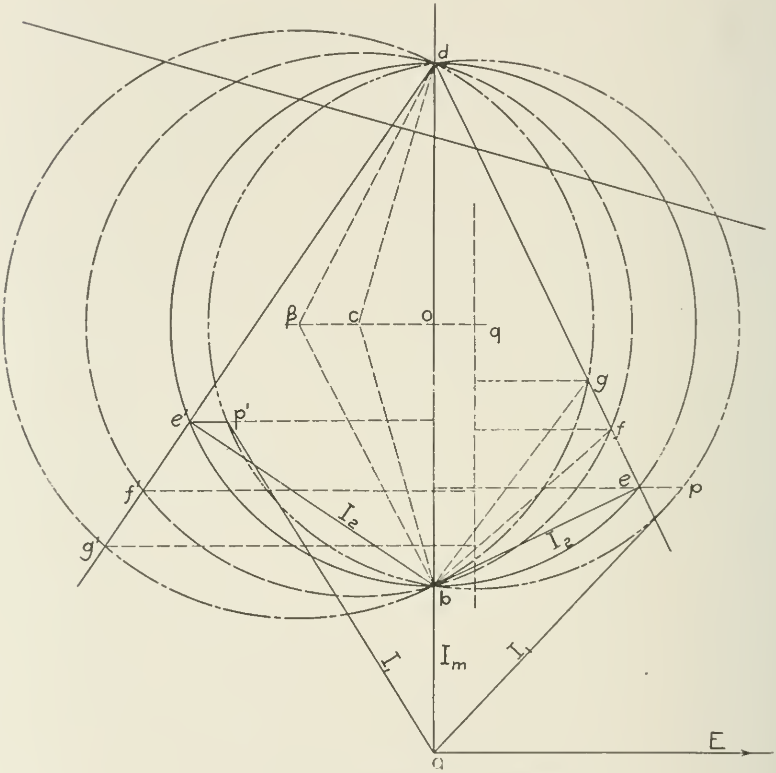

PLATE III.—HEUBACH'S DIAGRAM.

HEUBACH'S IMPROVEMENT

Julius Heubach shows his opinion as to the magnitude of the problem very succinctly in the preface to his book *Der Drehstrommotor*.

"The motor although simple in its mechanical relations is correspondingly complicated in the electrical phenomena which occur within the machine; yes, one can say that from the theoretical standpoint, the asynchronous (Induction) motor is the most difficult problem with which electrotechnics has to deal."

Plate III is based on the assumption that $\cos \phi_2 = 1$, and shows the condition of the induction machine from $+\infty$ to $-\infty$, the circle with center at o being the original circle used by Heyland. Heubach considers the electrical input of a motor and output of a generator as being on a circle whose center is at q so chosen that ep shall represent the losses due to hysteresis and eddy currents. The line ap, therefore, represents I_1; the perpendicular let fall from p to ad the electrical input: ep = hysteresis and eddy current losses; be $= I_2$; perpendicular from e to ad = electrical input minus hysteresis and eddy current losses. Now if de be drawn from d the effective flux is obtained, which is again reduced by losses due to leakage in stator and in rotor.

Laying off distances ef and fg such that $\frac{\text{e f}}{\text{b e}} = R_1 = \tan < \text{ebf}$ and $\frac{\text{f g}}{\text{b f}} = R_2 = \tan < \text{fbg}$

flux values df and dg are obtained proportional to input and output of the secondary respectively. Next lay off from the line ad the $<$s ob c = ebf $= \alpha$ and obβ = fbg $= \beta$ and describe circles whose centers lie on the points of intersection of the sides bα and bβ with a perpendicular to ad from the point o. Then draw a straight line parallel to ad and at such a distance as to represent the losses due to bearing friction and windage. Then perpendiculars let fall from f and g on this line will give by their length values of torque and mechanical power.

Output will increase in the motor as p swings around counterclockwise until g reaches the line oq prolonged, its maximum ordinate, thereafter though I_1 and I_2 increase the output decreases steadily until, when the line de becomes tangent to the circle whose center is B, the output becomes zero and g and d coincide. This is the point of standstill or 100% slip and a line drawn at right angles to ed through this point may be divided into 100 parts, each of which represents 1% slip. For any load the slip may be read directly from the slip-line, or any proportionally divided parallel line, being the length along the slip-line from ad to the intersection with the line de at that load.

Heubach says: "This figure shows the Heyland diagram for all possible conditions and it occurs peculiarly in it, that the scales for positive and negative slip are different. This peculiarity is demanded because the loss of potential in the stator winding is not considered with entire accuracy, since in this study Stator—is set equal to Rotor — current." The angle of inclination of the slip line is of course the same for positive or negative slip. On the motor side the intersection of the slip line with the solid circle is the point of 100% slip; while on the generator side the point of 100% slip is the intersection with the dot-dash circle whose center is at B.

As in the consideration of the induction machine as a motor so as a generator, the primary current I_1 is measured from a to the intersection of the dash-double-dot circle with a perpendicular from ad to the point of particular load. p′ to ad = electrical power output; e′p′ = loss through hysteresis and eddy currents; e′ to ad = total electrical power. Drawing de′ obtain points f′ and g′ giving the increased fields df′ and dg′ which must be developed to care for the stator and rotor losses. From f′ to the line parallel to ad gives the resistance moment or negative torque, while from g′ to the same line gives mechanical energy input. $I_2 = be'$, $I_m = ab$. As p′ revolves counter-clockwise the output rises to a maximum over point o and comes to zero when point p′ reaches d.

This is the point of — 100% slip and any further increase in speed throws the electrical power into the opposite direction, *i. e.* both mechanical and electrical power are consumed and turned into heat. This continues from — 100% to — ∞ slip and is the same condition of brake or sink of energy as is found from + 100% to + ∞ slip.

OSSANNA'S DIAGRAM

Ossanna has done a great deal toward the elucidation of induction motor problems by his diagram published in 1899.[9]

---

[9] *Zeitschrift für Elektrotechnik*, May, 1899. *Elektrotechnische Zeitschrift*, Aug. 23, 1900.

Of it Ossanna himself says, " . . . it is strictly accurate since in recognizing the voltage drop in the primary winding, the total primary current and not merely its watt component is considered, and further my representation of slip, torque, mechanical power and efficiency are simpler than in Heyland's diagram."

M. Breslauer says of it, "This corrected diagram is alone right and every graphical representation must be based upon it."[10]

Karl Kuhlmann says: "The Ossanna diagram in its ordinary form [see Plate IV] answers the following question: How does an asynchronous polyphase motor, with a rotor short-circuited and with a constant coefficient of self-induction, behave?"[11]

All of Ossanna's predecessors had built up diagrams for constant *back* e. m. f. and constant angle of secondary lag angle ϕ_2, but these are not the conditions in the actual motor where we have instead constant impressed e. m. f. and constant secondary inductance L_2.

Taking up the figures of those who had worked before him he showed them to be inaccurate although convenient, and developed his accurate figure. In this constant impressed e. m. f., varying I_1, slip, and efficiency η, are the only qualities represented since the loci of the free ends of the flux and I_2 vectors bear no simple relation to the rest of the figure although they may be drawn for any particular load.

Ossanna's development follows:

Take A_1 = terminal pressure
K = reactance of primary per phase
im $= \frac{A_1}{K}$
$\sigma = 1 - v_1 v_2$ (where v_1 and v_2 are less than unity. Stray factors)

$$\text{Then Xo} = \frac{A_1}{K} \frac{\beta}{2\alpha} \text{ and Yo} = \frac{A_1}{K} \frac{\gamma}{2\alpha}$$

$$\text{R (radius)} = \frac{A_1}{K} \frac{1}{2\alpha} \frac{1 - \sigma}{\sigma}.$$

---

[10] *Elektrotechnische Zeitschrift,* Mar. 3, 1904.

[11] *Ibid.,* Apr. 18, 1901.

Where $\alpha = 1 + \frac{2\pi n_1 L_1}{K} \cdot \frac{1+\sigma}{\sigma} + \frac{1}{\sigma} \frac{W_1{}^2 + 2\pi n_1 L_2{}^2}{K^2}$

$$\beta = \frac{1}{\sigma}\left(1 + \sigma + 2\,\frac{2\pi n_1 L_1}{K}\right)$$

$$\gamma = \frac{1}{\sigma}\,\frac{2W_1}{K}$$

These equations determine the circle with respect to the axes.

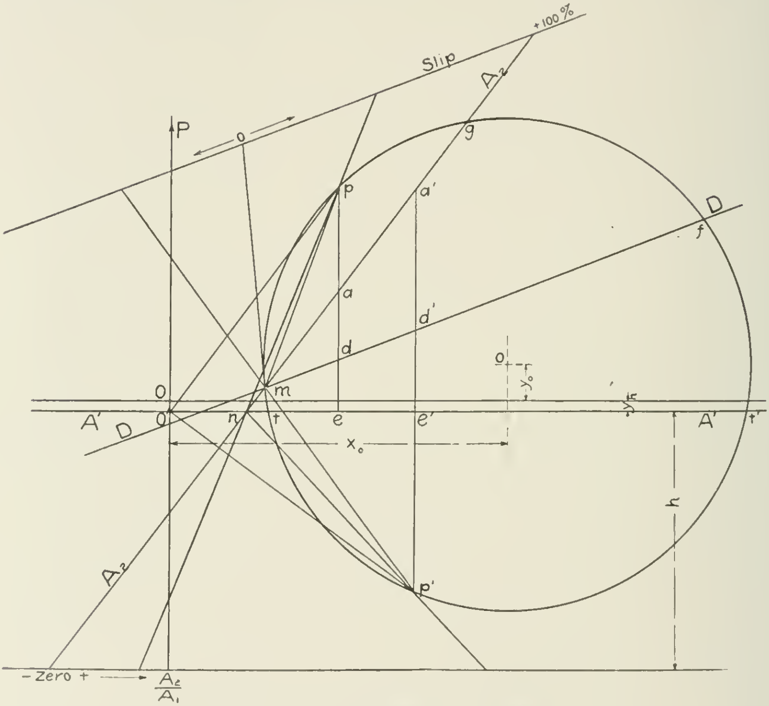

PLATE IV.—DIAGRAM OF OSSANNA.

Torque.—To obtain values of torque instead of drawing an extra circle as Heyland does, draw the line DD whose equation is $Z = rx - T$

(Z is ordinate, x abscissa)

$$r = \frac{w_1 \frac{\beta}{\alpha}}{K - w_1 \frac{\gamma}{\alpha}}, \text{ and } \mathbf{T} = \frac{l_1}{K} \cdot \frac{w_1 \frac{1}{\alpha\sigma}}{K - w_1 \frac{\gamma}{\alpha}}$$

Absolute torque in meter-kilogrammes may be obtained as

$$D = \frac{p}{9.81}\frac{v_1}{v_2}\cdot\frac{1}{2\pi n_1}\left(K - w_1\frac{\gamma}{\alpha}\right)\frac{I_1}{K}(y - z)$$

$(y - z)$ = the distance pd in the figure which for any load is representative of torque.

Mechanical Power.—Draw for mechanical power the line A_2A_2 whose equation is $Z = Vx - u$

$$\text{where } V = \frac{w_1\frac{\beta}{\alpha} + w_9{}^1 v}{K - w_1\frac{\gamma}{\alpha} - w_2{}^1\mu}$$

$$u = \frac{\frac{I}{K}\cdot\frac{w_1}{\alpha\sigma} + w_2{}^1\rho}{K - w_1\frac{\gamma}{\alpha} - w_2{}^1\mu}$$

$$\mu = \frac{\gamma}{\alpha}\frac{w_1{}^2 + (K + 2\pi n_1 L_1)^2}{K^2} - 2\frac{w_1}{K}$$

$$\text{and } w_2{}^1 = (w_2 \text{ reduced to primary}) = w_2\frac{1}{1-\sigma}\left(\frac{z_1}{z_2}\right)^2\left(\frac{f_1}{f_2}\right)^2$$

$$v = \frac{\beta}{\alpha}\cdot\frac{w_1{}^2 + (K + 2\pi n_1 L_1)^2}{K^2} - 2\frac{K + 2\pi n_1 L_1}{K}$$

$$\rho = \frac{1}{\alpha\sigma}\cdot\frac{w_1{}^2 + (K + 2\pi n^1 L_1)^2}{K} - 1$$

The absolute value in watts per phase

$$A_2 = \frac{\gamma_1}{\gamma_2}\left(K - w_1\frac{\gamma}{\alpha} - w_2{}^1\mu\right)\frac{I_1}{K}(y - z)$$

Here $(y - z)$ = distance pa in the figure which is proportional to mechanical power for any load.

Efficiency.—Parallel to the base line and at distances yh and h draw two right lines.

yh = watt component of I_1 which represents the hysteresis and eddy current losses.

All electric quantities are measured from the line A_1A_1 (distant yh from the X axis) as for instance pe = watts input, $O^1p = I_1$.

Call the point of intersection of A_1 and A_2 n.

$$h = 100 \frac{w_1 \frac{\beta}{\alpha} + w_2{}^1 v}{K}$$

Lay off along the line distant from the X axis yh + h parts proportional to the same scale as the line h and with the intersection with A_2 as zero. This will represent the relation $\frac{A_2}{A_1}$ which is efficiency η for a motor, $\frac{1}{\eta}$ for a generator, and negative for the positions of sink of energy.

Slip.—For slip draw parallel to DD a line, draw tangent to m a line to intersect the above and call the common point zero slip. The point of + 100% slip is at the intersection of the slip line and A_2 while — 100% is at an equal distance the other side of the line of zero slip.[12] To obtain the per cent slip for any line prolong pm to the slip line and read. Similarly for $\%\eta$ draw pn to the efficiency line and read.

From m to t both mechanical and electrical power are required to be put in and there is no output but heat. At t^1 the primary current has a lag of 90° ($\cos\phi = 0$) and I_1 is therefore entirely wattless, this being about the only place in electrotechnics where a lag of exactly 90° can be obtained.

From t to t^1 the machine acts as a generator, from m to g as a motor, and from g to t^1 through f as a sink of energy.

Plate IV shows a motor with highly exaggerated leakage, high resistance in both primary and secondary, and large iron losses, so that all the parts and processes may be made more clear.

The greatest values of mechanical power, torque and electric power, occur at points where the perpendicular to the lines A_2, D, and A_1, respectively, have their greatest lengths.

The difficulty of determining the distances y_0, X_0, yh and h and the points m and n, the fact that secondary current and the fluxes are not represented have prevented the adoption of Ossanna's diagram to so large an extent as its accuracy would seem to make probable. The necessity of converting experimental values into analytical geometry and then putting that into a figure also obscures the direct connection of machine and figure.

---

[12] The point of — 100 per cent. slip should be at the point where t'm prolonged cuts the slip line, but Ossanna's figures show an error in this point.

GROB'S DIAGRAM

Hugo Grob describes ". . . a theoretically absolutely correct polyphase induction motor diagram which has no negligibilities other than the inevitable assumption of constant permeability of the iron; of sine form of current, pressure and fields; and farther the not quite accurate allowance for iron losses."[13]

It is a diagram of constant terminal pressure and the main circle, the locus of the free terminus of primary current vector, is the same as Ossanna's although more readily located. Heyland's approximate diagram is easy to make but not nearly accurate, while his accurate one is very complicated. Ossanna brings to bear analytical geometry and deduces equations for circle and lines which represent primary current, phase angle, output, slip, etc., but has not the fluxes nor secondary current and does require some not inconsiderable calculation.

Grob develops his diagram without using analytical geometry nor higher mathematics as follows:

On a line OZ (Plate V) lay off

$$AD = \frac{1}{T_1 + T_2} \text{ OA or more accurately}$$

$$AD = \frac{1}{T_1 + T_2 + T_1 T_2} .OA$$

where T_1 and T_2 are the usual leakage factors (here taken equal to .2). Lay off $OB : BA = T_2 : T_1$ more accurately $= (T_2 + T_1 T_2) : T_1$, erect DG perpendicular to OZ at D so that $DG : OD = T_3 : (T_1 + T_2)$ more accurately $= T_3 : (T_1 + T_2 + T_1 T_2)$ where $T_3 = \dfrac{I_1 \, R_1 \text{ at no load}}{\text{Constant terminal e. m. f.}}$

Draw OG, and a perpendicular to OZ through A cutting OG in H. On BH and HD as diameters describe circles. Draw the pressure triangle with right angle at K such that $OK : OL = T_3 : 1$.

---

[13] *Elektrotechnische Zeitschrift*, Jan. 24, 1901.

OL is the constant terminal pressure and is at right angles to HMD.

The larger circle, the locus of the points N, is Ossanna's. ON representing primary flux or current, NHQ representing secondary flux or current. Parallel to HMD and therefore perpendicular to OL through O draw OJE. Parallel to OHG through E draw the slip line; calling the intersection with the line AH produced zero slip and the point E — 100% divide up the line. Draw a line from + 100% slip through H to cut the circle at F. The point of ± ∞ slip is marked ∞.

A method is now available for representing each of the three quantities, torque, electrical, and mechanical power.

Bisect the angle CHG and draw $N_+HQ_+U_+$ (OQ represents flux).

ON_+ is I_1 at time of greatest torque. Perpendicular to OG at H draw HV. Parallel to OD at U_+ draw U_+V (U_+ is any point on line U_+N_+).

With V as center and radius VH draw a circle. UW for any load = Torque. (W on the line AH) Torque is also represented by a perpendicular let fall from N on A ∞.

Let $VU = \frac{1}{2}$ maximum horse power $= 3/2. \frac{I_2^2 \text{ (max) } R_2}{746}$.

Draw with center *U*, and radius *UH* a circle. Parallel to AH draw a line such that *DW* is the power lost in bearing friction and windage. Then *BD* = mechanical power.

Electric power, since the pressure is constant, can be represented as the watt component of the primary current, therefore from N drop perpendiculars on OL and the watt component OP is obtained. Electric power is also represented by perpendiculars let fall on the line JE (since JE is at right angles to OL).

Starting at — ∞ with either Plate V or Plate XVIIa we find a region of sink of energy. Here $I_1 = O \infty$. $I_2 = \infty Q_0$, torque = O, electrical and mechanical power both absorbed. As we slow down I_1 and I_2 grow, reaching a maximum when I_1 passes through M_1 and I_2 is parallel to OD. Mechanical power and torque grow; electrical comes to zero at — 100% slip and thereafter becomes output. At — 100%, I_1 is perpendicular to OL and is pure wattless current.

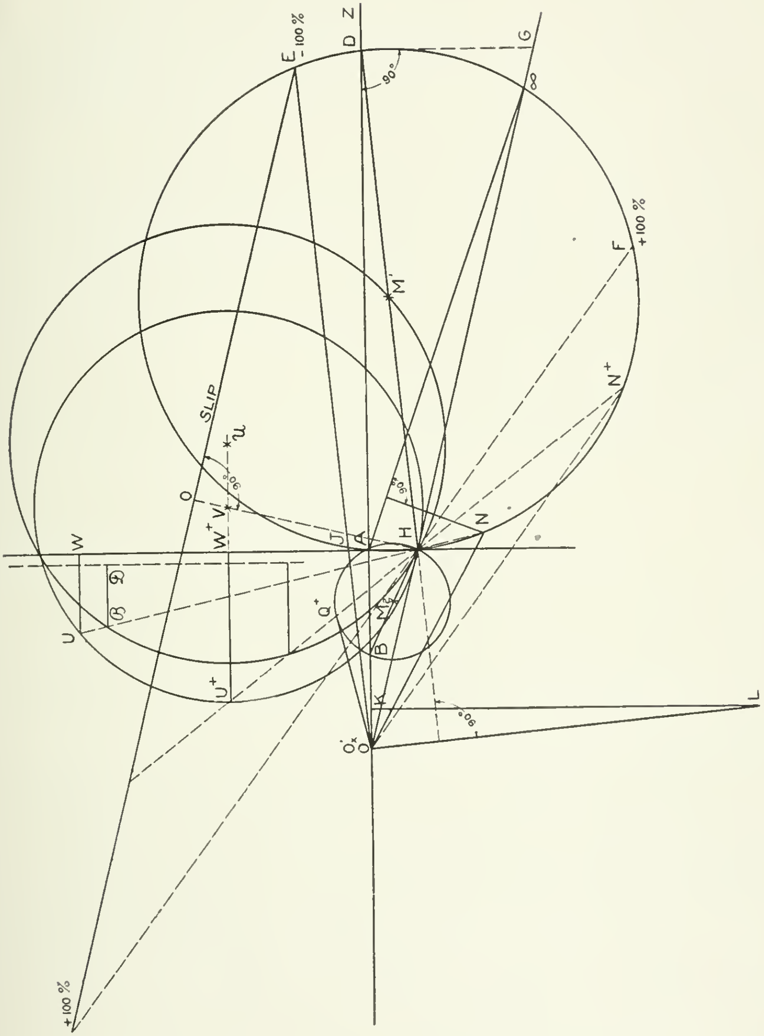

Plate V.—Hugo Grob's Diagram.

Generator.—Below —100% slip all three increase, reaching their maxima in the order, mechanical power, torque, and electrical power after which all decrease.

Sink of Energy.—At a small negative slip ($I_1 = OJ$) electrical power becomes zero again with I_1 wattless. At synchronism torque becomes zero, $I_1 = OA_1$, $I_2 =$ zero. From J to H both powers are absorbed. At a small positive slip (I_1 at H) mechanical power becomes zero.

Motor.—After passing through their zero points each has a sign opposite to that with which it started. Electrical is now input, mechanical and torque, output. All rise reaching their maxima in the order, mechanical, torque, electrical power. At + 100 per cent. or standstill mechanical power becomes zero, and electrical and torque give the starting values.

Sink of energy.—Mechanical power reverses and at $+ \infty$ we again strike the point of beginning with torque = o, mechanical and electrical power both consumed.

GROB'S 1904 DIAGRAM

In 1904[14] Grob developed another diagram, not mentioning his article of 1901 except in an introductory footnote.

The new figure (see Plate VI) differs in that it is more accurate, represents power and torque on the main circle by lines simply located, and determines the potential line somewhat differently.

He gives the method of construction and a concrete example from data for a particular motor. This example and diagrams for four other motors will be given. The constant pressure in the new figure is chosen as the basis and perpendiculars are erected to it. The leakage factors which for the 1901 circle had to be determined in order to construct the figure are now deduced from the figure. The value T_3 alone need be predetermined and it is easily obtained. The lines for torque and mechanical power (as will be proven shortly) are on the circle and he has corrected the torque line, making it the distance inter-

---

[14] *Ibid.*, June 2 and June 9, 1904.

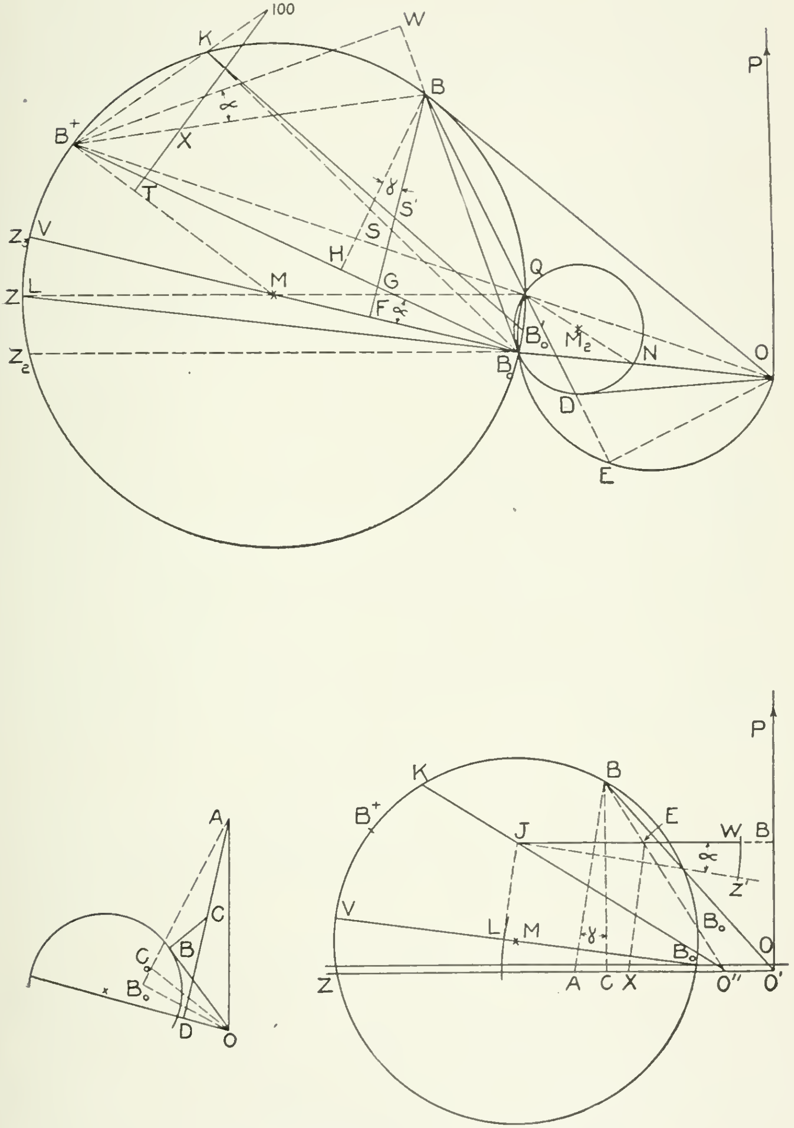

Plate VI.—Diagram of Hugo Grob, 1904.

cepted by the line B_0B^+ on the perpendicular let fall from B to the line B_0V instead of the length of the perpendicular to the line B_0B^+. Also mechanical power is obtained as the interception of the same perpendicular as for torque with the line $B_0'K$.

Total power equals the area of the triangle ODB = DB × OE. (Point E moves on the semicircle over OQ.)

The triangle BB_0D remains always similar to itself, peripheral angles of constant arc.

$$\frac{DB}{BB_0} = \text{constant} = \frac{LQ}{LN} \text{ (same peripheral angles)}$$

Therefore $I_2 = \text{chord } B_0B \times \frac{NL}{LQ}$

But $\frac{NL}{LQ} = \frac{OA}{AC_0}$

Therefore $DB = BB_0 \times \frac{OA}{AC_0}$

Also the arc OEB_0 is similar to the arc B_0BB^+, therefore the triangles also are similar and $OE = OB_0 \times \frac{B^+B}{B^+B_0}$

The vector OB_0 is the no load flux, which calls up the pressure left for developing power when ohmic and inductive drop have been deducted. This pressure is AC_0 perpendicular to OB_0.

$$OB_0 = P.\frac{AC_0}{OA} \text{ in volts.}$$

$$\text{Therefore } OE = P.\frac{AC_0}{OA} \cdot \frac{B^+B}{B^+B_0}$$

Torque:

$$DB.\ OE = B_0B.\frac{OA}{OC_0} \cdot P.\frac{AC_0}{OA} \cdot \frac{B^+B}{B^+B_0}$$

$$= P\,\frac{B_0B \,.\, B^+B}{B^+B_0} = \frac{P}{B^+B_0} \cdot B_0B \times \frac{B^+W}{\cos\alpha} \cdot \frac{2}{2}$$

$$= \frac{P \times 2}{B^+B_0 \cos\alpha} \text{ (area of triangle } B_0BB^{\times}\text{)}$$

$$= \frac{P \times 2}{B^+B_0} \times \frac{B^+B_0 \times BH}{2} = \frac{P.BH}{\cos\alpha} = P.\ BG$$

In absolute measure then

$$\text{Torque} = \frac{\dfrac{\text{P (volts)} \times \text{BG (amps.)} \times 3}{746} \times 75}{2\,\pi\,\dfrac{n}{60}} \text{ (In Kg — m)}$$

$$= 2.88\,\frac{P \times BG}{n} \text{ (In Kg — m)}$$

$$\text{or} = 208\,\frac{P \times BG}{n} \text{ (In lb. ft.)}$$

Mechanical Power: Loss in the rotor is proportional to I_2^2, or to $\overline{DB}^2$ or to $\overline{B_0B}^2$ or to B_0F, FS is proportional to the copper loss but since FG is also proportional to B_0F we can take GS as a measure of the copper losses.

Then BG — GS = BS = Power developed. To subtract bearing friction and windage, lay off B_0B_0' perpendicular to B_0V and equal to the watt current of the no load losses. Draw $B_0'K$, and BS′ is the actual mechanical power available. In absolute measure mechanical power is given by

$$\text{H. P.} = \frac{\text{P (volts)} \times \text{BS}^1 \text{ (amperes)} \times 3.}{746}$$

To care for iron losses drop O to O′.

Slip:

$$\text{Slip} = \frac{\text{Rotor losses in heat}}{\text{Energy output of rotor}} = \frac{B_0G}{BG}$$

Draw anywhere a perpendicular to B^+M, draw B^+K and prolong to intersection. The triangle B^+XT is similar to B_0GB.

$$\text{Therefore } \frac{B_0G}{GB} = \frac{XT}{TB^+} = \text{slip.}$$

Slip is measured along TX in per cent.[15]

Efficiency:

$$\text{Efficiency} = \eta = \frac{BS^1}{\text{OB projected on OP}} = \frac{BS^1}{BC} = \frac{BS^1}{BA}\,\frac{1}{\cos\alpha},$$ where α = the angle CBA.

---

[15] A very slight inaccuracy in the slip scale comes in for light loads from the neglect of rotor hysteresis.

Prolong KB_0' to O'' the intersection with $O'Z$. Erect JR perpendicular to OP. Draw $O''BE$. Draw EX parallel to BA.

$$\text{Then } \eta = \frac{EN}{EX}\frac{1}{\cos\alpha} = \frac{EN}{O''R}\frac{1}{\cos\alpha} = \frac{JE}{JR\cos\alpha}$$

Draw JZ parallel to B_0V and strike the arc ZW. Then the angle $RJZ = \alpha$ and $JW = JR \cos\alpha$

$$\text{Finally } \eta = \frac{JE}{JW}.$$

For simple construction, lay off $O''L = 100$ mm. along B_0V, erect a perpendicular to B_0V cutting $O''K$ in J. Draw JR at right angles to OP. Strike off $JW = 100$ mm.

Read η as length JE in mm., or per cent. E is determined as the intersection of JW and the line $O''B$ for each load.

Data, work up and curves now follow for five machines. The first is given by Grob, three are in the electrical laboratories of the University of Wisconsin, and one is derived from H. M. Hobart's book, *Electric Motors.*

OERLIKON TWENTY HORSE POWER THREE PHASE MOTOR

Data given by Grob. 380 volts; 1.500 rev. per. min.; 50 cycles; $R_1 = .212$ ohms; $R_2 = .0386$ ohms; Ratio of stator to rotor turns $= \frac{1}{.381}$.

No load.

$I_1 = 7.3$, $V = 380$, 50 cycles, 880 watts, 450 watts friction and windage, $\cos\phi_0 = .184$.

Short circuit. (Rotor slowly running.)

35 amperes, 50 frequency, 77 Volts, 2,050 watts, $\cos\phi_k = .437$.

I_k at 380 volts $= 35 \times \frac{380}{77} = 172.5$ amperes.

Eddy current loss in the Stator.

When $I_1 = 35$, $I_2 = \frac{I_1}{.381} = 92$, $I_2{}^2R_2 = 778$, $I_1{}^2R_1 = 980$

Total 1,758. The wattmeter read, however, 2,050. Then, since the current density should be about the same in stator and rotor, increase the stator. That is, eddy currents effectively increase the stator R.

$2050 - 1758 = 292$. Add $\frac{292}{2}$ to each then $I_1{}^2R_1 = 778 + 146 = 924$ and

$R_1{}^1 = .212 \times \frac{924}{778} = .252$ ohms.

Short circuit $I_2{}^2R_2$ at 380 volts $= 980 \left(\frac{380}{77}\right)^2 = 24{,}000$ watts

watt current $= \frac{24000}{380 \times \sqrt{3}} = 36.4$ amperes.

Construct on the pressure line a power factor semi-circle of 100 mm. diameter, lay off at the proper angle and to suitable

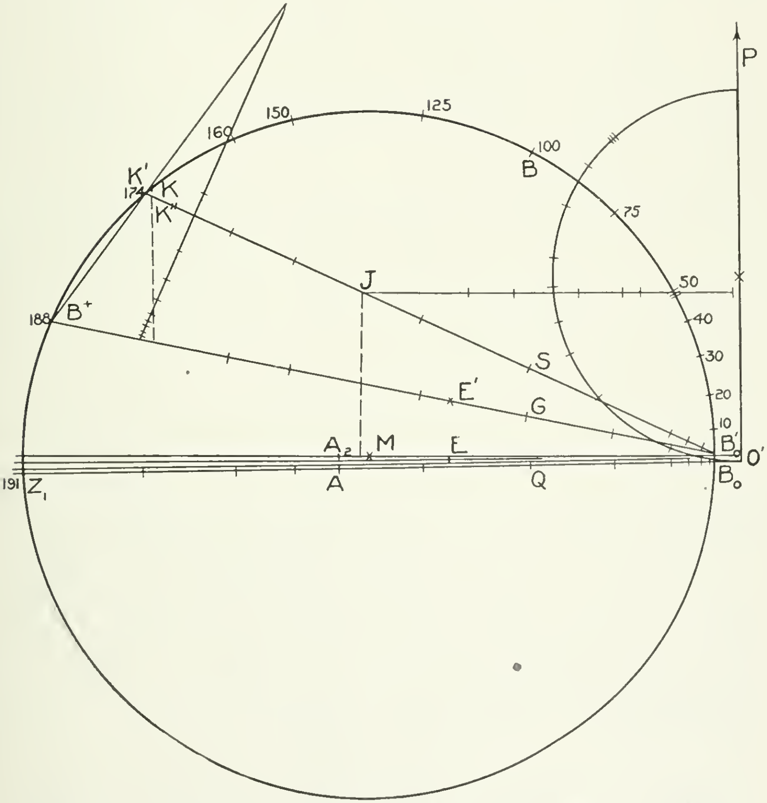

Plate VII.—Oerlikon 20 Horse Power 3 Phase Induction Motor.

scale the short circuit and no load vectors. Subtract the watt component of the no load current B_0B_0'. (See Plate VII.)

Draw perpendiculars to $O'P$ in O' and through B_0: draw B_0C_0.

$O'C_0$ = wattless component of no load current. $7.2 \times 0.252 = 1.82$

$$T_3 = \frac{1.82}{\left(\frac{380}{\sqrt{3}}\right)} = .00828$$

Lay off $B_0A = 100$ mm. $A_1A_2 = .828$ mm. Construct circle with center on B_0A_2 which shall pass through K and B_0.

$$T = \frac{OB_0}{B_0L} = .0392$$

Lay off $OE = T$ and $EE_1 = T_3$

Infinite slip is the intersection with the circle of OE_1 prolonged.

Draw B^+B_0

Drop a perpendicular from K toward diameter B_0V to intersection with B_0B^-; from this intersection backwards lay off the watt current of rotor loss at short circuit. Draw $B_0'K''$ through to intersection of line with the circle at K^1.

B_0B^+ is the torque line.

$B_0'K'$ is the mechanical power line.

$O'Z_1$ is the electrical power line.

Torque and mechanical power are the lengths for any load of the perpendicular to the diameter B_0V as far from the circles as the intersections with the torque and power lines respectively. Electrical power is the perpendicular distance to the line $O'Z_1$.

To lay off the slip line, draw and prolong B^+K'. Perpendicular to B^+H (a radius) erect TY so that the intercept between B_0B^- and B^+K' shall be for convenience, just 100 mm. Slip for any load is the distance TX the intercept with the line B^-B for that load read directly in mm. or per cent. [See Plate VI].

Scale of efficiencies. Prolong $K'B_0'$ to O'', its intersection with $O'Z_1$. Describe an arc 100 mm. long. Erect a tangent perpendicular to the diameter B_0V to intersection with the

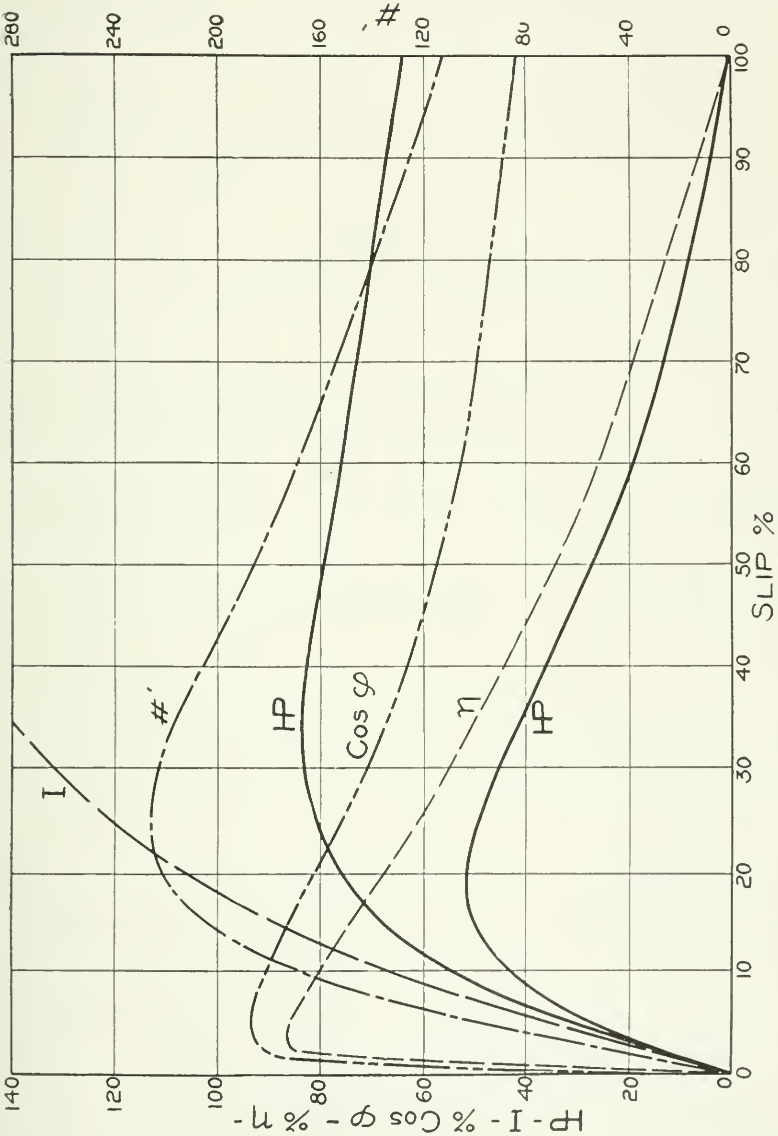

Plate VIII.—Oerlikon 20 Horse Power 3 Phase Induction Motor.

power line $B_o'K'$. Erect perpendicular to the pressure line and lay off on it an arc 100 mm. long. Read directly in mm. or per cent., the efficiency at any load as the intersection of line $O''B$ for that load with the efficiency line.

The motor was loaded both by brake and by a rated generator and the circle gave points between the fluctuations of the experimental data. The circle and curves derived therefrom follow.

OERLIKON MOTOR.

Data for circle, Grob.

Amperes.	Slip.	Cos ϕ	η	Torque lb. ft.	H. P. input.	H. P. output.	B. Q.	B. S.	B. G.
10	0.9	68.8	70.9	18.2	6.3	4.7	71	53	60
20	2.2	90.9	84.7	48.9	16.2	13.3	183	150	161
30	3.9	93.4	86.5	79.0	25.1	21.5	281	243	260
40	5.4	93.6	85.6	104.8	33.4	28.7	378	325	345
50	6.9	93	84.0	130.6	41.6	35.3	472	400	430
75	11.4	89.5	78.3	182.4	59.2	46.4	670	525	600
100	17.3	83.4	70.2	217.0	74.0	52.4	837	593	714
125	25.8	74.5	59.1	226.0	82.5	48.9	934	554	744
150	42.5	61.4	41.8	200.5	81.8	34.2	926	387	660
174*	100	41.5	0	112.5	64.0	0	735	0	320
7B†	0.1†	18.4	0	4	1.18	0	880‡	0	....
160	56	54.5	29.8	176	77.4	22.7	876	257	580

* Short circuit.
† No load.
‡ Watts.

GENERAL ELECTRIC CO.'S MOTOR NO. 71602

Form L; 60 frequency; 5 h. p.; 3 phase; volts between lines, 110; 4 pole, amperes per line, 28. The rotor has an internal clutched starting resistance.

No load.

110 volts, 14.5 amperes, 420 watts, cos $\phi_o = .1520$.

Short circuit.

I (av.)	V	W (total).	Cos ϕ_k	I_k (110 volts).	W_k (110 volts).
22.1	15.5	340	.497	156	17160
26.3	18.5	480	.493	156	17160
30.3	22.5	680	.497	156	17160
35.0	26.0	890	.481	156	17160
41.3	30.0	1,080	.503	156	17160
Av...	....	....	.494	....	....

$$I_1^2 R_1^1 = I_2^2 R_2 = \frac{17160}{2} = 8580 = 156^2 \times .353$$

The windings of rotor and stator are identical, therefore $R_1' = R_2' = .353$.

Direct current measurements gave $R_1 = R_2 = .3115$ which is raised to .353 by eddy current losses.

$$C_0O^1 = 14.4, \; T_3 = \frac{\frac{14.4}{\sqrt{3}} \times .353}{110} = .0267, \; T = \frac{OB_0}{B_0L} = .0870$$

Watt current of $I_2^2R_2$ loss is $\frac{8580}{3 \times 110} = 26$ amperes.

Circle, data scaled therefrom and curves follow.

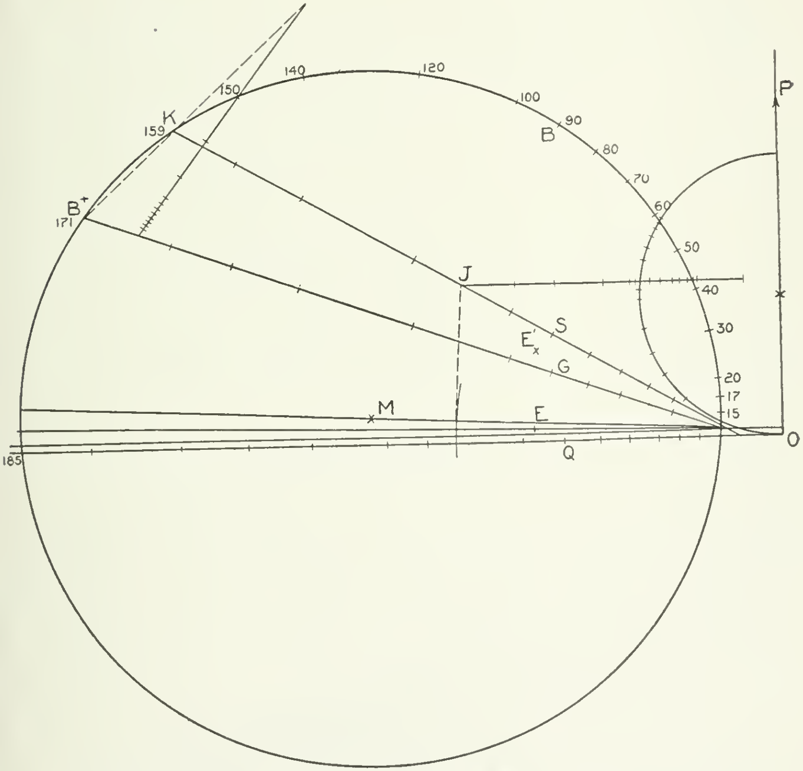

PLATE IX.—FIVE HORSE POWER INDUCTION MOTOR. G. E. No. 71602.

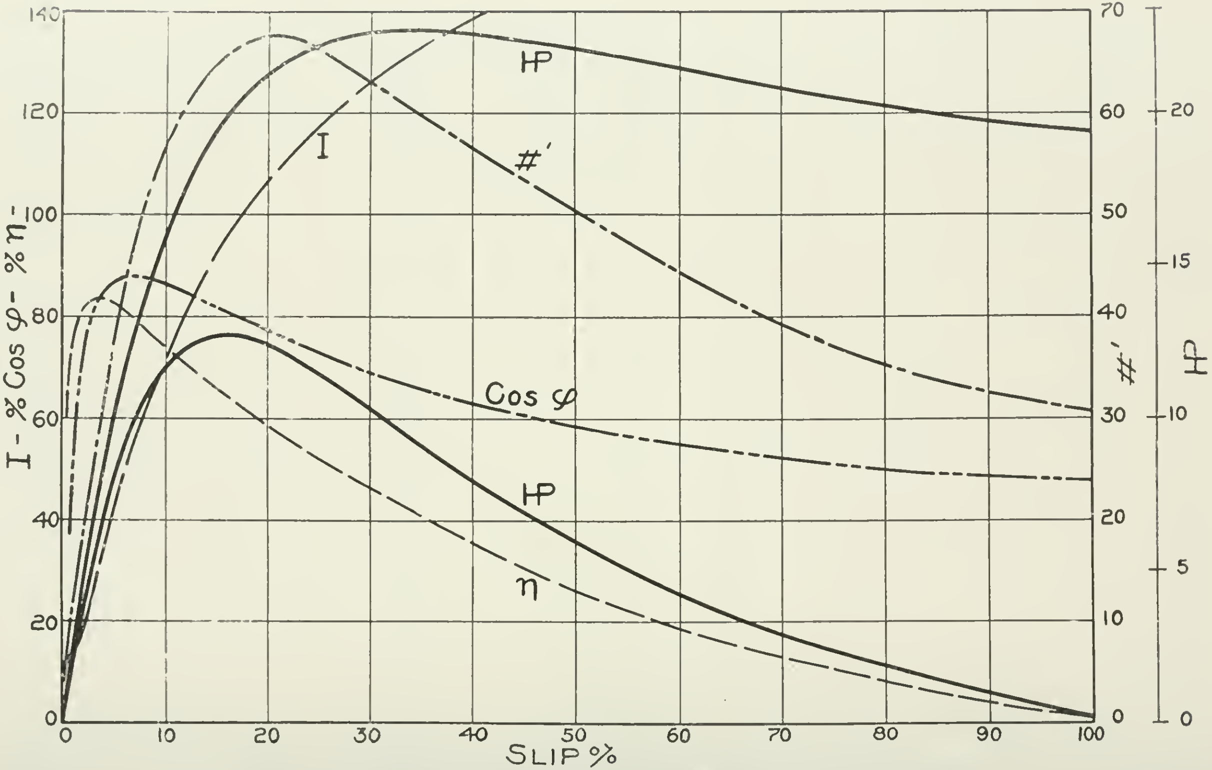

Plate X.—Five Horse Power Induction Motor. G. E. No. 71602.

General Electric Motor No. 71602.

Data for circle: Kyser, Fussell.

Amperes.	Slip.	Cos ϕ	Per ct. η	Torque lb. ft.	H. P. Output	H. P. Input.	BQ	BS	BG
15	.50	37.5	60.2	4.78	.85	1.53	90	50	65
17	1.15	55.5	74.8	8.81	1.78	2.46	145	105	120
20	1.90	69.5	80.2	13.4	2.81	3.73	210	165	182
30	3.5	83.8	83.6	25.0	5.35	6.46	380	315	340
40	4.9	86.3	82.6	34.6	7.33	8.83	520	432	470
50	6.2	88.0	80.3	43.0	9.08	11.28	665	535	585
60	7.9	87.4	77.6	50.0	10.36	13.40	790	610	680
70	10 1	86.3	74.5	56.6	11.52	15.40	910	680	770
80	11.9	84.5	70.8	61.0	12.20	17.30	1020	720	830
90	14.4	82.0	66.8	64.6	12.55	18.84	1110	740	880
100	17.3	79.3	62.2	66.9	12.42	20.30	1200	730	910
120	25.6	72.0	50.8	65.4	11.18	22.20	1310	660	890
140	42.0	62.0	33.3	55.2	7.36	22.20	1310	434	750
150	60.0	54.5	19 0	44.1	4.07	21.10	1240	240	600
159*	100.0	47.0	00.0	30.1	0.00	19.00	1120	0	410

*Short circuit.

Values scaled from circle agree very well with the results taken from brake tests.

General Electric Co's Motor No. 2577

Type I; form C; 3 phase; 60 frequency; 6 pole; 5 horse power; 1200 rev. per min.; 220 volts. Stator turns, 1728; rotor turns, 144.

No load.

219 volts, $I_o = 3.88$ amperes, $\cos \phi_o = .176$.

Watts friction and windage $= 115$

Watt current friction and windage $= \dfrac{115}{220 \times \sqrt{3}} = .302$ amperes

Watt current total $= \dfrac{258}{220 \times \sqrt{3}} = .678$ amperes

Short circuit.

220 volts; 48 amperes; $\cos \phi_k = .497$.

$R_1 = 1.21$ ohms (hot), $R_2 = .0086$ ohms (hot) $O'C_o = 3.64$.

$$T_s = \frac{\frac{3.64}{\sqrt{3}} \times 1.21}{220} = .01125$$

$$T = \frac{OB_0}{B_0L} = .0716$$

$$48^2 \times 1.21 = 2790$$

$$\overline{12 \times 48}^2 \times .0086 = 2850$$

$\frac{2850}{220} = 13$ amperes watt current to subtract along line KK″.

Circle, data and curves follow.

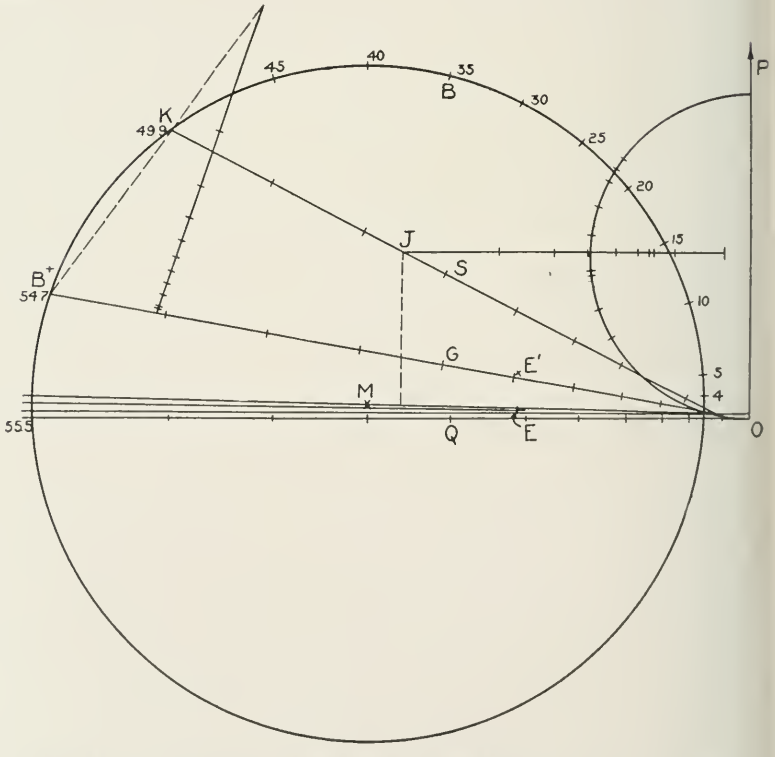

PLATE XI.—FIVE HORSE POWER INDUCTION MOTOR. G. E. No. 2577.

GENERAL ELECTRIC CO.'S MOTOR NO. 2577.

Amperes.	Slip.	Cos ϕ	Per ct. η	Torque lb. ft.	H. P. Input.	H. P. Output.	BQ	BS	BG
3.88*	.4	17.6	0	.6	.346	0	....	0	11
4	.9	41.0	54.4	2.8	.854	.459	67	36	50
5	1.9	66.2	76.0	6.5	1.78	1.29	140	101	118
10	5.8	87.6	84.0	18.1	4.52	3.75	355	294	327
15	9.4	89.2	81.4	27.2	6.89	5.61	540	440	492
20	13.2	87.4	77.2	35.7	9.04	7.00	708	548	645
25	18.0	84.8	72.4	42.0	10.84	7.84	850	614	760
30	23.4	80.2	65.9	46.6	12.33	8.15	967	639	844
35	31.0	74.5	57.8	49.3	13.40	7.78	1050	610	890
40	41.5	67.2	46.9	48.4	13.80	6.50	1080	510	875
45	59.0	57.0	30.0	43.2	13.27	4.08	1040	320	750
48	79.0	49.7	14.4	36.7	12.20	1.79	956	140	664
49.9†	100.0	44.2	0	31.2	11.22	0	880	0	565

* No load.
† Short circuit.

WESTERAS MOTOR

(Allmanna Svenska Elektriska Aktiebolaget.)
From H. M. Hobart's book *Electric Motors.*
12 pole; 50 frequency; 500 volt; 500 rev. min.; 3 ϕ; 100 orse power. Y connected. 288V per coil.

$$\text{er } \phi \left\{ \begin{array}{l} R_1 = .084 \qquad R_2 = .058 \\ \dfrac{\text{Primary turns}}{\text{Secondary turns}} = \dfrac{90}{72} = 1.25 \end{array} \right.$$

No load.

23 amperes, $\cos \phi_0 = .190$

$3 \times 288 \times 23 \times .19 = 3700$ watts

Bearing and windage = 1400 watts

$$\text{Watt current total} = \frac{3700}{500 \times \sqrt{3}} = 4.27 \text{ amperes}$$

$$\text{Watt current, bearing and windage} = \frac{1400}{500 \times \sqrt{3}} = 1.61 \text{ amperes.}$$

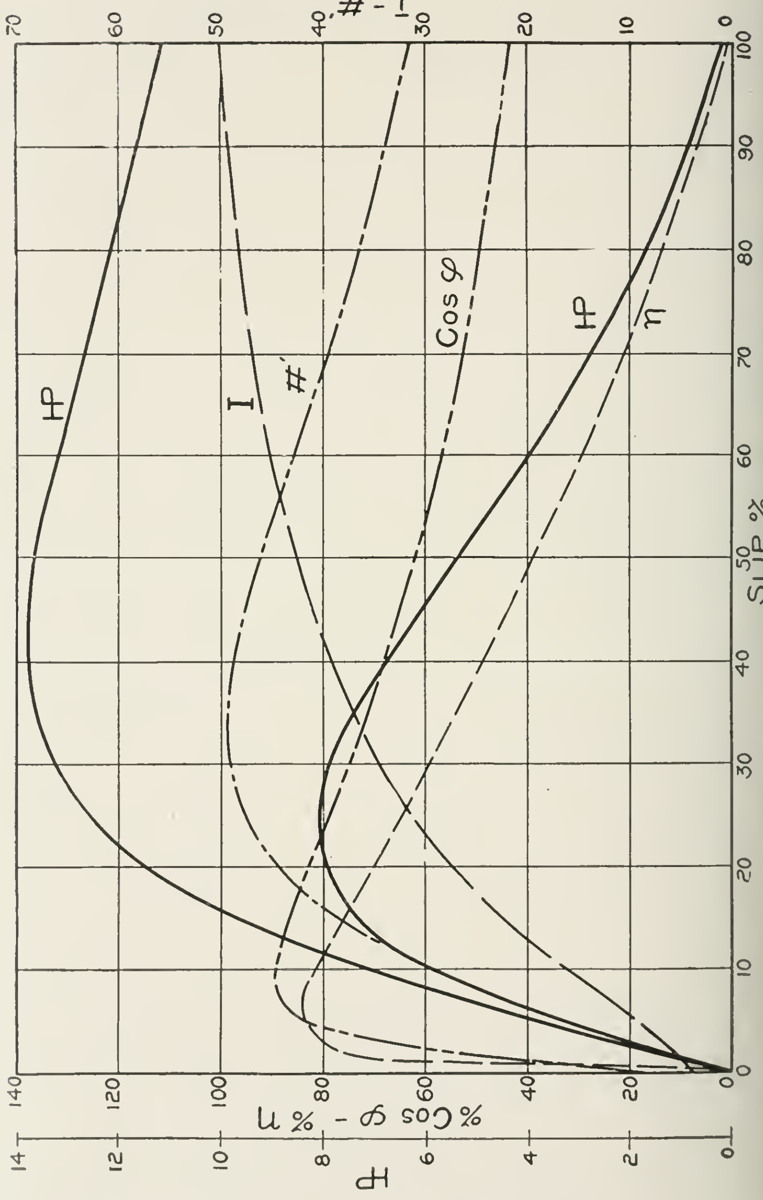

Plate XII.—Five Horse Power Induction Motor. G. E. No. 2577.

Short circuit.
438 amperes; 288 volts; $\cos \phi_k = .383$.

$O^1C_0 = 22.4$ amperes

$22.4 \times .084 = 1.88$ volt

$$T_3 = \frac{1.88}{\left(\frac{500}{\sqrt{3}}\right)} = .00651$$

$$T = \frac{OB_0}{B_0L} = \frac{1.12}{22.51} = .0498$$

$I_2{}^2R_2 = (438 \times 1.25)^2\ .\ 058 \times .383 = 65000$ watts

$$\text{Watt current at short} = \frac{65000}{500 \times \sqrt{3}} = 75.2 \text{ amperes}$$

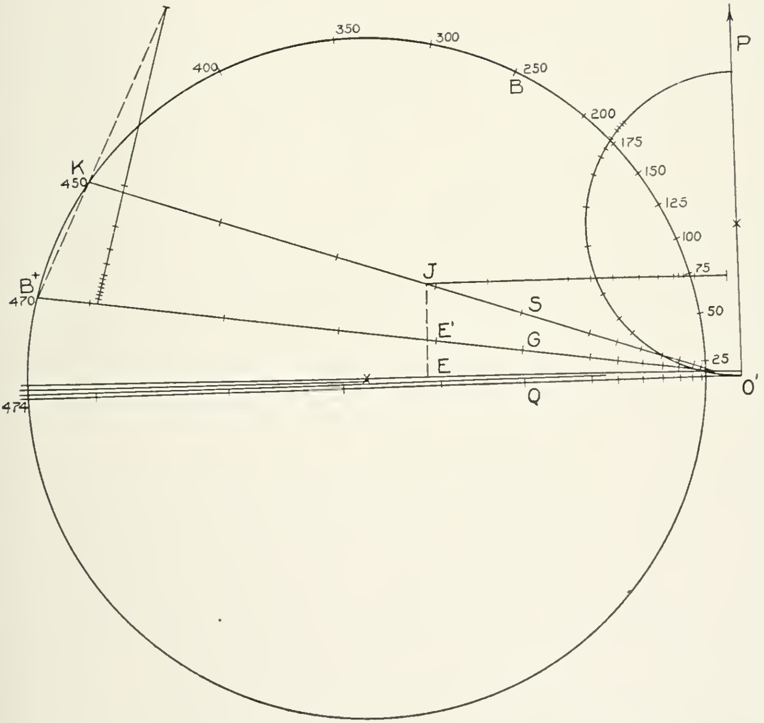

Plate XIII.—Westeras 100 Horse Power 3 Phase Induction Motor

WESTERAS 100 HORSE-POWER MOTOR.

Ampere.	Slip.	Cos ϕ	η	Torque lb. ft.	H. P. Input.	H. P. Output.	BG.	BQ.	BS.
23	.05	190	0	21.6	5	0	9	37	0
25	.2	440	547	98.4	13.5	7.9	41	58	34
50	1.8	853	860	460	48.7	41.7	192	210	180
75	3.0	905	880	768	80.6	69.6	320	335	300
100	4.1	917	881	1030	106.8	93.4	430	460	402
125	5.2	912	870	1292	133	116.0	538	573	500
150	6.8	902	858	1519	158	136.0	632	680	581
175	8.0	889	841	1730	181	152.5	721	780	657
200	9.7	870	822	1920	202	166.5	800	876	718
250	13.5	817	776	2210	238	184.5	922	1028	796
300	17.4	750	713	2360	262	186.5	983	1130	804
350	25.3	660	628	2305	268	167.0	960	1155	720
400	39.4	532	474	1960	246	116.0	815	1061	500
438	71.0	383	207	1320	195	40.4	550	840	174
450	100	320	0	960	164	0	400	708	0

BROWN, BOVERI MOTOR NO. 193,913

Type 6; 6 horse power; 4 pole; 1800 rev. per min.; 3 phase; 110 volts; 60 frequency.

$R_1' = .137$ ohms (hot)

$R_2' = .089$ ohms (hot)

No load.

110 volts, $I_o = 8.45$ amperes, $\cos \phi_o = .290$

160 Watts friction and windage

Watt current friction and windage $\frac{160}{110 \times \sqrt{3}} = .84$ amperes

Watt current total $\frac{466}{110 \times \sqrt{3}} = 2.45$ amperes

Short circuit.

110 volts, $I_k = 159$ amperes, $\cos \phi_k = .572$

$$T_3 = \frac{8. \times .137}{110} = .00996$$

$$T = .0432$$

Plate XVI shows this machine as a normal motor, solid line, and the dotted line shows a modified motor which is discussed later. Circle, data and curves are given. Plate XVIIa shows the curves for this machine and Plate XVIIb for the modified motor.

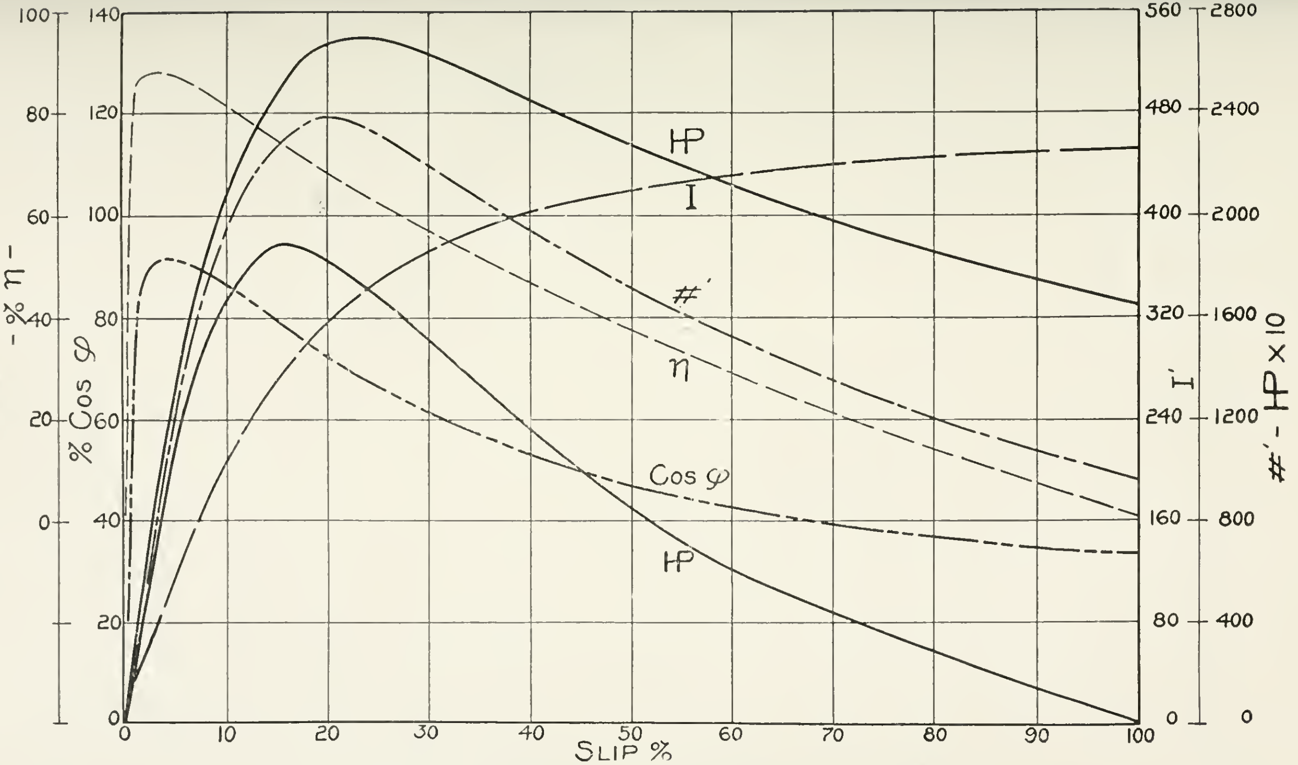

Plate XIV.—Westeras 100 Horse Power Induction Motor.

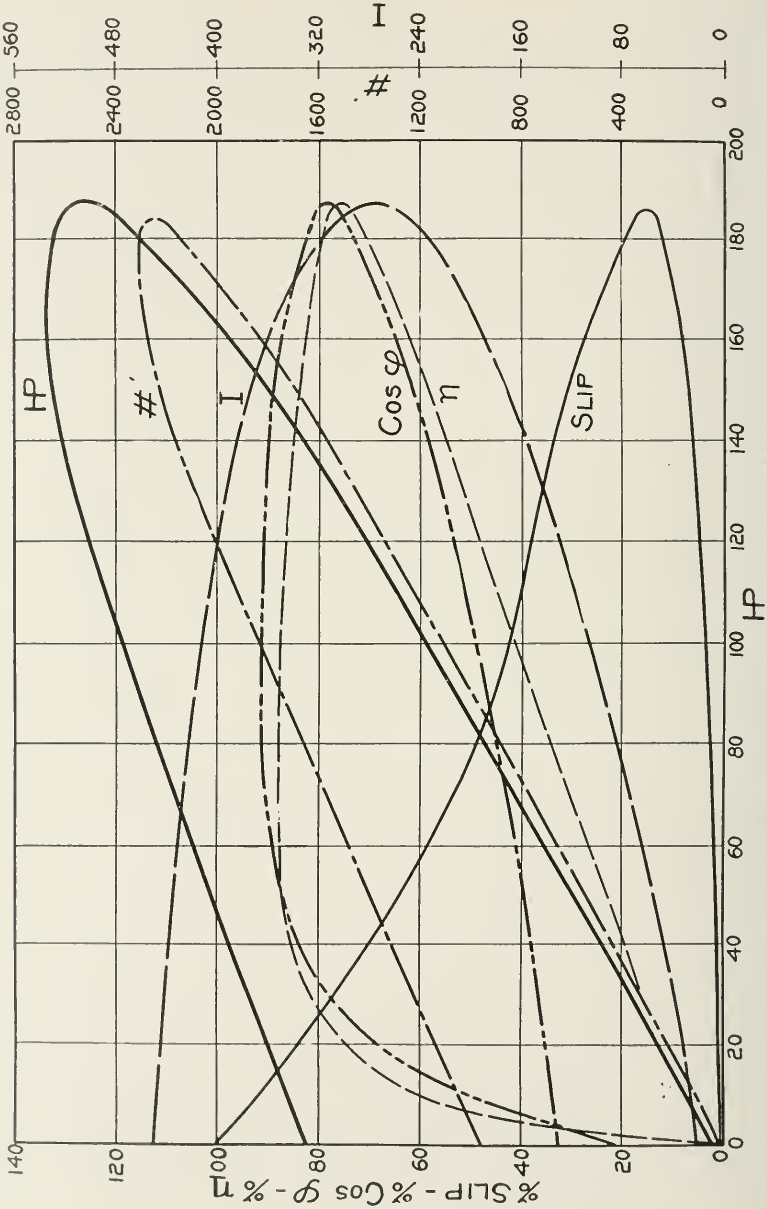

Plate XV.—Westeras 3 Phase Induction Motor.

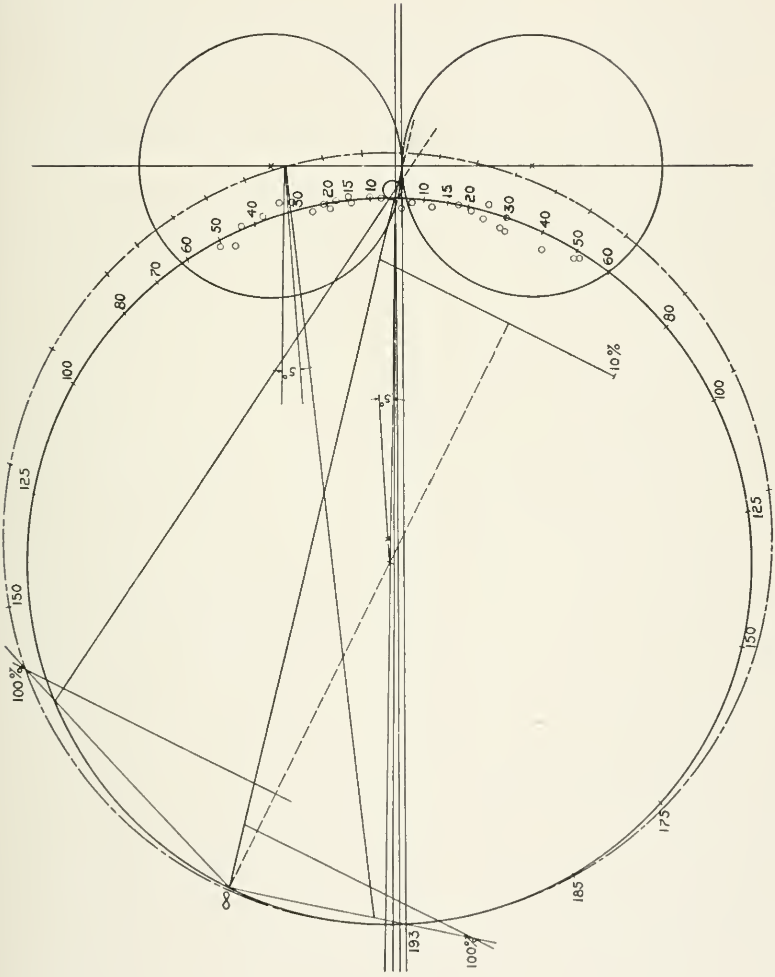

PLATE XVI.—GROB. DIAGRAM OF BROWN BOVERI 3 PHASE INDUCTION MOTOR.
(Normal and compensated with 5° brush displacement.) Small circles indicate experimental values.

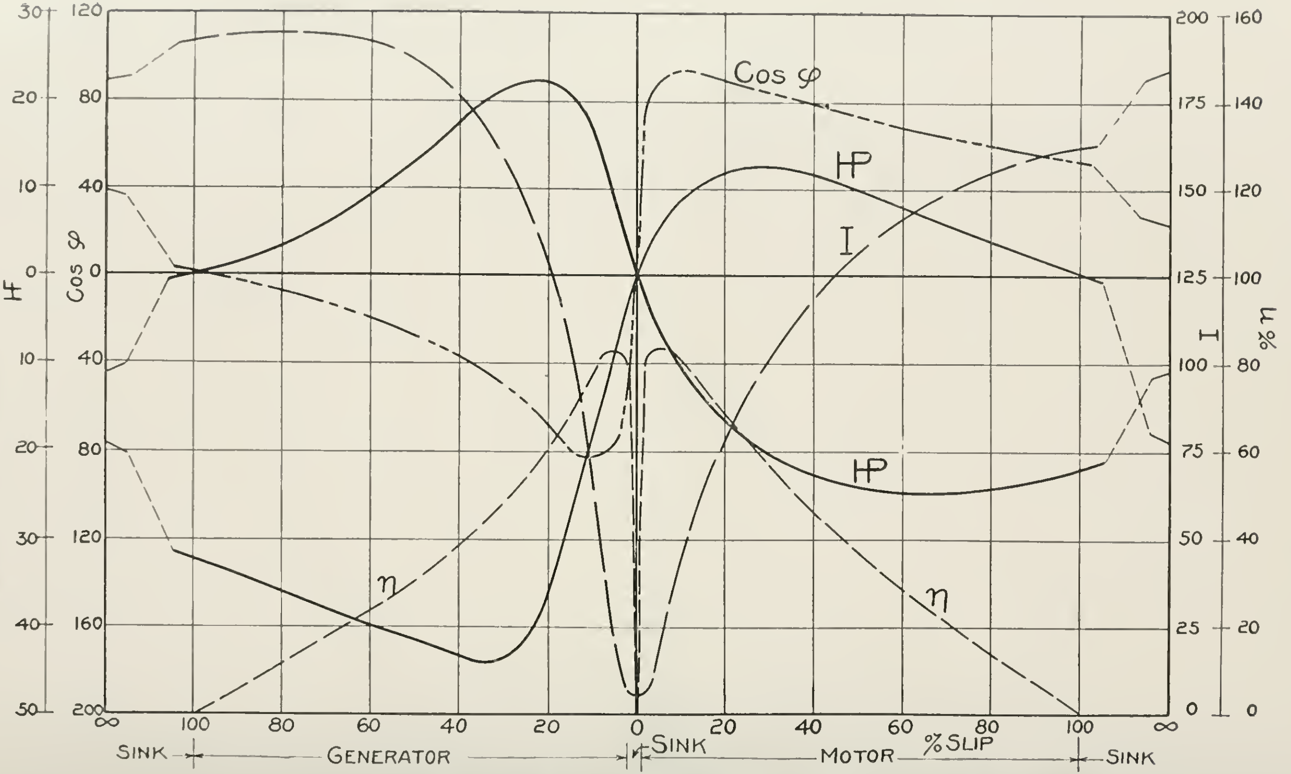

PLATE XVIIa.—BROWN BOVERI 5 HORSE POWER 3 PHASE INDUCTION MOTOR.
Normal operation.

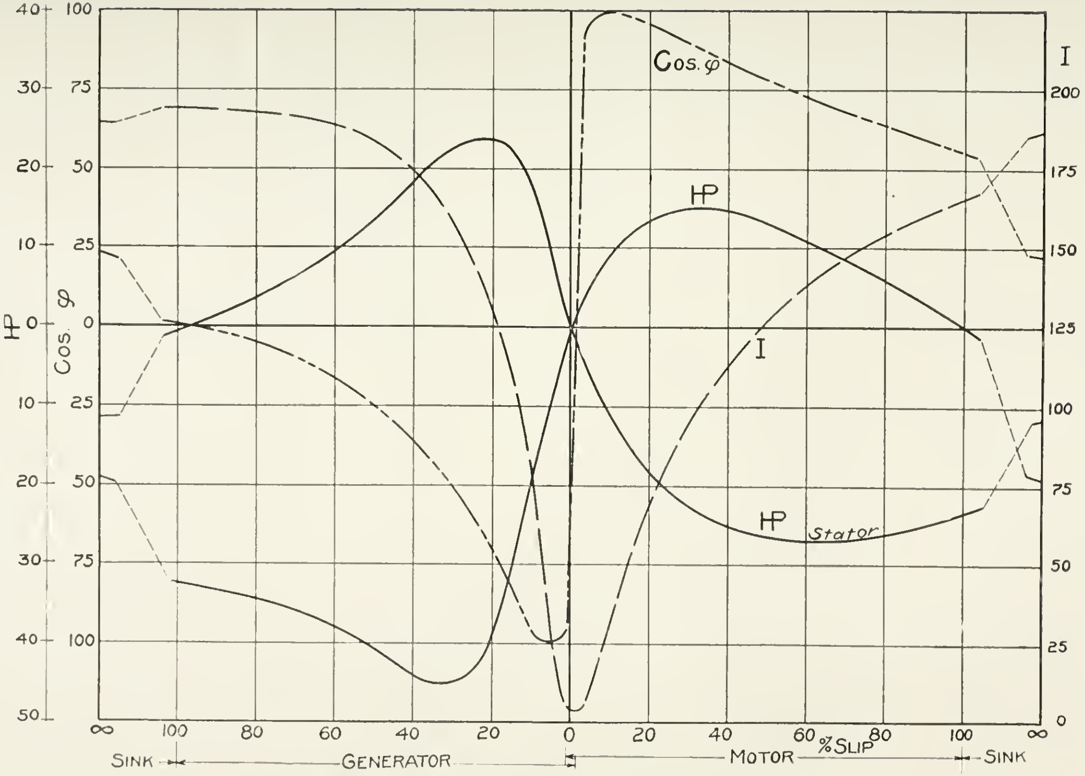

Plate XVIIb.—Brown Boveri Induction Motor. Compensated 5° Brush displacement.

Per cent. slip.	H. P. mechanical.	H. P. electrical.	I_1	Cos ϕ	η
∞	—19.80	11.80	188	24.0	....
Standstill					
1.00	0.00	23.20	162	55.0	0.00
.717	4.68	24.60	150	62.5	19.0
.446	10.40	24.40	125	75.0	42.5
.293	12.60	21.82	100	83.5	58.0
.212	12.30	18.36	80	88.0	67.0
.180	11.60	16.30	70	90.6	71.3
.148	10.57	14.20	60	91.8	74.4
.119	9.35	12.10	50	92.9	77.1
.094	7.80	9.70	40	93.5	80.4
.068	5.88	7.28	30	92.7	81.0
.040	3.81	4.68	20	89.0	81.5
.030	2.43	3.12	15	82.0	77.7
.010	1.04	1.73	10	61.0	60.0
.0098	0.52	1.21	9	45.0	42.9
Synchronism					
.0000	0.00	.69	8.06	29.0	0.00
.0097	2.25	1.38	10	54.0	61.5
.0176	3.81	3.12	15	78.2	81.7
.0247	5.36	4.33	20	86.0	80.6
.0382	8.50	6.93	30	90.3	81.6
.0519	11.60	9.35	40	91.0	80.6
.0646	14.50	11.60	50	90.5	79.7
.0780	18.20	13.70	60	89.0	75:2
0.1042	23.9	17.5	80	85.4	73.2
0.1370	30.3	20.8	100	80.0	68.6
0.1800	37.3	23.0	125	71.0	62.0
0.2500	43.2	22.5	150	58.0	52.5
0.3800	44.4	17.0	175	37.0	38.3
1.0000	33.0	0.	192	0	0.

BROWN, BOVERI, MOTOR BRAKE TEST.

I av.	Per cent. Cos ϕ	Slip.	B. H. P.
8.25	25.0	.22	.0
11.3	71.8	1.50	1.35
15.9	82.1	3.0	2.68
18.8	88.5	3.5	3.34
21.9	90.1	4.5	3.98
25.2	88.8	5.2	4.63
29.0	95.1	6.5	5.26
32.6	96.0	7.3	5.90
37.4	94.2	9.1	7.15
43.3	93.5	9.45	7.79
47.0	90.5	10.5	8.38
50.5	91.6	11.0	8.68
8.2	26.3	.187	0
9.8	49.2	.86	1.14
15.3	85.2	1.42	2.46
20.7	86.7	2.28	3.72
32.6	87.9	4.02	5.48

SLIP SCALE FOR HYPERSYNCHRONISM

In all of the foregoing diagrams, as well as in those given in the appendix to this chapter, the scales for slip are accurate for the condition of motor running since they represent all the limit conditions and agree with brake data. For generator slip, however, none are accurate since the authors have done one of three things: (a) evaded the issue entirely, Grob, 1904; (b) extended the motor slip scale proportionally which fails to represent the limit conditions, Ossanna; or (c) extended the generator slip scale set by the limits to motor action which fails to give the correct position for 100 per cent. motor slip (standstill), Grob, 1901.

If in a diagram, whose motor slip scale accurately agrees with data which are obtained from careful observation during a brake test, the motor slip line be prolonged the values scaled off from this prolongation do not agree with tests made during a generator run. In one test at about 50 per cent. overload they had the relation, scale to test equals 10.7 to 6.1, not a remarkable agreement.

If, however, parallel to the motor slip scale a line be drawn, so that its 100 mm. length fills the distance between the base line of slip and a line drawn from ∞ slip through Z the point where the energy component of the primary current changes direction and which must represent the point of 100 per cent. slip, it will represent to a very fair degree of approximation the conditions actually found to occur during careful measurements of a run of the machine as a generator.

The diagrams given show two of the possible schemes of connection, each employing a synchronous generator in parallel as the source of leading exciting current. One scheme loads with lamps or other dead resistance as absorption agent, while the other is a "pump back" system. The latter is the easier to operate by far; it being possible by the mere movement of a rheostat (that in the smaller DC machine "R" being most often used) to effect a change of the induction machine clear through by easy steps from 100 per cent. overload as a motor to 100 per cent. overload as a generator. This causes readily 20 h. p. to

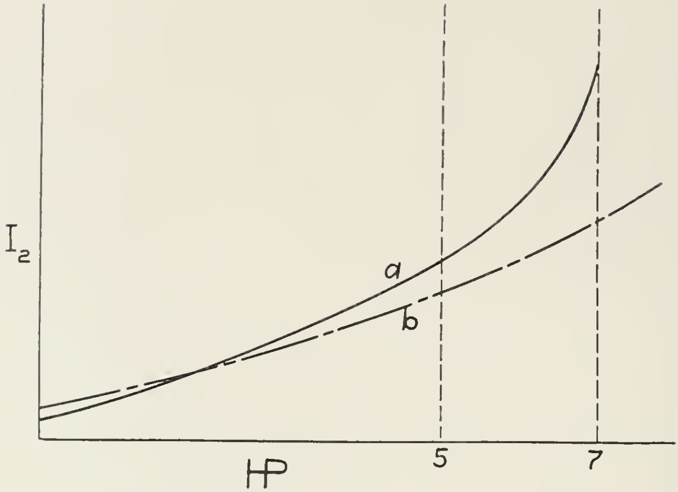

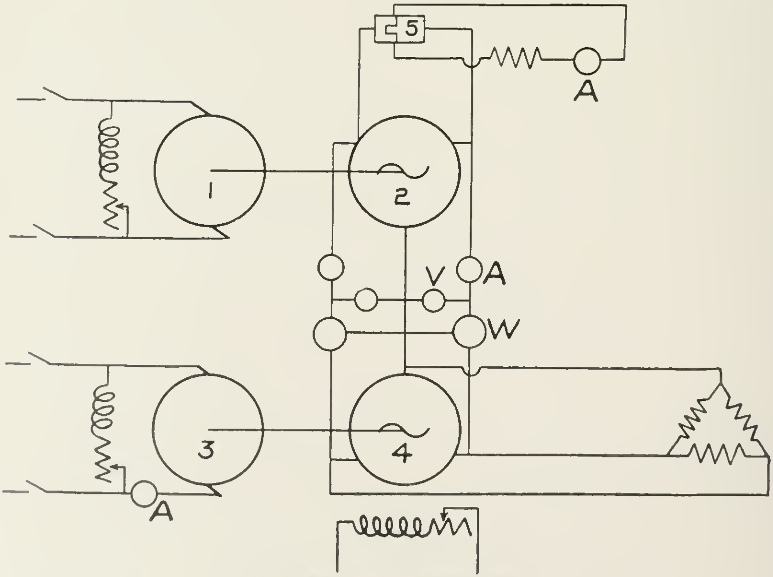

PLATE XVIII.—CONNECTIONS.

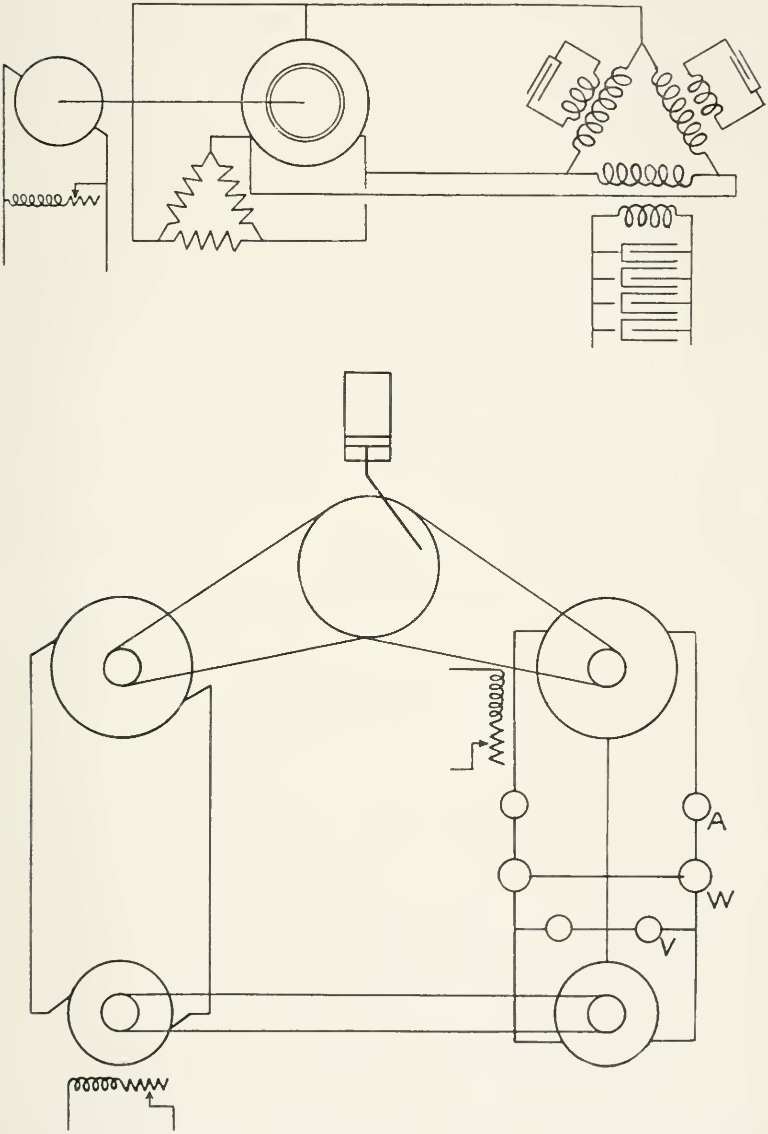

Plate XIX.—Condenser Excitation and Pump. Back Connections.

circulate with a total loss of less than 2 h. p., the machine under test being rated at 6 P. S. (German h. p. of 736 watts).

In order to test this theory, the following experiment was performed. Driving above speed an induction machine it was paralleled with a synchronous generator and the following values maintained constant while load was added in the shape of lamp banks in delta across the lines, primary frequency, held at 60 by keeping the speed of the synchronous generator at 1,200 rev. per min.; the line pressure by adjusting the synchronous machine field current; and approximately the input to the machine driving the synchronous generator and therefore to the synchronous generator itself. It was found that while remarkably stable and constant when once adjusted, the system was one of a very considerable flexibility, since it sufficed to change any one of the three field rheostats to throw the load of the whole system on to whichever prime mover was desired and to cause the other to act as a generator, or both could be adjusted to act as motors. The motor driving the synchronous generator, in order that the frequency might be maintained constant, was kept functioning as a motor but was not allowed to take more than a very little power input. Accurate readings of speed were taken on both generators and these were used as checks on the indications of the slip-indicator. This consists (See Plate XVIII) of a commutator capable of being driven by the rotor speed and having a number of segments equal to the number of poles. Stator frequency impressed electrically upon these bars and rotor frequency mechanically (by holding against the shaft as in a tachometer) the number of beats due to these two frequencies superimposed is indicated by the throws of a DC ammeter needle connected in the circuit of the indicator brushes. For a four-pole motor the indications per half minute equal the revolutions slip per minute.

For the low readings if the tachometers and slip indicator disagreed the latter was taken, when the slip rose to higher values (due to the difficulty of counting) discrepancies were adjusted by weighting the slip-indicator as four times as accurate as the tachometer. All the values are the average of a number of separate determinations taken after the constants had been adjusted and the performance stationary. The limit was placed by the sparking of the Westinghouse motor and not by the induction generator although it did get warm.

The slip $\frac{\overline{\lfloor}}{\underline{\rfloor}}$ is that scaled from the prolongation of the motor slip line while the slip S is from test values. The columns headed slip from XY and from YZ indicate the agreement obtainable from two diagrams, for the same motor, constructed entirely independently of one another, when scaled off my line.

The curves, Plates XX and XXI, between per cent. slip from test and per cent. slip from scale on my diagram is a most drastic test under which the diagram stands up well. The larger circles as indicated, represent the values as scaled from the correct lines, while the smaller circles are the values of generator slip as scaled from the prolongation of the motor slip line.

The agreement of the motor values with the 45° line is well-nigh perfect and the great improvement of the generator slip line is apparent to the most casual inspection. The greatest error of my values is large, 46.6 per cent., the average being high, however, about 15 per cent. or less.

The values of the prolonged motor slip line, however, are very much greater, the maximum *error* being 132 per cent. of the true value, while the average is more than 100 per cent. This means that the generator slip in diagrams heretofore employed gave values which were twice the real values as obtained by test.

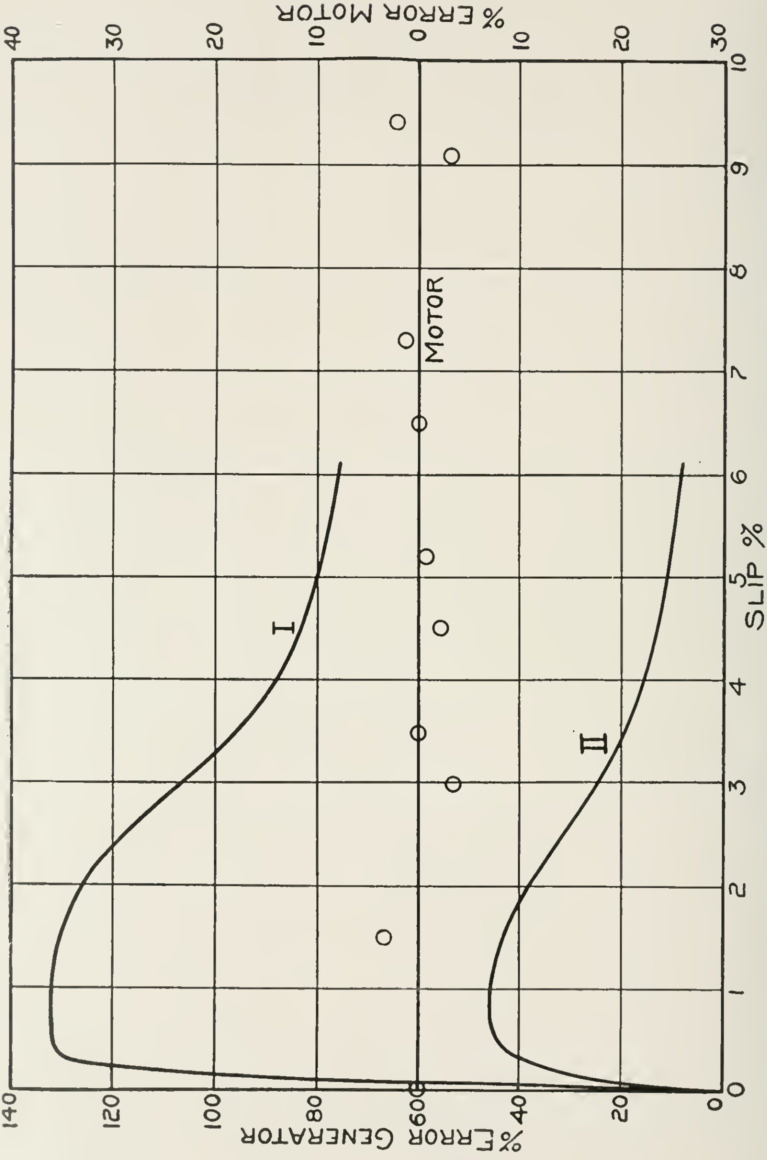

Plate XX. Curve I From Motor Slip Line Continued. Curve II From Corrected Slip Line.

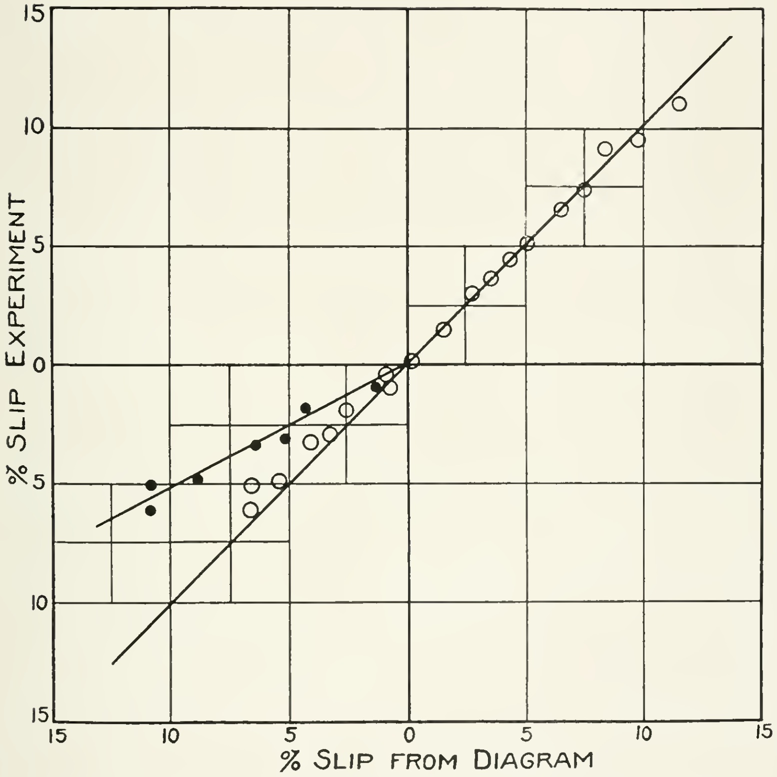

PLATE XXI.—COMPARISON OF SLIP SCALES.
Small circles give values from continuing the motor slip line.

No.	A_1 av.	V_1 av.	KW_1	KW_2	KW total.	$IE\sqrt{3}$
1	9.8	110.6	.91	1.01	1.92	1,870
2	21.3	109.2	2.25	1.14	3.39	4,040
3	31.3	109.3	3.35	1.67	5.02	5,940
4	41.9	108.5	4.42	2.33	6.75	7,860
5	50.8	110.2	5.57	2.91	8.48	9,680

No.	Cos ϕ	Stator rev. per min.	Rotor rev. per min.	Slip by difference.	Slip by indicator.	Slip rev. per min.
1	1.035	1,206.5	1.821	11	7.5	7.5
2	.840	1,206.5	1,845	35	34	34
3	.845	1,203	1,868	60	58	58.5
4	.858	1,200	1.889	89	85	86.8
5	.886	1,200	1.904	104	112	110

No.	Slip S per cent.	Slip **S** per cent.	Line frequency.	Lamps.	Westinghouse.	
					A total.	V
1	.41	.95	60.3	0	16.8	110.8
2	1.88	4.30	60.3	3 x 10	43.6	109.9
3	3.24	6.3	60.2	3 x 17	67.6	109.2
4	4.83	8.8	60.0	3 x 24	98.0	108.7
5	6.11	10.7	60.0	3 x 32	131.0	105.0

No.	Western A armature.	G.E. I_f	H. P. Output.	Slip from diagram.	
				Xy	yZ
1	16.0	4.68	....	.6	.60
2	16.6	4.62	4.54	2.6	2.63
3	16.2	4.75	6.72	4.1	3.94
4	17.0	4.87	9.04	5.4	5.38
5	17.2	4.90	11.39	6.6	6.59

No.	A_1	A_2	A av.	KW_1	KW_2	KW total.
1	9.4	10.9	10.45	.855	—.224	.631
2	25.6	23.8	25.10	1.465	2.620	4.085
3	30.8	29.8	30.70	1.865	3.310	5.175
4	50.8	50.0	50.40	3.070	5.675	8.745

	Cos ϕ	V_1N	V_2N	V av	Rev. per min.	
					Rotor.	Stator.
1	.318	110	111	110.5	1,810	1,200
2	.841	112	111	111.5	1,853	1,200
3	.853	113	112	112.5	1,844	1,195
4	.885	113	113	113.0	1,902	1,200

	Slip by		Slip rev. per min.	Slip S per cent.	**5** per cent.	Cycles.
	Difference.	Indicator.				
1	10	17	17	.945	1.0	60
2	53	53	53	2.94	5 1	60
3	52	61	59	3.30	6.4	59.7
4	102	88	91	5.05	10.7	60

	Lamps.	Amperes to rotary.	H. P. output.	X Y	Y Z	
1	0	14	.846	.70	.63	
2	3x10	4	5.47	3.2	3.14	
3	3x15	4	6.94	4.0	3.82	
4	3x25	1.5	11.7	6 5	6.47	

APPENDIX TO CHAPTER I

In chapter I credit must be given Adolph Thomälen for his work of November 26, 1903, and August 11, 1904, in *Elecktrotechnische Zeitschrift* following along the lines of Grob's diagram and giving the relation of the Heyland to the Ossanna circle. Of course, Heyland in 1894[1], gave the diagram with stator resistance represented and then in 1896 simplified so as to be applicable with ease. His 1894 work was, however, difficult of application and that of Ossanna much simplified this but was still complicated by requiring analytical geometry calculations.

Grob gave his 1901 method of drawing the circle followed by Thomälen in 1903 giving a slightly simpler method and showing the relation to the simple 1896 Heyland circle. Grob in 1904 gave his very much simplified diagram and Thomälen shows that his diagram is applicable.

KUHLMANN'S DIAGRAM

Karl Kuhlmann discusses[2] the general alternating current transformer under three heads "I. . . . without inductive resistance in the secondary circuit (Polyphase induction motor).

"II. . . . with constant secondary phase displacement ($< \phi_2$ constant).

"III. . . . with constant secondary self-induction L_2 and variable phase displacement $< \phi_2$, $[\tan \phi_2 = 2\pi (Y_1 - Y_2) \frac{L_2}{R_2}]$ the most general case."

His figure 17, reproduced here as Plate XXII, is based on the case number II. Like Ossanna, he takes currents as being in phase with and of same length as fluxes. That is, he considers OA = primary flux $F_1 = I_1$.

In Plate XXII from similar triangles GE is employed for I_1 instead of OA, since $GE = T_1 \times OA = T_1 \times I_1$. If the phase displacement is held constant, the angle FOD is constantly

---

[1] *Elektrotecnische Zeitschrift*, 1894, p. 561.

[2] *Ibid.*, Apr. 18, 1901.

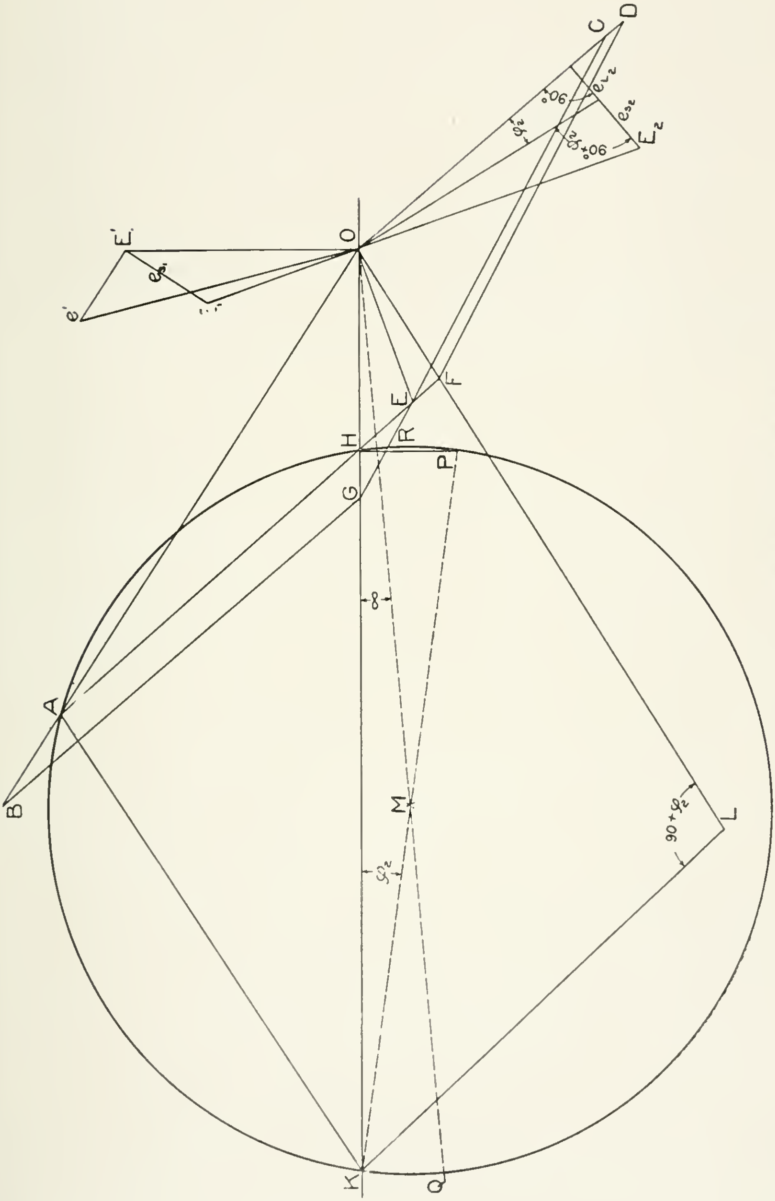

Plate XXII.—Karl Kuhlmann's Diagram.

equal to $90° + \phi_2$. Since AK is parallel to OF for all loads $HAK = 90° + \phi_2$

$$\frac{OK}{OH} = \frac{LK}{HF} \text{ where } OK = OH\frac{1}{\sigma} \text{ and } HK = OH\frac{1-\sigma}{\sigma}.$$

$$\text{Therefore } OK = \frac{1}{\sigma}OH \text{ for any load.}^3$$

Construct circle M through the three points H, A and K.

E_1' is constant and therefore OH is constant. Draw the diameter KP. Then KPHA is an inscribed quadrilateral and therefore

$$HPK = 180° - (90° + \phi_2)$$

$$= 90° - \phi_2$$

$$HK = PK \sin(90° - \phi_2) = PK \cos\phi_2 = RQ \cos\phi_2$$

Following the secant law

$OH \times OK = OR \times OQ = \overline{OM}^2 - \overline{MQ}^2 = \overline{OH}^2\frac{1}{\sigma}$ but $OA = I_1$; $OH = I_m$; $OM = \alpha$; $MQ = r$

Therefore

$$I^2_m\frac{1}{\sigma} = \alpha^2 - r^2 \text{ and } \alpha = \frac{I_m}{2\sigma\cos\phi_2}\sqrt{(1-\sigma)^2 + 4\sigma\cos^2\phi_2}.$$

In the triangle OAR

$I_1{}^2 - 2I_1\alpha\cos AOR + \alpha^2 - r^2 = 0$; $AOR = 90° - \phi_1 + \gamma$

in which only γ is unknown and it may be found from the triangle HOM.

$$\cos\gamma = \frac{I_m{}^2 + \alpha^2 - r^2}{2I_m \times \alpha} = \frac{I_m{}^2\left(1 + \frac{1}{\sigma}\right)}{2I_m \times \alpha}$$

$$= \frac{1 + \sigma\cos\phi_2}{\sqrt{(1-\sigma)^2 + 4\sigma\cos^2\phi_2}}$$

$$\sin\gamma = \frac{\sin\phi_2(1-\sigma)}{\sqrt{(1-\sigma)^2 + 4\sigma\cos^2\phi_2}}$$

---

[3] This value of dispersion coefficient σ is the same as Grob's T and is equal to $T_1 + T_2 + T_1T_2$ In terms of Heyland's coefficients. Also equal to $v_1v_2 - 1$ in terms of Hopkinson's coefficients and equal to $\frac{1}{v_1v_2} - 1$ in terms of Behrend's coefficients.

The coordinates of the center M are:

$$X_1 = \frac{e_1}{K} \cdot \frac{\beta}{2\alpha} \text{ and } y_1 = \frac{e_1}{K} \cdot \frac{\gamma_1}{2\alpha}$$

$$\text{The radius } R = \frac{e_1}{K} \cdot \frac{1}{2\alpha_1} \sqrt{\beta_1{}^2 + \gamma_1{}^2 - 4\alpha_1 \delta_1}$$

With $\phi_2 = 0$ these become

$$X_1 = X_0,\ y_1 = y_c,\ R_1 = R.$$

Several other diagrams were investigated but will not be given since they were found not applicable to the work of the second chapter.

CHAPTER II

SELF-EXCITING ASYNCHRONOUS GENERATORS

If an ordinary induction motor is driven above speed by mechanical power, it will operate as a generator and deliver current, provided a leading exciting current is supplied. This leading current may be produced by condenser, by an ordinary synchronous motor floating on the line, by a synchronous generator in parallel, or by means of modifications in the rotor to be described later.

The action of this leading current is to supply a wattless component which shall equal, approach or exceed the wattless magnetizing current.

The problem, then, of making an induction generator self-exciting is reduced to determining some method of supplying this wattless component from the machine itself; and the object of this investigation is to represent on a diagram the action of this exciting current. The historical development of the diagram for the ordinary induction machine has been taken up and several diagrams have been described in Chapter I.

The history of the diagram for the self-excited generator or the compensated motor has been extremely short. It will, however, be taken up and the self-exciting lines developed for the Heyland and the Grob diagram. The different developments which actually give these phenomena will be taken up individually and examined.

The representation on a diagram was first given for the compensated as for the ordinary motor by Alexander Heyland[1] whose work will be displayed shortly. Heubach, De Latour, Bragstad and La Cour seem, with Heyland, to have done most of the work with the actual machines. although Prof. C. A. Adams and Dr. A. S. McAllister in this country should be mentioned.

---

[1] *Elektrotechnische Zeitschrift*, July 23, 1903.

HEYLAND'S DIAGRAM FOR COMPENSATED MOTORS

Starting with the regular approximate Heyland construction. he briefly runs over the discussion of the diagram and then proceeds to the necessary modifications. The only difference occurs from the fact that the excitation field comes from the rotor. power being led into it from the external supply. This occasions a leakage in the direction opposite to that in the ordinary motor since the rotor has the larger flux.

In consequence of this externally applied e. m. f. in the rotor added to the electromotive force induced by its motion in the stator field. the secondary current no longer stands at a right angle to the rotor or secondary field. but makes a smaller angle with it, Plate XXIII.

In the current triangle we will have as before AC as the wattless magnetizing current of the stator field and AC^k the magnetizing current of the rotor field: AC being constant and AC_1^k parallel to the rotor field.

To determine the rotor current we must obtain the components of the e. m. f. which produces it and combine them. That produced by the motion in the stator field e^1 will vary in size with the slip and will always be perpendicular to the rotor field; the other e^k in the most general case of the application of a constant line pressure will have a constant length and a direction dependent upon the degree of brush displacement, here called the angle α.

This gives a figure with $AC = ADT$ all being constants. e^1 perpendicular to CK′D and e^k constant in length and direction. given.

As in the ordinary motor the corners of the triangle move on circles which may be determined as follows: Call the angle of brush displacement zero when the pressure impressed on the rotor is in line with the stator field. Any other brush angle

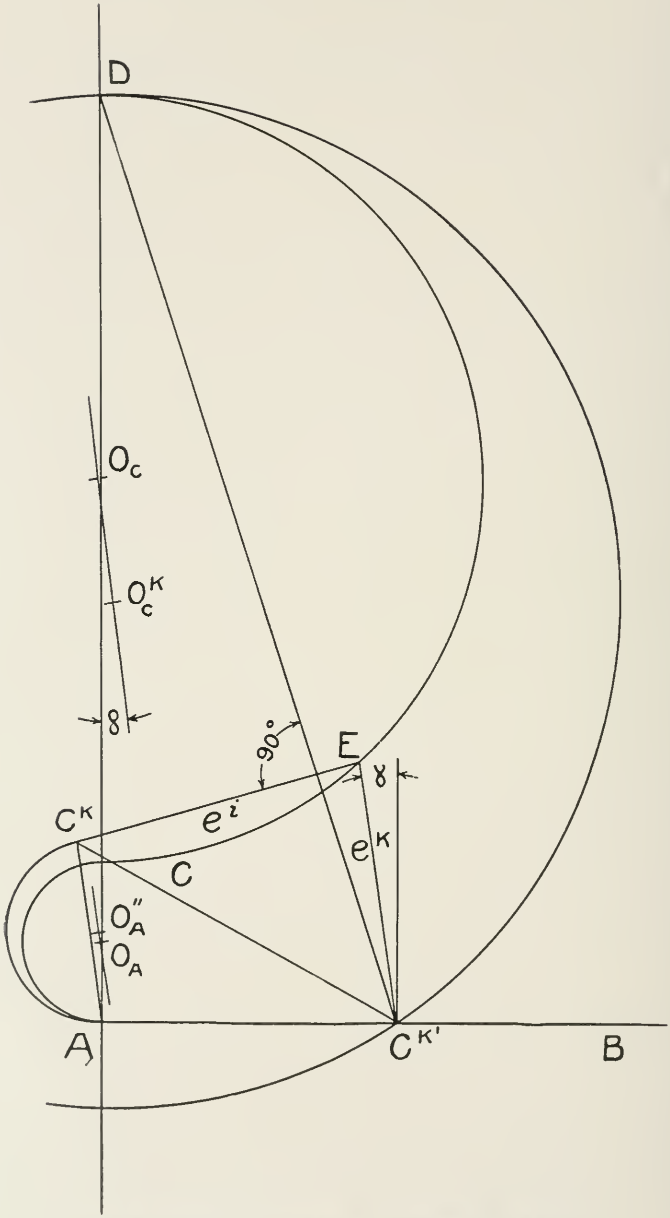

Plate XXIII.—Diagram Compensated Machine.

will be the angle α and is measured from the direction of AD. Lay off from O_c at the angle α a length $O_cO_c^k = \frac{e}{2}(1 - T)$, and from O_a at angle α a length $O_aO_a^k = \frac{e}{2}T$.

Draw a circle with O_c^k as center to pass through D; draw another with O_a^k as center to pass through A. The construction of the torque and mechanical power circles and of the slip line is made in the same way as for the ordinary motor.

This diagram yields a clear idea of the working of compensation in the motor, for, let the compensation be zero. e^k becomes zero. O_c^k falls back O_c and we have the original diagram. The greater the compensation the larger diameter has the circle and the more is the power output, (see later reference to an Observation of Heyland's ETZ 5/28/03). For but one load is the power factor exactly unity and in order to obtain this the no-load current must be a leading one, that is, the machine must be over-compensated.

Losses in the compensated are less than in the ordinary motor, the iron loss in stator is the same since it arises from the same stator field, while the rotor iron loss is slightly greater, due to greater flux but still negligible, while the copper losses in stator are smaller since for a given output the current is less with increased cos ϕ and similarly in the rotor from a certain load upwards the loss is less than in the ordinary motor.

This he shows[2] by data experimentally determined in a machine with a stator and two rotors, the first one employed being compensated, the second a wound rotor with slip rings. Measuring the rotor current revealed the fact that only on very low loads was the I_2 of the compensated greater than that of the ordinary motor. The explanation comes from the fact that power output equals common field times induced rotor current.

Since the flux is greater in the compensated motor to produce the same power output, a less current is needed in the secondary, or, to express it differently, for the same rotor current and therefore heat-loss the power output will be larger than in the ordinary motor. This effect is sufficient to more than allow for the increased current in the rotor due to compensation. He gives the following table:

---

[2] *Ibid.*, May 28, 1903.

	Normal motor.	Compensated Motor.	
		Same power.	Same heating.
H. P.	5	5	7
Iron and friction, per cent	14	14	10
Slip, per cent	4	2	4
Stator copper loss, per cent	4	2	3
Rotor copper loss, per cent	4	3.5	6
Per cent. efficiency	78	80.5	81

To return to the diagram, we see that the slip is for any load smaller than in the ordinary motor and varies inversely as the rotor current.

A figure (Plate XXIV) gives a very interesting comparison of the cos ϕ-output curves of the ordinary motor and of the compensated at various brush settings. As is noticed, the power factor rises much more quickly, attains and passes through unity but hugs it much more closely than does the ordinary motor going also to a greater output before it turns back and the output decreases. The greater the angular displacement, the quicker the power factor rises and the greater the output. It is found, however, that large brush displacement influences the efficiency unfavorably and this puts an effectual stop to too great a displacement.

As will be readily noted, the brush position which gives the best cos ϕ, at full load under motor action gives too small an output when the machine is run as a generator. Since there can never be inductive lagging power factor and any output from the machine, the output is limited by the intersection of the circle with the pressure line. This will be largely raised by increasing the brush displacement.[3]

---

[3] This does not mean that an inductive load cannot be supplied, but simply that there must be enough leading current to prevent the total power factor being a lagging one.

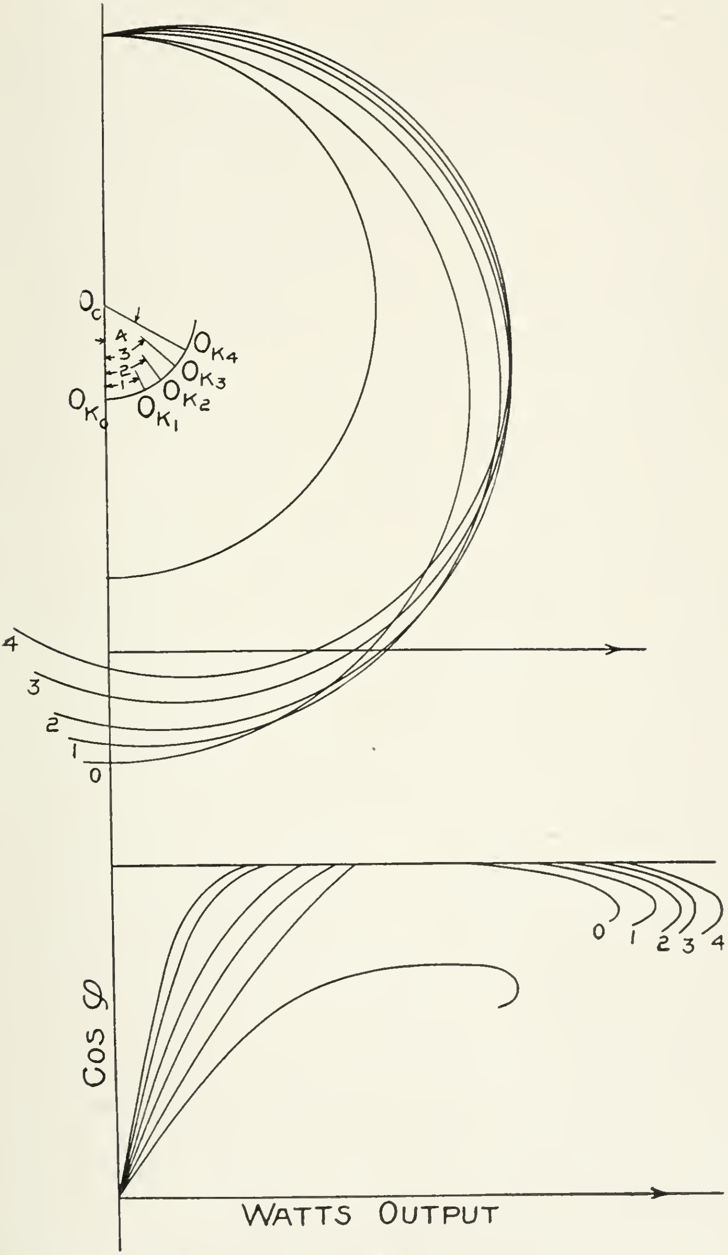

Plate XXIV.—Heyland, July 23, 1903.

The use of some motors over-compensated on light load upon the same mains as some regular induction motors with lagging cos ϕ, should be noted as an excellent and simple method for improving the general power factor of a system.

In chapter I, reference was made to the theory of the induction machine built up by Julius Heubach in his book, *Der Drehstrommotor* (Julius Springer, Berlin, 1903). In 1904, in the *Vorträge*, Heubach gives a *Theorie der Kompensierten Asynchronmaschine*, in which he develops working basis for the compensated machine along the same lines as in his book for the ordinary induction motor. He deals first with an ideal motor and gradually introduces the complications which are really met with, dealing, however, almost entirely with the motor and saying that the generator action may be obtained by completing to circles the five semi-circles which are the loci of the ends of the current pressure and flux vectors.

He offers no experimental verifications, nor has he any easy method of construction or reading off of the mechanical and other characteristics. Notwithstanding, however, his work is of a very high standard and is a noteworthy contribution to the literature. Since his method does not obviate the experimental errors in the determination of the various leakage factors, the results to be obtained from his diagrams are necessarily limited by the large per cent. of inaccuracy which is the best available in determining these leakage values. One reason why Grob's diagram stands preeminent is that instead of necessitating the observation of these various leakage factors, the data to be taken are easily and directly read and if desired the leakage factors may be deduced from the circles with a very considerable accuracy.

OSCILLOGRAMS

The theory assumes that pressure, current, and flux are all sine waves, and it is of interest to record the wave shapes used in taking the experimental data. The first data on generator test were taken with a pressure wave like No. 1, Plate XXV, which yields when subjected to the 80 part Harmonic Analyser of the mathematics department of the University of Wisconsin, the Fourier series,

$$57 \sin x - 8 \sin 3x + 17 \sin 5x \text{ (irregular)}$$

The current waves will be distorted as shown in Nos. 5 and 6 in the well-known way produced by a circuit containing inductance and resistance, the current wave being as shown practically independent of the shape of the pressure wave.

Pressure wave No. 2 was employed in the second set of generator experiments since it is much nearer the desired sine wave giving the following series.

$54 \sin x - 6 \sin 3x$

Oscillograms Nos. 3 and 4 are from the induction generator, capacity excited by condensors and thus free from the influence of any impressed wave shape. No. 3, the pressure wave at no load, is a very smooth curve with the formula:

$6 \sin x - 5 \sin 3x$, other terms negligible,

a very good approximation to the sine curve.

The current wave of No. 4 was taken when the current per ϕ was 18.3 amperes, the pressure 109, and the power factor $\cos \phi = .904$. The less apparent displacement of the oscillogram is without doubt due to the fact that the vibrator of the oscillograph was shunted across a lead through only a small part of which the total current flowed, much of the resistance drop being due to a current supplying lamp load only.

In connection with this curve, a rather peculiar phenomenon was observed. Superimposed upon the main current wave (appearing stationary in the oscillograph) was a ripple which appeared periodically and traveled from left to right over the wave, making difficult the accurate determination of the main wave. The period of recurrence of this traveling wave was rather long and its wave length much shorter than the main wave. This may be caused by the fact that, since the numbers of the stator and rotor teeth are made to have small greatest common divisor, there are only rare intervals when the flux path is highly good and the flux passes in a stronger tuft. If the rotor were running in synchronism with the stator frequency, these tufts would show up on the pressure wave also.

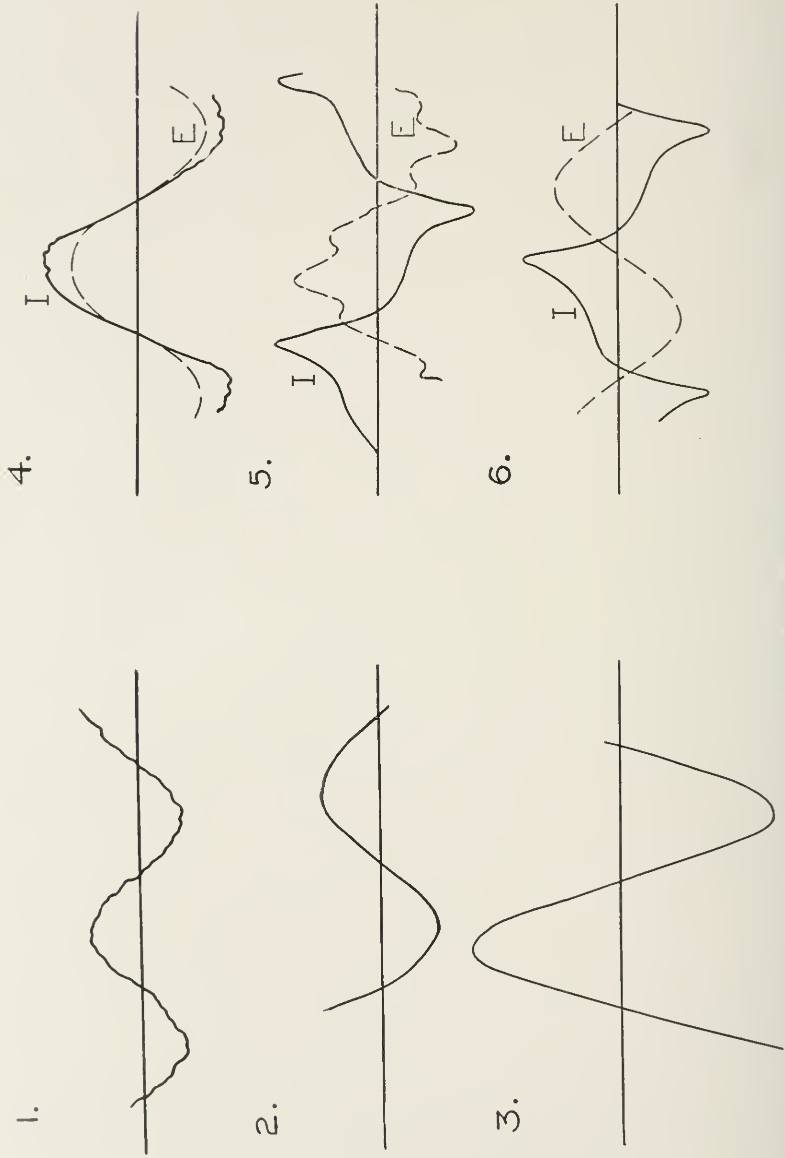

PLATE XXV.—OSCILLOGRAMS.

Since, however, there is a slip, the recurrence of this bunch of lines of force takes place only at a rate much slower than that of normal frequency, giving, in fact, a traveling wave whose rate of recurrence is equal to the slip. This is a rather interesting carrying through of stroboscopic revealing of hidden phenomena.

The oscillograms listed are

No. 1. No load 3ϕ pressure from a 3ϕ and 2ϕ synchronous machine. Wagner No. .919. 10 H. P. Type 6.

No. 2. No load pressure from a 3ϕ synchronous machine G. E. Co. No. 75654. 16 H. P. Type A. S. B.

No. 3. No load pressure from 3ϕ Induction Generator. Brown, Boveri No. 193913, 6 H. P. Condenser excited.

No. 4. Load pressure and current for No. 3 generator.

No. 5. Pressure and current on load composed of L and R in series. From one of the city supply generators.

No. 6. Same curves as No. 5 from a 3ϕ synchronous machine. National No. 1114. Type R. B. 200 kw.

In connection with the operation of the induction generator excited by condensers in the high pressure side of transformers in delta across the stator, (See Plate XIX) a rather interesting phenomenon was noted. As pointed out by A. S. McAllister, an induction generator will rise to the voltage represented by the intersection of the magnetization curve, plotted between volts and exciting current, and the line drawn to represent the condenser used to excite the machine. He also pointed out that there would be some capacities so low that they would nowhere intersect the curve and therefore give no pressure as A. Increasing the capacity increases the pressure as shown. If the capacity increases indefinitely, the pressure would theoretically soon come to a practically constant value and remain there, demanding a very much greater magnetizing current, provided the frequency remains constant. The limit of this action is when an infinite capacity, i. e., a conductor, is shunted across the stator. This infinite capacity line would cross the magnetization curve at ∞ and o giving maximum pressure with ∞ magnetizing current or zero pressure and current. As seen by experiment when an infinite capacity, in this case a severely punctured condenser, was put across the line the excitation was entirely lost. Ordinarily when the circuit to an induction machine is broken, magnetism must be left in at least two of the three phases, no matter at what point of the wave the switch is pulled, and upon again starting as a generator the machine will pick up by itself. After passing through the reduction to zero, however, by means of ∞ capacity all the magnetism is killed, there is no residual, and one phase must be primed from an external source in order to start the machine. In some cases when the punctured condenser was inadvertently left included, the machine would not excite even though primed, since it immediately returned to zero.

Heyland in describing some tests on his first machine says in this respect: "The chief difference in the asynchronous alternate current dynamo is the fact that it does not possess fixed poles as in the continuous current dynamo and *has therefore also no residual magnetism*. . . . residual magnetism is absent and after bringing the generator up to speed it must be separately excited from some external source."[4]

The machine which I used was regular stator construction without pole-pieces and yet picked up invariably, unless the magnetism had been killed by raising the capacity to an infinite value. It would appear that Mr. Heyland's machine should have picked up also. The phenomena attending critical speed were also observed. That is, there was a definite speed below which the machine would not pick up with a certain condenser and above which it worked nicely. It was noticed that the change of the capacity in any one leg influenced the voltage of the whole system so the experiment was tried, keeping the speed of prime mover constant, of adjusting the pressure with varying load by means of a variable condenser in one leg. It behaved admirably, acting, of course, simply as a field rheostat in a shunt direct current machine to vary the amount of the exciting current. With constant rotor speed, however, the increased slip

---

[4] *Electrician* (London), Jan 24, 1902.

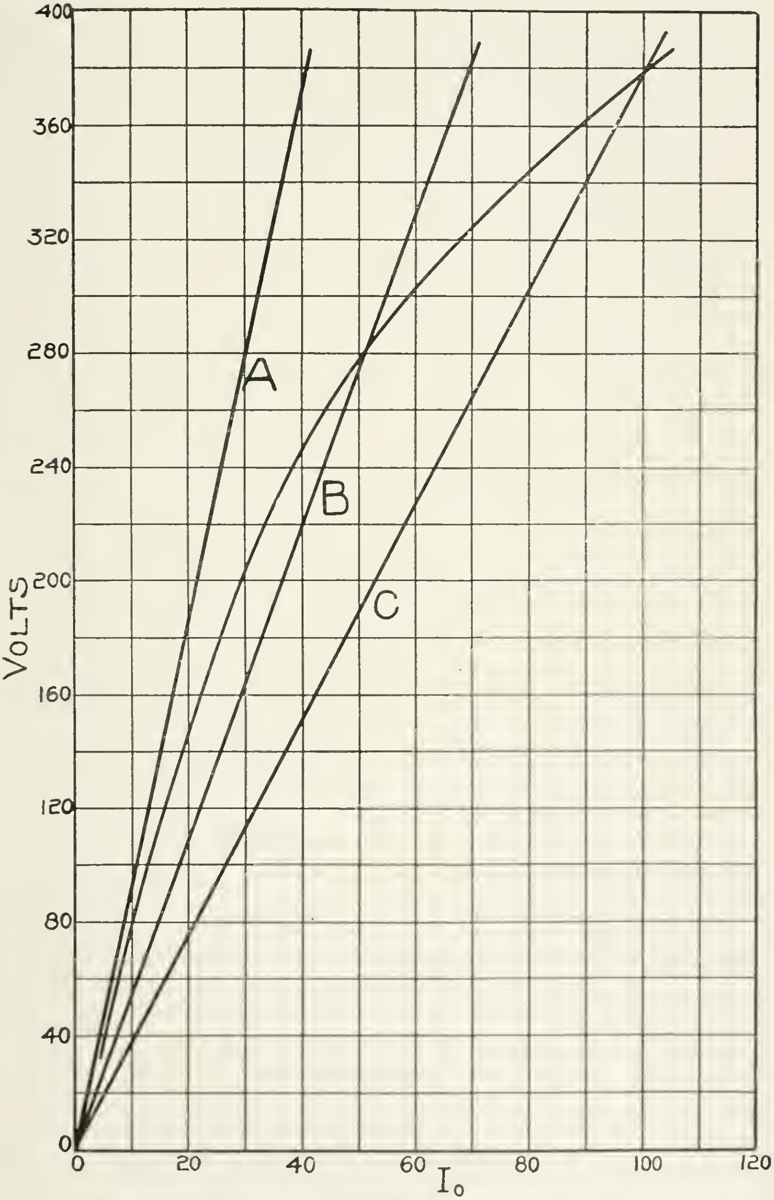

Plate XXVI.—Voltage Determined by Capacity.

under load necessarily gives a lowered line frequency; this lower frequency applied to the condenser requires for the same effective capacity-reactance a much larger capacity in microfarads than as though the line frequency were constant. This means that the regulation is very bad and with increasing load the attendant in charge of the condenser must be very active or his voltage will not only fall low but he will lose his excitation and have to begin anew. The curves, shown in Plates XXVII and XXVIII, are very ragged, following the variations in pressure. These, however, are as closely adjusted as the steps of the condenser would permit.

The lines for the compensated motor in the Grob diagram may be found as follows. In the Heyland diagram the secondary power factor is taken as unity, that is, secondary current I_2 in phase with E_2 and therefore at right angle to ϕ_2, the secondary flux. This cannot be true for any position except at synchronism where the frequency in the secondary circuit is zero, since there is some inductance even in a squirrel-cage rotor, and L combined with even a small f will inevitably produce its 2π fL and phase angle.

This angle will increase up to standstill where full frequency is impressed; in fact, in both directions from synchronism the frequency will increase until infinite frequency is reached; but by what law this variation occurs is not known. Some preliminary experimentation showed that this determination of law of change of cos ϕ_2 is far from free of complexities and, due to shortness of time, this particular line of investigation was abandoned for the time (although the author hopes later to take this point up much more fully) when it was found that variations in pressure much smaller than could be regulated varied the observations to such an extent as to make consistent data impossible.

The problem even for the ordinary motor is an interesting one, for we have in addition to the increasing frequency with increase of load the increase of saturation; and varying with that the increase of current, and flux—wave-distortion, which though small at no load due to the air-gap, soon becomes far from negligible. L_1 and M both vary with load also and like so many

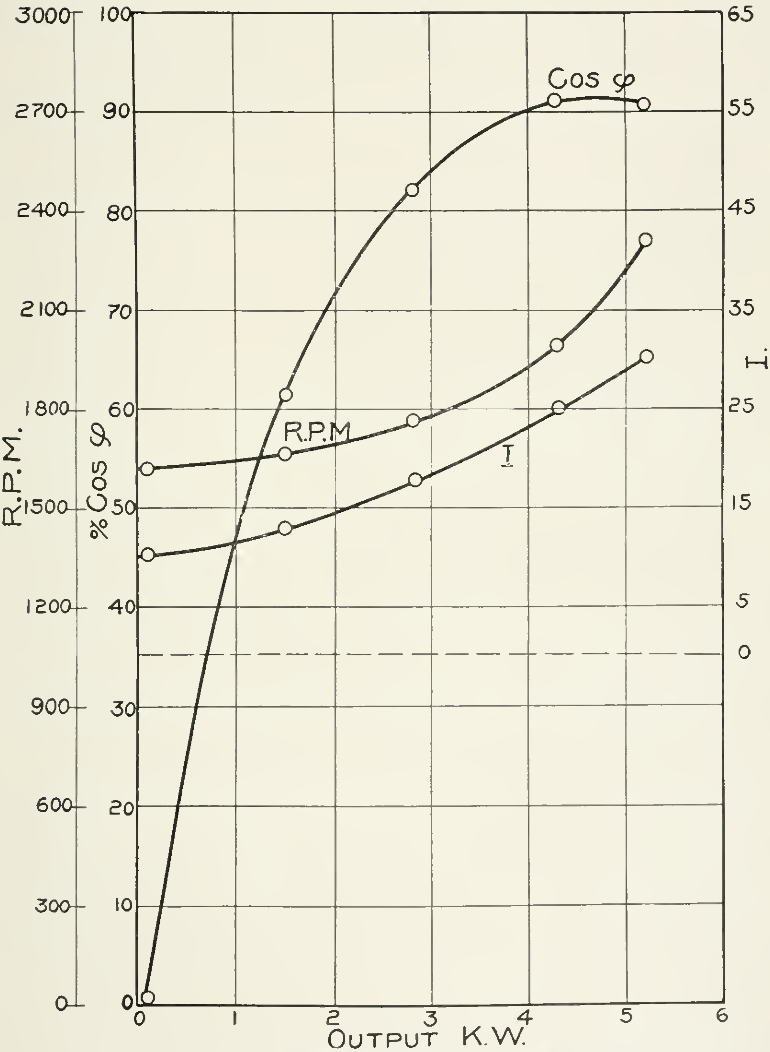

PLATE XXVII.—BROWN BOVERI INDUCTION GENERATOR.
Capacity excited.

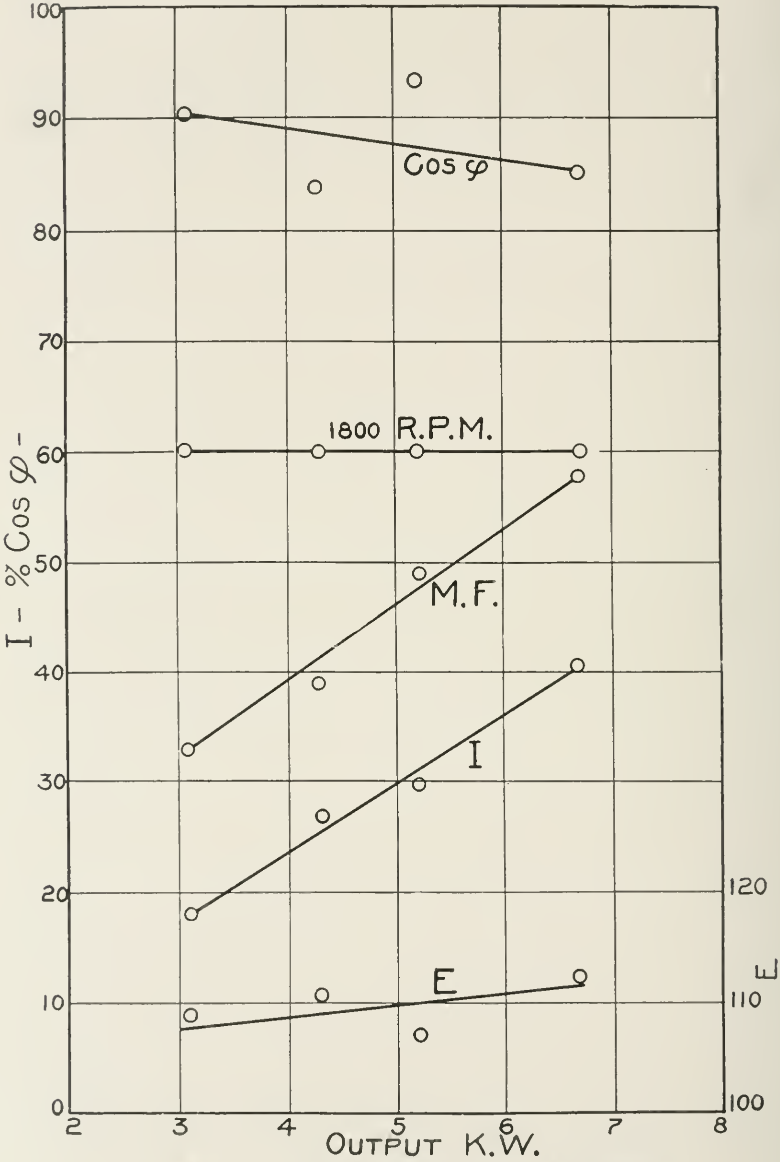

Plate XXVIII.—Brown Boveri Induction Generator.
Capacity excited. Constant speed.

of the functions in the motor with a most peculiar law of variation.

On the whole, to quote a member of the department of physics, "this point alone would make a most excellent and complete subject for an investigation for a Ph. D. thesis."

Acknowledging, then, the source of error involved in the compensated-motor diagram for which this is in a measure an underlying point, I proceed to the development, claiming, however, as is due, a much greater accuracy than is found in Heyland's. The limits upon the circle between which the free end of the secondary flux vector can move are a very small per cent. of the total circumference and thus the total error is not large.

Starting, then, with the Brown, Boveri motor, on which the most accurate work has been done here, let us consider that it is fitted with a direct current armature with shorted commutator and that the brushes are displaced five electrical degrees. (Plate XVI.) Let us further assume that we desire to obtain unity power factor at a load a little less than full load. The construction will proceed as follows:—parallel to the diameter through the no load current position, draw a line through the desired value on the pressure line (where, of course, I_1 and E_1 are in phase at unity $\cos \phi$).

Lay off an angle of 5° from this line and another at 5° from the center of the circle. Draw the flux line and perpendicular to it, through the intersection of the 5° line and the circle, a line to intersect the secondary circle. Draw a line from the new primary current end through the upper intersection of the circles; this is the new secondary current. The change in the secondary circle is so slight as to be inappreciable, the increase of secondary current coming at the other end. Now, with center on 5° line through the center of the original circle draw a circle through the end of the new primary current and through the far end of the flux line. This will be the circle for the compensated motor and self-excited generator under the conditions specified and to the same scale as the ordinary circle. The maximum motor output will exceed that of the uncompensated motor and the power factor will be much higher starting as a leading—passing through unity and continuing as a lagging-power factor. At the maximum output (about 15.6 h. p. with this arrangement as compared with 12.3 h. p. as a normal motor) the power factor is still as high as 91 per cent. As a generator, the machine will be self-exciting only so long as the circle stays on the right of the pressure line. With this particular brush position the output could rise only to about 6 h. p. This shows the necessity of a greater brush displacement for generator than for motor action and also that for best performance the brushes must be shifted when the change in function occurs. This is true since the position which would give proper output as a generator (a larger diameter circle) would give a motor power factor very bad as a leading current. To represent different brush displacements other circles are necessarily constructed in a manner just like the above except that some other number of degrees is selected and the new center is differently displaced. If it is desired to have unity power factor fall at some other load it may readily be done simply by choosing that point as the origin of field of flux, and of secondary current. As has been pointed out, it is entirely possible so to adjust a compensated motor that its leading current at light loads will just balance the lagging currents of similar uncompensated motors at light load. Curves have been drawn for the ordinary motor and generator and for the same machine compensated for unity power factor at normal full load and with 5° brush displacement.

As plotted, the curves for the 5° machine seem to point to error, since not alone is the ratio of mechanical to e. h. p. greater than one, during much of the range, but there is a time when both are output. It must be remembered, however, that the e. h. p. curve involves only the power brought to or taken from the stator and to represent the total this would need to have added to it the power to the rotor. The most interest attaches, however, to the relation between the stator currents in the two cases. The appearance of mechanical power from the rotor and electrical at the same time from the stator is like taking, in the ordinary motor, current and mechanical power both from the rotor. The machine acts in each case both as motor and as transformer being thus Steinmetz's "most general case of the alternating current transformer" since it gives out part of the energy as mechanical power and part as electrical at changed pressure and frequency. As shown. (Plate XVIIb) the compensated machine will give motor output nearly up to synchronism with input to both stator and rotor. Then the rotor becomes the only point of input and mechanical power and electrical from stator may be obtained up to a little *above* synchronism. Thereafter. mechanical power must be input and electrical output is derived from the stator. Self-excitation with 5° displacement continues only up to a trifle over 6. h. p. and thereafter some other source of leading current must be employed. although, as will be noted. the amount of this leading current is much less than is required by the normal motor.

It will be noted that while the power factor rises both in motor and generator much faster and higher than when uncompensated. although it reaches unity and passes through. it merely hovers near it and does not. as Heyland's early articles maintained. give "unity for all loads." It does stay good up to more than 100 per cent. overload as a motor (as a generator it soon falls off). but not at unity. and while .97 is good. it still represents an angle of 14° 4′ between pressure and current. while .95 is 18° 12′ and .90 (often reached by ordinary motors) is only 25° 50′. an angle of 8° 6′ with .99 power factor.

The curves of primary current for the two machines are much alike; the main difference being in their minima. the compensated falling much below the ordinary induction motor for its minimum current when power factor equals zero.

An efficiency curve can. of course. not be plotted for the compensated machine until the total input is known both to stator and rotor.

The rotor current flows due to a pressure which is the resultant of two components. one due to motion in stator field which is perpendicular to rotor field and varies directly with the slip. the other component is that which comes in from the line and is of constant value and is fixed in position by the degree of brush displacement.

At synchronism the first of these falls to zero since there is no relative motion and therefore no cutting of stator lines by the rotor. The current triangle falls into a straight line at synchronism in which case the equation $I_2 = I_1 + I_m$ holds algebraically, whereas in all other places it is merely a vector equation.

To determine rotor input for positions other than synchronism a knowledge of secondary power factor is requisite and since this is a variable of unknown law this solution will have to be postponed for some future investigation.

BROWN, BOVERI COMPENSATED 5° DISPLACEMENT

Scaled from diagram. Plate XVI.

Slip	I_1	STATOR H. P.		Per cent Cos ϕ
		Electrical.	Mechanical.	
∞	188	11.8	19.3	24.0
Standstill. 1.00	166	23.8	0.	55.0
.761	150	26.2	7.1	67.0
.470	125	26.0	13.3	79.7
.311	100	23.2	15.4	89.0
.229	80	19.6	15.2	94.0
.192	70	17.5	14.4	96.0
.163	60	15.2	13.5	97.7
.143	50	12.8	12.0	99.0
.109	40	10.4	10.4	99.8
.078	30	8.0	8.5	100.0
.052	20	5.2	6.4	99.0
.035	15	3.8	5.2	97.8
.029	10	2.6	3.8	93.4
.007	3.7	0.	1.5	0.
.000	4.0	.4	1.0	39.0
.005	6.3	1.4	0.	82.0
.010	10	2.6	1.2	96.2
.016	15	3.8	2.6	98.9
.023	20	5.2	4.2	99.9
.028	24	6.1	5.2	100.0
.036	30	7.6	7.1	99.9
.049	40	10.2	10.1	98.9
.062	50	12.7	13.4	97.6
.075	60	14.9	16.5	95.9
.102	80	18.9	22.7	91.3
.131	100	22.2	29.1	85.1
.178	125	24.4	36.6	75.0
.243	150	23.7	42.1	61.0
.400	175	18.2	44.7	39.0
.506	185	13.0	40.9	23.4
1.000	192	0.	33.0	0.
∞	188	11.8	19.3	24.0

THE MACHINES

In the production of a machine which will excite itself as a generator and have a good power factor as a motor, many hybrids have resulted some of which are important and others mere freaks.

The general scheme has been to place in the rotating field of an ordinary stator a rotor which consists essentially of a direct current armature, (modified in different ways to suppress sparking, etc.), into which current of the frequency of the line is led through brushes spaced around the commutator at electrical angles equal to the number of degrees of the system, 90° for two phase, 120° for three phase, etc.

The first schemes merely short circuited the commutators of ordinary direct current armatures through a low resistance, while the later ones have produced marked changes in the internal construction and winding, all retaining, however, the commutator and three brushes, which by their displacement determine where in space the exciting field, now coming from the rotor, shall be held fast.

Since compensation brings the slip to lower values, making more care requisite in paralleling though not needing synchronization, there have resulted as examples of the hybrids mentioned above, asynchronous motors which run at synchronous speed, and synchronous motors with a pronounced slip.

Any device by which we can produce the wattless component necessary for excitation, on the scene of action, and obviate its transmission with the accompanying lowered power factor, will be an immense improvement.

If with an ordinary induction rotor locked in position current of the line frequency be led to the slip rings, a revolving field will be set up in the rotor which will travel around at the same rate as that in the stator, and, by making its ampere-turn strength exceed that of the field by the proper amount, the wattless component of the stator current may be annulled. If the rotor be brought up to synchronous speed, the same results can be achieved by using a direct current of the proper value. (This becomes an induction motor running synchronously.)

For speeds other than standstill and synchronism the wattless primary current may be balanced and the line power factor raised to unity by impressing the proper frequency on the rotor.

This proper frequency may be obtained by supplying a commutator and brushes to which line frequency is led. No matter at what speed the armature may be rotated the commutator causes the current to pass through conductors having the same position in space and therefore the same relation to the magnetism of the stator.

The frequency necessary at any time is line frequency less the frequency of the rotation. Thus at standstill 60 frequency —0 frequency = 60 frequency. At synchronism 60 frequency —60 frequency = 0 frequency; at half speed 60 frequency—30 frequency = 30 frequency, etc.

An ordinary direct current armature would have no torque since no current would flow in it. We must, therefore, connect together points which have some difference of potential that current may flow and torque be exerted. To this end Heyland in his first machine simply shorted the whole commutator. (This was also done at practically the same period by Professor D. C. Jackson at the University of Wisconsin.) These shorting resistances form a shunt through which the reactance voltage at the instant of commutation may discharge and thus improve sparkless conditions at the brushes.

As to the degree to which commutation has been improved opinions differ. Most of the foreign comments are decidedly favorable, but as most of the writers were describing the machines they themselves had invented, we must remember that their panegyrics may, in a measure at least, be due to enthusiasm. In this country, Prof. C. A. Adams' experiments with a G. E. experimental model did not show perfection, though he admits his connections (for compounding) were a little questionable. Dr. A. S. McAllister in his most excellent treatise, *Alternating Current Motors*, says (p. 45): "So effective is the elimination of sparking that no observable result is produced by shifting the brushes into any position." Also: "The resistance forms a non-inductive shunt . . . which fact allows the use of copper brushes of cross section much less than that required for carbon brushes and the commutator is given a correspondingly smaller size." Prof. Adams says: "The large exciting currents used in the generator tests gave trouble on another score, that of sparking; in fact with any exciting current within the working range there was some sparking, but with the larger currents the sparking was so vicious as to require that the commutator should be turned down after a run of a few hours. It is thus evident that the damping effect of the low resistance squirrel cage is not sufficient to warrant the use of copper brushes, certainly not with such a small number of commutator bars."[5] (The squirrel cage mentioned is another device to obtain torque and supposedly to prevent sparking.)

Like so many other points, in a subject of this nature so far from being settled, it is necessary to weigh the evidence, in the absence of personal experimentation, and then draw your own conclusions.

The first motor was Görges,[6] a series polyphase motor, which was excellent at synchronous speed but execrable elsewhere and since the series motor characteristics do not leave it long at synchronous speed it met with no success.

Blondel[7] brought out a motor which was in a measure the complement of Heyland's since it consisted of the same stator and same short-circuited direct current armature but used in place of the polyphase rotor excitation, direct current excitation put into the armature through brushes rotated by a synchronous motor. The action of this motor was successful, it being in all essentials identical in theory with Heyland's, but the complication of the synchronous motor and keeping the pressure of brush on commutator uniform prevented commercial success.

It is regrettable that so many additions to knowledge are accompanied by discord. The compensated motor is not an exception; the discussion between Heyland and Latour as to priority of invention being almost as acrimonious as the Tesla-Ferraris controversy. Heyland's first article[8] appeared in 1901 and described the motor with direct current armature shorted through non-inductive resistances; and also the machine with two windings, one straight direct current, the other squirrel-cage. He noted that it would self-excite as a generator.

Latour describes[9] a very similar machine intended as a generator principally. It differs from Heyland's in having no squirrel-cage and is in fact as he calls it a "shunt-machine." The current of slip frequency finds a path, in lieu of any other, back through the supply lines.

---

[5] *A. I. E. E. Trans*, **20:** 780.

[6] *Elektrotechnische Zeitschrift*, Dec. 25, 1891.

[7] *Ec. El.*, Aug. 29, 1890.

[8] *Elektrotechnische Zeitschrift*, Aug. 8, 1901.

[9] *Industrie Electrique*, Feb. 25, Apr. 10 and 25, 1902.

Osnos has described[10] a machine in which the exciting current is commutated in a small auxiliary armature and then led in rotor through rings.

At the St. Louis Congress, where the compensated machine was severely criticized as being beautiful but not applicable to machines of sufficient size to be commercially practicable (500 Kilovolt-ampere machines have been built and run successfully), this device of external commutator was spoken of as the possible saving of the situation for the compensated machine. In all of Heyland's numerous machines this commutator (called "sifting device" by Prof. Karapetoff since it separates watt from wattless current and allows of real flat compounding regardless of power factor) is the one unchanged and unchangeable feature.

An alternator with a practically constant frequency and speed but requiring no synchronizing to parallel, which can be compounded to any desired extent and is absolutely self-contained except for static transformers, being thus independent of any exciting source whatsoever, is assuredly a desideratum. The statement made at St. Louis that in any plant large enough to need such regulation there would always be an attendant who could watch the voltage, does not appeal to me as at all removing the desirability of an absolutely *automatic* regulation. A synchronous alternator with a good Tirrell or similar regulator in the exciter circuit would be hard to beat on load of unity power factor but there is no other device than the compensated and compounded induction generator employing this sifting commutator which will automatically compound for the energy current alone in circuits of any power factor.

The figure (Plate XXIX) shows two rotors both essentially direct current armatures but modified; one by resistances shorting from one commutator bar to the next, the other by the addition of a regular squirrel-cage winding of medium resistance in the same iron with the direct current winding.

---

[10] *Elektrotechnische Zeitschrift*, Oct. 16, 1902.

The upper figure (Plate XXIX) shows a favorite connection which obviates the expense of a separate transformer for reducing line pressure to a value which can be successfully handled by the rotor commutator. As seen, it employs the stator iron as core for a polyphase transformer of which the normal stator winding is primary and the additional low tension winding shorted through the rotor, which may be of any type, is the secondary.

Heyland's most successful winding scheme is shown by the upper pair of figures which picture a two-pole three phase machine showing two conditions in the commutation cycle. The brushes are shown as moving, the armature stationary, of course identical in result with the actual condition since relative motion alone is essential. The winding shown has 2 bars per pole per phase that are active, and 1 per pole per phase inactive, thus making 18 in all. The winding is in six sections shorted inside the bars by 10 ohmic resistances by the proper proportioning of which the reactance voltage of commutation may be reduced theoretically with a sine wave to zero. Practically there exist enough harmonics in every wave to produce some sparking at any time, but a small minimum may be reached and it is interesting to note, as pointed out by Heyland's paper at St. Louis, that it is possible to reduce to zero with a perfect wave, a thing not ever possible with a direct current commutator.

The brushes are made wide enough to span the inactive segments as shown to the right where brush I is in the act of commutating, that is, short circuiting, the active segments of opposite sign. In these two figures is shown the action of this machine which is a successfully self-exciting and compounding *synchronous* generator. Though not coming strictly under the heading of this thesis this machine is included because it is a direct product of work on asynchronous machines and would never have been evolved save as the limit of gradual injection into the induction machine of characteristics of the synchronous. It becomes very difficult to tell to which class a machine really

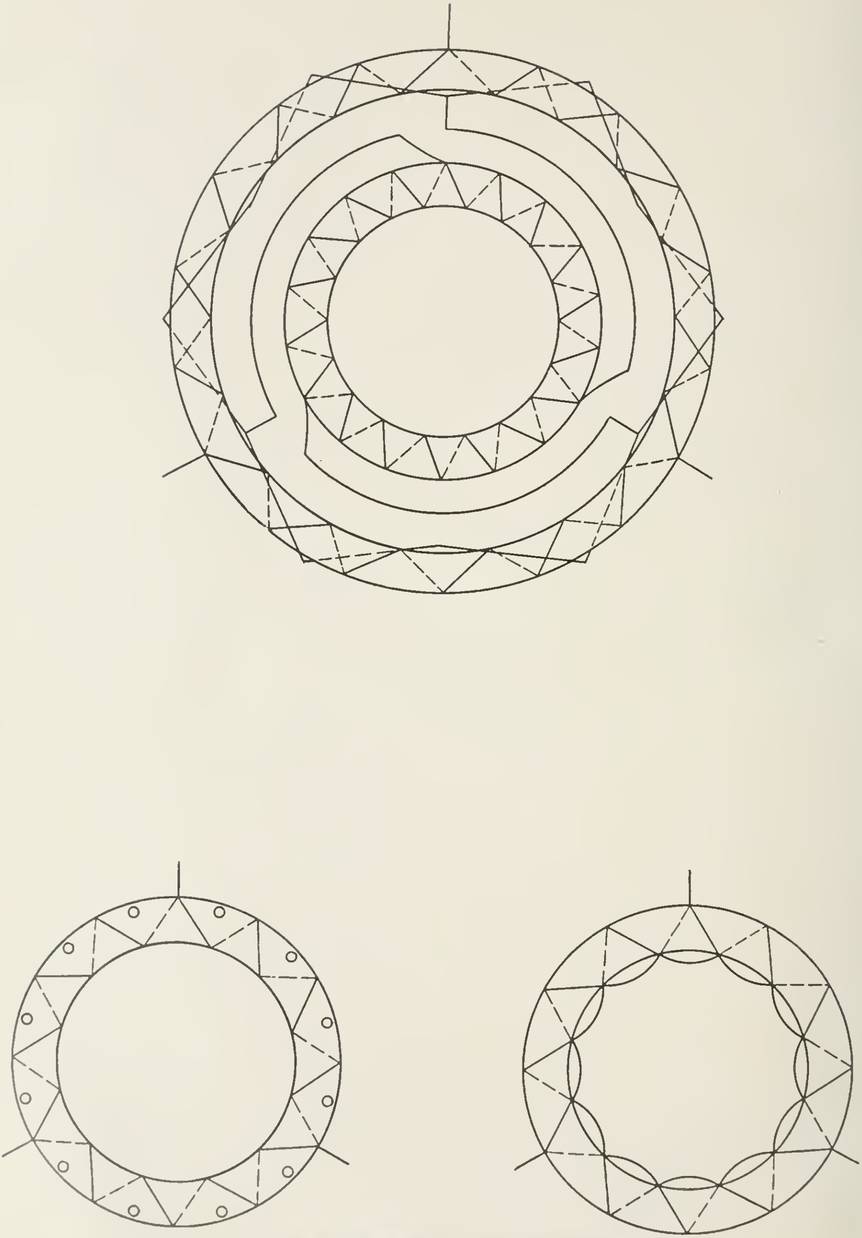

PLATE XXIX. WINDING DIAGRAMS.

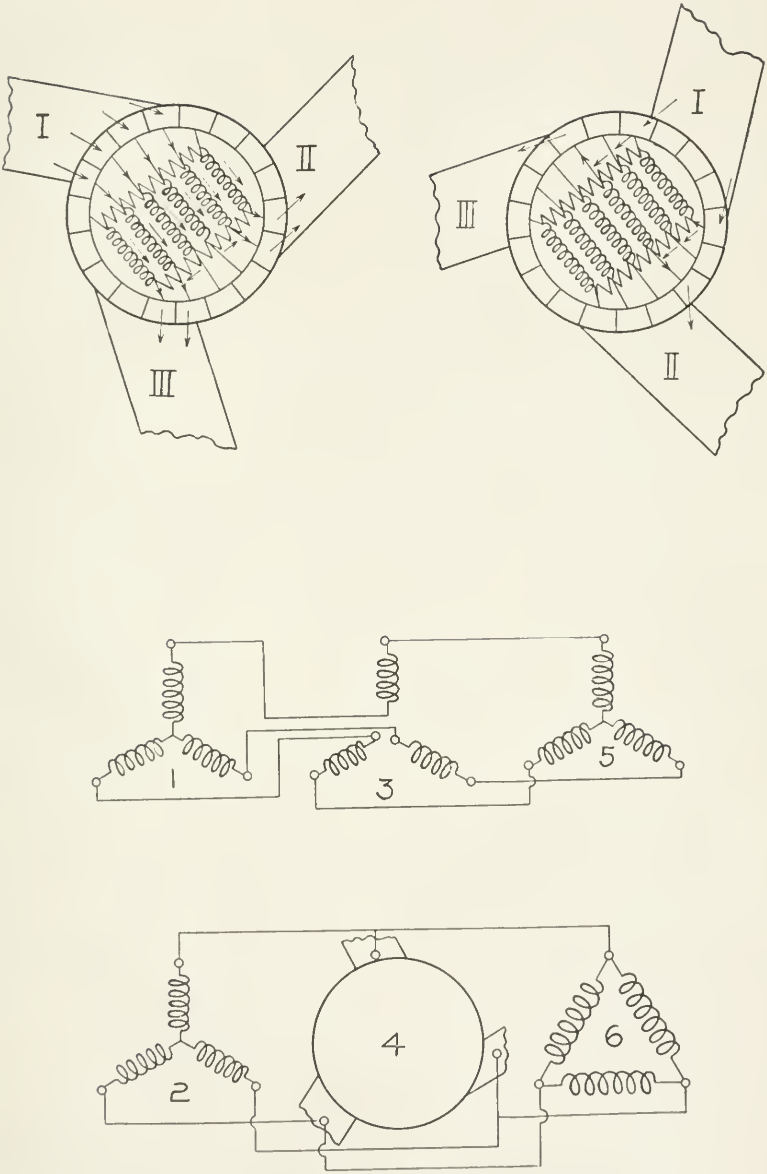

Plate XXX.—Heyland's Connections.

belongs when it partakes, as so many do, so very strongly of the characteristics of both. This commutator has the same function of sifting out watt from wattless as in the induction machine pure and simple and the method of compounding is identical.

At first, for compounding, Heyland used a second set of three brushes placed on the commutator 90° ahead of the first set (since there is a 90° lag of wattless current behind e. m. f.). This worked very satisfactorily but the six brushes looked formidable so he reduced them to three by using (as is necessary with large machines) transformers and connecting (as shown in lower figure) the secondaries of the exciting transformers in mesh whereas the primaries are in star. This gives an additional angle of 30°, which added to the 90° gives 120°, thus coinciding with the next brush and making but three requisite.

In the lower figure, No. 1 is the primary side of the compounding transformer and No. 2, the secondary. No. 3 is the generator armature (stationary) and No. 4 is armature and commutator as shown in upper figure, while No. 5 is primary and No. 6 secondary of the exciting transformer.

By adjusting the number of turns in the compounding transformer any desired degree of compounding may be obtained while the main exciting current is varied if desired by variable resistance, although the idea is to fix the adjustments once and then leave them alone unless it is desired to correct for greater line drop, etc.

BIBLIOGRAPHY

ARTICLES

Elektrotechnische Zeitschrift:

- Thomälen, A. November 26, 1903; August 11, 1904.
- Ossanna. August 2 . 1900.
- Heyland, A. Page 561, 1894; page 632, 1896; August 8, 1901; August 21, 1901; November 21, 1901; December 12, 1901; January 9, 1902; June 26, 1902; January 22, 1903; January 29, 1903; February 5, 1903; March 19, 1903; May 28, 1903; June 26, 1903; July 23, 1903; November 5, 1903; December 17, 1903; November 1, 1906; February 7, 1907; February 14, 1907.
- Grob, H. January 24, 1901; June 2, 1904; June 9, 1904.
- Kuhlmann, K. April 18, 1901; vol. 22, page 341.
- Neithammer, Dr. F. Vol. 22, page 474.
- Bragstad, and La Cour. Vol. 25, page 993.
- Beneschke, G. Vol. 25, page 738; vol. 25, page 1401.
- Kolben. November 8, 1903, et seq.
- Weisshaar, O. November 14, 1901.
- Osnos. October 16, 1902; November 27, 1902.
- Bodensteiner. August 21, 1902.
- Heubach, J. April 27, 1899; May 4, 1899. Page 73, 1900; page 97, 1906.
- Müller, P. Vol. 25, page 173.
- Behrend, B. A. January 30, 1896; January 24, 1901.
- Behn Eschenburg, Dr. Page 178, 1894.
- Behn Eschenburg, Dr. and Cohen. Page 284, 1894.
- Steinmetz, C. P. Page 78, 1896.
- Görges, M. April 9, 1903; December 25, 1891.
- Latour, M. May 22, 1902; July 3, 1902.
- Sievert, A. August 1, 1901.

Zeitschrift für Elektrotechnik:

- Sumec, J. K. January 4, 1903; April 14, 1901; August 27, 1905.
- Besig, F. July 10, 1904.
- La Cour, J. November 1, 1903, et seq.
- Breslaur, Dr. M. April 20, 1902.
- "E. A." Page 346, 1902.
- Ossanna. Page 223, 1899; page 236, 1899; page 248, 1899.
- Puluj, J. Page 63, 1904; page 80, 1904.
- Rosskopf, June 11, 1905.
- Hobart, H. M. March 13, 1904.
- Alexander, and Fleischman. May 3, 1903; May 10, 1903.
- Sartori. Page 188, 1903.

Electrical World and Engineer:

- Way, W. C. December 25, 1905.
- Press, A. September 9, 1905.
- McAllister, A. S. January 17, 1903; vol. 41, page 109.
- Averett. Vol. 46, page 270.

Electrical World and Engineer—Continued.
Reyval. October 7, 1905.
La Tour, M. Vol. 45, page 97; vol. 41, page 442; vol. 41, page 479; February 1, 1902; March 14, 1903; March 21, 1903.
Heyland, A. Vol. 40, page 817.
Danielson, E. Vol. 21, page 44.
Alexanderson, E. F. May 20, 1905.
Specht. February 25, 1905.
Heyland, A. Feburary 23, 1907.

American Electrician:
McAllister, A. S. January, 1903; July, 1903; November, 1903. Vol. 15, page 534.

Transactions, American Institute of Electrical Engineers:
Alexanderson, E. F. January, 1906.
Langsdorff, A. S. September, 1905.
Garfield, A. S. May, 1903.
Adams, C. A. May, 1903.
Franklin, W. S. May, 1903.
Behrend, B. A. Vol. 21, page 497; vol. 21, page 517.
Perkins. Vol. 24, page 649.

Sammlung Elektrotechnischer Vorträge (Volt):
Heyland, A. Vol. 2, paper 2.
Niethammer, Dr. F. Vol. 2, paper 3.
Arnold, E. and La Cour, J. Vol. 3, paper 1; vol. 6, paper 3.
Heubach, J. Vol. 4, paper 1; vol. 6, paper 1.
Breslaur, Dr. M. Vol. 4, paper 4.
Railing, Dr. Ing. A. Vol. 4, paper 6.

Electrician (London):
Butt, T. P. E. August 25, 1905.
Heyland, A. Vol. 36, page 505; vol. 36, page 578; vol. 36, page 651; vol. 36, page 719; vol. 36, page 753; vol. 53, page 509; January 24, 1902; October 26, 1906.
Breslaur, Dr. M. Vol. 51, page 803; vol. 51, page 903; vol. 51, page 940.
Eborall. Vol. 51, page 442; vol. 51, page 486.
Hawkins, C. C. January 27, 1899.
Ferraris, Prof. G. December 27, 1895.
(Translated entire from Turin Acad. Vol. 23, March, 1888. Rotazioni Elettrodynamische.)

Electric Journal:
Karapetoff. Vol. 1. ——.

Western Electrician:
Reist. Vol. 26, page 353.
Heyland, A. Vol. 37, page 144.

Electrical Review (London):
Parker, W. July 1, 1904.
Heyland, A. December 7, 1900.
Hooghwinkel, A. Vol. 53, page 122, et seq.

Industry and Iron:
Jackson, D. C. Vol. 21, page 124.

Electricien:
Aliamet. Vol. 23, page 113.
La Tour, M. Vol. 23, page 164.

Eclairage Electrique:
Blondel. August 29, 1896; May, 1895; April 25, 1903; May 2, 1903. Vol. 35, page 121; vol. 35, page 167.
Lehmann, Dr. Th. August 22, 1903. Vol. 36, page 281; vol. 36, page 351.

Eclairage Electrique—Continued.
Neithammer, Dr. F. Vol. 40, p. 5. July, 1904.
Bethenod. Vol. 40, p. 253; vol. 40, p. 281.
Adams, C. A. Vol. 38, p. 23.
Osnos. Vol. 31, p. 279.
Hutin, and Leblanc. Vol. 40, p. 373.
Leblanc. August 29, 1896; October 26, 1901. Page 161, 1899; page 376, 1899.
La Tour, M. November 30, 1901; April 12, 1902.
Poincaire. January 18, 1902.
Heyland, A. March 22, 1902.

Schweizerische Electrotechnische Zeitschrift:
Lehmann, Dr. Th. Serials in 1904.
Niethammer, Dr. F. Serials in 1904.
Behn Eschenburg, Dr. Serials in 1904.

Elektrotechnische Anzeiger:
Zeigenberg. July 17, 1902; July 24, 1902; August 10, 1902; August 17, 1902; September 21, 1902; September 28, 1902; October 21, 1902; October 28, 1902.
Hahn. Page 678, 1904.

Bulletin de la Societie International des Electriciens:
Leblanc. Vol 15, p. 488.

Industrie Electrique:
Latour, H. B. Vol. 11, page 148; vol. 11, page 172; vol. 11, page 245; vol. 11, page 149.
Heyland, A. Vol. 11, page 244.

Proceedings of the Institution of Electrical Engineers (London):
Walker, S. F. April, 1905.

Sibley Journal;
McAllister, A. S. November, 1902.
Norris. March, 1901.

Elektrotechnics und Maschinenbau:
Lombardi. September 30, 1906.

Electrical Engineer (London):
Pensabene. February 12, 1904.
Davies. January 27, 1904.
Heyland, A. November 9, 1906.
Butt. Vol. 91, page 36.

Proceedings of the International Electric Congress;
La Tour. St. Louis, 1904.
Steinmetz, C. P. St. Louis, 1904.
Heyland, A. St. Louis, 1904.
Leblanc. Paris, 1900.

THESES UNIVERSITY OF WISCONSIN.

Whiting, M. A., *Induction Generator and Booster.* (For B. S.)
Foote, F. J., *Design of Induction Motors.* (For E. E.)
Feige, H. *The Rotor Pressure Waves of Induction Motors at Synchronous Speed.* (For B. S.)
Scott, A. C. *Rotations Single-phase Alternator.* (For Ph. D.)

Books.

McAllister, Dr. A. S., *Alternating Current Motors.*
Thompson, S. P., *Polyphase Electric Currents.*
Bedell, F., and Crehore, *Alternating Currents.*
Russell, A. S., *Alternating Currents* (2 vols.).
Raymond, E. B., *Alternating Current Engineering.*
Blondel, ——. and DuBois, *La Traction Electrique* (vol. 2).
Hobart, H. M., *Electric Motors.*
Jackson, D. C., *Alternating Currents.*
Hay, A., *Alternating Currents.*
Oudin, M. A., *Standard Polyphase Apparatus and Systems.*
La Tour, H. B., *The Induction Motor.*
Behrend, B. A., *Induction Motor.*
Heubach, J., *Der Drehstrommotor.*
Feldmann, C., *Asynchrone Generatoren.*
Niethammer, Dr. F., *Moteurs à Collecteur à Courants Altérnatifs.*
Steinmetz, C. P., *Alternating Current Phenomena.*
Benischke, Dr. G., *Die Asynchronen Drehstrommotoren.*
Tesla, N., *Patents of.*
Kapp, G., *Transformers.*
Emde, F., *Die Arbeitsweise der Wechselstrommaschinen.*
Roessler, *Elektromotoren für Wechsel—und Dreh-strom.*

P
Univ
W

Wisconsin, University of
Bulletin. v.4

122486

DATE

NAME OF BORROWER

UNIVERSITY OF TORONTO
LIBRARY

Do not
remove
the card
from this
Pocket.

Acme Library Card Pocket
Under Pat. "Ref. Index File."
Made by LIBRARY BUREAU